APR 29 1989

NAS1.55:3031/pt.3

Mf-0830-H-10
(330)

NASA Conference Publication 3031
Part 3

Recent Advances in Multidisciplinary Analysis and Optimization

Proceedings of a symposium held in
Hampton, Virginia
September 28-30, 1988

NASA

VL

COMPLETED

NASA Conference Publication 3031
Part 3

Recent Advances in Multidisciplinary Analysis and Optimization

Jean-François M. Barthelemy, *Editor*
NASA Langley Research Center
Hampton, Virginia

Proceedings of a symposium cosponsored by
NASA Langley Research Center, NASA Lewis
Research Center, and the Wright Research
Development Center, and held in
Hampton, Virginia
September 28–30, 1988

NASA
National Aeronautics and
Space Administration
Office of Management
Scientific and Technical
Information Division
1989

BLANK PAGE

PREFACE

This publication contains papers presented at the Second NASA/Air Force Symposium on Recent Advances in Multidisciplinary Analysis and Optimization held September 28-30, 1988 in Hampton, Virginia. The symposium was cosponsored by NASA Langley, NASA Lewis, and the Wright Research Development Center. The meeting was attended by 195 participants, with 41% from industry, 35% from academia, and 24% from government organizations.

The aim of the symposium was to provide a forum for researchers, software developers, and practitioners of multidisciplinary analysis and optimization to learn of the latest developments and to exchange experiences in this burgeoning field of engineering.

Ninety-two papers were presented (83 of which are published here). Of the papers originally presented, 58% discussed method development, 30% applications, and 12% software development or implementation. Most (72%) of the contributions to the symposium were strictly multidisciplinary. There were 15 papers dealing with the combination of structures and control systems, 10 with aeroelastic problems, and 5 with aeroservoelastic problems. Eight papers dealt with generic developments in multidisciplinary design. The keynote address was a review of the role of knowledge-based systems in analysis and optimization.

The papers are grouped by sessions and are identified in the Contents. Papers were edited to conform to the technical standards set by NASA for conference publications. A list of addresses of all registered participants is included.

Jean-François M. Barthelemy
Technical Program Chairman

BLANK PAGE

CONTENTS

PREFACE iii

ATTENDEES xiii

Part 1*

Session 1: Plenary
Chairman: Owen F. Hughes

APPLICATIONS OF INTEGRATED DESIGN/ANALYSIS SYSTEMS IN AEROSPACE STRUCTURAL DESIGN 3
Philip Mason, Edwin Lerner, and Lawrence Sobel

INTEGRATED DESIGN OPTIMIZATION RESEARCH AND DEVELOPMENT IN AN INDUSTRIAL ENVIRONMENT 39
V. Kumar, M. D. German, and S.-J. Lee

OPTIMIZATION BY DECOMPOSITION: A STEP FROM HIERARCHIC TO NON-HIERARCHIC SYSTEMS 51
Jaroslaw Sobieszczanski-Sobieski

OVERVIEW OF DYNAMICS INTEGRATION RESEARCH (DIR) PROGRAM AT LANGLEY RESEARCH CENTER: Goals and Progress 79
Steven M. Sliwa and Irving Abel

SESSION 2: HELICOPTERS
Chairmen: D. Anderson and R. G. Kvaternik

AN INITIATIVE IN MULTIDISCIPLINARY OPTIMIZATION OF ROTORCRAFT 109
Howard M. Adelman and Wayne R. Mantay

STRUCTURAL OPTIMIZATION OF ROTOR BLADES WITH STRAIGHT AND SWEPT TIPS SUBJECT TO AEROELASTIC CONSTRAINTS 145
Peretz P. Friedmann and Roberto Celi

OPTIMIZATION OF ROTOR BLADES FOR COMBINED STRUCTURAL, PERFORMANCE, AND AEROELASTIC CHARACTERISTICS 163
David A. Peters and Y. P. Cheng

TRANSONIC AIRFOIL DESIGN FOR HELICOPTER ROTOR APPLICATIONS 181
Ahmed A. Hassan and B. Jackson

EFFICIENT SENSITIVITY ANALYSIS AND OPTIMIZATION OF A HELICOPTER ROTOR 195
J. W. Lim and I. Chopra

STRUCTURAL OPTIMIZATION OF ROTOR BLADES WITH INTEGRATED DYNAMICS AND AERODYNAMICS 209
Aditi Chattopadhyay and Joanne L. Walsh

---

*Presented under separate cover.

MULTI-OBJECTIVE/LOADING OPTIMIZATION FOR ROTATING COMPOSITE FLEXBEAMS 235
Brian K. Hamilton and James R. Peters

SESSION 3: ARTIFICIAL INTELLIGENCE
Chairmen: K. H. Abbott and P. Hajela

NEW DIRECTIONS FOR ARTIFICIAL INTELLIGENCE (AI) METHODS IN OPTIMUM DESIGN 259
Prabhat Hajela

DEVELOPMENT OF A MICRO-COMPUTER BASED INTEGRATED DESIGN SYSTEM FOR HIGH ALTITUDE LONG ENDURANCE AIRCRAFT 275
David W. Hall and J. Edward Rogan

DEMONSTRATION OF DECOMPOSITION AND OPTIMIZATION IN THE DESIGN OF EXPERIMENTAL SPACE SYSTEMS 297
Sharon L. Padula, Chris A. Sandridge, Raphael T. Haftka, and Joanne L. Walsh

STRUTEX - A PROTOTYPE KNOWLEDGE-BASED SYSTEM FOR INITIALLY CONFIGURING A STRUCTURE TO SUPPORT POINT LOADS IN TWO DIMENSIONS 317
James L. Rogers and Jaroslaw Sobieszczanski-Sobieski

TRUSS: AN INTELLIGENT DESIGN SYSTEM FOR AIRCRAFT WINGS 333
Preston R. Bates and Daniel P. Schrage

REAL-TIME APPLICATION OF KNOWLEDGE-BASED SYSTEMS 357
Randal W. Brumbaugh and Eugene L. Duke

THE DESIGNER OF THE 90'S: A LIVE DEMONSTRATION 373
Tommy L. Green, Basil M. Jordan, Jr., and Timothy L. Oglesby

SESSION 4: AEROELASTIC TAILORING
Chairmen: B. A. Rommel and T. A. Weisshar

STRUCTURAL TAILORING OF COUNTER ROTATION PROPFANS 389
K. W. Brown and D. A. Hopkins

COMPOSITE SIZING AND PLY ORIENTATION FOR STIFFNESS REQUIREMENTS USING A LARGE FINITE ELEMENT STRUCTURAL MODEL 403
N. A. Radovcich and D. P. Gentile

AEROELASTIC TAILORING AND INTEGRATED WING DESIGN 431
Mike Love and Jon Bohlmann

INTEGRATED AERODYNAMIC-STRUCTURAL DESIGN OF A FORWARD-SWEPT TRANSPORT WING 445
R. T. Haftka, B. Grossman, P. J. Kao, D. M. Polen, and J. Sobieszczanski-Sobieski

STATIC AEROELASTIC ANALYSIS AND TAILORING OF MISSILE CONTROL FINS 465
S. C. McIntosh, Jr., and M. F. E. Dillenius

EFFECTS OF NONLINEAR AERODYNAMICS AND STATIC AEROELASTICITY ON MISSION PERFORMANCE CALCULATIONS FOR A FIGHTER AIRCRAFT 477
Gary L. Giles, Kenneth E. Tatum, and William E. Foss, Jr.

OPTIMUM STRUCTURAL DESIGN WITH STATIC AEROELASTIC CONSTRAINTS 497
K. B. Bowman, R. V. Grandhi, and F. E. Eastep

OPTIMUM DESIGN OF SWEPT-FORWARD HIGH-ASPECT-RATIO GRAPHITE-EPOXY WINGS 509
M. J. Shuart, R. T. Haftka, and R. L. Campbell

PART 2*

SESSION 5: SOFTWARE I
Chairmen: G. N. Vanderplaats and R. E. Fulton

ASTROS - A MULTIDISCIPLINARY AUTOMATED STRUCTURAL DESIGN TOOL 529
D. J. Neill

A GENERALIZED SOFTWARE EXECUTIVE FOR MULTIDISCIPLINARY COMPUTATIONAL STRUCTURAL DYNAMICS 545
Alex Berman

RESEARCH ON OPTIMIZATION-BASED DESIGN AT THE ENGINEERING DESIGN METHODS LAB, BRIGHAM YOUNG UNIVERSITY 565
R. J. Balling, A. R. Parkinson, and J. C. Free

RECENT EXPERIENCES USING FINITE-ELEMENT-BASED STRUCTURAL OPTIMIZATION 581
B. K. Paul, J. C. McConnell, and M. H. Love

THE SIZING AND OPTIMIZATION LANGUAGE (SOL) - A COMPUTER LANGUAGE TO IMPROVE THE USER/OPTIMIZER INTERFACE 601
S. H. Lucas and S. J. Scotti

ROBUST COMPUTER-AIDED SYNTHESIS AND OPTIMIZATION OF LINEAR MULTIVARIABLE CONTROL SYSTEMS WITH VARYING PLANT DYNAMICS VIA AUTOCON 621
C. P. Lefkowitz, J. A. Tekawy, P. K. Pujara, and M. G. Safonov

COMPUTERIZED DESIGN SYNTHESIS (CDS), A DATA BASE-DRIVEN MULTIDISCIPLINARY DESIGN TOOL 639
D. M. Anderson and A. O. Bolukbasi

SESSION 6: SENSITIVITY ANALYSIS
Chairmen: R. T. Haftka and B. Prasad

ON EQUIVALENCE OF DISCRETE-DISCRETE AND CONTINUUM-DISCRETE DESIGN SENSITIVITY ANALYSIS 653
Kyung K. Choi and Sung-Ling Twu

AN INVESTIGATION OF USING AN RQP BASED METHOD TO CALCULATE PARAMETER SENSITIVITY DERIVATIVES 673
Todd J. Beltracchi and Gary A. Gabriele

---

*Presented under separate cover.

GRID SENSITIVITY CAPABILITY FOR LARGE SCALE STRUCTURES 697
Gopal K. Nagendra and David V. Wallerstein

ITERATIVE METHODS FOR DESIGN SENSITIVITY ANALYSIS 713
A. D. Belegundu and B. G. Yoon

RESULTS OF AN INTEGRATED STRUCTURE/CONTROL LAW DESIGN SENSITIVITY ANALYSIS 727
Michael G. Gilbert

ON THE CALCULATION OF DERIVATIVES OF EIGENVALUES AND EIGENVECTORS IN THE SIMULTANEOUS DESIGN AND CONTROL OF STRUCTURES 747
Luis Mesquita and Manohar P. Kamat

TREATMENT OF BODY FORCES IN BOUNDARY ELEMENT DESIGN SENSITIVITY ANALYSIS 759
Sunil Saigal, R. Aithal, and Jizu Cheng

DESIGN SENSITIVITY ANALYSIS OF BOUNDARY ELEMENT SUBSTRUCTURES 777
James H. Kane, Sunil Saigal, and Richard H. Gallagher

SESSION 7: CONTROL OF AEROELASTIC STRUCTURES

Chairmen: I. Abel, and N. A. Radovcich

AEROSERVOELASTIC TAILORING FOR LATERAL CONTROL ENHANCEMENT 803
Terrence A. Weisshaar and Changho Nam

RESULTS OF INCLUDING GEOMETRIC NONLINEARITIES IN AN AEROELASTIC MODEL OF AN F/A-18 815
Carey S. Buttrill

FLUTTER SUPPRESSION USING EIGENSPACE FREEDOMS TO MEET REQUIREMENTS 837
William M. Adams, Jr., Robert E. Fennell, and David M. Christhilf

AEROELASTIC MODELING FOR THE FIT TEAM F/A-18 SIMULATION 861
Thomas A. Zeiler and Carol D. Wieseman

DIGITAL ROBUST CONTROL LAW SYNTHESIS USING CONSTRAINED OPTIMIZATION 879
Vivekananda Mukhopadhyay

AN INTEGRATED APPROACH TO THE OPTIMUM DESIGN OF ACTIVELY CONTROLLED COMPOSITE WINGS 897
E. Livne

CONTROL SURFACE SPANWISE PLACEMENT IN ACTIVE FLUTTER SUPPRESSION SYSTEMS 919
E. Nissim and J. J. Burken

SESSION 8: STRUCTURES

Chairmen: R. Levy and P. Papalambros

AN APPROXIMATION FUNCTION FOR FREQUENCY CONSTRAINED STRUCTURAL OPTIMIZATION 937
R. A. Canfield

STRUCTURAL OPTIMIZATION OF FRAMED STRUCTURES USING GENERALIZED OPTIMALITY CRITERIA 955
R. M. Kolonay, V. B. Venkayya, V. A. Tischler, and R. A. Canfield

FINITE ELEMENT FLOW-THERMAL-STRUCTURAL ANALYSIS OF AERODYNAMICALLY HEATED LEADING EDGES 971
Pramote Dechaumphai, Allan R. Wieting, and Ajay K. Pandey

INVOLUTE COMPOSITE DESIGN EVALUATION USING GLOBAL DESIGN SENSITIVITY DERIVATIVES 991
J. K. Hart and E. L. Stanton

OPTIMIZING FOR MINIMUM WEIGHT WHEN TWO DIFFERENT FINITE ELEMENT MODELS AND ANALYSES ARE REQUIRED 1009
Jeffrey C. Hall

PART 3

SESSION 9: LARGE ENGINEERING SYSTEMS
Chairman: G. L. Giles

ENGINEERING APPLICATIONS OF HEURISTIC MULTILEVEL OPTIMIZATION METHODS 1029 2
Jean-François M. Barthelemy

RECENT DEVELOPMENTS IN MULTILEVEL OPTIMIZATION 1039 11
G. N. Vanderplaats and D-S Kim

A DECOMPOSITION-BASED DESIGN OPTIMIZATION METHOD WITH APPLICATIONS 1055 27
S. Azarm, M. Pecht, W.-C. Li, and S. Praharaj

MULTILEVEL DECOMPOSITION OF COMPLETE VEHICLE CONFIGURATION IN A PARALLEL COMPUTING ENVIRONMENT 1069 41
Vinay Bhatt and K. M. Ragsdell

SESSION 10: SHAPE OPTIMIZATION
Chairman: G. A. Gabriele

DESIGN OPTIMIZATION OF AXISYMMETRIC BODIES IN NONUNIFORM TRANSONIC FLOW 1085 57
C. Edward Lan

PROCEDURES FOR SHAPE OPTIMIZATION OF GAS TURBINE DISKS 1097 69
Tsu-Chien Cheu

SESSION 11: ENGINEERING SYSTEM DESIGN
Chairmen: M. D. German and D. P. Schrage

A DECISION-BASED PERSPECTIVE FOR THE DESIGN OF METHODS FOR SYSTEMS DESIGN 1111 83
Farrokh Mistree, Douglas Muster, Jon A. Shupe, and Janet K. Allen

THE ART OF SPACECRAFT DESIGN: A MULTIDISCIPLINARY CHALLENGE 1137 **109**
F. Abdi, H. Ide, M. Levine, and L. Austel

HYPERSONIC AIRBREATHING VEHICLE CONCEPTUAL DESIGN (FOCUS ON AERO-SPACE PLANE) 1157 **129**
James L. Hunt and John G. Martin

OPTIMIZING CONCEPTUAL AIRCRAFT DESIGNS FOR MINIMUM LIFE CYCLE COST 1195 **167**
Vicki S. Johnson

AIRCRAFT DESIGN OPTIMIZATION WITH MULTIDISCIPLINARY PERFORMANCE CRITERIA 1219 **191**
Stephen Morris and Ilan Kroo

SESSION 12: METHODS
Chairmen: M. P. Kamat and J. E. Rogan

AN INTERPRETATION AND SOLUTION OF ILL-CONDITIONED LINEAR EQUATIONS 1239 **211**
I. U. Ojalvo and T. Ting

GENERALIZED MATHEMATICAL MODELS IN DESIGN OPTIMIZATION 1253 **225**
Panos Y. Papalambros and J. R. Jagannatha Rao

OPTIMUM DESIGN OF STRUCTURES SUBJECT TO GENERAL PERIODIC LOADS 1265 **237**
R. Reiss and B. Qian

FUZZY SET APPLICATIONS IN ENGINEERING OPTIMIZATION 1279 **251**
Alejandro R. Diaz

A PENALTY APPROACH FOR NONLINEAR OPTIMIZATION WITH DISCRETE DESIGN VARIABLES 1291 **263**
Dong K. Shin, Z. Gurdal, and O. H. Griffin, Jr.

MULTIPLIER-CONTINUATION ALGORITHMS FOR CONSTRAINED OPTIMIZATION 1303 **275**
Bruce N. Lundberg, Aubrey B. Poore and Bing Yang

SESSION 13: SOFTWARE II
Chairmen: R. A. Canfield and J. L. Rogers, Jr.

A LARGE SCALE SOFTWARE SYSTEM FOR SIMULATION AND DESIGN OPTIMIZATION OF MECHANICAL SYSTEMS 1319 **291**
Bernhard Dopker and Edward J. Haug

THE ROLE OF OPTIMIZATION IN THE NEXT GENERATION OF COMPUTER-BASED DESIGN TOOLS 1335 **307**
J. E. Rogan

AN OVERVIEW OF THE DOUGLAS AIRCRAFT COMPANY AEROELASTIC DESIGN OPTIMIZATION PROGRAM (ADOP) 1359 **331**
Alan J. Dodd

MEETING THE CHALLENGES WITH THE DOUGLAS AIRCRAFT COMPANY AEROELASTIC DESIGN OPTIMIZATION PROGRAM (ADOP) 1369 **341**
Bruce A. Rommel

SESSION 14: DYNAMICS AND CONTROL OF FLEXIBLE STRUCTURES
Chairmen: J.-N. Juang and E. Livne

OPTIMIZATION OF STRUCTURE AND CONTROL SYSTEM 1381 **353**
N. S. Khot and R. V. Grandhi

STRUCTURAL OPTIMIZATION AND RECENT LARGE GROUND ANTENNA INSTALLATIONS 1393 **365**
Roy Levy

A NOVEL IMPLEMENTATION OF METHOD OF OPTIMALITY CRITERION IN SYNTHESIZING SPACECRAFT STRUCTURES WITH NATURAL FREQUENCY CONSTRAINTS 1417 **389**
B. P. Wang and F. H. Chu

COMPUTATIONAL EXPERIMENTS IN THE OPTIMAL SLEWING OF FLEXIBLE STRUCTURES 1427 **399**
T. E. Baker and E. Polak

OPTIMAL PLACEMENT OF EXCITATIONS AND SENSORS BY SIMULATED ANNEALING 1441 **413**
M. Salama, R. Bruno, G-S. Chen, and J. Garba

EXPERIENCES IN APPLYING OPTIMIZATION TECHNIQUES TO CONFIGURATIONS FOR THE CONTROL OF FLEXIBLE STRUCTURES (COFS) PROGRAM 1459 **431**
Joanne L. Walsh

AN IMPROVED ALGORITHM FOR OPTIMUM STRUCTURAL DESIGN WITH MULTIPLE FREQUENCY CONSTRAINTS 1489 **461**
Oliver G. McGee and Khing F. Phan

ADDITIONAL PAPERS

The following paper is being included in this publication although time restrictions did not permit its presentation at the September conference.

STRUCTURAL DAMAGE ASSESSMENT AS AN IDENTIFICATION PROBLEM 1507 **479**
P. Hajela and F. J. Soeiro

The following paper arrived during the printing process and was originally included in Session I.

RECENT DEVELOPMENTS IN LARGE-SCALE STRUCTURAL OPTIMIZATION 1521 **493**
V. B. Venkayya

BLANK PAGE

ATTENDEES

Mrs. Kathy H. Abbott
NASA/Langley Research Center
MS 156A
Hampton, VA 23665-5225

Mr. Irving Abel
NASA/Langley Research Center
MS 242
Hampton, VA 23665-5225

Mr. William M. Adams Jr.
NASA/Langley Research Center
MS 489
Hampton, VA 23665-5225

Dr. Howard M. Adelman
NASA/Langley Research Center
MS 246
Hampton, VA 23665-5225

Dr. Don Anderson
McDonnell Douglas Helicopter Co.
Bldg. 530/B327
5000 E. McDowell Rd.
Mesa, AZ 85205

Mr. Ernest S. Armstrong
NASA/Langley Research Center
MS 499
Hampton, VA 23665-5225

Prof. Shapour Azarm
The University of Maryland
Department of Mechanical
Engineering
College Park, MD 20742

Dr. Richard J. Balling
Brigham Young University
Engineering Design Methods
Laboratory
368R Clyde Building
Provo, UT 84602

Dr. Dey Banerjee
McDonnell Douglas Helicopter Co.
Bldg. 530, MS/B 346
5000 E. McDowell Rd.
Mesa, AZ 85205

Mr. Paul Barnhart
Sverdrup Technology, Inc.
P.O. Box 30650, Midpark Branch
Middleburg Heights, OH 44130

Dr. Bruno Barthelemy
Ford Research and Engineering
Center
Room E31[illegible]/SCI-LAB
P. O. Box 2053
Dearborn, MI 48121-2053

Dr. Jean-Francois M. Barthelemy
NASA/Langley Research Center
MS 246
Hampton, VA 23665-5225

Mr. Oscar Barton, Jr.
Howard University
Department of Mechanical
Engineering
2308 6th St. N.W.
Washington, DC 20059

Mr. P. R. Bates
Georgia Institute of Technology
School of Aerospace Engineering
P. O. Box 30302
Atlanta, GA 30332-0150

Prof. Ashok D. Belegundu
Penn State University
Mechanical Engineering
University Park, PA 16802

Mr. Todd J. Beltracchi
Rensselaer Polytechnic Institute
2418 Huntington Lane #3
Redondo Beach, CA 90278

Dr. Laszlo Berke
NASA/Lewis Research Center
MS 4907
21000 Brookpark Road
Cleveland, OH 44135

Mr. Alex Berman
Kaman Aerospace Corp.
Old Windsor Road
P.O. Box 2
Bloomfield, CT 06002

Mr. Vinay Bhatt
University of Missouri-Columbia
Mechanical and Aerospace
Engineering
1080 Engineering UMC
Columbia, MO 65201

Mr. Robert Blackwell
Sikorsky Aircraft
No. Main Street
Stratford, CT 06601-1381

Mr. Chris Borland
Boeing Military Airplane Co.
P.O. Box 3707
Mail Code 33-04
Seattle, WA 98124

Mr. Keith Bowman
US Air Force
AFWAL/FIBCA
Wright AFB
Wright-Patterson AFB, OH 45433

Mrs. Lynn M. Bowman
Planning Research Corporation
303 Butler Farm Rd, Suite 100
Hampton, VA 23666

Mr. Kenneth W. Brown
Pratt & Whitney Aircraft
400 Main Street, M.S. 163-09
East Hartford, CT 06108

Mr. Randal W. Brumbaugh
Planning Research Corporation
PO Box 273
NASA Dryden Bldg. 4839
Edwards, CA 93323

Mr. Christopher N. Butten
Digital Equipment Corporation
4417 Corporation
Virginia Beach, VA 23462

Mr. Carey S. Buttrill
NASA/Langley Research Center
MS 494
Hampton, VA 23665-5225

Mr. Charles Camarda
NASA/Langley Research Center
MS 396
Hampton, VA 23665-5225

Mr. Frank Campisano
Northrop Corporation
One Northrop Ave
Hawthorne, CA 90250

Capt. Robert A. Canfield
AF Wright Aeronautical
Laboratories
AFWAL/FIBRA
Wright-Patterson AFB, OH
45433-6553

Mr. Richard G. Carter
ICASE
NASA/Langley Research Center
MS 132C
Hampton, VA 23665

Mr. Jeffrey A. Cerro
Planning Research Corporation
303 Butler Farm Rd, Suite 100
Suite 100
Hampton, VA 23666

Dr. Christos C. Chamis
NASA/Lewis Research Center
MS 49-8
21000 Brookpark Road
Cleveland, OH 44135

Prof. A. Chandra
University of Arizona
Aerospace and Mechanical
Engineering
Aero Bldg #16
Tucson, AZ 85721

Dr. Kwan J. Chang
Planning Research Corporation
303 Butler Farm Rd, Suite 100
Hampton, VA 23666

Dr. Mladen Chargin
NASA/Ames Research Center
MC 213-3
Moffett Field, CA 94035

Dr. Aditi Chattopadhyay
Analytical Services and
Materials Inc.
NASA/Langley Research Center
MS 246
Hampton, VA 23665-5225

Dr. Tsu-Chien Cheu
Textron Lycoming, Dept. LSK-5
550 S. Main Street
Stratford, CT 06497

Prof. Kyung K. Choi
The University of Iowa
Dept.of Mechanical Engineering
2132 Engineering Bldg
Iowa City, IA 52242

Mr. Choon T. Chon
Ford Motor Company
S-1108, SRL
P.O. Box 2053
Dearborn, MI 48121

Prof. Inderjit Chopra
University of Maryland
Dept. of Aerospace Engineering
College Park, MD 20742

Mr. David M. Christhilf
Planning Research Corporation
NASA/Langley Research Center
MS/489
Hampton, VA 23665-5225

Mr. Ching-Hung Chuang
Old Dominion University
937 Rockbridge Ave. #244
Norfolk, VA 23508

Prof. Young W. Chun
Villanova University
Dept. of Mechanical Engineering
Villanova, PA 19085

Mr. Robert D. Consoli
General Dynamics
P. O. Box 748
Fort Worth, TX 76102

Mr. Mark W. Davis
United Technologies Research
Center
MS 19
Silver Lane
E. Hartford, CT 06108

Mr. Randall C. Davis
NASA/Langley Research Center
MS 396
Hampton, VA 23665-5225

Dr. Pramote Dechaumphai
NASA/Langley Research Center
MS 395
Hampton, VA 23665-5225

Prof. Alejandro Diaz
Michigan State University
Dept. of Mechanical Engineering
Room 200, Engineering Building
East Lansing, MI 48824-1226

Mr. Alan J. Dodd
Douglas Aircraft Company
C1-E84, Mail Code 212-10
3155 Lakewood Blvd.
Long Beach, CA 90815

Mr. Auqustine R. Dovi
Planning Research Corporation
303 Butler Farm Rd, Suite 100
Hampton, VA 23666

Mr. Rodney Dreisbach
The Boeing Company
P. O. Box 707
Mail Stop 9W-22
Seattle, WA

Mr. Delmar W. Drier
NASA/Lewis Research Center
MS 86-12
21000 Brookpark Road
Cleveland, OH 44135

Dr. Ernest D. Eason
Modeling & Computing Services
1153 Bordeaux Drive
Suite 107
Sunnyvale, CA 94089

Dr. Peter A. Fenyes
General Motors Research
Laboratories
Engineering Mechanics Department
30500 Mound Rd Dept 15
Warren, MI 48090-9055

Mr. Brian Fite
NASA/Lewis Research Center
21000 Brookpark Road
MS 86-10
Cleveland, OH 44135

Dr. Donald Flaggs
Lockheed Palo Alto Research
Laboratory
Lockheed M&S 93-30/251
3251 Hanover ST.
Palo Alto, CA 94304

Prof. Claude Fleury
University of California
Dept. of Mech. Aero. & Nuclear
Engrg.
5732 Boelter Hall
Los Angeles, CA 90024

Mr. Williard E. Foss Jr.
NASA/Langley Research Center
MS 412
Hampton, VA 23665

Prof. Joseph Free
Brigham Young University
Department of Mechanical
Engineering
242 Clyde Building
Provo, UT 84602

Prof. Peretz P. Friedmann
University of California-Los
Angeles
5732H Boelter Hall
Los Angeles, CA 90024

Prof. Robert E. Fulton
Georgia institute of Technology
Mechanical Engineering
Atlanta, GA 30332

Dr. Gary A. Gabriele
Rensselaer Polytechnic Institute
Dept. of Mechanical Engineering
Johnson Engineering Center,
Rm. 4026
Troy, NY 12180-3590

Mr. James E. Gardner
NASA/Langley Research Center
MS 246
Hampton, VA 23665

Mrs. Marjorie German
G. E. Research and Development
1 River Road, Bldg. K-1, Room
3A20
Schenectady, NY

Mr. D. Ghosh
Planning Research Corporation
303 Butler Farm Rd, Suite 100
Hampton, VA 23665

Mr. Daniel P. Giesy
Planning Research Corporation
303 Butler Farm Rd, Suite 100
Suite 100
Hampton, Va 23666

Mr. Michael G. Gilbert
NASA/Langley Research Center
MS 243
Hampton, VA 23665-5225

Dr. Gary L. Giles
NASA/Langley Research Center
MS 246
Hampton, VA 23665-5225

Mr. David E. Glass
Analytical Services & Materials
107 Research Drive
Hampton, Va 23666

Prof. Ramana Grandhi
Wright State University
Mechanical Systems and
Engineering
Dayton, OH 45435

Mr. Philip C. Graves
Vigyan Research Association
30 Research Drive
Hampton, Va 23666

Mr. Tommy L. Green
LTV Aerospace and Defense
Company
Aircraft Products Group
P.O. Box 655907, MS 194-24
Dallas, TX 75265-5907

Mr. William H. Greene
NASA/Langley Research Center
MS 190
Hampton, VA 23665-5225

Prof. Bernard Grossman
Aerospace and Ocean Engineering
VPI & SU
Blacksburg, VA 24061

Prof. Zafer Gurdal
VPI & SU
Engineering Science and
Mechanics Dept.
Norris Hall
Blacksburg, VA 24061

Prof. Raphael T. Haftka
VPI&SU
Dept. of Aerospace & Ocean
Engineering
Blacksburg, VA 24061

Prof. Prabhat Hajela
University of Florida
Dept. of Aero. Eng., Mech. and
Eng. Sci.
231 Aerospace, Aero
Gainesville, FL 32611

Mr. David W. Hall
David Hall Consulting
1158 South Mary Avenue
Sunnyvale, CA 94087-2103

Dr. Jeffrey C. Hall
General Dynamics Corp./Elec.
Boat Div.
Department 443
Eastern Point Road
Groton, CT 06340

Mr. Stephen A. Hambric
David Taylor Research Center
Code 1844
Bethesda, MD 20084

Dr. M. Nabil Hamouda
Planning Research Corporation
NASA/Langley Research Center
MS 340
Hampton, VA 23665-5225

Mr. Jonathan K. Hart
PDA Engineering, Inc.
2975 Redhill Avenue
Costa Mesa, CA 92626-5923

Mr. Ahmed A. Hassan
McDonnell Douglas Helicopter
Company
5000 E. McDowell
Bldg 530, MS B346
Mesa, AZ 85205-9797

Mr. T. K. Hasselman
Engineering Mechanics Assoc.,
Inc.
3820 Del Amo Boulevard, Suite
318
Torrance, CA 90503

Ms. Jennifer Heeg
Planning Research Corporation
303 Butler Farm Rd, Suite 100
Hampton, Va 23666

Mr. Charles Holland
AF Office of Scientific Research
Department of the Air Force
Bolling Air Force Base, DC
20332-6458

Prof. Jean Win Hou
Old Dominion University
Dept. Mech. Engineering and
Mechanics
Norfolk, VA 23462

Prof. Owen F. Hughes
VPI & SUN
1745 Jefferson Davis Highway
STE 300
Arlington, VA 22202

Mr. Amir Izadpanah
Vigyan Research Association
NASA/Langley Research Center
MS 340
Hampton, VA 23665

Mr. Burton H. Jackson
McDonnell Douglas Helicopter
5000 E. McDowell
Mesa, AZ

MS. Cheryl C. Jackson
Old Dominion University
Dept. of Mech. Eng. and Mech.
Norfolk, VA 23529-0247

Mr. Benjamin B. James III
Planning Research Corporation
303 Butler Farm Rd, Suite 100
Hampton, VA 23666

Ms. Vicki Johnson
NASA/Langley Research Center
MS 412
Hampton, VA 23665-5225

Mr. B. M. Jordan, Jr.
LTV Aerospace & Defense Company
P.O. Box 655907
MS 194-24
Dallas, Texas 75265-5907

Mr. Suresh M. Joshi
NASA/Langley Research Center
MS 161
Hampton, VA 23665-5225

Dr. Jer-Nan Juang
NASA/Langley Research Center
MS 230
Hampton, VA 23665-5225

Prof. Manohar P. Kamat
Georgia Institute of Technology
School of Aerospace Engineering
Atlanta, GA 30332

Mr. James Kane
Clarkson University
Mech. and Ind. Engineering Dept.
Potsdam, NY 13676

Mr. Pi-Jen Kao
VPI&SU
Dept. of Aerospace & Ocean
Engineering
Blacksburg, VA 24061

Mr. Mordechay Karpel
Technion -Israel Institute of
Technology
Dept. of Aero Engineering
Haifa 32000 Israel

Mr. Sean P. Kenny
Old Dominion University
Norfolk, VA 23508

Mr. Suresh Khandelwal
Sverdrup Technology
16530 Commerce Ct.
Middleburg Hts, OH 44130

Prof. Noboru Kikuchi
University of Michigan
Department of Mechanical
Engineering
Ann Arbor, MI 48109

Prof. Rex K. Kincaid
College of William and Mary
Dept. of Mathematics
Williamsburg, VA 23185

Dr. Norman F. Knight, Jr.
NASA/Langley Research Center
MS 244
Hampton, VA 23665-5225

Mr. Raymond M. Kolonay
AF Wright Aeronautical
Laboratories
AFWAL/FIBRA
Wright-Patterson AFB, OH 45433

Prof. Ilan Kroo
Stanford University
Dept. of Aero/Astro
Stanford, CA 94305

Dr. Raymond G. Kvaternik
NASA/Langley Research Center
MS 340
Hampton, VA 23665-5225

Prof. C. Edward Lan
The University of Kansas
Aerospace Engineering Dept.
Room 2004, Learned Hall
Lawrence, KS 66045

Mr. Jerry Lang
NASA/Lewis Research Center
21000 Brookpark Rd.
Cleveland, OH 44135

Mr. M. Levine
Rockwell International
P.O. Box 92098
Los Angeles, CA 90245

Dr. Roy Levy
Jet Propulsion Laboratory
MS 144-201
4800 Oak Grove Drive
Pasadena, CA 91109

Mr. Joon W. Lim
University of Maryland
College Park, MD

Mr. Kyong B. Lim
Planning Research Corporation
303 Butler Farm Rd
Suite 100
Hampton, Va 23666

Mr. Eli Livne
University of California Los
Angeles
4531 Boelter Hall, UCLA
Los Angeles, CA 90024

Mr. Andrew Logan
McDonnell Douglas Helicopter Co.
Bldg. 503, MSB 325
5000 E. McDowell Rd.
Mesa, AZ 85205

Mr. Michael G. Long
Cray Research. Inc.
1333 Northland Drive
Mendota Heights, MN 55120

Dr. Robert V. Lust
General Motors Research
Laboratories
Engineering Mechanics Department
30500 Mound Road, MS 256 Rm B
Warren, MI 48090-9057

Mr. Peiman G. Maghami
Old Dominion University
Norfolk, VA 23508 23508

Mr. Wayne R. Mantay
US Army Aerostructures
Directorate
NASA/Langley Research Center
MS 266
Hampton, VA 23665-5225

Mr. Carl J. Martin
Planning Research Corporation
303 Butler Farm Rd, Suite 100
Hampton, Va 23666

Mr. John G. Martin
Planning Research Corporation
303 Butler Farm Rd, Suite 100
Hampton, Va 23666

Mr. Zoran N. Martinovic
Analytical Mechanics
Associates, Inc.
17 Research Drive
Hampton, VA 23666

Mr. Philip Mason
Grumman Aerospace Corp.
B-35, Dept. 430
Stewart Ave.
Bethpage, NY 11714

Mr. Oliver G. McGee
Ohio State University
Department of Civil Engineering
417B Hitchcock Hall
Columbus OH 43210

Mr. Niki Mehta
Old Dominion University
Dept. of Mechanical Eng. and
Mechanical
College of Engineering and
Technology
Norfolk, VA 23529-0247

Prof. Luis Mesquita
University of Nebraska
Department of Enigneering
Mechanics
217 Bancroft
Lincoln, NE 68588

Prof. Farrokh Mistree
University of Houston-Univ. Park
Dept. of Mechanical Engineering
4800 Calhoun Road
Houston, TX 77204-4792

Dr. Hiro Miura
NASA/Ames Research Center
Ames Research Center
Attn: 237-11
Moffett Field, CA 94035

Mrs. Arlene A. Moore
Planning Research Corporation
303 Butler Farm Rd, Suite 100
Hampton, Va 23666

Prof Subrata Mukherjee
Cornell University
Dept of T & AM
Kimball Hall
Ithica, NY 14853

Dr. T. Sreekanta Murthy
Planning Research Corporation
MS 340
NASA/Langley Research Center
Hampton, VA 23665-5225

Mr. Evhen M. Mychalowycz
Boeing Vertol Company
MS P32-15
P. O. Box 16858
Philadelphia, PA 19142

Dr. Gopal K. Nagendra
Mac Neal-Schwendler Corp.
815 Colorado Blvd.
Los Angeles, CA 90041-1777

Mr. Changho Nam
Purdue University
School of
Aeronautice/Astronautics
West Lafayette, IN 47907

Mr. D. J. Neill
Northrop Corporation, Aircraft
Division
Dynamics & Loads Research
3854/82
One Northrop Avenue
Hawthorne, CA 90250

Dr. Elli Nissim
NASA Dryden
CODE OFV
Edwards, CA 93523-5000

Mr. Kevin W. Noonan
NASA/Langley Research Center
MS 266
Hampton, VA 23665-5225

Dr. Ahmed K. Noor
The George Washington University
NASA/Langley Research Center
MS269
Hampton, VA 23665-5225

Mr. T. L. Oglesby
LTV Aerospace & Defense Company
P. O. Box 655907
MS 194-24
Dallas, TX 75265-5907

Prof. Irving U. Ojalvo
University of Bridgeport
Dept. of Mechanical Engineering
Bridgeport, CT 06601

Mrs. Sharon L. Padula
NASA/Langley Research Center
IRO Office
MS 246
Hampton, VA 23665

Mr. Ajay K. Pandey
Planning Research Corporation
303 Butler Farm Rd, Suite 100
Hampton, VA 23666

Prof. Alan Parkinson
Department of Mechanical Engineering
Brigham Young University
242 CB
Provo, UT 84602

Mr. Bernhard Pepker
CCAD, EB
University of Iowa
Iowa City, IA 52242

Prof. David Peters
Georgia Institute of Technology
School of Aerospace Engineering
Atlanta, GA 30332

Mr. James Peters
McDonnell Douglas Helicopter Co.
Bldg. 530/B346
5000 E. McDowell Rd.
Mesa, AZ 85205-9797

Prof. Lucian Elijah Polak
University of California
Dept. of Electrical Engineering
565 Cory Hall
Berkeley, CA 94720

Mr. Dave Polen
VPI&SU
Dept. of Aerospace & Ocean Engineering
400 H. Foxridge
Blacksburg, VA 24061

Prof. Aubrey Poore
Colorado State University
Dept. of Mathematics
Fort Collins, CO 80523

Dr. Biren Prasad
Electronic Data Systems Corporation
5555 New King Street
Troy, MI 48007-7019

Dr. Thomas K. Pratt
Pratt & Whitney
Engineering Building, 161-16
400 Main Street
East Hartford, CT 06108

Dr. N. A. Radovcich
Lockheed Aeronautical Systems Co.
D/76-12, Bldg 63-G, Plant A-1
P.O. Box 551
Burbank, CA 91520

Mr. Charles C. Rankin
Lockheed Missiles and Space
Palo Alto Research Lab.
0/93-30 B/251
Palo Alto, CA 94304-1191

Dr. S. M. Rankin
Mathematics Dept.
Worcester Poly. Tech.
Worcester, Ma 01609

Mr. Jagannatha Rao
The University of Michigan
2212 G. G. Brown Lab.
Ann Arbor, MI 48109

Mr. John J. Render
NASA/Langley Research Center
MS 365
Hampton, VA 23665-5225

Prof. Robert Reiss
Howard University
Department of Mechanical Engineering
2300 Sixth Street, N.W.
Washington, DC 20059

Mr. J. Edward Rogan
Georgia Institute of Technology
School of Aerospace Engineering
Atlanta, GA 30332-0150

Mr. James. L. Rogers
NASA/Langley Research Center
IRO Office
MS 246
Hampton, VA 23665

Mrs. V. Aileen Rogers
Planning Research Corporation
303 Butler Farm Rd, Suite 100
Hampton, VA 23666

Mr. Bruce A. Rommel
Douglas Aircraft Company
C1-E84, Mail Code 212-10
3855 Lakewood Blvd.
Long Beach, CA 90846

Dr. Sunil Saigal
Worcester Polytechnic Institute
Mechanical Engineering Department
Institute Road
Worcester, Mass 01069

Dr. Moktar Salama
Jet Propulsion Laboratory
Applied Mechanics Div. - MS 157-316
California Institute of Technology
Pasadena, CA 91109

Mr. Chris A. Sandridge
VPI & SU
Aerospace & Ocean Engineering
Blacksburg, VA 24061

Prof. Lucien A. Schmit
University of California, Los Angeles
4531K Boelter Hall
Los Angeles, CA 90024

Prof. Daniel P. Schrage
Georgia Institute of Technology
School of Aerospace Engineering
250 Drummen Ct
Atlanta, GA 30332-0150

Mr. Stephen J. Scotti
NASA/Langley Research Center
MS 396
Hampton, VA 23665-5225

Mr. Jeen S. Sheen
Old Dominion University
Dept. of Mechanical Eng. and Mechanics
College of Engineering and Technology
Norfolk, VA 23529-0247

Mr. Joram Shenhar
Planning Research Corporation
303 Butler Farm Rd, Suite 100
Hampton, VA 23665

Dr. Mark J. Shuart
NASA/Langley Research Center
MS 190
Hampton, VA 23665-5225

Mr. J. A. Shupe
B. F. Goodrich
9921 Brecksville Road
Brecksville, OH 44141

Mr. Walter A. Silva
Planning Research Corporation
303 Butler Farm Rd, Suite 100
Hampton, VA 23666

Mr. James A. Simak
General Dynamics
Data Systems Division
P.O. Box 748
Fort Worth, TX 76102

Dr. Jaroslaw Sobieski
NASA/Langley Research Center
MS 246
Hampton, VA 23665-5225

Mr. Andy H. Soediono
Georgia Institute of Technology
P. O. Box 34091
225 North Avenue
Atlanta, GA 30332

Dr. James H. Starnes, Jr.
NASA/Langley Research Center
MS 120
Hampton, VA 23665-5225

Mr. Frank J. Tarzanin
Boeing Vertol Company
MS P32-15
P. O. Box 16858
Philadelphia, PA 19142

Mr. Kenneth E. Tatum
Planning Research Corporation
SSD/ATD
303 Butler Farm Rd., Suite 100
Hampton, VA 23666

Mr. Rajiv Thareja
Planning Research Corporation
303 Butler Farm Rd, Suite 100
Hampton, VA 23666

Prof. Garret N. Vanderplaats
University of California, Santa
Barbara
Dept. of Mechanical &
Environmental Eng.
Santa Barbara, CA 93160

Dr. Vipperla B. Venkayya
AF Wright Aeronautical
Laboratories
AFWAL/FIBR
Wright-Patterson AFB, OH 45433

Dr. A. V. Viswanathan
Boeing Commercial Airplane Co.
P. O. Box 3707
Seattle, WA 98124

Mr. A. Von Flotow
MIT
37-335, MIT
Cambridge, MA 02139

Ms. Joanne L. Walsh
NASA/Langley Research Center
MS 246
Hampton, VA 23665-5225

Prof. Bo Ping Wang
The University of Texas
Dept. of Mechanical Engineering
P.O. Box 19023
Arlington, TX 76019

Mr. Bryan Watson
Spectragraphics Corporation
9125 Rehco Road
San Diego, CA 92121

Prof. Terrence A. Weisshaar
Purdue University
School of
Aeronautics/Astronautics
West Lafayette, IN 47907

Mr. W. H. Weller
United Technologies Research
Center
M. S. 19, Silver Lane
East Hartford, CT 06108

Ms Carol D. Wieseman
NASA/Langley Research Center
MS 243
Hampton, VA 23665-5225

Mr. James L. Williams
NASA/Langley Research Center
MS 499
Hampton, VA 23665-5225

Mrs. Jessica A. Woods
Planning Research Corporation
NASA Langley Research Center
Mail Stop 243
Hampton, VA 23665-5225

Mr. Gregory A. Wrenn
Planning Research Corporation
NASA/Langley Research Center
MS905
Hampton, VA 23665-5225

Mr. Ren-Jye Yang
Ford Motor Company
Scientific Research Labs
P. O. Box 2053, RM E-1134
Dearborn, MI 48212

Dr. E. Carson Yates
NASA/Langley Research Center
MS 246
Hampton, VA 23665-5225

Mr. Chao-Pin Yeh
Georgia Tech
Atlanta, Georgia 30332

Mr. John W. Young
NASA/Langley Research Center
MS 499
Hampton, VA 23665-5225

Mrs. Katherine C. Young
NASA/Langley Research Center
IRO Office
MS 246
Hampton, VA 23665

Mr. Rudy Yurkovich
McDonnell Aircraft Co.
P.O. Box 516
St. Louis, MO 63166

Dr. Thomas A. Zeiler
Planning Research Corporation
NASA/Langley Research Center
MS 243
Hampton, VA 23665-5225

PART 3

SESSION 9: LARGE ENGINEERING SYSTEMS

Chairman: G. L. Giles

ENGINEERING APPLICATIONS OF HEURISTIC MULTILEVEL OPTIMIZATION METHODS

Jean-François M. Barthelemy
NASA Langley Research Center
Hampton, VA

2

Abstract Some engineering applications of heuristic multilevel optimization methods are presented and the discussion focuses on the dependency matrix that indicates the relationship between problem functions and variables. Decompositions are identified with dependency matrices that are full, block diagonal and block triangular with coupling variables. Coordination of the subproblem optimizations is shown to be typically achieved through the use of exact or approximate sensitivity analysis. Areas for further development are identified.

Introduction

Ever since optimization methods have been applied in engineering, practitioners have attempted to use them in multilevel schemes. These are procedures where a large problem is broken down in a number of smaller subproblems; this phase is referred to as *decomposition*. These subproblems are optimized separately and an iterative process is then devised which accounts for the coupling so that when it is converged, the resulting optimum is that of the original non-decomposed problem; this phase is referred to as *coordination*.

Multilevel methods can be classified as formal or heuristic according to whether the decomposition and the coordination phases are exclusively based on the mathematical form of the problem or on understanding of the underlying physics. In general, formal methods are more amenable to convergence studies than heuristic methods. The distinction between the two classes of methods is somewhat arbitrary, however, and, depending on how it is presented, a method may be shown to belong to either class.

This paper covers applications of heuristic multilevel optimization methods in engineering design. Problems are assumed to be formulated as static nonlinear parametric programming problems. While most applications are for structural design problems, reference will be made also to selected papers in mechanical, power and electrical engineering.

The paper begins with a review of the objectives of multilevel optimization and a description of typical applications. The two following sections address the decomposition problem and the coordination problem. The paper concludes with an assessment of the state-of-the-art and recommendations for further work. While the paper discusses primarily two-level formulations, most methods may be adapted to decompositions with more than two levels. For the sake of generality, the presentation remains in terms of a generic design problem. Only a limited number of representative papers will be cited.

Objectives and Examples of Application

Some design problems naturally have a multilevel structure as the calculation of their constraints or objective functions are themselves the results of minimization or maximization problems. Haftka [1] showed that the design of damage tolerant space trusses and wing boxes can be formulated with a constraint on maximum collapse load.

By far, the most commonly cited reason for resorting to multilevel optimization is the improvement of the numerical performance of optimization algorithms. In structural optimization, early attempts were direct extensions of the fully stressed design methodology. Using methods devised by Giles [2] and Sobieszczanski and Loendorf [3], Fulton et al. [4] designed a complete aircraft model that involved on the order of 700 design variables and 2500 constraints. Schmit and Mehrinfar [5] followed with optimization of truss and wing box models that included local and global constraints while Hughes [6] developed similar ideas for naval structures. Using a method first proposed by Sobieszczanski [7], Wrenn and Dovi [8] optimized a fairly complex transport wing model with 1200 variables and 2500 nonlinear constraints. Substructuring has also been used to decompose optimization problems. Nguyen [9] used it to reduce the cost of the sensitivity analysis phase. Schmit and Chang [10] and Svensson [11] have looked at optimizing substructures independently. In other engineering applications, multilevel approaches were used to design underground energy storage systems (Sharma, [12]), speed reducers (Datseris, [13]), microwave systems (Bandler and Zhang, [14]) and to solve the optimum power flow problem (Contaxis et al. [15]).

Formulating a multilevel problem can also be used to improve its mathematical conditioning since variables that have different orders of magnitudes and rates of change can be kept separate in the optimization process. Probably the most common example of such application is the simultaneous sizing and optimization of the geometry of structures in which the sizing problem is solved for fixed geometry in an inner loop, while in the outer loop, the geometry is modified to optimize the design. This approach has been used primarily for space trusses and frameworks, examples are given by Felix [16]. Kirsch [17] used a similar formulation to conduct the simultaneous analysis and optimization of reinforced concrete beams.

The design of complex engineering systems is by nature multilevel. Designers carry out the effort by breaking the total problem into subproblems and assigning each to different units of the engineering team. Each unit has developed its own design methodologies and successful designs result from skillful integration of objectives, requirements and constraints from each unit. This becomes a coordination problem. Sobieszczanski [7] was the first to propose to use multilevel coordination methods to solve multidisciplinary design problems. Rogan and Kolb [18] showed how a transport aircraft preliminary design problem can be treated as a multilevel optimization problem.

Decomposition

The general form of the original, non-decomposed optimization problem is as follows (vectors are boldfaced and scalars use normal script):

$$\min_{\mathbf{X}} f(\mathbf{X}), \text{ st } \mathbf{g}(\mathbf{X}) \leq 0, \ \mathbf{h}(\mathbf{X}) = 0 \qquad (1)$$

The relationship between variables and functions (objective and constraints) can be described symbolically by the dependency matrix (Fig. 1). There is one column in the matrix for each variable (or vector of similar variables) and one row for each function (or vector of similar functions); the objective function is listed first. Entry i,j indicates qualitatively the relation between function j and variable i. In our figures an entry (X) indicates function i depends on variable j; no entry indicates function i does not depend on variable j. Figure 1 corresponds to Prob. 1, a general nonlinear programming problem where all functions are assumed to depend on all variables.

As discussed by Carmichael [19], "...decomposition implies breaking the system into subsystems with interactions and breaking the problem [variables,] constraints and [objective] into [variables], constraints and [objectives] associated with the subproblems. Decoupling... may be carried out by the introduction [or identification] of interaction variables such that there results independent optimization problems at the lower level." Typical approaches to decomposition are discussed below.

Decomposition of the Variable Vector

Without any special structure (that is with a fully populated dependency matrix), Prob. 1 may always be decomposed by partitioning the variable vector:

$$\mathbf{X} = \mathbf{X}_1,\ldots,\mathbf{X}_n \qquad (2)$$

It may then be replaced by n problems, the ith of which is

$$\min_{\mathbf{X}_i} f(\bar{\mathbf{X}}_1,\ldots,\bar{\mathbf{X}}_{i-1},\mathbf{X}_i,\bar{\mathbf{X}}_{i+1},\ldots,\bar{\mathbf{X}}_n), \text{ st } \mathbf{g}(\bar{\mathbf{X}}_1,\ldots,\bar{\mathbf{X}}_{i-1},\mathbf{X}_i,\bar{\mathbf{X}}_{i+1},\ldots,\bar{\mathbf{X}}_n) \le 0,$$

$$\text{and } \mathbf{h}(\bar{\mathbf{X}}_1,\ldots,\bar{\mathbf{X}}_{i-1},\mathbf{X}_i,\bar{\mathbf{X}}_{i+1},\ldots,\bar{\mathbf{X}}_n) = 0 \qquad (3)$$

where an overbar on a variable indicates that the variable is held fixed. This approach has been used for simultaneous configuration optimization and sizing (Lev, [20]) and optimal load flow control (Contaxis *et al*. [15]). Typically, no real decoupling results from such a decomposition (the dependency matrix remains fully populated), unless one of the subproblems can be further decomposed as in Kirsch [17] or Vanderplaats *et al*. [21].

Block-Diagonal Dependency Matrix

From the standpoint of decomposition, a problem having an additively separable objective function and a dependency matrix as in Fig. 2a (assuming suitable re-ordering of the variables and constraints) is ideal, since it yields totally uncoupled subproblems which can be solved independently of each other. The original problem formulation reads:

$$\min_{\mathbf{X}=\mathbf{X}_1,\ldots,\mathbf{X}_n} f(\mathbf{X}) = \sum_1^n f_i(\mathbf{X}_i) \text{ st } \mathbf{g}_i(\mathbf{X}_i) \le 0 \; i=1,n; \; \mathbf{h}_i(\mathbf{X}_i) = 0 \; i=1,n \qquad (4)$$

resulting in n independent subproblems:

$$\min_{\mathbf{X}_i} f_i(\mathbf{X}_i) \text{ st } \mathbf{g}_i(\mathbf{X}_i) \le 0, \; \mathbf{h}_i(\mathbf{X}_i) = 0 \qquad (5)$$

While design problems seldom have such form, it is often assumed that they have a similar form in which some functions depend strongly on some variables and only weakly on others. This situation is described in Fig. 2b where dots denote weak dependency. Assuming additively separable objective function, this yields the following n subproblems:

$$\min_{\mathbf{X}_i} f_i(\bar{\mathbf{X}}_1,\ldots,\bar{\mathbf{X}}_{i-1},\mathbf{X}_i,\bar{\mathbf{X}}_{i+1},\ldots,\bar{\mathbf{X}}_n), \text{ st } \mathbf{g}_i(\bar{\mathbf{X}}_1,\ldots,\bar{\mathbf{X}}_{i-1},\mathbf{X}_i,\bar{\mathbf{X}}_{i+1},\ldots,\bar{\mathbf{X}}_n) \le 0,$$

$$\text{and } \mathbf{h}_i(\bar{\mathbf{X}}_1,\ldots,\bar{\mathbf{X}}_{i-1},\mathbf{X}_i,\bar{\mathbf{X}}_{i+1},\ldots,\bar{\mathbf{X}}_n) = 0 \qquad (6)$$

One of the major shortcomings of this method is that it cannot explicitly handle constraints which strongly depend on variables belonging to different subsystems. Sobieszczanski and Loendorf [3] and Hughes [6] devised an ad hoc procedure to correct the overall design for violations of these constraints.

Generally, the decomposition of the problem is arrived at in a very natural way; it is imposed by the structure or the layout of the engineering system considered. Therefore, very few systematic approaches to decomposition exist. An exception is that used by Datseris [13] for the design of mechanisms. Here the key idea is to divide the set of design variables in mutually exclusive subsets so that some measure of the coupling between the variable subsets is minimized. Coupling is measured by an interdependence function based on the design problem objective function. If a decomposition in two subsets is desired, the first step is to randomly identify two subsets of variables. Then a systematic approach is used to exchange variables among the subsets in an effort to lower the value of the interdependence function.

Another approach to systematic decomposition is proposed by Bandler and Zhang [14] in their optimization of large microwave systems. Their starting point is a matrix similar to the dependency matrix introduced above. They use a matrix whose i,j entry is the normalized sensitivity derivative of function i with respect to variable j (or a sum of sensitivity derivatives calculated at various points in the design space). They manipulate the rows and columns of the matrix to finally identify the subproblem to optimize starting with the reference function group (with the worst contribution to the objective) and the candidate variable groups (those that affect that reference function group). Optimization proceeds with repeated redefinition of the variable and function groups making up the subproblem, which as the optimum design is reached, includes all variables and functions.

Block-Angular Dependency Matrix with Coupling Variables

Reasonably complex engineering design problems cannot typically be formulated with a block-diagonal (Fig. 2a) or even a quasi-block diagonal (Fig. 2b) structure. Indeed, as alluded to before, some constraints depend strongly on variables belonging to several subproblems. A more typical structure is the block-angular structure with coupling variables of Fig. 3a. This may result from the existence of a hierarchical structure in the model in which two levels of variables and functions exist. At the higher level, the higher level (or system or global) variables affect directly the higher level constraints. At the lower level, for fixed higher level variables, the lower level (or subsystem or local) variables affect directly the lower level constraints. Further decoupling may exist that results in a number of independent lower level subproblems. The coupling higher level variables are the interaction variables. Assuming additively separable objective function, the starting problem would be given by

$$\min_{\mathbf{Y},\mathbf{X}_1,\ldots,\mathbf{X}_n} f_0(\mathbf{Y}) + \sum_1^n f_i(\mathbf{Y},\mathbf{X}_i) \text{ st } \mathbf{g}_0(\mathbf{Y}) \le 0,\ \mathbf{g}_i(\mathbf{Y},\mathbf{X}_i) \le 0 \ i=1,n \tag{7}$$
$$\text{and } \mathbf{h}_0(\mathbf{Y}) = 0,\ \mathbf{h}_i(\mathbf{Y},\mathbf{X}_i) = 0 \ i=1,n$$

The resulting higher level subproblem would then be

$$\min_{\mathbf{Y}} f_0(\mathbf{Y}) \text{ st } \mathbf{g}_0(\mathbf{Y}) \le 0,\ \mathbf{h}_0(\mathbf{Y}) = 0 \tag{8a}$$

while there would be n independent lower level subproblems:

$$\min_{\mathbf{X}_i} f_i(\bar{\mathbf{Y}},\mathbf{X}_i) \text{ st } \mathbf{g}_i(\bar{\mathbf{Y}},\mathbf{X}_i) \le 0,\ \mathbf{h}_i(\bar{\mathbf{Y}},\mathbf{X}_i) = 0 \tag{8b}$$

Haftka [22] gave a penalty formulation for the same initial problem.

To derive a problem structure as in Eq. 7 from a general nonlinear programming problem as described in Eq. 1, equality constraints sometimes need to be introduced. They typically express the consistency between the higher level and the lower level models of the system. These can impede convergence of the process. Thareja [23] proposed to linearize them at each optimization step and to use them to eliminate some variables of the problem and thus reduce its size. Schmit and Merhinfar [5] transformed these equality constraints in penalty-type objective functions for the lower level subproblems allowing for incomplete satisfaction of the equalities at the beginning of the optimization process, and in effect, only achieving a quasi-block-angular structure as in Fig. 3b.

The issue of automatically generating a problem structure as in Eq. 7 for complex engineering systems was first addressed by Rogan and Kolb [18] who suggested handling it as scheduling problem.

Coordination

Coordination amounts to devising a scheme iterating among the subproblem optimizations such that the final solution is that of the original problem (or one of its solutions). Central to the coordination process is the identification of coordination variables (Carmichael [19]). These variables are held fixed at the lower level, giving independent subproblems which are solved separately, and then information is returned to the higher level to update the value of the coordination variables. This cycle is repeated until convergence is achieved. Some modification of the higher level subproblem is necessary to ensure coordination.

Applications that rely on variable vector or block-diagonal (or quasi-block-diagonal) decompositions generally do not possess any coordination mechanism. In the former case, coordination is really not necessary since each subproblem deals with all the functions of the problem. In the latter case, this lack of coordination has been long known to prevent finding even a local minimum of the problem and probably accounts for some of the disappointing results reported by Svensson [11]. In the context of structural applications, Sobieszczanski [24] indicated: "...Minimization of the individual component masses does not guarantee minimization of the total mass. This situation is caused by the inability to control the load path on the assembled structure level...". Schmit and Chang [10] offer a unique approach to coordinating problems using a substructuring formulation. They write the problem variable vector:

$$\mathbf{X} = \sum_{1}^{n} \alpha_i \mathbf{X}_i \tag{9}$$

Each vector $\mathbf{X}i$ is manipulated at the local level to satisfy local constraints while minimizing stiffness (hence boundary force) changes; vector $\boldsymbol{\alpha}$ is manipulated at the global level to minimize the global objective, satisfy the global constraints and some local constraints that cannot be satisfied at the local level.

Block-angular decompositions with coupling variables provide an explicit coordination mechanism. A feasible coordination technique is always used in which the higher level variables are taken as the coordination variables. Generally, to provide a means of coordination at the higher level, the effect of changes in lower level designs due to changes in higher level variables must be known.

For example, at the end of each lower level optimization, Schmit and Merhinfar [5] update limits on higher level behavioral (dependent) variables to reflect new lower level designs. To coordinate the lower level designs Felix [16] suggests to take a search direction at the higher level that will minimize the system objective function while continuing to satisfy the constraints active at the conclusion of the lower level optimizations. A one dimensional search is performed at the higher level that accounts for possible higher level constraints.

Since lower level optima are obtained for fixed value of the coordination variables, they really are implicit functions of these variables. For the subproblem of Eq. (8b), denoting optimum quantities with an (*), we have

$$f_i^*(\mathbf{Y}, \mathbf{X}_i^*) = f_i^*(\mathbf{Y}, \mathbf{X}_i^*(\mathbf{Y})) = f_i^*(\mathbf{Y}) \tag{10}$$

Optimization at the higher level must therefore continue in a direction that maintains these lower level optima. To achieve coordination, the problem of Eq. (8a) must then be restated:

$$\min_{\mathbf{Y}} f_0(\mathbf{Y}) + \sum_{1}^{n} f_i^*(\mathbf{Y}) \text{ st } \mathbf{g}_0(\mathbf{Y}) \le 0,\ \mathbf{h}_0(\mathbf{Y}) = 0 \tag{11}$$

One approach to constructing approximations to the implicit relations of Eq. (10) is to repeat the lower level solutions for several combinations of higher level variables. The resulting information can be used in non-gradient optimization schemes or in gradient schemes with finite-difference-based derivative estimates. Kunar and Chan [25] used the conjugate direction and the conjugate gradient method. In addition to being computationally expensive, this approach is prone to round-off and truncation errors. Alternately, as proposed by Sharma et al. [12] the information can be used in surface-fitting procedures to construct approximate response surfaces giving the lower level optima explicitly as functions of the higher level variables. While this approach appears effective for small problems, the size of the sample necessary for large problems with large numbers of higher level variables will become prohibitive.

Another approach proposed by Sobieszczanski [7], and Sobieszczanski et al. [26] is to resort to sensitivity analysis of optimum solutions. This technique provides exact derivatives of the solution of lower level subproblems with respect to higher level variables and permits the generation of first-order approximations:

$$f_i^*(Y) \equiv f_i(\bar{Y}) + \sum_1^n \frac{\partial f_i^*(\bar{Y})}{\partial \bar{Y}_j} (Y_j - \bar{Y}_j) \qquad (12)$$

Haftka [22] used a similar approach for penalty function formulations.

Complete sensitivity analysis of optimum solutions (variables, objective and constraints) is numerically costly since it requires second-order derivatives of these functions. However, as shown by Barthelemy and Sobieszczanski [27], if only the lower level objectives must be known for the coordination mechanism, the additional calculations are limited to the problem first-order derivatives.

Sensitivity derivatives are also discontinuous functions of higher level variables (Barthelemy and Sobieszczanski, [28]). Presumably, lower level subproblem unconstrained formulations based on penalty function formulations (Haftka [22]) or envelope functions (Sobieszczanski [7]) should eliminate that difficulty. However, as shown by Barthelemy and Riley [29] in the case where envelope functions are used, driving the solution of the approximate unconstrained subproblems to that of the original constrained ones often results in rapidly varying (albeit still continuous) gradients, a phenomenon that all but brings back the derivative discontinuity issue. It is likely that the same problem occurs with penalty functions formulation. Haftka [22] proposed to limit the effect of discontinuity by restricting optimization to one step at each level in each cycle. Vanderplaats and Cai [30] proposed an interesting approach to approximate sensitivity analysis that should anticipate constraint switching. No definitive solution exists for this difficulty, but no example was ever shown where the derivative discontinuity precluded convergence of the procedure.

Concluding Remarks

This brief review shows that heuristic multilevel optimization methods have a demonstrated potential in engineering design. The most promising decomposable problem statement considered is block-diagonal with coupling variables. These variables are used at the higher level of the decomposition to provide for decoupling of the lower level subproblems and coordination of their optimization. The lower level subproblems communicate with the higher level subproblem with sensitivity information that may be based on formal sensitivity analysis. Various schemes have been proposed and some have been demonstrated on very large problems.

Very little work focuses on the decomposition process itself that is on the approach to be taken to obtain such a block angular structure. If multilevel optimization is to be applied to truly large engineering systems, then the ideas of Rogan and Kolb [18] on scheduling must be further developed. One direction is to account not only on the existence of coupling as they have done but also on the strength of coupling between variables and functions as was done by Bandler and Zhan [14].

As stated above, efficiency of the algorithm is one of the most cited reasons to resort to multilevel optimization. Yet few of the results in the literature are concerned with more than convergence of the algorithm. Haftka [22] showed that significant savings could result from limiting iteration of the subproblems to as little as one iteration per cycle, while Thareja and Haftka [23] showed how further gains could be made by exploiting the structure of the problem when calculating and storing derivatives. Barthelemy and Riley [29] and Vanderplaats *et al*. [21] showed good results combining decomposition and approximations. The works of Bandler and Zhan [14], as well as Barthelemy and Riley [29] indicate that it is worthwhile in each cycle to optimize only those subproblems that have the strongest influence on the problem objective.

Multilevel procedures are ideally suited for execution in parallel. Surprisingly, no engineering application of multilevel methods on parallel processors has ever been implemented. Young [31] demonstrated the feasibility of using Sobieszczanski's [7] approach on a network of engineering workstations.

Finally, as all methods developed for design, multilevel methods must be made to conform better to the design process itself. Most complex engineering systems require more than two levels for modelization. Initial work by Sobieszczanski et al. [32] and Kirsch [17] should be pursued. Likewise, particularly in the multidisciplinary context, problems are likely to have several objectives. Multilevel/multiobjective formulations are necessary to determine what design is obtained when each discipline-subproblem deals with its own variables, objective and constraints.

References

[1] Haftka, R.T., "Damage Tolerant Design Using Collapse Techniques", AIAA J., Vol. 21, No. 10, Oct. 1988, pp. 1462-1466.

[2] Giles, G.L. "Procedure for Automating Aircraft Wing Structural Design", J. Struc. Div., ASCE, Vol. 97, ST1, Jan. 1971, pp. 99-113.

[3] Sobieszczanski-Sobieski, J. and Loendorf, D. "A Mixed Optimization Method for Automated Design of Fuselage Structures" J. Aircraft, Vol 9, No. 12, Dec. 1972, pp. 805-811.

[4] Fulton, R.E., Sobieszczanski, J., Storaasli, O., Landrum, E.J. and Loendorf, D., "Application of Computer-Aided Aircraft Design in a Multidisciplinary Environment", in Proc. 14th AIAA/ASME/SAE SDM Conf., Williamsburg, VA, Mar. 1973.

[5] Schmit, L.A. and Merhinfar, M.,"Multilevel Optimum Design of Structures with Fiber-Composite Stiffened-Panel Components", AIAA J., Vol. 20, No. 1, Jan. 1982, pp. 138-147.

[6] Hughes, O.F., "A Method for Nonlinear Optimum Design of Large Structures, and Applications to Naval Ship Design", in Proc. Int. Symp. on Optimum Structural Design, Tucson, AZ, Oct. 1981, pp. 10.5-10.12.

[7] Sobieszczanski-Sobieski, J., "A Linear Decomposition Method for Large Optimization Problems - Blueprint for Development", NASA TM 83248, Feb. 1982.

[8] Wrenn, G.A. and Dovi, A.R., "Multilevel/Multidisciplinary Optimization Scheme for Sizing a Transport Aircraft Wing", Proc. 28th AIAA/ASME/ASCE/AHS SDM Conf., Monterey, CA, Apr. 1987.

[9] Nguyen, D.T, "Multilevel Substructuring Sensivity Analysis", Comp. & Struct., Vol. 25, No. 2, 1987, pp. 191-202.

[10] Schmit, L.A. and Chang, K.J. "A Multilevel Method for Structural Synthesis" Proc. 25th AIAA/ASME/ASCE/AHS SDM Conf., Palm Springs, CA, May 1984.

[11] Svensson, B., "A Substructuring Approach to Optimum Structural Design", Comp. and Struct., Vol. 25, No. 2, 1987, pp. 251-258.

[12] Sharma, A., Chiu, H.H., Ahrens, F.W., Ahluwalia, R.K. and Ragsdell, K.M., "Design of Optimum Compressed Air Energy-Storage System", Energy, Vol. 4, 1979, pp. 201-216.

[13] Datseris, P. "Weight Minimization of a Speed Reducer by Heuristic and Decomposition Techniques", Mech. Mach. Th., vol. 17, no. 4, 1982.

[14] Bandler, J.W. and Zhang, Q.-J. "An Automatic Decomposition Approach to Optimization of Large Microwave Systems", IEEE Trans. Micr. Th. Tech., Vol. MTT-35, No. 12, 1987, pp. 1231-1239.

[15] Contaxis, G.C., Delkis, C. and Korres, G. "Decoupled Optimal Load Flow Using Linear or Quadratic Programming", IEEE Trans. Pwr. Sys., Vol. PWRS-1, No. 2, May 1986, pp. 1-7.

[16] Felix, J.E. "Shape Optimization of Trusses Subject to Strenght, Displacement and Frequency Constraints", M.S. Thesis, Naval Postgraduate School, Monterey, CA, 1981.

[17] Kirsch, U., "An Improved Multilevel Structural Synthesis Method", J. Struct. Mech., Vol. 13, No. 2, 1985, pp. 123-144.

[18] Rogan, J.E. and Kolb, M.A. "Application of Decomposition Techniques to the Preliminary Design of a Transport Aircraft", NASA CR 178239, Feb. 1987.

[19] Carmichael, D.G. Structural Modelling and Optimization, Chichester, Ellis Horwood Ltd., 1981.

[20] Lev, O.E. "Sequential Geometric Optimization", J. Struct. Div., ASCE, Vol. 107, No. ST10, Oct. 1981, pp. 1935-1943.

[21] Vanderplaats, G.N., Yang, Y.G. and Kim, D.S. "An Efficient Multilevel Optimization Method for Engineering", Proc. 29th AIAA/ASME/ASCE/AHS SDM Conf., Williamsburg, VA, Apr. 1988, pp. 125-132.

[22] Haftka, R.T. "An Improved Computational Approach for Multilevel Optimization Design", J. Struct. Mech., Vol. 12, No. 2, 1984, pp. 245-261.

[23] Thareja, R.R. and Haftka, R.T. "Efficient Single-Level Solution of Hierarchical Problems in Structural Optimization", Proc. 28th AIAA/ASME/ASCE/AHS SDM Conf., Monterey, CA, 1987, pp. 59-75.

[24] Sobieszczanski-Sobieski, J. "An Integrated Computer Procedure for Sizing Composite Airframe Structures", NASA TP 1300, Feb. 1979.

[25] Kunar, R.R. and Chan, A.S.L. "A Method for the Configurational Optimization of Structures", Comp. Meth. Appl. Mech Eng., Vol. 7, pp.331-350, 1976.

[26] Sobieszczanski-Sobieski, J., Barthelemy, J.F. and Riley, K.M. "Sensitivity of Optimum Solutions to Problem Parameters", AIAA J., Vol. 20, No. 9, pp. 1291-1299, Sep. 1982.

[27] Barthelemy, J.-F.M. and Sobieszczanski-Sobieski, J. "Optimum Sensitivity Derivatives of Optimum Objective Functions in Nonlinear Programming", AIAA J., Vol 21, No. 6, pp. 913-915, Jun. 1983.

[28] Barthelemy, J.-F.M. and Sobieszczanski-Sobieski, J. "Extrapolation of Optimum Design Based on Sensitivity Derivatives", AIAA J., Vol. 21, No. 5, pp. 797-799, May 1983.

[29] Barthelemy, J.-F.M. and Riley, M.F. "Improved Multilevel Optimization Approach for the Design of Complex Engineering Systems", AIAA J., Vol. 26, No. 3, pp. 353-360, Mar. 1988.

[30] Vanderplaats, G.N. and Cai, H.D. "Alternative Methods for Calculating Sensitivity of Optimized Designs to Problem Parameters" in Sensitivity analysis in Engineering, Adelman H.M. and Haftka, R.T. Eds., NASA CP-2457, 1987.

[31] Young, K.C., Padula, S.L. and Rogers, J.L.Jr. " A Strategy for Reducing Turnaround Time in Design Optimzation Using a Distributed Computer System" in Proc. 1988 Des. Autom. Conf., Orlando, FL, Sep. 24-26, 1988.

[32] Sobieszczanski-Sobieski J., James, B.B. and Riley, M.F. " Structural Optimization by Generalized, Multilevel Optimization" Proc. 26th AIAA/ASME/ASCE/AHS SDM Conf., Orlando, FL, Apr. 15-17, 1985.

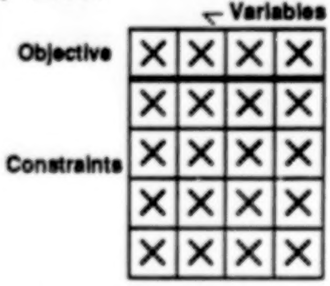

Fig. 1. Full dependency matrix

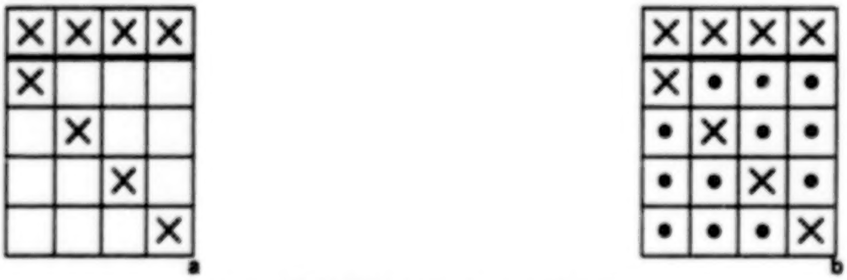

Fig 2. (a) block-diagonal, (b) quasi-block diagonal dependency matrix

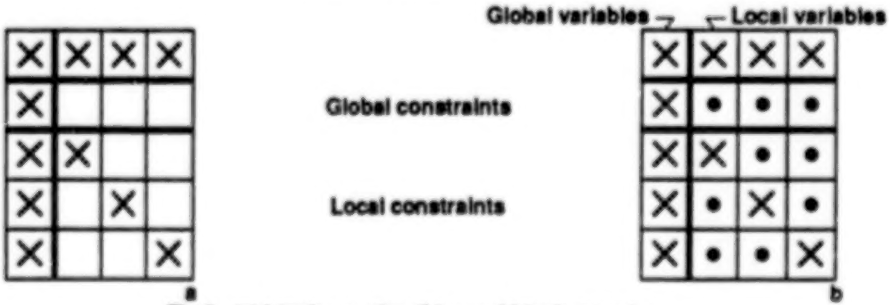

Fig 3. (a) block-angular, (b) quasi-block- angular dependency matrix with coupling variables

RECENT DEVELOPMENTS IN MULTILEVEL OPTIMIZATION

G. N. Vanderplaats

and

D-S Kim

Department of Mechanical & Environmental Engineering
The University of California
Santa Barbara, California 93111

Figure 1 identifies the general nature of the multidiscipline design task. The key point is that there are relatively few system level design variables, while there may be a great many subsystem design variables. For example, the overall length and diameter of the fuselage, the thickness, aspect ratio, sweep, etc. of the wing, and the maximum thrust may generally define the design of an aircraft as a system. On the other hand, the design of a subsystem such as a wing, consists of hundreds or even thousands of variables defining the aerodynamic shape, skin thickness distribution, spars, webs, etc. Also, this subsystem may be considered to be itself a collection of subsystems, including aerodynamics, structures, controls, hydraulics and others. There is seldom a clear mathematical structure to the overall design task which would make it amenable to efficient solution techniques such as are available for many structural subsystem design problems. Also, the analysis tools for the various components range from purely experimental to empirical to formal solution of the governing equations by finite element or finite difference methods. In view of these complexities, it must be said at the outset that formal multidiscipline optimization is a technology that is still in its infancy.

FEATURES OF THE MULTIDISCIPLINE PROBLEM

RELATIVELY FEW SYSTEM DESIGN VARIABLES

OFTEN COMPLEX/EXPENSIVE ANALYSIS

ANALYTIC GRADIENTS ARE SELDOM AVAILABLE

THERE IS NO CLEAR MATHEMATICAL STRUCTURE

OPTIMIZATION IS TYPICALLY SEEN AS A "BLACK BOX"

FIGURE 1

A key element in engineering design is the use of approximations to develop and solve the analysis/design task. These approximations may be very simple, such as empirical estimates of component weights based on historical data or they may be quite sophisticated such as the formal solution of the Navier Stokes equations. The motivation is usually to provide the efficiency necessary to the real design environment. Figure 2 lists some of the motivations for making approximations. It is noteworthy that in the relatively well developed subsystem field of structural optimization, the technology was pursued for over fifteen years before a formal approach to creating high quality approximations was developed. In other areas such as aerodynamic or propulsion system optimization, this has yet to be pursued to a significant extent.

APPROXIMATIONS

AT THE SUBSYSTEM LEVEL

- PROVIDE NECESSARY EFFICIENCY
- IN STRUCTURAL OPTIMIZATION
  - LINEARIZATION WITH RESPECT TO SOME INTERMEDIATE VARIABLES

AT THE SYSTEM LEVEL

- DEAL WITH SUBSYSTEM RESPONSES
- ACCOUNT FOR INTERACTIONS AMONG SUBSYSTEMS
- SEND SYSTEM LEVEL INFORMATION TO SUBSYSTEMS
- SEND INTERACTION INFORMATION TO SUBSYSTEMS

FIGURE 2

Figure 3 depicts the structure of the formal multidiscipline optimization problem. It is noteworthy that this is a tree structure similar to the general design environment where the system may be thought of as the chief designer and the subsystems as engineering departments. Whenever the system variables are changed, the effects on the subsystems must be accounted for. Similarly, when the subsystem variables are changed, the effect of the overall system must be considered. Subsystems may be defined along discipline lines or by other criteria. For example, the design of a wing may be considered as a subsystem including aerodynamic, structural and other considerations. Alternatively, aerodynamics and structures may be considered to be separate subsystems or lower level subsystems within the general category of wing design. It is clear that aerodynamics and structures play interacting and competing roles in the overall design and so these interactions must be properly accounted for via the system design control. Ideally, aerodynamic and structural design must be done simultaneously. However, this is counter to the usual division along discipline lines and so little emphasis has been directed toward the combined design process, even at the research level.

FORMAL MULTIDISCIPLINE OPTIMIZATION

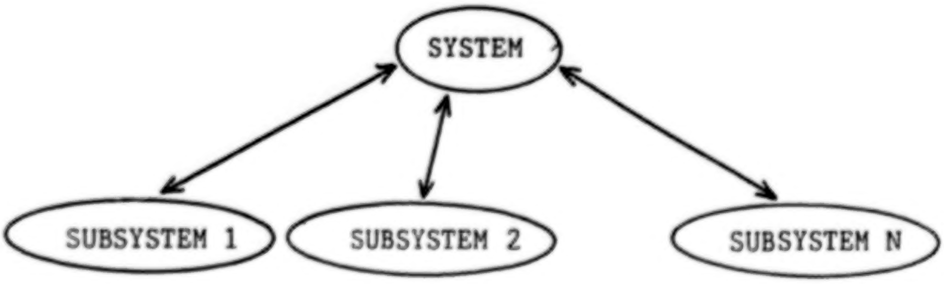

ADDITIONAL LEVELS OF SUBSYSTEMS MAY EXIST

FIGURE 3

Figure 4 presents a simple cantilevered beam which demonstrates the concepts of multilevel design. The objective is to minimize the material volume subject to limits on the deflection at the beam junction and at the tip, and on the maximum bending stresses and height to width ratios of the members. The design variables of interest are the width, B_i, and height, H_i, of each element, and the length, L_1 ($L_2 = L - L_1$). Clearly, for such a simple problem, this would be solved directly. However, for demonstration purposes, it is possible to formulate it as a multilevel problem with a system level and two subsystems.

The system level problem may be stated as, find the beam length, L_1, and dimensions B_1, H_1, B_2 and H_2 to minimize the volume subject to constraints on the deflections. Additionally, in the present method, subsystem constraints will be imposed, in linearized form, on the stresses and the height to width ratio on the members. Each member can be taken as a subsystem and, during subsystem optimization, the member volume will be minimized subject to constraints on the member stresses and height to width ratio. At this level, the purely system level design variable, L_1, will be held fixed, but the system level constraints (deflections) will be included in linearized form.

Note that, at the system level, all design variables are included. At the subsystem, the design variables that are important to the subsystem are considered, but the strictly system level variable, L_1, is held fixed.

Because of the interdependence between the system and subsystem variables, each level will affect the other. The key issue is how to account for these interactions and how to account for competition between subsystems.

MULTILEVEL DESIGN OF A CANTILEVER BEAM

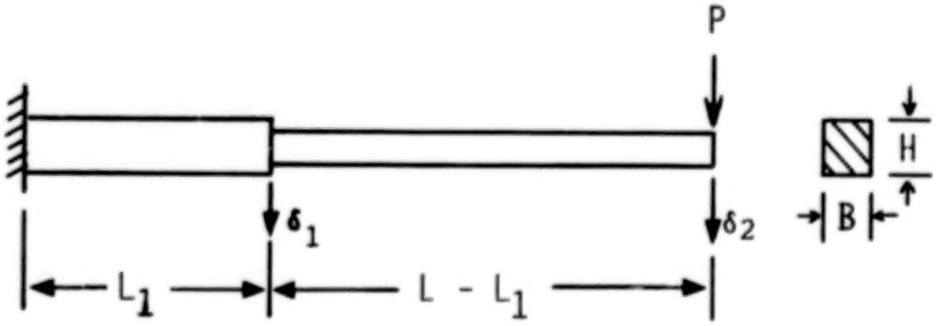

FIGURE 4

A variety of methods have been proposed to deal with the multidiscipline design task in a formal way. Figure 5 presents a recent method developed in an effort to simplify the overall process while maintaining the traditional separation of disciplines [1]. Initially, all system level functions (objective and constraints) are linearized. Each of the subsystem optimizations is then performed, presumably in parallel. At the optimum for the subsystem, its constraints (or a critical and near critical subset) are linearized and returned to the system. The system level optimization is then performed, including these linearized subsystem constraints. Also, at this point, the subsystem design variables are included along with the strictly system level variables. The process is repeated until it has converged to an optimum. As with any linearization technique, move limits must be imposed at each level and these are reduced as the optimization proceeds.

MULTILEVEL OPTIMIZATION PROCESS

EVALUATE SYSTEM LEVEL FUNCTIONS

CREATE LINEAR APPROXIMATION TO SYSTEM LEVEL FUNCTIONS

SOLVE EACH SUBSYSTEM PROBLEM,
INCLUDING LINEARIZED SYSTEM LEVEL CONSTRAINTS

CREATE LINEAR APPROXIMATION TO ALL SUBSYSTEM CONSTRAINTS

SOLVE SYSTEM LEVEL PROBLEM
INCLUDING LINEARIZED SUBSYSTEM CONSTRAINTS

REPEAT TO CONVERGENCE

MOVE LIMITS ARE USED AT EACH LEVEL

FIGURE 5

Figure 6 provides the basic mathematical details of the optimization task at the system level. Here, capital letters indicate strictly system level design variables, objective and constraints, and lower case letters indicate subsystem level variables and constraints. Here, the subsystem variables are included along with the system variables. The subsystem constraints are included in their linearized form. Note that the number of design variables, as well as the number of constraints to be considered here is greatly increased from the number of strictly system level variables and constraints. However, the subsystem constraints are linearized and so are relatively easily dealt with. This is a departure from previous methods which used a cumulative constraint for each subsystem as well as a set of "optimum sensitivities" from the subsystems. The tradeoff is that the functions here are linearized at the expense of an increase in the number of design variables and constraints. However, the need to deal with nonlinear inequality constraints at the subsystem, as well as the need to calculate sensitivities of the optimized subsystems is avoided.

PRESENT METHOD

AT THE SYSTEM LEVEL

DESIGN VARIABLES, $X, x_1, x_2, \ldots x_N$

OBJECTIVE, $F(X, x_1, x_2, \ldots x_N)$

SYSTEM CONSTRAINTS, $G_j(X, x_1, x_2, \ldots x_N)$

SUBSYSTEM CONSTRAINTS, $g_j(X, x_1, x_2, \ldots x_N)$

WHERE

$$g_j = g_j^0 + \sum_{i=1}^{nss} \underline{\nabla}_x g_j \cdot (\underline{x}_i - \underline{x}_i^0) + \underline{\nabla}_X g_j \cdot (\underline{X} - \underline{X}^0)$$

FIGURE 6

The basic mathematical details for the subsystem optimization are given in Figure 7. The inputs to the subsystem problem include the boundary conditions, system level variables and system level constraints, all in linearized form. The reason that the system level variables and boundary conditions must be linearized is that these may be functions of the subsystem variables and are not assumed to be constant in the present method. For example, the forces in the members of a structure may be functions of the local variables. Also, if the strictly system variables are functions of the subsystem variables, this must be accounted for. Then, when the approximate system level constraints are calculated, it is first necessary to calculate the approximate values of the system variables and subsystem boundary conditions since the system constraints are functions of these. While this appears to be a bit cumbersome, it must be remembered that these computations are relatively simple matrix operations and so are efficiently performed. Also, if sufficient information is available to calculate these parameters precisely, this may be done to improve the overall efficiency.

PRESENT METHOD

AT EACH SUBSYSTEM

DESIGN VARIABLES x_i

OBJECTIVE, $f(BC, X, x_i)$

SUBSYSTEM CONSTRAINTS $g_j(BC, X, x_i)$

SYSTEM CONSTRAINTS, $G_J(BC, X, x_1, x_2, \ldots x_N)$

WHERE

$$BC = BC^0 + \underline{\nabla}_x BC . (x - x^0)$$

$$X = X^0 + \underline{\nabla}_x X . (x - x^0)$$

$$G_j = G_j^{\,0} + \underline{\nabla}_X G_j . (\underline{X} - \underline{X}^0) + \underline{\nabla}_x G_j . (\underline{x} - \underline{x}^0) + \underline{\nabla}_{BC} G_j . (\underline{BC} - \underline{BC}^0)$$

FIGURE 7

Figure 8 presents the iteration history for the cantilevered beam shown in Figure 4. The problem was also solved by direct application of optimization and those results are shown also. The initial design violated constraints, so the direct method first increased the volume in order to overcome these constraint violations. While it appears from the figure that the multilevel method provided an equivalent convergence rate, it must be remembered that one iteration of the multilevel method consists of optimization of all subsystems followed by a system level optimization. Thus, for this simple example, the direct method is much more efficient computationally. This is generally true for problems that can be solved directly. The value of the multilevel method is for design problems where it is necessary to separate the problem for other reasons.

ITERATION HISTORY FOR CANTILEVER BEAM

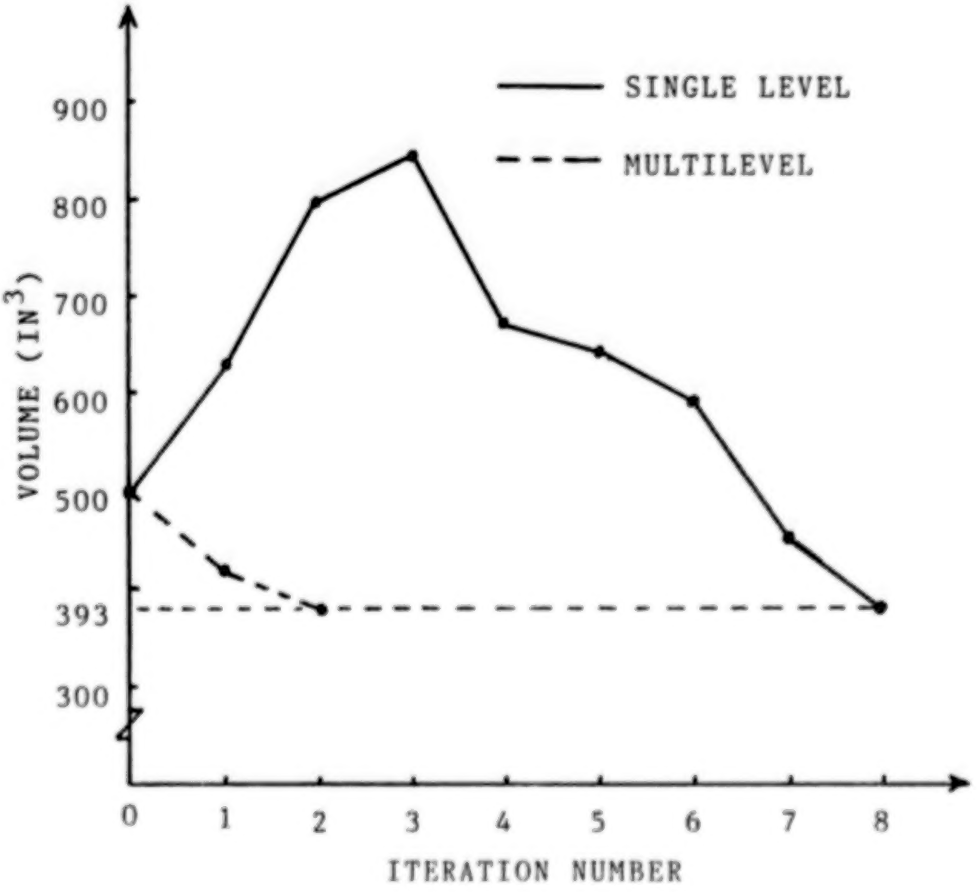

FIGURE 8

The portal frame shown in Figure 9 was designed using the proposed method. This is considered to be a standard test case, and the details of the loads, materials, system and subsystem constraint calculations are presented in Reference 2. The system level constraints are displacement and rotation limits at the joint where the loads are applied. The subsystem constraints included stress, local buckling, and sizing limits. There are three subsystems, being the design of the individual beam elements. The subsystem design variables are the six individual dimensions of the cross-section of each element. The objective function at both the system and subsystem levels is to minimize the volume of material.

Two cases were considered. In the first, the initial design was well within the feasible region, while in the second, the initial design was quite infeasible. The iteration histories for the two cases are shown in Figures 10 and 11. The multilevel approach did not produce as good an optimum in either case, but did produce a near optimum. There is no clear reason for the differences, although this structure is known to have relative minima.

MULTILEVEL OPTIMIZATION OF A PORTAL FRAME

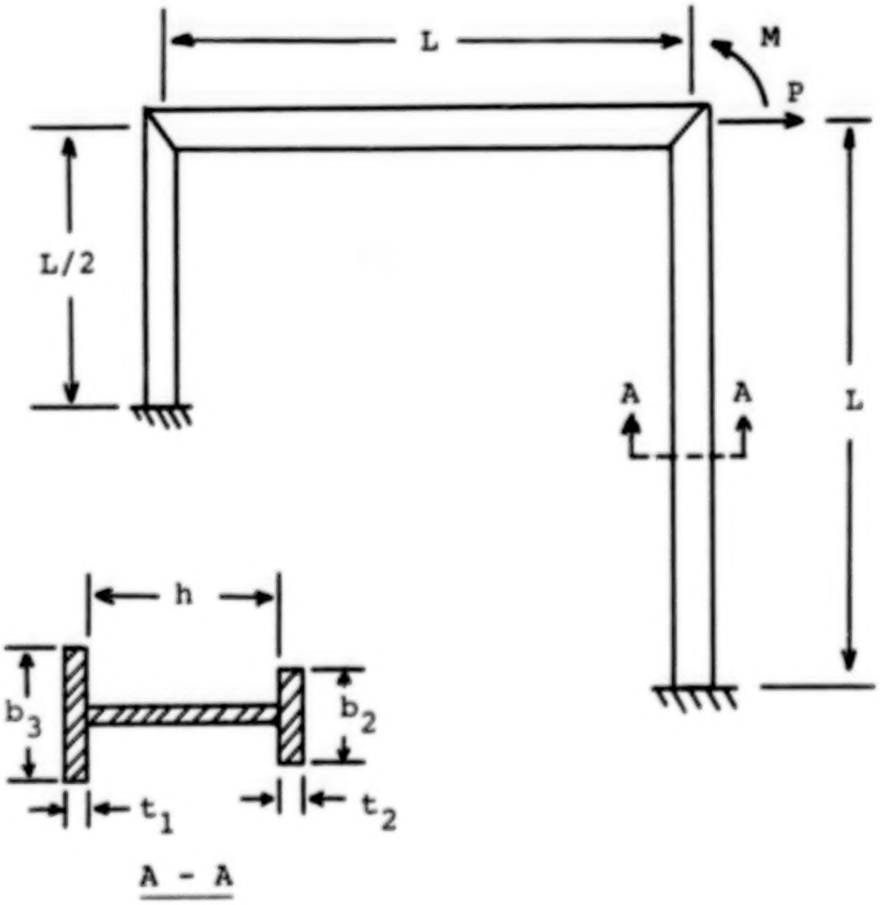

FIGURE 9

ITERATION HISTORIES FOR PORTAL FRAME CASE I

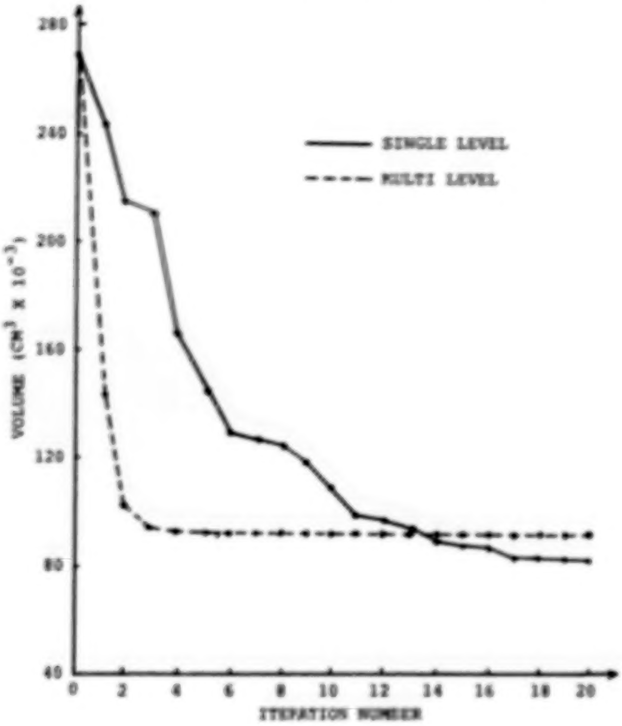

FIGURE 10

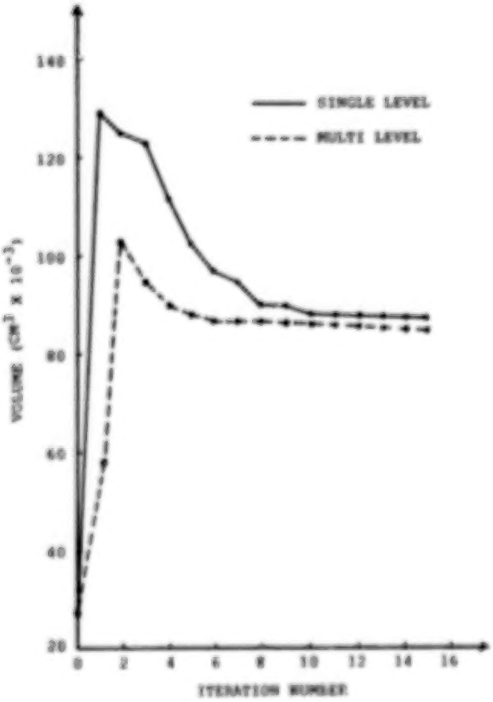

FIGURE 11

The two-bay frame shown in Figure 12 was designed for minimum material using the proposed method. The design variables and material properties for each beam and the subsystem constraints are the same as for the portal frame. The system level constraints are shown in the figure, as well as the loading conditions. Symmetry was used so the system is comprised of four subsystems, being the vertical members of each bay and the floor members of each bay. Each subsystem consists of six design variables for a total of twenty four independent design variables.

The results for single level and multilevel optimization are shown in Figures 13 and 14 for an initially feasible design and an initially infeasible design, respectively.

MULTILEVEL DESIGN OF A TWO-BAY FRAME

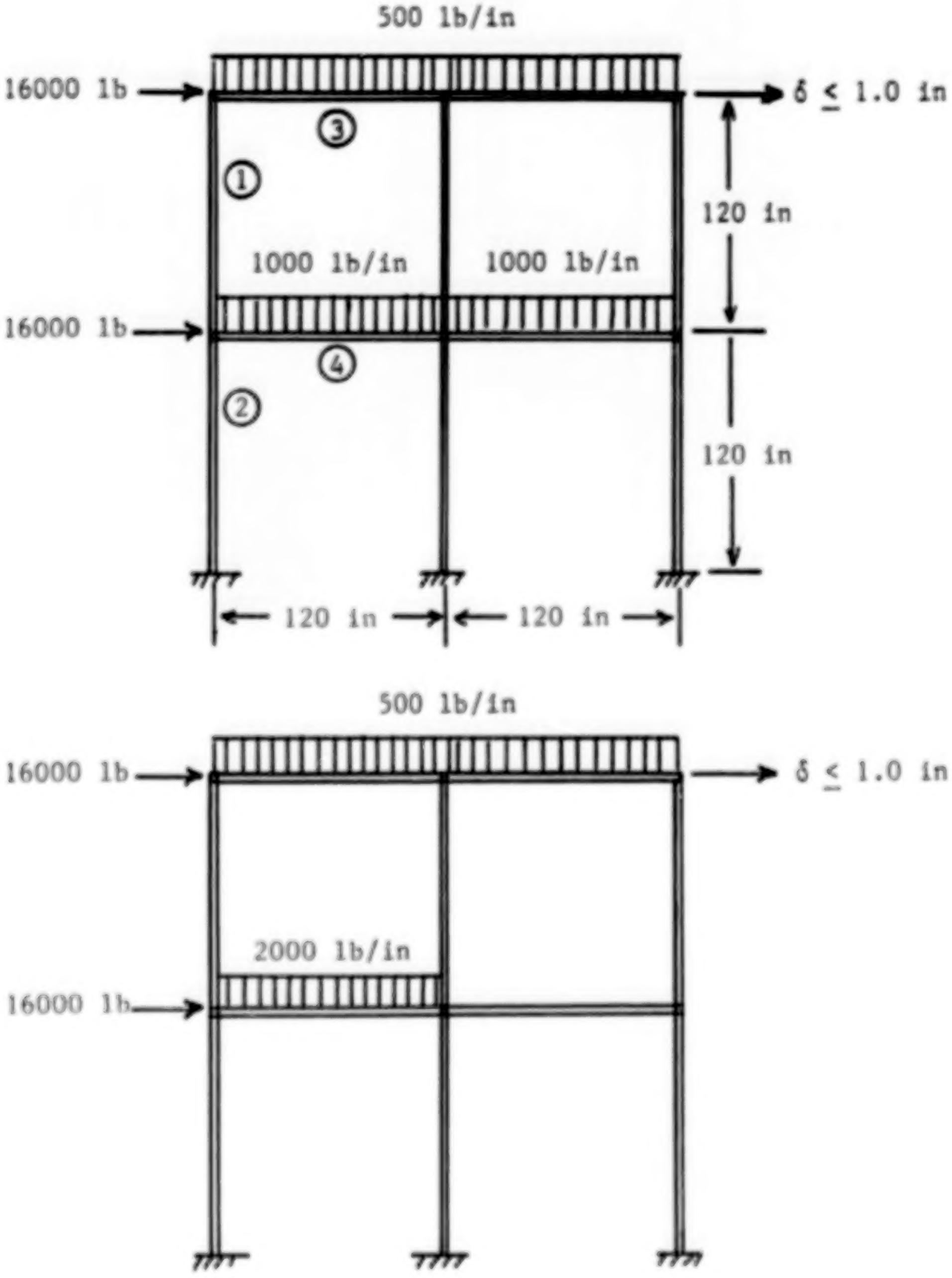
500 lb/in
16000 lb
$\delta \leq 1.0$ in
③
①
120 in
1000 lb/in
1000 lb/in
16000 lb
④
②
120 in
120 in
120 in
500 lb/in
16000 lb
$\delta \leq 1.0$ in
2000 lb/in
16000 lb

FIGURE 12

ITERATION HISTORIES FOR A TWO-BAY FRAME

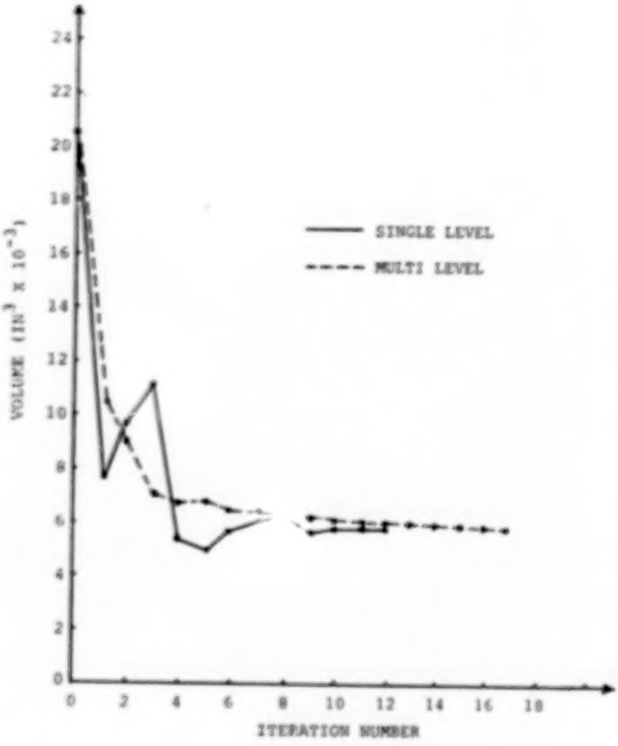

FIGURE 13

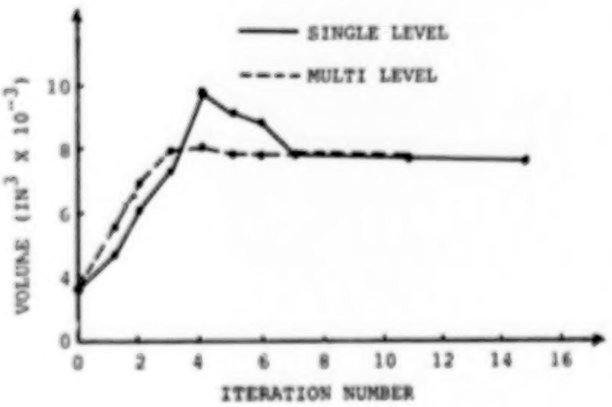

FIGURE 14

Figure 15 lists the advantages and disadvantages of the present approach. A key advantage is that the concept is relatively simple. It does not require the use of nonlinear equality constraints at the subsystem level or the calculation of sensitivities of the subsystem optimum with respect to the system variables as are required in earlier methods. The principal disadvantages are that the number of system level variables is greatly increased and that the quality of the linearizations is important. Regarding this last issue, it should be remembered that the term "linearization" used here does not infer strict linearizations. For example linearizations in reciprocal space may be preferred for structural design problems. The key idea is that the approximations used at each level are explicit.

In summary, it is clear that much research remains to be done before decomposition methods such as this reach the state of reliability that is available in standard structural optimization today. However, for optimization to find widespread use in the multidiscipline environment, it is clear that methods must be developed that will interface with designers with a minimum of disruption to the traditional design environment.

ADVANTAGES OF PRESENT APPROACH

EACH SUBSYSTEM IS SOLVED AS THE ENGINEER CHOOSES

ONLY A SIMPLE SET OF LINEAR CONSTRAINTS MUST BE ADDED

THE SYSTEM AND SUBSYSTEM OBJECTIVES MAY BE DIFFERENT DEPENDING ON THE NEEDS/MOTIVATIONS OF THE INDIVIDUAL LEVEL

THE SYSTEM LEVEL CONTROLS THE OVERALL OBJECTIVE

THE CONCEPT IS SIMPLE

DISADVANTAGES OF THE PRESENT APPROACH

THE NUMBER OF SYSTEM LEVEL DESIGN VARIABLES IS GREATLY INCREASED

THE QUALITY OF THE LINEARIZATIONS IS IMPORTANT

MOVE LIMITS ARE IMPORTANT

THE METHOD HAS THE SAME OVERALL ADVANTAGES AND DISADVANTAGES AS SEQUENTIAL LINEAR PROGRAMMING

FIGURE 15

A key issue in the development of "user friendly" multilevel and multidiscipline optimization methods is the user interface. Figure 16 is a general diagram showing the essential components of such a system, and this is the subject of current research at UC Santa Barbara. The control module directs the activities relative to the system and subsystem tasks, as well as basic data management. All data transfer between modules is via a data management system which may be a general system or may be a specialized system for the multidiscipline optimization task. The important aspect of this approach is that the system and subsystems are provided with a specific form of their input and output which is general enough to accommodate the need to operate either independently or within the multidiscipline environment. This only requires a general degree of standardization and the individual disciplines are otherwise free to operate as usual. Also, at the subsystem level, a similar standardization is required to allow the user to perform analysis alone, optimization without an interface to a controlling system, and optimization within the overall system. The purpose of the pilot code being developed is to create such an environment for testing on a variety of multilevel and multidiscipline problems. This is expected to identify more clearly the strengths and weaknesses of the present method as well as identify future research needs.

DATA TRANSFER

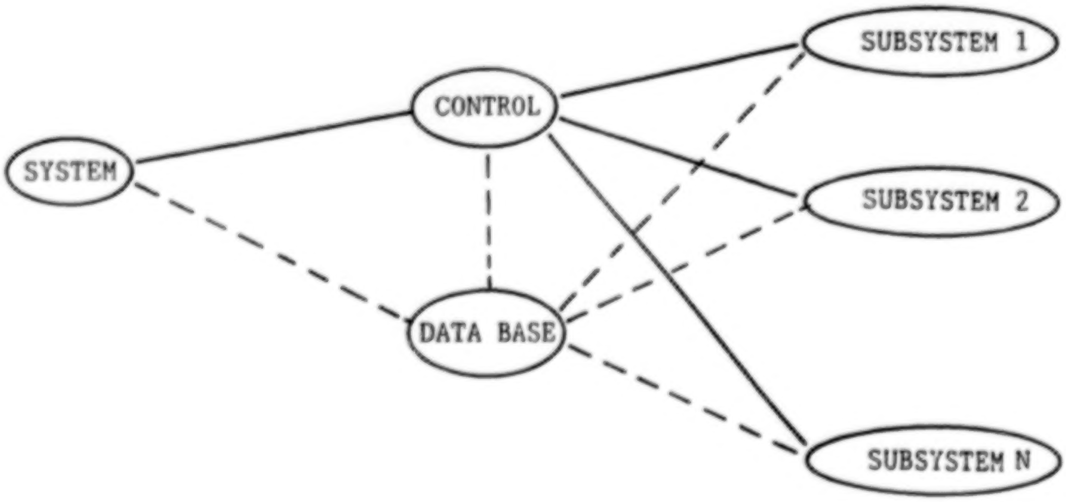

FIGURE 16

25

REFERENCES

1. Vanderplaats, G. N., Yang, Y. J. and Kim, D. S., "An Efficient Multilevel Optimization Method for Engineering Design, Proc. 1988 AIAA/ASME/ASCE/AHS Structures, Structural Dynamics and Materials Conference, Williamsburg, Virginia.

2. Sobieszczanski-Sobieski, J., "A linear Decomposition Method for Large Optimization Problems - Blueprint for Development," NASA Technical Memorandum 83,248, February 1982.

26

A DECOMPOSITION-BASED DESIGN OPTIMIZATION METHOD WITH APPLICATIONS

S. Azarm, M. Pecht, W.-C. Li, and S. Praharaj
Department of Mechanical Engineering
The University of Maryland
College Park, Maryland

TOPICS

There are many real-world engineering design problems which cannot be effectively handled using conventional design optimization methods. Special techniques and/or modifications of the conventional methods are necessary to handle such complex problems. One solution involves two-level decomposition, whereby a problem is divided into smaller subproblems, each with its own design objective and constraints (refs. 1,2).

Here, we will describe a two-level design optimization methodology and give a progress report of its application to Printed Wiring Board (PWB) assembly examples.

1. **Two-Level Design Optimization**
    - **Formulation**
    - **Procedure**
2. **Example: PWB Assembly**
3. **Summary**

29

FORMULATION

We consider a problem which may be decomposed into two-levels, each having several local variables. Here, i,j are the indices corresponding to the number of subproblems and number of constraints in each subproblem, respectively. Furthermore, x_i is the vector of "local" design variables in the lower-level subproblem i, and y is the vector of "global" design variables in the top-level problem.

$$\text{Minimize } f(y;x) = f_o(y) + \sum_{i=1}^{I} f_i(y;x_i)$$

$$\text{Subject: } g_\ell(y)<0 \qquad \ell=1,\ldots,L$$

$$g_{i,j}(y;x_i)<0 \qquad j=1,\ldots,J$$

29

PROCEDURE

The procedure is to

(1) Select the starting value for the global variables y,
(2) find x_i (y is fixed), i=1,...,I, in subproblem i,
(3) find a new y in the top-level problem such that f(y,x) is decreased,
(4) return to step (2) until the minimum for f(y;x) is obtained.

Subproblem i:

Minimize $f_i(y;x_i)$

Subject to: $g_{i,j}(y;x_i)<0 \qquad j=1,\ldots,J$

Top-level problem:

$$\text{Minimize } f(y;x) = f_o(y) + \sum_{i=1}^{I} f_i(y;x_i)$$

Subject to: $g_\ell(y)<0 \qquad \ell=1,\ldots,L$

EXAMPLE: PWB ASSEMBLY

Design optimization of a PWB assembly is considered. The objective is to determine the required component redundancy and fluid flow-rate for each PWB such that the reliability of the assembly is maximized. This is a mixed-integer nonlinear programming problem.

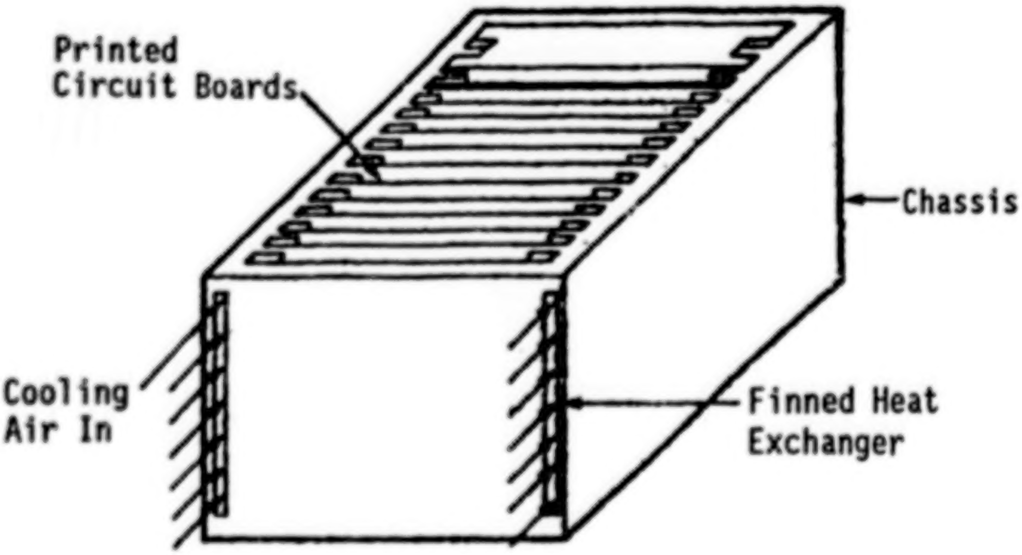
Printed Circuit Boards
Chassis
Cooling Air In
Finned Heat Exchanger

EXAMPLE: TWO-LEVEL MODEL OF A PWB ASSEMBLY

Here, a two-level design optimization model for an assembly of PWBs is presented. Allocation of fluid flow-rates (continuous variables) is performed at the top-level problem, while, allocation of component redundancy (integer variables) for each PWB is performed at the bottom-level subproblems.

MODEL

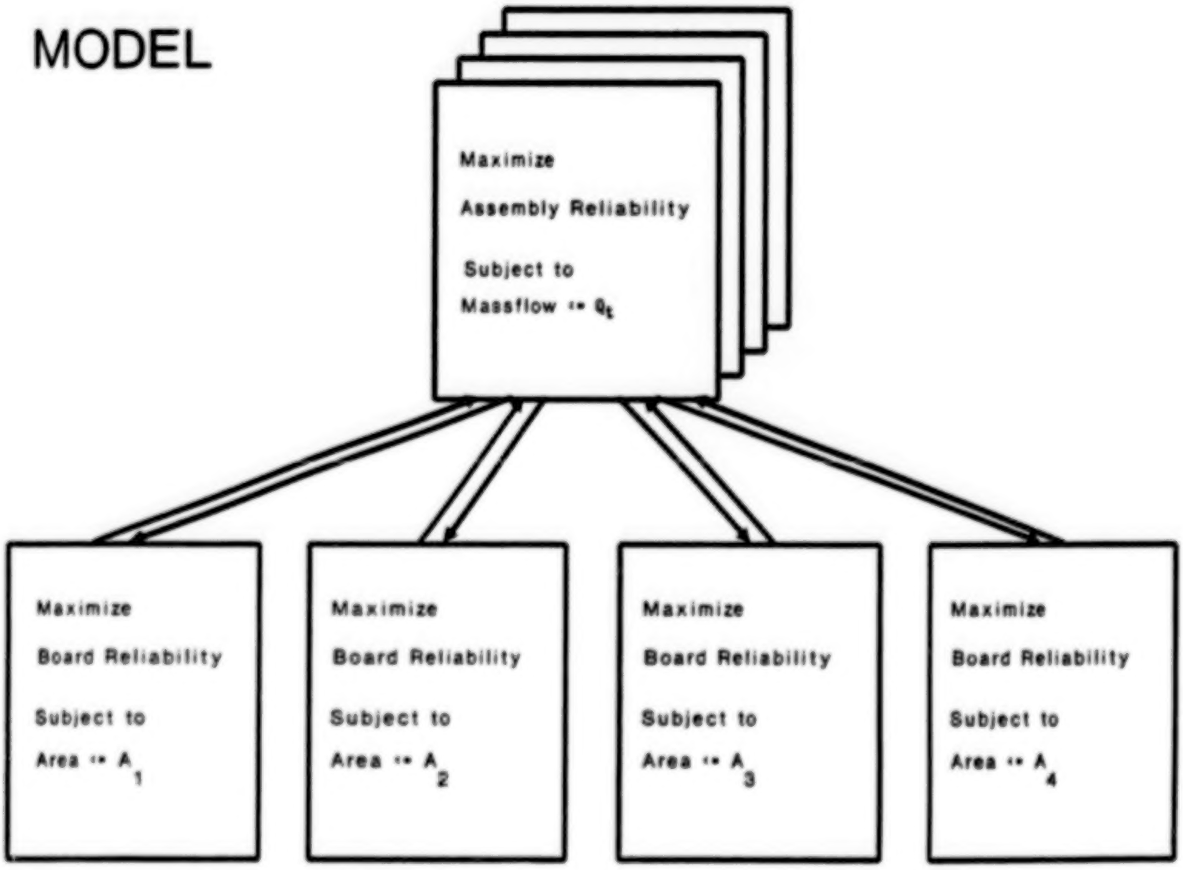
Maximize
Assembly Reliability
Subject to
Massflow <= Q_t
Maximize
Board Reliability
Subject to
Area <= A_1
Maximize
Board Reliability
Subject to
Area <= A_2
Maximize
Board Reliability
Subject to
Area <= A_3
Maximize
Board Reliability
Subject to
Area <= A_4

EXAMPLE: REDUNDANCY ALLOCATION FOR A PWB (Ref. 3)

It is assumed that each PWB consists of a series of N stages, where each stage n, is a parallel combination of M_n redundant components. All components in a stage are active. Thus, for a stage to fail, all components in that stage must fail. Furthermore, it is assumed that for a PWB, all components at a given stage are identical and equally reliable.

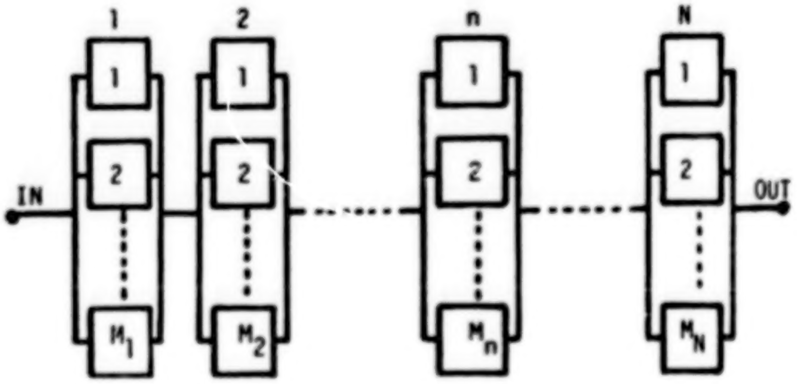

EXAMPLE: TWO-LEVEL OPTIMIZATION FORMULATION

In the two-level formulation of the PWB assembly, subproblem i corresponds to PWB i in which the reliability (R_i) is maximized. In the top-level problem, fluid flow-rates (Q_i, $i=1,\ldots,I$) are allocated to maximize the assembly reliability (R). It is assumed that the assembly is a series system of I PWBs.

Subproblem i:

$$\text{Maximize } R_i = \prod_{n=1}^{N} \left(1-q_n^{M_n}\right)$$

$$\text{Subject to: } \sum_{n=1}^{N} A_n M_n e^{M_n \beta} - A_{avi} < 0$$

$$M_n > 1 \qquad n=1,\ldots,N$$

Top-Level Problem:

$$\text{Maximize } R = \prod_{i=1}^{I} R_i$$

$$\text{Subject to: } \sum_{i=1}^{I} Q_i - Q_t < 0$$

$$Q_i > 0 \qquad i=1,\ldots,I$$

where:

q_n = nth stage component unreliability of ith PWB
M_n = nth stage component redundancy of ith PWB
A_{avi} = available area of ith PWB
A_n = area of a component at nth stage of ith PWB
Q_t = total fluid flow-rate of assembly

EXAMPLES

Three PWB assembly examples were solved. The first example was an assembly of 2 PWBs, each PWB having 5 stages. The second example was an assembly of 4 PWBs, each PWB having 15 stages. The third example was an assembly of 4 PWBs, each PWB having 30 stages. The overall design objective in each example was to maximize assembly reliability.

Example	No. of stages/PWB	No. of PWBs	Variables	Constraints
1	5	2	12	15
2	15	4	64	69
3	30	4	124	129

EXAMPLE: RESULTS

Initial and final solutions for an assembly of two PWBs are given:

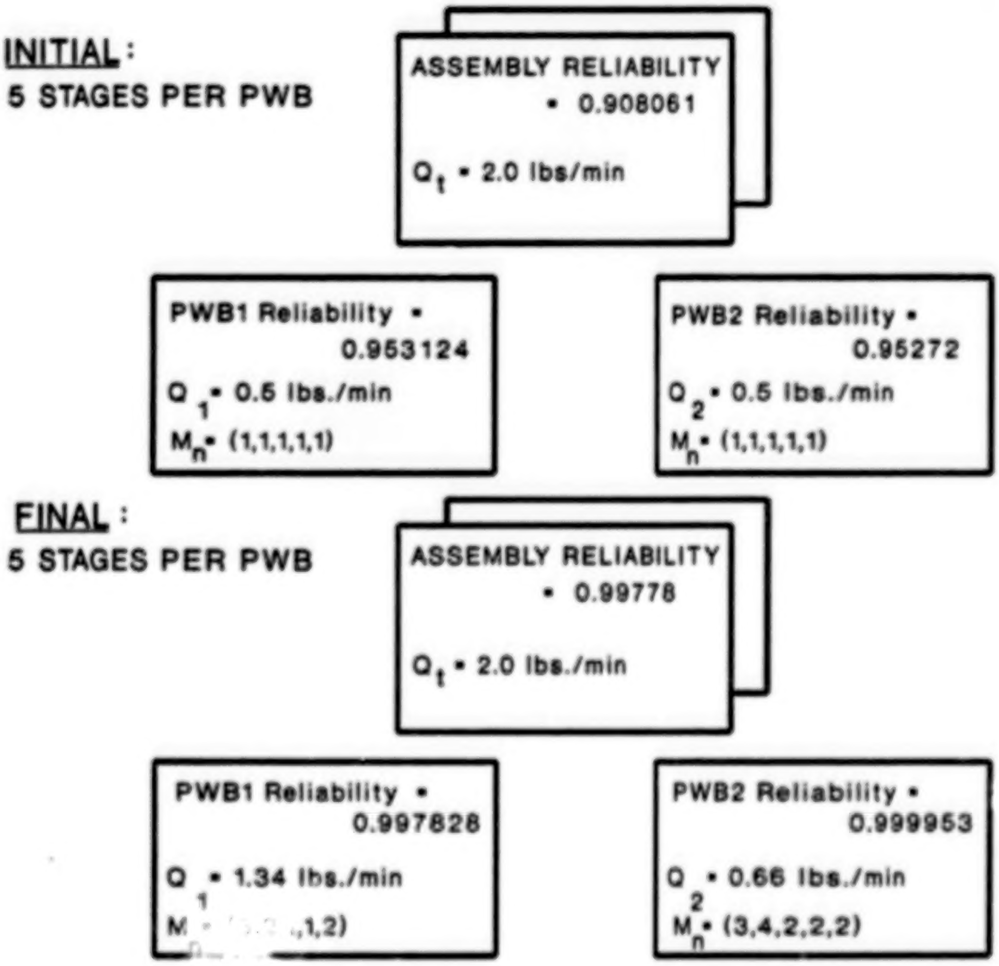

INITIAL:
5 STAGES PER PWB

ASSEMBLY RELIABILITY
• 0.908061
Q_t • 2.0 lbs/min

PWB1 Reliability •
0.953124
Q_1• 0.5 lbs./min
M_n• (1,1,1,1,1)

PWB2 Reliability •
0.95272
Q_2• 0.5 lbs./min
M_n• (1,1,1,1,1)

FINAL:
5 STAGES PER PWB

ASSEMBLY RELIABILITY
• 0.99778
Q_t • 2.0 lbs./min

PWB1 Reliability •
0.997828
Q_1 • 1.34 lbs./min
M_n • ([illegible],1,2)

PWB2 Reliability •
0.999953
Q_2 • 0.66 lbs./min
M_n• (3,4,2,2,2)

EXAMPLE: RESULTS

Initial and final solutions for two assemblies of four PWBs are given.

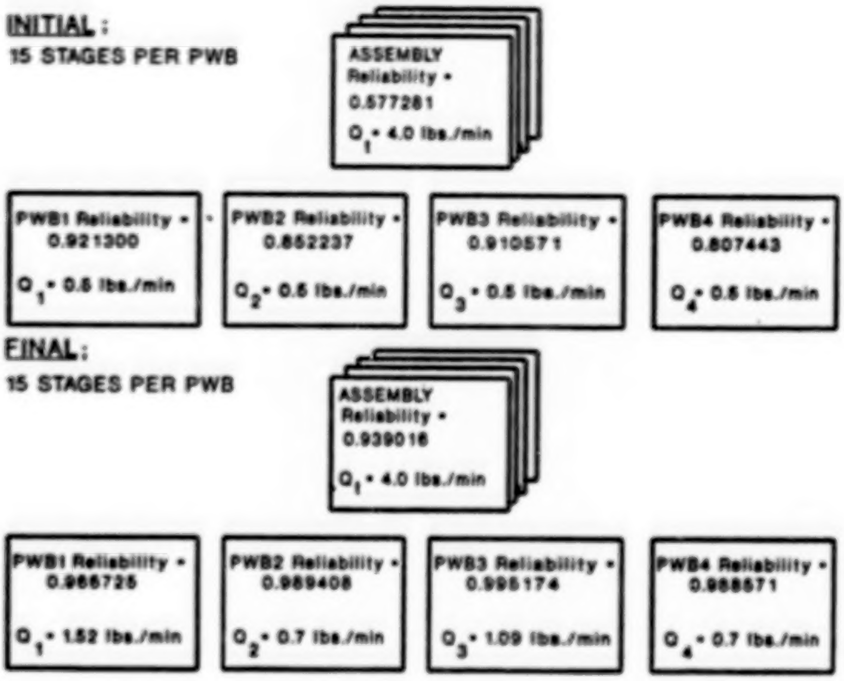

INITIAL:
15 STAGES PER PWB
ASSEMBLY Reliability = 0.577281
Q_1 = 4.0 lbs./min
PWB1 Reliability = 0.921300
Q_1 = 0.5 lbs./min
PWB2 Reliability = 0.852237
Q_2 = 0.5 lbs./min
PWB3 Reliability = 0.910571
Q_3 = 0.5 lbs./min
PWB4 Reliability = 0.807443
Q_4 = 0.5 lbs./min
FINAL:
15 STAGES PER PWB
ASSEMBLY Reliability = 0.939016
Q_1 = 4.0 lbs./min
PWB1 Reliability = 0.986725
Q_1 = 1.52 lbs./min
PWB2 Reliability = 0.989408
Q_2 = 0.7 lbs./min
PWB3 Reliability = 0.995174
Q_3 = 1.09 lbs./min
PWB4 Reliability = 0.966571
Q_4 = 0.7 lbs./min

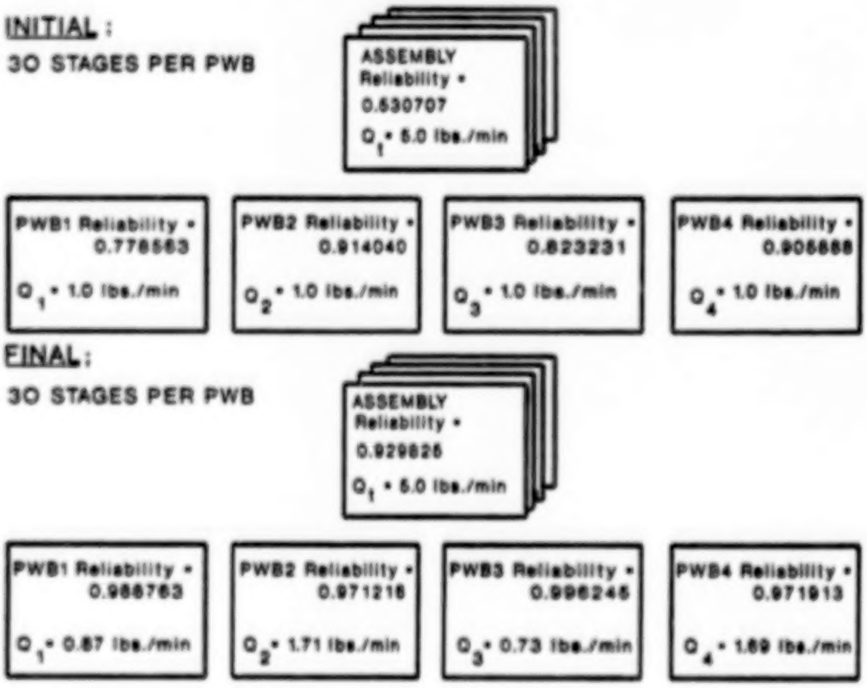

INITIAL:
30 STAGES PER PWB
ASSEMBLY Reliability = 0.530707
Q_1 = 5.0 lbs./min
PWB1 Reliability = 0.778563
Q_1 = 1.0 lbs./min
PWB2 Reliability = 0.914040
Q_2 = 1.0 lbs./min
PWB3 Reliability = 0.823231
Q_3 = 1.0 lbs./min
PWB4 Reliability = 0.905888
Q_4 = 1.0 lbs./min
FINAL:
30 STAGES PER PWB
ASSEMBLY Reliability = 0.929826
Q_1 = 5.0 lbs./min
PWB1 Reliability = 0.988763
Q_1 = 0.87 lbs./min
PWB2 Reliability = 0.971216
Q_2 = 1.71 lbs./min
PWB3 Reliability = 0.996245
Q_3 = 0.73 lbs./min
PWB4 Reliability = 0.971913
Q_4 = 1.69 lbs./min

SUMMARY

The design of PWB assemblies is a complex task which is generally conducted as a "sequential process." Individual PWBs are usually designed first, followed by the composition of the PWBs into an assembly. As a result, optimizing design considerations such as assembly reliability cannot be accomplished. This study showed that a two-level decomposition method can be employed to optimize for reliability at both the PWB- and the assembly-level in a coupled manner. The two-level decomposition method also resolved the mixed-integer nonlinear programming nature of the problem rather easily.

- **The sequential design process makes system optimization impossible**
- **A mixed-integer nonlinear optimization problem modelled and solved using a two-level optimization technique**
- **More research is needed to improve the performance of the two-level optimization method**

38

REFERENCES

1. Azarm, S., Li, W.-C.: A Two-Level Decomposition Method for Design Optimization, Engineering Optimization, vol. 13, pp. 211-224, 1988.

2. Azarm, S., Li, W.-C.: A Multi-Level Optimization-Based Design Procedure Using Global Monotonicity Analysis, Proceedings of 1988 ASME Design Automation Conference, Orlando, Florida, Advances in Design Automation, ASME publication DE, vol. 14, pp. 115-120, 1988.
3. Pecht, M., Azarm, S. Praharaj, S.: Optimized Redundancy Allocation for Electronic Equipment, Engineering Optimization, vol. 14, pp. 101-114, 1988.

MULTILEVEL DECOMPOSITION of COMPLETE VEHICLE CONFIGURATION in a PARALLEL COMPUTING ENVIRONMENT

VINAY BHATT
and
K. M. RAGSDELL
Design Productivity Center
University of Missouri
Columbia, MO

40

ABSTRACT

This research summarizes various approaches to multilevel decomposition to solve large structural problems. A linear decomposition scheme based on the Sobieski algorithm is selected as a vehicle for automated synthesis of a complete vehicle configuration in a parallel processing environment. The research is in a developmental stage. Preliminary numerical results are presented for several example problems.

NOMENCLATURE

SS_{ijk} - j^{th} subsystem at level i with parent k at level (i-1)

x^{ijk} - vector of design variables for SS_{ijk}

y^{ijk} - vector of design parameters for SS_{ijk}

$C^{ijk}(x^{ijk},y^{ijk})$ - cumulative constraint violation function for SS_{ijk}

$F^{ijk}(x^{ijk},y^{ijk})$ - penalty function for SS_{ijk}

$f^{ijk}(x^{ijk},y^{ijk})$ - objective function for SS_{ijk}

$g_W^{ijk}(x^{ijk},y^{ijk})$ - vector of inequality constraints for SS_{ijk}

$h_v^{ijk}(x^{ijk},y^{ijk})$ - vector of equality constraints for SS_{ijk}

KS - Kresselmeir - Steinhauser function

INTRODUCTION

A modern vehicle (aircraft or automobile) is a complex engineering system composed of many subsystems that are tightly coupled. Often, the number of design variables involved and constraints imposed is large. The total amount of data handled becomes so large that synthesis of such a system is both intractable and costly and can easily saturate even the most advanced supercomputers available today. A remedy is to break the large problem into several manageably smaller subproblems; and solve these subproblems independently without loosing integrity with the main or parent problem and ultimately achieve satisfactory results for the original problem. This method of problem solving is known as decomposition.

Decomposition is the technique of dividing a large task into a set of smaller, self-contained subtasks that can be solved concurrently [1].

In a multilevel decomposition technique, the main structure at the top level is decomposed into a hierarchical tree consisting of substructures at different levels. A typical multilevel decomposition tree is shown in Figure 1. The main advantage of the multilevel optimization scheme lies in the fact that all substructures can be analyzed and optimized independently with convenient coupling. This application makes such an algorithm appropriate for parallel computing technology existing today.

Several studies have been devoted to the decomposition of large-scale optimization problems [2]. Mainly two classes of decomposition methods exist: ***formal methods*** and ***intuitive methods.*** *Formal methods* decompose a problem using its mathematical structure. Such a decomposition may be fully automatic and can be built-in within the design cycle. However, in *intuitive methods*, an understanding of the physics of the system is the prime factor directing the decomposition. These intuitive methods provide an alternative for decomposing those problems which do not possess the structure for which a formal decomposition method exists.

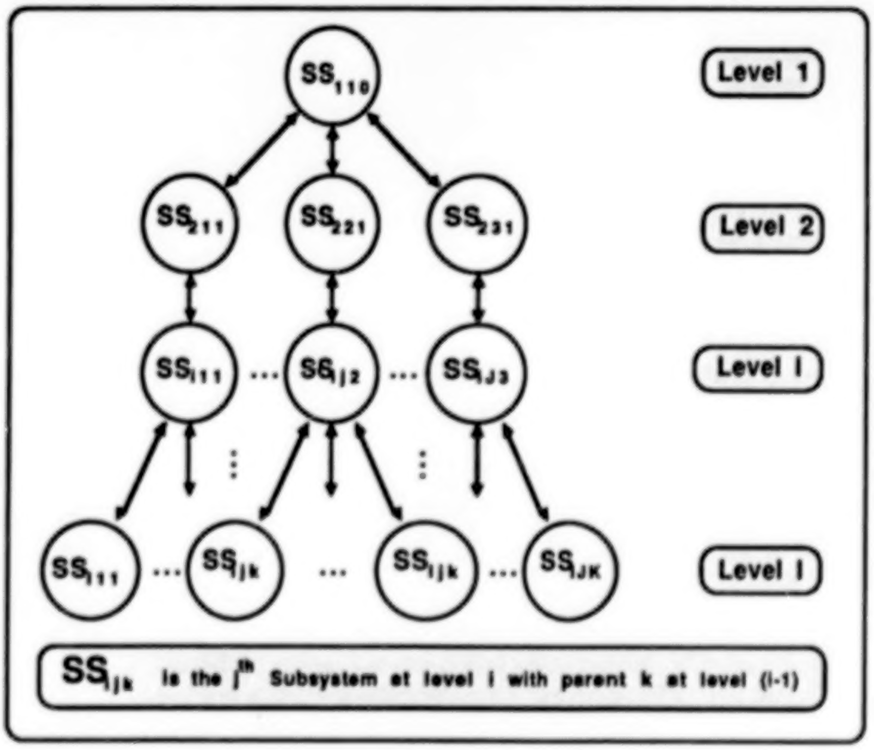

Figure 1
A general, Multilevel Decomposition Tree

PARALLEL PROCESSING

In a broader sense, the terms parallel computing or concurrent processing are used to define simultaneous execution of multiple tasks on multiple CPU's. This is achieved either by synchronizing the tasks on a multiprocessor or by effectively distributing the tasks among a network of computers. Parallel computing operations are classified in a number of ways depending upon the architecture of available computing resources and the granularity of the applications.

Flynn [3] has divided computer architectures from a macroscopic point of view using stream concept. Stream in this context simply means a sequence of items (instructions or data) as executed or operated on by a processor. The four broad classifications of machine organizations are:

(1) ***The Single Instruction stream - Single Data stream (SISD)***, which represents most conventional, uni-processor computing equipments available today.

(2) ***The Single Instruction stream - Multiple Data stream (SIMD)***, which includes most array processors; for example, Illiac IV.

(3) ***The Multiple Instruction stream - Single Data stream (MISD)*** type organizations; for example pipeline computers like CYBER 205.

(4) ***The Multiple Instruction stream - Multiple Data stream (MIMD)*** machines, which include the multiprocessor systems and distributed computing networks. It is possible to classify the MIMD architecture further according to coupling of the multiple processors as ***Tightly-Coupled*** and ***Closely-Coupled*** systems.

Various parallel computing applications are also classified based on granularity ranging from infinite grain size to very fine grain size. Granularity is measured by synchronization interval which is in fact the period between synchronization events measured in number of instructions for multiple processors or processing elements.

Concurrent processing computers set new demands on data structure, data management, organization, program coding, and adaptability considerations. These computers offer the possibility for significant gains in computational speed for structural synthesis based on multilevel optimization. Experience in parallel processing on NASA Langley's first multiple instruction, multiple data (MIMD) computer has shown that the greatest computational gains are obtained by writing special-purpose codes based on "rethinking" the solution method; somewhat smaller gains have resulted from "recoding" an existing algorithm, and no gain has resulted from the approach of just running an existing program on a parallel computer [4].

In recent years, significant research effort has been reported in applying linear and nonlinear finite element algorithms on concurrent processing computers using substructuring methods. Kowalik [5] has projected the potential for impact of parallel computers on numerical algorithms. Lootsma and Ragsdell [6] have described the state-of-the-art work in parallel nonlinear optimization area. A unique feature of this research is that this is the first attempt to implement a multilevel decomposition code on a network of computers. For this a VAX 8650 will be used as a host to load applications on a number of microvax stations available in a network of computers at the Design Productivity Center, University of Missouri, Columbia.

MULTILEVEL DECOMPOSITION

Most of the multilevel optimization algorithms developed so far involve intuitive or physical decomposition of the large-scale system into its component subsystems. All these algorithms exhibit a general philosophy of design. The subsystems are designed separately as component level synthesis problems. Then, the main system and all the subsystems are coupled appropriately and synthesized so as to achieve overall convergence of the system. A few approaches to multilevel decomposition are described now.

Review of Multilevel Decomposition Algorithms

Lucien Schmit Jr. and Ramanathan [7] introduced a multilevel approach to the design of minimum weight structures so as to include both local and global buckling of the elements and the system. In a two-level formulation of their decomposition algorithm, they treated total structural weight as the system level objective function whereas at component level, instead of component weight as an objective function, they considered minimization of change in equivalent system stiffness of the component. This is due to the fact that a structure made up of minimum weight components is not necessarily a minimum weight system. Schmit & Ramanathan observed that an efficient multilevel decomposition scheme should inherently lead to a weaker and weaker coupling between the subsystems as the iterations proceed.

Another interesting decomposition approach is by Uri Kirsch [8]. In this approach, the design quantities are divided into a set of dependent design variables and another set of independent quantities called behavior variables. The design variables and the behavior variables are optimized at different levels leading to a minimum two-level optimization algorithm. In the proposed scheme, the top level system is decomposed into a number of subsystems as second level problems. At the first level, dependent design variables are optimized for any assumed behavior (independent) variables. Then, at second level behavior quantities are optimized for each subsystem separately. The third level is an optional level in which elastic analysis is repeated only after a complete solution of both the first and the second levels. The main advantages of this algorithm are that the number of elastic analyses required is small, the first level is decomposable and the number of

44

independent variables is not affected by the number of loading conditions the structure is subjected to.

One of the most irksome problems with the multilevel or hierarchical decomposition approach is the discontinuous behavior of derivatives that is transferred from the lower levels of the hierarchy to the upper levels. Raphael Haftka [9] has proposed a hierarchical algorithm that is free of such difficulties. In this algorithm, a penalty function method is employed in combination with Newton's method with approximate second derivatives to perform the optimization.

Jaroslaw Sobieski at NASA LangleyResearchCenter proposed an intuitive scheme of multilevel decomposition in 1982 which is not only versatile but also convenient. In the Sobieski approach, a large-scale system is physically decomposed into a number of subsystems at multiple levels with the complex system at the top level and the detailed most elements at the lower most level. For each subsystem the design space is divided into a set of constant design parameters and another set of design variables. A unique feature of the algorithm is **Optimum Sensitivity Analysis (OSA)**. Sensitivity of the subsystems to problem parameters is determined and this information provides for the vertical coupling between a subsystem and its parent subsystem. In order to optimize a complete vehicle configuration, the Sobieski algorithm is selected as a vehicle for structural synthesis [10].

Optimum Sensitivity Analysis

In a multilevel decomposition algorithm it is essential to estimate the sensitivity of a problem at its optimum to the assumed constant parameters of the problem. This information provides for necessary coupling between various subsystems in the decomposition tree. The optimum sensitivity coefficients are essentially the Lagrange Multipliers. Numerically, they correspond to total derivatives of the objective function and the design variables with respect to the design parameters. A number of methods have been developed to compute the sensitivity coefficients directly. These methods include: Lagrange multiplier method, penalty function methods, feasible directions methods with the extension of the latter method to incorporate higher order coefficients and discontinuities.

In the Lagrange multiplier method [11], one starts with the Kuhn-Tucker conditions for a constrained minimum. Noting that the optimum value of the design variable is given by $x^* = x^*(y)$ where, y is the vector of design parameters, one can differentiate the Kuhn-Tucker conditions with respect to y, using the chain rule of partial differentiation. On simplification, we get a set of simultaneous linear equations with the sensitivity derivatives $\left(\frac{\partial x^*}{\partial y}\right)$ as unknowns.

In the penalty function methods, the penalty function: $F(x,y) = f(x,y) + rP$ is differentiated with respect to the design parameter y. Here, f is the objective function, r is the penalty parameter and P is the penalty term which could be either an interior function, or an exterior function or in case of coupled constraints, a Kresselmeir - Steinhauser function which is essentially the envelope of the constraint surface. Depending upon the choice of penalty term, different sets of linear equations can be developed to solve for the unknown sensitivity values. Optimum sensitivity analysis based on penalty function formulation is adopted in this research.

Vanderplaats [12] has developed algorithm based on the method of feasible directions to compute linear and higher order sensitivity coefficients.

The Sobieski Algorithm

The Sobieski algorithm for multilevel decomposition is depicted in an easy to comprehend flow chart as shown in Figure 2.

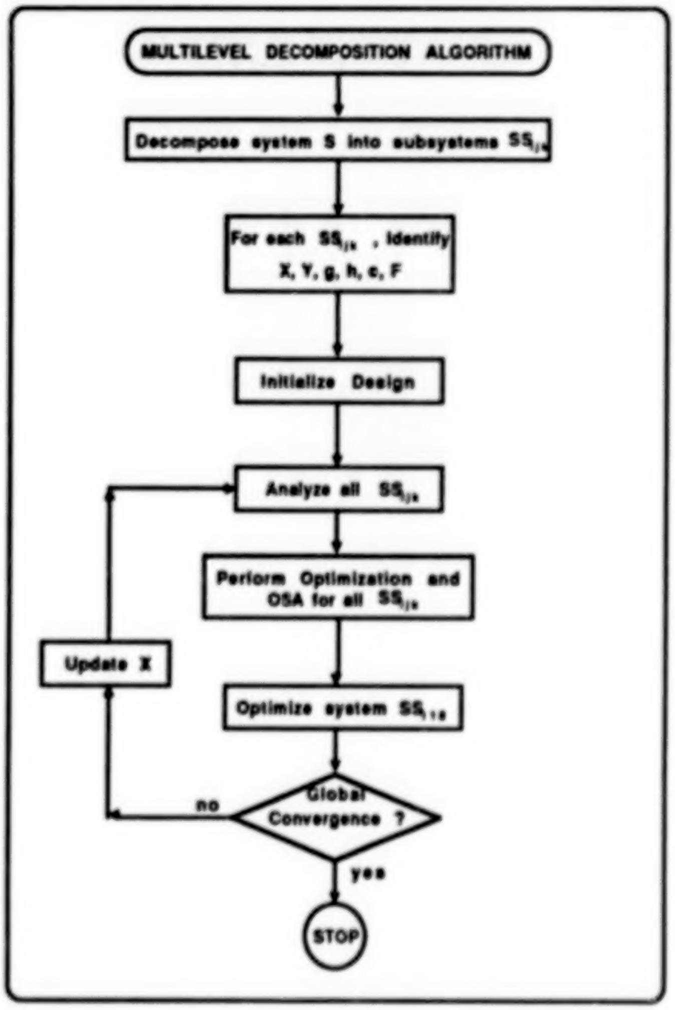
MULTILEVEL DECOMPOSITION ALGORITHM
Decompose system S into subsystems SS_{ijk}
For each SS_{ijk} , Identify X, Y, g, h, c, F
Initialize Design
Analyze all SS_{ijk}
Perform Optimization and OSA for all SS_{ijk}
Update X
Optimize system SS_{1k}
Global Convergence ?
no
yes
STOP

Figure 2
A Flow Chart for Multilevel Decomposition

The system $S=SS_{110}$ is decomposed into a number of subsystems SS_{ijk}. The design variables and the design parameters for the subsystems are x^{ijk} and y^{ijk} respectively. The design variables at the system level are essentially a set of design parameters for all the subsystems. The design procedure begins with initializing the design and analyzing all the subsystems. The objective functions for subsystem optimization are formulated by a cumulative constraint violation function C^{ijk} using, for example, a Kresselmeir-Steinhauser function of the form:

$$C^{ijk} = \frac{1}{p}\ln\left[\sum_{w} e^{-pg_w^{ijk}}\right] + p\sum_{v}\left(h_v^{ijk}\right)$$

During the system optimization, when the design variables x^{110} are perturbed, the changes in subsystem objective function and design variables can be predicted using linear the Taylor series extrapolation:

$$C_e^{ijk} = C^{ijk^{(*)}} + \sum\left(\frac{dC^{ijk^{(*)}}}{dx^{110}}\right)\left(\delta x^{110}\right)$$

$$x_e^{ijk} = x^{ijk^{(*)}} + \sum\left(\frac{dx^{ijk^{(*)}}}{dx^{110}}\right)\left(\delta x^{110}\right)$$

where, $\left\{\frac{dC^{ijk^{(*)}}}{dx^{110}}\right\}$ and $\left\{\frac{dx^{ijk^{(*)}}}{dx^{110}}\right\}$ are the total derivatives computed by Optimum Sensitivity Analysis. The procedure terminates when, (i) system response constraints are met, (ii) cumulative constraint violation for all the subsystems is reduced to at least zero and (iii) no further reduction of system mass appears possible.

EXAMPLES

The multilevel decomposition algorithm based on the Sobieski approach is being coded on VAX 8650 using FORTRAN 77 in double precision. In order to check the validity of the OSA algorithm and the multilevel decomposition algorithm various example problems have been set up. Closed-form analyses are generated for a three-bar truss problem and a portal frame involving beam elements. A highly simplified finite element model of an automobile configuration is also created using beam elements.

Three-Bar Truss Problem

The optimum sensitivity analysis is applied to a simple Three-Bar Truss (Figure 3), where the design variables are the areas of cross-section and the design parameters are the applied load P and the angle α which P makes with the y-axis. The weight of the structure is to be optimized with respect to the design variables. The behavior constraints correspond to simple upper and lower limits on stresses within the rods while the variable bounds ensure nonnegative areas of cross-section. Numerical results, shown in Figure 4, are in agreement with published results.

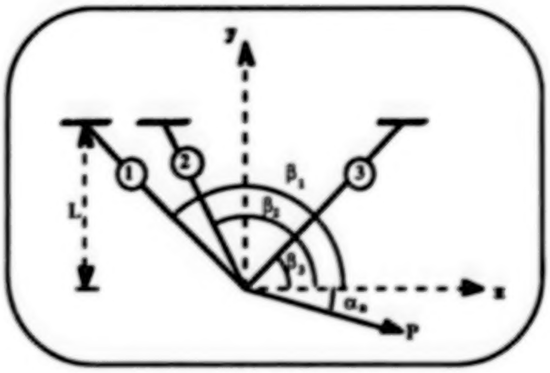

Figure 3
A Three-Bar Truss

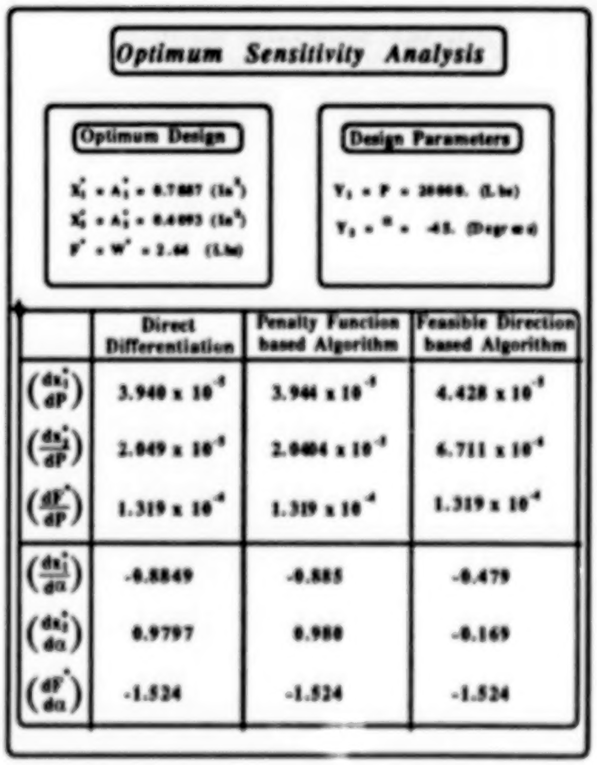

Optimum Sensitivity Analysis

Optimum Design

$X_1^* = A_1^* = 0.7887$ (In^2)
$X_2^* = A_2^* = 0.4083$ (In^2)
$F^* = W^* = 2.64$ (Lbs)

Design Parameters

$Y_1 = P = 20000.$ (Lbs)
$Y_2 = \alpha = -45.$ (Degrees)

	Direct Differentiation	Penalty Function based Algorithm	Feasible Direction based Algorithm
$\left(\frac{dx_1^*}{dP}\right)$	3.940×10^{-5}	3.944×10^{-5}	4.428×10^{-5}
$\left(\frac{dx_2^*}{dP}\right)$	2.049×10^{-5}	2.0404×10^{-5}	6.711×10^{-6}
$\left(\frac{dF^*}{dP}\right)$	1.319×10^{-4}	1.319×10^{-4}	1.319×10^{-4}
$\left(\frac{dx_1^*}{d\alpha}\right)$	-0.8849	-0.885	-0.479
$\left(\frac{dx_2^*}{d\alpha}\right)$	0.9797	0.980	-0.169
$\left(\frac{dF^*}{d\alpha}\right)$	-1.524	-1.524	-1.524

Figure 4
Three-bar Truss Results

Portal Frame Problem

A portal frame with three beam elements is selected for testing the two-level decomposition algorithm. Figure 5 displays the complete frame as a top level system whereas, the individual beam elements are three subsystems for the problem. The portal frame structural weight is minimized subject to stress, deflection and buckling constraints. The simple statically indeterminate frame is analyzed using a variational method based on the minimization of the total complementary energy functional. Figure 6 shows the iteration history for "one-level" optimization versus "two-level" optimization.

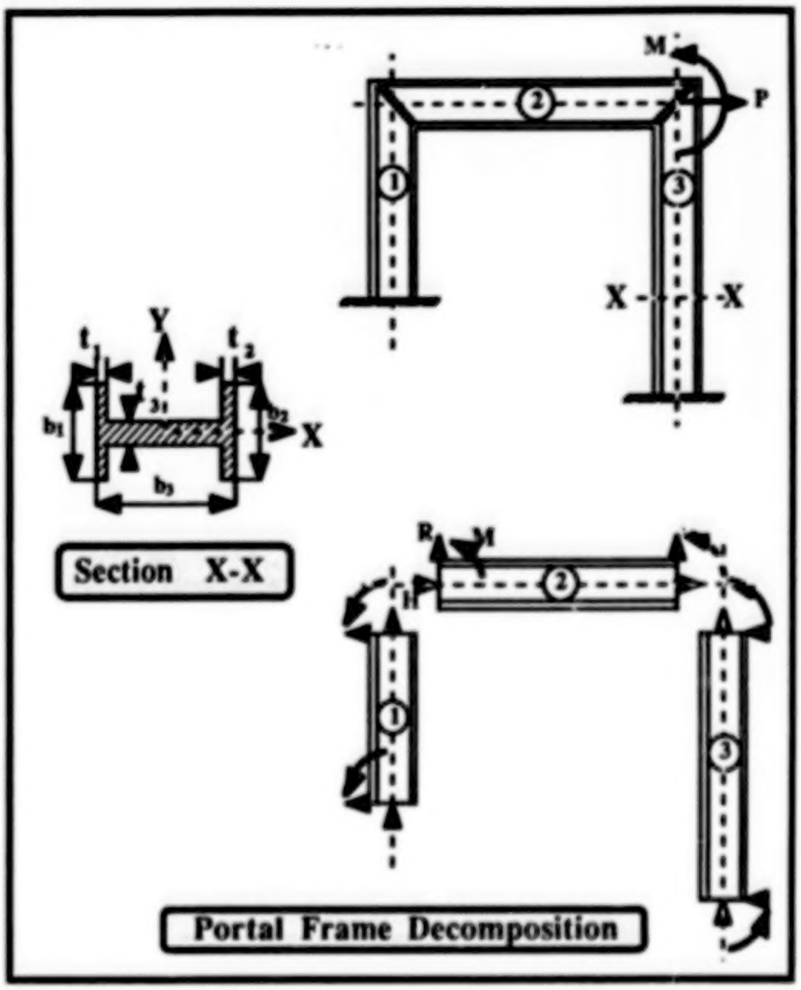
M
P
②
①
③
X
X
Y
t_1
t_2
t_{31}
b_1
t_{32}
X
b_3
Section X-X
R
M
H
②
①
③
Portal Frame Decomposition

Figure 5
Portal Frame Problem

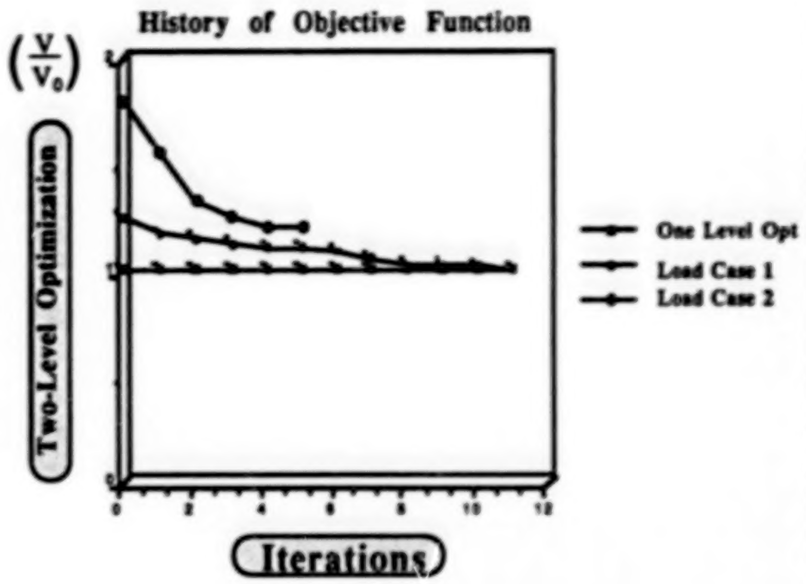

V = Objective Function value for Two Level Optimization
V_0 = Objective Function value for One Level Optimization

Portal Frame Decomposition Results

Figure 6
Portal Frame Decomposition Results

Optimum Vehicle Configuration Problem

A major objective of the study is to demonstrate the applicability of the multilevel decomposition algorithm to produce an optimum automobile configuration from a generic model of a complete automotive structure. As a first step in this direction, a simplified uniframe car model is developed [13]. Figure 7 shows the car frame selected to develop a simplified finite element model containing 22 nodes with 33 beam elements. The model is being studied for its static and dynamic response using NASTRAN. The automobile configuration is ideally suited for multilevel decomposition. In a three level decomposition strategy, the complete frame is selected as the top level which is decomposed into three middle level subsystems as shown in Figure 8. The third or bottom level corresponds to a box beam cross section.

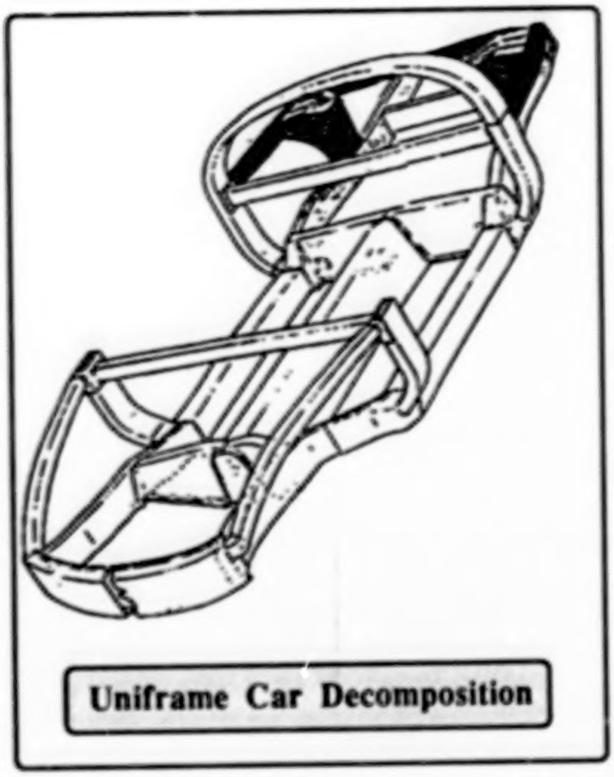
Uniframe Car Decomposition

Figure 7
Uniframe Car Model

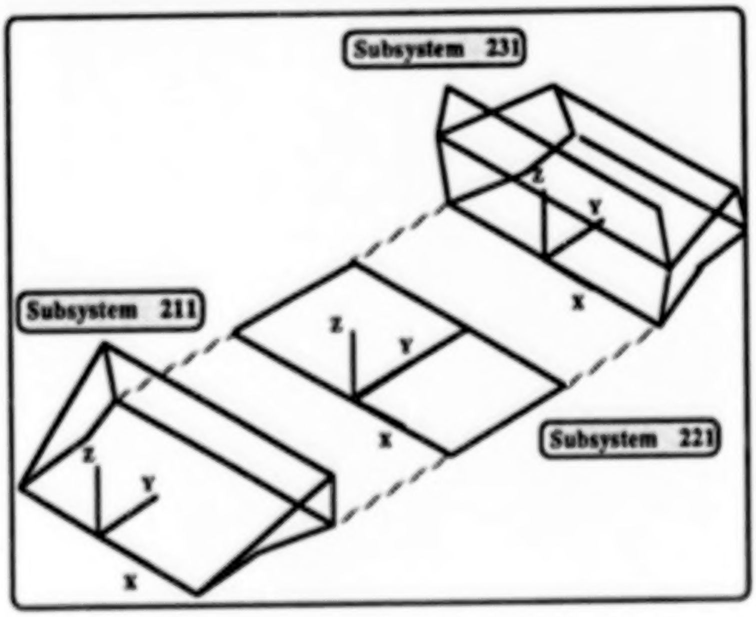
Subsystem 231
Z
Y
X
Subsystem 211
Z
Y
X
Subsystem 221
Z
Y
X

Figure 8
Second Level of Decomposition

CLOSURE

Multilevel decomposition is a multidisciplinary area. Here, we have concentrated on the study of large-scale structural synthesis in a parallel computing environment. A long term commitment to research in this area will have a significant impact on the design productivity of the automobile and aerospace industry of the future.

REFERENCES

1. Sobieski, J., "A Linear Decomposition Method for Large Optimization Problem - Blueprint for Development", NASA Technical Memorandum # 83248, Feb. 1982.

2. Barthelemy, J.,"Development of a Multilevel Optimization Approach to the Design of Modern Engineering Systems", NASA Contractor Report #172184, VPI, Virginia, Aug. 1983.

3. Flynn, M. J., "Some Computer Organizations and their Effectiveness", IEEE Transactions onComputers, Vol. C-21, No. 9, Sept. 1972.

4. Storaasli, O. and Bergan, Pal, "Nonlinear Substructuring Method for Concurrent Processing Computers", AIAA Journal, Vol. 25, No. 6, June 1987.

5. Kowalik, J. S., "Parallel Computers and their Impact onNumerical Algorithms and Related Software", Nonlinear Optimization 1981, NATO conference series, Academic Press, 1982.

6. Lootsma, F. A. and K. M. Ragsdell, "State-of-the-Art in Parallel Nonlinear Optimization", Design Productivity Center Report #86DPC027, University of Missouri, Columbia, Nov. 1986.

7. Schmit, L. A. and Ramanathan, R. K., "Multilevel Approach to Minimum Weight Design including Buckling Constraints", AIAA Journal, Vol. 16, No. 2, Feb. 1978.

8. Kirsch, U., "An Improved Multilevel Structural Synthesis Method", Journal of Structural Mechanics, #13(2), 1985.

9. Haftka, R., "An Improved Computational Approach for Multilevel Optimum Design", Journal of Structural Mechanics, 12(2), pp. 245 - 261, 1984.

10. Bhatt, V., Linden, S. and Ragsdell, K., "Optimal Synthesis of Large-Scale Systems using Decomposition Techniques and Parallel Processing", Design Productivity

Center Technical Report # 88DPC002, University of Missouri, Columbia, Feb. 1988.

11. Sobieski, J., J. Barthelemy and K. Riley, "Sensitivity of Optimum Solutions of Problem Parameters", AIAA Journal, Vol. 20, No. 9, Sept. 1982.

12. Vanderplaats, G., "Efficient Calculation of Optimum Design Sensitivity", AIAA Journal, Vol. 23, No. 11, Nov. 1985.

13. Linden, S., "Decomposition and Multilevel Optimization of Large Scale Systems", Final Report, Design Productivity Center, Columbia, May 1987.

SESSION 10: SHAPE OPTIMIZATION

Chairman: G. A. Gabriele

54

DESIGN OPTIMIZATION OF AXISYMMETRIC BODIES IN NONUNIFORM TRANSONIC FLOW

C. Edward Lan
Department of Aerospace Engineering
The University of Kansas
Lawrence, Kansas

55

FORMULATION OF ANALYSIS PROBLEM

For an axisymmetric body immersed in a propfan slipstream, or a jet, the effect of freestream nonuniformity must be accounted for to calculate the wave drag in a transonic flow. Since the flow field is rotational, in the present approach a rotation function (F) and a velocity function (ϕ) are introduced in Euler's equations to result in a governing equation which is similar, in mathematical structure, to a full-potential equation as shown in figure 1 (refs. 1 and 2). The equation is solved with the algorithm of reference 3. Following reference 3, the equation is cast in curvilinear coordinate systems with a body-normal coordinate system covering the front portion and a sheared cylindrical system used in the aft. The rotation function is calculated through Crocco's relation. In figure 1, only the equation in body-normal coordinates is shown. Details can be found in reference 2.

- **Equation in Body Normal Coordinates:**

$$\left(1-\frac{u^2}{a^2}\right)\frac{1}{H}\left(\frac{1}{H}\phi_\xi\right)_\xi-\frac{2uv}{a^2H}\phi_{\xi\eta}+\left(1-\frac{v^2}{a^2}\right)\phi_{\eta\eta}+\left(\frac{2uv}{a^2}\frac{\kappa}{H}+\frac{\sin\theta}{r}\right)\frac{1}{H}\phi_\xi+\left[\left(1-\frac{u^2}{a^2}\right)\frac{\kappa}{H}+\frac{\cos\theta}{r}\right]\phi_\eta$$

$$+\left[\frac{uv}{a^2}\sin\theta+\left(1-\frac{u^2}{a^2}\right)\cos\theta\right]\frac{1}{H}F_\xi-\left[\frac{uv}{a^2}\cos\theta+\left(1-\frac{v^2}{a^2}\right)\sin\theta\right]F_\eta=0$$

- **Velocity Components:**

$$u=\frac{1}{H}\phi_\xi+(1+F)\cos\theta \qquad v=\phi_\eta-(1+F)\sin\theta$$

- **Crocco's Relation for the Rotation Function:**

$$\frac{\sin\theta}{H}F_\xi+F_\eta\cos\theta=\frac{\gamma}{u\left(1+\frac{\gamma-1}{2}M^2\right)}\left(\frac{M^2}{2}T_{o\eta}+\frac{T_\eta}{\gamma P_o}P_{o\eta}\right)$$

T_o = Stagnation temperature $\qquad$ P_o = Stagnation pressure

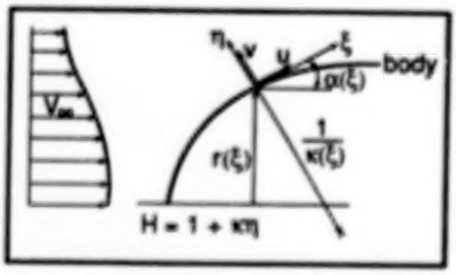

Figure 1

DESIGN FORMULATION

The analysis program is coupled with the CONMIN optimizer (ref. 4) to design an axisymmetric body for minimal wave drag. The constraints include a specified maximum thickness and a tail thickness. To reduce the number of design variables, the shape is represented by a modified Fourier series with its coefficients being the design variables (fig. 2).

- **Objective Function to be Minimized:**

$$OBJ = -0.1/(0.001 + C_{d_w})$$

- **Constraints:**

$$G(1) = 10(r_{max}/r_u - 1) < 0$$
$$G(2) = 10(1 - r_{max}/r_\ell) < 0$$
$$G(3) = r_{te}/r_u - 1 < 0$$
$$G(4) = 1 - r_{te}/r_\ell < 0$$

where r_u, r_ℓ, t_u, and t_ℓ are the specified upper and lower bounds of maximum thickness and the tail thickness, respectively

- **Body Shape Representation:**
  1. Rounded Nose and Tail

$$r = \frac{\ell}{2}\left\{\frac{A_{N+1}}{2}(\theta + \sin\theta) - \frac{A_{N+2}}{2}(\theta - \sin\theta) + \frac{A_1}{2}\left(\theta - \frac{\sin 2\theta}{2}\right) + \sum_{n=2}^{N} A_n\left[\frac{\sin(n-1)\theta}{n-1} - \frac{\sin(n+1)\theta}{n+1}\right]\right\}$$

  2. Rounded Nose only

$$r = \frac{\ell}{2}\left\{A_{N+1}\sin\theta\cos\frac{\theta}{2} + \sum_{n=2}^{N} A_n\cos(n-1)\theta\right\},\quad \theta = \cos^{-1}\left(\frac{2x}{\ell} - 1\right),\quad \ell = \text{body length}$$

Figure 2

DESIGN ALGORITHM

The design process is started by identifying the design variables from the input shape through a Fourier analysis. By perturbing the design variables (i.e., the Fourier coefficients) one at a time, gradients of the objective function and constraint equations can be calculated. To reduce the computing time, these gradient calculations are made with a small change in the design variables. Typically, the change (to be called the step size) is taken to be 0.1% ~ 0.5% of each design variable, but not less than 0.00035 ~ 0.0005. These gradients are all calculated with the same starting ϕ-values. These ϕ-values are updated if the design is feasible (fig. 3).

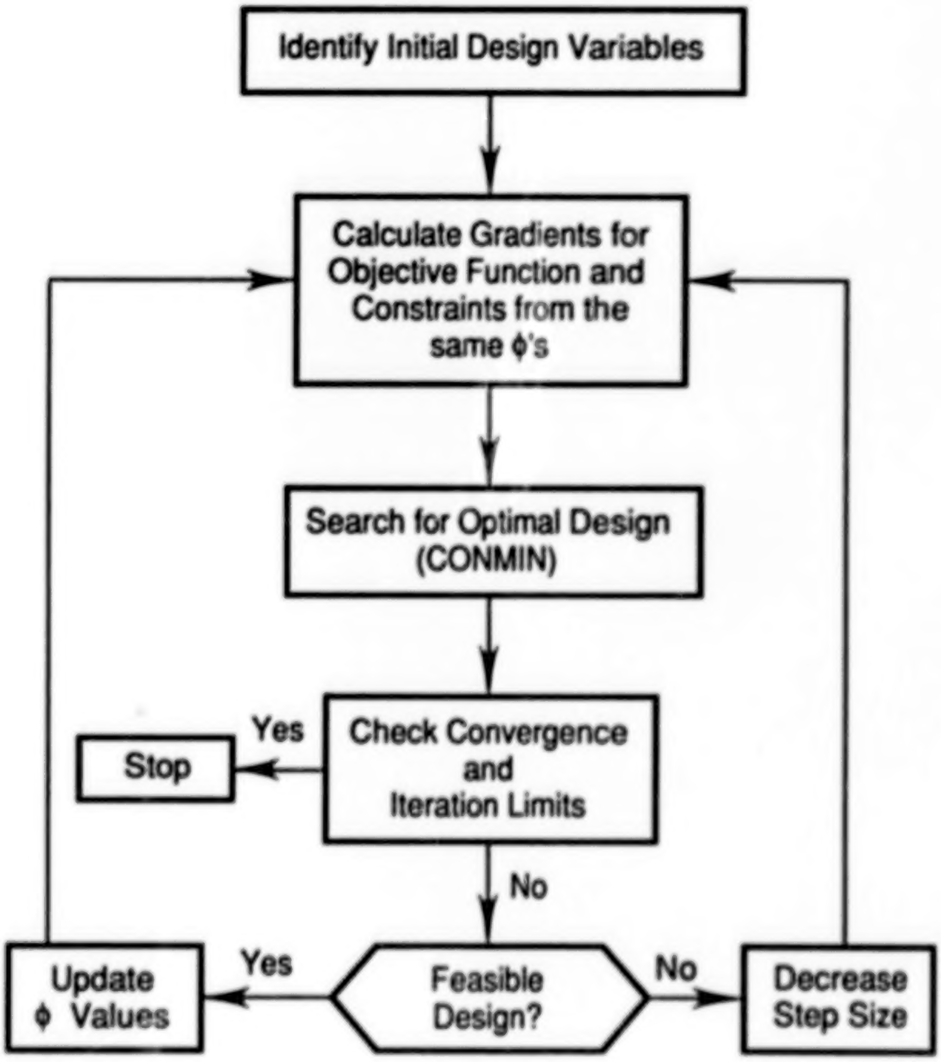
Identify Initial Design Variables
Calculate Gradients for Objective Function and Constraints from the same ϕ's
Search for Optimal Design (CONMIN)
Yes
Stop
Check Convergence and Iteration Limits
No
Yes
Update ϕ Values
Feasible Design?
No
Decrease Step Size

Figure 3

SUMMARY OF SOME OPERATIONAL EXPERIENCE

1. To reduce the computing time, an improved design was chosen by comparing all calculated results at the same numerical accuracy. That is, in analysis, convergence to a very small residual was not demanded. Instead, evaluation of all gradients was based on convergence to the same maximum residual. All starting values of the velocity function (ϕ) for gradient calculation were the same. The velocity function was updated only when the design has improved.

2. Typically, 2 to 3 iterations were performed in each run to allow manual adjustment in step size for gradient evaluation. If the design was not improved, the step size should be reduced. For this purpose, the solution was always saved in a file for possible re-use.

3. Since a smooth input shape was highly desirable, it was found advantageous to Fourier-analyze the input shape separately and then use the resulting Fourier coefficients, or modified values if desired, to generate a starting shape with more defining coordinate points.

4. All design exercises have been achieved with 81 x 81 grid points. Attempt with 41 x 41 grid points has not been successful.

DESIGN OF AN AXISYMMETRIC BODY WITH A FINENESS RATIO OF 8.33 IN A NONUNIFORM FLOW

The initial shape was assumed to be given by the NACA-0012 contour. Six design variables (A_n) were used. The tail thickness was constrained to be between 0 and 1%. The Mach number in the external flow was 0.98, and that over the body was 0.995. The results in figure 4 indicated that reducing the nose radius and increasing the thickness in the aft portion would reduce the wave drag (c_{d_w}) by 29%.

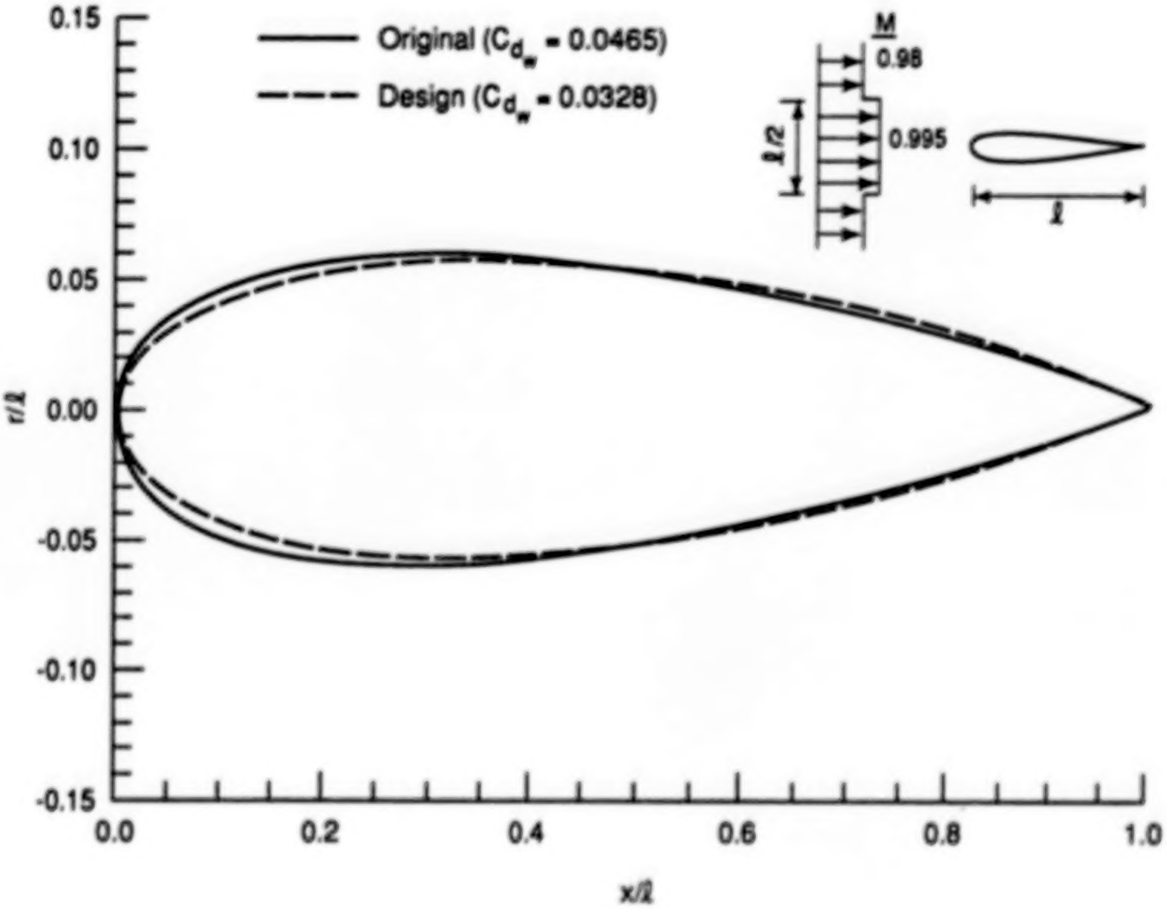

Figure 4

DESIGN OF AN AXISYMMETRIC BODY WITH A FINENESS RATIO OF 5.0 IN A TRANSONIC UNIFORM FLOW

The initial shape was generated from the NACA-0020 contour. The freestream Mach number was 0.925. The step size used in gradient evaluation was 0.1% of the design variables with a minimum change of 0.0005. The results in figure 5 showed that to reduce the wave drag, the pressure peak in the nose region must be reduced. As a result, the shock strength could also be decreased. A reduction in wave drag by 41% was achieved.

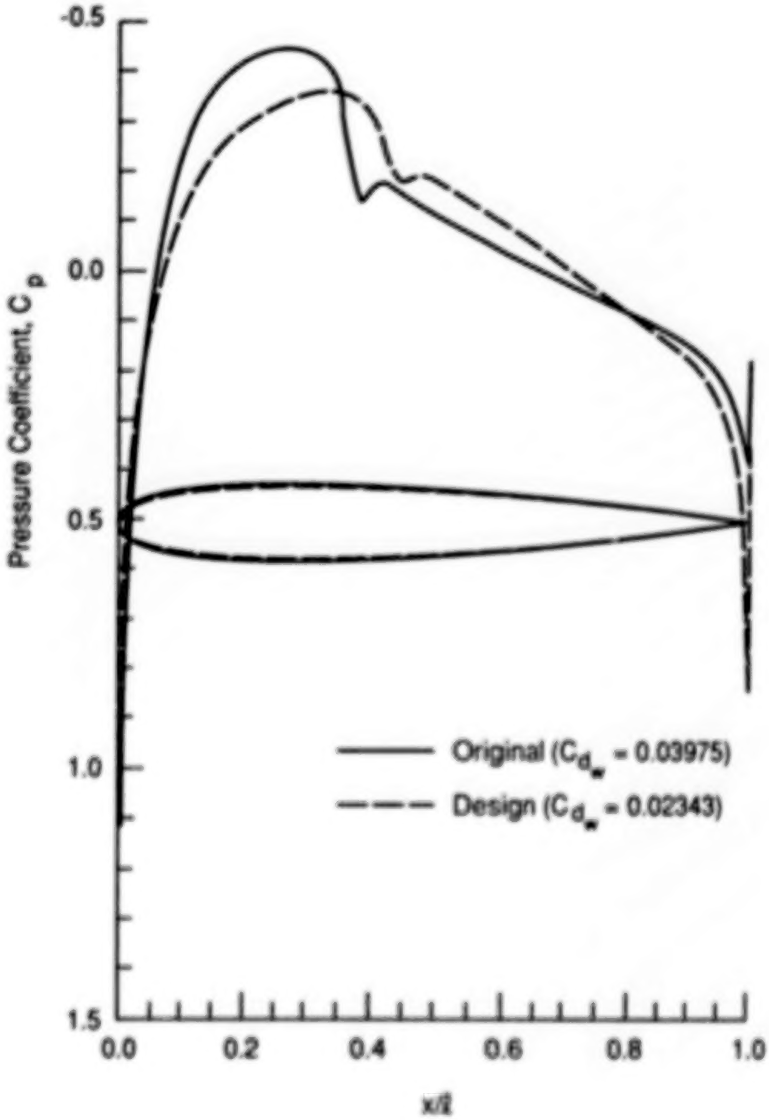

Figure 5

DESIGN OF AN AXISYMMETRIC BODY WITH A FINENESS RATIO OF 5.0 IN A TRANSONIC UNIFORM FLOW

The final body shape given in figure 6 indicated, again, that to reduce the wave drag, the nose radius should be reduced and the maximum thickness location moved aft. Further improvement could be made only if a larger tail thickness was allowed.

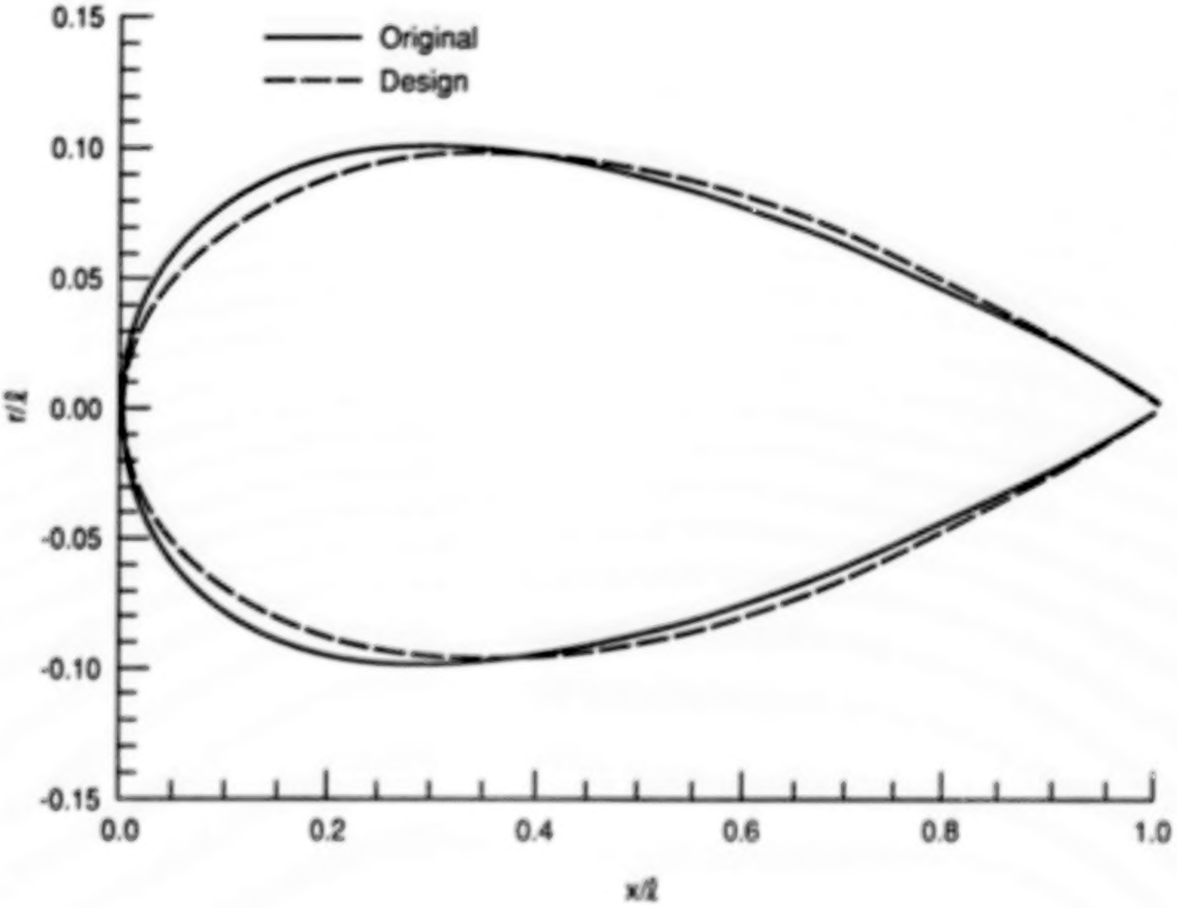

Figure 6

DESIGN OF AN AXISYMMETRIC BODY WITH A FINENESS RATIO OF 5.0 IN A TRANSONIC NONUNIFORM FLOW

The initial shape was again generated with the NACA-0020 contour. The freestream Mach number varied from 0.90 away from the body and a 0.95 near the body, with an average of 0.925. The step sizes in gradient evaluation used ranged from 0.1% at the beginning to 1%. The final value used was 0.5%. It was found that if the step size was greater than 0.5%, little improvement could be made. The results in Figure 7 showed that the change in shape successfully reduced the shock strength. The wave drag was reduced by 65%. A larger drag reduction was possible in this case perhaps because the external Mach number was lower than that in figure 5.

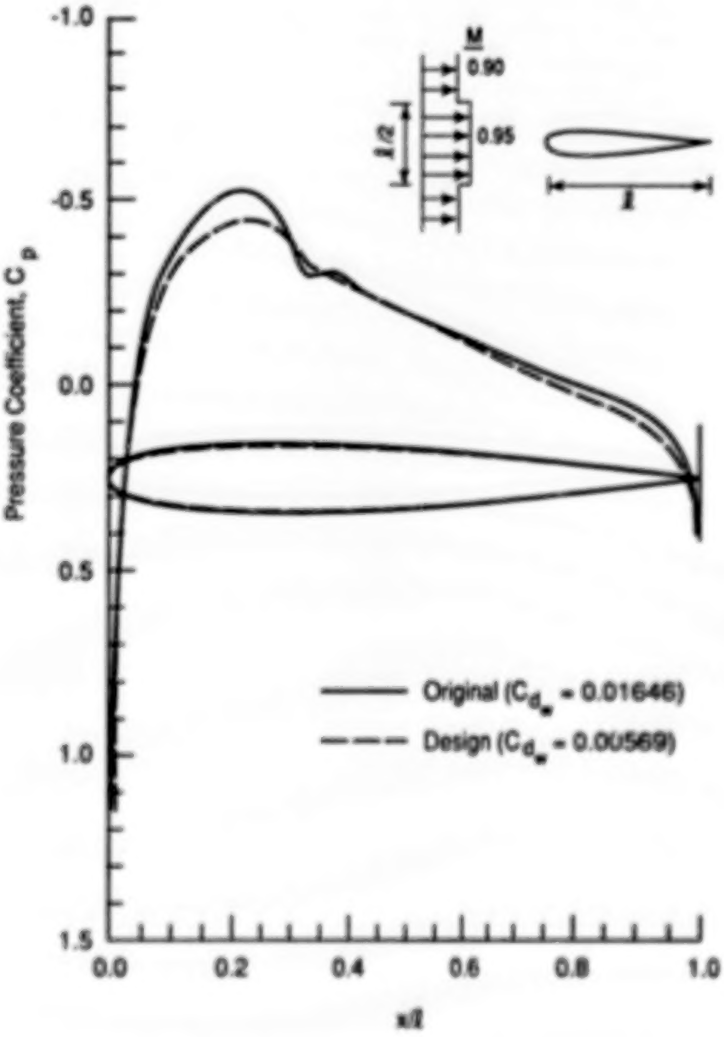

Figure 7

DESIGN OF AN AXISYMMETRIC BODY WITH A FINENESS RATIO OF 5.0 IN A TRANSONIC NONUNIFORM FLOW

Again, a favorable shape was one with a reduced nose radius and a thicker aft portion as shown in figure 8. Further change was difficult because of the constraints of maximum thickness and tail radius.

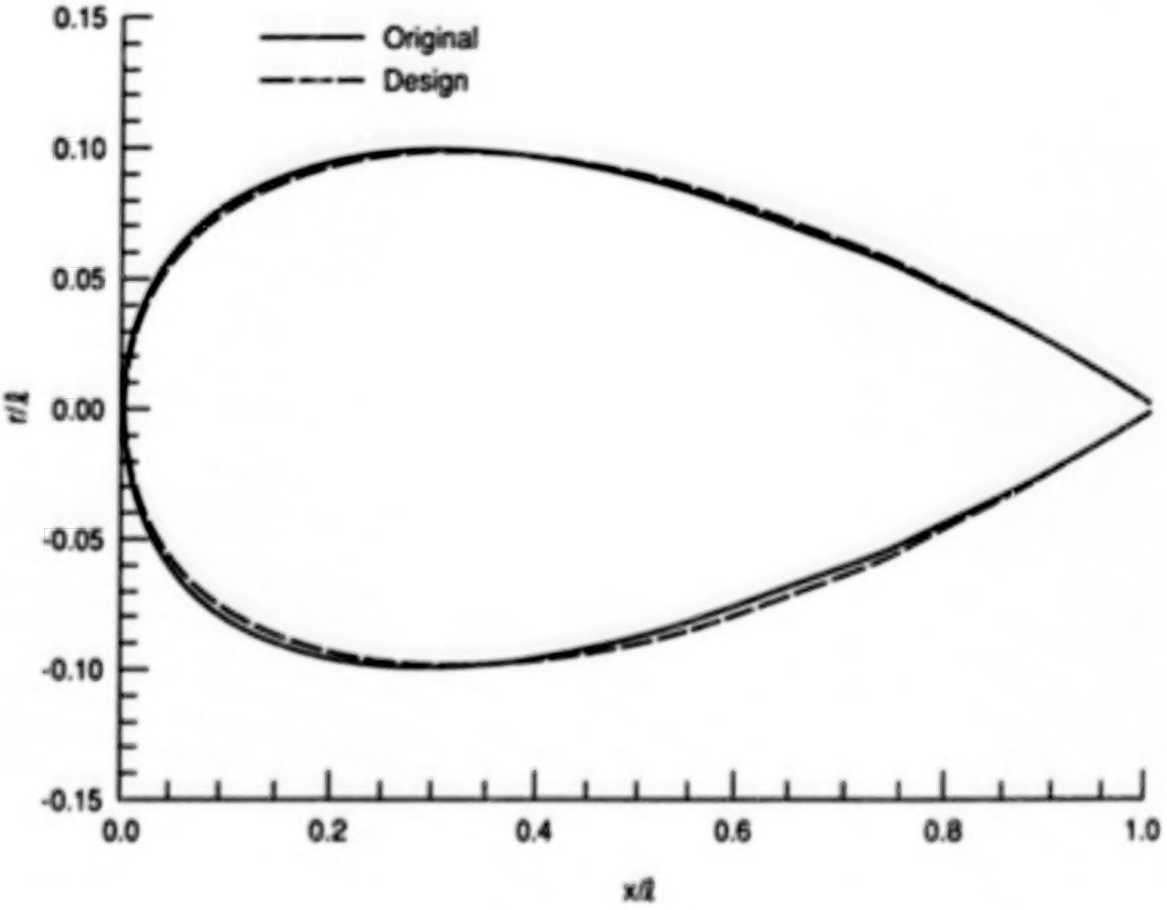

Figure 8

CONCLUSIONS

An inviscid transonic code capable of designing an axisymmetric body in a uniform or nonuniform flow was developed. The design was achieved by direct optimization by coupling an analysis code with an optimizer.

Design examples were provided for axisymmetric bodies with fineness ratios of 8.33 and 5 at different Mach numbers. It was shown that by reducing the nose radius and increasing the afterbody thickness of initial shapes obtained from symmetric NACA four-digit airfoil contours, wave drag could be reduced by 29% for a body of fineness ratio 8.33 in a nonuniform transonic flow of M = 0.98 to 0.995. The reduction was 41% for a body of fineness ratio 5 in a uniform transonic flow of M = 0.925 and 65% for the same body but in a nonuniform transonic flow of M = 0.90 to 0.95.

REFERENCES

1. Chang, J. F.; and Lan, C. E.: Transonic Airfoil Analysis and Design in Nonuniform Flow. NASA CR-3991, June 1986.

2. Chang, J. F.; and Lan, C. E.: Transonic Analysis and Design of Axisymmetric Bodies in Nonuniform Flow. NASA CR-4101, November 1987.

3. Keller, J. D.; and South, J. C.: RAXBOD: A Fortran Program for Inviscid Transonic Flow over Axisymmetric Bodies. NASA TMX-72831, February 1976.

4. Vanderplaats, G. N.: CONMIN--A Fortran Program for Constrained Function Optimization. NASA TMX-62282, August 1973.

PROCEDURES FOR SHAPE OPTIMIZATION OF GAS TURBINE DISKS

Tsu-Chien Cheu
Textron Lycoming
Stratford, Connecticut

46

ABSTRACT

Two procedures, the feasible direction method and sequential linear programming, for shape optimization of gas turbine disks are presented in this paper. The objective of these procedures is to obtain optimal designs of turbine disks with geometric and stress constraints. The coordinates of the selected points on the disk contours are used as the design variables. Structural weight, stress and their derivatives with respect to the design variables are calculated by an efficient finite-element method for design sensitivity analysis. Numerical examples of the optimal designs of a disk subjected to thermo-mechanical loadings are presented to illustrate and compare the effectiveness of these two procedures.

1. INTRODUCTION

The problem of how to efficiently minimize the weight of a gas turbine engine disk while satisfying the stress design requirement and keeping the disk size within a prescribed geometric envelope is an important topic in the gas turbine industry. A stress function in common use is the Von Mises stress. Therefore, a requirement can be to limit the value of the von Mises stress anywhere on the disk to a prescribed value.

This task becomes one of shape optimization of an axisymmetric structure with the objective of minimizing the weight while meeting the geometric and the stress constraints. Each of the procedures involved requires a solver and an optimizer. The solver provides weight, stress and their derivatives with respect to the design variables. An optimizer must be selected which can effectively utilize the solver.

It has been shown that the weight and stress gradients can be obtained directly from a finite-element program [1-5]. In this paper, two optimization procedures which can effectively utilize the weight and stress gradients are proposed for disk shape optimization. These two methods are the feasible direction method [6] and sequential linear programming [1,4,7].

In structural optimization, design variables may be finite-element nodal coordinates, element thickness, etc. The derivatives of the objective function and the constraint functions with respect to the design variables provide the variational trends of the structures for optimization. Calculation of these derivatives is known as design sensitivity analysis.

In this paper, an efficient method is used for design sensitivity analysis [5]. The technique of isoparametric mapping is used to generate a finite-element mesh from a small set of master nodes. In order to assure that a general boundary shape can be achieved for the optimal design of a complex structural shape, selected coordinates of the master nodes are used as the design variables. These variables are permitted to change within a specified design envelope.

67

The formulations and computational results of these two optimization procedures are presented in the following sections.

2. FORMULATION

2.1 PROBLEM STATEMENT

The general statement of the problem to be dealt with in this paper is to minimize an objective function

$$F = f(A) \tag{1}$$

while satisfying the constraints

$$g_j(A) \leq 0 \qquad j = 1,\ldots,M \tag{2}$$

where the N dimensional hyperspace design point, A, is a vector of design variables initially lying in the feasible region with side constraints

$$a_i^l \leq a_i \leq a_i^u \qquad i = 1,\ldots,N \tag{3}$$

In this paper, the objective function is W, the structural weight, the constraint functions are the structural response such as σ, the stress, and the design variables are the coordinates of the selected points on the structural contours with upper and lower constraints a_i^u and a_i^l.

2.2 FEASIBLE DIRECTION METHOD

The feasible direction method efficiently uses weight and constraint gradients. This method requires two operational phases. The first one is the steepest decent phase (SD) which requires only the weight gradients, the second one is a linear programming phase (LP) which requires both the weight and constraint gradients.

Starting with a feasible design point, A^0, a better point

$$A = A^0 + \alpha S \tag{4}$$

can be achieved by moving A^0 in the feasible region a distance of α in the direction S.

The feasible region is bounded by the constraint limits with the constraint margins, e_j, as shown in Figure 1. The boundary zones which are thus formed by the hypersurfaces parallel to the constraint limit hypersurfaces are known as the LP region. The rest of the feasible space is known as the SD region. The design points within either regions are the feasible design points.

48

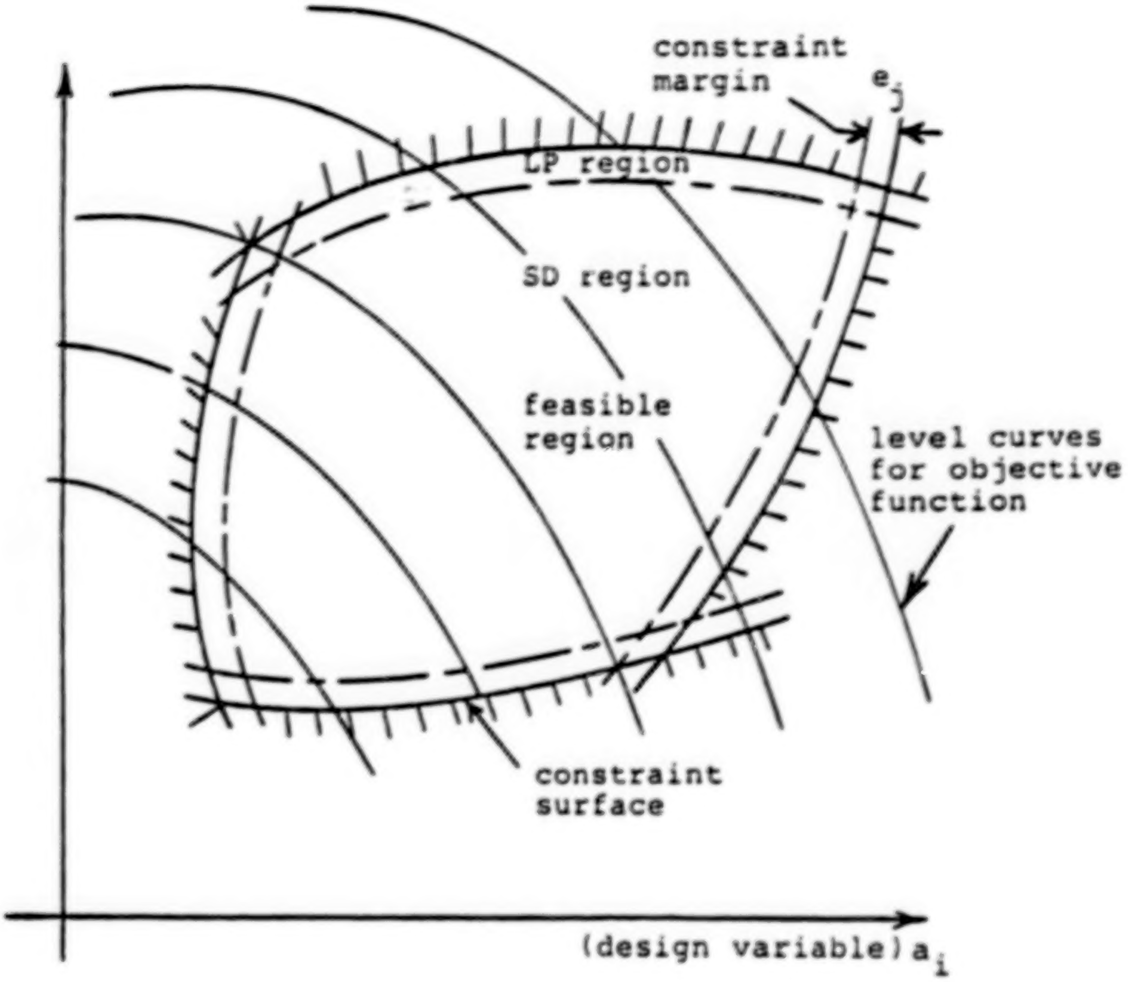
constraint
margin
e_j
LP region
SD region
feasible
region
level curves
for objective
function
constraint
surface
(design variable) a_i

Figure 1. Design space for feasible direction method.

In the SD region S is the negative of the weight gradients, while in the LP region S is calculated by a linear programming procedure, [8], with the formulations

$$S^T \nabla g_j(A) + \theta_j \beta \leq \sum_i \frac{\partial g_j}{\partial a_i} \qquad j = 1,\ldots,M \tag{5}$$

$$S^T \nabla f(A) + \beta \leq \sum_i \frac{\partial f}{\partial a_i} \tag{6}$$

and side constraints on directions are

$$s_i \leq 2 \qquad i = 1,\ldots,N \tag{7}$$

$$s_i \geq 0 \qquad i = 1,\ldots,N \tag{8}$$

where θ_j are the pushoff factors and β is the objective function.

After a feasible direction to proceed is found, the distance to travel in that direction is calculated by using a Powell's univariate search. The minimum distance to be traveled is 0. The maximum distance is taken to be the maximum of all the permissible variation of each design variable in the feasible region. The actual distance will occur at any point along the line between 0 and the maximum distance point.

Before engaging in Powell's search, the finite-element method is used to check if a negative determinant of Jacobi transformation matrix occurs at any Gauss integration point [9]. If a design point yields a negative value, then the design point is moved back along the line by a specified fraction. If a negative value still results, the process is repeated until a positive value occurs. This positive value is taken as the maximum distance for a Powell's univariate search. If the new design point is in the feasible region, a new direction and univariate search will be made again for the next iteration. If this new point is in the infeasible region, then an interpolation scheme is used to bring the design point back into the feasible region [6]. If the geometric constraints are violated, a linear interpolation routine is used. If the stress constraint is violated, a quadratic interpolation procedure is used.

After a new feasible design point is found, the process is repeated until the convergence criteria are satisfied.

2.3 SEQUENTIAL LINEAR PROGRAMMING

The sequential linear programming procedure linearizes the nonlinear objective and constraint functions within a specified range where the linear programming procedure will be applied repeatedly. This method efficiently utilizes the gradients of the objective and the constraint functions and has been shown to be reliable in many different applications.

The structural weight and responses generally are nonlinear functions of the design variables. Using a first order Taylor series expansion centered at the current design, these functions can be approximated by

$$W = W^o + \sum_i \frac{\partial W}{\partial a_i}(a_i - a_i^o) \tag{9}$$

$$\sigma = \sigma^o + \sum_i \frac{\partial \sigma}{\partial a_i}(a_i - a_i^o) \tag{10}$$

where the superscript o denotes the current design.

These equations are used to form a linear programming problem

$$-\sum_i \frac{\partial W}{\partial a_i} a_i = C = W^o - W - \sum_i \frac{\partial W}{\partial a_i} a_i^o \tag{11}$$

$$\sum_i \frac{\partial \sigma}{\partial a_i} a_i \leq \sigma_d - \sigma^o + \sum_i \frac{\partial \sigma}{\partial a_i} a_i^o \tag{12}$$

and the side constraints on design variables

$$a_i \leq a_i^o(1+\Delta) \tag{13}$$

$$-a_i \leq -a_i^o(1-\Delta) \tag{14}$$

where

$$\Delta = \text{Max}\,(\Delta_{min}, \Delta_c)$$

$$\Delta_i = \text{Min}\,\left(\left| \frac{\sigma_d - \sigma^o}{\frac{\partial \sigma}{\partial a_i}} \right| ,\ \Delta_{max} \right)$$

$\Delta_c = \text{Max}\,(\Delta_i)$ for the beginning of each LP iteration

$\Delta_c = r \cdot \Delta$ for the subsequent LP iteration

and r is the step size reduction factor.

The linear programming problem is solved by a revised simplex method [8]. After a new design is found, the process is repeated until the convergence criteria are satisfied.

3. Numerical Examples

Shape optimization of an actual gas turbine disk subjected to thermo-mechanical loadings is used as an illustration. The flow chart of the design optimization process is shown in Figure 2.

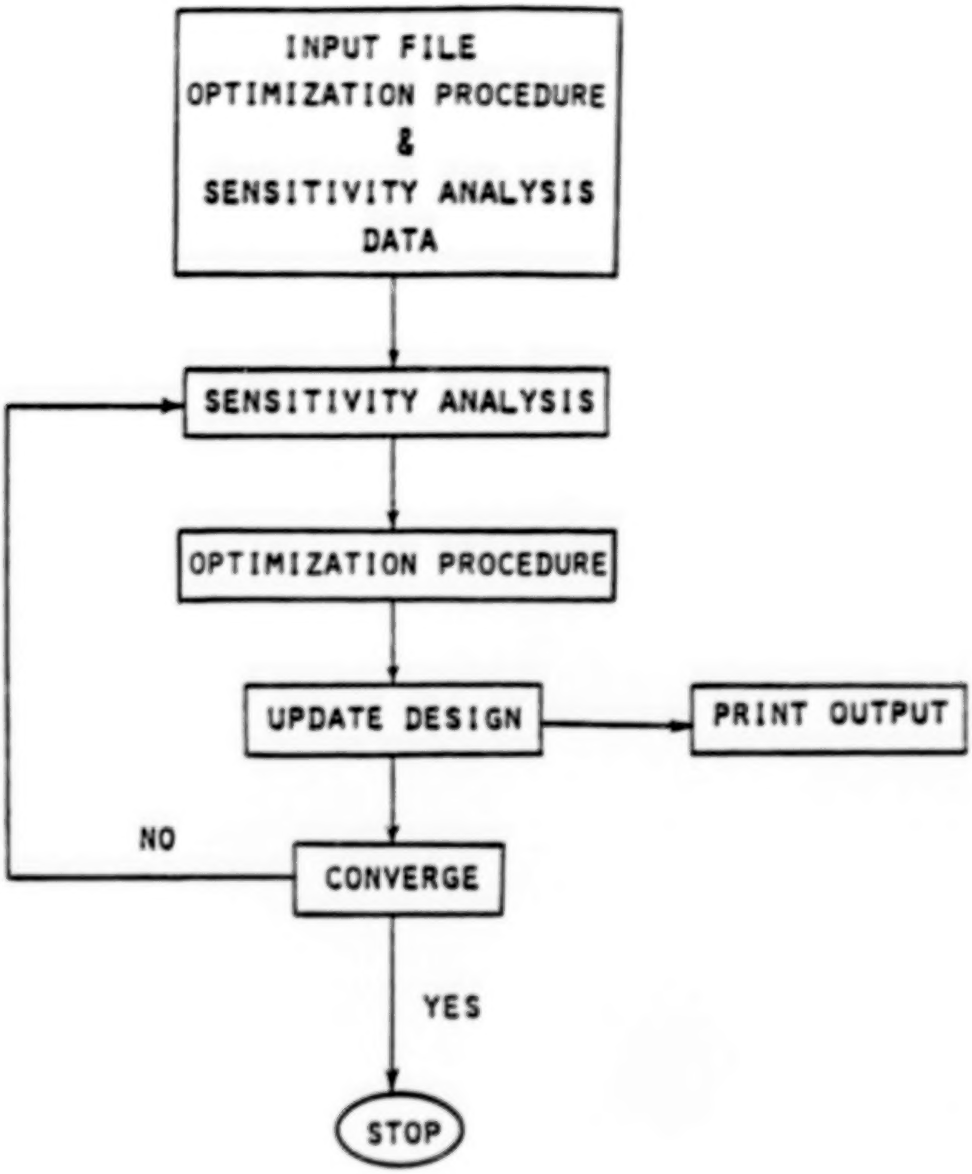
INPUT FILE
OPTIMIZATION PROCEDURE
&
SENSITIVITY ANALYSIS
DATA
SENSITIVITY ANALYSIS
OPTIMIZATION PROCEDURE
UPDATE DESIGN
PRINT OUTPUT
NO
CONVERGE
YES
STOP

Figure 2. Disk design optimization system flow chart

72

The master finite-element mesh and the generated finite-element mesh are shown in Figures 3a and 3b. Seventy master nodes are used to form 38 4-noded linear master elements for the disk. Both radial and axial coordinates of master nodes numbered from 1 through 30 are used as design variables. The finite-element mesh generated from the master finite-element mesh has 130 8-noded quadratic elements and 469 nodes.

This disk has a uniform initial temperature of 70° F. The radial coordinates at the hub and the tip of the disk are 0.8 inch and 4.85 inches, respectively. The operating temperatures of the disk are set arbitrarily to vary linearly from 80° F at the hub to 485° F at the tip.

The disk rotates at a constant speed of 22,000 rpm. It has a distributed load of 24,000 psi acting radially outward on the tip circumferential surface. Axial coordinates of the points on side A-B are fixed as boundary conditions. The yield stress of the disk is specified at 125,000 psi. The maximum Von Mises stress is used as the stress design criterion.

Feasible direction method and sequential linear programming are used in the first and the second examples, respectively. The computer software developed was executed on the IBM 3090 using a VS 2.2 compiler. The optimization procedures are considered to have converged if the change of the structural weight is less than 0.1% for the two successive iterations. The computational results are listed in Tables 1 and 2.

In the first example, the feasible direction method is used. Convergence is achieved in 8 iterations with 216 CPU seconds of computational time. The total weight is reduced from 18.0 pounds to 13.978 pounds. The maximum Von Mises stress is increased from 91,914 psi to 124,668 psi.

In the second example, the sequential linear programming is used. Convergence is achieved in 9 iterations with 369 CPU seconds of computational time. The total weight is reduced from 18.0 pounds to 13.873 pounds. The maximum Von Mises stress is increased from 91,914 psi to 124,999 psi.

The optimal designs of both examples satisfy the stress design criterion. However, slightly different weight reductions, 22.35% and 22.93%, respectively, are achieved for the first and the second examples. For the same convergence criterion the first example requires about 40% less computational time than the second example. However, for the same percentage of weight reduction both methods require about the same computational time.

The shapes of the optimal designs of the two examples are almost identical. The shape of the optimal design obtained with the sequential linear programming is shown in Figure 4.

The computational results indicate that by using the procedures developed, shape optimization of gas turbine disks with complicated

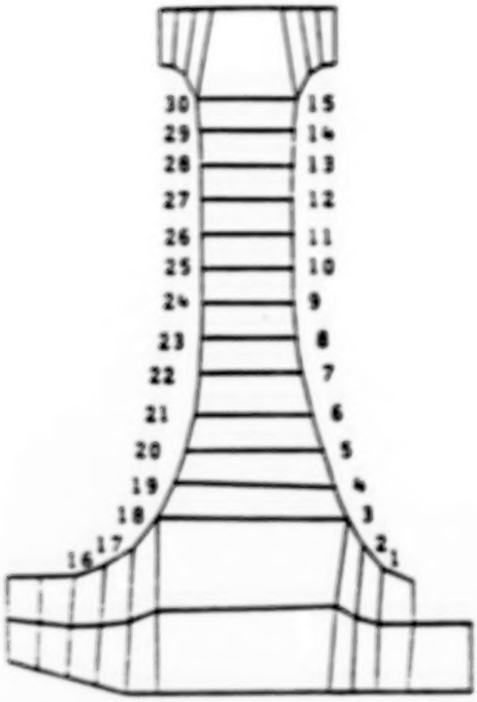
30
29
28
27
26
25
24
23
22
21
20
19
18
17
16
15
14
13
12
11
10
9
8
7
6
5
4
3
2
1

Figure 3a. Master finite-element model for the initial disk design

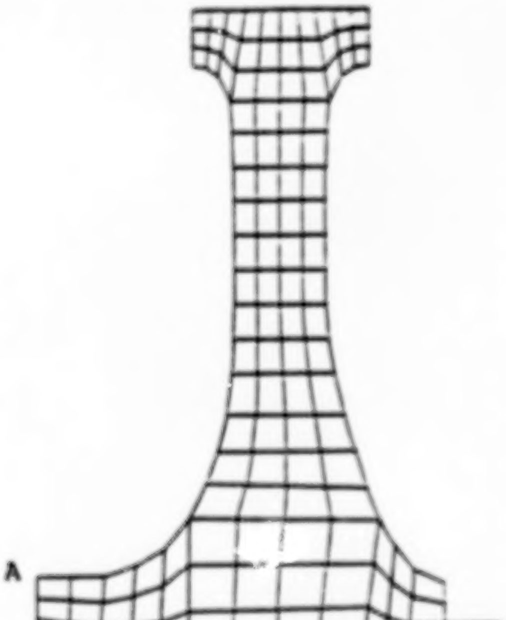

Figure 3b. Generated finite-element model for the initial disk design

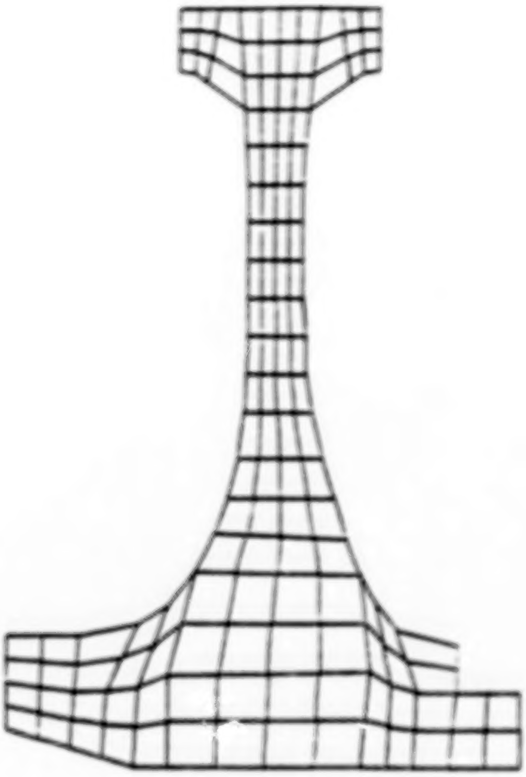

Figure 4. Optimal disk design

Table 1. Computation results for example 1.

Iteration No.	Iteration Type	Max. Von Mises Stress (psi)	Weight lb	Successive Reduction (%)	Total Reduction (%)
0	Original	91914	18.000		
1	SD	91478	16.943	5.869	5.869
2	SD	97185	15.872	6.322	11.820
3	SD	110374	14.784	6.856	17.865
4	SD	116609	14.350	2.937	20.278
5	SD	122822	14.027	2.249	22.071
6	LP	123243	14.000	0.195	22.223
7	LP	124921	13.979	0.149	22.339
8	LP	124688	13.978	0.008	22.345

Table 2. Computation results for example 2.

Iteration No.	Max. Von Mises Stress (psi)	Weight lb	Successive Reduction (%)	Total Reduction (%)
0	91914	18.000		
1	110802	15.012	16.602	16.602
2	121876	14.287	4.824	20.625
3	124964	13.918	2.586	22.678
4	124755	13.896	0.161	22.802
5	124989	13.884	0.086	22.868
6	124994	13.878	0.042	22.901
7	124997	13.875	0.020	22.916
8	124999	13.874	0.011	22.924
9	124999	13.873	0.006	22.929

contour shapes and loading conditions can be achieved with relatively short computational time.

REFERENCES

1. Zienkiewicz, O.C.; and Campbell, J.S.: 'Shape Optimization and Sequential Linear Programming', Optimum Structural Design (Edited by Gallagher R.H. and Zienkiewicz O.C.), Wiley, New York, 1973

2. Ramakrishnan, C.V.; and Francavilla, A.: 'Structural Shape Optimization Using Penalty Functions', J. Struc. Mech., 3(4), pp. 403-422, 1974-75.

3. Botkin, M.E.: 'Shape Optimization of Plate and Shell Structures', AIAA J., Vol. 20, pp. 268-273, 1981.

4. Wang, S.Y.; Sun, Y.; and Gallagher, R.H.: 'Sensitivity Analysis in Shape Optimization of Continuum Structures', Comp. Struc., Vol. 20, pp. 855-867, 1985.

5. Cheu, T.C.: 'Sensitivity Analysis and Shape Optimization of Axisymmetric Structures', Vol. 28, pp. 95-108, January 1989.

6. Fox, R.L.: Optimization Methods for Engineering Design, Addison-Wesley, London, 1970.

76

BEST COPY AVAILABLE

7. Pederson, P.: 'The Integrated Approach of FEM-SLP for Solving Problems of Optimal Designs', Optimization of Distributed Parameter Structures, (Edited by Hang and Cea) Sijthoff and Nourdhoff, pp. 757-780, 1981.

8. Hanson, R.J.; and Wisniewski, J.A.: 'A Revised Simplex Code for LP Problems Using Orthogonal Decomposition - A User's Guide', Sandia Lab. Report Sand 78-2322, 1979.

9. Zienkiewicz, O.C.: The Finite Element Method, 3rd edition, McGraw-Hill, New York, 1977.

SESSION 11: ENGINEERING SYSTEM DESIGN

Chairmen: M. D. German and D. P. Schrage

BLANK PAGE

A DECISION-BASED PERSPECTIVE
for the
DESIGN OF METHODS
for
SYSTEMS DESIGN

Farrokh Mistree and Douglas Muster
Systems Design Laboratory
Department of Mechanical Engineering
University of Houston
Houston, Texas

Jon A. Shupe
BF Goodrich Company R&D Center
9221 Brecksville Road
Brecksville, Ohio 44141

Janet K. Allen
Janco Research
4501 University Oaks Boulevard
Houston, Texas 77004

MOTIVATION

By system definition we mean the establishment of a construct which characterizes the needs and requirements of a system for a particular application. The importance of system definition and concept design in the development of new, major engineering systems cannot be overemphasized. A popular representation that has been used to illustrate this importance with respect to life cycle cost is reproduced below. As can be seen design freedom or management leverage rapidly decreases once a project is underway. In other words, the freedom to make modifications to a concept becomes increasingly expensive as one gets further into the project. In effect, a significant amount of the life cycle costs have been committed at the time when relatively little knowledge about the object of design has been generated. Usually, this occurs by the end of the conceptual and preliminary design phases.

We believe that the design research community --- the theorists, the academics and engineers in industry --- must all contribute to the common goal of striving to develop a recognized science of design. In an ultimate sense, the purpose of developing the science of design is to ensure that our manufacturing industries can become more effective as well as efficient and that the designers, manufacturers and maintainers of our products will be working in an environment where their subdisciplines are considered simply as parts of the continuous technological spectrum which spans what we have come to call life cycle engineering.

Our recent work and research interests suggest that there is a viewpoint of design research - three-faceted and tightly organized within itself - which should be considered. The issues we include in our view of design research do not exist separately but as a single interactive entity. They are

1 Meta-design - the way in which we define and partition a problem using generic discipline-independent modeling techniques.
2 Computer-based design supports holistic or systems thinking.
3 Adaptive Action Learning - a way of learning through doing.

We believe this tripartite view of design research is unique and is essentially congruent with the principal elements required to establish the philosophy and practice of the science of design which, when accepted and used in industry and academe, will ensure the continued growth and improved productivity of our industries.

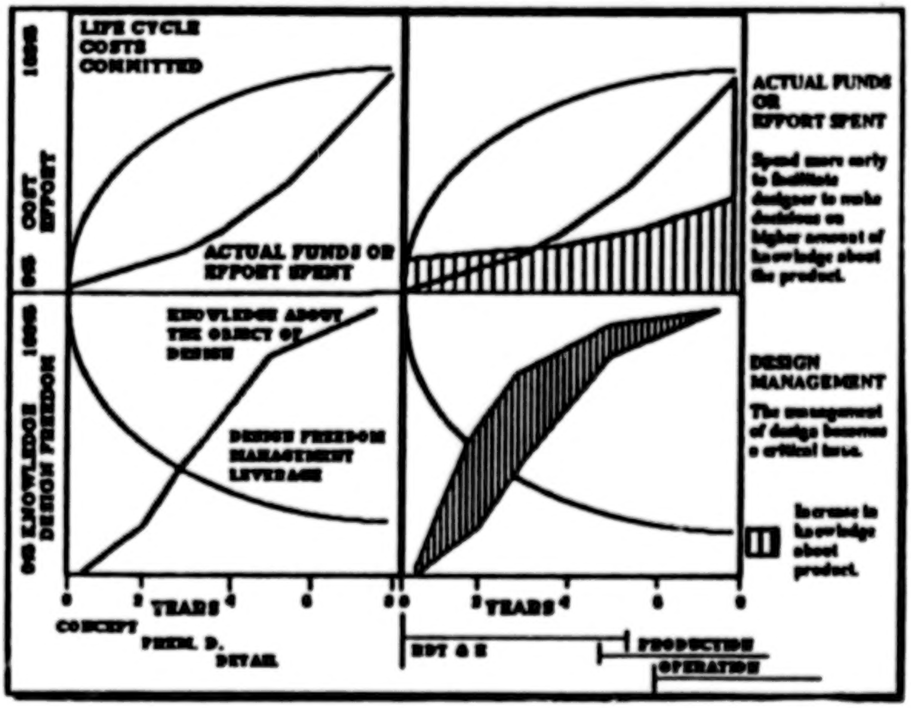

ORGANIZATION OF MATERIAL

"Everyone designs who devises courses of action aimed at changing existing situations into preferred ones." Simon [1, p 129].

The preceding definition is not discipline specific. It can be used as the basis for categorizing the activities of groups of individuals in other science-based disciplines than engineering, for example, management science, systems science, economics and the social and behavioral sciences. The members of the groups are designers in the context of Simon's definition. They design artifacts and machines (engineers), industrial organizations (managers), including their communication and information networks (behavioral scientists and experts in information science) and accounting information systems (accountants, managers and experts in information science). We subscribe to Simon's definition of a designer. In this paper our comments are directed principally towards engineering design, but are not limited to it. The organization of the material is given below.

DEFINITIONS

- **Decision-Based Design**
- **Heterarchy and Hierarchy**
- **System**

THE DECISION SUPPORT PROBLEM TECHNIQUE: CONCEPTUAL MODELS

- **Short Term Goal: Design that can be Produced and Maintained**
- **Long Term Goal: Design, Manufacture and Maintenance as a Continuous Process**

DECISION-BASED DESIGN

- **Meta-Design, Computer-Based Design and Adaptive Action Learning**
- **The Characteristics of Decisions**
- **Decision Activities to Decision Entities**
- **Types of Design**

THE DECISION SUPPORT PROBLEM TECHNIQUE: STATUS

- **Designing for Concept and Designing for Manufacture**
- **Designing for Concept: A Scenario**
- **Status: Software, Decision Hierarchies and Applications**

ISSUES THAT NEED TO BE CONSIDERED TO FOSTER DEVELOPMENT

DECISION-BASED DESIGN

Decision-Based Design [2,3] is a term we have introduced to provide a new focus from which design methods can be developed. In the context of Decision-Based Design, we assert that the principal role of an engineer is to make decisions associated with the design of an artifact. This seemingly limited role ascribed to engineers is useful to provide a starting point for developing design methods based on paradigms that spring from the perspective of decisions made by designers (who may use computers) as opposed to design that is assisted by or based on the use of computers, optimization methods (computer-aided design optimization) or methods that evolve from specific analysis tools such as finite element analysis. In other words, we do not consider Decision-Based Design as a subset or superset of Computer-Aided Design or Computer-Based Design. We see it in another role. Many design approaches were developed originally for purposes and uses now considered outmoded. Their continued use by designers is contingent largely upon custom, tradition and familiarity, and the innate conservatism of most engineers. Enter Decision-Based Design; considering design as a decision-based process offers designers a new and different perspective for viewing established approaches and provides them with the basis for extending and developing anew these established tools of the trade.

The implementation of DBD can take many forms. One implementation of Decision-Based Design is the Decision Support Problem Technique [4,5].

- **A new term - to provide a new focus from which to develop methods that support**
  - **systems thinking, and**
  - **the making of decisions by designers of engineering systems.**

- **Principal role of engineer in DBD is to make decisions associated with the design of an artifact.**

- **Starting point for developing design methods based on paradigms that spring from the perspective of decisions made by designers (with or without computers).**

- **DBD has as its content a heterarchical set of constructs that embody a researcher's perception of the design environment and the real world.**
  - **definition of "system"**
  - **types of design: original, adaptive and variant**
  - **open and closed environments**
  - **the nature of decisions and the type of decision activities.**

- **There is NO SINGLE unique TECHNIQUE or METHOD for the implementation of DBD. The development of a major class of design technique or method will be a result of a researcher selecting a subset of constructs and establishing a hierarchy between them.**

DECISION-BASED DESIGN: DEFINITION

We define Decision-Based Design as a heterarchical set of constructs that embody a developer's perceptions of the design environment and the real world.

The heterarchical constructs associated with a product's life-cycle are the product's market, the product (the design must meet or exceed the criteria related to the product's function, meeting its market, its capability for being manufactured in serial and, when it reaches its market, that it be free of unreasonable dangers), its manufacture (tooling and assembly), its maintenance and its subsequent retirement. A portion of the heterarchical set of constructs for a product's life-cycle are shown below. The relationships between the constructs are not ordered and hence not directed.

DECISION-BASED DESIGN is a heterarchical set of constructs that embody a designer's perception of the real world.

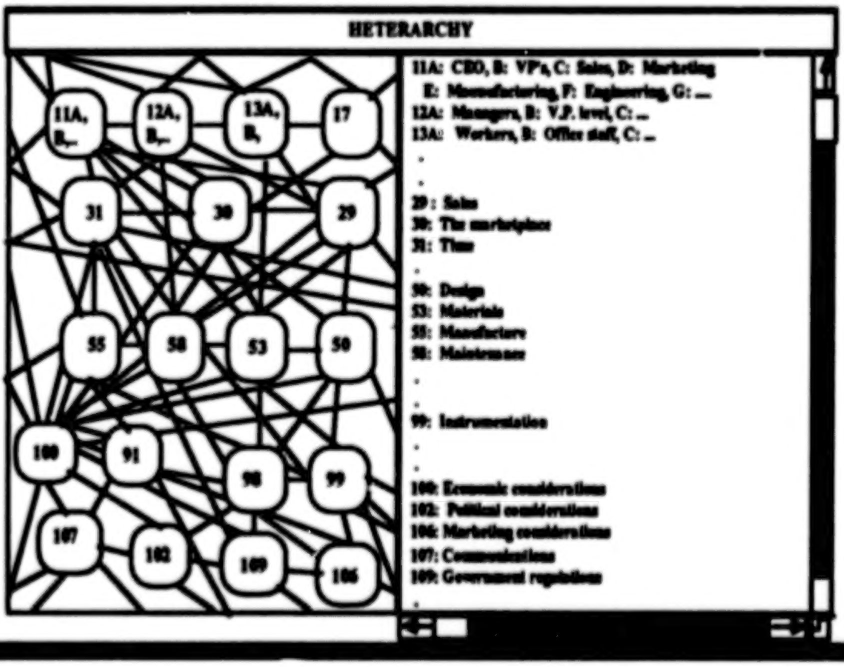

11A: CEO, B: VP's, C: Sales, D: Marketing
E: Manufacturing, F: Engineering, G: ...
12A: Managers, B: V.P. level, C: ...
13A: Workers, B: Office staff, C: ...
.
.
29: Sales
30: The marketplace
31: Time
.
50: Design
53: Materials
55: Manufacture
58: Maintenance
.
.
99: Instrumentation
.
.
100: Economic considerations
102: Political considerations
106: Marketing considerations
107: Communications
109: Government regulations
.

DECISION-BASED DESIGN: HIERARCHY

Different hierarchies can result from the same heterarchy. A heterarchy is transformed into a hierarchy once the **goal** for the transformation is identified and the subsystems that can contribute to the achievement of the goals are selected and placed in the hierarchy.

HIERARCHY OF CONSTRUCTS FOR THE DEVELOPMENT OF TECHNIQUES AND METHODS IN DECISION-BASED DESIGN: AN EXAMPLE

ASSERTION:

The development of a major class of design method will be the result of a researcher selecting a subset of constructs from a HETERARCHY and establishing a HIERARCHY.

GOAL

DESIGN,
MANUFACTURE
AND
MAINTENANCE
AS A
UNIFIED
AND
CONTINUOUS PROCESS

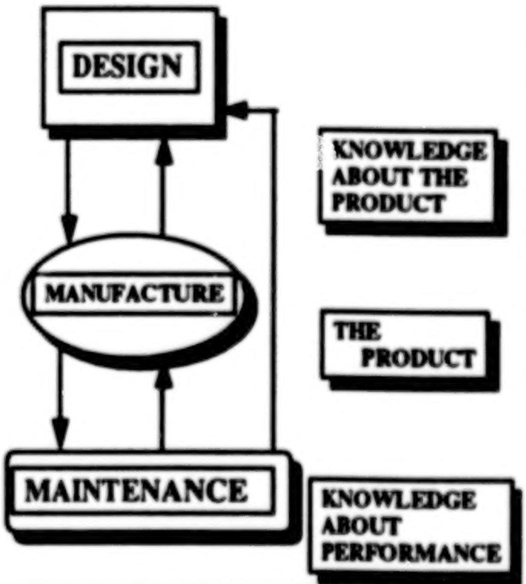

DESIGN

MANUFACTURE

MAINTENANCE

KNOWLEDGE ABOUT THE PRODUCT

THE PRODUCT

KNOWLEDGE ABOUT PERFORMANCE

THE DECISION SUPPORT PROBLEM TECHNIQUE: GOALS AND REPRESENTATION

The implementation of Decision-Based Design can take many forms. A comprehensive approach called the Decision Support Problem Technique [3,4,5] is being developed and implemented at the University of Houston to provide support for human judgment.

Different hierarchies can result from the same heterarchy. A heterarchy is transformed into a hierarchy once the goal for the transformation is identified. In the long term our goal is to unify the processes of design, manufacture and maintenance.

In the short term our goal, for the UH Decision Support Problem Technique, is to develop processes and tools to support the making of decisions associated with the design of an artifact that can be produced and maintained. In the long term we would like to develop the capability to design, manufacture and maintain as a unified continuous process. Note that the representations for the two cases are different.

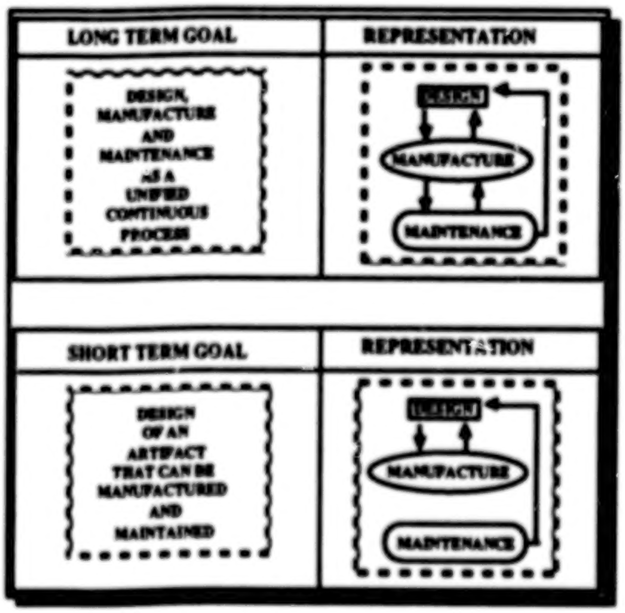
LONG TERM GOAL
REPRESENTATION
DESIGN, MANUFACTURE AND MAINTENANCE AS A UNIFIED CONTINUOUS PROCESS
DESIGN
MANUFACTURE
MAINTENANCE
SHORT TERM GOAL
REPRESENTATION
DESIGN OF AN ARTIFACT THAT CAN BE MANUFACTURED AND MAINTAINED
DESIGN
MANUFACTURE
MAINTENANCE

DECISION-BASED DESIGN: THE FIRST CONSTRUCT

We define the term system to mean a grouping of associated entities which is characterized by a mental construct. The terms in this definition were selected for the specific meanings and associations they can convey. The term grouping conveys the impression that an act of forming and arranging is involved. Associated is used to indicate that there is an association among or that relationships may exist between the entities in a grouping without indicating the precise natures of the association or relationships. The entities could be any thing with an essential nature that can be conceptualized, including other systems, concepts, ideas, symbols, and objects in the real world. The term characterized is meant to convey that the characterization of the grouping is unique and that it is coupled to the grouping and mental construct which have been selected. Only with both can a mental image of the system be created. A construct is "a complex idea resulting from a synthesis of simpler ideas" . The redundant qualifier mental serves to highlight the involvement of the human mind in the process of creating a construct. This definition is, as will become evident from the following sections, of primary importance for the development of methods rooted in Decision-Based Design.

SYSTEM a grouping of associated entities which is characterized by a mental construct.

THE PROCESS OF DECISION MAKING AS A SYSTEM

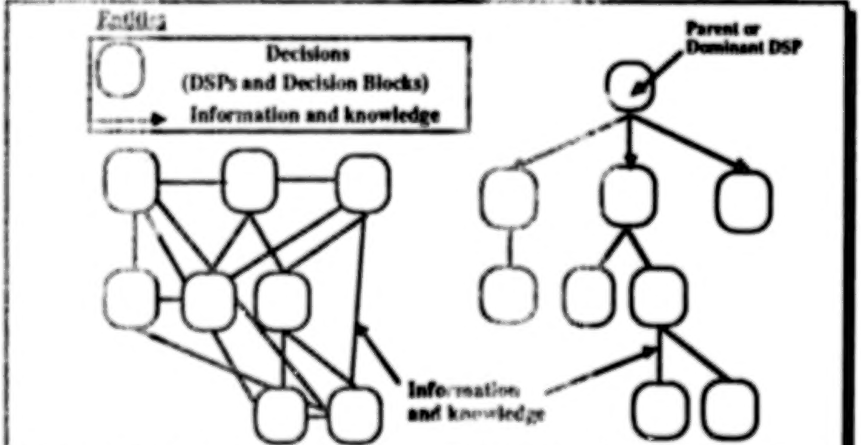
Entities
Decisions
(DSPs and Decision Blocks)
Information and knowledge
Parent or Dominant DSP
Information and knowledge

HETERARCHICAL REPRESENTATION
The relationships between decision blocks are not ordered and hence not directed.

HIERARCHICAL REPRESENTATION
The relationships between decision blocks are ordered and hence are directed.

CONCEPTUAL MODEL
DESIGN THAT CAN BE MANUFACTURED AND MAINTAINED

A process, according to our earlier definition, can be modeled as a system. In the DSP Technique unification of process is sought through the harmonious 'hierarchical' integration of

- **DESIGN** - a process of converting information that characterizes the needs and requirements for a product into knowledge about a prototype of the product,
- **MANUFACTURING** - a process in which the knowledge about a prototypical version of the product is converted into replicates of the product, and
- **MAINTENANCE** - a process in which information that characterizes the performance of a product in terms of its function and its effects on its environment is monitored and analyzed in order to
  - maximize the performance/cost ratio (thereby enhancing customer satisfaction)
  - gain knowledge for design modifications (thereby increasing industrial competiveness).

This hierarchical construct of design for the life-cycle provides the conceptual model of design (see below) for which the Decision Support Problem Technique is being developed. It is clear that the conceptual model can be modeled in its entirety using the entities of DSPs and information/knowledge.

A conceptual model representing the short term goal for the Decision Support Problem Technique is shown below.

Continued on next page.

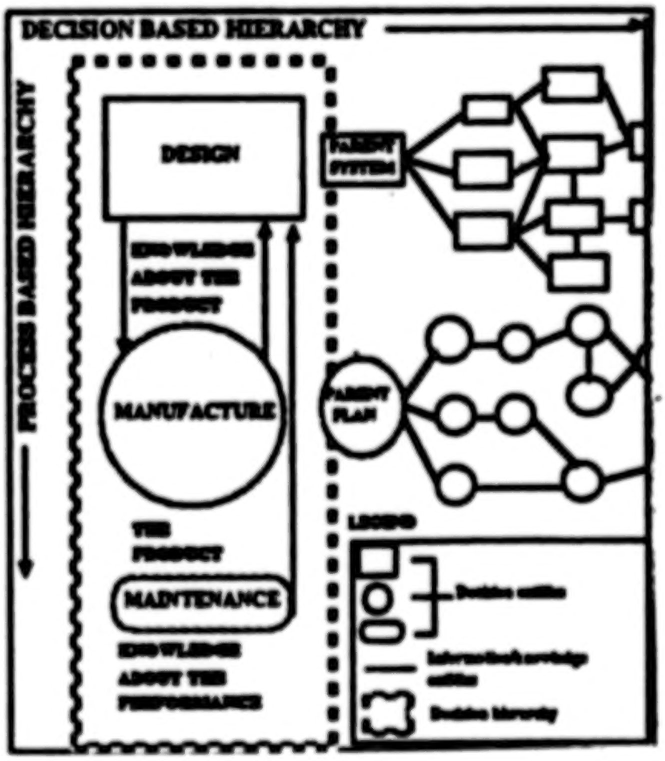
DECISION BASED HIERARCHY
PROCESS BASED HIERARCHY
DESIGN
KNOWLEDGE ABOUT THE PRODUCT
MANUFACTURE
THE PRODUCT
MAINTENANCE
KNOWLEDGE ABOUT THE PERFORMANCE
PARENT SYSTEM
PARENT PLAN
LEGEND
Decision entities
Information/knowledge entities
Decision hierarchy

CONCEPTUAL MODEL
UNIFIED DESIGN, MANUFACTURE AND MAINTENANCE

Continued from previous page.

The relation between the processes of design, manufacturing and maintenance is below and in the next slide. Within the checkered box, the three processes contain knowledge about the interaction between them. This establishes a process-based hierarchy in the creation of an artifact. Outside the checkered box, the rectangles, circles and ovals are used to represent collections of related decisions within design, manufacturing and maintenance, respectively. These decisions correspond to systems and subsystems when dealing with design and plans and subplans when dealing with manufacturing and maintenance. The interaction between the DSPs within each of the processes is represented by the lines connecting the rectangles, circles and ovals. The lines represent the passing of information and knowledge. The patterns of the networks shown are possible hierarchical representations of the decision process in design, manufacturing and maintenance . These hierarchies are based on the types of decisions made in each process. Hence they are called decision-based hierarchies which engineers recognize today as being common to the three linked processes of design, manufacturing and maintenance.

A conceptual model representing the long term goal for the Decision Support Problem Technique is shown below.

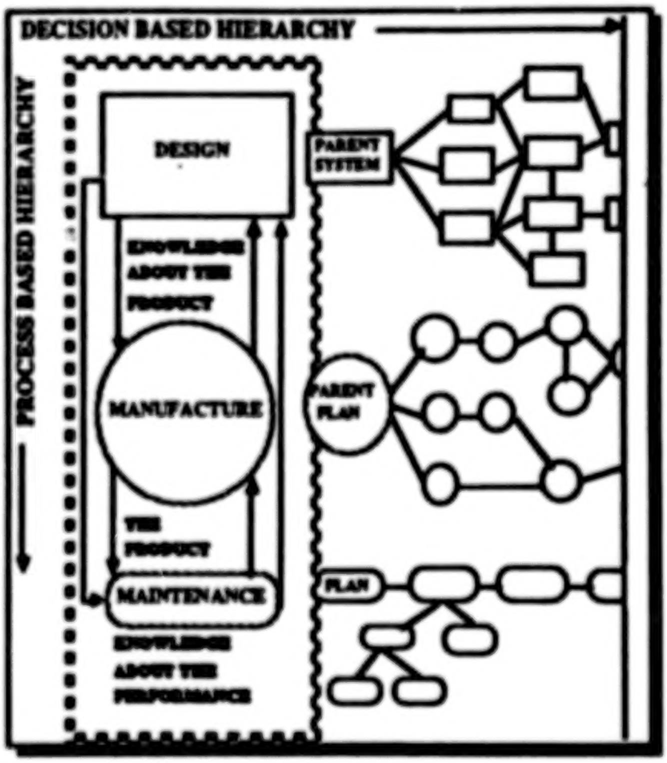
DECISION BASED HIERARCHY
PROCESS BASED HIERARCHY
DESIGN
KNOWLEDGE ABOUT THE PRODUCT
MANUFACTURE
THE PRODUCT
MAINTENANCE
KNOWLEDGE ABOUT THE PERFORMANCE
PARENT SYSTEM
PARENT PLAN
PLAN

DECISION-BASED DESIGN: SOME OBSERVATIONS

The design of most real-life engineering systems is characterized by the following descriptive sentences:

- The problems are multi-leveled, multi-dimensional and multi- disciplinary in nature.
- Most of the problems are loosely defined and open; virtually none of which has a singular, unique solution, but all of which must be solved. The solutions are less than optimal and are called satisficing solutions.
- There are multiple measures of merit for judging the "goodness" of the design, all of which may not be equally important.
- All the information required may not be available.
- Some information may be hard, that is, based on scientific principles and some information may be soft, being based on the designer's judgment and experience. The design environment is invariably fuzzy.
- Design is the process of converting information that characterizes the needs and requirements of a system into knowledge about the system itself.

The design of a complex engineering system involves partitioning of the system into smaller manageable parts which in turn require the formulation and solution of a series of problems involving decisions to be made by the designer.

A Decision-Based Design Technique is based on the following assertions:

- Design involves **a series of decisions,** some of which may be made sequentially and others that must be made concurrently.

- Design involves hierarchical **decision making,** and the interaction between these decisions must be taken into account.

- Design productivity can be increased through the use of analysis, visualization and synthesis in complementary roles, and by augmenting the recognized capability of computers in analysis to include the use of expert systems with limited (at present) capability in synthesis.

- Symbols are processed to support human decisions:
  - Analog/signals
  - Numbers
  - Graphs/Pictures/Drawings
  - Words

A technique that supports human decision making, ideally,

- must be process-based and discipline-independent,
- must be suitable for solving open problems that are characteristic of a fuzzy environment, and
- must facilitate self-learning.

META-DESIGN, COMPUTER-BASED DESIGN AND ACTION LEARNING

Central to the development of Decision-Based Design are the following major areas of research:

1 Meta-Design: This consists of two parts, namely, partitioning and planning. Partitioning deals with the way in which we define and partition a problem using a generic discipline-independent modeling technique. Planning involves the way in which we organize the expertise of individuals, the information (and knowledge) embodied in databases, and computers.

2 Computer-based Design: The use of discipline-independent processes to facilitate the generation domain-dependent information and knowledge that are needed to negotiate satisficing solutions to problems.

3 Adaptive Action Learning: A way of learning through doing.

Meta-design: Meta-design consists of two parts, namely, partitioning and planning.

Partitioning: In each of the areas of overlap in a multidisciplinary program engineers and scientists from one discipline bring with them the intellectual baggage of the technical culture in which they have been trained. They work as, say, engineers who have knowledge of the problems and methods in another area, but they tend to abide in their discipline and use its approaches and methods without changing their mindset. Recently, as designers move towards each other and seek out common ground, they have redefined their problems and in the process defined a meta-level on which to approach them. This meta-level represents the common ground on which, say, engineers and managers can meet . These meta-engineers and meta-managers operate at a level where the commonalties and only the commonalties of their disciplines exist; thus they are of this common ground with a mutually understood mindset and not simply (as in the case of a multidisciplinary approach to a problem) engineers and managers working in the overlapping areas of each others disciplines with the mindset from which they come.

Planning: The process of planning decisions is crucial for effective implementation of Decision-Based Design. The decisions themselves are not made in this phase; rather, the decisions that need to be made, to convert information that characterizes the needs and requirements for a product into knowledge about a prototype of a product that can be manufactured and maintained, are placed in a decision plan. This plan is created with the knowledge of what will be needed in implementing a designer's tasks and their relationships one to another and on the knowledge gained from meta-engineering, the design organization and its resources, the time scale and the anticipated costs.

Computer-based Design: The pervasive influence of computer-based thinking has spread to every part of every science-based discipline like a benign virus, creating an environment that has encouraged the parallel growth of systems thinking and an appreciation of the practical limits of analysis-based science in design. These events have encouraged designers to look afield for new paradigms and new approaches and methods. The computer-based approach we espouse is captured in its essence in some later discussions here and elsewhere [2,6,7]. In a sense it is the antithesis of computer-aided design; in detail at least for us a term which is used to characterize methods of automating calculations and visualization essentially without interaction by the designer. Our computer-based approach to design requires the constant interaction between two entities - a human designer and a computer.

META-DESIGN, COMPUTER-BASED DESIGN AND ACTION LEARNING ... continued

Adaptive Action Learning: The focus of effort at present in Decision-Based Design is to increase the knowledge about the object of design early on and to develop computer tools for supporting human decision making in the very early stages of project initiation. In our opinion, the development of design theory will improve design practice only under certain conditions. We offer for consideration one condition that we feel is of paramount importance. Unlike the practitioners in other fields of science, academics in design must be concerned with the pedagogical aspects of how design skills (associated with both theory and practice) can be passed on to their students. We believe that, in the long term, only that portion of theory that can be taught (or as we prefer to say learned) to a large number of students will influence design practice. We have found that what we call "adaptive action learning" with its emphasis on the synergistic effects associated with teamwork [4,7] is an essential ingredient in our research and in assuring that our students do, in fact, understand the approach, methods and design philosophy we espouse. Over two thousand years ago, Confucius is quoted as having said,

"Tell me, and I will forget.

Show me, and I will remember.

Let me do it, and I will understand."

This captures our feeling and belief that only through a hands-on learning process coupled with participation in a goal-oriented design process can our students truly become the designers we want them to be.

Central to the development of Decision-Based Design are the following major areas of research:

META-DESIGN

Partitioning **deals with the way in which we define and partition a problem, using a generic discipline-independent modeling technique.**

Planning **involves the way in which we organize the expertise of individuals, the information (and knowledge) embodied in databases, and computers.**

COMPUTER-BASED DESIGN

The use of discipline-independent processes to facilitate the generation domain-dependent information and knowledge that are needed to negotiate satisficing solutions to problems. Our computer-based approach supports systems thinking and requires the constant interaction between two entities - a human designer and a computer.

ADAPTIVE ACTION LEARNING

Confucius is quoted as having said,

> **"Tell me, and I will forget.**
> **Show me, and I will remember.**
> **Let me do it, and I will understand."**

THE DECISION SUPPORT PROBLEM TECHNIQUE PROCESS

The principal role of any Decision-Based Design process is to convert information that characterizes the needs and requirements for a product into knowledge about the product itself. The DSP Technique facilitates the conversion of information for the product into knowledge about the product that can be used for its manufacture. In the DSP Technique identification, decomposition, organization and synthesis are used:

- to **identify** the information that characterizes the needs and requirements for the design and is necessary for the process of design,
- to **partition** and decompose a design problem into appropriate Decision Support Problems,
- to **organize** the domain dependent information in a form suitable for solution, and
- to **synthesize** the component solutions into one "system" solution and thereby gain knowledge about the product being designed.

In the DSP Technique the process, for converting information into knowledge, consists of two phases (meta-design and design) and six steps as shown below. These steps are valid for any stage in the design process and the DSP Technique can be used for designing systems and components.

Our efforts to date have been directed to developing the second phase, namely, design. In the process we have identified various decision hierarchies (see later) and developed software to solve them (see later). These developments, we believe, are of value to industry and are appropriate for use in a classroom.since Decision Support Problems can be formulated and solved as an activity in any other design scheme; particularly if designing for concept is involved.

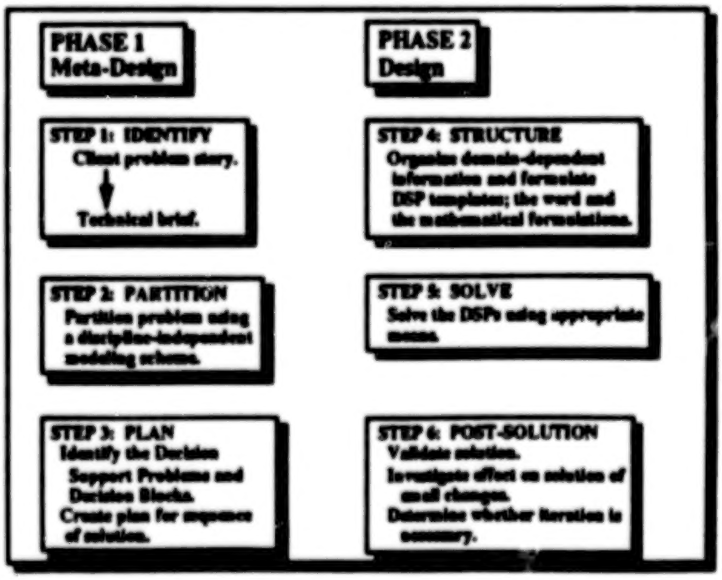
PHASE 1
Meta-Design
PHASE 2
Design
STEP 1: IDENTIFY
Client problem story.
Technical brief.
STEP 4: STRUCTURE
Organize domain-dependent information and formulate DSP templates; the word and the mathematical formulations.
STEP 2: PARTITION
Partition problem using a discipline-independent modeling scheme.
STEP 5: SOLVE
Solve the DSPs using appropriate means.
STEP 3: PLAN
Identify the Decision Support Problems and Decision Blocks.
Create plan for sequence of solution.
STEP 6: POST-SOLUTION
Validate solution.
Investigate effect on solution of small changes.
Determine whether iteration is necessary.

93

CHARACTERISTICS OF DECISIONS

In engineering a designer often walks a fine line between developing and maintaining a model that is amenable to solution and one whose results yield information and knowledge that is usable in practice. In engineering, decisions involving design are characterized by the following descriptive sentences:

- Decisions involve information that comes from different sources and disciplines.
- Decisions are governed by multiple measures of merit and performance.
- The measures of merit may not be of equal importance to the final decision and may conflict with each other.
- All of the information for making an adequate decision may not be available to a designer.
- Some of the information may be hard (based on scientific principles), some may be soft (based on the perceptive judgment of the designer) and some may be partially soft (empirical in nature).
- The problem for which the decision is being made is open.

These characteristics dictate the mathematical form of the DSPs and govern the type of solution algorithms appropriate for solving them. For example, these characteristics virtually rule out the use of traditional single objective optimization in Decision-Based Design.

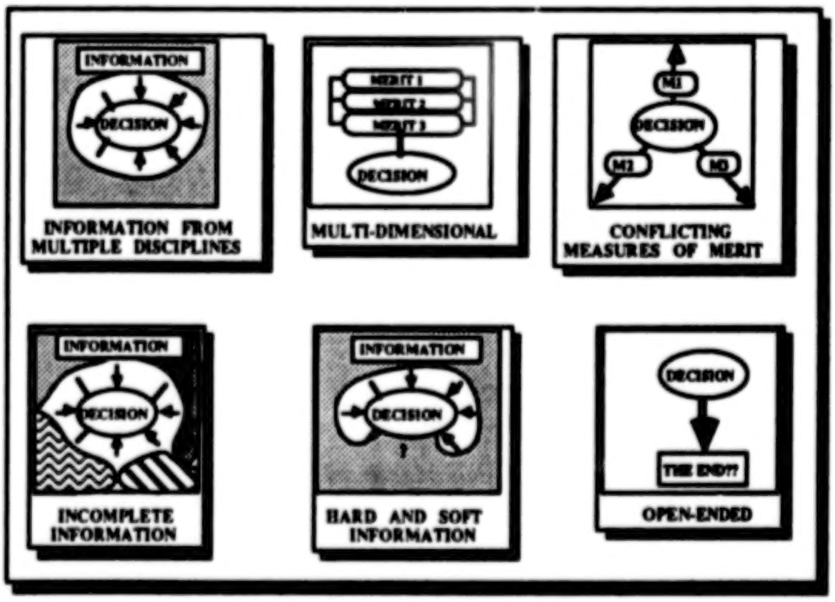
INFORMATION
DECISION
INFORMATION FROM MULTIPLE DISCIPLINES
MERIT 1
MERIT 2
MERIT 3
DECISION
MULTI-DIMENSIONAL
M1
DECISION
M2
M3
CONFLICTING MEASURES OF MERIT
INFORMATION
DECISION
INCOMPLETE INFORMATION
INFORMATION
DECISION
HARD AND SOFT INFORMATION
DECISION
THE END??
OPEN-ENDED

DECISION ACTIVITIES TO DECISION ENTITIES

An abstract, conceptual statement about the relationship between decisions as people discuss them and how they could be structured for computer-based solution is made in in the figure below [2,8]. The Decision Support Problems and Decision Blocks are also shown in the Figure. The transformation of decision activities into decision blocks is based on the inherent characteristics of decisions in engineering design. The transformation of DSPs into DBs depends on the type, separability and order in which the decisions have to be made to effect a solution. As is evident from the figure the process of this transformation is modeled using the decision and knowledge/information entities described earlier. Further, the transformation process complies with our earlier definition of system. The set of Decision Support Problems shown in the figure is incomplete.

PRELIMINARY SELECTION
The selection of the top-of-the-heap concepts for further development.

SELECTION
The indication of a preference based on multiple attributes for one amongst several feasible alternatives.

COMPROMISE
The improvement of an alternative through modification.

HIERARCHICAL
Decisions, within a decision entity in which both selection and compromise occur.
Decisions, between decision entities, which involve subplan interaction and compromise.

CONDITIONAL
Decisions in which the risk and uncertainty of the outcome are taken into account.

HEURISTIC
Decisions which are made on the basis of a knowledge base of facts and rules of thumb.

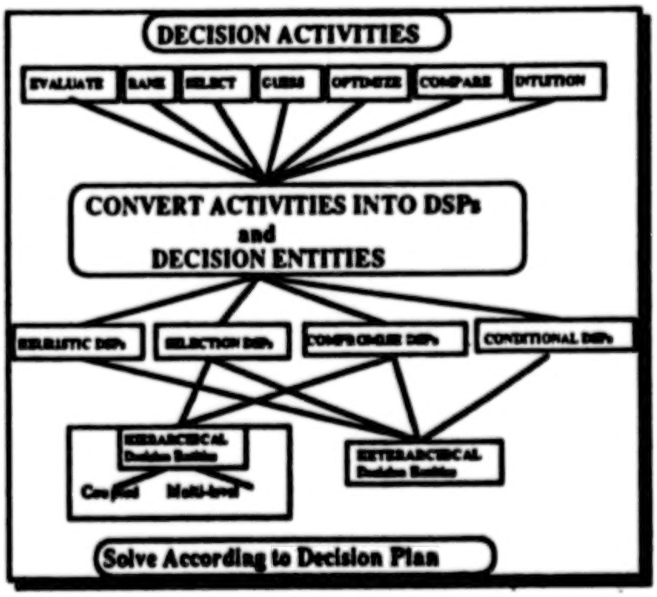
DECISION ACTIVITIES
EVALUATE
RANK
SELECT
GUESS
OPTIMIZE
COMPARE
INTUITION
CONVERT ACTIVITIES INTO DSPs
and
DECISION ENTITIES
HEURISTIC DSPs
SELECTION DSPs
COMPROMISE DSPs
CONDITIONAL DSPs
HIERARCHICAL
Decision Entities
Coupled
Multi-level
HETERARCHICAL
Decision Entities
Solve According to Decision Plan

TYPES OF DESIGNS

- **Original Design** - The design specification for the system may require the system to perform the same, similar or a new function altogether. An original solution principle is defined for a desired system and used to create the knowledge and information so that it can be manufactured and maintained.
- **Adaptive Design** - An original design is adapted to meet a modified set of specifications. The solution principle, in the main, remains the same but the product will be sufficiently different so that it can meet the changed specifications.
- **Variant Design** - The size and/or arrangement of parts or subsystems of the chosen system are fine-tuned, say, to meet a set of specifications more cheaply; the specifications and solution principle remain the same.

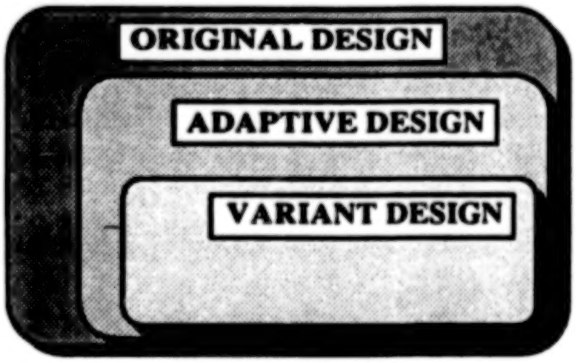

ORIGINAL DESIGN

ADAPTIVE DESIGN

VARIANT DESIGN

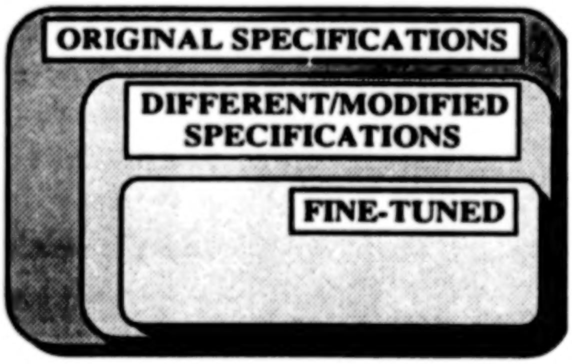

ORIGINAL SPECIFICATIONS

DIFFERENT/MODIFIED SPECIFICATIONS

FINE-TUNED

CHARACTERISTICS OF DESIGN GUIDANCE SYSTEM

IT MUST BE COMPATIBLE WITH ALL THREE TYPES OF DESIGN.

ELEMENTS OF IT MUST BE USABLE INTERCHANGEABLY.

DESIGNING FOR CONCEPT

According to our definition, the principal role of any design process is to convert information that characterizes the needs and requirements for a product into knowledge about the product itself. Further, it is safe to assume that because of the complexity of the product (an engineering system) the conversion of information into knowledge will have to be accomplished in stages. In the traditional design process names have been given to the stages such as feasibility, conceptual, preliminary and detail. The names and the number of stages, from the standpoint of the information necessary for making decisions in each of the stages, are not important. What is important is that

- the types of decisions being made (e.g., selection and compromise) are the same in all stages, and
- the amount of hard information increases as the knowledge about the product increases.

It appears to us that, in Decision-Based Design, the ratio of soft to hard information available is a key factor in determining the nature of the support that a human designer needs as he/she negotiates a solution to a design problem. Our current efforts are focused on understanding what is needed and developing the tools to support human decision making in the early stage of a project. We assert that it is possible, based on the ratio of hard to soft information that is available, to make a distinction between designing for concept and designing for manufacture (see below). Based on this distinction it is possible to categorize computer-based aids into two categories, namely, tools that provide support for human decision making and tools for automation.

DESIGNING FOR CONCEPT AND MANUFACTURE: A DECISION-BASED PERSPECTIVE

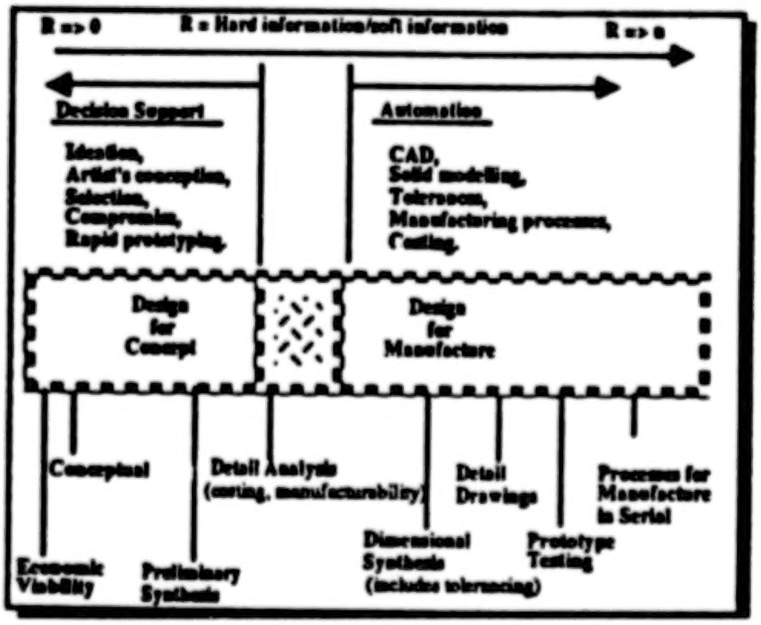
R => 0
R = Hard information/soft information
R => ∞
Decision Support
Ideation,
Artist's conception,
Selection,
Compromise,
Rapid prototyping,
Automation
CAD,
Solid modelling,
Tolerances,
Manufacturing processes,
Costing,
Design for Concept
Design for Manufacture
Conceptual
Detail Analysis (costing, manufacturability)
Detail Drawings
Processes for Manufacture in Serial
Economic Viability
Preliminary Synthesis
Dimensional Synthesis (includes tolerancing)
Prototype Testing

DESIGNING FOR CONCEPT: A SCENARIO

In designing for concept we seek to cast a wide net, that is, generate many concepts and then systematically home-in on a concept that meets its functional specifications and can be produced and maintained. In other words we are involved in the process of converting information that characterizes the needs and requirements for a product into specific knowledge that can be used in designing for manufacture. In designing for manufacture we attempt to ensure that the product can be manufactured cost-effectively. Of course we recognize that in practice iteration will occur and this, for convenience, has not been illustrated in the figure.

A schematic of designing for concept is shown below. Let us assume that the process is underway and the problem definition is available. This permits ideation that results in the identification of alternative ways (concepts) of achieving the objectives embodied in the problem definition. Ideally, a large number of concepts should be generated. At this stage most of the information will be soft and there should be many concepts. We envisage a **preliminary selection** DSP being formulated and solved to identify the more promising "top-of-the-heap" or "most-likely-to-succeed" concepts. In preliminary selection we start with concepts, the end product of ideation. We evaluate the concepts based on criteria. The criteria are quantified using experience-based judgment (or soft information) only. The solution to the preliminary selection DSP involves the rank ordering of concepts. Therefore one cannot automatically infer, from the rankings, by how much one concept is preferred to another and hence it is injudicious to use this approach to identify the "best concept". At this stage we expect engineering analysis to be used to convert as many of the top-of-the-heap concepts one can afford into feasible alternatives. These alternatives will be characterized by both hard and soft information. We envisage a **selection** DSP being formulated and solved to identify one or two alternatives that should be further developed. In selection we start with feasible alternatives. We evaluate the feasible alternatives based on attributes (using both hard and soft information). We solve the selection DSP to identify the best alternative. The solution to the selection DSP involves the ordering of alternatives. One can infer from the ranking by how much one alternative is preferred to another and therefore the best alternative is known. Further development involves improvement through modification and we believe that the **compromise** DSP is appropriate for this task. Iteration is necessary and is not precluded from the scenario just presented.

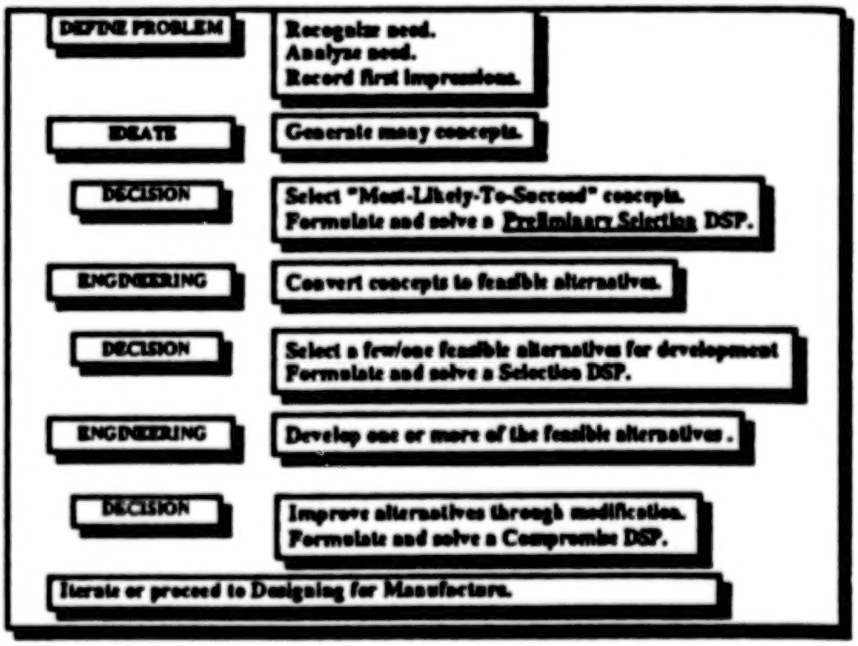
DEFINE PROBLEM
Recognize need.
Analyze need.
Record first impressions.
IDEATE
Generate many concepts.
DECISION
Select "Most-Likely-To-Succeed" concepts.
Formulate and solve a Preliminary Selection DSP.
ENGINEERING
Convert concepts to feasible alternatives.
DECISION
Select a few/one feasible alternatives for development
Formulate and solve a Selection DSP.
ENGINEERING
Develop one or more of the feasible alternatives .
DECISION
Improve alternatives through modification.
Formulate and solve a Compromise DSP.
Iterate or proceed to Designing for Manufacture.

THE DSIDES SOFTWARE

The software for the Decision Support Problem Technique continues to be developed by the Systems Design Laboratory at the university of Houston. The software is called DSIDES (Decision Support In the Design of Engineering Systems). At this time, we provide no computer-based support for the planning and structuring steps of the DSP Technique. An experimental system for partitioning is available [2].

Software to solve preliminary selection and selection DSPs in an interactive and extremely user-friendly environment has been written in PASCAL for the Apple Macintosh computers. This software is called MacDSIDES. A version for the IBM PC/AT is also available. The algorithm used is summarized in [9,10,11]. This software has been used, in industry, in two major projects involving designing for concept.

Software to solve the compromise DSPs is called DSIDES and has been written in FORTRAN 77. DSIDES can also be used to solve selection and hierarchical DSPs. To date, ship design has been the largest single application of the compromise DSP formulation [12,13,14]. Applications involving the design of damage tolerant structural [15,16] and mechanical systems [17,18,19], the design of aircraft [11,20], mechanisms [17,21], a solar-thermal-powered agricultural-water pumping system [22,23], design using composite materials [24,25] and data compression [22]. DSPs have been developed for hierarchical design; selection- compromise [13,26,27], compromise-compromise [28] and selection-selection [10]. An overview of DSIDES (its function and structure) is presented in [6]. The compromise DSP is solved using a unique optimization scheme called Adaptive Linear Programming. This scheme is described in references [29,30].

Current projects include the development of templates for designing thermal energy systems [22] templates to study the interaction between design and manufacturing [24,25] and the conceptual design of automobile tires [31]. Other projects include the incorporation of intelligence into the DSIDES software, the development of a method for data compression and the development of the capability to design lubricants using information obtained from condition monitoring.

The software for the Decision Support Problem Technique is called:

Decision	**D**
Support	**S**
In the	**I**
Design of	**D**
Engineering	**E**
Systems	**S**

MacDSIDES: Macintosh Plus, SE and II (PC-DSIDES end of summer)

PSELECT   Preliminary Selection
Identify top-of-the-heap concepts
Use information that is "soft" only.

SELECT   Selection
Identify the most appropriate alternative for further development
Use both "hard and "soft" information

DSIDES: Mini-computers

SELECT   As above
SLIPML   Compromise
Improve alternative through modification - multiobjective optimization.
SLIPML   Coupled
Hierarchical problems involving both Selection and Compromise

BEST COPY AVAILABLE

DECISION HIERARCHIES

Some decision-based hierarchies and their status of development (and availability for use in industry and in the classroom) are shown below. One construct may be of particular importance to this audience and is briefly described. A coupled selection-selection DSP arises whenever we have a system that can be decomposed into several inter-dependent subsystems that have to be selected by the designer. It is always present in "Catalog Design" a procedure in which a system is assembled by selecting standard components from catalogs of available components. The performance of the overall system depends on all of the components, which are dependent on each other. It is not appropriate to select any component without taking into account the effect it has on the other components and the performance of the system as a whole. Further information is provided in reference [10]. The same construct is also appropriate for use in identifying an initial layout in the early stages in designing for concept.

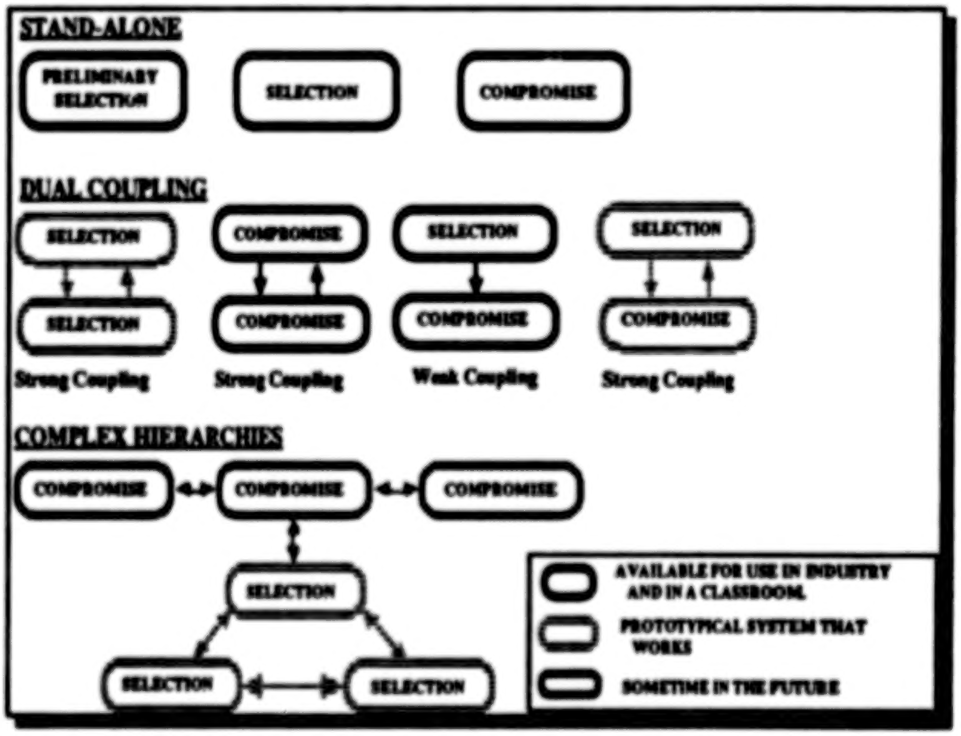
STAND-ALONE
PRELIMINARY SELECTION
SELECTION
COMPROMISE
DUAL COUPLING
SELECTION
SELECTION
Strong Coupling
COMPROMISE
COMPROMISE
Strong Coupling
SELECTION
COMPROMISE
Weak Coupling
SELECTION
COMPROMISE
Strong Coupling
COMPLEX HIERARCHIES
COMPROMISE
COMPROMISE
COMPROMISE
SELECTION
SELECTION
SELECTION
AVAILABLE FOR USE IN INDUSTRY AND IN A CLASSROOM.
PROTOTYPICAL SYSTEM THAT WORKS
SOMETIME IN THE FUTURE

CLOSURE

In a recent paper [32], Dixon (who is currently the Director of the NSF Design Theory and Methodology Program) offered his viewpoint of engineering design as he sees it today --- no longer only an art and not yet a recognized science. He raises four issues which comprise his view of the status of engineering design science today, namely,

(a) that researchers in design theory constitute a single goal-directed research community

(b) that the development of design theory is essentially still in a pre-theory stage

(c) that the goal of the design research community should be the development of a formal scientific theory or theories of design that will enable the generation of hypotheses for testing by traditional scientific methods

(d) that the development of design theory will improve design practice

We are in agreement with the sense of his observations. In another paper [33] we offer an interpretative commentary on their scope and impact. We start by presenting a historical perspective of the centuries-long evolution of design from a wholly intuitive art to the beginnings of becoming a rational science. We comment on Dixon's four observations in the context of this view of the origins and present state of design and offer a fifth perspective which takes into account the discipline-specific origins of design in several fields and is focussed forward in time. In this new view, we introduce the notion of meta-design. Finally, we offer our views on the process of identifying research activities worthy of support in today's yeasty environment of change-just-over the horizon. Some of these views are summarized below.

1 **DEVELOPMENT OF DESIGN METHODS THAT ARE BASED A HOLISTIC, SYSTEMATIC VIEWPOINT OF DECISION MAKING, NAMELY, DECISION-BASED DESIGN IS RECOMMENDED.**

2 **THERE ARE MANY DIFFERENT WAYS OF IMPLEMENTING DECISION-BASED DESIGN. OUR APPROACH IS CALLED THE DECISION SUPPORT PROBLEM TECHNIQUE.**

3 **FOR LONG TERM COST-EFFECTIVENESS RESEARCH IN THIS AREA SHOULD:**

- **SUPPORT THE DEVELOPMENT OF A DOMAIN INDEPENDENT PROCESS AND THE DEVELOPMENT OF DOMAIN DEPENDENT INFORMATION.**
- **BE OF A KIND THAT MAKES CONTACT AT SOME LEVEL WITH THE PRACTICAL WORLD.**
- **PROVIDE FOR GAINING INSIGHT AND UNDERSTANDING THAT COULD BE USED FOR INCREASING DESIGN PRODUCTIVITY.**
- **CONTRIBUTE TO OUR UNDERSTANDING OF THE PROCESS OF DESIGN.**
- **INCLUDE SOME MEANS TO FACILITATE AN EVALUATION OF THE EFFECTIVENESS OF THE DEVELOPMENT.**
- **CONTAIN A COMPONENT THAT IS TEACHABLE AND/OR LEARNABLE.**

CLOSURE continued

There is much that remains to be done and as we have learned to say, since we came to Texas - *y'all come! There is so much to do!*

ACKNOWLEDGMENT

The financial contribution of our corporate sponsor, the BF Goodrich Company, to further develop the Decision Support Problem Technique is gratefully acknowledged.

4 SOME SPECIFIC RESEARCH ISSUES

- THE DEVELOPMENT OF A TAXONOMY AND CONCEPTUAL MODELS FOR PROCESSES IN DESIGN IS CRUCIAL. FOR EXAMPLE, DESIGN FOR MANUFACTURE, DESIGN FOR THE LIFE-CYLE, HETRARCHY AND HIERARCHY, PARTITIONING, PLANNING, ETC.
- THE DEVELOPMENT OF THE CAPABILITY TO MODEL SYSTEM) BEHAVIOR IS CRUCIAL.
- THE DEVELOPMENT OF THE CAPABILITY TO MODEL FEATURES ASSOCIATED WITH REAL-WORLD DECISIONS IS IMPORTANT.
- EVENT-BASED DESIGN GUIDANCE SYSTEMS WILL BE NEEDED.
- INTELLIGENT DATA REDUCTION SCHEMES AND REPRESENTATION SCHEMES FOR USE IN DESIGN GUIDANCE SYSTEMS WILL BE NEEDED.
- DESIGN OF A COMPUTER ENVIRONMENT TO SUPPORT THESE ACTIVITIES IS NECESSARY.

5 IN AN AGE CHARACTERIZED BY RAPID CHANGES IN TECHNOLOGY AND AN ABUNDANCE OF INFORMATION ANY SIGNIFICANT INCREASE IN PRODUCTIVITY WILL, TO A LARGE MEASURE, DEPEND ON THE EDUCATION THE ENGINEERS HAVE RECEIVED. WE WILL GAIN MOST FROM THOSE WHO HAVE, AS PART OF THEIR EDUCATION PROCESS, BEEN GIVEN THE OPPORTUNITY TO LEARN HOW TO COPE WITH CHANGE.

REFERENCES

1 H.A. Simon, *Sciences of the Artificial*, 2nd Edition, MIT Press, 1982.

2 J.A. Shupe, J.K. Allen, D. Muster and F. Mistree, *Decision-Based Design: Some Concepts and Research Issues*, Expert Systems: Design and Management of Manufacturing Systems, A. Kusiak (ed.), Society of Manufacturing Engineers, June 1988.

3 J.A. Shupe, *Decision-Based Design: Taxonomy and Implementation*, Ph.D. Dissertation, Department of Mechanical Engineering, University of Houston, May 1988.

4 D. Muster and F. Mistree, *The Decision Support Problem Technique in Engineering Design*, The International Journal of Applied Engineering Education, Vol. 4, No. 1, 1988, pp. 23-33.

5 F. Mistree, H.M. Karandikar, J.A. Shupe and E. Bascaran, *Computer-based Design Synthesis: An Approach to Problem Solving*, Systems Design Laboratory Report, Department of Mechanical Engineering, University of Houston, August 1988.

6 S.Z. Kamal, H.M. Karandikar, F. Mistree and D. Muster, *Knowledge Representation for Discipline-Independent Decision Making*, Expert Systems in Computer-aided Design, J.S. Gero (ed.), Elsevier Science Publications, 1987, pp. 289-321.

7 F. Mistree and D. Muster, *Mechanical Design: An Undergraduate Curriculum for Design in the Systems Age*, 1984 ASEE Annual Conference Proceedings, Salt Lake City, Utah, June 1984, pp. 818-826.

8 F. Mistree and D. Muster, *Designing for Concept: A Method that Works*, Proceedings International Workshop on Engineering Design and Manufacturing Management, The University of Melbourne, Melbourne, Australia, November 21-23, 1988.

9 N. Kuppuraju, P. Ittimakin and F. Mistree, *Design through Selection: A Method that Works*, Design Studies, Vol. 6, No. 2, 1985, pp. 91-106.

10 E. Bascaran, R.B. Bannerot and F. Mistree, *Hierarchical Selection Decision Support Problems in Conceptual Design*, Systems Design Laboratory Report, Department of Mechanical Engineering, University of Houston, June 1988.

11 F. Mistree, S. Marinopolous, D. Jackson.and J.A. Shupe, *The Design of Aircraft using the Decision Support Problem Technique*, NASA Contractor Report 4134, April 1988.

12 T.D. Lyon and F. Mistree, *A Computer-based Method for the Preliminary Design of Ships*, Journal of Ship Research, Vol. 29, No. 4., December 1985, pp. 251-269.

13 W.F. Smith and F. Mistree, *The Influence of Hierarchical Decisions on Ship Design*, Marine Technology, Vol. 24, No. 2, April 1987, pp. 131-142.

14 W.F. Smith, T.D. Lyon and B. Robson, *AUSEVAL - A Systems Approach for the Preliminary Design of Naval Ships*, Proceedings Bicentennial Maritime Symposium, Sydney Australia, Jan. 18-20, 1988, pp. 1-29

15 J.A. Shupe and F. Mistree, *Compromise: An Effective Approach for the Design of Damage Tolerant Structural Systems*, Computers and Structures, Vol. 27, No. 3, pp. 407-415, 1987.

16 J.A. Shupe, F. Mistree and O.F. Hughes, *A Conceptual Basis for the Design of Damage Tolerant Structural Systems*, Recent Experiences in Multidisciplinary Analysis and Optimization, NASA CP 2327, April 1984, pp. 907-942.

17 S. Mudali, *Dimensional Synthesis of Mechanical Linkages using Compromise Decision Support Problems*, M.S. Thesis, Department of Mechanical Engineering, University of Houston, October 1987.

REFERENCES continued

18 N. Nguyen and F. Mistree, *A Computer-based Method for the Rational Design of Horizontal Pressure Vessels*, ASME Journal of Mechanism, Transmissions and Automation in Design, Vol. 108, June 1986, pp. 203-210.

19 A. Jivan and F. Mistree, *A Computer-based Method for Designing Statically Loaded Helical Compression Springs*, ASME 11th Design Automation Conference, Cincinnati, Ohio, September 10-13. ASME Paper Number 85-DET-75.

20 S. Marinopolous, D. Jackson, J. Shupe and F. Mistree, *Compromise: An Effective Approach for Conceptual Aircraft Design*, Paper No. AIAA-87-2965.

21 Q-J. Zhou, *The Compromise Decision Support Problem: A Fuzzy Formulation*, M.S. Thesis, Department of Mechanical Engineering, University of Houston, May 1988.

22 E. Bascaran, F. Mistree and R.B. Bannerot, *Compromise: An Effective Approach for Solving Multi-objective Thermal Design Problems*, Engineering Optimization, Vol. 12, No. 3, pp. 175-189, 1987.

23 E. Bascaran, R.B. Bannerot and F. Mistree, *The Conceptual Development of a Method for Solving Multi-objective Hierarchical Thermal Design Problems*, 1987 National Heat Transfer Conference, Pittsburgh, August 1987. Paper No. 87-HT-62.

24 H.M. Karandikar, W.J. Fuchs, F. Mistree and H. Eschenauer, *Compromise: An Effective Approach for Designing Composite Conical Shell Structures*, Proceedings 1988 Design Automation Conference, September 1988.

25 F. Mistree, W.J. Fuchs, H.M. Karandikar, R. Srinivasan, *Design of Composite Material Systems using the Decision Support Problem Technique*, Systems Design Laboratory Report, Department of Mechanical Engineering, Houston, October 1987, 157 pages.

26 N. Kuppuraju, S. Ganesan, F. Mistree and J.S. Sobieski, *Hierarchical Decision Making in System Design*, Engineering Optimization, Vol. 8, March 1985, pp. 223-252.

27 J.A. Shupe, F. Mistree and J.S. Sobieski, *Compromise: An Effective Approach for Design of Hierarchical Structural Systems*, Computers and Structures, Vol. 26, No. 6, pp. 1027-1037, 1987.

28 W.F. Smith, *The Development of AUSEVAL: An Automated Ship Evaluation System*, M.S. Thesis, Department of Mechanical Engineering, University of Houston, December 1985.

29 F. Mistree and O.F. Hughes, *Adaptive Linear Programming: An Algorithm for Solving Multi-objective Decision Support Problem*, Systems Design Laboratory Report, University of Houston, November 1986.

30 F. Mistree, O.F. Hughes and H.B. Phuoc, *An Optimization Method for the Design of Large, Highly Constrained, Complex Systems*, Engineering Optimization, Vol. 5, No. 3, Aug./Sept., 1981, pp. 141-144.

31 N. Bhattacharya, R.P. Reddy, L. Velez, V. Tsikkinis, L. Koszegi, *A Decision Support Problem Template for the Preliminary Design of Automobile Tires*, Systems Design Laboratory Report, Department of Mechanical Engineering, University of Houston, May 1988.

32 J.R. Dixon, *On Research Methodology Towards A Scientific Theory of Engineering Design*, Artificial Intelligence for Engineering Design, Analysis and Manufacturing, Vol. 1, No. 3, June 1988.

33 D. Muster and F. Mistree, *Engineering Design as it Moves from an Art to a Science*, Proceedings NSF Grantee Workshop on Design Theory and Methodology, Rensselaer Polytechnic Institue, Troy, New York, June 3-5, 1988.

THE ART OF SPACECRAFT DESIGN: A MULTIDISCIPLINARY CHALLENGE

F. Abdi, H. Ide, M. Levine, and L. Austel
Rockwell International, NAA
Los Angeles, CA

INTRODUCTION

It is an engineer's dream to have all aspects of analysis done in a relatively short time period so that many different configurations can be examined. Hence, the best suitable design product can be delivered on time. Although this may still be a dream, actual design turn-around time has become shorter due to the use of optimization techniques which have been introduced into the design process. It seems that what, how and when to use these optimization techniques may be the key factor for future aircraft engineering operations.

Another important aspect of this technique is that complex physical phenomena can be modeled by a simple mathematical equation. For example, it is known that interactions among aerodynamic, structure, control and thermal are strong in the hypersonic flow regime[1]. Often, each analysis may fail due to highly complex, nonlinear conditions. Engineers, however, wish to understand the coupling effect and relationships between these disciplines even in the preliminary design stage. Traditionally, this type of analysis takes a long time because all disciplines are depending on one anothers results. Therefore, a small change in one of the disciplines results may cause long delay in analysis since all the disciplines must be reanalyzed.

The new powerful multilevel methodology reduces this time-consuming analysis significantly while maintaining the coupling effects. This simultaneous analysis method stems from the implicit function theorem and system sensitivity derivatives of input variables.[2,3,4] Use of the Taylor's series expansion and finite differencing technique for sensitivity derivatives in each discipline makes this approach unique for screening dominant variables from nondominant variables.[5]

In this study, the current CFD* aerodynamic and sensitivity derivative/optimization techniques are applied for a simple cone-type forebody of a high-speed vehicle configuration to understand basic aerodynamic/structure interaction in a hypersonic flight condition.

---

*Computational fluid dynamics (CFD).

(06

PROBLEM IDENTIFICATION

The performance of hypersonic vehicles largely depends on shock strength and position at the engine's inlet. For example, a shock which is introduced at the nose of vehicle must be ingested by the inlet in order to avoid spillage of mass flow. Optimum performance can be expected when the shock impinges on the cowl's lip due to maximum mass flow and ram recovery. This condition, however, is marginally unstable in actual applications because small changes in angles of attack, yaw, boundary-layer separation (with or without thermal effects) and other changing conditions can induce the shock to move.

The main task of this study is to examine the effects of static aeroelasticity on the optimization of the forebody shape which is greatly dependent on the changes in the shock position.

FOREBODY/INLET AND SHOCK PATTERN

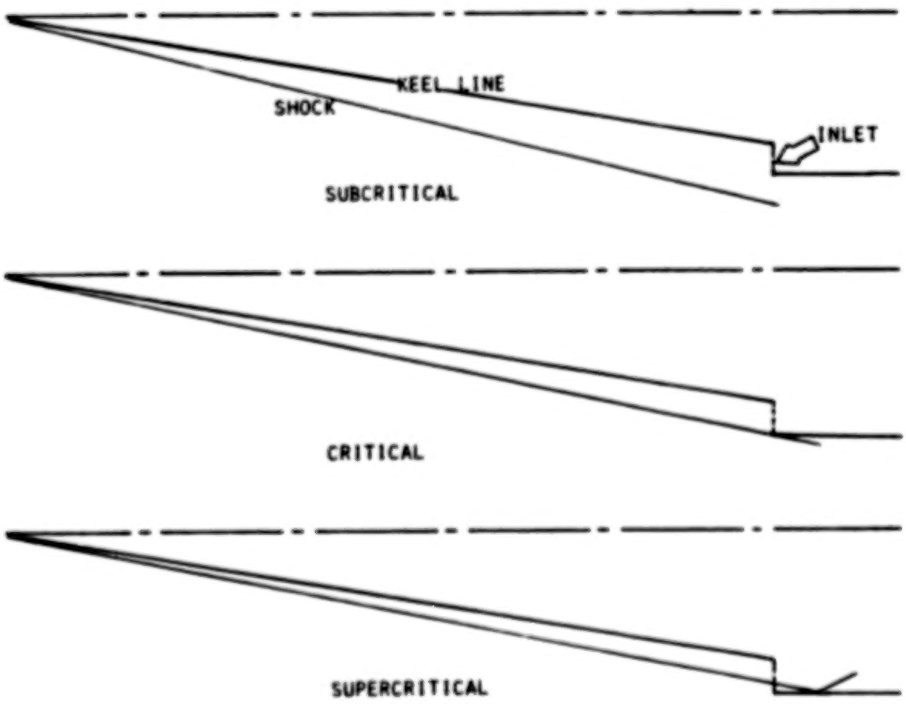

OBJECTIVES

Objectives of this study are two-fold: (1) finding the design parameters of a hypersonic forebody configuration which gives the maximum mass flow rate over the drag ratio at a specified inlet station and (2) examining the effect of the forebody static aeroelasticity.

The first level is the aerodynamic analysis for a rigid forebody. Sensitivity derivatives of the rigid body will be analyzed in this level. The second level is a structure analysis in terms of elastic boundary condition application. A vibration analysis is performed based on the predetermined FEM[*] and structural condition. Several mode shapes will be extracted from this level.

In the actual hypersonic flight regime, these two disciplines are uniquely coupled, and their interaction has a significant effect on the shock location. A new method to solve this type of coupled problems based on the implicit function theorem will be used to compute global sensitivity derivatives and these derivatives will be passed to an optimizer.

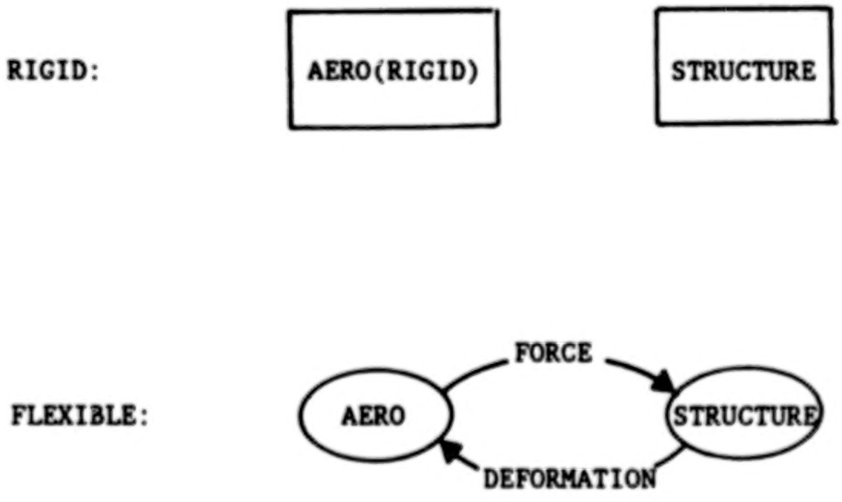

---

[*] Finite-element method (FEM).

APPROACHES

A new approach to analyze interaction between the design disciplines (aero, structure and dynamics) simultaneously and optimize required design parameters is introduced based on the implicit function theorem. The use of Taylor's series expansion and finite differencing technique for computing local sensitivity derivatives in each discipline make this approach unique since all discipline analyses can be performed concurrently.

The definition of objective function, in general, is a difficult task mainly due to unknown mathematical functions. Use of CFD analysis bypasses this time-consuming mathematical function identification by evaluating a series of digital points. Using these point distributions, one can create a simple mathematical model based on linear or quadratic function.

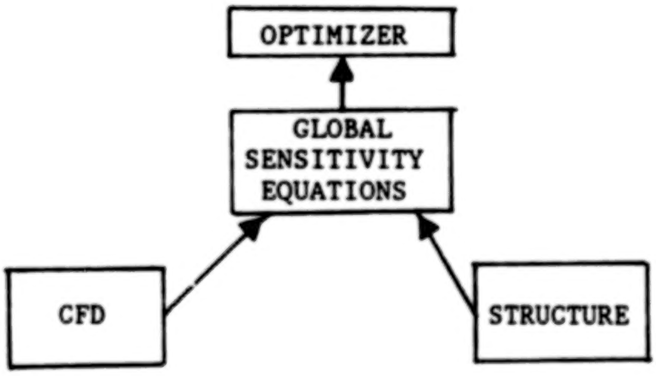

ADVANTAGES OF NUMERICAL SENSITIVITY DERIVATIVE/ OPTIMIZATION METHOD

- NO MATHEMATICAL FUNCTION DEFINITION IS REQUIRED
- CFD AND STRUCTURE ANALYSES ARE DONE INDEPENDENTLY
- SCREENING OF DESIGN OR LOCAL PARAMETERS IS EASY
- COUPLING EFFECT BETWEEN DISCIPLINES IS INCORPORATED

FORMULATION OF THE PROBLEM

A simple problem is assumed in this study. Since a basic configuration already exists, the sensitivity derivative and optimization technique is used to indicate the most feasible direction in which to find the optimum forebody shape. In order to set the correct direction in optimizing the objective function, a small perturbation technique based on the Taylor's series expansion method is used.[5] Therefore, the sensitivity derivatives are also evaluated at the initially known condition of the objective function.

Optimization of the ratio of mass flow rate ($\dot{m}_a$) and drag at a given station by changing design parameters X_i can be expressed as

$$\dot{m}_a/D = f\ (X_i) \tag{1}$$

where $\dot{m}_a/D$, or μ, is the mass flow rate-drag ratio at a given station, and X_i is the independent design variable.

By the use of Taylor's series expansion, Eqn. (1) is rewritten as

$$\dot{m}_a/D = (\dot{m}_a/D)_0 + \frac{\partial f}{\partial X_i} \Delta X_i \tag{2}$$

where $(\dot{m}_a/D)_0$ is the known initial condition.

TASKS

OBJECTIVE: maximize $\dot{m}_a/D$

CONSTRAINT: volume = volume required

VARIABLES: X_i

PROCEDURE: evaluate $\partial f/\partial X_i$

CFD ROLE IN OPTIMIZATION

One of the objectives of this study is to show how CFD and products of CFD are used in an optimization technique.[2,5] The purpose of CFD analysis is to compute the aerodynamic flow and forces for a given object shape. Therefore, the input shape geometry is the most important factor that determines flow characteristics.[6,7,8]

CFD methods are the main tool to analyze and generate the aerodynamic sensitivity derivatives. Normally, CFD analysis is performed for at least three different points for a given variable. For example, to compute $\partial L/\partial\alpha$ as an element of the local sensitivity derivatives matrix, L must be evaluated at three different α's. By using three points, the nonlinear effect due to α change can be easily integrated into the optimization process.

If the nonlinear effect is very strong, more than three points can be used. Also, if L is evaluated for wide range of α once the same curve can be used for the optimization without reconstructing $\partial L/\partial\alpha$ curve.

C_L VS ANGLES OF ATTACK OF STATICALLY DEFORMED WING FOR

TRANSONIC AND SUPERSONIC FLOW CONDITIONS

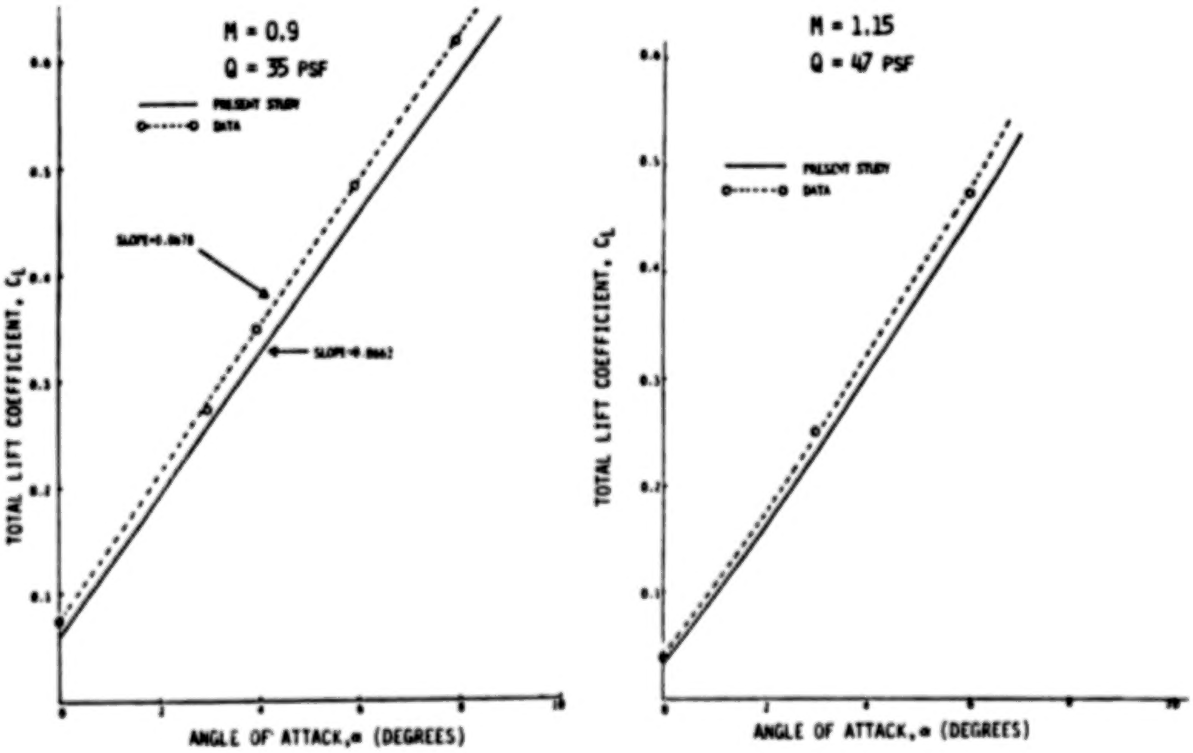

EULER-MARCHING CODE

The current NAA Euler marching code (EMTAC-MZ)[9] solves a set of Euler equations for a complex 3-D configuration across the Mach number range. In the code, a finite volume, multizone implementation of high accuracy total variation diminishing (TVD) formulation (based on Roe's scheme) is used. This code has been applied for numerous configurations including shuttle orbiter with external tank and solid rocket boosters, and the F-14 fighter. It has proved to be accurate as well as robust.

Aerodynamic pressure forces are computed on the 3-D body surface which is contoured in the perpendicular plane to the longitudinal direction as shown in figure below. The pressure forces are summed in the mean plane where structural influence coefficients (SIC) are defined. This process is repeated for each station where SIC's are present.

CONE SHAPE FOREBODY EULER-MARCHING MODEL

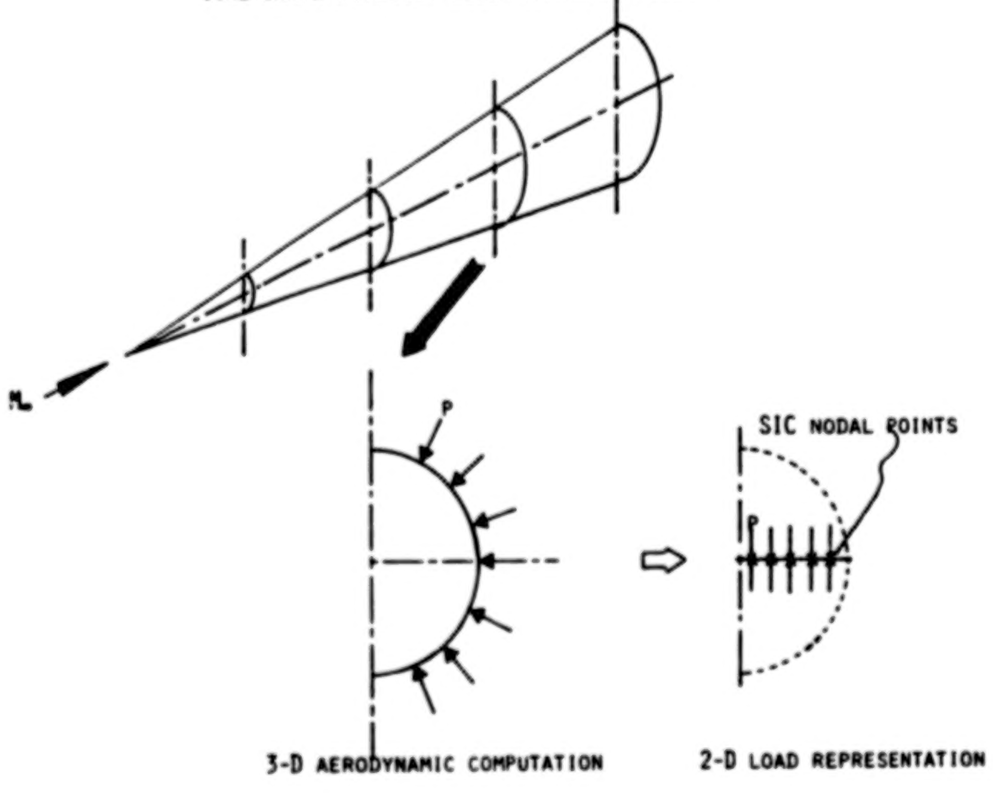

SIC VS MODAL APPROACH

While it is possible to conduct static and dynamic aeroelastic analyses starting either with direct SIC's or with modal data, the modal approach has some advantages in providing a measure of physical insight into the aeroelastic phenomena. Also, there is a very serious disadvantage to the SIC approach: the SIC approach tends to produce surface ripples which are not present in the modal approach. This type of ripple could produce unwanted shocks or the code may blow up if it is severe enough. In order to avoid this problem, the modal approach was taken for this study. The modal approach can reduce the size of the sensitivity derivatives matrix significantly due to utilization of generalized coordinates.

ADVANTAGES OF MODAL APPROACH

- The deformed shape is smooth and does not have any abrupt geometry slope changes (good for aerodynamic analysis)
- No need for extra smoothing operation of body geometry
- The system is considered a summation of known shapes (modal data); thus, variables can be reduced significantly by generalization
- Each mode shape has a physical meaning and is easy to identify, ie., 1st bending, 1st torsion, etc

ISSUES OF GRID TRANSFORMATION

- CFD - FEM grid transformation

  through interpolation techniques

- CFD - generalized coordinates transformation

  through MODE shapes

- FEM - generalized coordinate transformation

  through CFD-generalized coordinate transformation

SENSITIVITY DERIVATIVES

The two disciplines in this study are aerodynamics and structure. Aerodynamic discipline computes generalized lift and drag. Also, $\dot{m}_a/D$ is computed at a specified location. Structure discipline computes SIC with FEM model and mode shapes from vibrational analysis. Thus, the following is the sensitivity derivative matrix

$$\begin{array}{c|ccc|} & L_i & \mu & M_j \\ L_i & 1 & 0 & -\frac{\partial f(L)}{\partial M} \\ \mu & 0 & 1 & -\frac{\partial f(\mu)}{\partial M} \\ M_j & -\frac{\partial f(M)}{\partial L} & \cancelto{0}{-\frac{\partial f(M)}{\partial \mu}} & 1 \end{array} \left\{ \begin{array}{c} \frac{\partial L}{\partial X} \\ \frac{\partial \mu}{\partial X} \\ \frac{\partial M}{\partial X} \end{array} \right\} = \left\{ \begin{array}{c} \frac{\partial f(L)}{\partial X} \\ \frac{\partial f(\mu)}{\partial X} \\ \frac{\partial f(M)}{\partial X} \end{array} \right\}$$

where $\mu = \dot{m}_a/D$, $f(L)$, $f(\mu)$ and $f(M)$ are functions of aerodynamic force, mass flow rate and mode shape respectively. Also,

$\partial f(L_i)/\partial M_j$ - change in aerodynamic force due to change in mode shape

$\partial f(\mu)/\partial M_j$ - change in mass flow rate due to change in mode shape

$\partial f(M_j)/\partial L_i$ - change in mode shape due to change in aerodynamic force

$\partial L_i/\partial X_k$, $\partial \mu/\partial X_k$ and $\partial M_j/\partial X_k$ - global sensitivity derivatives with respect to the design parameter X_k

$\partial f(L_i)/\partial X_k$, $\partial f(\mu)/\partial X_k$ and $\partial f(M_j)/\partial X_k$ - change in aerodynamic force, mass flow rate, mode shape due to design parameter change

i is generalized force index
j is mode shape index
k is design parameter index

ISSUES OF GENERATING SENSITIVITY DERIVATIVES

The terms $\partial f(L)/\partial M$, $\partial f(\mu)/\partial M$, $\partial f(L)/\partial X$ and $\partial f(\mu)/\partial X$ are easy to compute since CFD operation requires geometry input and M and X relate this input geometry directly. The $\partial f(M)/\partial L$ and $\partial f(M)/\partial X$ computations, on the other hand, are not easy due to introduction of the generalized coordinate which requires special treatment. This special treatment is shown below.

COMPUTATION OF $\partial f(M)/\partial L$

$$\text{Given } \{p_G\} = [M]^T\{p_D\} \text{ and } \{\delta_D\} = [M]\,\{\delta_G\}$$

where P is load, δ is deflection, [M] is mode shape matrix, subscript G is generalized, and D is SIC nodal coordinate systems. The potential energy, U, is

$$U = (1/2)\{\delta_D\}^T\{p_D\} = (1/2)\{\delta_G\}^T\{p_G\}$$

Since $\{\delta_D\}=[sic]\{p_D\}$, the above equation will take the following form:

$$\begin{aligned} U &= (1/2)\{\delta_D\}^T\{p_D\} \\ &= (1/2)\{\delta_D\}^T[sic]^{-1}\{\delta_D\} \\ &= (1/2)\{\delta_G\}^T[M]^T[sic]^{-1}[M]\{\delta_G\} \\ &= (1/2)\{\delta_G\}^T\{p_G\} \end{aligned}$$

Therefore, $\{\delta_G\} = [\ [M]^T[sic]^{-1}[M]\ ]^{-1}\ \{p_G\} = [B]\{p_G\}$ and the specific relationship matrix [B] is the sensitivity.

COMPUTATION OF $\partial f(M)/\partial X$

Based on the sensitivity matrix [B], $\partial f(M)/\partial X$ is computed as;

$$\begin{tikzcd}
 & FEM^+ \arrow[r] & {[sic]^+} \arrow[r] & {[B]^+} \arrow[r] & \{\delta_G\}^+ = [B]^+\,\{p_G\}_0 \\
FEM_0 \arrow[ur, "+\Delta X"] \arrow[dr, "-\Delta X"'] & & & & \\
 & FEM^- \arrow[r] & {[sic]^-} \arrow[r] & {[B]^-} \arrow[r] & \{\delta_G\}^- = [B]^-\,\{p_G\}_0
\end{tikzcd}$$

where 0 is the fixed condition, ΔX is the perturbation. From this process, $\partial f(M)/\partial X = (\{\delta_G\}^+ - \{\delta_G\}^-)/(2\Delta X)$ is computed.

CONFIGURATION CRITERIA

A simple cone type forebody hypersonic configuration has been selected. Flow condition is selected as $M_\infty = 16$, $\alpha = 0.0$ and the dynamic pressure, Q, of 1500 psf. Also, this study is a simulation of a wind tunnel model so that the aft section of the vehicle is fixed in space. Consequently, no free-free mode shapes are introduced. The three mode shapes used here are all structural mode shapes.

FLOW CONDITION

$M_\infty = 16.0$

$\alpha = 0.0$

$Q = 1{,}500$ psf

HYPERSONIC VEHICLE FOREBODY CONFIGURATION

3-D VIEW

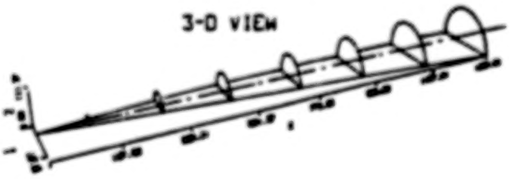

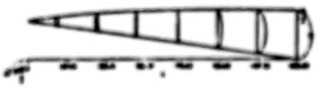

AERODYNAMIC MODEL

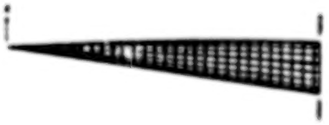

FEM MODEL

VIBRATIONAL ANALYSIS AND MODE SHAPES

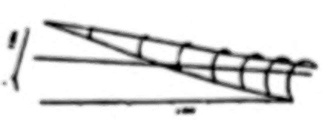

1ST BENDING 0.76 HZ

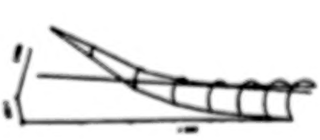

2ND BENDING 2.3 HZ

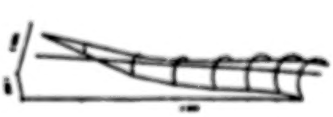

3RD BENDING 3.5 HZ

DESIGN PARAMETER SELECTIONS

A total of four design parameters are selected from previous experiences. They are length, vertical nose position, keel line shape, and fuselage radius. A volume constraint (equality type) is also included.

SELECTED DESIGN PARAMETERS

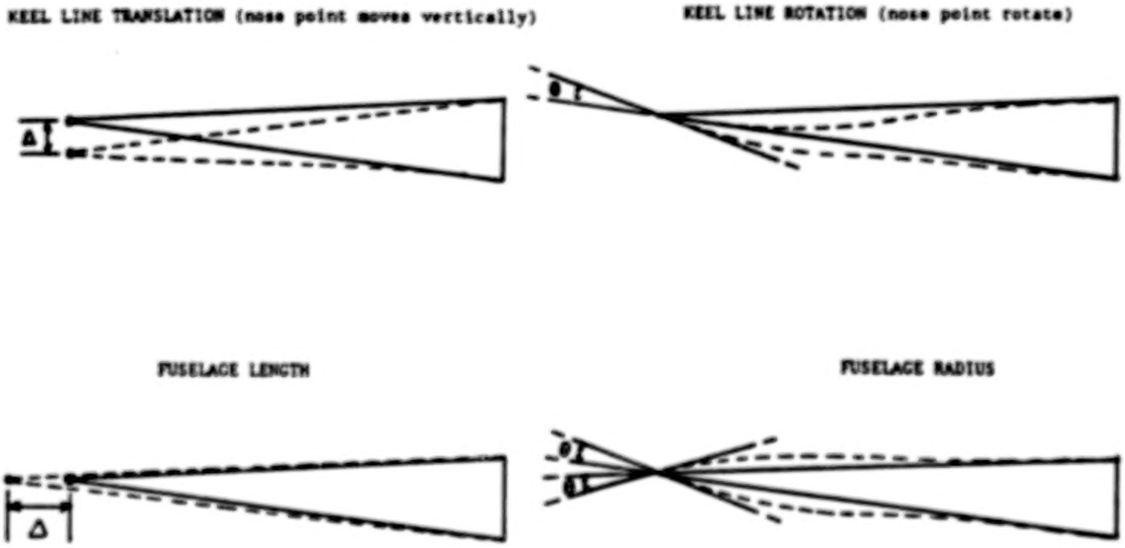

KEEL LINE TRANSLATION (nose point moves vertically)

KEEL LINE ROTATION (nose point rotate)

FUSELAGE LENGTH

FUSELAGE RADIUS

EFFECT OF THE MODAL SHAPE ON AERODYNAMICS

The three mode shapes computed by the structural analysis were analyzed by the Euler marching code. The results are shown in the figure below. They were then used to calculate the local sensitivities which were fed into the global sensitivity equations. The first and second bending modes produced a decrease in $\dot{m}_a/D$, while mode three showed a considerable increase.

HYPERSONIC FLOW CHANGES DUE TO ELASTIC EFFECT

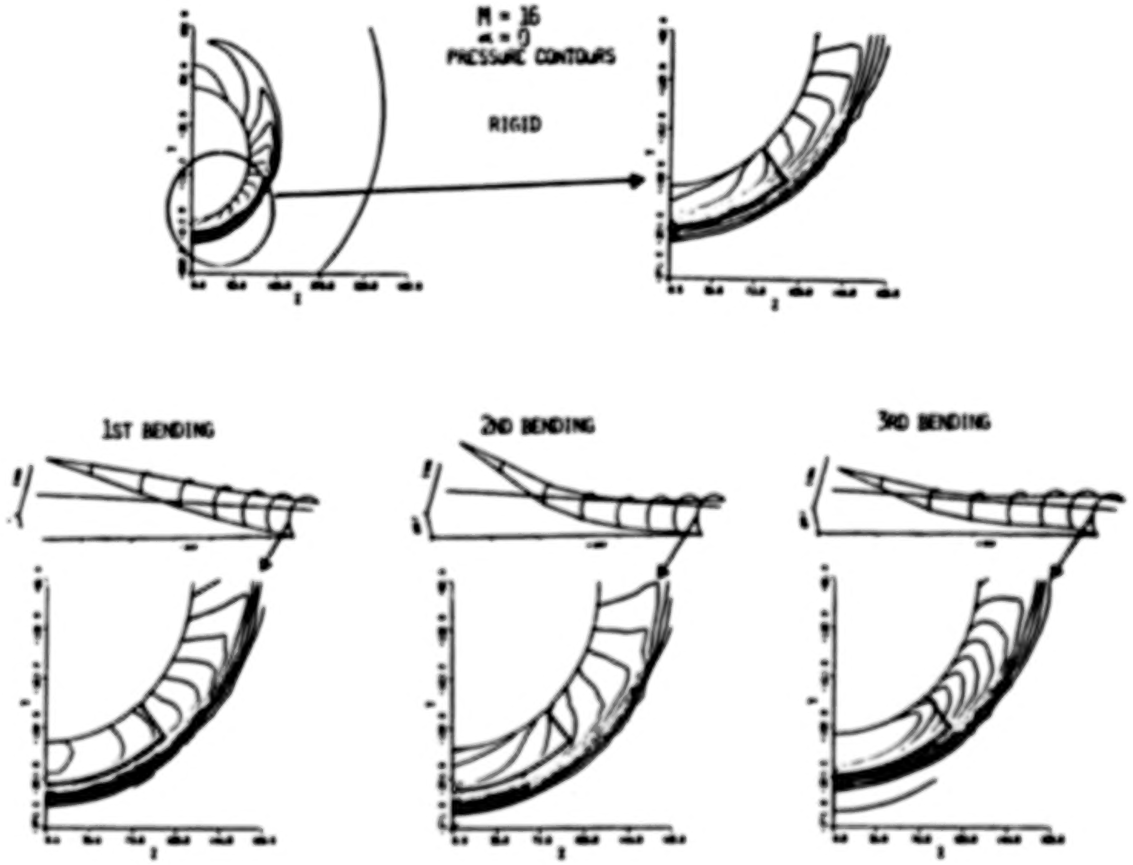

AERODYNAMIC SENSITIVITIES TO DESIGN PARAMETERS

The aerodynamic sensitivities were obtained using computational fluid dynamics (CFD). A baseline analysis was computed. Then, analysis was performed for a positive and a negative perturbation of each design parameter. The results for the two design parameters which effect the translation and rotation of the keel line are presented in the figure below. These parameters affect the objective function, but they have no effect on the volume constraint.

SENSITIVITY OF OBJECTIVE FUNCTION TO KEEL LINE SHAPE

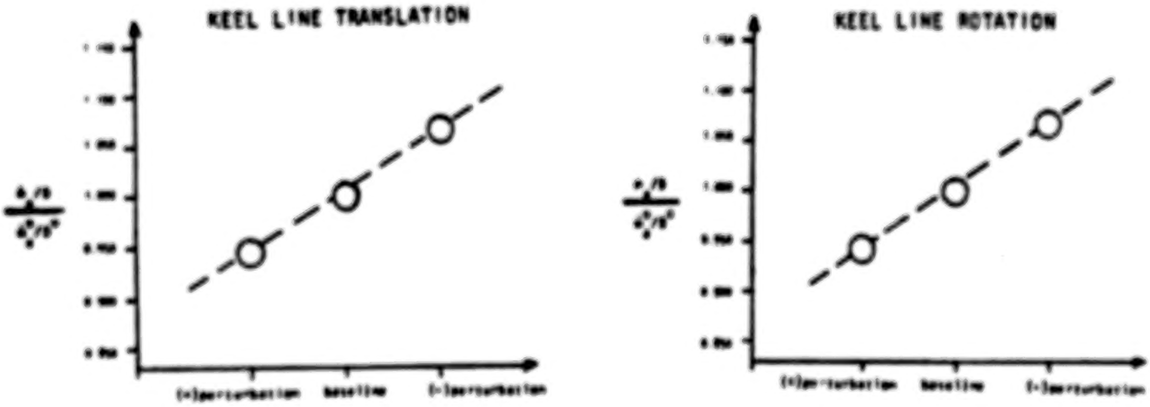

AERODYNAMIC SENSITIVITIES (CONCLUDED)

The length and radius of the fuselage directly affect the volume constraint. The results for these two parameters are shown in the figure below. During the optimization process, there will be a trade-off between these two variables inorder to maintain the same volume.

SENSITIVITY OF OBJECTIVE FUNCTION
TO THE LENGTH AND RADIUS OF THE FUSELAGE

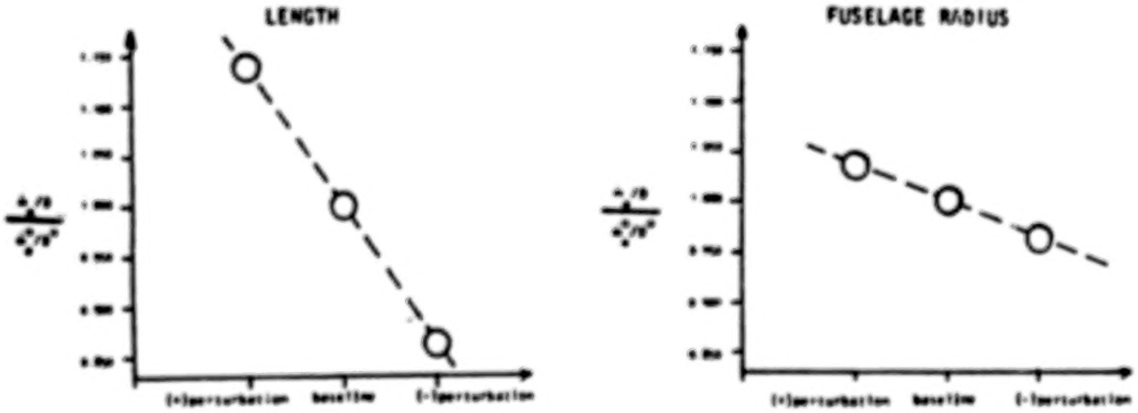

BEST COPY AVAILABLE

STRUCTURAL ANALYSIS

Structural sensitivity derivatives are generated by using Rockwell, NAA's rapid structural optimization program (RSOP)[10] which includes FEM generation, structural analysis and optimization, thermal analysis and automatic data/grid transformation. The trend study of the RSOP analysis for the selected design parameters shows that the fuselage radius is the dominant parameter. The results of the RSOP analysis of the forebody shapes due to parameter change are shown below.

DESIGN PARAMETERS TREND FOR STRUCTURAL ANALYSIS

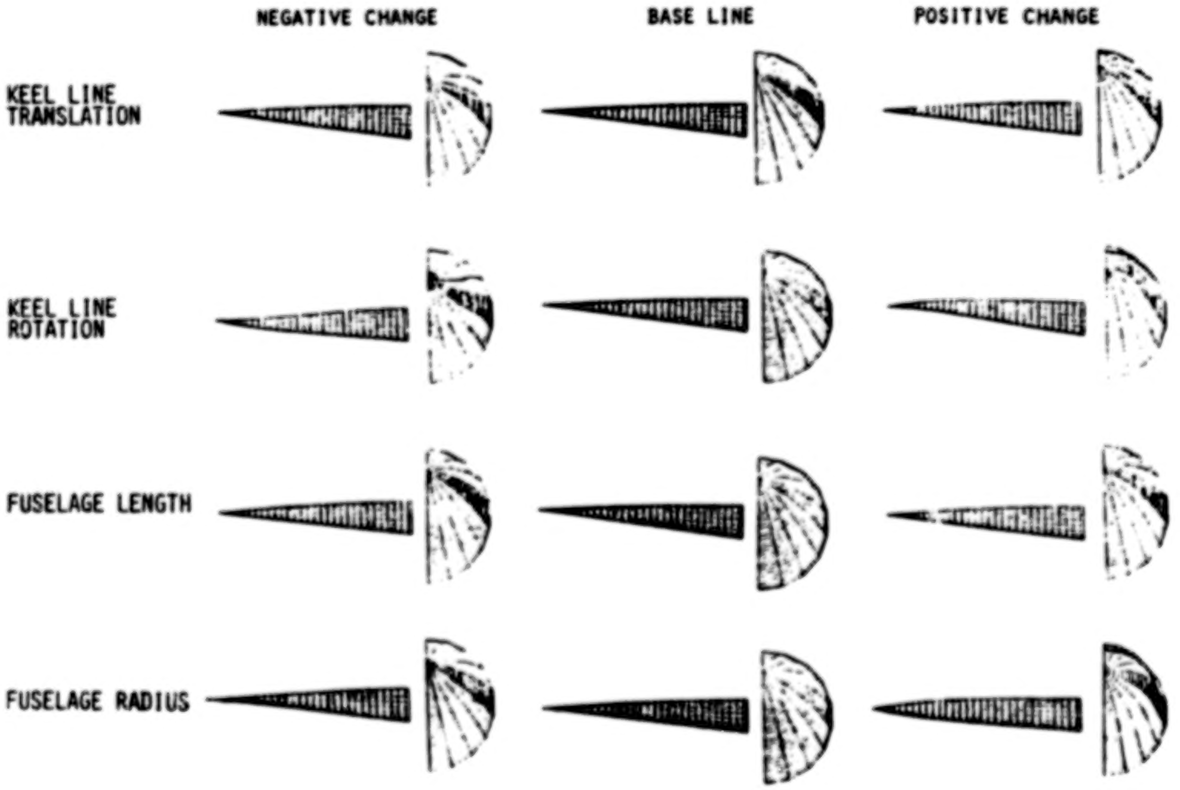
NEGATIVE CHANGE
BASE LINE
POSITIVE CHANGE
KEEL LINE TRANSLATION
KEEL LINE ROTATION
FUSELAGE LENGTH
FUSELAGE RADIUS

BEST COPY AVAILABLE

OPTIMIZATION RESULTS

Optimization was performed for a rigid (aerodynamics only) and a flexible (aerodynamics and structures) forebody. The results for each are presented in the figure below. The results were computed using ADS[11] with ISTRAT-0 (no strategy, go directly to optimizer), IOPT-4 (Method of Feasible Directions), and IONED-7 (find the minimum of an constrained function by first finding bounds and then using polynomial interpolation). A volume equality constraint was employed. The results shown are a first pass through the optimizer. At this point the process would continue by first analyzing the present shape, this shape then becomes the new baseline. Next, the local sensitivity analysis is performed about the new baseline and they are fed into the global sensitivity equations. The new global sensitivities are then used by the optimizer to produce a new optimized shape. This process is repeated until a converged shape is obtained.

FIRST PASS OPTIMIZATION RESULTS

Rigid	Flexible
Change in design parameters	
- increased length (31.36 in.)	- decreased length (0.55 in.)
- decrease in fuselage radius	- increase in fuselage radius
- nose tip moved downward	- nose tip moved downward
- negative keel line rotation	- negative keel line rotation
Objective function value (normalized)	
OBJECTIVE - 1.08345	OBJECTIVE - 1.05871

REFERENCES

1. Shih, P. K., Prunty, J. and Mueller, R. N., "Thermostructural Concepts for Hypervelocity Vehicles," AIAA paper No. 88-2295, Presented at 29th SDM Conference, Williamsburg, VA, April 1988.

2. Sobieski, J. S., "The Case for Aerodynamic Sensitivity Analysis," NASA-CP 2457, Sensitivity Analysis in Engineering Proceedings, NASA Langley, Hampton, VA.

3. Sobieski, J. S., "On the Sensitivity of Complex, Internally Coupled Systems," AIAA paper No. 88-2378, Presented at 29th SDM Conference, Williamsburg, VA, April 1988.

4. Sobieski, J. S., Bloebaum, C. L., and Hajela, P., "Sensitivity of Control-Augmented Structure Obtained by a System Decomposition Method," AIAA Paper No. 88-2205, Presented at 29th SDM Conference, Williamsburg, VA, April 1988.

5. Ide, H., Abdi, F. F. and Shankar, V. J., "CFD Sensitivity Study for Aerodynamic/Control Optimization Problems," AIAA Paper 88-2336, Presented at 29th SDM Conference, Williamsburg, VA, April 1988.

6. Shankar, V. J., and Ide, H., "Treatment of Steady and Unsteady Flows Using a Fast, Time-Accurate Full Potential Scheme," AIAA Paper No. 85-4060, Presented at 3rd Applied Aerodynamics Conference, Colorado Springs, Colorado, Oct. 14-16, 1985.

7. Ide, H., and Shankar, V. J., "Applications of A Fast, Time Accurate Full Potential Scheme to A Statically Flexible Wing in the Transonic Regime," AIAA Paper 87-0707-CP, AIAA/ASME/ASCE/AHS 28th Structures, Structural Dynamics and Material Conference, April 6-8, 1987.

8. Ide, H., and Shankar, V. J., "Unsteady Full Potential Aeroelastic Computations for Flexible Configurations," AIAA Paper No. 87-1238, AIAA 19th Fluid Dynamics, Plasma Dynamics and Laser Conference, Hawaii, June 8-10, 1987.

9. Szema, K. Y., Chakravarthy, S. R., Pan, D., Bihari, B. L., Riba, W. T., Akdag, V. M. and Dresser H. S., "The Application of a Unified Marching Technique for Flow Over Complex 3-Dimensional Configurations Across the Mach Number Range," AIAA paper NO. 88-0276, Presented at 26th Aerospace Sciences Meeting, Reno, Nevada, Jan 1988.

10. Abdi, F. F., Austel, L. G. and Chang, P. W., "An Approach to an Aero/Thermal/Elastic Design System," AIAA Paper No.88-2383, Presented at 29th SDM Conference, Williamsburg, VA, April 1988.

11. Vanderplaats, G. N., Sugimoto, H. and Sprague, C. M., "ADS-1: A New General Purpose Optimization Program," AIAA Journal, Vol. 22, NO. 10, Oct 1984.

HYPERSONIC AIRBREATHING VEHICLE CONCEPTUAL DESIGN
(FOCUS ON AERO-SPACE PLANE)

James L. Hunt
NASA Langley Research Center
Hampton, Virginia
and
John G. Martin
Planning Research Corporation
Hampton, Virginia

FUNDAMENTALS OF AERO-SPACE PLANE DESIGN

INTRODUCTION

Hypersonic airbreathing vehicles are highly integrated systems involving strongly coupled, multi-discipline technologies. These vehicular visions and/or applications are now guiding a hypersonic technology maturation effort. In prioritizing the technology issues and focusing the research activity as well as setting goals for this endeavor, it is important to be able to examine the vehicle design options and performance envelope. This vehicle examination, the conceptual design process, requires unique evaluation procedures and analytical tools in all major technical disciplines.

The design procedure, to a considerable extent, depends on the nature of the vehicle to be examined and the design philosophy. In todays hypersonic scenarios, both cruise and accelerator type vehicles are of interest with visions such as the aero-space plane embodying both capabilities. The commonality shared by these hypersonic vehicles is that all operate within an airbreathing corridor; they will be powered by air breathing engines -- a subsidiary engine cycle for low-speed acceleration, ramjets to Mach 5, and scramjets to potentially Mach 20 plus -- and will take off and land horizontally on standard runways. Some will be designed to ascend to cruise at hypersonic speeds, Mach 6 to 12, twenty or more miles above the ground; others will continue to accelerate upward through an airbreathing corridor to Mach 25 and, with minimal rocket power, transition to a low earth orbit, one hundred miles up.

CRUISER VERSUS ACCELERATOR (ORBITER)

The technology itself represents the capability to cruise and maneuver into and out of the atmosphere, to provide rapid response for low-earth-orbit missions, or to attain very rapid transport service between remote Earth destinations. But, there are differences between configurations dedicated to cruise and those that accelerate to orbit. The accelerator must have a much bigger inlet area relative to body cross-section than the cruiser in order to facilitate sufficient thrust margin, and thus sufficient acceleration, to reach orbital speed. Acceleration time must be minimized so that the integrated drag loss in the air-breathing corridor is kept within manageable bounds. On the other hand, the cruiser requires no thrust margin at the design cruise speed. For the accelerator, the primary aerodynamic issue is minimizing configuration drag near zero angle of attack, while for the cruiser, the task is to maximize configuration lift-to-drag ratio at the design point; both are performed under specific volume-to-planform-area constraints. In structures, the differences are mainly in the design of the leading edges (materials and/or cooling) and the tank insulation -- the accelerator is heating rate impacted while the concern for the cruiser is heat load.

Basic Equation

Cruise:

$$\text{RANGE} = \frac{V\, I_{sp} \frac{L}{D} \ln \frac{w_i}{w_f}}{1 - \frac{V^2}{V_s^2}}$$

Where: V = Velocity
I_{sp} = Specific impulse
L/D = Lift to drag ratio
w_i/w_f = Initial to final weight ratio
V_s = Orbital velocity

Acceleration:

$$\Delta V = g\ I_{sp_{eff}}^{*}\ \ln \frac{w_i}{w_f}$$

$$\text{where}\quad I_{sp_{eff}}^{*} = \frac{\Delta V}{\int_{\Delta V} \frac{dV}{I_{sp_{eff}}}}$$

$$\text{and}\quad I_{sp_{eff}} = \frac{T-D}{\dot{m}} = \frac{\text{Thrust - Drag}}{\text{Fuel flow rate}}$$

ENGINE/AIRFRAME INTEGRATION

Of the three distinguishing factors mentioned, the inlet area and in turn propulsion/airframe integration will be the dominant factor in shaping both the cruiser and accelerator configurations. This is because the propulsion system is sized at hypersonic speeds and must add minimum drag and weight to the vehicle while still processing as much air as possible. These stipulations are best met by considering the entire underside of the vehicle as part of the propulsion system such that the inlet is contiguous with the fuselage and captures nearly all the air processed by the bow shock. This concept, (ref. 1) referred to as the airframe-integrated design, is illustrated in figure 1. The vehicle forebody will have to provide inlet precompression without seriously compromising the aerodynamics, packaging, and Thermal Protection System (TPS) requirements. Not only must the precompression be efficient, but with modular engines closely stacked side-by-side (shown in figure), the flow must be relatively uniform in the lateral direction, across the speed range and during minor maneuvers, to avoid a complex engine operating schedule. The vehicle afterbody must also serve as a nozzle expansion surface in order to provide net installed performance at the high speeds. Both the hypersonic accelerator and cruiser must rely on this engine/airframe integration scheme; the distinguishing factor(s) between the two become the extent of the engine modular stack within the shock layer (inlet size) and/or the amount of inlet over speed (inlet size) and the amount of LOX augmentation (increases thrust levels at the expense of engine specific impulse.)

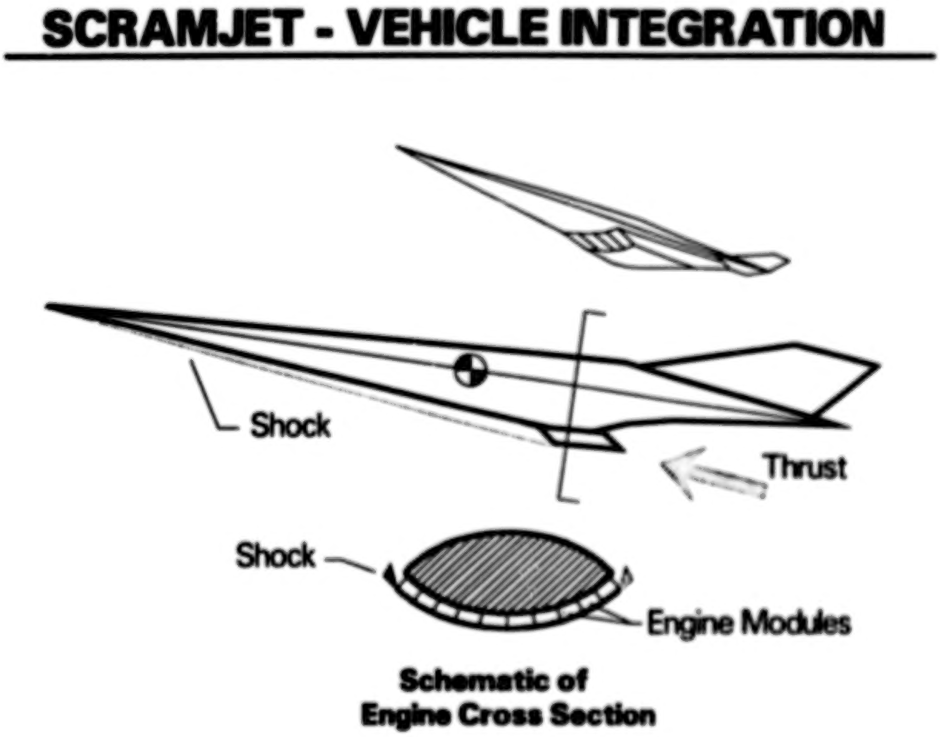

Figure 1

THE AERO-SPACE PLANE MATRIX

If the design is restricted to no inlet overspeed, and extremely light weight materials are available for engine nacelle construction, then the most optimum vehicle configuration could be a flying engine or cone -- cone derivative. But the use of inlet over speed and rocket thrust augmentation opens up the configuration matrix to underslung engine configuration -- especially when more conventional materials are considered for the engine structure and engine weight becomes a factor. See figure 2.

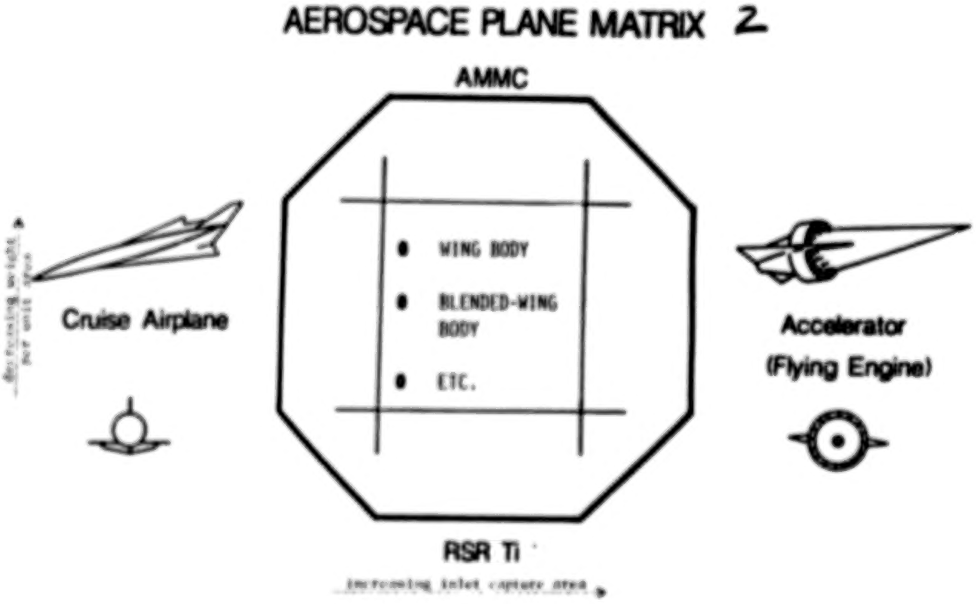
AEROSPACE PLANE MATRIX 2
AMMC
decreasing weight per unit area
Cruise Airplane
WING BODY
BLENDED-WING BODY
ETC.
Accelerator
(Flying Engine)
RSR Ti
increasing inlet capture area

Figure 2

VEHICLE SYNTHESIS

The purpose of this text is to present the conceptual design procedures and tools used for these hypersonic aircraft. Any aircraft design process is a compromise of all the engineering disciplines. An effective design is the integration of aerodynamics, propulsion, structures, and material, flight control, avionics and subsystems, blended in just the right manner to give a complementary effect. This is amplified in hypersonic aircraft design because of the additional acceleration requirements on the vehicle, the high degree of engine airframe integration, and the intrusion of aerothermal loads at the hypersonic speeds; the coupling between the technical disciplines are much stronger and the sensitivities much more intensified. The design process and analytical tool requirements for the hypersonic accelerator and cruiser are similar. Of course, for an orbiter, accomodations must be made for airbreathing acceleration to Mach 20 plus, rocket acceleration to Mach 24, orbital insertion and circulation, deorbit, and reentry; the discipline analytical tools must include the additional Mach delta, stronger viscous interactions, real gas effects in the vehicle flow field -- especially in the boundary layer, finite rate chemistry in the combustor/nozzle, frozen chemistry in the aftbody nozzle, and the transitional and rarefied flow regimes.

DESIGN/SYNTHESIS FLOW CHART

A vehicle design/synthesis flow chart is presented in figure 3. A vehicle concept, once conceived, is evaluated through this process. First, the airframe shape, engine flow path, and area distribution are defined and refined. Options on fuselage structural design (integral, non-integral tank, or aeroshell), and substructure (ring frames and bulkheads, ribs and spars, etc.) wing box and carry-thru, and materials are considered along with internal packaging arrangements. Engine structural design is usually selected between stiffened panel and/or honeycomb with or without ring frame or stringer supports.

Engine/airframe integration is the center of the design process. Here, load paths throughout the vehicle are optimized with particular emphasis on the synthergistic transfer of the thrust load from the engine to the airframe. Inlet and nozzle contours are laid-out; not only are these surfaces common to both the airframe and engine in the nested engine integration approach, they are absolutely crucial to the net performance of the propulsion system, and their importance increases with Mach number. Also, since the aftbody nozzle plays a key role in the trim of the vehicle at hypersonic speeds, control of the vehicle must now be considered.

At this point the design process becomes a true synthesis activity. Sizing and flight performance definition can be, and often is, performed in one synthesis operation with direct constraint coupling, but for the sake of explanation simplicity the discussion shall proceed along parallel fronts.

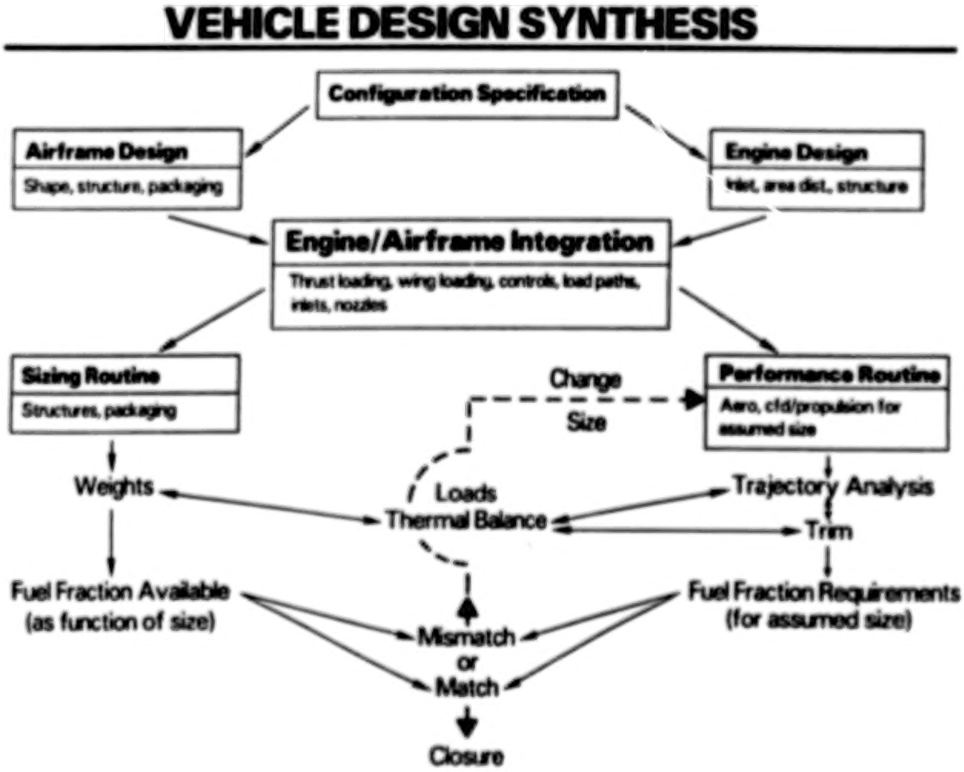
VEHICLE DESIGN SYNTHESIS
Configuration Specification
Airframe Design
Shape, structure, packaging
Engine Design
Inlet, area dist., structure
Engine/Airframe Integration
Thrust loading, wing loading, controls, load paths, inlets, nozzles
Sizing Routine
Structures, packaging
Change
Size
Performance Routine
Aero, cfd/propulsion for assumed size
Weights
Loads
Thermal Balance
Trajectory Analysis
Trim
Fuel Fraction Available (as function of size)
Fuel Fraction Requirements (for assumed size)
Mismatch
or
Match
Closure

Figure 3

DESIGN ASSESSMENT FLOW CHART

The design assessment process with the emphasis on the disciplines and their couplings is shown in figure 4 (ref. 2)

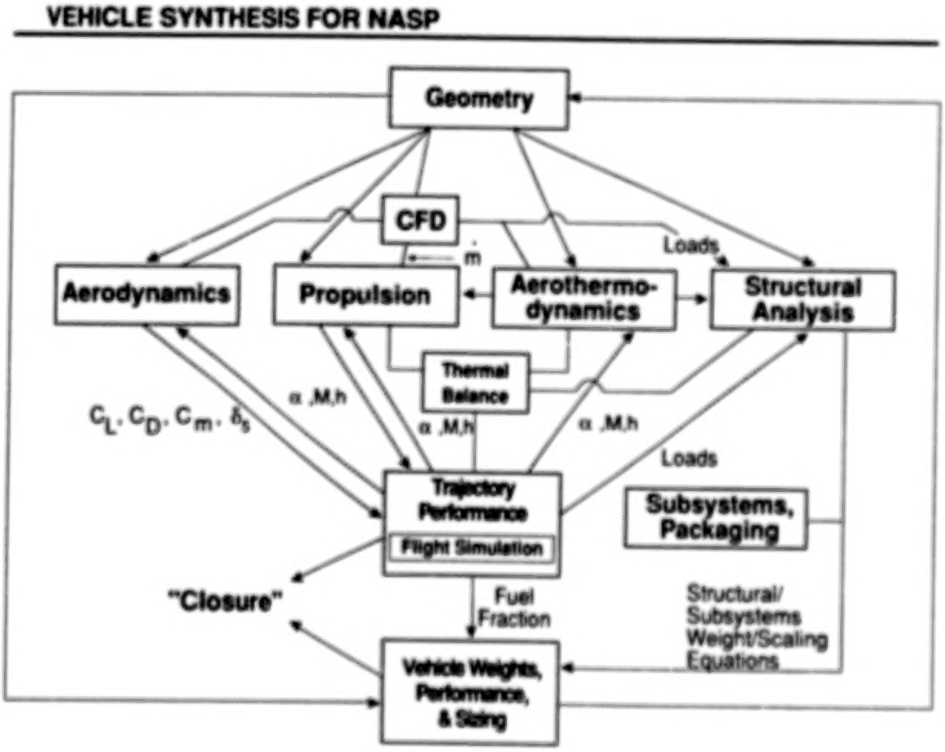
VEHICLE SYNTHESIS FOR NASP
Geometry
CFD
Loads
$\dot{m}$
Aerodynamics
Propulsion
Aerothermo-dynamics
Structural Analysis
Thermal Balance
C_L, C_D, C_m, δ_s
α ,M,h
α ,M,h
α ,M,h
Loads
Trajectory Performance
Flight Simulation
Subsystems, Packaging
"Closure"
Fuel Fraction
Structural/ Subsystems Weight/Scaling Equations
Vehicle Weights, Performance, & Sizing

Figure 4

SIZING

The sizing routine requires scaling relationships for the vehicle subsystem and structure. Subsystem weights are based on a technology enhancement extrapolation of historical algorithms; the scaling relationships are based on vehicle length, gross weight, and applicable areas such as inlet or control surfaces.

Structural weights/scaling are generally based on historical data bases; (ref. 3) such has been used in parametric first order sensitivity screening for the aero-space plane. But, because of the uniqueness of the aero-space plane design and performance sensitivity to weight, higher fidelity options are required. One method is to calculate structural weights based on vehicle loads and failure mode criteria and TPS weights based on a transient thermal analysis of the internal wall construction. Insulation requirements are determined by minimum weight to keep internal structure below material temperature limits -- minimum of combined boil-off and TPS* weight for tank region. Weights of segments of the structure are expressed in power law form as a function of component length or area. From this information set and the fuel density, the sizing routine calculates the fuel fraction available as a function of vehicle gross weight and/or length (figure 5).

---

*Thermal Protection System

VEHICLE SIZING

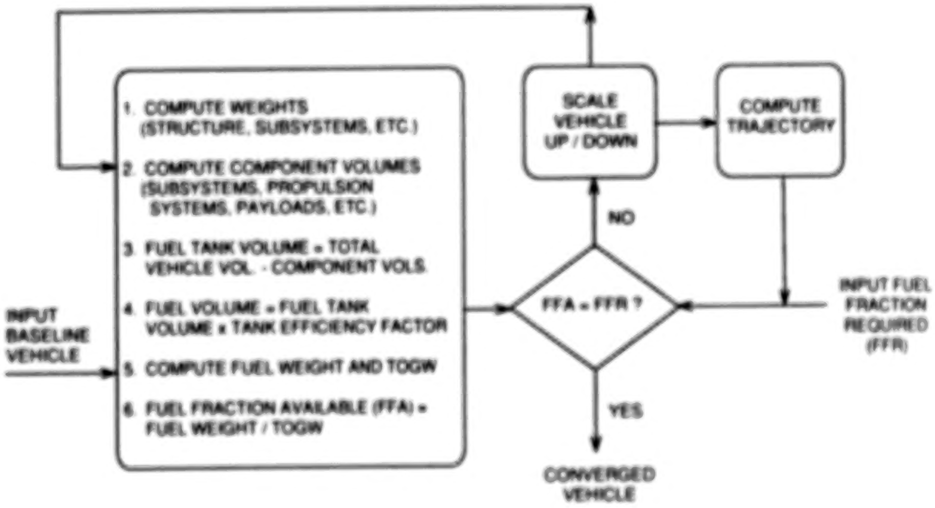
1. COMPUTE WEIGHTS (STRUCTURE, SUBSYSTEMS, ETC.)
2. COMPUTE COMPONENT VOLUMES (SUBSYSTEMS, PROPULSION SYSTEMS, PAYLOADS, ETC.)
3. FUEL TANK VOLUME = TOTAL VEHICLE VOL. - COMPONENT VOLS.
4. FUEL VOLUME = FUEL TANK VOLUME x TANK EFFICIENCY FACTOR
5. COMPUTE FUEL WEIGHT AND TOGW
6. FUEL FRACTION AVAILABLE (FFA) = FUEL WEIGHT / TOGW
SCALE VEHICLE UP / DOWN
COMPUTE TRAJECTORY
NO
FFA = FFR ?
YES
INPUT BASELINE VEHICLE
INPUT FUEL FRACTION REQUIRED (FFR)
CONVERGED VEHICLE

Figure 5

PERFORMANCE/TRAJECTORY

The performance routine is a trajectory code, whether a simple energy-state integration approach or a three-degree of freedom dynamic version. Aerodynamic and propulsion performance are the required inputs. A force accounting scheme is selected -- free stream to free stream or inlet ramp to free stream. In the first, any surface that is washed by flow that goes through the engine is a propulsion surface; in the second, only the surfaces that are washed by engine flow from the beginning of the inlet ramping or cowl lip to the afterbody nozzle exit (free stream) is a propulsion surface. The latter is chosen here, again to expedite the discussion. Since the vehicle size and weight are not yet known, nominal values are selected to begin the iteration. The aerodynamic matrix (lift and drag coefficient, C_L and C_D, as a function of Mach number, angle of attack and altitude, M, α, and h) is calculated for an assumed trajectory bandwidth on dynamic pressure ($500 \text{ psf} \le q \le 2000 \text{ psf}$). Since the ramjet/scramjet cycle performance prediction codes require inlet flow conditions (mass flow, total pressure recovery, and enthalpy) that are contingent on the airframe forebody precompression, forebody flow field solutions over the range of hypersonic flight conditions are required; the boundary layer must be included in these calculations because of the substantial displacement thicknesses at the high speeds that rob the scramjet of air -- thrust is proportional to air mass flow. The cycle calculation provides the internal engine performance and cowl exit conditions for starting the aft body nozzle flow field calculations which are constrained by an external flow boundary. Integration of the pressures on the aftbody wall provides the nozzle forces.

The net engine performance matrix (thrust coefficient and specific impulse as a function of Mach number, angle of attack and fuel equivalence ratio) is then assembled, with the thrust coefficients vectored along the vehicle wind axis and referenced to free stream static in the same manner as the aero coefficients. With this aero/propulsion performance set, the fuel fraction required to perform the ascent (98 percent of fuel requirement), orbital insertion, circularization, and deorbit is determined from the trajectory analysis.

Iterations are now required in the synthesis process to adjust the structure and insulation for the optimum (off-nominal) ascent and descent trajectory and vice versa and to perform an iteration on size/weight in the performance routine. Trim also comes into play here since the afterbody nozzle must be shaped to minimize the trim penalties, especially at the high speeds (Mach 10 plus) and, of course, there is a trajectory and structure coupling in this nozzle tuning.

CLOSURE

The closure of the synthesis process is represented in figure 6 in terms of fuel weight-fraction required and fuel weight-fraction achievable as a function of gross weight for an airbreather ascent to orbital conditions and return with a fixed payload. The closure point is where the two curves cross. The fuel-fraction-required line is nearly independent of gross weight; however, as the vehicle is scaled up geometrically, the increase in wing loading and resultant drag due to lift induces a slight positive slope. The fuel fraction achievable curve increases significantly with gross weight, at least to a point; the bending of the curve to the right (knee) at the larger gross weights is due to the negative influence of size on the structural efficiency. The closure point provides the gross weight/size of the vehicle -- and more: the magnitude of the difference in the slope of the two curves at the closure point is indicative of the margins achievable or viability of the vehicle to performing the mission. If the closure point is near the knee on the fuel-fraction-achievable curve, then a small increase in the fuel fraction requirement to achieve orbit could move the closure point far to the right and substantially increase the gross weight of the vehicle required to perform the mission. In this undesirable closure region, the validity of conceptual design methods are suspect because of the extreme sensitivity; very high fidelity number sets are required to resolve the design.

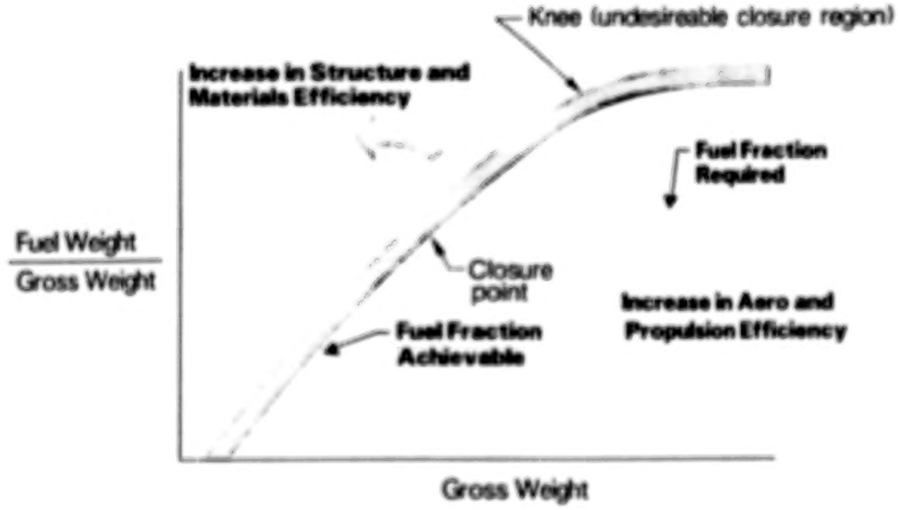

Figure 6

CONE CONFIGURATION SYNTHESIS

The conical configuration shown in figure 7 provides a good starting point/example with regard to configuration synthesis and the aero-space plane problem. In terms of desirable characteristics, its forebody, which provides an excellent precompression surface, also has a relatively thin boundary layer -- more mass flow and momentum to inlet. Also the circular cross-section is desirable from a structural perspective. More important, however, is the flexibility afforded by the conical configuration in such critical areas as engine inlet area which allows the necessary parametrics that provide understanding to the design problem. Also, the ability to make credible analytical predictions required for performance estimates because of the simplicity of the forebody shape is not a small advantage in starting with a conical configuration.

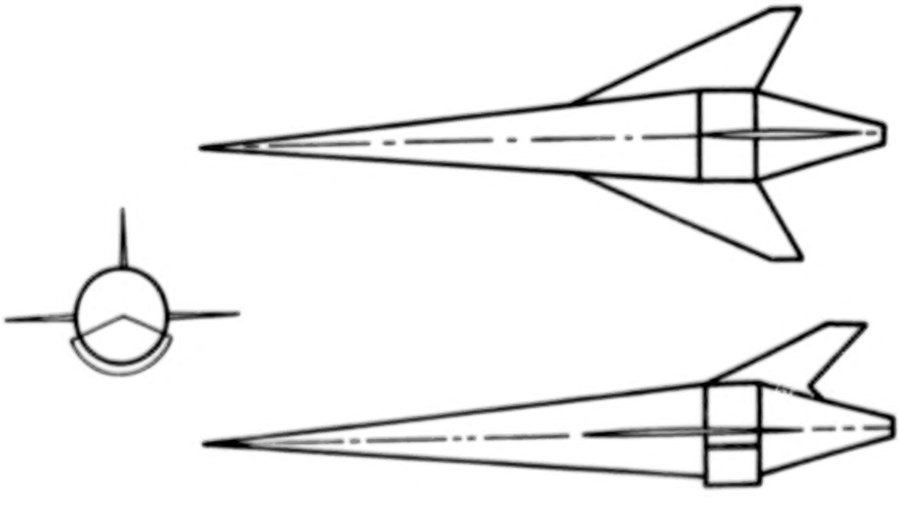

Figure 7

135

BEST COPY AVAILABLE

BOOKKEEPING

A force accounting scheme is selected -- free stream to free stream or inlet ramp to free stream. In the first, any surface that is worked by flow that goes through the engine is a propulsion surface; in the second, only the surfaces that are washed by engine flow from the beginning of the inlet ramping to the afterbody nozzle exit (free stream) is a propulsion surface. For this particular discussion, the classical route of free stream to free stream is used.

In the cycle analysis process, the increased pressure on the captured streamtube due to spillage at the cowl lip is not accounted for. This additive drag must be substracted from the thrust. Also, there is a spillage lift term which must be accounted for -- usually in the aerodynamic matrix.

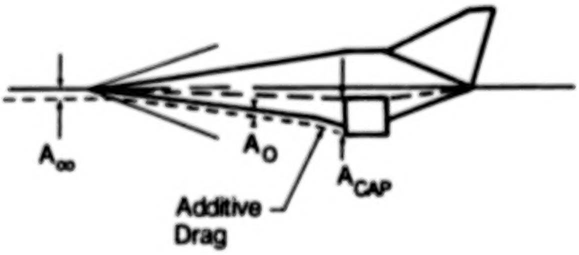

Thrust ➡ Accounts for all forces on surfaces wetted by engine flow

Net propulsive force (NPF)

↳ Thrust- Additive drag

Figure 8

VEHICLE DRAG

In the free-stream to free-stream accounting system, the larger the engine wrap angle, the more surface area that is accounted for in the propulsion matrix, as demonstrated in figure 9. Therefore, for a full engine wrap on a conical configuration, only the lifting and stabilizing/control surface appear in the aerodynamics.

Vehicle Drag Includes All Surfaces Not Wetted By Engine Flow

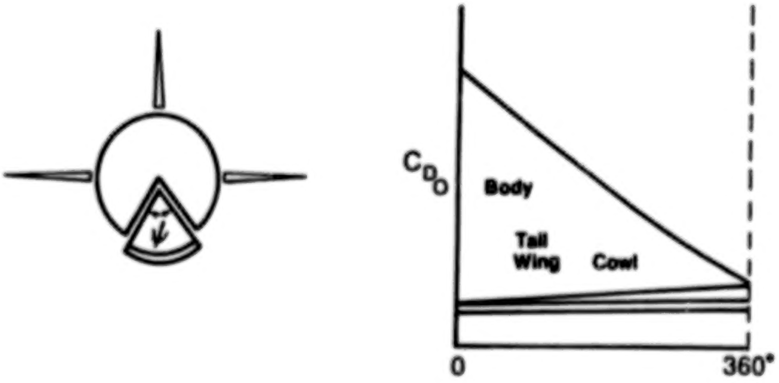

Figure 9

BEST COPY AVAILABLE

CONE CONFIGURATION PERFORMANCE

The cone configuration performance sensitivity can be ascertained from the w/P_s (fuel flow divided by specific excess power) distribution in figure 10 (the trend applies to much higher Mach numbers). Minimizing the area under the curve is minimizing the fuel consumed for the mission. Increasing the thrust to weight or the dynamic pressure (up to a point) for the cone reduces the fuel consumed. Increasing the throttle setting much above an equivalence ratio of 1 increases the fuel consumed (decreases engine I_{sp}).

$$T - D = (C_T - C_D)\, q\, A = (\text{thrust coefficient} - \text{drag coefficient}) \times (\text{dynamic pressure})(\text{reference area})$$

where $C_D = f(M, \text{alt}, \alpha)$ and $C_T = f(M, \text{alt}, \alpha, \phi)$

IMPACT OF T/W ON FUEL FLOW PARAMETER

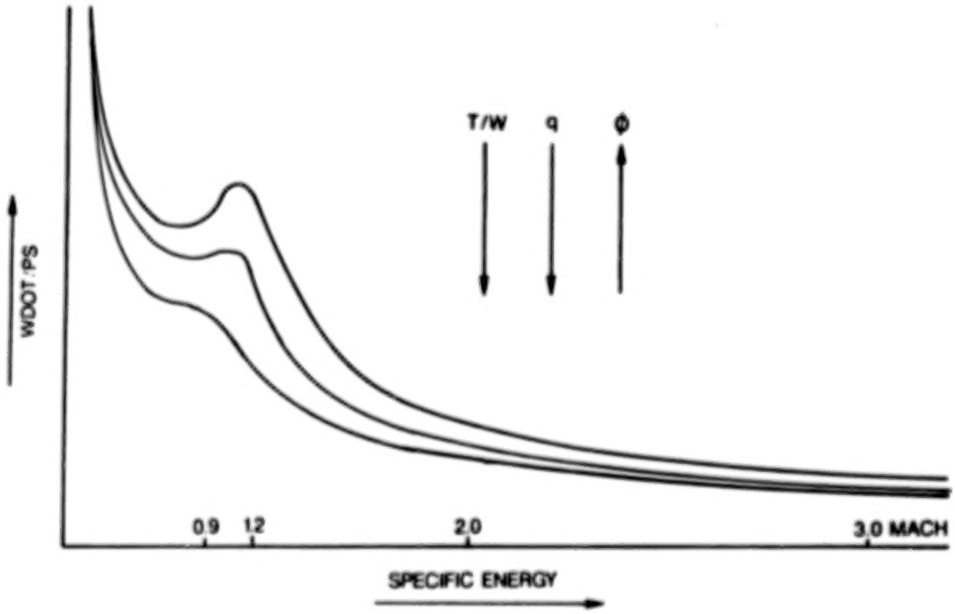

Figure 10

DESIGN TRADES AND SENSITIVITIES

In the design process for SSTO's, the emphasis is on trades that will impact favorably on vehicle closure. Reduction in the fuel weight-fraction required can be realized with improvements in propulsion efficiency and reduction in vehicle drag. The influence of the drag on fuel fraction required is shown in figure 11 for a typical axisymmetric configuration. (The eight percent delta shown in fuel fraction required can be enormous in terms of closure capability.) The fuel weight-fraction achievable curve (fig. 6) moves to the left and rotates counter clockwise (increases) as the structural design and subsystems improve in efficiency and/or the materials advance in terms of strength-to-weight and stiffness-to-weight properties. The immediate discussion focuses on ways of reducing the fuel fraction required which will prove to have indirect and, in some cases, direct coupling to the fuel fraction achievable.

FUEL FRACTION REQUIREMENT SENSITIVITY TO AIRFRAME DRAG LOSS

(CONSTANT q TRAJECTORY)

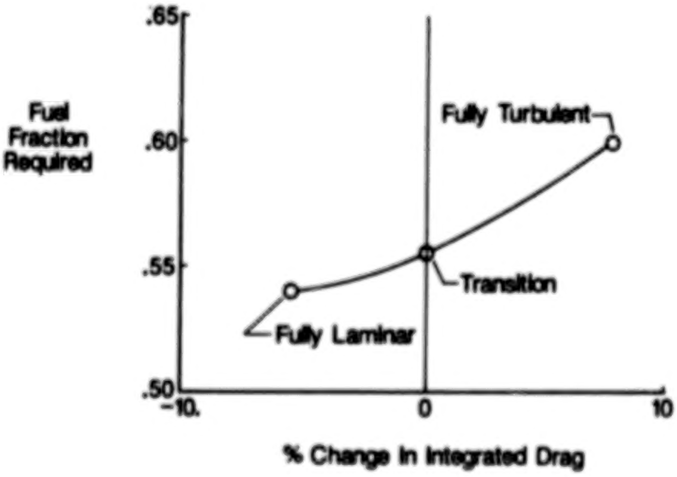

Figure 11

THRUST MARGIN

For an accelerating vehicle, the time derivative of its specific energy is equal to its specific excess power. That is:

$$\frac{d}{dt}\left(\frac{V^2}{2} + gh\right) = \frac{\overset{\text{velocity}}{V}(\overset{\text{thrust margin}}{T-D})}{\underset{\text{weight}}{W}} = P_s = \text{specific excess power}$$

Increasing the thrust margin and/or decreasing the weight of the vehicle for a given velocity increases the instantaneous energy imparted to the vehicle and, as shown in the preceeding article, increasing the ratio of the propulsion energy imparted to the vehicle to that left in the atmosphere reduces the fuel fraction required. The thrust margin is the difference between two large numbers, thrust and drag, which makes it sensitive to small changes in either; both are functions of dynamic pressure:

$$T - D = (C_T - C_D)\underset{\text{dynamic pressure}}{q}\overset{\text{reference area}}{A}$$

Increasing the flight dynamic pressure by flying lower in the atmosphere increases the thrust margin assuming constant thrust and drag coefficients. But the vehicle drag coefficient decreases with increasing dynamic pressure because of the reduction in skin friction coefficient with increasing Reynolds number (the caveat here is boundary-layer transition) and lower drag due-to-lift with decreasing angle of attack since the angle of attack decreases with increasing dynamic pressure in order to maintain a given lift. Also, the thrust coefficient increases with increasing dynamic pressure because of a favorable trend in the ratio of inviscid to viscous forces inside the scramjet engine. Increasing dynamic pressure at the high Mach numbers also maintains a given pressure in the engine combustor at lower inlet contraction ratios so that less energy is lost to gas kinetics in the nozzle expansion process.

DYNAMIC PRESSURE

However, increasing flight dynamic pressure is advantageous only so long as the structure/weight of the vehicle is not unduly affected, which can easily happen because of increased heating rates, loads, and flutter tendencies. Also, the advantages and disadvantages of increasing dynamic pressure are configuration dependent. For example, the thrust margin of axisymmetric configurations should benefit from higher dynamic pressure because these vehicles are being driven toward zero angle of attack where they perform best. This is indicated in figure 12 where the nondimensional take-off gross weight for such a configuration is shown to decrease substantially with increasing dynamic pressure of the trajectory. (The caveats here are boundary layer transition and weight of engines, actively cooled airframe surface area, etc.) On the other hand, the thrust margin for vehicles with underslung engines, such as that shown in figure 1, peaks at modest angles of attack; the thrust increases faster than drag with properly shaped forebodies up to some small angle of attack because of the increase in the air flow and pressure recovery to the inlet system. Any increase in flight dynamic pressure that drives the angle of attack below that for which the thrust margin peaks is detrimental. (This type vehicle could be shaped for high dynamic pressure trajectories but the fineness ratio may be driven to a point of diminishing return.)

EFFECT OF DYNAMIC PRESSURE ON GROSS WEIGHT FOR AN AXISYMMETRIC VEHICLE

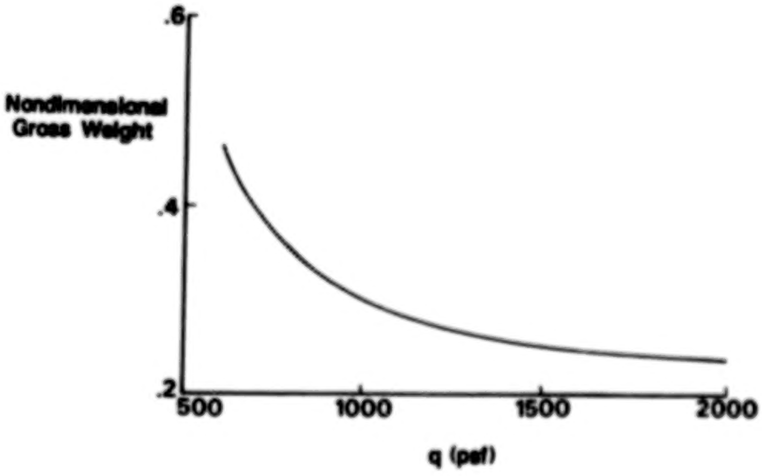

Figure 12

INLET AREA

Of course, there are ways of increasing the thrust margin of these vehicles other than just increasing dynamic pressure -- increasing inlet area and/or air capture area, increasing the fuel equivalence ratio beyond stoichiometric in the combustor, or rocket augmentation. For a given vehicle shape and size, increasing the inlet area decreases the fuel weight-fraction required, but it also decreases the fuel weight-fraction achievable because the engine weight, and thus vehicle dry weight, is increasing (not necessarily linearly) while the fuel weight remains constant. So, as illustrated in figure 13 for a given size vehicle, there is an optimum inlet area that maximizes the payload weight-fraction deliverable to orbit. This is also the case for a vehicle optimized to deliver a fixed payload to orbit as indicated in terms of TOGW (take-off gross weight) in figure 14.

EFFECT OF INLET AREA ON WEIGHT FRACTION

(Fixed size vehicle)

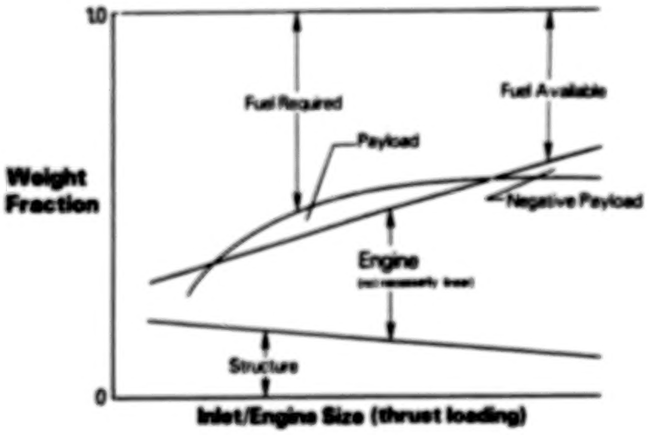

Figure 13

EFFECT OF INLET AREA ON TOGW

(Fixed payload size/weight)

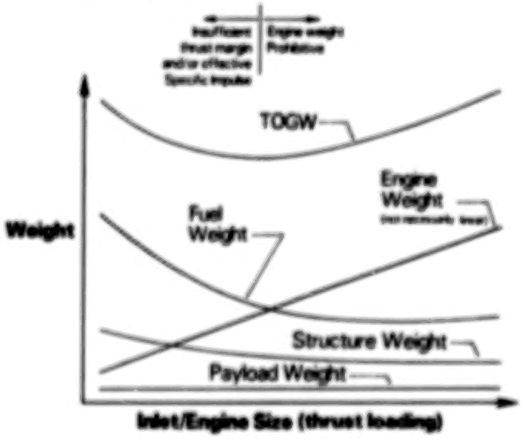

Figure 14

INLET AREA (Continued)

The optimum inlet area depends not only on the engine weight per unit inlet area, but on the engine performance per unit inlet area which is affected by where and how the inlet area is added. The inlet area can be added such that the cowl lip is kept within the shock layer throughout the airbreathing ascent or oversized such that the vehicle bow shock crosses the cowl lip at some designated top-end Mach number, and more of the inlet area protrudes into the free stream as the acceleration proceeds (inlet overspeed). In the first situation there are more limits on increases in inlet area since the shock layer has only a finite amount of thickness at the top end Mach numbers; also, the inlet air capture suffers at the lower Mach numbers. For the overspeed case, more inlet area is possible, and the air capture is greater at the lower Mach numbers; however, the mass flow per unit inlet area is less at the high Mach numbers and so is engine efficiency, but not thrust, since the inlet area is larger.

Rather than, or in addition to, increasing the physical inlet area to facilitate thrust margin, the inlet air capture area can be increased by the optimization of the forebody precompression contour and the trim attitude of the vehicle -- the result of effective engine/airframe integration. The objective is to maximize the capture area while minimizing the parasitic drag area (surfaces that compress air-flow that does not pass through the engines) and still provide the appropriate lift to sustain the vehicle in the airbreathing corridor.

THROTTLE

As for increasing the fuel equivalence ratio beyond stoichiometric, such may be required at the very high Mach numbers to cool the engine, but fortunately the decreases in specific impulse that nominally accompany fuel rich conditions are somewhat nulled; at the very high speeds the thrust benefits of mass injection of the hot, low-molecular-weight hydrogen can be very significant.

ANALYTICAL TOOLS FOR HYPERSONIC VEHICLE DESIGN

AEROSPACE VEHICLE INTERACTIVE DESIGN

Vehicle design codes that consist of an executive with interfaces to geometry generation and to discipline data sets or data set generation capability are essential in conceptual design studies of hypersonic vehicles because of the many variables and couplings involved. The Aerospace Vehicle Interactive Design (AVID) (ref. 2) is a computer-aided design system based on designer participation. Its development began in the mid 1970s using interactive graphics on a minicomputer for geometry modeling of configurations and for interpreting a large volume of data generated on a mainframe computer. The current architecture of the AVID system is shown in figure 15. The core system consists of four separate modules. The key module is the engineering data management system that controls all data and programs. The user interface module aids in the utilization of the system by providing a standard set of commands for system operation. The program interface module utilizes a standard technique for integrating analysis programs into the system or short-circuiting to data sets generated externally. The final module is the geometry system for generating, displaying, modifying and sizing both externally and internally generated configuration data.

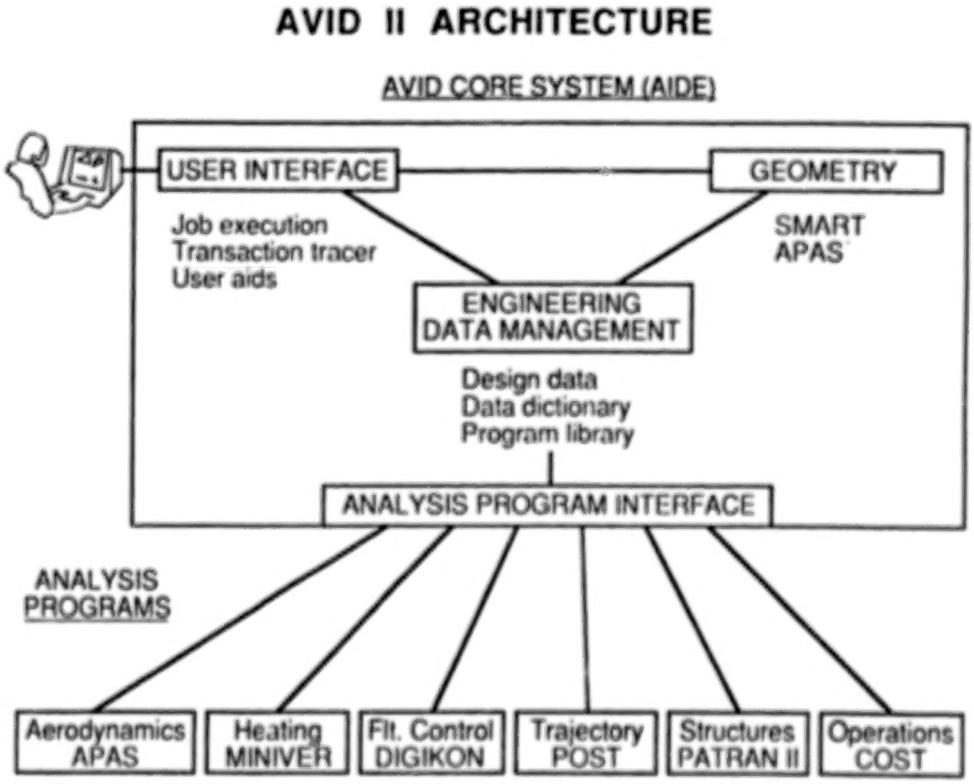
AVID II ARCHITECTURE
AVID CORE SYSTEM (AIDE)
USER INTERFACE
GEOMETRY
Job execution
Transaction tracer
User aids
SMART
APAS
ENGINEERING
DATA MANAGEMENT
Design data
Data dictionary
Program library
ANALYSIS PROGRAM INTERFACE
ANALYSIS
PROGRAMS
Aerodynamics
APAS
Heating
MINIVER
Flt. Control
DIGIKON
Trajectory
POST
Structures
PATRAN II
Operations
COST

Figure 15

AVID GEOMETRY

The geometry capabilities (figure 16) in AVID[*] include external lofting, internal arrangement, and geometry analysis. Present geometry programs in the AVID network are APAS, CDS, GEOMOD, and SMART.

- Capabilities
  - External lofting (creative and duplication modes)
  - Internal arrangement
  - Geometric analysis (areas, volume, cg's, I's)
- Present programs
  - Aerodynamic Preliminary Analysis System (APAS-Rockwell)
  - Configuration Development System (CDS-Rockwell Proprietary)
  - GEOMOD (SDRC-vendor)
  - SMART - LaRC Real Time Solid Modeling

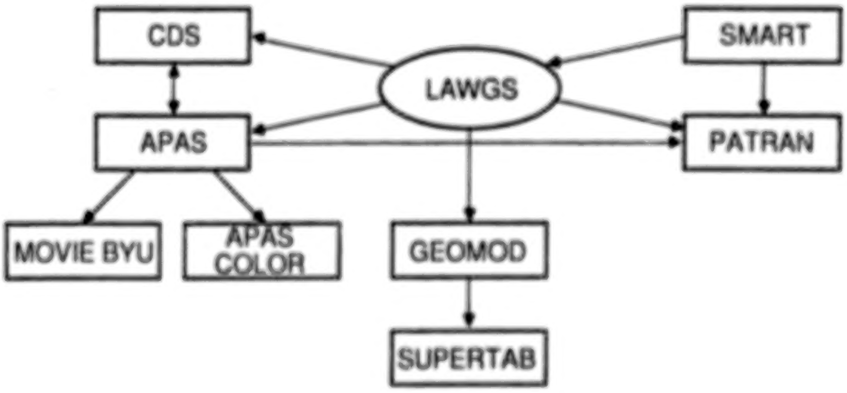
CDS
LAWGS
SMART
APAS
PATRAN
MOVIE BYU
APAS COLOR
GEOMOD
SUPERTAB

Figure 16

---

[*] Advanced Vehicle Interactive Design

AVID's AERODYNAMIC PREDICTION CAPABILITY (APAS)

(As conveyed by Alan W. Wilhite, NASA Langley Research Center)

The Aerodynamic Preliminary Analysis (APAS) (ref. 4) is used to create a total aerodynamic profile for trajectory analysis. In the subsonic/supersonic region, slender-body theory is used to predict fuselage forces and vortex panels to predict wing/tail forces. Skin-friction, wave, and base-drag theories are combined with induced drag to predict total configuration drag. For high speeds, the Hypersonic Arbitrary Body (HAB) program has been integrated into APAS (figure 17). APAS program capabilities and related programs can be seen in figure 18.

AERODYNAMIC PRELIMINARY ANALYSIS SYSTEM

(APAS)

- Rockwell developed and is using for NASP studies
- Subsonic/supersonic analysis
  - Distribute vortex panels with leading edge suction
  - Slender body theory
  - Laminar - Blasius with Echert's compressibility
  - Turbulent - Van Driest
  - Wave drag at angle of attack
  - Hoerner corrections for thickness
  - Base drag derived from Shuttle databook
- Hypersonic arbitrary body program

Figure 17

INTERACTIVE APAS

- Geometry
  - Digitizing
  - Interactive
  - Editing
  - Component panelling
  - Display

- Analysis
  - Geometric parameters
  - Wave drag
  - Viscous drag

- Analysis setup
  - Mach, altitude, α sweep, β
  - Hypersonic method selection
  - Analysis model display

- Output display
  - Coefficients
  - C_p

BATCH APAS

- UDP
  - Vortex panel
  - Viscous drag
  - Wave drag
  - Base Drag

- HABP
  - Impact methods
  - Viscous drag/heating

RELATED PROGRAMS

- Movie BYU – Shaded image

- PATRAN – C_p, T_w display

Figure 18

DRAG PREDICTIONS WITH APAS

The minimum drag coefficient on a five-degree half-angle cone configuration is given in figure 19 as a function of Mach number. Base drag, wavedrag, and viscous plus profile drag are shown. The flipper-door drag is that which resulted from the inward deflection of a flap at the trailing edge of the cowl in order to keep the afterbody nozzle plume attached (fill the nozzle) at transonic speeds.

5° CONE CONFIGURATION DRAG PREDICTIONS

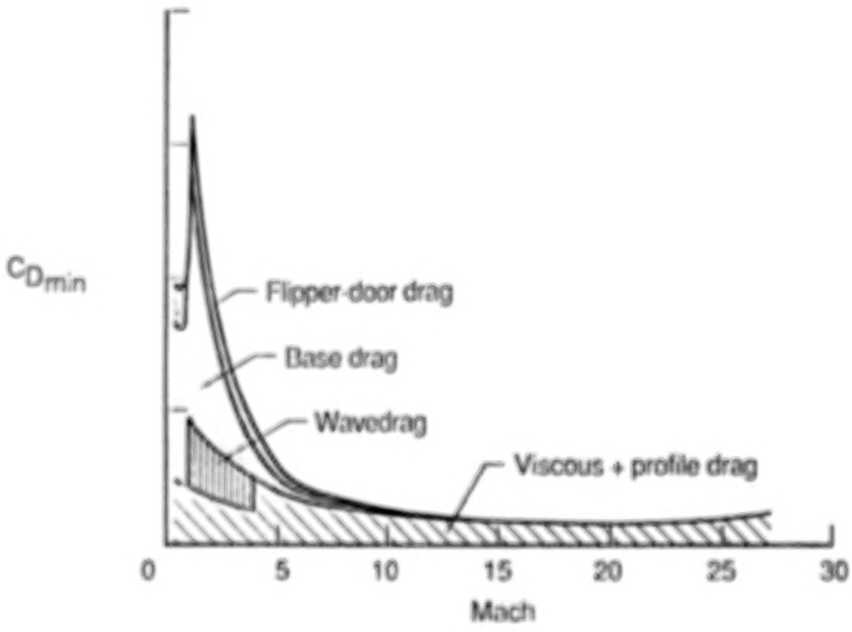

Figure 19

APAS DRAG PREDICTION ON CONE

Minimum drag coefficient is presented as a function of Mach number as shown in figure 20. The APAS predictions (UDP, unified dispersive panel -- vortex panel, viscous drag, wavedrag, and base drag, and the Hypersonic Arbitrary Body Code) are compared with wind tunnel data.

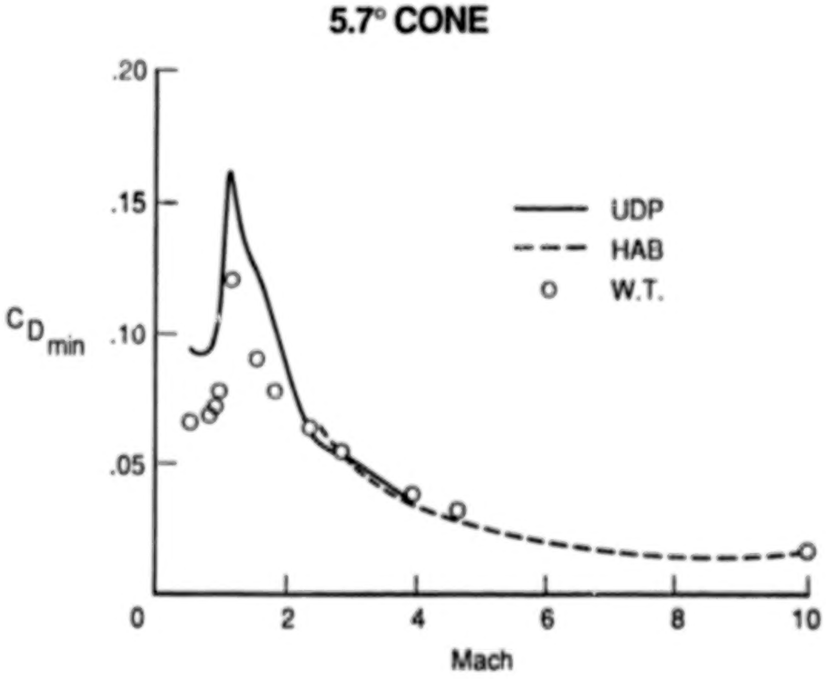

Figure 20

BEST COPY AVAILABLE

AERODYNAMIC COEFFICIENTS COMPARISON

A comparison of the aerodynamics generated on a cone with APAS and a PNS code are shown in figure 21 for Mach 20. A comparison of viscous and inviscid drag contributions, as calculated by APAS and PNS code for a cone at Mach 15 is shown in figure 22.

5° SPHERE-CONE

AOA	CODE	C_A	C_N	C_L	C_D	L/D	C_M
0	APAS	0,0232	0,0	0,0	0,0232	0,0	0,0
	PNS	0,0204	0.0	0,0	0,0204	0.0	0,0
2,5	APAS	0,0251	0,0920	0,0909	0,0291	3,12	-0,7068
	PNS	0,0218	0,0833	0,0823	0,0254	3,24	-0,6412
5,0	APAS	0,0308	0,1849	0,1815	0,0468	3,88	-1,4190
	PNS	0,0256	0,1681	0,1652	0,0405	4,08	-1,2920

Figure 21

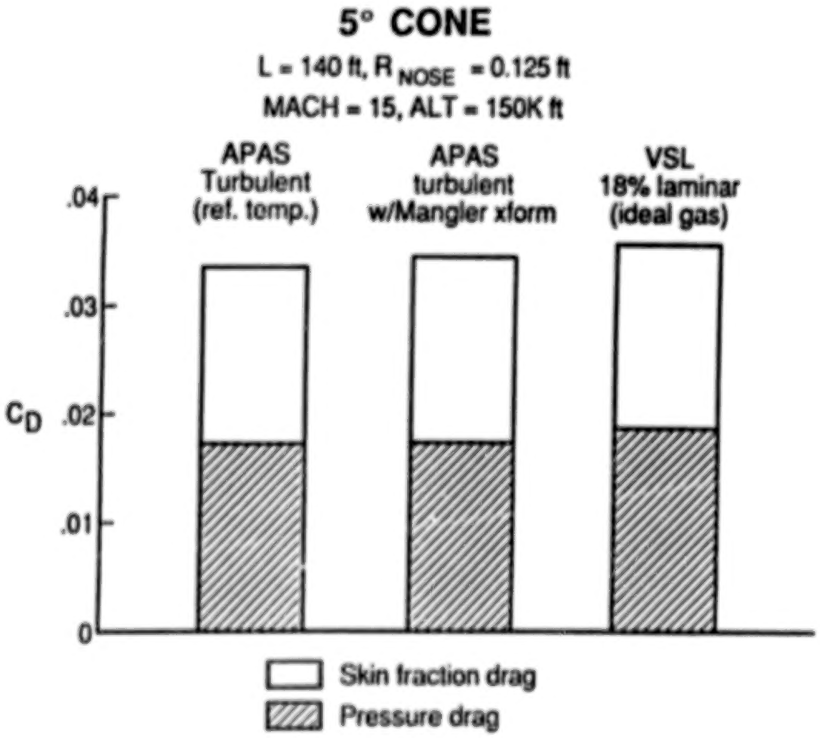

Figure 22

HEATING PREDICTIONS FROM GENTRY (HAB, APAS)

Heating predictions on a 5° half-angle cone assuming a laminar boundary layer is shown in figure 23. The difference in the Mark 3 Reference Enthalpy and the Mark 3B Reference Enthalpy levels is mainly that of the Mangler transformation (Mark 3B). The Mark 3B predictions agree with those given by the Viscous Shock Layer code. Heating predictions assuming a turbulent boundary layer are shown in figure 24.

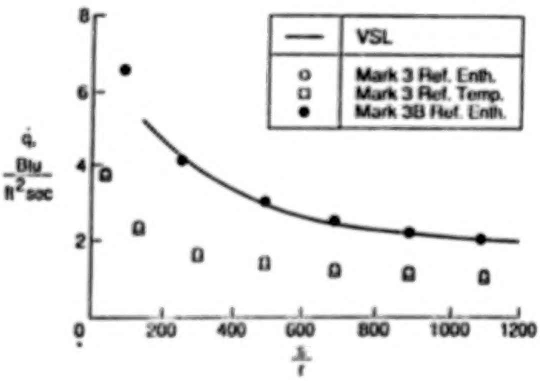
5° CONE LAMINAR BOUNDARY LAYER CONVECTIVE HEATING RATE

Mach 15, α = 0°

Figure 23

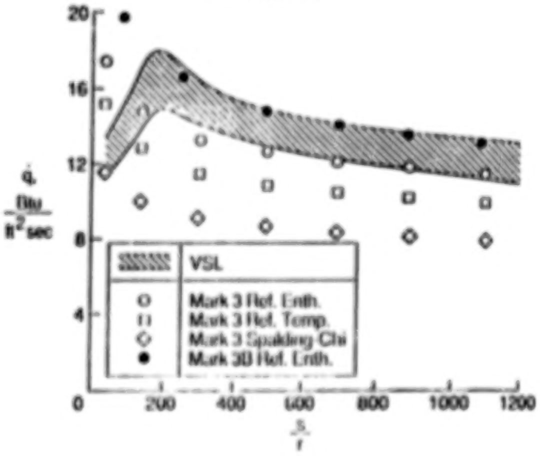
5° CONE TURBULENT BOUNDARY LAYER CONVECTIVE HEATING RATE

Mach 15, α = 0°

Figure 24

TRANSITION CRITERIA

High Mach numbers tend to laminarize the flow on a 5° half-angle cone as indicated by the merger of the solid line drag prediction containing Beckwith's transition criteria (figure 25) with the dashed line representing predictions for laminar flow, as shown in figure 26. Thus above Mach 14, the flow on the cone appears to be all laminar. This is for a trajectory having a dynamic pressure of 1,000 psf.

APPROXIMATE TRANSITION CRITERIA FOR APAS

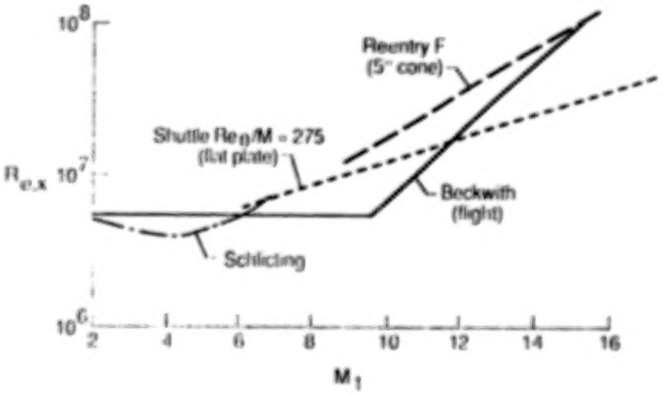

Figure 25

5° CONE CONFIGURATION DRAG WITH TRANSITION

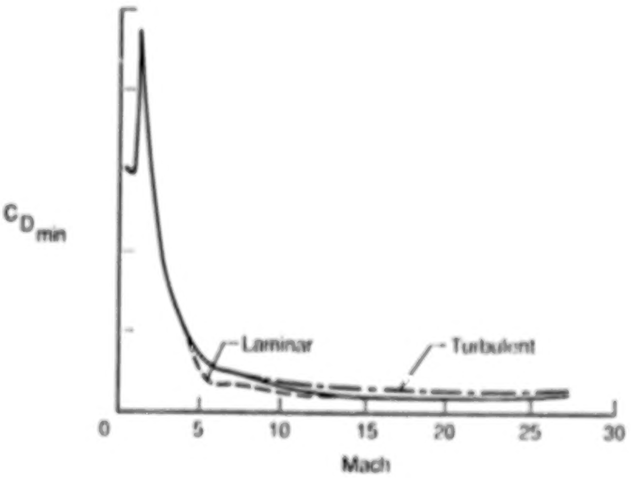

Figure 26

TRAJECTORY ANALYSIS (POST)

(As conveyed by Richard W. Powell, NASA Langley Research Center)

PROGRAM TO OPTIMIZE SIMULATED TRAJECTORIES (ref. 5)
(POST)

1. Three degree of freedom version
2. Suitable for ascent, entry, and orbital problems
3. Multiple guidance options and integration techniques
4. Powered (rocket and airbreathing) or unpowered vehicles
5. Option to calculate engine gimbal angles or flap deflections required to balance moments due to thrusting and aerodynamics
6. Simulate winds, horizontal take-off, hold down for vertical take-offs
7. Optimizes trajectory while meeting equality or inequality constraints
8. Optimization and constraint variables can be any calculated variable

PROGRAM TO OPTIMIZE SIMULATED TRAJECTORIES (POST)
APPLICATIONS TO NASP

A. CAPABILITIES

1. Both a 3 degree-of-freedom and a 6 degree-of-freedom version are available.
2. Flexible enough to apply to virtually any aerospace trajectory problem (ascent-orbital maneuvers, entry).
3. General targeting (including both equality and inequality constraints) and optimization capability.
4. Optimization criteria, constraints, and controls may be virtually any input or calculated parameter.
5. Modularity design allows for easy modification or addition of mathematical models.
6. Becoming an industry standard.

B. ENHANCEMENTS FOR NASP STUDIES

1. Propulsion module updated to simulate air-breathing propulsion used by candidate NASP vehicles.
2. Guidance system modified to allow for easy acquisition of desired dynamic pressure profile.
3. Additional output variables are calculated (ISP, effective ISP, propulsive efficiency, etc.)

PROPULSION FOR INPUT TO POST

The propulsion data set is generated external to AVID. The procedure and tools used in generation of this input performance data set for the scramjet is shown in figure 27. Flow field solutions (CFD) to check the forebody/inlet starting profiles for the scramjet analysis are also generated external using VSL, PNS, TLNS, and FNS codes.

SCRAMJET PERFORMANCE ANALYSIS

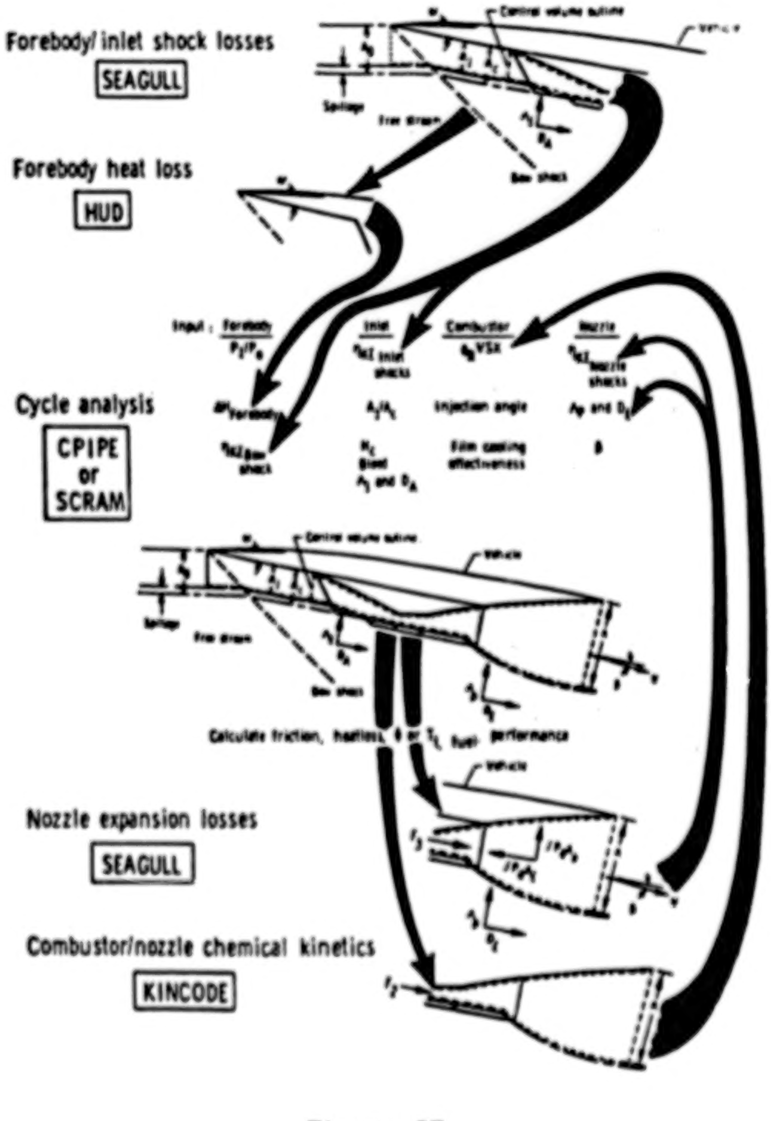
Forebody/inlet shock losses
SEAGULL
Control volume outline
Vehicle
Spillage
Free stream
Bow shock
Forebody heat loss
HUD
Input : Forebody
Inlet
Combustor
Nozzle
Inlet shocks
Nozzle shocks
Cycle analysis
CPIPE or SCRAM
Injection angle
Film cooling effectiveness
Bow shock
Control volume outline
Vehicle
Spillage
Free stream
Bow shock
Calculate friction, heatloss, fuel performance
Vehicle
Nozzle expansion losses
SEAGULL
Combustor/nozzle chemical kinetics
KINCODE

Figure 27

BEST COPY AVAILABLE

COMPUTATIONAL FLUID DYNAMICS (CFD)

The flow field over the vehicle is calculated external to AVID with CFL3D (ref. 6). This is a thin layer Navier Stokes program that utilizes an upwind difference scheme; integration is performed in the physical plane. The primary purpose of calibrating the flow field is to provide a high fidelity solution of the air-flow properties at the inlet face and eventually at the inlet throat in order to adjust the scramjet performance analysis. These solutions are increasingly being sought to calibrate/adjust aerodynamic and heat transfer data sets generated from less sophisticated means.

AEROTHERMODYNAMICS

The aerothermodynamic slot in APAS makes use of both internal and external data generation sources. The MINIVER code is used to provide engineering heating predictions with such methods as Fay and Ridell (stagnation point), Cohen and Beckwith (leading edge), and Shultz and Grueno (fuselage). This analysis is agumented with the CFD solutions mentioned earlier.

THERMAL MANAGEMENT

The goal of the thermal management analysis effort is to analyze hypersonic vehicle concepts with realistic thermal loads applied and realistic thermal management system installed to obtain temperature distributions, cooling loads, hydrogen flow conditions, system weights, and system volumes. Once the thermal management system is designed and integrated, the challenge is a thermal balance of the vehicle that sets the fuel cooling equivalence ratio of the vehicle and the delta on engine performance due to the heat addition to the hydrogen before injection into the engine.

The tasks are to develop and/or obtain:

1. Surface heat loads for airframe and engine. (From MINIVER and SRGULL).
2. Thermal model of overall vehicle. (PATRAN generated condition models and translated into SINDA.)
3. Thermal model of coolant flow network. (Established in SINDA -- uses GASPLUS for fluid properties.)
4. Engine and airframe temperature. (From SINDA)
5. Hydrogen network flow rates, temperatures, and pressure. (From SINDA, ref. 7.)

156

STRUCTURAL ANALYSIS, WEIGHTS

The structural analysis is performed external to AVID. Weight of the structural architecture is estimated through a finite element/failure mode analysis (ref. 8). The procedure is as given below.

LOADS AND FAILURE MODE WEIGHT PREDICTION METHODOLOGY

A. Create a PATRAN finite element model of the desired component and include:

1. nodes and connectivities
2. rigid masses
3. external loads
   a. distributed and point forces
   b. temperature loading
   c. inertial loading
4. constraint cases
5. element construction type, and material data
   a. bar
   b. beam
   c. honeycomb plate
   d. corrugated web
   e. hat stiffened skin

B. Translate PATRAN data to an EAL runstream.

C. Run the model through each applied loadset, or loadset combination. Use the element sizing code to calculate structural gages based on, minimum gage, buckling, yield, and ultimate strength design criteria.

D. Summarize calculated gages for each loadset and create a file of new element dimensions based on the heaviest of each element for each loadset.

E. Update the EAL runstream with new element stiffnesses reflecting dimensions from the worst case element dimension file. Repeat steps C through E until element dimensions remain unchanged between iterations.

F. Postprocess the converged element dimensions with appropriate non-optimum factors to permit the integration of calculated structural weights into a vehicle performance sizing program.

SIZING

Vehicle sizing is conducted external to AVID. The primary criteria for sizing a vehicle is propellant mass fraction (propellant weight/take-off gross weight). Vehicles are scaled to achieve a given (required) propellant mass fraction (PMF) as described below:

1. The vehicles airframe, wings, and tails are scaled photographically. Structural weight is based on unit weight scaling laws as determined by structural analysis conducted on various size vehicles; the weight per unit area of various components are fit to a quadratic equation form ($C_1 + C_2\ell + C_3\ell^2$) where ℓ is a nondimensional representative length or scale factor.
2. Engine weight and volume is scaled by engine inlet area which is scaled photographically, W_{Engine} = Const. × Inlet Area.
3. Subsystems weights and volumes are based on emperical/historical equations with advanced technology factors included.
4. Payload bay and crew compartment are fixed.
5. Available volume for propellant tanks is the total vehicle volume minus the volumes of items 1 through 4. Propellant volume available is the tank volume minus volume lost to tank packaging efficiency.
6. The vehicle is then scaled up or down in an iterative manner until a given PMF is achieved.

CLOSURE

The fuel fraction required as calculated from the POST trajectory code (for ascent, transition to orbit, orbit, deorbit, reentry and decent, and landing -- complete trajectory) and the fuel fraction achievable as calculated from the sizing code provide the closure point as indicated in figure 28.

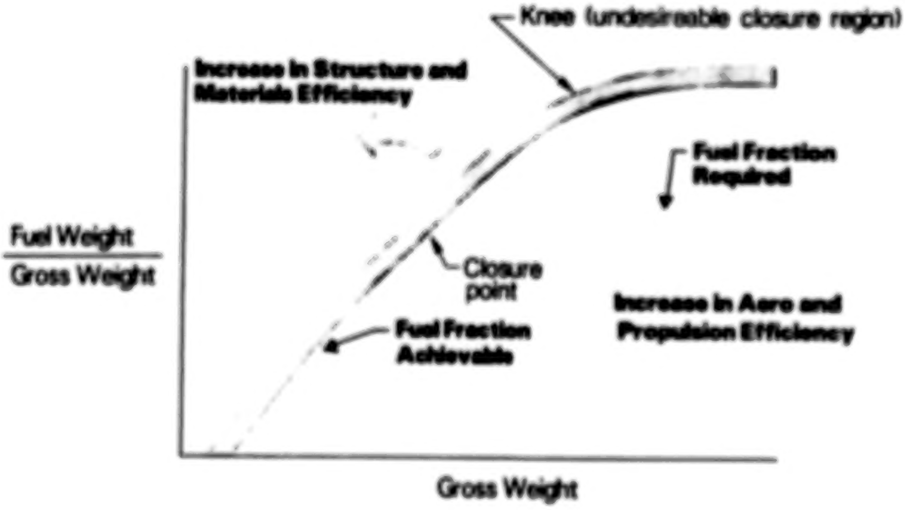

Figure 28

BEST COPY AVAILABLE

CONCLUDING REMARKS

The airbreathing SSTO vehicle design environment is variable-rich, intricately networked and sensitivity intensive. As such, it represents a tremendous technology challenge. Creating a viable design will require sophisticated configuration/synthesis and the synergistic integration of advanced technologies across the discipline spectrum. In design exercises, reductions in the fuel weight-fraction requirements projected for an orbital vehicle concept can result from improvements in aerodynamics/controls, propulsion efficiencies and trajectory optimization; also, gains in the fuel weight-fraction achievable for such a concept can result from improvements in structural design, heat management techniques, and material properties. As these technology advances take place, closure on a viable vehicle design will be realizable.

REFERENCES

1. Becker, J. V.: New Approaches to Hypersonic Aircraft. Presented at the 7th Congress of the International Council of the Aeronautical Sciences (ICAS), Rome, Italy, 1970.

2. Wilhite, A.; and Johnson, S. C.: Integrating Computer Programs for Engineering Analysis and Design. AIAA Paper No. 83-0597, January 1983.

3. Dixon, S. C.; Tenney, D. R.; Rummler, D. R.; Wieting, A. R.; and Bader, R. M.: Structures and Materials Technology Issues for Reusable Launch Vehicles. NASA TM-87626, October 1985.

4. Divan, P.: Aerodynamic Preliminary Analysis System II, Part II--User's Manual. NASA CR-165628, April 1981.

5. Brauer, G. L.; Cornick, D. E.; and Stevenson, R.: Capabilities and Applications for the Program to Optimize Simulated Trajectories (POST). NASA CR-2770, February 1977.

6. Thomas, J. L.; Walters, R. W.; Rudy, D. H.; and Swanson, R. C.: Upwind Relaxation Algorithm for Euler/Navier Stokes Equations. NASA CP-2397, April 1985, pp. 89-107.

7. SINDA '85/FLUINT Systems Improved Numerical Differencing Analyzer and Fluid Integrator, Version 2.1, User's Manual Appendix F, Martin Marietta, November 1987.

8. Rummler, D. R.; Cerro, J. A.; and Dixon, S. C.: Structures and Materials Requirements for Reusable Hypervelocity Vehicles. Proceedings of Seventh Metal Matrix Composites Technology Conference, Naval Surface Weapons Center, Silver Spring, Maryland, May 26-28, 1987, pp. 3-1 through 3-7.

OPTIMIZING CONCEPTUAL AIRCRAFT DESIGNS FOR MINIMUM LIFE CYCLE COST

Vicki S. Johnson
NASA Langley Research Center
Hampton, Virginia

162

IMPORTANCE OF COST IN CONCEPTUAL DESIGN

Engineers have traditionally designed systems that maximize performance while minimizing size and weight. Current practice in the conceptual design process tends toward approximation of minimum cost by either using minimum takeoff gross weight, empty weight, or fuel burned. It is generally accepted that between 70 and 80 percent of the life cycle cost of a configuration is locked in during the concept stage of development when very little actual money has been spent, as shown for military aircraft in figure 1 (taken from ref. 1). Reference 2 illustrates the same trend for commercial aircraft programs at the Boeing Company. During the early stages of development, commitments are made to increased performance over existing systems, thus implying the need to consider new technologies.

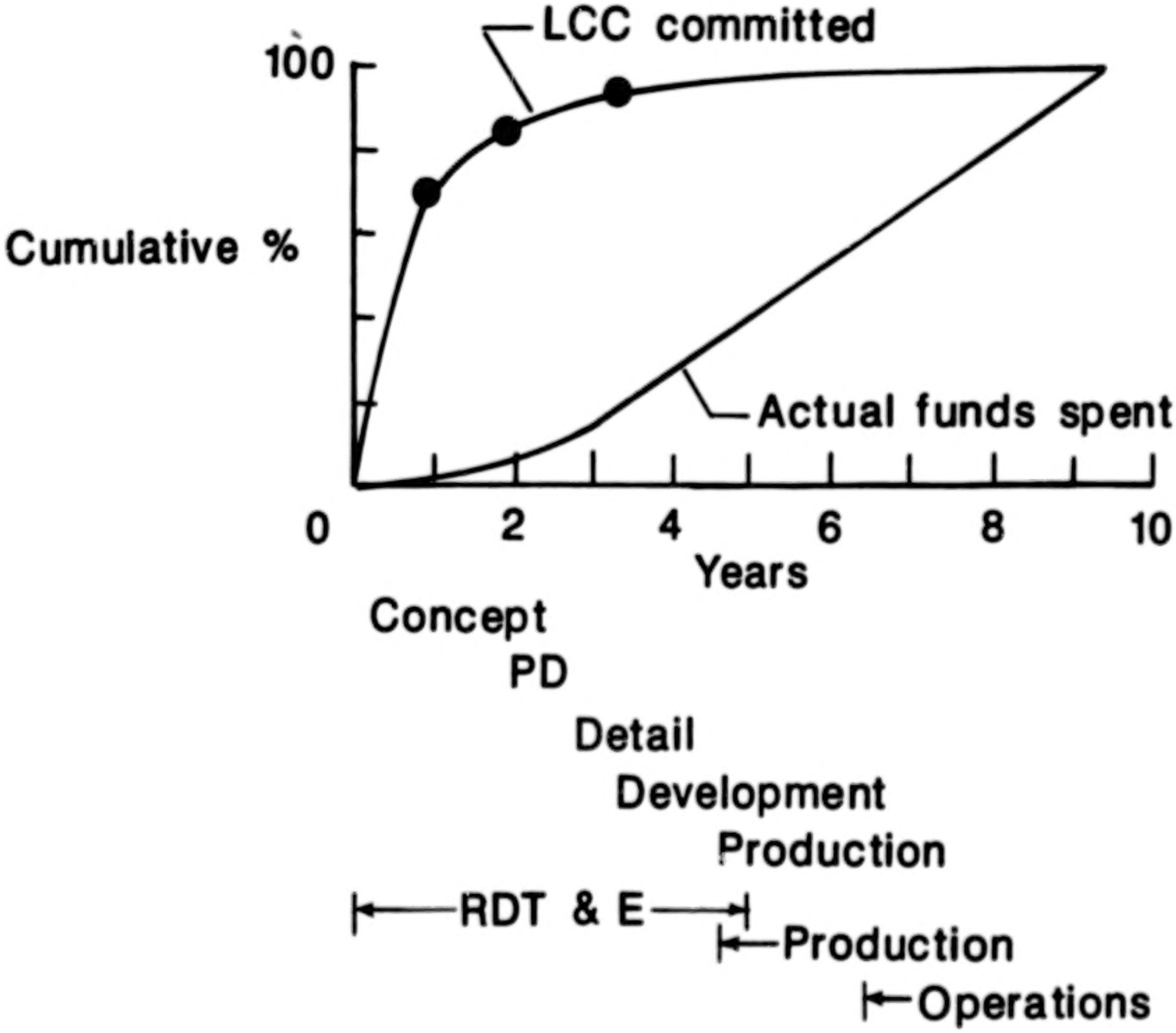

Figure 1

LIFE CYCLE COST

The life cycle cost (LCC) of an aircraft is the total cost associated with that aircraft from initial inception through the aircraft leaving service at the end of its life. The two major components of LCC are acquisition and operating costs (fig. 2). Acquisition cost is composed of research, development, testing and evaluation (RDT&E), and production costs, and is primarily associated with the manufacturer. Operating cost includes DOC (direct operating cost) and IOC (indirect operating cost) and is primarily associated with the customer or airline. Using LCC in the conceptual design process emphasizes the importance of balancing the design between potentially conflicting parameters. For example, low acquisition cost may be associated with low technology level and high operating cost. The prevailing economic conditions strongly influence how much technology can be included on the aircraft.

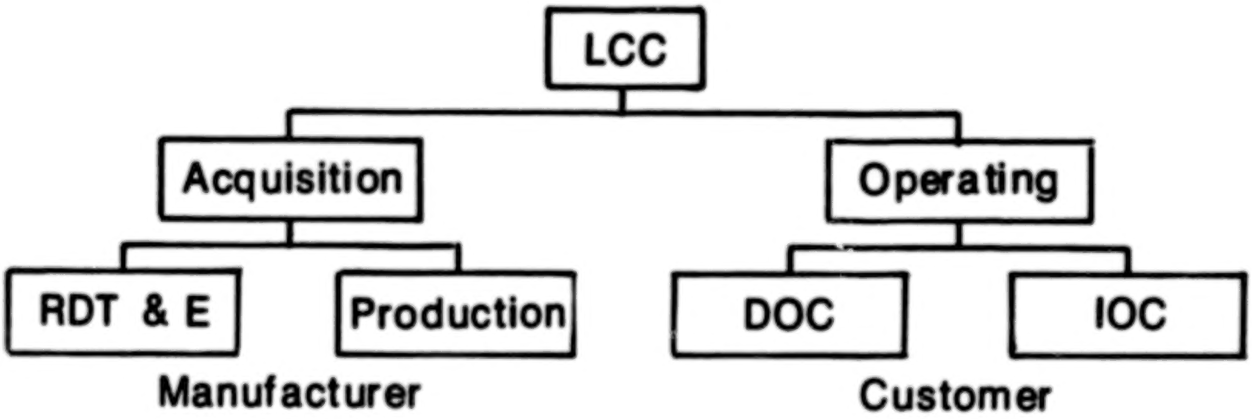

Considering LCC in the conceptual design process emphasizes the importance of balancing the design between potentially conflicting parameters

Figure 2

LCC CONCEPTUAL DESIGN SYSTEM

Figure 3 shows a schematic diagram of the system developed to include LCC in the conceptual design process. The system includes an existing conceptual design and analysis code called FLOPS (Flight Optimization System) and a LCC model developed for this effort. Input to the system includes a baseline mission, aircraft (geometry and propulsion data minimally), and economic assumptions. FLOPS and the LCC model will be described in more detail in the following two figures.

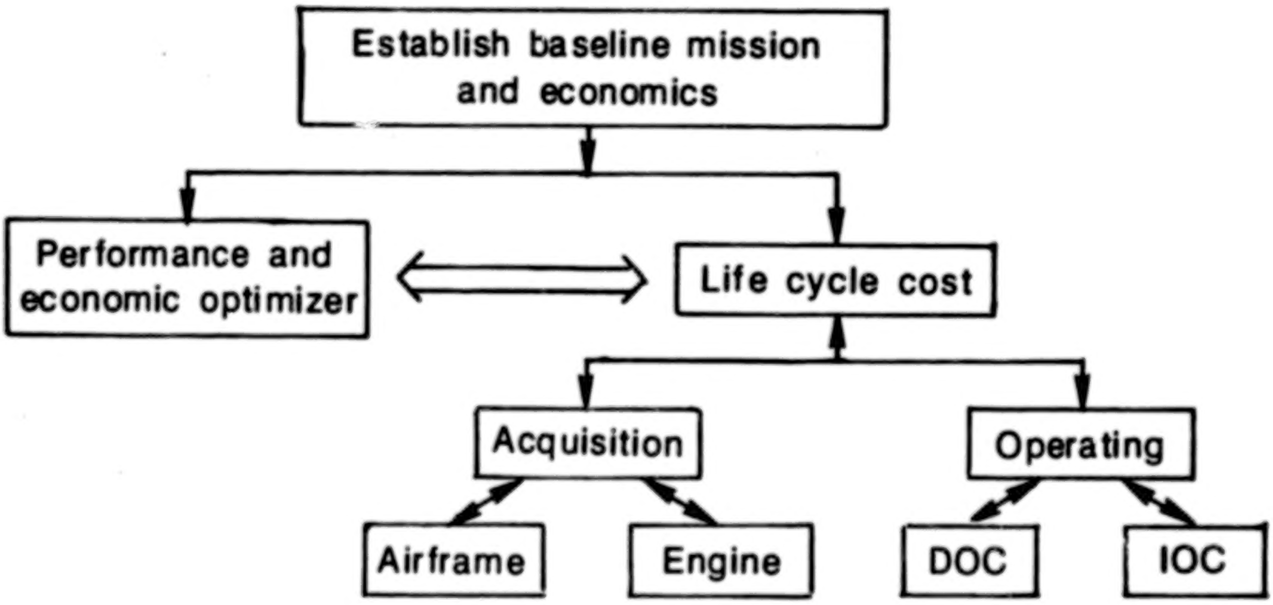
Establish baseline mission and economics
Performance and economic optimizer
Life cycle cost
Acquisition
Operating
Airframe
Engine
DOC
IOC

Figure 3

FLOPS CONCEPTUAL DESIGN PROGRAM

The major features of FLOPS (ref. 3) are discussed in figure 4. FLOPS is a multidisciplinary system of computer programs for conceptual and preliminary design and evaluation of advanced aircraft concepts. It originally consisted of four primary modules: weights, aerodynamics, mission performance, and takeoff and landing. FLOPS may be used to analyze a point design, parametrically vary certain design variables, or optimize a configuration with respect to these design variables using nonlinear programming techniques. The available design variables are wing area, wing sweep, wing aspect ratio, wing taper ratio, wing thickness-chord ratio, gross weight, thrust (size of engine), cruise Mach number, and maximum cruise altitude. Additionally, complexity factors can be used to account for advanced technologies in weights, aerodynamics, and propulsion. Previously, optimization could be done for minimum gross weight, minimum fuel burned, maximum range, or some combination of these. The addition of the LCC module to this conceptual design system allows cost to become an additional optimization parameter, making it possible to specify life cycle cost, acquisition cost, direct operating cost, total operating cost, or return on investment as the parameter to be optimized.

- ORIGINAL MODULES FOR WEIGHTS, AERODYNAMICS, MISSION PERFORMANCE, AND TAKEOFF AND LANDING
- ANALYZE DESIGN, VARY DESIGN PARAMETERS, OR OPTIMIZE CONFIGURATION
- DESIGN VARIABLES ARE S, Λ, AR, λ, T/C, TOGW, T_{MAX}, M_{CR} AND H_{CR}
- TECHNOLOGY LEVEL VARIATION THROUGH COMPLEXITY FACTORS
- OPTIMIZE FOR MINIMUM GROSS WEIGHT, MINIMUM FUEL BURNED, MAXIMUM RANGE, OR SOME COMBINATION

Figure 4

LCC MODEL

The LCC model is composed of elements to calculate RDT&E cost, production costs, DOC and IOC. Existing cost models (fig. 5) were selected for each of these elements based on their applicability to subsonic commercial aircraft and their connection to the conceptual design phase of development. These models are described in greater detail in reference 4.

The airframe acquisition cost is computed from the RDT&E cost model of reference 5 and the SAI (Scientific Associates, Inc.) production cost model of reference 6. The RDT&E model uses weight, speed and production quantity; weight and quantity are the primary cost drivers in the SAI model but weight is dependent on conceptual design type variables. A Rand model (ref. 7) is used to predict engine acquisition cost. The model uses engine size, weight, and performance parameters as variables affecting cost. The model is for military turbojet and turbofan engines; it was modified to produce results correct for commercial engines. The operating cost models include the American Airlines DOC model (ref. 8) and the Lockheed-Georgia IOC model (ref. 9). The DOC model is a modification of the ATA-67 model (ref. 10) which accounts for more of the conceptual design variables and includes more recent real world experience. The IOC model is the industry standard and includes some conceptual design variables.

ACQUISITION COST
- AIRFRAME
    - RDT&E - EIDE MODEL (WEIGHT, SPEED, QUANTITY)
    - PRODUCTION - SAI MODEL (WEIGHT, QUANTITY)
        - WEIGHT FUNCTION OF CONCEPTUAL DESIGN VEHICLES
- ENGINE - MODIFIED RAND MODEL
    - COST FUNCTION OF ENGINE SIZE, WEIGHT, AND PERFORMANCE

OPERATING COST
- DOC - AMERICAN AIRLINES DOC
    - MODIFICATION OF ATA-67 MODEL
    - INCLUDES CONCEPTUAL DESIGN VARIABLES AND REAL WORLD EXPERIENCE
- IOC - LOCKHEED GEORGIA IOC
    - INDUSTRY STANDARD
    - SOME CONCEPTUAL DESIGN VARIABLES

Figure 5

BEST COPY AVAILABLE

BASELINE MISSION AND ECONOMICS

For this study, three different classes of subsonic commercial aircraft were used (short,[*] medium,[†] and medium-to-long range[‡]). The baseline missions and economic assumptions are shown in figure 6. The missions are intended to be representative of realistic missions; therefore, range is not the only difference. The same economic assumptions were used for all aircraft. Baseline aircraft geometries were developed from existing aircraft of the same class. Scalable engine data appropriate to each vehicle size was used as input to FLOPS. Design variables for these aircraft were aspect ratio, wing area, wing sweep, wing thickness-chord ratio, engine thrust, and takeoff gross weight. In order to see the full effect of the optimization process, the design variables were not constrained to realistic values. The mission requirements (in particular takeoff field length) did help maintain a certain amount of realism in the designs. Only selected results of the study will be presented in the following discussion due to limitations of time and space.

	[*]SRAC	[†]MRAC	[‡]LRAC
RANGE, N.MI.	1000	2500	4500
CRUISE MACH	0.78	0.80	0.82
MAX CRUISE ALT., FT.	35000	40000	45000
PASSENGERS	100	200	500
TOFL, FT.	6000	7000	10000
NO. OF ENGINES	2	2	4

BASELINE ECONOMIC ASSUMPTIONS
(FOR ALL AIRCRAFT)

YEAR FOR CALCULATIONS = 1987
SPARES FACTOR FOR AIRFRAME = 0.10
SPARES FACTOR FOR ENGINES = 0.30
AIRFRAME PRODUCTION QUANTITY = 400
NO. OF PROTOTYPE AIRCRAFT = 2
NO. OF FLIGHT TEST AIRCRAFT = 2
PRIOR NO. OF ENGINES PROCURED = 0
DEPRECIATION PERIOD = 14 YEARS
LIFETIME = 14 YEARS
RESIDUAL VALUE AT END OF LIFE = 15%
FUEL PRICE = $0.50/GALLON

Figure 6

EFFECT OF OPTIMIZATION PARAMETER ON WING PLANFORM

A comparison of the wing planform obtained for the medium-range aircraft when optimized for minimum acquisition cost, takeoff gross weight, life cycle cost, direct operating cost, and minimum fuel burned is shown in figure 7. The aspect ratio, wing area, and wing sweep are represented in the planform sketch. The wings are drawn with a common root quarter-chord location. In terms of increasing aspect ratio and wing area, the planforms start with minimum acquisition cost, TOGW, LCC, DOC, and end with minimum fuel. Aspect ratio can be used as a measure of technology by recognizing that a larger aspect ratio wing is going to be more aerodynamically efficient but also more expensive to build. The minimum acquisition cost airplane is primarily dependent on the structural weight of the airplane, the minimum fuel airplane is primarily dependent on the fuel weight, and the TOGW airplane depends on both the structural weight and the fuel weight. The DOC airplane is dependent on the cost of fuel, the cost of maintenance, and has a secondary dependence on the acquisition cost of the aircraft. The LCC airplane balances both the operating and acquisition costs of the airplane. The next three figures will investigate the differences between these configurations further.

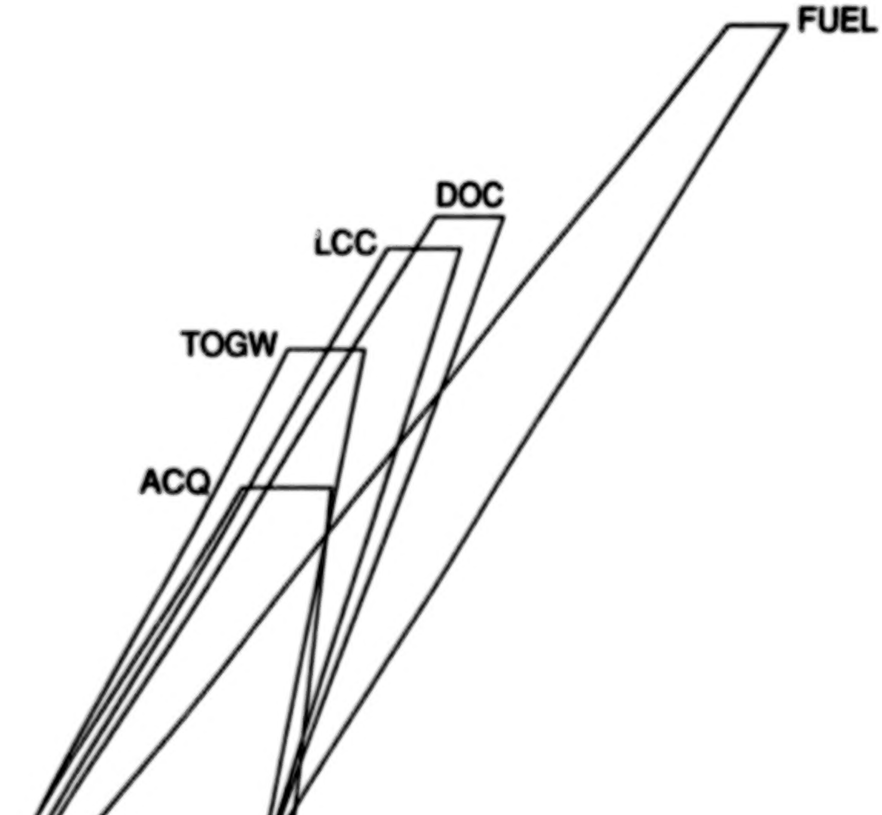

Figure 7

GROSS WEIGHT AND FUEL CONSUMPTION

The bars in the graphs of figure 8 each represent the value of TOGW and fuel burned per flight associated with the medium-range aircraft which have been optimized for minimum acquisition cost, TOGW, LCC, DOC, and fuel burned. The minimum fuel airplane has the highest TOGW while the minimum acquisition cost airplane burns the most fuel. With the exception of the minimum acquisition cost airplane, TOGW increases with increasing aspect ratio and wing area. The amount of fuel burned decreases for all cases with increasing aspect ratio.

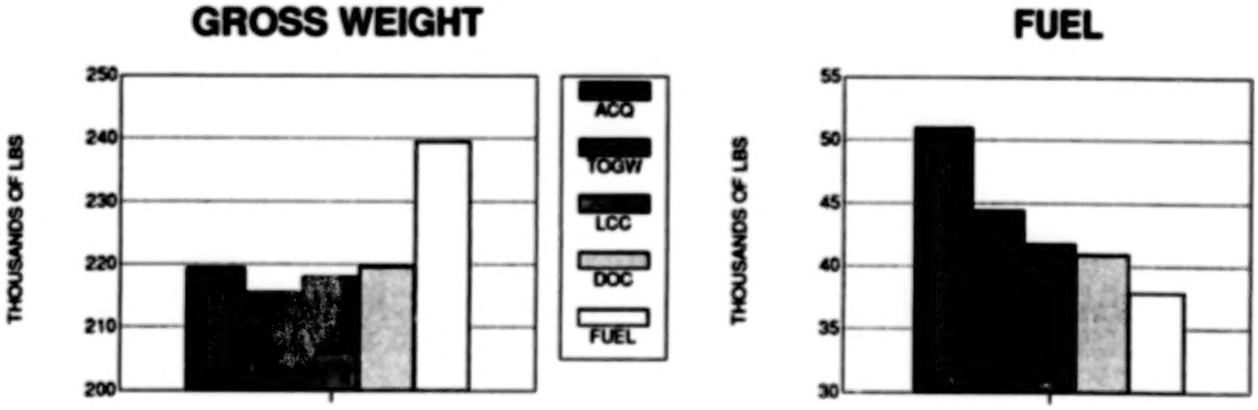

Figure 8

WEIGHT AND COST

Figure 9 illustrates the direct relationship between empty weight, acquisition cost and technology level. The minimum acquisition cost airplane has the lowest empty weight while the minimum fuel airplane has both the highest empty weight and highest acquisition cost. The minimum LCC airplane has a slightly higher empty weight and acquisition cost than the minimum TOGW airplane.

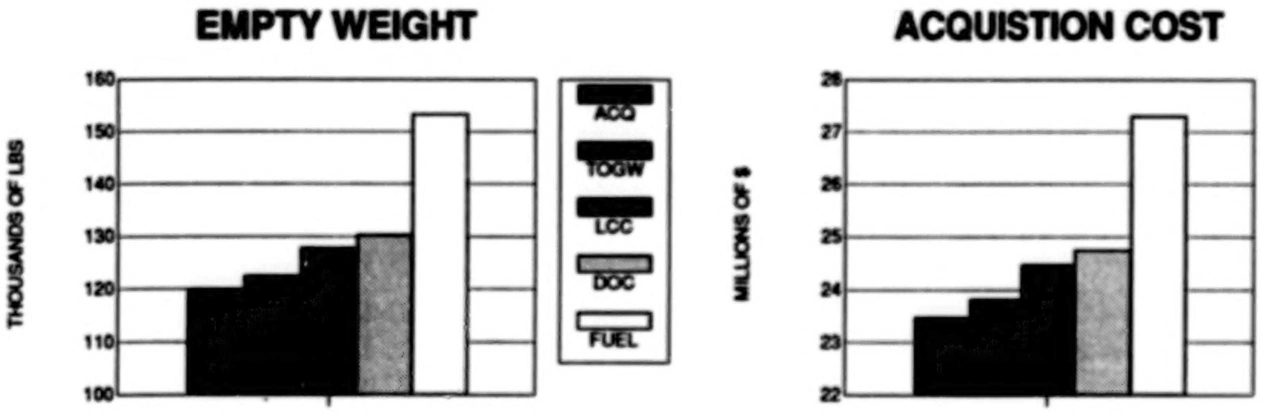

Figure 9

DIRECT OPERATING AND LIFE CYCLE COSTS

The direct operating cost and life cycle cost for the various optimized aircraft are shown in figure 10. Direct operating cost is the total over the lifetime of the aircraft. With the exception of the minimum fuel airplane, DOC decreases with increasing aspect ratio. The LCC of the configuration follows the technology trends with the extremes (minimum fuel and acquisition cost airplanes) having very high LCC and the minimum TOGW, LCC, and DOC airplanes having lower LCC. Both the short- and medium-to-long range airplanes showed similar results, although fuel played a much more important role in the medium-to-long range airplane. The minimum LCC and DOC airplanes are dependent on the economic assumptions. The DOC and LCC airplanes are very similar because with these economic conditions the elements that determine DOC (fuel, maintenance, salaries, acquisition cost, and so on) are of equal importance with the elements that determine LCC (acquisition cost and DOC). In the following discussion the effects of economic assumptions such as fuel cost and lifetime will be examined.

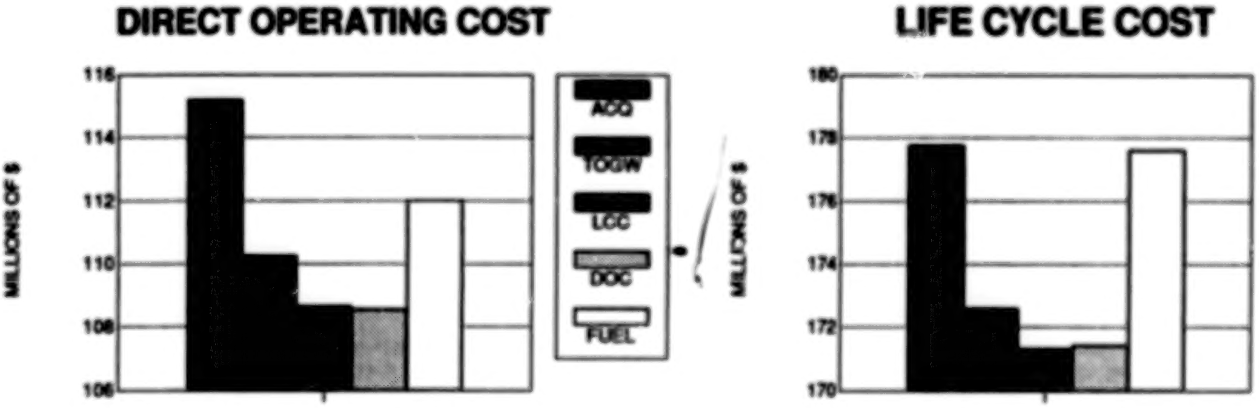

Figure 10

FUEL PRICE SENSITIVITY

Wing planforms resulting from optimization runs for minimum LCC and DOC for the medium-range airplane with fuel at \$2.00 per gallon are shown in figure 11. For reference the baseline minimum fuel, LCC, and DOC planforms are also shown. The effect of increasing fuel price is to increase the amount of technology that can be included for both the minimum LCC and DOC airplanes. In fact, the minimum DOC wing planform becomes nearly identical to the minimum fuel planform.

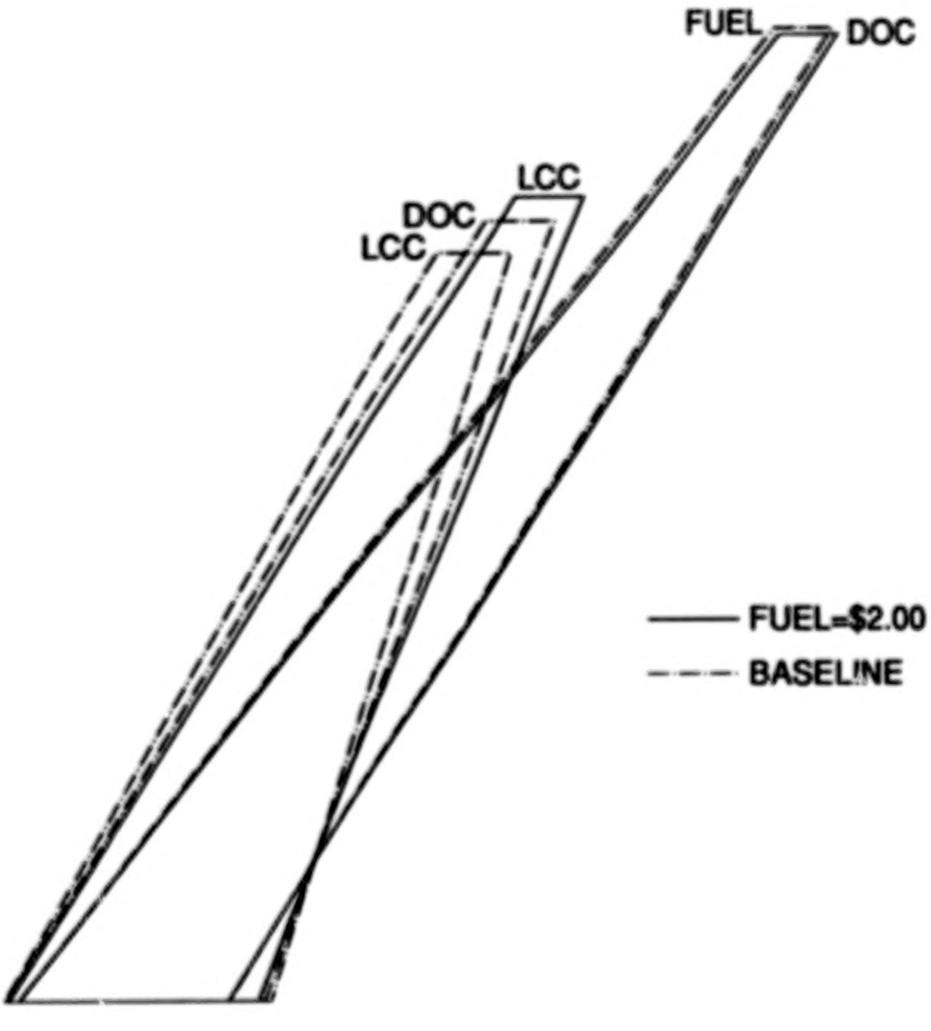

Figure 11

COSTS FOR INCREASED FUEL PRICE

Acquisition and life cycle cost for all of the medium-range aircraft with fuel cost of $2.00 per gallon are shown in figure 12. Once again acquisition cost increases with increasing technology level. The minimum LCC and DOC airplanes have higher acquisition costs than before. As might be expected, the minimum DOC and minimum fuel aircraft have nearly identical acquisition cost and life cycle cost. This is because the fuel cost has become a much more important element than acquisition cost in determining DOC. The amount of technology that can be included on the minimum LCC airplane is restricted by the balance between increases in acquisition cost and decreases in direct operating cost. Additionally, the difference in life cycle cost between the minimum LCC, DOC, and fuel airplanes is not that great.

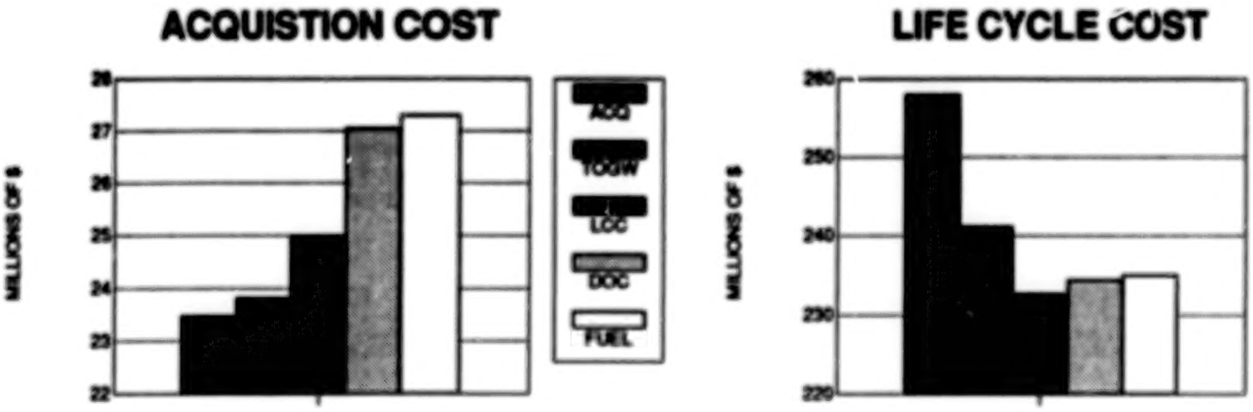

Figure 12

EFFECT OF LIFETIME AND RESIDUAL ON PLANFORM

Another important set of economic assumptions are the lifetime of the aircraft and its residual value at the end of that lifetime. Figure 13 shows the wing planform resulting from optimizing the medium-range aircraft for minimum DOC and LCC with a lifetime of eight years and a residual of 30 percent. For reference, the baseline minimum TOGW, LCC, and DOC airplane planforms are shown. Utilization of these aircraft in terms of number of flights per year is identical to the baseline. In this case, the LCC and DOC airplanes are identical. They have greater sweep but less aspect ratio than the baseline DOC and LCC aircraft. Wing areas are nearly identical.

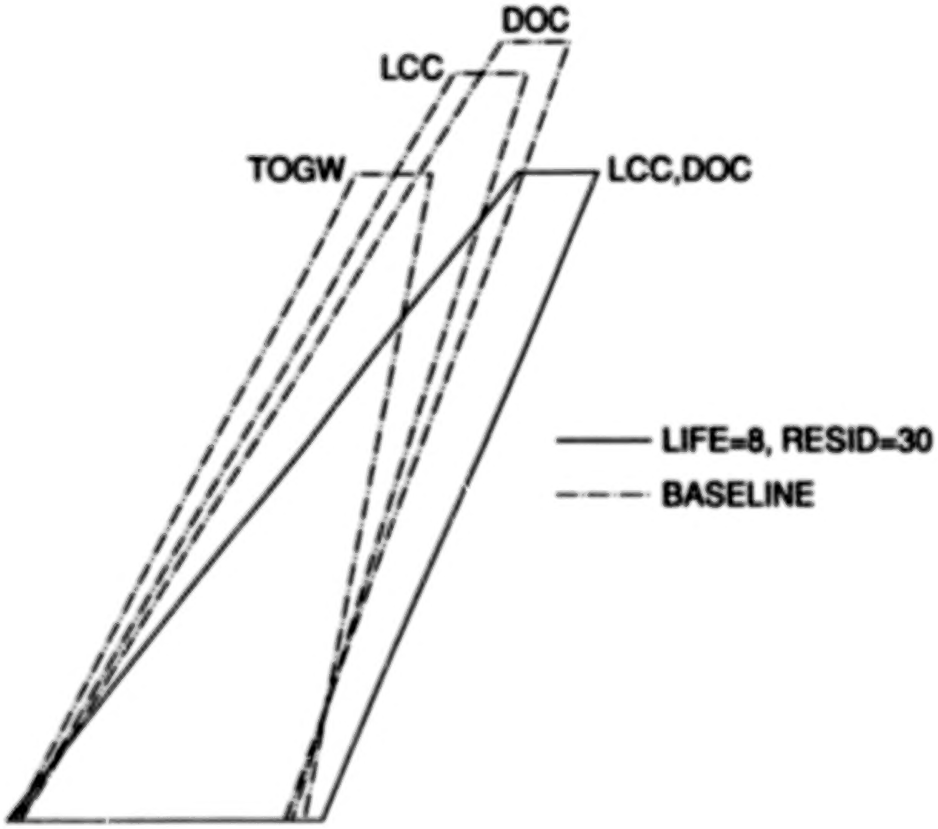

Figure 13

EFFECT OF LIFE AND RESIDUAL ON COST

Figure 14 shows the acquisition cost and LCC for all medium-range airplanes with a lifetime of eight years and residual value of 30 percent. The trends are the same as before but the reduced lifetime makes lowered acquisition cost and technology level more important than saving fuel in order to keep the life cycle cost low for both the minimum LCC and DOC airplanes.

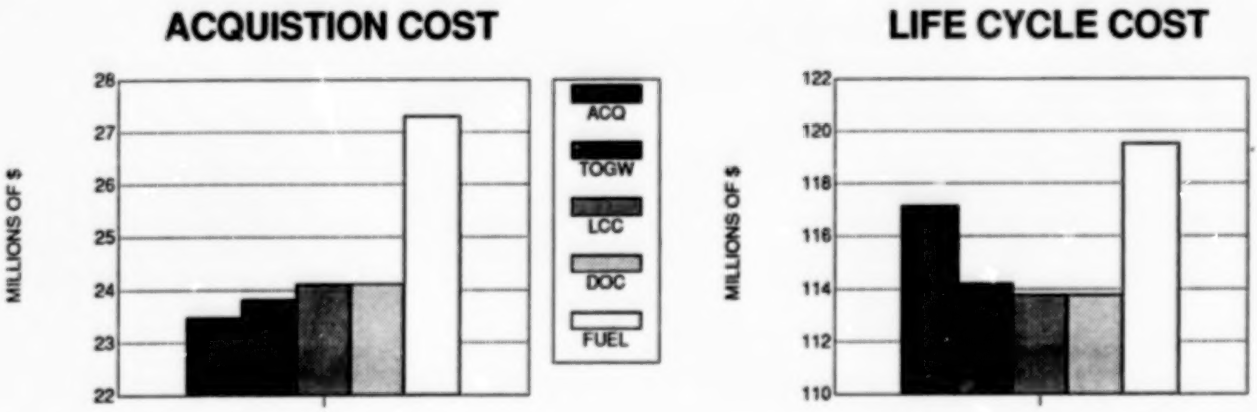

Figure 14

NUMBER OF ENGINES

The table in figure 15 illustrates one of the real payoffs of including cost in conceptual design. Each of the three classes of aircraft was optimized for minimum life cycle cost with two, three, and four engines. If the number of engines is selected based on minimum TOGW, empty weight, or fuel burned, in all cases four engines would be chosen. However, if the number of engines is based on minimum LCC or DOC, only in the case of the medium-to-long range aircraft would four engines be chosen. The short- and medium-range aircraft both have minimum DOC and LCC with two engines. If minimum acquisition cost is the criterion for selection, four engines would be chosen for the medium- and medium-to-long range aircraft; once again two engines would be selected for the short-range aircraft. For the short- and medium-range aircraft, the total cost for two engines is less than the cost for four engines. Additionally, the maintenance cost is a much greater function of number of engines than it is of engine size. Therefore, from an economic viewpoint, two engines is the logical choice. For the medium-to-long range aircraft, however, the total engine cost is approximately constant. The one-engine out requirements drive this very large airplane to very large engines. All costs increase with decreasing number of engines, making four the correct choice. This exercise was also conducted based on minimum TOGW aircraft; the results were identical. This type of application makes a very strong argument for considering cost in the conceptual design process.

	SRAC			MRAC			LRAC		
	4	3	2	4	3	2	4	3	2
TOGW, LB	86705	92014	90064	201616	215645	218086	753658	807769	948147
EW, LB	50386	54939	52613	113551	125856	127938	379740	409937	497152
FUEL, LB	12402	13031	13541	39686	41212	41784	251055	274610	327932
THRUST, LB	5218	8184	13839	14384	21437	34542	33750	54994	122863
T/W	0.24	0.27	0.31	0.29	0.30	0.32	0.18	0.20	0.26
LCC, M$	114.50	118.36	114.14	173.11	176.25	171.32	395.40	414.28	457.42
DOC, M$	79.20	81.62	78.37	111.28	112.39	108.67	250.03	264.55	301.71
ACQ, M$	11.90	12.92	11.81	23.49	25.44	24.48	55.92	59.48	64.14
COST/ENG, M$	0.38	0.51	0.72	0.71	0.86	1.15	1.14	1.49	2.26
TOT. ENG COST, M$	1.52	1.53	1.44	2.84	2.58	2.30	4.56	4.47	4.52

Figure 15

TECHNOLOGY EFFECT ASSUMPTIONS

As mentioned earlier, FLOPS has the capability to account for advanced technologies through the use of complexity factors. Similar factors were included in the LCC module. Complexity factors can be applied to airframe RDT&E, engine RDT&E, and manufacturing and operating costs associated with the individual aircraft components and systems. Using these factors it is possible to specify a technology improvement (or decrement) and a corresponding cost increase (or decrease). If these increments are known, they may be used to determine their effect on the configuration. However, one of the true values of this conceptual design system is the capability to evaluate the sensitivities of the aircraft to these technology and cost increments. An example is presented for an increase in aerodynamic technology for the medium-range aircraft. Figure 16 shows the aerodynamic performance improvements assumed and the corresponding cost increments. Three sets of cost increments (no additional cost, 20 percent additional cost and 40 percent additional cost in each element shown) were used to evaluate the sensitivity of this configuration to the change in cost. (All other economics are the baseline assumptions.) The results will be described in the next three figures.

PERFORMANCE IMPROVEMENTS IN AERODYNAMICS

ADVANCED TECHNOLOGY AIRFOIL
40% LAMINAR FLOW ON
  WING, HORIZONTAL TAIL, VERTICAL TAIL,
  BODY AND NACELLES

COST INCREASES

0%	20%	40%	IN AIRFRAME R&D
0%	20%	40%	IN MANUFACTURING OF WING, BODY, NACELLES, TAIL
0%	20%	40%	IN OPERATING OF WING, BODY, NACELLES
0%	20%	40%	IN MAINTENANCE LABOR RATE

Figure 16

TECHNOLOGY EFFECT ON WING PLANFORM

The wing planform for the medium-range aircraft when optimized for minimum life cycle cost with the aerodynamic performance improvements and 40% cost increase is shown in figure 17. For comparison the baseline minimum LCC planform is also shown. The advanced aerodynamic technology allows the wing to use less sweep, span, and area and more thickness to obtain an optimum wing for minimum LCC.

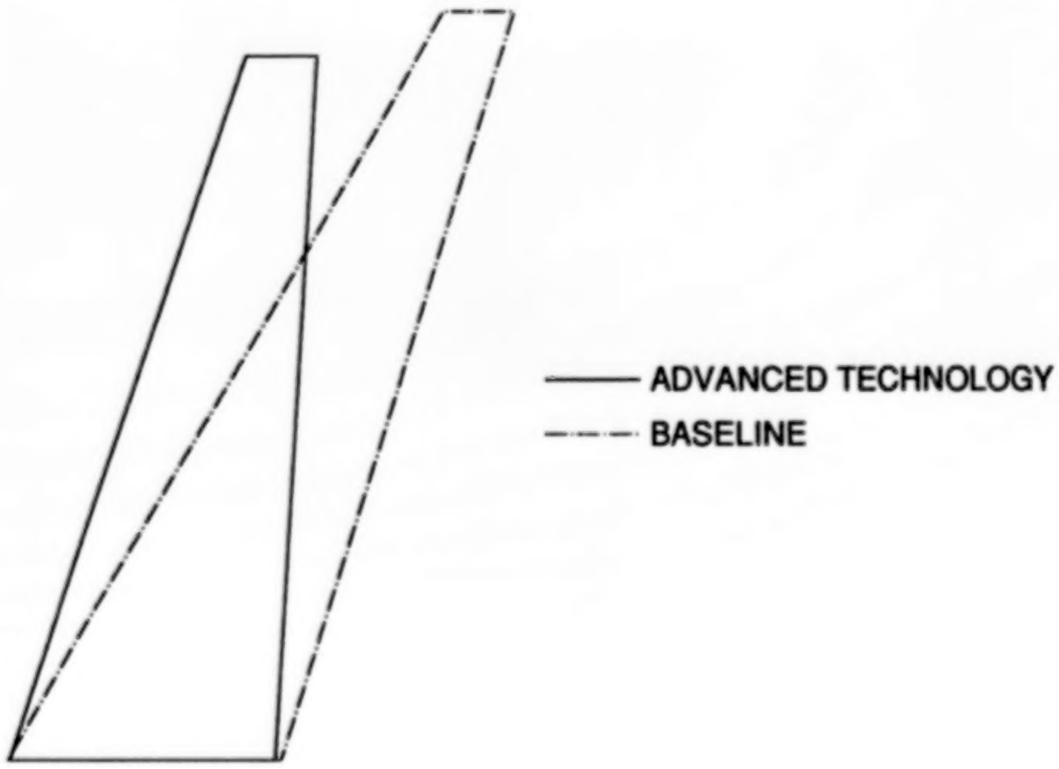

Figure 17

TECHNOLOGY EFFECT ON TOGW AND LCC

The TOGW and LCC of the medium-range aircraft when optimized for minimum LCC are shown in figure 18. Applying the aerodynamics technology results in a large decrease in TOGW. When there is no associated cost increase, the LCC is also dramatically reduced. With a 20 percent cost increase the LCC is still less than the baseline. If the cost increase is as much as 40 percent, the resulting LCC is greater than the baseline. For this set of economic conditions, a cost increase of up to approximately 30 percent appears to be tolerable for this technology set.

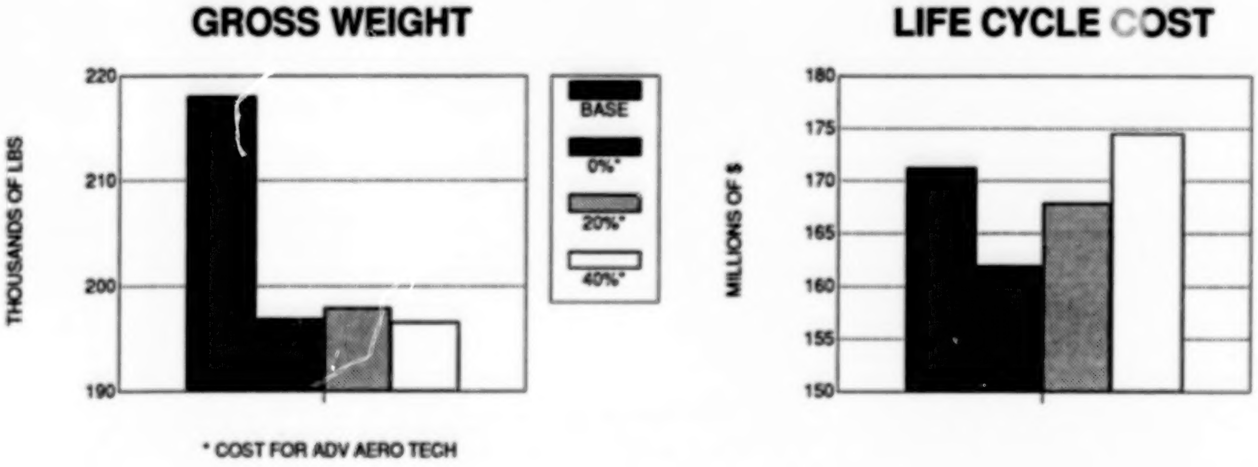

Figure 18

TECHNOLOGY EFFECT ON ACQUISITION COST AND DOC

Figure 19 shows the acquisition cost and direct operating cost for the configuration discussed in the previous figure. As would be expected, for no increase in cost associated with advanced technology, the acquisition and direct operating costs are less than for the baseline aircraft. For a 20 percent increase in cost, the acquisition cost is somewhat greater than the baseline and the direct operating cost is still significantly less. A 40 percent increase in cost leads to higher acquisition and direct operating costs. Similar results were obtained for the configuration when optimized for minimum takeoff gross weight. The point where advanced technology is affordable is highly dependent on the assumed economic conditions. In addition to aerodynamics this system can handle weight, propulsion and systems technologies and costs. They may be evaluated individually or combined.

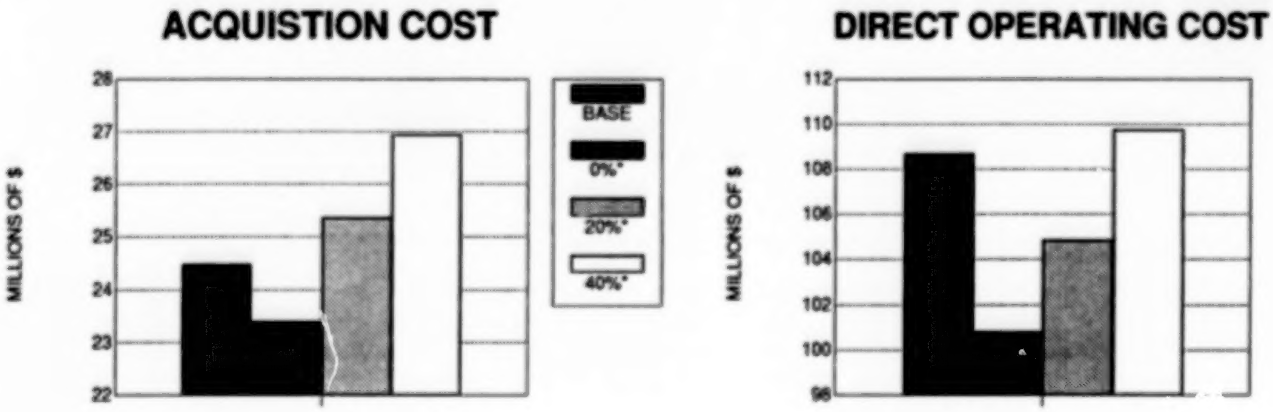

* COST FOR ADV AERO TECH

Figure 19

OPTIMIZATION OBSERVATIONS

The FLOPS optimization capability already existed and was in current use. The goal of this study was to extend the capability to include cost in the process. The modularized nature of FLOPS made this extension relatively easy. Some observations about the optimization process for this study are summarized in figure 20. For the airplanes used in this study the optimizations for TOGW and fuel generally converged without any problem. The acquisition cost optimization also succeeded in finding the global minimum during the first run. The LCC and DOC optimizations generally converged but not to the global minimum the first time. It was usually necessary to restart the runs at least once. During all of the optimization runs there was a lot of movement of the design variables. However, runs did tend to encounter problems and abort if the starting point was too far from the optimum. It was interesting to note that this study did uncover two problems with the FLOPS analysis. In trying to optimize the medium-range aircraft for minimum fuel burned, the aspect ratio went to 26, the wing sweep to 88 degrees, and the wing span to 225 feet. The problem was an error in the sweep portion of the wing weight equation. When that was corrected everything worked fine. Another problem uncovered was a weakness between the aerodynamics and weights for taper ratio. For all aircraft the taper ratio optimized to near zero. The final solution to this problem was to recognize that taper ratio is not a critical parameter and to leave it fixed for all configurations.

- EXISTING FLOPS OPTIMIZATION FOR TOGW AND FUEL WORKED VERY WELL FOR THESE AIRPLANES
- TYPICALLY GLOBAL MINIMUM FOUND DIRECTLY FOR MINIMUM ACQUISITION COST
- GENERALLY NECESSARY TO RESTART DOC AND LCC OPTIMIZATIONS AT LEAST ONCE
- DESIGN VARIABLES CHANGED SIGNIFICANTLY DURING OPTIMIZATION PROCESS; HOWEVER, SOMETIMES TOO MUCH CHANGE ABORTED THE PROCESS
- THIS STUDY DID UNCOVER TWO PROBLEMS WITH THE ANALYSIS:
  - -- ERROR IN WING SWEEP EQUATION FOUND BY MEDIUM-RANGE AIRCRAFT MINIMUM FUEL CASE
  - -- WEAK LINK BETWEEN AERODYNAMICS AND WEIGHTS FOR TAPER RATIO -- ALWAYS OPTIMIZED TO TAPER RATIO ≈ 0

Figure 20

CONCLUSIONS

Figure 21 summarizes conclusions from this study. A life cycle cost module has been added to FLOPS, allowing the additional optimization variables of life cycle cost, direct operating cost, and acquisition cost. Extensive use of the methodology on short-, medium-, and medium-to-long range aircraft has demonstrated that the system works well. Results from the study show that optimization parameter has a definite effect on the aircraft, and that optimizing an aircraft for minimum LCC results in a different airplane than when optimizing for minimum TOGW, fuel burned, DOC, or acquisition cost. Additionally, the economic assumptions can have a strong impact on the configurations optimized for minimum LCC or DOC. Also, results show that advanced technology can be worthwhile, even if it results in higher manufacturing and operating costs. Examining the number of engines a configuration should have demonstrated a real payoff of including life cycle cost in the conceptual design process: the minimum TOGW or fuel aircraft did not always have the lowest life cycle cost when considering the number of engines.

- A LCC MODULE HAS BEEN ADDED TO FLOPS, ALLOWING THE ADDITIONAL OPTIMIZATION VARIABLES OF LCC, DOC, AND ACQUISITION COST
- EXTENSIVE USE OF THE METHODOLOGY ON THREE DIFFERENT SUBSONIC TRANSPORT AIRCRAFT HAS DEMONSTRATED THAT THE SYSTEM WORKS WELL AND IS USEFUL
- RESULTS SHOW THAT
    - OPTIMIZATION PARAMETER HAS A DEFINITE EFFECT ON THE AIRCRAFT
    - OPTIMIZING FOR LCC RESULTS IN A DIFFERENT AIRCRAFT THAN OPTIMIZING FOR TOGW, FUEL BURNED, DOC, OR ACQUISITION COST
    - THE MINIMUM LCC AND DOC AIRPLANES TEND TO BE SIMILAR AND ARE DEPENDENT ON ECONOMIC CONDITIONS
    - THE MINIMUM TOGW OR FUEL AIRCRAFT DO NOT ALWAYS HAVE THE LOWEST LIFE CYCLE COST WHEN CONSIDERING THE NUMBER OF ENGINES
    - ADVANCED TECHNOLOGY CAN BE WORTHWHILE EVEN IF IT RESULTS IN HIGHER MANUFACTURING AND OPERATING COSTS

Figure 21

SYMBOLS

ACO	Acquisition cost
ATA	Air Transport Association
DOC	Direct operating cost
IOC	Indirect operating cost
LCC	Life cycle cost
RDT&E	Research, development, testing and evaluation
TOGW	Takeoff gross weight

REFERENCES

1. Nicolai, Leland M.: Fundamentals of Aircraft Design. METS, Inc., 6520 Kingsland Court, San Jose, California, 95120, 1975.

2. Brown, Robert B.: Design of Very Large Airplanes for Least System Cost. Aircraft Design, Integration and Optimization--Volume 1. AGARD CP-147, 1973, paper 15.

3. McCullers, L. A.: Aircraft Configuration Optimization Including Optimized Flight Profiles. Multidisciplinary Analysis and Optimization--Part I. NASA CP-2327, 1984, pp. 395-412.

4. Johnson, Vicki S.: Life Cycle Cost in the Conceptual Design Process. AIAA Paper 87-2889, 1987.

5. Eide, Donald G.: Cost Estimating Relationships for Airframes in the Development and Production Phases. NASA TM-80229, 1980.

6. Beltramo, Michael N.; and Morris, Michael A.: Application of Parametric Weight and Cost Estimating Relationships to Future Transport Aircraft. SAE Paper 1292, 1979.

7. Nelson, J. R.; and Timson, F. S.: Relating Technology to Acquisition Costs: Aircraft Turbine Engines. The Rand Corporation, R-1288-R, 1974.

8. A New Method for Estimating Current and Future Transport Aircraft Operating Economics. American Airlines, NASA CR-145190 (Revised), 1978.

9. Stoessel, Robert R.: A Proposed Standard Method for Estimating Airline Indirect Operating Expense. Lockheed-Georgia Company, LW70-500R, 1970.

10. Standard Method of Estimating Comparative Direct Operating Costs of Turbine Powered Transport Airlines. Air Transport Association of America, December 1967.

AIRCRAFT DESIGN OPTIMIZATION
WITH MULTIDISCIPLINARY PERFORMANCE CRITERIA

Stephen Morris and Ilan Kroo
Department of Aeronautics and Astronautics
Stanford University
Stanford, California

185

ABSTRACT

The presence of multidisciplinary performance criteria and constraints complicates the process of aircraft design and optimization. This paper addresses some of the problems that arise as performance measures from very different fields are compared and tradeoffs are made. The work focuses on the interaction between structural weight, aerodynamic performance, and handling qualities. A method for dealing with such design problems is described and several example cases are considered.

By minimizing a cost function consisting of both conventional performance criteria and a measure of aircraft handling qualities, a design with maximum performance for a specified level of handling can be achieved. Handling qualities are measured using a quadratic cost function similar to that used in the design of optimal feedback control systems. This function is proportional to the difference between the unforced response of the aircraft and a "model" case with dynamics that are considered acceptable. The variables to be optimized may include both aircraft design parameters (e.g. span, tail area, skin thickness) and control system feedback gains. The design variables are determined by an unconstrained numerical optimization procedure, using penalty functions to enforce both explicit and implicit constraints. The method is most useful in the simultaneous design of airframe and flight control systems to achieve improved handling, and for cases in which the handling and performance are highly coupled by the design parameters. In certain cases results obtained by this simultaneous design procedure are substantially better than those obtained by the usual sequential design methods.

Three example design problems using this methodology are discussed: tail sizing for minimum trimmed drag with longitudinal handling qualities constraints; wing weight minimization with aeroelastic constraints; and oblique-wing aerodynamic design for dynamic mode decoupling.

INTRODUCTION

The dynamic response of an aircraft is often an important aspect of its design; yet the analysis of handling qualities and control system design are often performed after the major aerodynamic and structural properties have been established. In many cases, this sequential approach to multidisciplinary design leads to suboptimal results. The current work was motivated by one such case — the design of an oblique wing aircraft — in which achieving the desired aerodynamic performance with acceptable handling requires an integrated approach.

The design method used in this case and in the two other examples discussed here, includes a measure of the aircraft dynamic response as an integral part of the overall objective function. Numerical optimization is used to determine the values of various design parameters which minimize the composite performance index. These design variables may include both geometric properties and control system feedback gains but are not limited to full state feedback. This means that the method can be used to design a system to meet desired dynamic response requirements without a feedback control system at all, provided sufficient degrees of freedom are available in the design variables.

Sequential Design

- Sub-optimal performance achieved with sequential disciplinary approach to design optimization

Integrated Design

- Objective function is a weighted combination of a handling qualities measure and other performance quantities
- Aircraft configuration variables and / or control system gains used as design variables
- Method is not restricted to full-state feedback (optimal control theory) — passive designs possible

COMPOSITE OBJECTIVE FUNCTION

A variable-metric, quasi-Newton method (QNMDIF, Ref. 1) is used to determine values of the design variables that minimize the composite objective function. This function consists of three terms: the non-dynamic performance measure, the weighted dynamic performance, and the constraint violation penalty function.

The non-dynamic performance variable may include such quantities as structural weight, drag, or direct operating cost. This component may be excluded if the goal is solely to improve dynamics.

J_d provides a measure of the aircraft's dynamic response by comparison with the unforced response of a model case. This term is identical to the performance index used in optimal control design, but the feedback controller in this method is not restricted to full-state feedback. As the weighting parameter, K_d, is varied from zero to a large number, the optimal solution moves from one in which dynamics are not considered to one which is required to achieve the specified dynamics. This permits a designer to evaluate the significance of dynamic performance constraints on the final solution. J_d is normalized so that it approaches 1.0 as the design approaches neutral stability.

The third term in the objective function includes penalty functions, used to enforce explicit and implicit constraints in the synthesis.

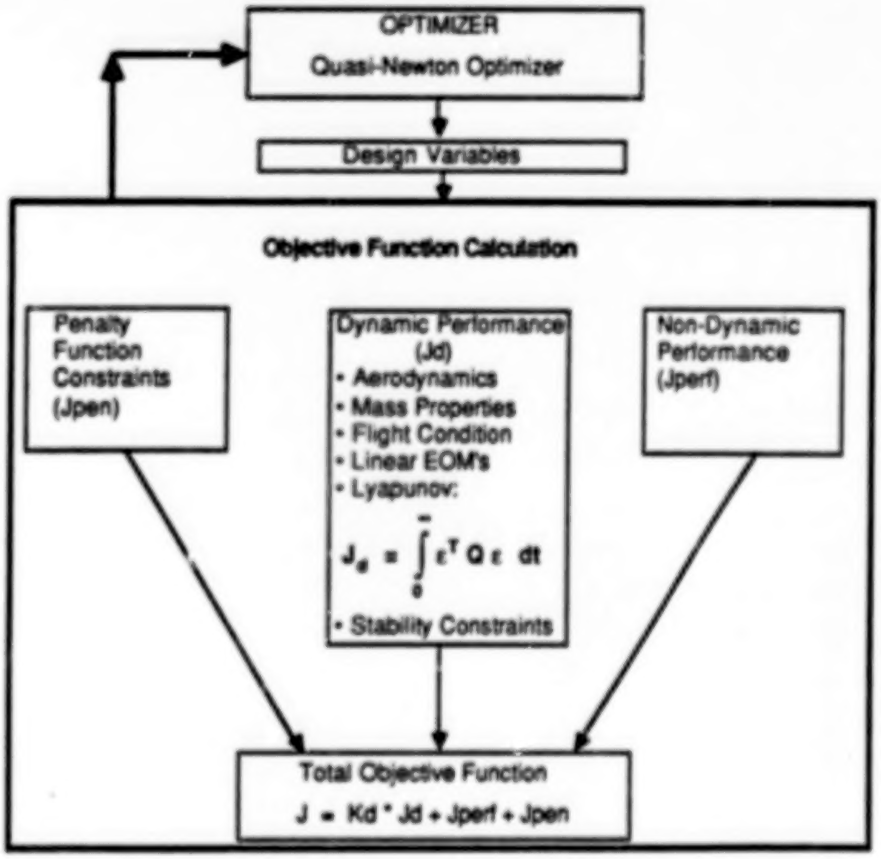
OPTIMIZER
Quasi-Newton Optimizer
Design Variables
Objective Function Calculation
Penalty Function Constraints (Jpen)
Dynamic Performance (Jd)
• Aerodynamics
• Mass Properties
• Flight Condition
• Linear EOM's
• Lyapunov:
$J_d = \int_0^\infty \epsilon^T Q \epsilon \, dt$
• Stability Constraints
Non-Dynamic Performance (Jperf)
Total Objective Function
J = Kd * Jd + Jperf + Jpen

DYNAMIC PERFORMANCE INDEX

A key aspect of this approach is the calculation of the dynamic performance index, Jd. It consists of a weighted integral over time of the difference in the state vectors of the current system and a model system whose dynamics are considered ideal. An additional term representing the control surface activity may also be included. The matrices [Q] and [R] (see below) contain weighting factors for the state error and control activity, respectively. The solution for the scalar handling quality index is obtained by solving three Lyapunov matrix equations.

The non-dynamic performance and penalty function constraints are problem specific quantities and their evaluation will be discussed in the design examples only. The dynamic performance index calculation requires that the linearized equations of motion for the aircraft be created as a function of the design variables at each objective function evaluation. This portion of the synthesis can be the most costly in terms of CPU time, particularly if the aerodynamic stability derivatives must be re-evaluated. The overall utility of this method relies on the careful choice of the analysis routines which evaluate the matrices shown in the equations of motion below. Methods which capture the essential physical phenomena and minimize computation time are desired.

Because the control gains are design variables in the optimizer loop, the controller can have any linear feedback architecture, including no controller (passive design). If full-state feedback is desired the optimal control gains may be calculated within the objective function evaluation by solving the associated algebraic Riccati equation (Refs. 2,3). This removes the control gains from the optimization loop but fixes the control system architecture.

Linearized Equations of Motion

$\dot{X} = [A]X + [B]U$

$U = [C]X$ (Any Linear Feedback Control Law)

Model Following Design

$\varepsilon = X - X_m$ where $\dot{X}_m = [A_m]X_m$

Dynamic Performance

$$J_d = \int_0^{\infty} (\varepsilon^T Q \varepsilon + U^T R U)\, dt$$

Solution is found from three Lyapunov Equations:

1. $[A - BC]^T [P1] + [P1][A - BC] + [Q + C^T H C] = 0$
2. $[A - BC]^T [P2] + [P2][Am] + [Q] = 0$
3. $[Am]^T [P3] + [P3][Am] + [Q] = 0$

$$Jd = \mathrm{Trace}[P1 - P2 - P2^T + P3]$$

AFT TAIL DESIGN FOR MINIMUM TRIMMED DRAG

Three examples are presented to illustrate the use of this method. The first of these, and the simplest, is the design of a wing and tail system. The configuration is required to trim at a selected lift coefficient while minimizing drag and retaining adequate longitudinal handling qualities. Variables include horizontal trail area, and wing location; in some of the designs a reduced order controller (consisting of angle of attack feedback to the elevator) is also synthesized.

The performance index is a weighted combination of drag and J_d, the handling quality parameter. J_d is computed based on a "model" case with tail area and wing location that provide Mil. Spec. 8785C level 1 response.

In this simple example the trimmed drag is calculated analytically assuming elliptic loading on the wing and tail. Drag includes parasite drag, lift dependent viscous drag, and the vortex drag associated with the interfering lifting surfaces. Designs are also required to trim at maximum lift without tail stall. This constraint is enforced using penalty functions.

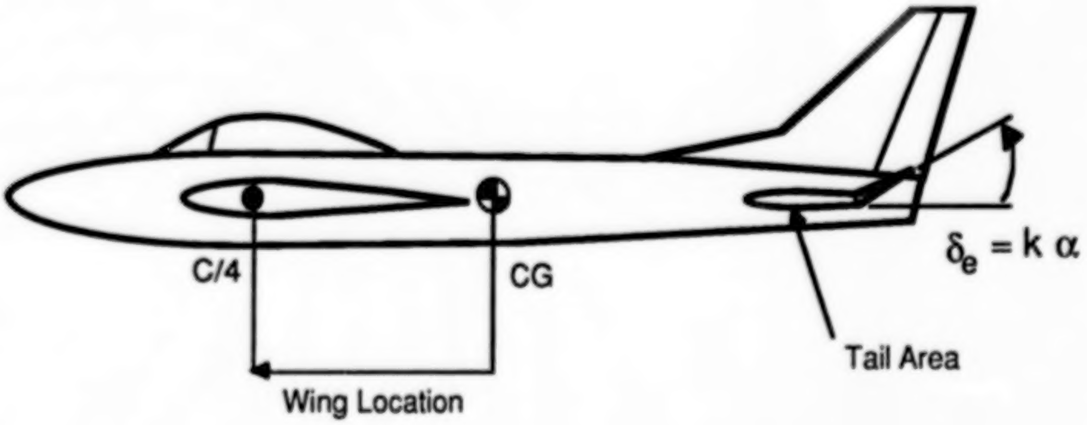

Goal: Minimize Trimmed Drag With a Given Level of Handling Quality

Design Variables: Tail Area, Wing Location, Feedback Gain (optional)

AFT TAIL DESIGN RESULTS

The plot below shows the tradeoff between trimmed drag and handling quality parameter for the aft tail design synthesis. Curves are shown for designs with and without a feedback control system. Each point on the curves represents a unique design which is optimal for a fixed weighting of handling qualities. As the weighting on handling is increased, J_d decreases and the dynamic response of the designed aircraft approaches that of the model case. Note also that the trimmed drag increases with improved handling quality. This occurs because tail size and static margin increase as J_d decreases, with a subsequent increase in parasite and trim drag. Designs with feedback control show reduced trimmed drag for a fixed level of handling compared to designs without control systems. The synthesis method has recognized that relaxed static stability and smaller tail size can reduce trimmed drag, while feedback control can ensure adequate handling qualities by providing artificial stability. As a result, designs are automatically synthesized which are statically unstable and have an optimally designed reduced order controller to provide stability. The values of J_d where the longitudinal dynamics meet the Mil. Spec. 8785C level (1) handling quality requirements are marked on each curve.

Because the control system does not provide rate feedback, adequate damping requires some tail area; thus it is not possible to eliminate the tail completely. Even if large values of Jd (poor handling) are accepted, trim constraints still yield a non-zero tail area when the wing pitching moment at zero lift is not zero. This leads to the flat part of the curve with feedback at higher values of J_d.

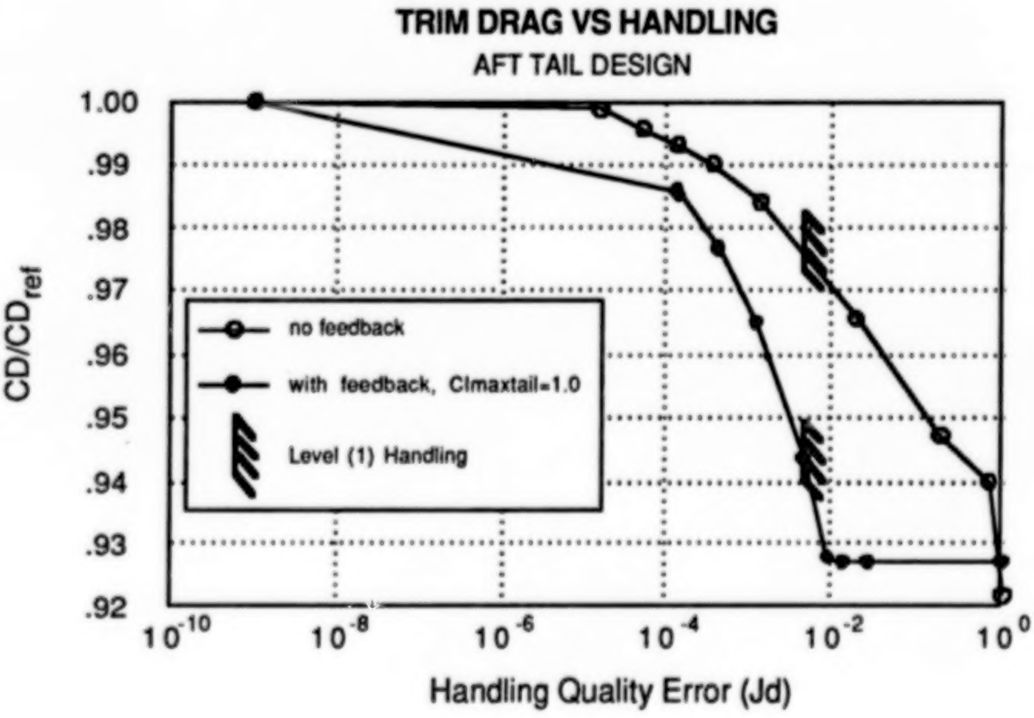

AFT TAIL RESULTS (CONTINUED)

This plot shows the eigenvalues of each optimal design as the handling qualities weighting factor K_d is increased. When the weighting is large, the eigenvalues associated with both the short period and phugoid modes are driven to those of the model case.

The synthesis method ensures that designs with small J_d will handle better than those for which J_d is large, but because J_d is only a scalar quantity representing the sum of dynamic errors in all modes, additional information is required to determine when the response of particular modes becomes acceptable. Analysis of eigensystems or time histories of the motion allows the designer to transform the values of J_d into standard handling quality ratings (e.g. Mil. Spec. 8785).

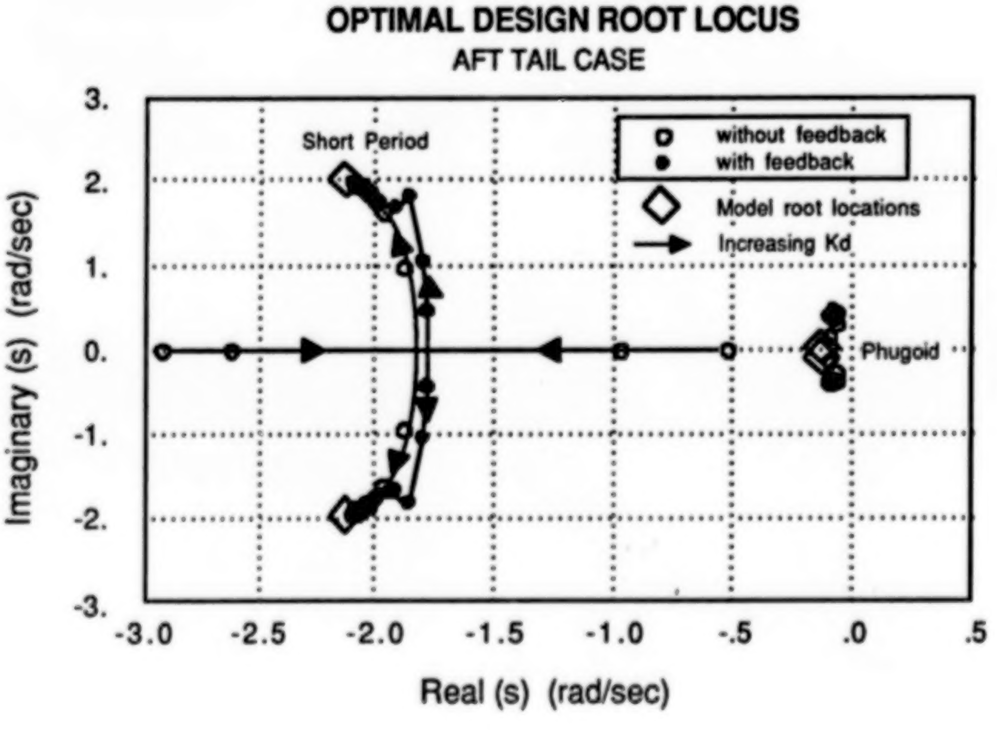

TAILLESS AIRCRAFT FLUTTER SUPPRESSION

The second example deals with the design of a tailless aircraft for minimum wing weight and an acceptable level of handling quality. The trimmed flight condition is at a high enough speed that flutter will occur unless the wing is stiffened. The goal of this design problem is to find the wing skin thickness (along the span) which achieves acceptable longitudinal dynamics with the smallest weight penalty. Two classes of designs are considered, those without any control system and those with a reduced order feedback controller consisting of wing tip deflection fed back to symmetric elevon deflection. The dynamics model for handling quality evaluation is the same tailless aircraft with a rigid wing. The integrated design procedure improves the handling by simultaneously suppressing the flutter and driving the unrestrained dynamic modes to be most like that of a rigid aircraft. This differs from conventional flutter suppression techniques which only guarantee flutter stability and do not attempt to restore acceptable handling qualities to the unrestrained modes of the free flying aircraft.

The critical flutter mode experienced by a high aspect ratio, swept tailless aircraft consists of a coupling between the aircraft's short period and wing bending modes (Ref. 4). The unstable mode is of low frequency (2 Hz) because the structural dynamics are coupled to the rigid body modes (i.e. short period mode). The reduced frequency of this motion is small enough that quasi-steady aerodynamic theory is appropriate for modelling this instability. The equations of motion describing these dynamics include all longitudinal rigid body degrees of freedom and two elastic wing bending modes. Aerodynamic stability derivatives are predicted by a vortex lattice method (quasi-steady aerodynamics) and all mass properties in the equations of motion are updated as skin thickness changes.

Constraints are imposed on maximum allowable stress (at a maximum load factor of 3 g's) and minimum skin gauge. Maximum skin stresses are calculated using a static aeroelastic analysis which accounts for inertia relief and the effect of wing deformation on the spanwise loading.

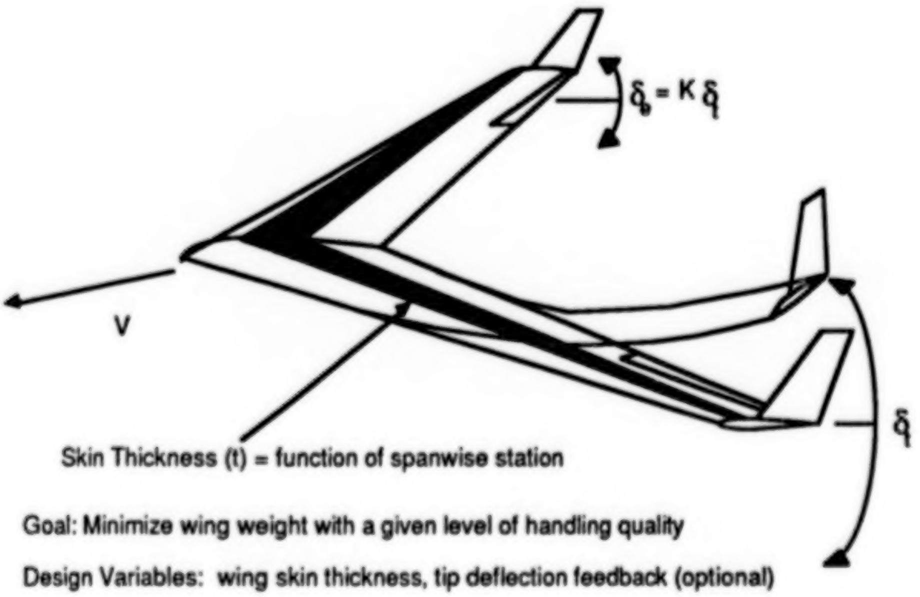

Goal: Minimize wing weight with a given level of handling quality

Design Variables: wing skin thickness, tip deflection feedback (optional)

UNRESTRAINED VEHICLE AEROELASTIC ANALYSIS

Formulation of the elastic, unrestrained vehicle's equations of motion in state vector form:
$dX / dt = [A] X + [B] U$
is necessary to evaluate the dynamic performance index, J_d, in this example. This is done by defining a new state vector that consists of both rigid body modes and a finite number of elastic degrees of freedom. Lagrange's method is then used to derive the equations of motion, given below in linearized form. With the equations expressed in this way, the designer can see the influence of structural flexibility explicitly, as an addition to the already familiar rigid body dynamic terms. The method can be extended to include unsteady aerodynamics by augmenting the state vector to include additional aerodynamic states with Pade approximates for the unsteady loading functions.

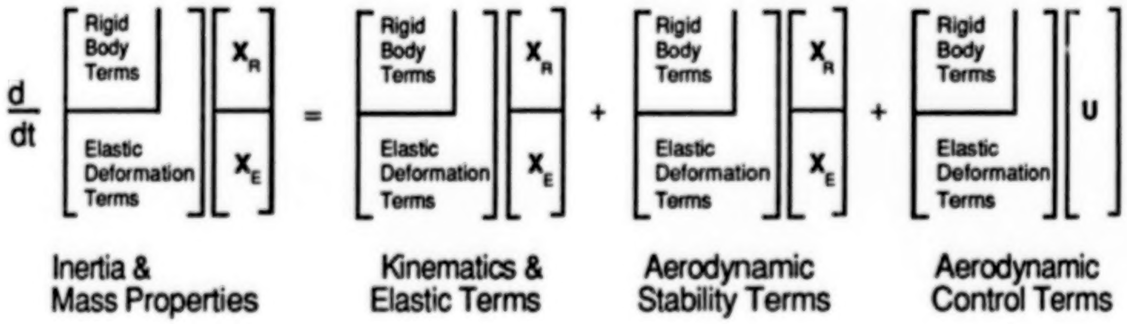
d/dt
Rigid Body Terms
Elastic Deformation Terms
X_R
X_E
=
Rigid Body Terms
Elastic Deformation Terms
X_R
X_E
+
Rigid Body Terms
Elastic Deformation Terms
X_R
X_E
+
Rigid Body Terms
Elastic Deformation Terms
U
Inertia & Mass Properties
Kinematics & Elastic Terms
Aerodynamic Stability Terms
Aerodynamic Control Terms

$$X = \begin{bmatrix} X_R \\ X_E \end{bmatrix}$$

$$\dot{X} = [A]\,X + [B]\,U$$

TAILLESS FLUTTER DESIGN RESULTS

Results for the tailless aircraft design example are shown below. As in the previous case, each point on the curves represents an optimal design with a specific value of handling quality weighting. Smaller values of J_d indicate improved handling, and increased values of weight ratio correspond to increased wing weight. The regions in which handling quality becomes acceptable lie to the left of the "level 1" limiting marks. Designs with feedback control show reduced wing weight since elevon deflection can provide artificial stiffness without additional material in the skins.

In a sequential design procedure the wing structure is first sized for minimum weight based on static aeroelastic loading and minimum gauge requirements. The control system (reduced order) is then designed for the best handling quality with a fixed wing design. The resulting sequentially designed aircraft has a stable flutter mode but its short period and phugoid dynamics are still highly coupled to the wing bending mode giving poor handling qualities. This design is represented by the point marked with an asterisk in the plot below.

By contrast, the integrated design procedure achieves a stable flutter mode with acceptable rigid body dynamics and does so with the least penalty in wing weight. Examination of the eigenvalues and eigenvectors shows that each of these approaches the model case as the handling quality weighting is increased. This is important to note, because the handling qualities for this example only become acceptable when the short period, phugoid, and wing bend modes are distinct and properly damped.

WING WEIGHT VS HANDLING

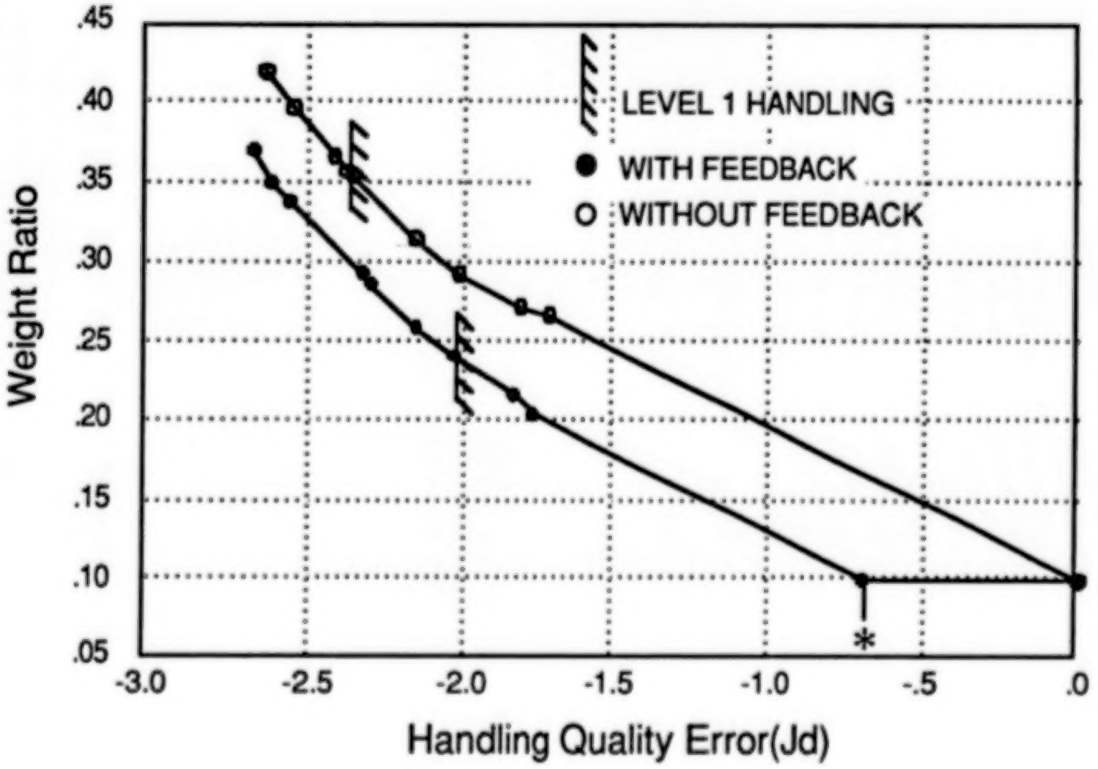

OPTIMAL SKIN THICKNESS DISTRIBUTION

The optimal solutions for the skin thickness as a function of semi-span are shown below. Aeroelastic stability requires that the skin thickness be increased at the wing root with greater thickness required for cases without a feedback controller. Interestingly, the results also show increased skin thickness at the wing tip, which acts as a concentrated tip mass. The presence of this material further separates the frequencies of wing bending and short period dynamic modes and is a significant factor in achieving flutter stability.

In a sequential design procedure skin thickness might be increased uniformly to achieve flutter stability. It is evident from these results that a uniform distribution is far from optimal and the weight penalty incurred in the sequential design procedure would be significant.

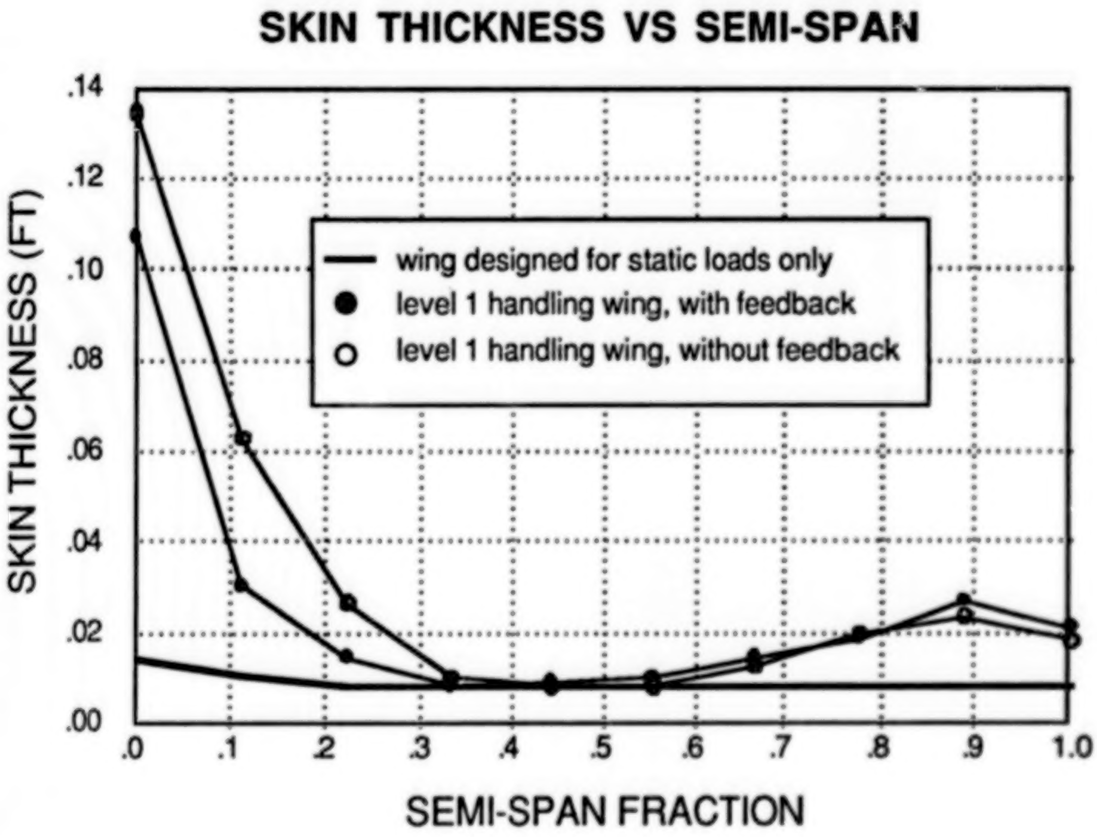

DYNAMIC DECOUPLING OF OBLIQUE WING AIRCRAFT

The oblique wing configuration exhibits reduced transonic and supersonic drag in a lightweight variable sweep configuration. At high sweep angles (greater than 25 degrees) asymmetries in the design produce a strong coupling between the lateral and longitudinal dynamics, which results in poor handling qualities. Previous efforts to decouple the response with feedback controllers have produced less than acceptable results because of insufficient control authority and lack of controllability in certain modes (Ref. 5). By including variables related to the aircraft's geometry within the feedback control system design, however, additional degrees of freedom are available to more thoroughly decouple the aircraft's dynamic response.

In this example, six variables are optimized to achieve the maximum decoupling of lateral and longitudinal dynamics. These variables include the x and y location of the pivot relative to the fuselage and wing, the wing bank angle with respect to the fuselage, and the wing dihedral. Control system feedback gains are purposely omitted from the design variables to illustrate the use of the method for "passive" design. The results show that small variations in geometric parameters can be utilized to reduce the demands placed on the control system design. The design could be improved further by including both geometric variables and feedback gains in the optimization.

Vortex Lattice Geometry of NASA/Rockwell F-8 OWRA

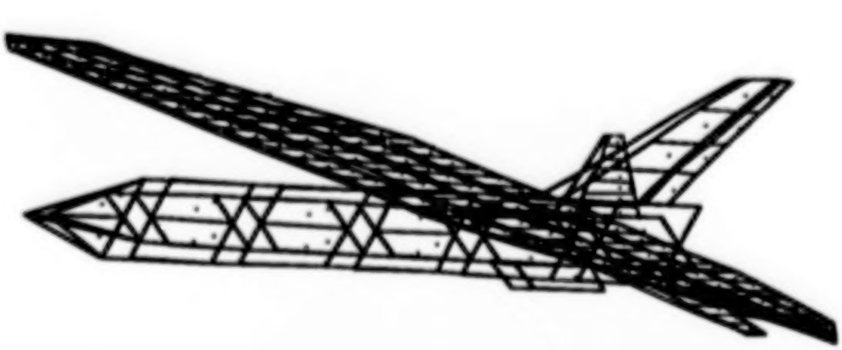

Goal: Achieve maximum decoupling in lateral and longitudinal dynamic modes by changing wing position relative to fuselage

Design Variables: Wing pivot location on fuselage, pivot location on wing, wing bank angle, dihedral

OBLIQUE WING AERODYNAMIC COUPLING

The oblique wing asymmetry gives rise to aerodynamic and inertial couplings which are not experienced by conventional symmetric aircraft. The first figure below shows the sideforce produced as angle of attack changes with zero sideslip. This coupling force is due to the low pressure region on the leading edge which produces a sideforce when the wing is swept obliquely. Rolling moments (lower figure) are caused by a distorted wing lift distribution and wing sideforce acting above the c.g. The nonlinear character of the aerodynamic coupling suggests that consideration of multiple flight conditions is required. Additional aerodynamic coupling exists in all six forces and moments.

Sideforce vs Angle of Attack

65 (deg) Sweep Oblique Wing Aircraft

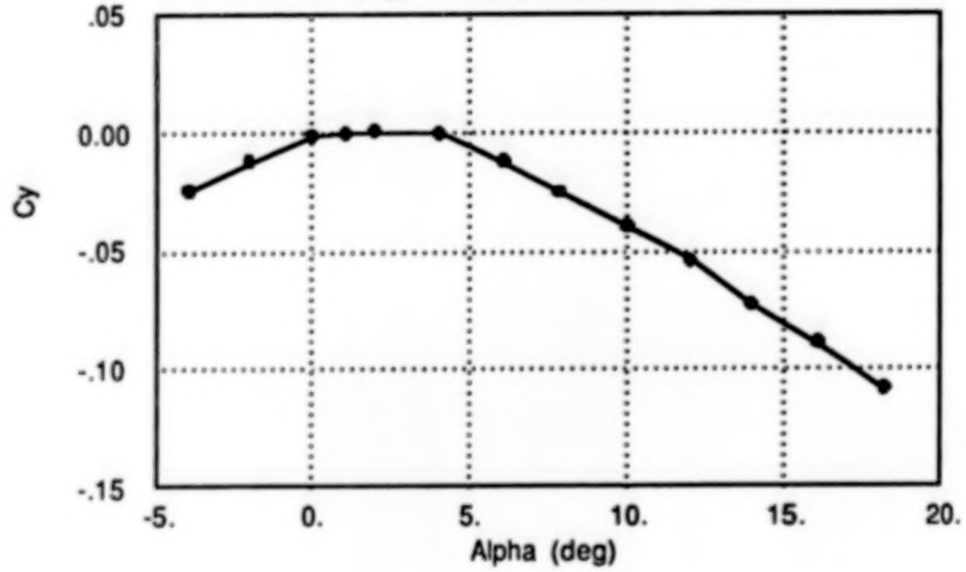

Rolling Moment vs Angle of Attack

65 (deg) Sweep Oblique Wing Aircraft

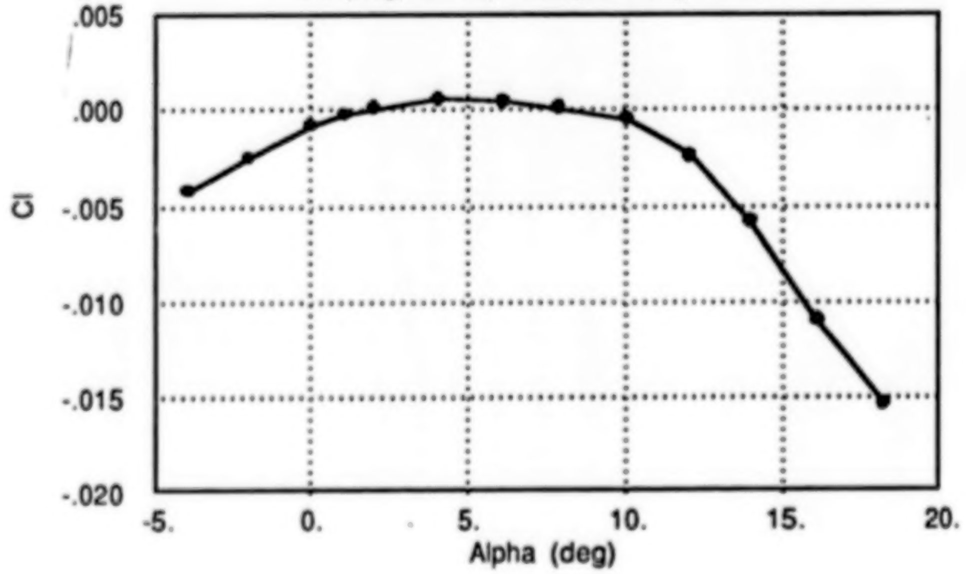

OBLIQUE WING DESIGN RESULTS

The vortex lattice geometries for the initial guess and the optimal solution configurations are shown below. The design synthesis is carried out for a fixed oblique wing sweep of 45 degrees. The optimizer forces the dynamic response to be as close as possible to the model case, a configuration with zero oblique sweep. The optimal solution shows the wing banked 8 degrees (forward wing low) and the wing displaced slightly from the initial guess position.

All six degrees of freedom are modeled in the equations of motion. As the configuration shape is changed, the aerodynamic stability derivatives and mass properties of the aircraft are recalculated. All aerodynamics are modeled using a vortex lattice method. The final design is constrained to satisfy trim requirements (with constraints on control surface deflection) at a specified design flight condition.

In this example vertical gusts are modeled as initial condition disturbances on angle of attack. The basic design procedure weights all possible initial conditions equally, but specific perturbations can be included by using a weighted trace of the three matrices associated with the Lyapunov equations. The integrated error in the vehicle's response to these excitations is weighted for minimum lateral acceleration and roll rate response by using an appropriate Q matrix. (See discussion of dynamic performance index.)

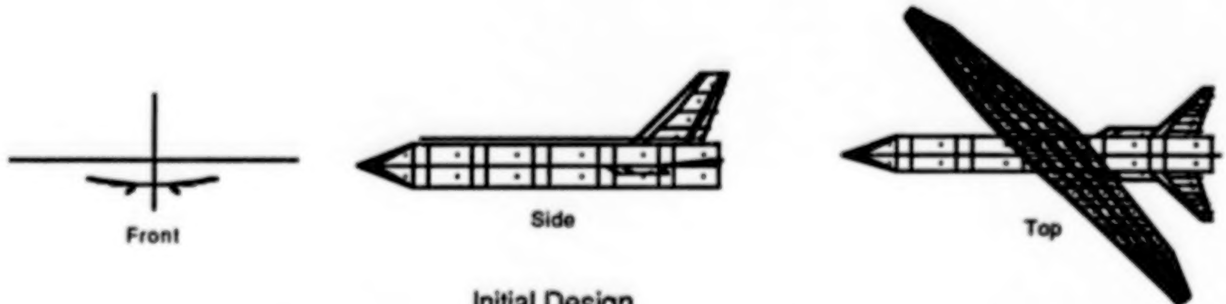

Initial Design

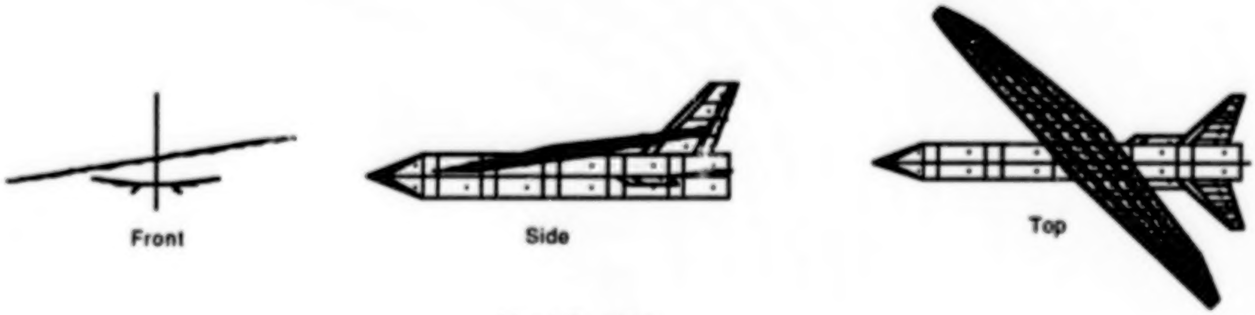

Final Design

OBLIQUE WING DYNAMIC RESPONSE

The performance of the optimized design is shown below in terms of the time histories of the aircraft's motion in response to a 50 ft/sec vertical gust. The results show significant reductions in peak lateral acceleration and roll angle when compared with the initial design case. Similar reductions occur in the sideslip and yaw rate response for the same gust excitation.

It was previously assumed that the best way to improve the oblique wing's handling qualities was to minimize the aerodynamic couplings present in the design. The optimal solution for this design synthesis shows, however, that the aerodynamic coupling terms for the optimal design are nonzero. This is understandable because decoupled dynamic response requires that the aerodynamic and inertial couplings cancel each other. Only an integrated design procedure, which simultaneously analyzes the effects of configuration changes on the inertia and aerodynamics of the vehicle, is capable of solving for the configuration which maximizes the dynamic response decoupling.

Lateral Acceleration vs Time
Response To Vertical Step Gust

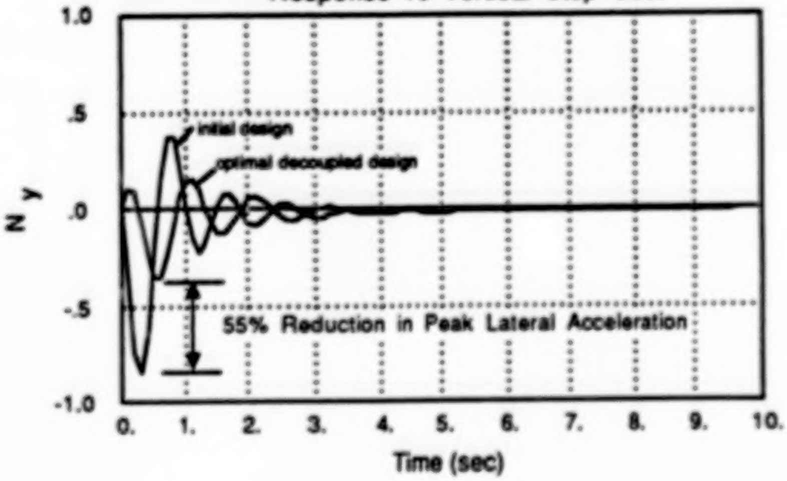

Roll Angle vs Time
Response To Vertical Step Gust

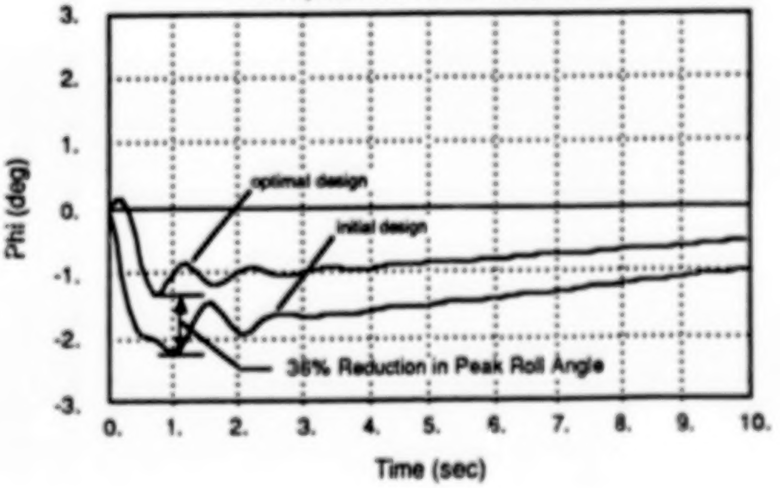

SUMMARY AND CONCLUSIONS

The method described here for aircraft design optimization with dynamic response considerations provides an inexpensive means of integrating dynamics into aircraft preliminary design. By defining a dynamic performance index that can be added to a conventional objective function, a designer can investigate the tradeoff between performance and handling (as measured by the vehicle's unforced response.) The procedure is formulated to permit the use of control system gains as design variables, but does not require full-state feedback. The examples discussed here show how such an approach can lead to significant improvements in the design as compared with the more common sequential design of system and control law.

REFERENCES

1. Gill, P., Murray, W., Pitfield, R., "The Implementation of Two Revised Quasi-Newton Algorithms for Unconstrained Optimization," National Physical Laboratory Rpt. NAC 11, April 1972.

2. Zeiler, T., Weisshaar, T., "Integrated Aeroservoelastic Tailoring of Lifting Surfaces," Journal of Aircraft, Vol 25, No. 1, Jan. 1988, pp 76-83.

3. Sawaki, E., Kobayakawa, M., Imai, H., "A Design Method of an Aircraft with ACT by Nonlinear Optimization," Trans. Japan Soc. of Aerospace Sciences, Vol. 29, No. 85, Nov. 1986, pp 142-162.

4. Schweger, J., Sensburg, O., Berns, H., "Aeroelastic Problems and Structural Design of a Tailless CFC Sailplane," 2nd International Symposium on Aeroelasticity in Structural Dynamics, 1985.

5. Alag, G., Kempel, R., Pahle, J., "Decoupling Control Synthesis for an Oblique-Wing Aircraft," NASA TM 86801, June 1986.

- Method provides an inexpensive way of integrating dynamic performance considerations into aircraft preliminary design

- Composite performance index allows designers to investigate tradeoffs between handling and performance

- Control gains or configuration variables are selected simultaneously permitting reduced-order controllers

- Approach can yield increased performance compared with sequential design of configuration and control system

SESSION 12: METHODS

Chairmen: M. P. Kamat and J. E. Rogan

AN INTERPRETATION AND SOLUTION OF ILL-CONDITIONED LINEAR EQUATIONS

I.U. Ojalvo and T. Ting
Mechanical Engineering Department
University of Bridgeport
Bridgeport, CT

INTRODUCTION

Data insufficiency, poorly conditioned matrices and singularities in equations occur regularly in complex optimization, correlation, and interdisciplinary model studies. This work concerns itself with two methods of obtaining certain physically realistic solutions to ill-conditioned or singular algebraic systems of linear equations arising from such studies.

Two efficient computational solution procedures that generally lead to locally unique solutions are presented when there is insufficient data to completely define the model, or a least-squares error formulation of this system results in an ill-conditioned system of equations.

If it is assumed that a "reasonable" estimate of the uncertain data is available in both cases cited above, then we shall show how to obtain realistic solutions efficiently, in spite of the insufficiency of independent data.

The proposed methods of solution are more efficient than singular-value decomposition [1] for dealing with such systems, since they do not require solutions for all the nonzero eigenvalues of the coefficient matrix.

OBJECTIVES

REVIEW MATHEMATICAL FORM OF ILL-CONDITIONING

OUTLINE PHYSICAL SOURCES OF ILL-CONDITIONING

REVIEW SINGULAR-VALUE DECOMPOSITION SOLUTION APPROACH

PRESENT A COMPUTATIONALLY SIMPLER METHOD

OFFER MATHEMATICAL & GEOMETRIC INTERPRETATION OF SOLUTIONS

DISCUSS PHYSICAL INTERPRETATION AND RELATIONSHIP TO:

1. MATH MODEL IMPROVEMENT
2. GRADIENT METHODS
3. BAYESIAN ESTIMATION

PROBLEM STATEMENT

Given the physical system with "m" bits of experimental data, $\{Y_e\}$ and "n" uncertain parameters $\{r\}$,

assume that a math model exists which yields the "m" values $\{Y_a\}$ based upon the "m" estimated parameters $\{r_o\}$.

It is desired to determine the "best" fit of parameters $\{r\}$ so that $\|y_e - y_a\|$ is a minimum.

A one-term Taylor approximation yields:

$$\left\{Ye - Ya\right\} = \left[\frac{\partial\{Ya\}}{\partial\{r\}}\right] \left\{r - r_o\right\} + \left\{R\right\}$$

where $\{R\}$ is the Taylor series truncation error plus experimental error.

The mXn sensitivity matrix [S] is then defined below.

SENSITIVITY MATRIX: $\underset{M \times N}{[S]} = \left[\frac{\partial\{Y_A\}}{\partial\{\Delta R\}}\right]$

NO. PARAMETERS: $\underset{N \times 1}{\{\Delta R\}} = \{R - R_0\}$

SOLUTION AND OUTPUT DATA: $\underset{M \times 1}{\{\Delta Y\}} = \{Y_E - Y_A\}$

RESIDUAL: $\underset{M \times 1}{\{R\}} = \{\Delta Y\} - [S]\{\Delta R\}$

TAYLOR SERIES: $\{Y_E\} = \{Y_A\} + [S]\{\Delta R\} + \text{Res}$

LEAST-SQUARES MINIMUM RESIDUAL: $[S^T S]\{\Delta R\} = [S]^T \{\Delta Y\}$

CONDITIONING

1. If $m > n$, there are more data than parameters, and so we shall seek a least-error-squared fit.

2. If $m < n$, then there are an infinite number of solutions and it is not clear which one to use.

Let us pursue case (1) first (i.e. $m > n$). If $[S^T S]$ is numerically invertible, then a least-error-squared solution is possible by efficient triangular factorization of $[S^T S]$ into $[LL^T]$, and subsequent forward and backward substitution. However, if "n" is only moderately large, then solutions can become difficult due to ill-conditioning. Also, if the rank of $[S^T S]$ is less than n, factorization is not possible. Now, if $m < n$ and a solution is somehow obtained, what is its interpretation?

One possible approach to these problems is to use the singular-value decomposition (SVD) solution approach [1]. This technique requires obtaining all the q ($\leq n$) nonzero eigenvalues $[\diagdown\lambda\diagdown]$ of $[S^T S]$ and the corresponding nxq modal matrix, [U]. If the rank of $[S^T S]$ is n, then the interpretation of SVD is clear. However, if the rank is less than n (as it may be for $m > n$ and will be for $m < n$), interpretations of the SVD solutions are not obvious.

$M > N$:	1.	$S^T S$	WELL CONDITIONED (NUMERICALLY & PHYSICALLY)
	2.	$S^T S$	ILL-CONDITIONED (NUMERICALLY, BUT NOT PHYSICALLY)
$M < N$:	3.	$S^T S$	ILL-CONDITIONED (NUMERICALLY & PHYSICALLY)

CASE OF WELL-CONDITIONED NUMERICALLY, BUT NOT PHYSICALLY, IS NOT CONSIDERED

IF CASE 1: $[S^T S] = [L]\,[L]^T$, L = CHOLESKY DECOMPOSITION = $[\ddots\ ^{0}]$

IF CASE 2: $\underset{N \times N}{[S^T S]^{-1}} \doteq \underset{NXQ}{U}\ \underset{QXQ}{[\diagdown\lambda\diagdown]^{-1}}\ \underset{QXN}{U^T}$ SINGULAR-VALUE DECOMP.

$\lambda = (Q \leq N)$ NON-ZERO EIGENVALUES OF $[S^T S]$

[U]=CORRESPONDING MODAL MATRIX

EPSILON DECOMPOSITION

The previously discussed procedure is laborious at best. A much simpler procedure is now presented. First, pick a small value ϵ, and set

$$[\underline{S^TS}] = [S^TS] + \epsilon[I]$$

such that $[\underline{S^TS}]$ may be efficiently factored into $[\underline{LL}^T]$ where $[\underline{L}]$ is lower triangular. This is then used to solve

$$[\underline{S^TS}]\{\Delta r\} = [S]^T\{\Delta y\}$$

Next, decrease ϵ until $\{\Delta r\}$ approaches an asymptote, or the factorization of $[\underline{S^TS}]$ into $[\underline{LL^T}]$ breaks down due to ill-conditioning.

This method has been termed a "Levenberg-Marquardt" method by Luenberger [2], who considers it to be a modification of Newton's Method and steepest-descent (see pp. 225-227 of Reference 2).

(SIMPLER PROCEDURE)

$$\overline{[S^TS]} = [S^TS] + \epsilon[I] = [\bar{L}][\bar{L}]^T$$

$$\epsilon_1 > \epsilon_2 > \epsilon_3 > \cdots\ 0$$

BUT, WHAT DO SOLUTIONS MEAN?

EXPLANATION BASED ON SIMPLE 2-DOF INTERPRETATION

TWO DOF EXAMPLE

Consider the two degree-of-freedom (DOF) example with m=1, where we are given:

$$[S] = [a \quad b]$$

Therefore,

$$[\underline{S}^T S] = \begin{bmatrix} a^2 + \varepsilon & a \cdot b \\ a \cdot b & b^2 + \varepsilon \end{bmatrix}, \quad |S^T S| = 0$$

$$[S^T S]^{-1} = \frac{1}{\varepsilon\,(\varepsilon + a^2 + b^2)} \begin{bmatrix} b^2 + \varepsilon & -a\,b \\ -a\,b & a^2 + \varepsilon \end{bmatrix}$$

Thus, the least-error-squared solution becomes $\{\overline{\Delta r}\} = [\underline{S}^T S]^{-1}[S]^T \{\Delta y\}$

or

$$\lim_{\varepsilon \to 0} \{\overline{\Delta r}\} = \lim_{\varepsilon \to 0} \begin{Bmatrix} \dfrac{a\,\Delta y}{a^2 + b^2 + \varepsilon} \\ \dfrac{b\ \Delta y}{a^2 + b^2 + \varepsilon} \end{Bmatrix} = \begin{Bmatrix} \dfrac{a\ \Delta y}{a^2 + b^2} \\ \dfrac{b\ \Delta y}{a^2 + b^2} \end{Bmatrix}$$

GEOMETRIC INTERPRETATION

A geometrical interpretation of the solution shows that the ideal solution occurs for the point on the line $[S]\{\Delta r\} = \{\Delta y\}$ which is closest to the origin.

Note that if $\varepsilon > 0$, then the solutions fall short of this ideal point.

A comparison of our proposed epsilon-decomposition approach with the method of singular-value decomposition yields the identical result for $\{\Delta r\}$, but through different computational steps.

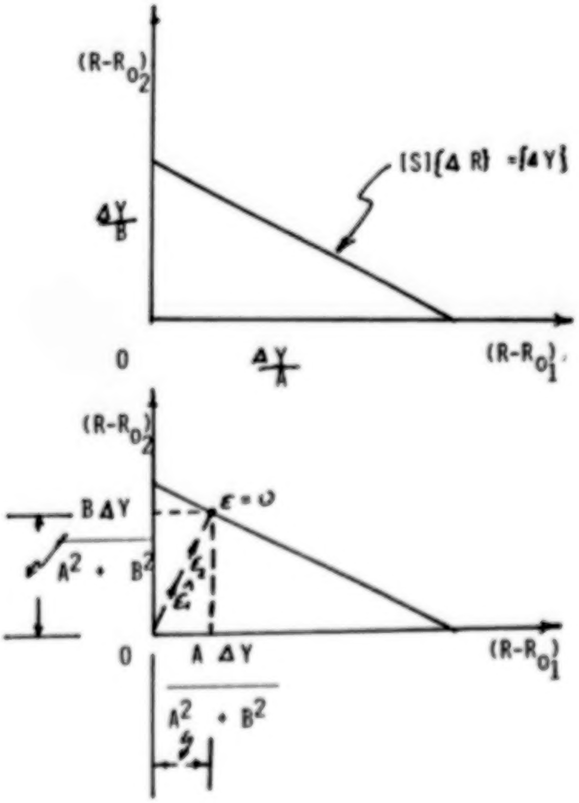
$(R-R_o)_2$
$[S]\{\Delta R\} = \{\Delta Y\}$
$\frac{\Delta Y}{B}$
0
$\frac{\Delta Y}{A}$
$(R-R_o)_1$
$(R-R_o)_2$
$\frac{B\,\Delta Y}{\sqrt{A^2+B^2}}$
$\varepsilon = 0$
ε_1
ε_2
0
$\frac{A\,\Delta Y}{\sqrt{A^2+B^2}}$
$(R-R_o)_1$

MATHEMATICAL INTERPRETITION

The previous two-pages suggest that an n-DOF solution approach is not only to minimize the sum of the residuals squared but also to minimize the distance on this line to the origin of $\{\Delta r\}$ space, i.e.

$$\underline{\Phi} = R^T R + \varepsilon \Delta r^T \Delta r$$

If $[S^T S]$ is not ill-conditioned, simply set ε to zero and solve by $[LL^T]$ decomposition. However, if it is ill-conditioned, choose an ε and solve by $[\underline{LL}^T]$ decomposition. Keep reducing ε until the solution asymptotes to certain values, or this type of factorization breaks down numerically.

Choosing a starting ε is arbitrary, but the two-DOF example suggests that ε should be small compared to the smallest eigenvalue of $[S^T S]$. However, it is dangerous to generalize.

We have shown that this procedure works, not only when $m > n$, but also when $m < n$ (which was initially called case 2 here). However, a more direct solution is possible if $m < n$ and this is shown on the following page.

$$\{R\} = \{\Delta Y\} - [S]\{\Delta R\}$$

$$\bar{\Phi} = \{R\}^T\{R\} + \varepsilon\{\Delta R\}^T\{\Delta R\}$$

$$\left\{\frac{\partial \bar{\Phi}}{\partial\{\Delta R\}}\right\} = \{0\}, \quad ([S^T S] + \varepsilon[I])\{\Delta R\} = [S]^T\{\Delta Y\}$$

UNDER-DETERMINED SYSTEMS

For the case where $m<n$, $[S^TS]^{-1}$ will not exist. However, if the rank of $[SS^T]$ is m, then its inverse will exist, and it is possible to show that $[S^TS]^{-1}[S]^T$ is equivalent to $S^T\,[SS^T]^{-1}$ (as ϵ approaches zero). Therefore, it is not necessary to use epsilon in determining $\{\Delta r\}$, for $m<n$, when the rank of $[SS^T]$ is m. However, if its rank is less than m, we may still wish to use the present method on either $[S^TS]$ or $[SS^T]$. Our method will yield almost identical results if epsilon is sufficiently small, as compared to the smallest non-zero eigenvalue of either $[S^TS]$ or $[SS^T]$.

$M<N$ CASE, $\overset{M\times M}{|S\,S^T|} \neq 0$

GIVEN: $[S^TS]\{\Delta R\} = [S]^T\{\Delta Y\}$, $\underset{N\times N}{|S^TS|} = 0$, $\{\overline{\Delta R}\} = [\overline{S^TS}]^{-1}\,[S]^T\{\Delta Y\}$

CONSIDER: $\lim\limits_{\epsilon\to 0}\,[\overline{S^TS}]^{-1}\,[S^T] = \lim\limits_{\epsilon\to 0}\,(S^TS + \epsilon\,I)^{-1}\,[S^T]$

$$\therefore\ [S^TS]\,[S]^T = \lim_{\epsilon\to 0}\,(S^TS + \epsilon\,I)\quad S^T \quad \ldots\ldots (1)$$

ASSUME: $|S\,S^T| \neq 0$. POST-MULTIPLY EQ (1) BY $[S\,S^T]^{-1}$

$$\therefore S^T = \lim_{\epsilon\to 0}\,(S^TS + \epsilon\,[I])\quad S^T\quad [S\,S^T]^{-1} \quad \ldots\ldots (2)$$

ASSUME: $|\overline{S^TS}| \neq 0$, $\epsilon > 0$

PREMULT. EQ(2) BY $\lim\limits_{\epsilon\to 0}\,[\overline{S^TS}]^{-1}$

THEN, $\lim\limits_{\epsilon\to 0}\,[\overline{S^TS}]^{-1}\quad S^T = S^T\quad [S\,S^T]^{-1}$

AND SO $\{\Delta R\} = S^T\quad [S\,S^T]^{-1}\,\{\Delta Y\}$

PHYSICAL INTERPRETATION OF PROPOSED PROCEDURE

Strictly speaking, the unique solution of an ill-conditioned system of equations is nonsense. What we have shown is that a unique solution is possible if an additional condition is introduced, in the form of a constraint, upon the minimization problem; namely, that the solution must not only satisfy the original "m" equations in a least-squared error sense, but if the resulting nxn system is ill-conditioned, then the proper solution should be closest to the initial math model. This latter condition is sufficient to uniquely determine the solution in most cases. In our minimization formulation, epsilon represents a weighting of the closeness-to-the-origin constraint, $|r-r_o| = \min$, relative to the size the m-equation residual, $|R|$, minimization. Thus, if we wish to minimize $|R|$, ϵ should be made as small as practically possible while still delivering a unique solution for $\{\Delta r\}$.

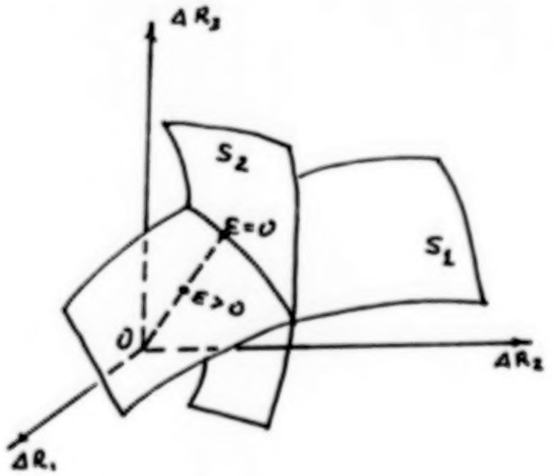

(NON-UNIQUE SOLUTIONS TO S_1 & S_2 EXIST ALONG INTERSECTION)

$\bar{\bar{\Phi}} = \{R\}^T\{R\} + \epsilon\{\Delta R\}^T\{\Delta R\} = $ MIN (MAKES PROBLEM WELL-POSED & SOLUTION-UNIQUE)

$\{\Delta R\} = \{0\}$ IS THE INITIAL GUESS

RELATIONSHIP TO EXISTING METHODS

Physically speaking, our approach implies that the initial solution-guess, $\{r_o\}$, is reasonable and that if the formulation leads to some insufficiency in uniquely defining the system (i.e. an ill-conditioned $[S^T S]$ matrix) then the criterion of closeness of $\{r\}$ to $\{r_o\}$ shall be imposed to uniquely define the system. By making ε as small as is practical, we are simply weighting this closeness of $\{r\}$ to $\{r_o\}$ condition as secondary to the least-square-error criterion. Viewed in this way, we may consider a different weighting of the various parameters of $\{r\}$ through the diagonal weighting matrix $[\diagdown W_r \diagdown]$. Continuing this concept for the various residuals, $\{R\}$, as well as through the weighting matrix $[W_y]$ we arrive at a Bayesian formulation i.e. to find the minimum of Φ where Φ is given by:

$$\Phi = \{R\}^T [W_y] \{R\} + \{r - r_o\}^T [\diagdown W_r \diagdown] \{r - r_o\}.$$

NEWTON METHODS: $\varepsilon_1 > \varepsilon_2 \cdots$ TRAVEL ALONG GRADIENT TO SOLUTION FROM INITIAL GUESS

BAYESIAN ESTIMATION:

MINIMIZE: $$\Phi = \{R\}^T \underset{\substack{\uparrow \\ \text{WEIGHTED} \\ \text{RESIDUALS}}}{[W_Y]} \{R\} + \{\Delta R\}^T \underset{\substack{\uparrow \\ \varepsilon\,[I] \\ \text{PROPOSED SOLUTION} \\ \text{APPROACH}}}{[W_R]} \{\Delta R\}$$

CONCLUSIONS

We have derived a numerical technique for solving ill-conditioned systems of equations which does not rely upon computation of the system's non-zero eigenvalues and eigenvectors (as is necessary with singular-value decomposition) . While others have proposed this same procedure, it is felt that we have given it a more formal and less heuristic derivation. In addition, we have supplied a physical interpretation which gives insight into the results which the method yields, as well as its relation to Bayesian estimation methods.

AVOIDED USE OF SINGULAR-VALUE DECOMPOSITION
(COMPUTATIONALLY HARDER)

PROVIDED MATHEMATICAL BASIS FOR PROPOSED SOLUTION APPROACH

PRESENTED A GEOMETRIC INTERPRETATION

PRESENTED A PHYSICAL INTERPRETATION

IMPROVED INSIGHT INTO SOLUTION OF ILL-CONDITIONED EQS.

REFERENCES

1. Dahlquist, G. and Bjurck, A., "Numerical Methods", Prentice-Hall, N.J., 1974

2. Luenberger, D.G., "Linear and Nonlinear Programming", 2nd Ed., Addison-Wesley, Reading, Mass, 1984.

BIBLIOGRAPHY

Isenberg, J., "Progressing from Least Squares to Bayesian Estimation", ASME Paper 79-WA/DSC-1, Dec. 1979.

SYMBOLS

a, b	Elements of a matrix
$\{r\}$	Parameters (or solution) of math model being sought
$\{r_o\}$	Starting estimate of math model parameters
$\{\Delta r\}$	$r - r_o$
$\{Y_a\}$	Analytically determined solution vector
$\{Y_e\}$	Experimental determined values
$\{\Delta Y\}$	$Y_e - Y_a$
R	Residual
S_1, S_2	2-dimensional surfaces in 3-dimensional space
ε	Epsilon parameter
$\Phi, \underline{\Phi}$	Functions to be minimized
$[I]$	Identity matrix
$[L]$	Lower triangular matrix
$[S]$	Senitivity matrix
$[U]$	Modal matrix corresponding to non-zero eigenvalues
$[W_r]$	Initial parameter confidence weighting matrix
$[W_y]$	Experimental data confidence weighting matrix
$[\lceil\lambda\rfloor]$	Diagonal eigenvalue matrix
T	Transpose of a matrix (used as a superscript)
-1	Inverse of matrix (used as a superscript)
-p	Pseudo-inverse (used as a superscript)

GENERALIZED MATHEMATICAL MODELS IN DESIGN OPTIMIZATION

Panos Y. Papalambros
and
J. R. Jagannatha Rao*
Department of Mechanical Engineering
and Applied Mechanics
The University of Michigan
Ann Arbor, MI

---

*Graduate Student

Introduction

We make the usual distinction between the vector of parameters and the vector of variables in an optimization problem. A parametric optimal design problem is considered as a system whose input is the vector of parameters. Corresponding to each input parameter vector, the output is, collectively, the feasible domain, the optimal objective value and the optimal variable vector. Hence, this input to output relation is characterized by a point-to-set map. When the stability arguments of such a map are augmented with the need to identify the optimal *input* for a given system, a very useful framework emerges for design problems. Recent results seem to indicate that such an approach would address the issue of studying the *modeling of the design itself,* in conjunction with the numerical procedures that are used to solve the optimization problem. While the concept of parametric optimization is not new, its interpretation in the form of an input to output mapping, and the associated solution strategy that could make explicit the inner stability of a problem, are considered very useful generalizations of traditional design optimization models (see fig. 1).

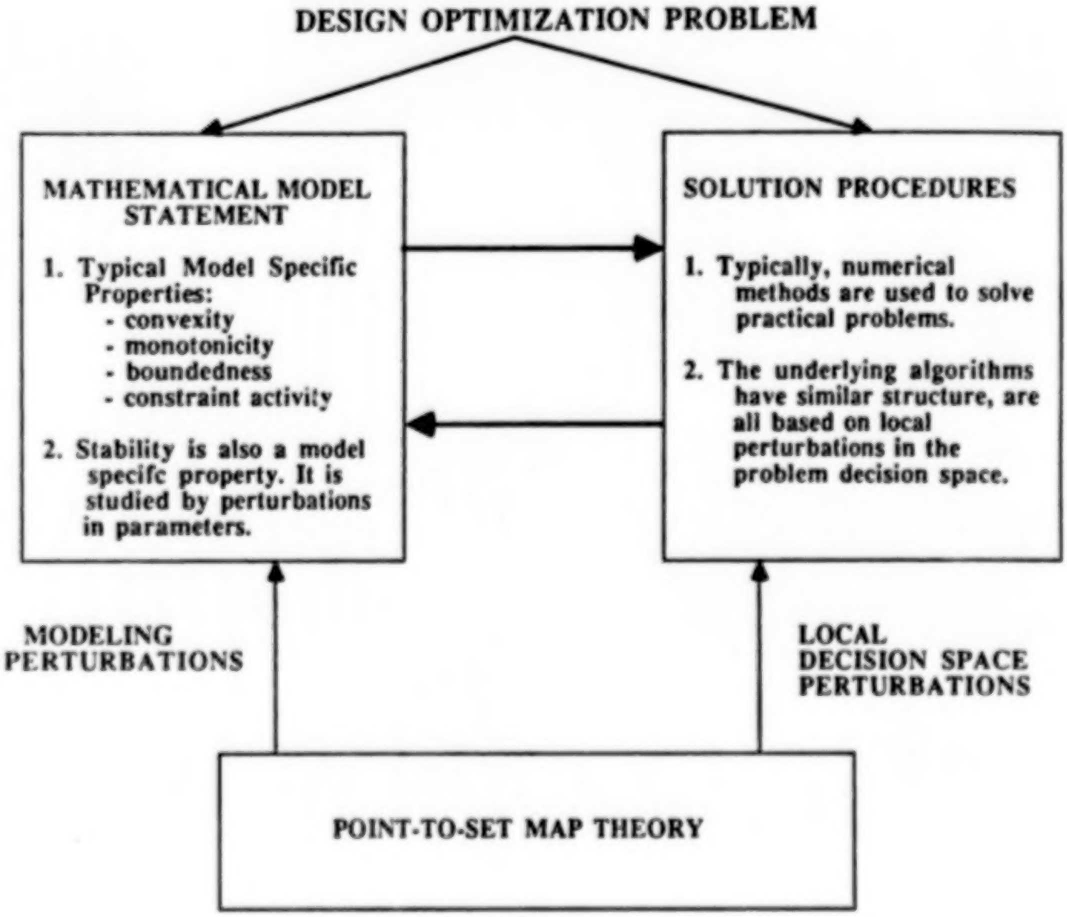
DESIGN OPTIMIZATION PROBLEM
MATHEMATICAL MODEL STATEMENT
1. Typical Model Specific Properties:
- convexity
- monotonicity
- boundedness
- constraint activity
2. Stability is also a model specifc property. It is studied by perturbations in parameters.
SOLUTION PROCEDURES
1. Typically, numerical methods are used to solve practical problems.
2. The underlying algorithms have similar structure, are all based on local perturbations in the problem decision space.
MODELING PERTURBATIONS
LOCAL DECISION SPACE PERTURBATIONS
POINT-TO-SET MAP THEORY

Figure 1

Problem Statement

The terminology used here closely follows that used in ref. 1. The general design optimization model is assumed to be stated as:

$$
\begin{array}{lll}
 & \textit{minimize} & f(x,p) \\
\boldsymbol{P(x,p)} & \textit{subject to} & \\
 & & g_k(x,p) \leq 0 \quad k \in L = \{1,\ldots,l\} \\
 & & h_i(x,p) = 0 \quad i \in M = \{1,\ldots,m\} \\
 & & p = (p_i) \qquad \in P \subset \Re^p \\
 & & x = (x_i) \qquad \in X \subset \Re^n
\end{array}
\tag{1}
$$

where f, g_k and h_i are the scalar objective, inequality, and equality constraint functions respectively. The variable vector $x = (x_i)$ usually describes the conventional design variables such as member areas in a truss structure. The vector p is a parameter that could describe, for example, the allowable yield stress for a truss member.

For any particular $p = p^* \in P$, the model $\boldsymbol{P(x,p)}$ is the usual mathematical programming statement:

$$
\begin{array}{ll}
\textit{minimize} & f(\mathbf{x}), \quad \mathbf{x} \in \Re^n \\
\textit{subject to} & \\
 & \mathbf{h}(\mathbf{x}) = \mathbf{0} \\
 & \mathbf{g}(\mathbf{x}) \leq \mathbf{0}
\end{array}
\tag{2}
$$

A Generalized Model as an Input-Output System

The basic idea in *input-output* (IO) formulations is as follows (fig. 2). We consider the model $\boldsymbol{P(x,p)}$ to be a system whose input is a particular $p \in P$. Corresponding to each such admissible input, the output is defined as collectively $\{F(p), F^*(p), f^*(p)\}$ where

$F(p) = \{x \in \Re^n : g_k(x,p) \leq 0 \; k \in L, h_i(x,p) = 0, \; i \in M\}$ is the feasible set

$F^*(p) = \{x^*(p)\}$, is the set of optimal solutions x^*

$f^*(p) = f(x^*(p),p)$, the optimal value function

STRUCTURE OF AN IO FORMULATION

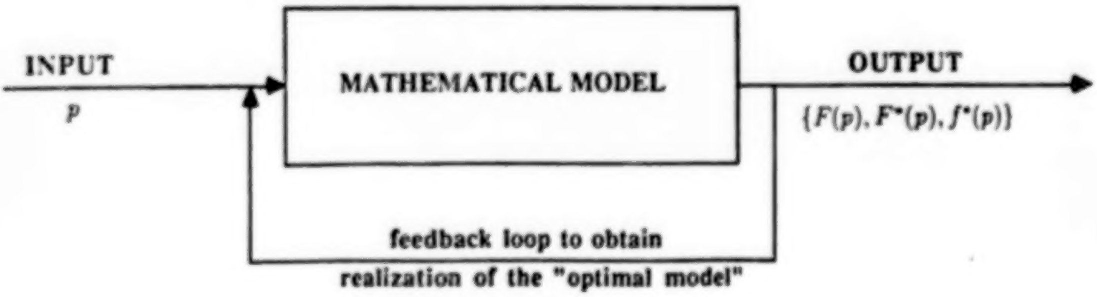
INPUT
p
MATHEMATICAL MODEL
OUTPUT
{F(p), F*(p), f*(p)}
feedback loop to obtain
realization of the "optimal model"

DESIRED OUTCOME FROM AN IO FORMULATION

- **OPTIMAL REALIZATION OF THE MATHEMATICAL MODEL**
- **THE BEST STABLE (AND FEASIBLE) PATH FROM THE INITIAL INPUT TO THE OPTIMAL INPUT**

Figure 2

IO and Conventional NLP*

One must at the outset try to answer under what circumstances would such an input-output formulation be more useful than the following single problem formulation:

$$\begin{array}{ll} \textit{minimize} & f(\mathbf{z}), \quad \textit{where } \mathbf{z} = (\mathbf{x}, \mathbf{p}) \in \Re^{n+p} \\ \textit{subject to} & \\ & \mathbf{h}(\mathbf{z}) = \mathbf{0} \\ & \mathbf{g}(\mathbf{z}) \leq \mathbf{0} \end{array} \qquad (3)$$

While the formulation above appeals to simplicity in its treatment since conventional optimality conditions and numerical methods apply to it, there are however some issues of note (fig. 3):

- **THE SOLUTIONS TO THE PROBLEMS (1) and (3) MAY NOT COINCIDE.** In some cases, a new set of necessary conditions can be derived for the IO solution (ref. 1).
- **A SIMPLER (such as convex or monotonic) SUBPROBLEM** can sometimes be derived by splitting the original variable vector z into a new variable x, of smaller dimension, and a *parameter* θ. Relates to decomposition techniques used in large-scale programming.

- Most importantly, an IO formulation, if successfully implemented, would **CHARACTERIZE THE INNER STABILITY OF THE PROGRAM.** The behavior of critical points on an IO path is identified as explicit model specific properties and enables us to view *modeling* and *solution techniques* in a unified way.

Figure 3

---

*Nonlinear Programming (NLP).

Stability Properties in Generalized Modeling

Following the usual notion of well-posedness, we say that a mathematical problem is well-posed if its solution is continuous w.r.t.* to the data. As we have seen, $\boldsymbol{P}(\boldsymbol{x},\boldsymbol{p})$ is an imbedded or parametrized family of mathematical programs. For these programs, the notion of stability is defined directly in terms of the continuity of the solution w.r.t. the perturbation vector p. In any study of such a perturbed family of related problems, the question of stability becomes central for two important reasons: Unstable points or regions should be identified to see if there is an attendant physical interpretation to the loss of stability; and if the problem is stable everywhere then standard optimality conditions would apply in the problem $\boldsymbol{P}(\boldsymbol{z})$ where $z = (x,p)$. The continuity of parameter-dependent feasible sets, solution sets and extremal value functions is useful to answer many questions such as:

- For which optimal design models, the intuitive argument that the accuracy of the solution obtained increases with the degree of approximation of the initial data, is indeed justified.

- If an exact solution can be viewed as an approximation to a solution of the problems that correspond to small perturbations of the initial parameters. This is particularly important if the calculation of solution requires substantial time and expense.

- Finally, what are the quantitative bounds on the solution as the initial data is substantially varied.

The stability information that we refer to here is directly related to (upper and lower) continuity properties of certain point-set-maps. As an example of such a map, we have:

$$\Omega : \Re^p \rightarrow \Re^n \times \Re^n \times \Re, \ \Omega(\theta) = \{F(\theta), F^*(\theta), f^*(\theta)\}$$

Several studies have been reported on the theoretical properties of such maps (e.g. ref. 2 and ref. 3).

Many of the early results in stability of optimal value function in nonlinear programming were obtained for right–hand–side perturbations of constraints (ref. 4). While studying general perturbations in the problem $\boldsymbol{P}(\boldsymbol{x},\boldsymbol{p})$:

$$\boldsymbol{P}(\boldsymbol{x},\boldsymbol{p}) : min\{f(x,p) : g(x,p) \leq 0, h(x,p) = 0, (x,p) \in X \times P\},$$

an interesting observation from ref. 5 is that at least when the dependence of f, g, and h on p is locally Lipschitz, a problem $\boldsymbol{P}(\boldsymbol{x},\boldsymbol{y},\boldsymbol{p})$ with equal $f^*(p)$ can be formulated having only right-hand-side perturbations (Note that now the variable vector is (x,y)) :

$$\boldsymbol{P}(\boldsymbol{x},\boldsymbol{y},\boldsymbol{p}) : min\{f(x,y) : g(x,y) \leq 0, h(x,y) = 0, -y + p = 0, (x,y,p) \in X \times P \times P\}$$

---

*with respect to (w.r.t.)

Regularity of Constraints and Stability

The study of constraint qualifications and nontrivial abnormality in Lagrange multiplier values is closely related to the study of stability of the optimal value function (ref. 5 and ref. 6). For example, if the second order sufficiency conditions hold at a local minimizer at which the constraints are *regular*, then that local minimizer persists under small perturbations (ref. 7). And the well known Mangasarian-Fromovitz constraint qualification is a necessary and sufficient condition for the set of Lagrange multiplier vectors associated with a stationary solution to form a compact polyhedron (ref. 8). While stability of optimal value function has been treated extensively in literature, the stability properties of the optimal solution set have also been considered (ref. 3 and ref. 9). From a computational standpoint, numerical continuation and bifurcation techniques can be applied to the critical points characterized by some suitable first-order necessary conditions (ref. 10 and also ref. 11). One can then classify the singularities based on:

1. Loss of the strict complementarity condition (see fig. 4)
2. Linear dependence of the gradients of the active constraints
3. Singularity of the Hessian of the Lagrangian on the tangent space

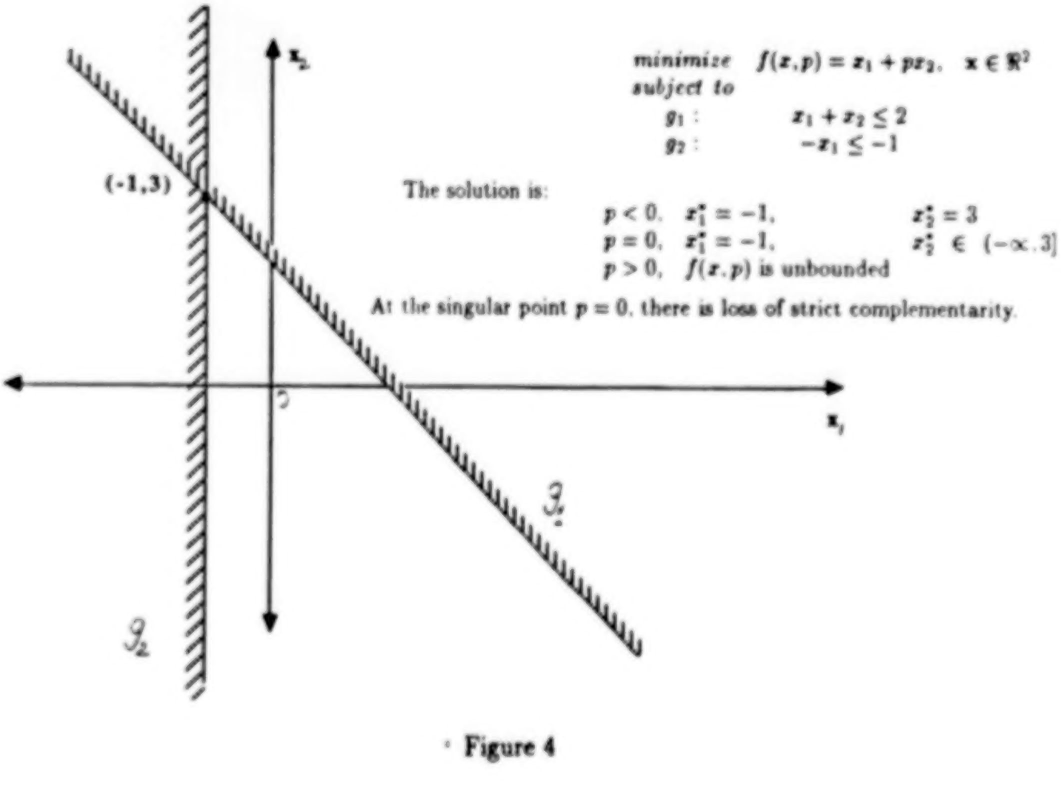

minimize $f(x,p) = x_1 + px_2, \quad \mathbf{x} \in \Re^2$
subject to
$g_1: \quad x_1 + x_2 \leq 2$
$g_2: \quad -x_1 \leq -1$

The solution is:

$p < 0, \quad x_1^* = -1, \quad x_2^* = 3$
$p = 0, \quad x_1^* = -1, \quad x_2^* \in (-\infty, 3]$
$p > 0, \quad f(x,p)$ is unbounded

At the singular point $p = 0$, there is loss of strict complementarity.

· **Figure 4**

223

BEST COPY AVAILABLE

A Design Plus Processing Model

A common characteristic of traditional design optimization models is that they operate on a single hierarchical level, with the possible exception of some decomposition strategies. However, there still does not exist a way to properly study the *modeling interactions* that occur in such practical systems where a model structure appears not just because the overall system is made up of individual components or subsystems, but rather because the same system can be viewed from two or more viewpoints. For example, a typical structural design model may be developed from its functional viewpoint, and another one from a fabrication or processing viewpoint. Usually, to study such an *integrated* system, models are blended in a single formulation by treating many additional constants (parameters) as variables and/or by introducing a rather arbitrary multiobjective formulation. In these cases, it is very difficult to understand and represent explicitly the relation of different quantities in the solution, or interpret their physical meaning. It is hoped that an input- output formulation will make more explicit the properties of model interactions. Figure 5 below depicts a typical system level abstraction in a design plus processing model.

Definition: Drawing is the process of reducing the cross-sectional area and/or the shape of a rod, bar, tube or wire (cold or hot) by pulling through a die.

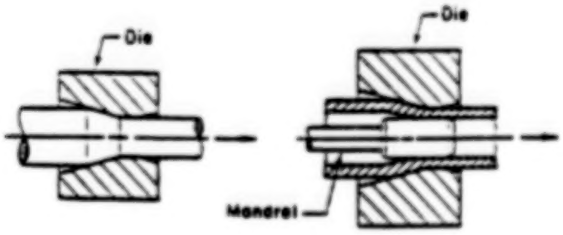
Die
Die
Mandrel

Figure: Drawing of (left) rod or wire and (right) tube

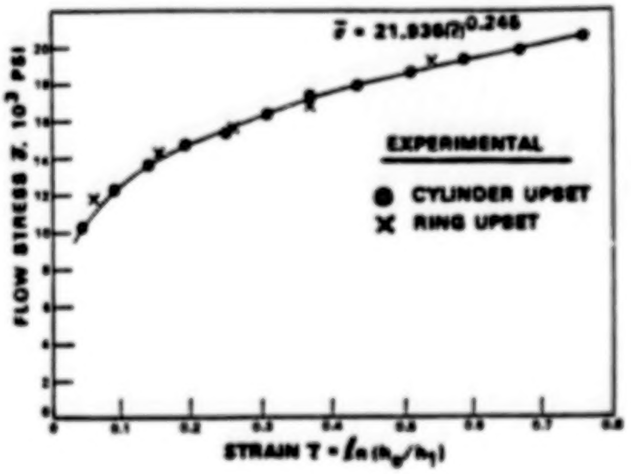

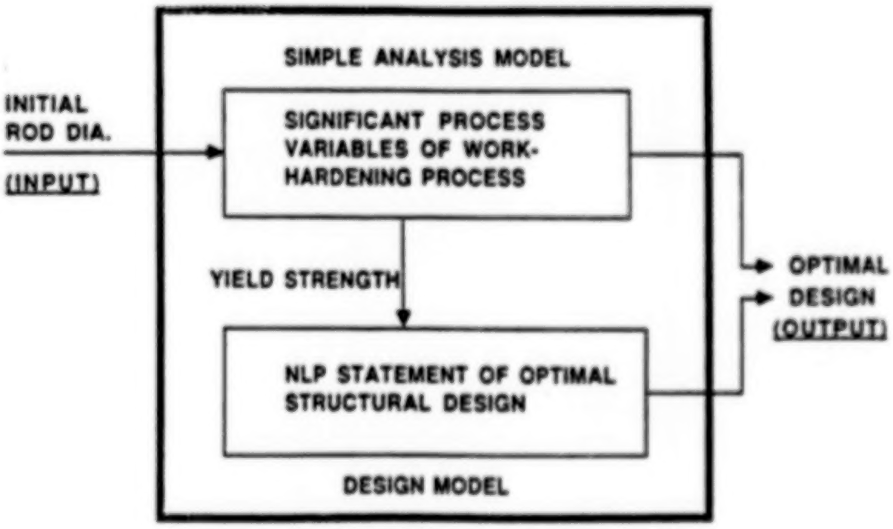
SIMPLE ANALYSIS MODEL
INITIAL
ROD DIA.
(INPUT)
SIGNIFICANT PROCESS
VARIABLES OF WORK-
HARDENING PROCESS
YIELD STRENGTH
NLP STATEMENT OF OPTIMAL
STRUCTURAL DESIGN
DESIGN MODEL
OPTIMAL
DESIGN
(OUTPUT)

MODEL INTERACTIONS IN IO FORMULATION

Figure 5

224

BEST COPY AVAILABLE

An Example of IO Formulation

As mentioned previously, it is of considerable importance to be able to study the behavior of optimum *design models* in conjunction with some model representation (referred to here as the processing model) of a class of suitable fabrication processes. Detailed processing models are in general much harder to obtain as compared to the *design* models, so one is often left with highly simplified processing models having a very limited range of validity. A natural approach seems then to take the more tractable *design* model and treat the *processing variables* as input. One then hopes to study the extremal behavior of *optimal design models* when the input (or in generic terms the *process*)is perturbed in a well-defined way. Using a stress-strain power law as being the simplest representation of those processes where the material work hardens, an IO formulation for a simple cantilever beam is described below. The design variables are the moments of inertia of the two segments of the stepped cantilever beam and the design objective is to minimize the weight of the beam subject to a deflection constraint at the tip load as well as a constraint on the stress at the fixed end (fig. 6).

$$
\begin{array}{lll}
\mathit{min} & f = \gamma(\sqrt{x_1} + \sqrt{x_2}) & (\mathit{weight}) \\
\mathit{Sub.\ to} & & \\
\mathbf{h}: & \mathbf{K}(\mathbf{X})\mathbf{U} = \mathbf{F} & (\mathit{equilibrium}) \\
g_1: & u_3 + lu_4 - c \leq 0 & (\mathit{deflection}) \\
g_2: & (64.0/\pi)^{0.25} p\, l/x_1^{0.75} - (K/s)\left(2\ln \frac{d_i}{(64x_1/\pi)^{0.25}}\right)^n \leq 0 & (\mathit{stress}) \\
g_3: & 2\ln \frac{d_i}{(64x_1/\pi)^{0.25}} \leq 0.7 & (\mathit{processing}) \\
g_4: & -2\ln \frac{d_i}{(64x_1/\pi)^{0.25}} \leq -0.1 & (\mathit{processing})
\end{array}
$$

$$p = (d_0) \in P = [d_{imin}, d_{imax}] \subset \Re$$

where K and n are material constants for the flow stress-strain equation.
and

$$\mathbf{K} = (E/l^3)\begin{bmatrix} 12(x_1 + x_2) & -6(x_1 - x_2)l & -12x_2 & 6x_2 l \\ & 4l^2(x_1 + x_2) & -6x_2 l & 2x_2 l^2 \\ & & 12x_2 & -6x_2 l \\ \mathit{symm} & & & 4x_2 l^2 \end{bmatrix}$$

and

$$\mathbf{F} = (0, 0, p, 0)^T$$

Variables: $(x_1, x_2, u_1, u_2, u_3, u_4)^T$

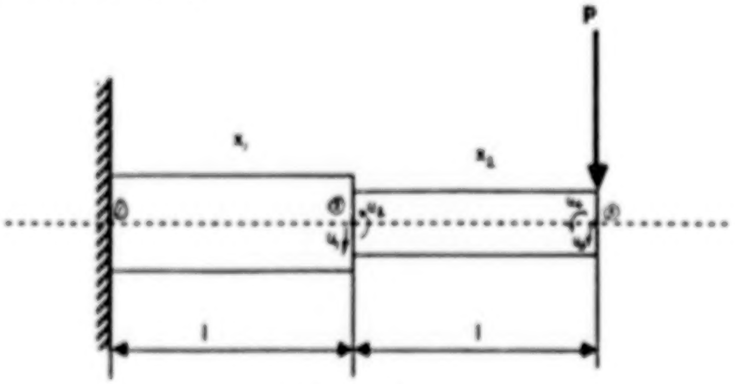

Figure 6

Proposed Numerical Procedure

Note that in this IO formulation, the standard design problem has been imbedded in a family of programs, parametrized by the scalar input parameter d_i, the initial stock diameter. For a fixed input (leading to a standard NLP), the problem can be solved by a generalized reduced gradient algorithm to get:

Design Variables $x_1 = 30.89\,, x_2 = 11.17$
for Input d_i=3.5 leading to $\epsilon^* = 0.434$

Solving the problem again for different values of input, a trend is obtained as shown in the figure below. This should give an indication of the IO solution strategy where we need to track the solution continuously as the input varies and to see if any critical or unstable points lead to bifurcation of the Kuhn-Tucker curve. Given an initial input p_0 for a feasible program, a rough outline of a numerical procedure to accomplish this can be presented as follows:

Step 1 From the solution of the IO problem at p_0, obtain a descent direction δp in the p space for the problem.

Step 2 Using this direction, obtain a step size $\bar{t}$ in the p space.

Step 3 Using $p = p_0 + t\delta p$, $t \in (0, \bar{t}\,]$, formulate the equations of appropriate first order necessary conditions (such as Fritz-John) in the reduced, scalar parameter space of t. Apply a continuation method for this locally parametrized process to identify the nature of critical points along this curve in the reduced t space.

Step 4 At a bifurcation point, identify the type of singularity, and continue if a minimum persists along a branch.

Note that in effect, we have here a combination of a descent and a continuation method (ref. 1 and ref. 12). It remains to be seen if the conjectured prevalence of singular critical points in practical IO problems justifies what appears to be a costly computational procedure. (**Fig. 7.**)

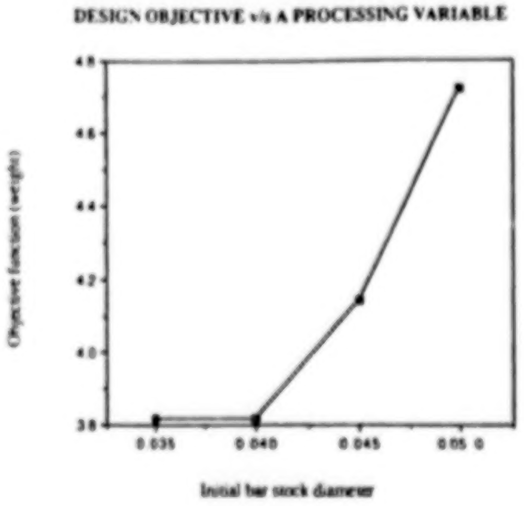

Figure 7

Conclusions

The theory of optimality conditions of extremal problems can be extended to problems continuously deformed by an input vector. The connection between the sensitivity, well-posedness, stability and approximation of optimization problems is steadily emerging. We believe that the important realization here is that the underlying basis of all such work is still the study of point-to-set maps and of small perturbations, yet what has been identified previously as being just related to *solution procedures* is now being extended to study *modeling* itself in its own right.

Many important studies related to the theoretical issues of parametric programming and large deformation in nonlinear programming have been reported in the last few years, and the challenge now seems to be in devising effective computational tools for solving these generalized design optimization models.

Acknowledgements

This research was partially supported by NSF grant DMC-85-14721 and also by the General Motors Corporation Contract "Generalized Models for Optimal Preliminary Design of Unconventional Vehicle Systems," at the University of Michigan. This support is gratefully acknowledged.

References

[1] Zlobec S., 1987, "Survey of Input Optimization," *Optimization*, Vol 18, No. 3, 309-348.

[2] Huard P., ed., 1979, **Point-to-Set Maps and Mathematical Programming**, Mathematical Programming Study - 10, North Holland.

[3] Robinson S. M., and Day, R. H., 1974, "A Sufficient Condition for Continuity of Optimal Sets in Mathematical Programming," *Jl. of Mathematical Analysis and Applications*, 45, 506-511.

[4] Evans J. P., and Gould F. J., 1970, "Stability in Nonlinear Programming," *Operations Research*, 18(1), 107-118.

[5] Clarke Frank H., 1983, **Optimization and Nonsmooth Analysis,** John Wiley, New York.

[6] Fiacco A. V., 1983, **Introduction to Sensitivity and Stability Analysis in Nonlinear Programming,** Academic Press, New York.

[7] Robinson S, M., 1974, "Perturbed Kuhn-Tucker Points and Rates of Convergence for a Class of Nonlinear-Programming Algorithms," *Math. Programming* 7, 1-16.

[8] Gauvin J., 1977, "A Necessary and Sufficient Regularity Condition to have Bounded Multipliers in Nonconvex Programming," *Math. Programming 12*, 136-138.

[9] Malanowski K., 1987, **Stability of Solutions to Convex Problems of Optimization,** Springer-Verlag, Berlin.

[10] Poore A B., and Tiahart C. A., 1987, "Bifurcation Problems in Nonlinear Parametric Programming," *Math. Programming 39*, 189-205.

[11] Kojima M., and Hirabayashi R., 1984, "Continuous Deformation of Nonlinear Programs," *Math. Programming Study 21*, 150-198. North-Holland.

[12] Rheinboldt W, C., 1986, **Numerical Analysis of Parametrized Nonlinear Equations,** John-Wiley, New York.

OPTIMUM DESIGN OF STRUCTURES SUBJECT TO GENERAL PERIODIC LOADS

R. Reiss and B. Qian
Large Space Structure Institute
Howard University
Department of Mechanical Engineering
Washington, D.C. 20059

229

INTRODUCTION

The optimum design of structures subject to a single harmonic load has been considered by Icerman [1] and Plaut [2]. Icerman [1] studied a rod acted upon by a single harmonic tip load, and he minimized the amplitude of the tip's steady state displacement subject to fixed volume. His derivation of the necessary optimality criterion required a steady state extension to the principle of minimum potential energy. This new extremum principle can be used to establish the global sufficiency of the optimality condition, provided sufficiently restrictive conditions are placed upon the admissible designs.

Plaut [2] generalized Icerman's work by minimizing the amplitude of the steady state deflection at any specified location of the structure. His problem allowed for several harmonic loads provided all were driven at the same frequency. He derived the necessary optimality condition by first extending the principle of mutual stationary potential energy to the steady state. He did not address whether the optimality condition was also sufficient for the optimal design.

This paper initially addresses a simplified version of Icerman's problem. The nature of the restrictive conditions that must be placed on the design space in order to ensure an analytic optimum are discussed in detail. Icerman's problem is then extended to include multiple forcing functions with different driving frequencies. And the conditions that now must be placed upon the design space to ensure an analytic optimum are again discussed. An important finding is that all solutions to the optimality condition (analytic stationary design) are local optima, but the global optimum may well be non-analytic.

The more general problem of distributing the fixed mass of a linear elastic structure subject to general periodic loads in order to minimize some measure of the steady state deflection is also considered. This response is explicitly expressed in terms of Green's functional and the abstract operators defining the structure. The optimality criterion is derived by differentiating the response with respect to the design parameters [3]. The theory is applicable to finite element as well as distributed parameter models.

AN ELEMENTARY FORCED VIBRATION

Consider a rod of length L whose cross-sectional area S is piecewise constant. In the simplest case $S = S_1$ for $0 \le x < L/2$ and $S = S_2$ for $L/2 < x \le L$ (Fig. 1). The design ratio S_1/S_2 is denoted by R. The tip load is $F \cos \omega_D t$. The steady state response can be represented by $U(x) \cos \omega_D t$, where $|U(L)|$ is the amplitude of the tip response. Figures 2 and 3 show, respectively, the natural frequency of the design and tip amplitude as a function of the design ratio R. For designs with $R = R^*$, the design and driving frequencies coincide and hence the resonance condition shown, Iceman's [1] optimality condition is sufficient provided only designs $R > R^*$ are considered.

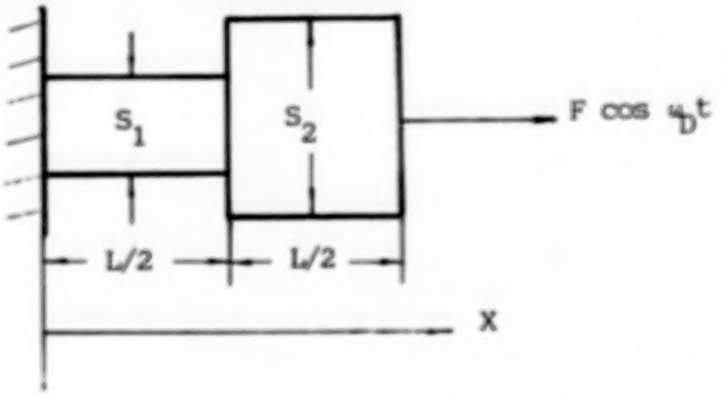

Figure 1. Two-Segment Rod Subject To A Single Driving Frequence

FREQUENCY AND TIP-DEFLECTION AMPLITUDE VS DESIGN

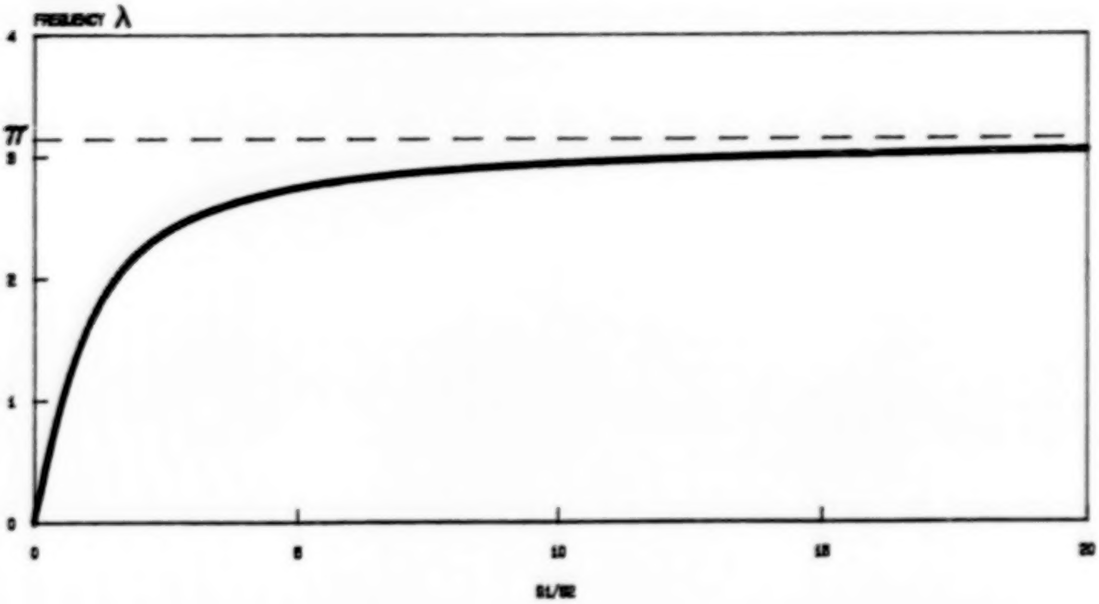

Fig. 2. Non-Dimensional Frequency vs. Design. The non-dimensional frequency λ is defined as $\omega L\sqrt{\rho/E}$ where ρ is mass per unit length and E is Young's modulus.

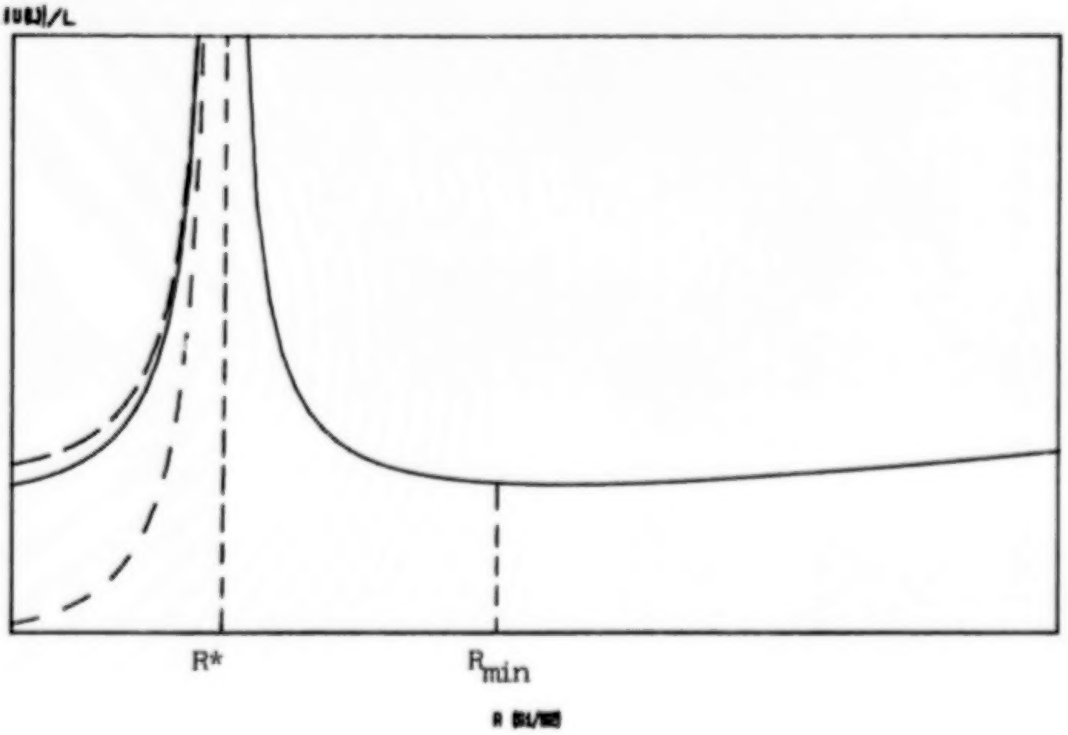

Fig. 3. Tip Deflection vs. Design. R_{min} is the analytic local optimum. Depending upon the value of U(0), R_{min} may or may not be globally the optimum.

232

TWO ELEMENT ROD SUBJECTED TO TWO DRIVING FREQUENCIES

The rod shown in Figure 1 is now subjected to a tip load consisting of two frequencies - $F=F_1 \cos \omega_D t + F_2 \cos 2 \omega_D t$. While the addition of the second driving frequency does not affect the period of the response, it does add a minor complication to the calculation of the maximum response. The response can be expressed in the form $U_1(x) \cos \omega_D t + U_2(x) \cos 2\omega_D t$. The maximum tip response U_{max} is obtained by setting x=L and maximizing the magnitude of the response over one period.

There are two resonant frequencies and, in general, two designs R_1^* and R_2^* for which the fundamental frequency equals one of the resonant frequencies. A typical response is depicted in Figure 4. Clearly, there are up to three local extrema; all are minima and one is not analytic. Analogous to the simpler case of only one forcing frequency, one or both of the resonant designs may not exist.

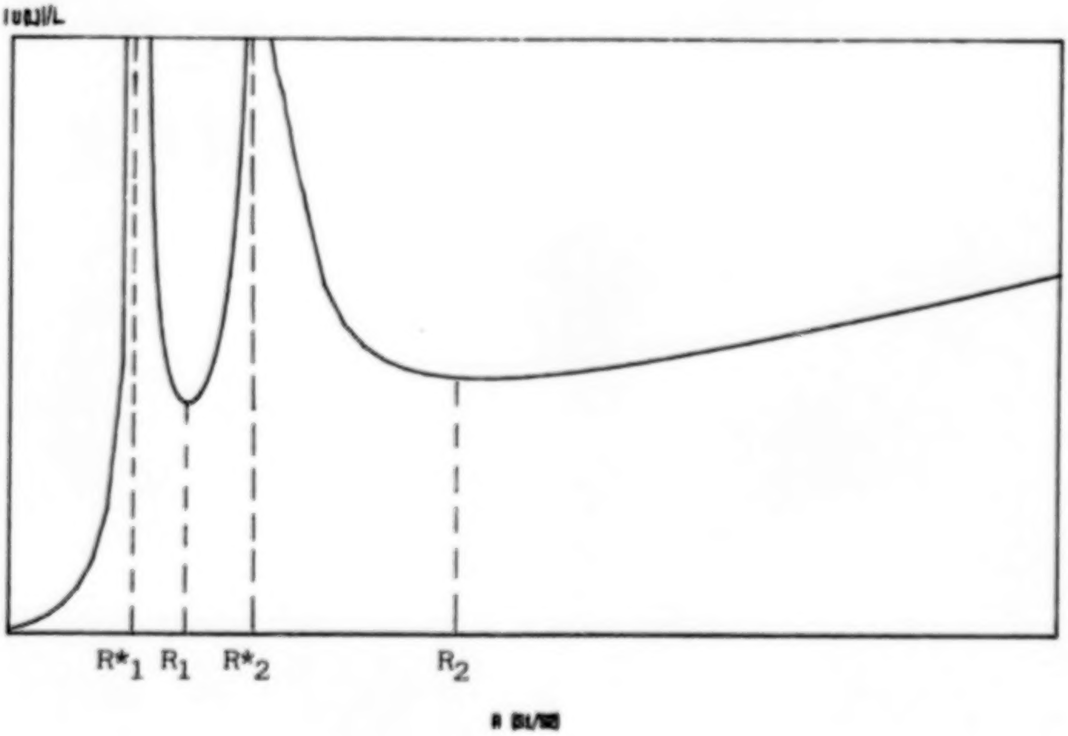

Figure 4. Typical Maximum Response as a Function of the Design Parameter. R_1 and R_2 are analytic local optimum designs.

OPTIMIZATION USING GREEN'S FUNCTIONAL

Consider the following boundary value problem

$$\begin{aligned} (T^* ET + \alpha M)u &= f \text{ in } \Omega \\ B\gamma u &= g \text{ in } \partial\Omega_1 \\ B^* \gamma^* ET\, u &= h \text{ in } \partial\Omega_2 \end{aligned}$$

where T, T^* ...L_2 adjoint operators

$E(S)$ ... Linear stiffness operator

$M(S)$ ... Linear mass operator

α ...... A scalar

γ, γ^* ... Trace operators mapping functions defined in Ω onto functions defined on $\partial\Omega_1$ and $\partial\Omega_2$, respectively.

B, B^* ... Boundary operators

$\partial\Omega_1, \partial\Omega_2$..Complementary subsets of $\partial\Omega$

S ...... Design variable(s)

The following integration by parts formula, due to Oden and Reddy [4], is postulated

$$\begin{aligned} &(Tu,\ ETv)_\Omega - (u, T^* ETv)_\Omega \\ &\qquad = (\gamma u, B^* \gamma^* ETv)_{\partial\Omega_2} - (B\gamma u, \gamma^* ETv)_{\partial\Omega_2} \end{aligned}$$

Also E,M satisfy

$$(u, Ev)_\Omega = (v, Eu)_\Omega$$

$$(u, Mv)_\Omega = (v, Mu)_\Omega \text{ for every admissible } u \text{ and } v.$$

STRUCTURAL DYNAMICS

The equations governing linear structural dynamics can be expressed as

$$T^{*} ET\, u + M\ddot{u} = f \quad \text{in } \Omega$$

$$B\gamma u = g \quad \text{on } \partial\Omega_1$$

$$B^{*}\gamma^{*} ET\, u = h \quad \text{on } \partial\Omega_2$$

If f,g, and h all have the same periodicity,

$$f = \sum_{1}^{N} f_n(x) \cos n\, \omega_D t$$

$$g = \sum_{1}^{N} g_n(x) \cos n\, \omega_D t$$

$$h = \sum_{1}^{N} h_n(x) \cos n\, \omega_D t$$

The solution u (x,t) satisfies

$$u = \sum_{1}^{N} U_n(x) \cos n\, \omega_D t$$

The Fourier coefficients satisfy

$$L_n \equiv (T^{*}ET - n^2 \omega_D^2 M)\, U_n = f_n \quad \text{in } \Omega$$

$$B\gamma\, U_n = g_n \quad \text{on } \partial\Omega_1$$

$$B^{*}\gamma\, ET\, U_n = h_n \quad \text{on } \partial\Omega_2$$

It can be shown that the solution is

$$U_n = (f_n, G_n)_{\Omega} + (g_n, \gamma^{*} ETG_n)_{\partial\Omega_1} + (h_n, \gamma G_n)_{\partial\Omega_2}$$

where G_n is the Green's function corresponding to the operator L_n.

SOLUTION TO VARIATIONAL EQUATIONS

Define

$$\delta U_n = U_n(x,S+\delta S) - U_n(x,S)$$

Then, by using Oden and Reddy's integration by parts formula and taking the first variation of the differential equation specifying U_n, it can be shown that

$$\delta U_n = -(\delta E\ TU_n,\ TG_n)_\Omega + n^2\omega_D^2\,(\delta MU_n, G_n)_\Omega$$

Consequently,

$$\delta u(x,t) = \sum_1^N [n^2\omega_D^2(\delta MU_n, G_n)_\Omega - (\delta ETU_n, TG_n)_\Omega] \cos n\ \omega_D t$$

To determine whether any particular design which causes a stationary response at fixed x and t also minimizes the response can be obtained by variational calculus. The second variation $\delta^2 u$ clearly involves the terms $\delta^2 E$, $\delta U_n, \delta^2 M$. However, δU_n is determined above, and

$$\delta G_n = -(TG_n\ \delta E\ TG_n)_\Omega + n^2\ \omega_D^2\ (\delta MG_n, G_n)_\Omega$$

Consequently, $\delta^2 u$ is completely determined by the variations in the operators E and M.

APPLICATIONS TO A ROD

A rod with varying cross-sectional area $A(x)$ is fixed at $x=0$ and acted upon by the horizontal periodic force

$$\Sigma F_n \cos n \omega_D t$$

at the tip $x=L$. The steady state equations are

$$-(E_o A U_n')' - c^{-2} E_o A \omega_D^2 n^2 U_n = F_n \delta(L-x)$$

$$U_n(0) = E_o A U_n'(L)=0$$

where E_o is Young's modulus and $c^{-2} = \rho/E$. Clearly

$$U_n(x) = F_n G_n(L,x)$$

Upon making the following identification for the operators:

$$T = - T^* = d/dx , \quad E=E_o A=S(x), \quad M=\rho A = c^{-2}S(x)$$

the solution for $\delta U_n(L)$ becomes

$$\delta U_n(L) = \frac{1}{F_n} \{ \int_o^L \{ U_n'^2 - n^2 \omega_D^2 c^{-2} U_n^2\} \delta S \, dx$$

Now, let T be selected so that

$$u(L,T) \equiv U_{max}$$

By imposing the fixed mass constraint

$$\int_o^L \delta S \, dx = 0,$$

the optimality condition for minimizing U_{max} over all admissible designs S is obtained, i.e.

$$\sum_{n=1}^{N} \frac{\cos n \omega_D T}{F_n} (U_n'^2 - n^2 \omega_D^2 c^{-2} U_n^2) = \lambda$$

For rods consisting of piecewise constant cross-sections S_i in the domain $x_{i-1} < x < x_i$, the optimality condition takes the form

$$\sum_{n=1}^{N} \frac{\cos n \omega_D T}{F_n} \int_{x_{i-1}}^{x_i} (U_{ni}'^2 - n^2 \omega_D^2 c^{-2} U_{ni}^2) dx = \lambda_i$$

RESULTS FOR A TWO-SEGMENT ROD WITH ONE DRIVING FREQUENCY

Table 1 shows results for a single driving. The non-dimensional frequency Ω is $\omega_D L/c$, the analytic optimum design stiffness ratio R is S_1/S_2, U_{opt} is the analytic minimum, U_{unif} is the amplitude of vibration for R=1 and U_o is the non-analytic minimum obtained by letting R approach zero.

It is observed that for low frequencies, the analytic optimum is clearly superior to any other design. For $\Omega > 0.854$, the awkward non-analytic optimum provides a smaller amplitude for the response than does the analytic design. For still larger frequencies $\Omega > 1.743$, even the uniform design is preferable to the analytic local optimum.

TABLE 1. Comparison of Analytic Optimum to Non-Analytic Optimum and Uniform Designs.

Ω	R	U_{opt}/U_{unif}	U_{opt}/U_o
0.1	1.005	0.99999	0.010
0.3	1.046	0.999	0.093
0.5	1.130	0.996	0.278
0.7	1.266	0.982	0.604
0.854	1.415	0.957	1.000
1.0	1.597	0.911	1.625
1.4	2.419	0.497	4.066
1.743	3.828	1.000	13.657
1.8	4.176	2.824	19.734

RESULTS FOR A TWO-SEGMENT ROD WITH TWO DRIVING FREQUENCIES

Table 2 shows numerical results for two driving frequencies. The symbols Ω and R are defined the same as in the previous example. Here, U_{opt}, U_{unif} and U_o are, respectively, the maximum absolute value of the displacement over one period for a local analytical optimal design, uniform design, and a rod for which S_1 tends to zero. The forcing function is $F_1 \cos \omega_D t + F_2 \cos 2\omega_D t$. The non-dimensional frequency Ω_D is fixed at 0.6 for this example. Note that there are two analytic local optimal designs R_1 and R_2. In the third and fourth columns in Table 2 are comparisons based upon the design R_1 while the sixth and seventh columns are comparisons based upon R_2.

The global optimum is obtained by searching the fourth and seventh columns. Since the entries in Column 4 always exceed the corresponding entry in Column 7, it follows that R_2 always provides a better solution than R_1. Further, for $F_1 \geq F_2$, R_2 is the global optimum but for $F_1 < F_2$, R=0 is the global optimum.

TABLE 2. Comparison of Both Analytic Optimal Designs with Non-Analytic Optimal Designs with Non-Analytic Optimum and Uniform Designs. All data is for $\Omega_D = 0.6$

F_1/F_2	R_1	$\frac{U_{opt}}{U_{unif}}$	$\frac{U_{opt}}{U_o}$	R_2	$\frac{U_{opt}}{U_{unif}}$	$\frac{U_{opt}}{U_o}$
1/9	0.168	0.81	2.02	1.89	0.80	1.99
2/8	0.194	0.99	1.88	1.85	0.81	1.54
3/7	0.213	1.15	1.72	1.79	0.83	1.24
4/6	0.234	1.29	1.56	1.74	0.85	1.03
5/5	0.250	1.42	1.41	1.68	0.87	0.87
6/4	0.270	1.53	1.27	1.61	0.89	0.74
7/3	0.288	1.63	1.13	1.54	0.92	0.64
8/2	0.313	1.69	1.00	1.45	0.94	0.55
9/1	0.347	1.69	0.85	1.34	0.97	0.48

ADDITIONAL RESULTS FOR TWO DRIVING FREQUENCIES

The identical problem as the preceding one is considered. Here, however, results are presented for fixed force amplitudes where $F_1=F_2$. The driving frequency Ω_D is varied in Table 3.

Of the analytic solutions, it is clear that R_1 is superior to R_2 for values of Ω_D closer to 1.0, but R_2 is better for the smaller driving frequencies. However R_1 never provides the optimum global design. For forcing frequencies $\Omega_D < 0.6$, R_2 is the global optimum; otherwise the global optimum is not analytic.

TABLE 3. Comparison of Both Analytic Optimal Designs with Non-Analytic Optimum and Uniform Designs. All data is for $F_1/F_2 = 1$.

Ω_D	R_1	$\frac{U_{opt}}{U_{unif}}$	$\frac{U_{opt}}{U_o}$	R_2	$\frac{U_{opt}}{U_{unif}}$	$\frac{U_{opt}}{U_o}$
0.2	0.025	16.6	1.10	1.05	0.999	0.07
0.4	0.105	3.93	1.27	1.24	0.985	0.30
0.6	0.251	1.42	1.40	1.68	0.87	0.87
0.8	0.482	0.14	1.76	2.67	0.18	2.31
1.0	0.824	0.96	2.36	5.09	2.84	7.00

TWO SEGMENT ROD SUBJECT TO THREE FREQUENCIES

The two segment rod is now subjected to the tip force $F_1 \cos \omega_D t + F_2 \cos 2\omega_D t + F_3 \cos 3\omega_D t$. There are now three resonant designs and three local optimal designs in addition to the non-analytic optimal design as $R \to 0$. Table 4a contains results for the lowest driving frequency $\Omega_D = 0.3$. In all cases R_3 provides the global optimum. However, if $\Omega_D = 0.6$ (Table 4b), then R_2 is the global optimum.

TABLE 4. Comparison of Three Analytic Local Optimum Designs with Non-Analytic Local Optimum Design. $\Omega_D = 0.3$ for (4a) and $\Omega_D = 0.6$ for (4b).

F_2/F_1	F_3/F_1	R_1	$\frac{U_{opt}}{U_o}$	R_2	$\frac{U_{opt}}{U_o}$	R_3	$\frac{U_{opt}}{U_o}$
0.50	0.50	0.065	0.82	0.157	0.40	1.22	0.18
0.75	0.75	0.061	0.89	0.158	0.52	1.25	0.21
1.00	1.00	0.058	0.94	0.158	0.54	1.27	0.34

(4a)

0.50	0.50	0.286	1.07	0.825	0.67	3.12	1.38
0.75	0.75	0.267	1.15	0.830	0.76	3.24	1.72
1.00	1.00	0.254	1.20	0.838	0.95	3.32	2.02

(4b)

REFERENCES

1. Iceman, L.J.: Optimal Structural Design for Given Dynamic Deflection. Int. J. Solids and Structures, Vol. 5, 1969, pp. 473-490.

2. Plaut, R.H.: Optimal Structural Design for Given Deflection under Periodic Loading. Q. Appl. Math., July 1971, pp. 315-318.

3. Reiss, R.: On Singular Cases in the Design Derivative of Green's Functional, Symposium: Sensitivity Analysis in Engineering. NASA Conference Publication 2457, 1986, pp. 319-328.

4. Oden, J.T. and Reddy, J.N.: Variational Methods in Theoretical Mechanics. Springer-Verlag, Berlin, 1976.

FUZZY SET APPLICATIONS IN ENGINEERING OPTIMIZATION

Multilevel Fuzzy Optimization

Alejandro R. Díaz
Mechanical Engineering
Michigan State University
East Lansing, MI

243

INTRODUCTION

Since the landmark paper by Bellman and Zadeh in 1970 [1], fuzzy sets have been used to solve a variety of optimization problems. In mechanical and structural design, however, relatively few applications of fuzzy optimization have appeared in the literature, even though the formulations and algorithms developed in management science are readily applicable in engineering fields. In engineering design fuzzy optimization has most often been suggested as a mechanism to represent 'soft' constraints (e.g. [2]) and as an alternative formulation to solve multiobjective optimization problems (e.g. [3,4].) A formulation for multilevel optimization with fuzzy objective functions is presented in this paper.

With few exceptions, formulations for fuzzy optimization have dealt with a one- level problem in which the objective is the membership function of a fuzzy set formed by the fuzzy *intersection* of other sets. This concept dates back to the original work by Bellman and Zadeh in which objective and constraints are handled in identical fashion: if $f(\mathbf{x})$ is the function to be minimized under constraints $g_i(\mathbf{x}) \leq 0$, $i=1,2,...,m$, the fuzzy optimization problem maximizes the membership function μ_G of

$$G=G_0 \cap G_1 \cap ,..,\cap G_m \quad \text{with} \quad \mu_G=\min(\mu_0,\mu_1,...,\mu_m)$$

The set G_0 has membership function μ_0 such that

$\mu_0(f) \rightarrow 1$ as f *decreases*

while, for other G_j's,

$\mu_j(g_j) \rightarrow 1$ as g_j *decreases* from 0, and

$\mu_j(g_j) \rightarrow 0$ as g_j *increases* from 0.

This model has been used extensively to relax ('fuzzify') the constraint set and to deal with multiple objectives.

A somewhat different problem is discussed here. First, the goal set G is defined in a more general way, using an aggregation operator H that allows arbitrary combinations of set operations (union, intersection, addition) on the individual sets G_i. This is a straight-forward extension of the standard form, but one that makes possible the modeling of interesting evaluation strategies. This feature has been discussed in detail elsewhere [3,4] but, for completeness, it will be briefly outlined in the next section.

A second, more important departure from the standard form will be the construction of a multilevel problem analogous to the design decomposition problem in optimization [5-8]. This arrangement facilitates the simulation of a system design process in which

- Different components of the system are designed by different teams.
- Different levels of design detail become relevant at different time stages in the process: global design features early, local features later in the process.

SINGLE -LEVEL PROBLEM

The optimization problem can be solved in a single level when a design alternative can be fully described and evaluated using local design variables and functions. Let $\mathbf{x} \in R^n$ represent the vector of design variables. The goal of the problem is to find the design $\mathbf{x}$ that

maximizes $\mu_G = h(\mu_1, \mu_2, \ldots, \mu_p)$,

the membership in the design goal

$G = H(G_1, G_2, \ldots, G_p)$,

subject to *crisp* constraints

$\mathbf{x} \in X = \{\mathbf{x} \in R^n : g_i(\mathbf{x}) \leq 0,\ i = 1, 2, \ldots, m\}$.

Each individual goal G_i has membership μ_i and represents a desirable design quality such as strength, low cost, or reliability. The mapping from $\mathbf{x}$ to each of the μ_i's depends on specific details of the design process and designer's preferences and it is assumed to be known. The function $h: [0,1]^p \rightarrow [0,1]$ is an acceptable connective associated with H, as defined in [3,9]. For instance, in a standard 3- objective fuzzy optimization problem

$H(G_1, G_2, G_3) = G_1 \cap G_2 \cap G_3$ and $h(\mu_1, \mu_2, \mu_3) = \min\{\mu_1, \mu_2, \mu_3\}$.

This is by no means the only possible or meaningful choice for H and h. For instance, the choice

$H(G_1, G_2, G_3) = (G_1 \cap G_2) \cup (G_1 \cap G_3) \cup (G_3 \cap G_2)$

indicates that the optimum solution needs to satisfy only 2 out of 3 objectives. The connective h can be built using different intersection and union operators. An extensive review of these connectors can be found in [10].

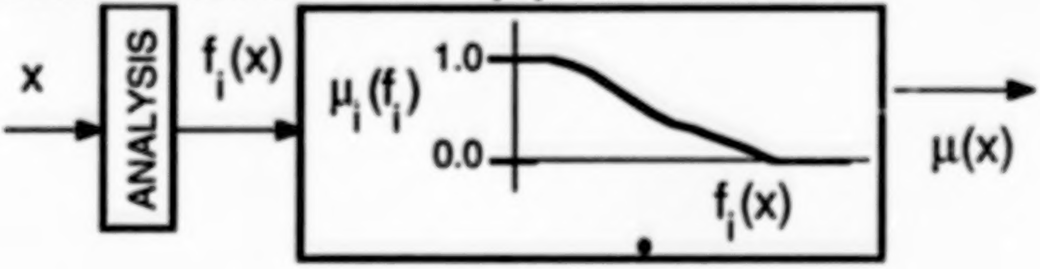

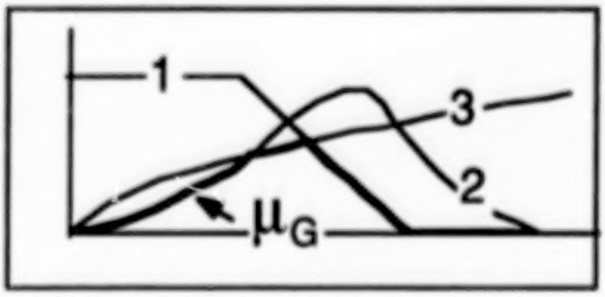

$G = G_1 \cap G_2 \cap G_3$

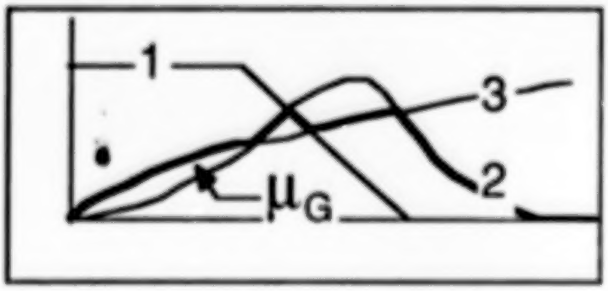

$G = (G_1 \cap G_2) \cup (G_2 \cap G_3) \cup (G_1 \cap G_3)$

MULTILEVEL PROBLEM

In a multilevel approach the system being designed is decomposed into several sub-systems. This decomposition is often made along boundaries determined by the organization and expertise of design teams involved in the design task. Each team becomes responsible for the design of its own sub- system and is an expert only in this limited area. Sobieszczanski-Sobieski, J. [5,7,8], Haftka [6], and Parkinson et. al. [11], among others, have suggested different approaches to the optimization problem in this setting.

Two important questions arise in the multilevel optimization problem: what is a meaningful objective function to guide the optimization and how to maintain feasibility when only local constraints can be evaluated exactly. The fuzzy set approach offers an operationally useful answer to the first question. The second question will be addressed using convex approximations to non- local functions.

In the fuzzy multilevel problem each sub- problem (j) has its own variables $\mathbf{x}^{(j)}$ and goal $G^{(j)}$. The sub- problems contribute their goals to the overall design objective G, formed in a hierarchical fashion using set operations on the sub-problem goals. This arrangement:

- Introduces the flexibility of the fuzzy formulation at the sub- problem level. All of the tools from fuzzy optimization are available there, including the traditional 'crisp' optimization problem.

- Facilitates the comparison of dissimilar objectives arising in different environments: membership functions are dimensionless.

- Makes possible the construction of a design goal that varies as the design process unfolds. The vagueness that characterizes the early stages of the design can be easily modeled at the local level in the definition of the local goal.

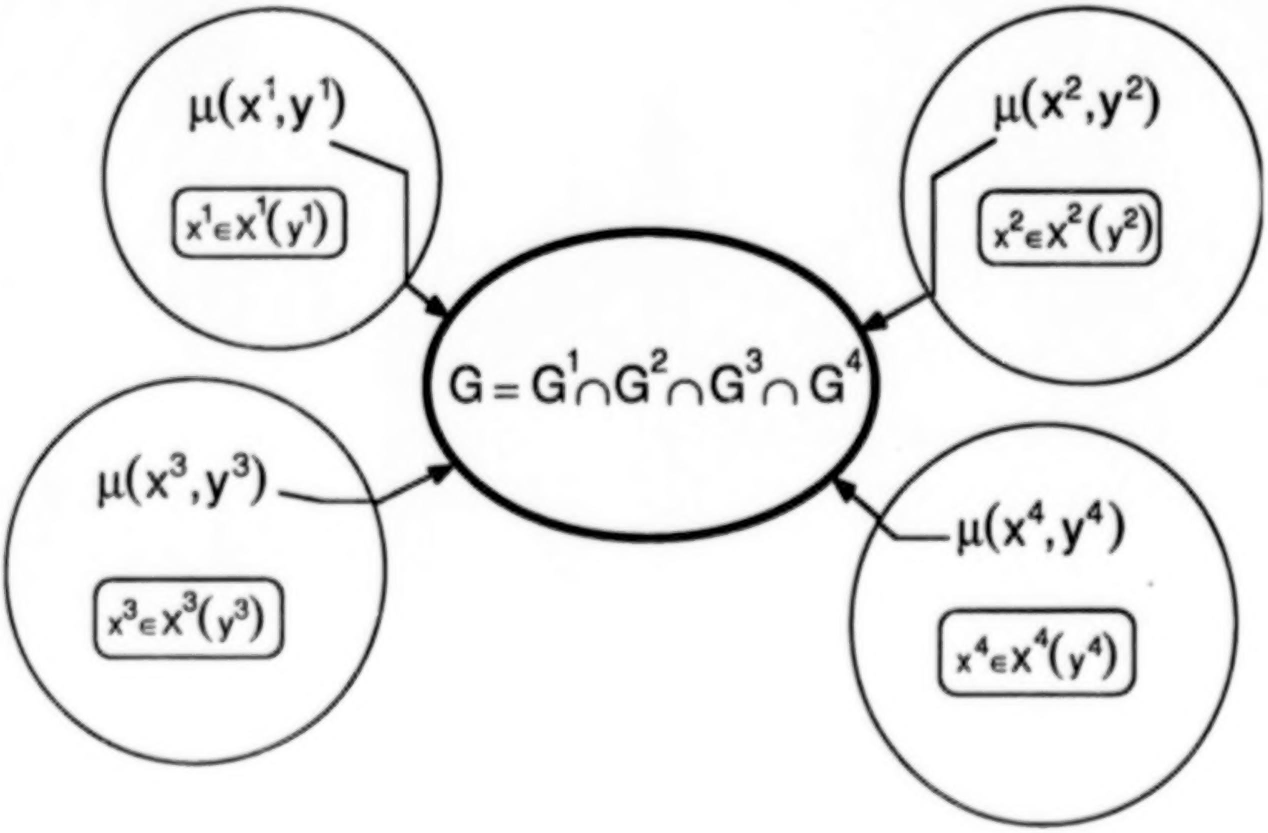

GLOBAL PROBLEM

Let $\mathbf{x}\in R^N$ be the vector of all design variables. The solution to the global optimization problem

maximizes $\mu_G(\mathbf{x})=h_G(\mu^{(1)},\mu^{(2)},\ldots,\mu^{(p)})$

under the constraints of the local problems defined below. The functions $\mu^{(j)}$ are membership functions of the sets $G^{(j)}$ corresponding to acceptable solutions to the j-th sub- problem and the function μ_G corresponds to the fuzzy set G that describes the optimum global solution,

$G=H_G(G^{(1)},G^{(2)},\ldots,G^{(p)})$

The operators h_G and H_G describe the way different sub- problems interact and, in general, change to reflect different stages in the design problem.

LOCAL PROBLEM $P^{(j)}$

Let $\mathbf{x}^{(j)}\in R^{n(j)}$ represent the vector of local design variables and let $\mathbf{y}^{(j)}\in R^{N-n(j)}$ represent design variables outside the j-th problem, i.e., $\mathbf{y}^{(j)}=\mathbf{x}-\mathbf{x}^{(j)}$. Problems are assumed to be coupled: objectives and constraints in the j-th problem are functions of $\mathbf{y}^{(j)}$. However, while $\mathbf{x}^{(j)}$ varies in the j-th problem, $\mathbf{y}^{(j)}$ remains fixed. The goal of the local problem is to find the design $\mathbf{x}^{(j)}$ that

maximizes $\mu_G(\mathbf{x}^{(j)};\mathbf{y}^{(j)},\mathbf{f}^{(j)}(\mathbf{x}^{(j)},\mathbf{y}^{(j)}))$

subject to *crisp* constraints

$\mathbf{x}^{(j)}\in X^{(j)}=\{\mathbf{x}^{(j)}\in R^{n(j)} : g^{(j)}_i(\mathbf{x}^{(j)};\mathbf{y}^{(j)},\mathbf{f}^{(j)}(\mathbf{x}^{(j)},\mathbf{y}^{(j)}))\le 0,\ i=1,2,\ldots,m(j)\}$

Local goals are coupled with other sub-problems via $\mathbf{y}^{(j)}$ and $\mathbf{f}^{(j)}$. The $f^{(j)}_i$'s are functions evaluated *outside* problem $P^{(j)}$. Convex approximations are used to evaluate these functions.

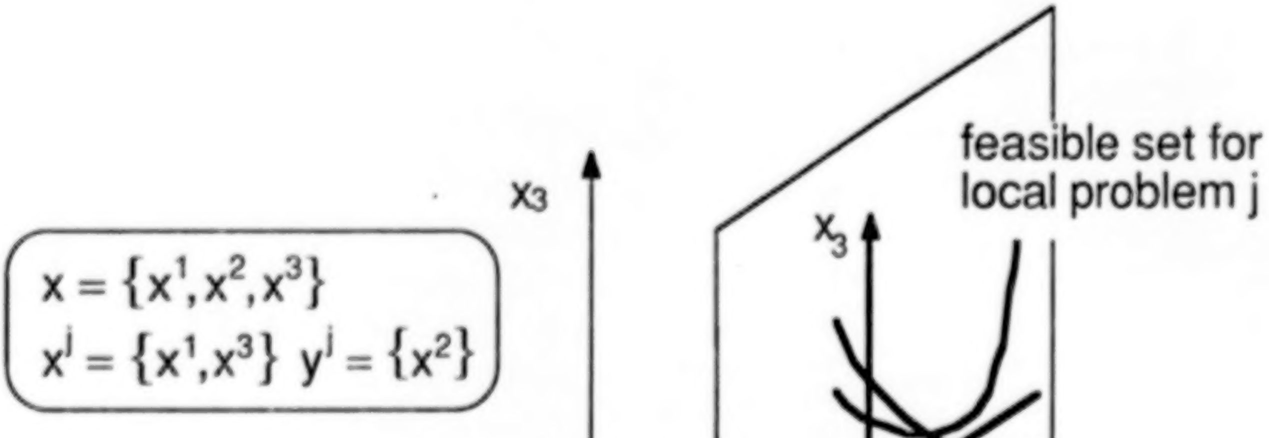

feasible set for local problem j
x_3
x_3
$x = \{x^1,x^2,x^3\}$
$x^j = \{x^1,x^3\}\ y^j = \{x^2\}$
$x_2 = y_1^j$
x_1
x_1
x_2^o

EVALUATING NON-LOCAL FUNCTIONS: Maintaining feasibility.

A challenging difficulty in the multilevel problem involves maintaining global feasibility while solving the sub-problems. The question is, how to insure that all variables, not just the local variables, remain feasible without actually evaluating non-local constraints. An answer to this question will be attempted using convex approximations of non-local functions.

Convex approximations were introduced by Starnes and Haftka [12] and used by Fleury and Braibant [13] to solve a range of structural optimization problems. If f($\mathbf{x}$) is a differentiable function in R^N, the convex approximation of f at $\mathbf{x}^o$ is the function

$$\tilde{f}(\mathbf{x}) \equiv \sum_{(+)} \left(\frac{\partial f}{\partial x_i} \right)_{x^o} (x_i - x_i^0) + \sum_{(-)} \left(\frac{\partial f}{\partial x_i} \right)_{x^o} \frac{x_i^0}{x_i} (x_i - x_i^0)$$

where the (+) sum is over positive derivatives while the (-) sum is over the negative derivatives of f. It is easy to show that for positive variables the convex approximation is the more 'conservative' approximation out of the linear, reciprocal, or concave approximations of f [12] . Indeed, the set f(x)≤0 is often contained in the set $\tilde{f}(x) \leq 0$. This motivates the following variation of the problem $P^{(j)}$:

Find $\mathbf{x}^{(j)} \in R^{n(j)}$ that maximizes μ_G subject to the local constraints

$$\mathbf{x}^{(j)} \in \tilde{X}^{(j)} = \left\{ \mathbf{x}^{(j)} \in R^{(n(j))} : g_i^{(j)}\left(\mathbf{x}^{(j)}; \mathbf{y}^{(j)}, \tilde{\mathbf{f}}^{(j)}(\mathbf{x}^{(j)}, \mathbf{y}^{(j)}) \right) \leq 0,\ i = 1, \ldots, m(j) \right\}$$

and the convex approximations of the non-local constraints at the starting point,

$$\mathbf{x}^{(j)} \in \tilde{X}^{(k)} = \left\{ \mathbf{x}^{(j)} \in R^{(n(j))} : \tilde{g}_i^{(k)}(\mathbf{x}^{(j)}) \leq 0,\ i = 1, \ldots, m(k) \right\}, k = 1, \ldots, p; k \neq j$$

Along with a step-size restriction, the addition of these constraints is often enough to insure that $\mathbf{x}^{(j)}$ remains within all feasible sets, local and non-local, without need to evaluate the non-local constraints $\mathbf{g}^{(k)}$ and functions $\mathbf{f}^{(j)}$ exactly. The convex approximations are easy to compute and only require the kind of sensitivity information that is often available in many nonlinear programming algorithms. Efficient methods to compute these derivatives have been reported in the literature [14].

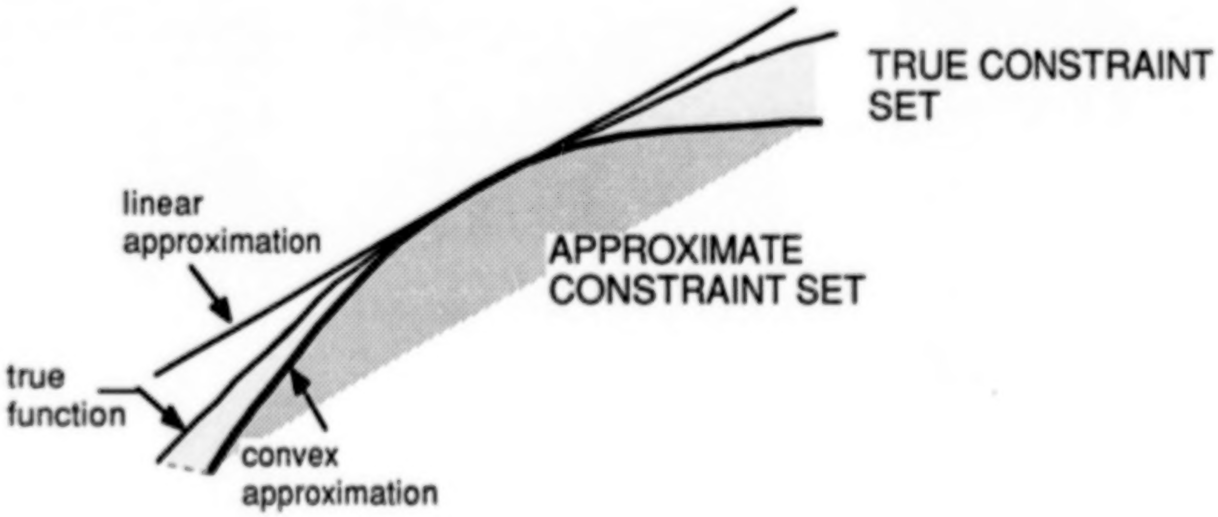

SEQUENCE OF SOLUTION

In the solution strategy of the multilevel problem one local problem, the *active problem* $P^{(j)}$, is solved at a time by searching only in the space of local variables $\mathbf{x}^{(j)}$. The choice of operator h_G determines the relative importance of each sub-problem and hence the order in which problems will be solved. Consider for example a non-associative connective such as

$$h_G(\mu^{(1)},\mu^{(2)})=\min\{\mu^{(1)},\mu^{(2)}\} \quad (G=G^{(1)}\cap G^{(2)})$$

If $\mu^{(1)}>\mu^{(2)}$ at a given point $\mathbf{x}$, the global problem is dominated by the sub-problem goal $G^{(2)}$ at that point and efforts should be directed to improve $\mu^{(2)}$. If, on the other hand,

$$h_G(\mu^{(1)},\mu^{(2)})=\mu^{(1)} \times \mu^{(2)}$$

some gain is possible even if only $\mu^{(1)}$ is improved. Indeed, sub-problem goal $G^{(1)}$ dominates with possibility $\mu^{(2)}$. In general, goal $G^{(j)}$ will dominate with possibility

$$m_j = \max\left\{\left(\frac{\partial h_G}{\partial \mu^{(j)}}\right)^+, \left(\frac{\partial h_G}{\partial \mu^{(j)}}\right)^-\right\},$$

(+)=right, (-)=left derivatives

To simplify the solution strategy only the 'min' operator will be used to connect sub-goals (any operator can be used *within* each problem). With this simplification m_j is always 1 for the dominant goals (0 otherwise) and the procedure is simplified.

In some steps, $\mu^{(j)}$ can be improved within $X^{(j)}$. It may happen, however, that an increase in a dominant $\mu^{(j)}$ is possible only after relaxing some constraint that depends on a non-local variable $\mathbf{y}^{(j)}$. When this happens it may be necessary to make another problem, say $P^{(k)}$, $k \neq j$, active and seek to relax the troublesome constraint in $X^{(k)}$ instead of improving its natural local objective. A robust strategy to select the next active problem and its objective function is essential to the success of the approach. Efforts are being directed toward this goal but more research is still required. An example that applies to the 'min' operator is outlined below.

At $\mathbf{x}^o$, after solving P^i, $M \equiv \{j: \mu_j=1\}$ $S^j_G=$ feasible descent direction for μ_G in X^j $S^j =$ feasible descent direction for μ^j in X^j			
IF	$S^j_G \neq 0,\ j \in M,$	THEN	$\underset{x^j}{\text{MAX}}\ \mu^j_G$
IF	$S^j_G \neq 0,$ any j,	THEN	$\underset{x^j}{\text{MAX}}\ \mu^j_G$
IF	$S^j \neq 0, j \in M\ j \neq i$	THEN	Set relaxation: $r_k>0$, $k\neq j$, $k\in M$ $r_k=0$, otherwise. $\underset{x^j}{\text{MAX}}\ \underset{k}{\text{MIN}}\left\{\mu^{(k)} + r_k\right\}$
ELSE for $j \in M$, $k^* \equiv \left\{k \notin M: g^k_r(\mathbf{x}) = 0,\ \left\langle \nabla^k\mu^j, \nabla^k g^k_r \right\rangle \to \min_{k \notin M}\right\}$ $\underset{x^*}{\text{MIN}}\ g^{k^*}_r,\ \mu_G(\mathbf{x}) \geq \mu_G(\mathbf{x}^o)$			

EXAMPLE

The multilevel problem with fuzzy objectives can be illustrated by the following simple model of support system for a heavy piece of machinery. The problem is modeled by a flexible beam supported by three spring- dashpot components. To illustrate the approach the device will be decomposed in two subsystems: the suspension (springs) and the structure (beam).

1. Suspension: Spring stiffnesses are to be selected to transmit a periodic load to the foundation. The amount of force transmitted and the maximum deflection are relevant performance measures. In this problem the flexibility of the structure is ignored.

1.1 At a detailed level, the springs themselves are to be designed. Stiffness, stress, clearance, and natural frequency are relevant measures. Coil and wire diameters are design variables.

2. Structure: Beam cross-sectional properties are to be selected to support a load. Amount of material, stresses and deflections are relevant performance measures. In this problem dynamic effects are ignored.

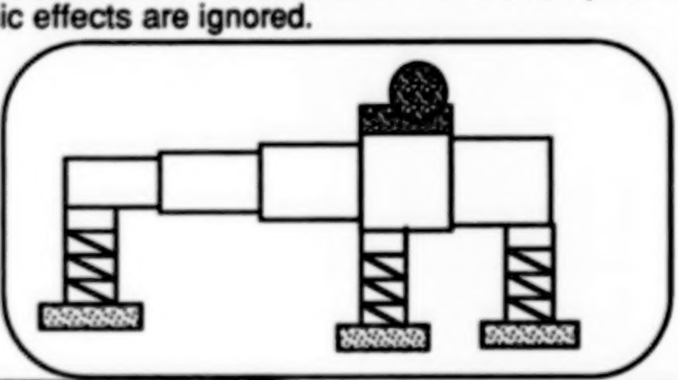

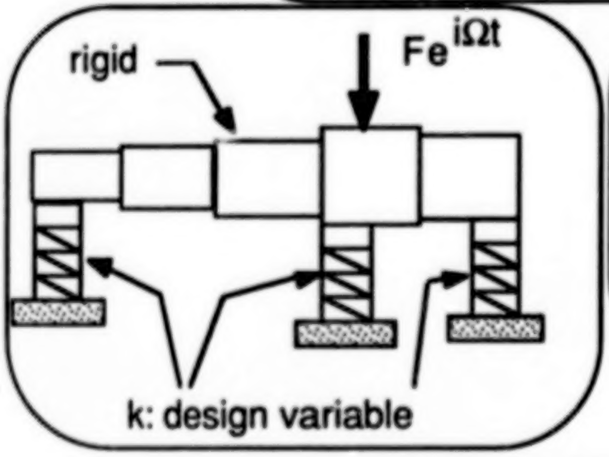

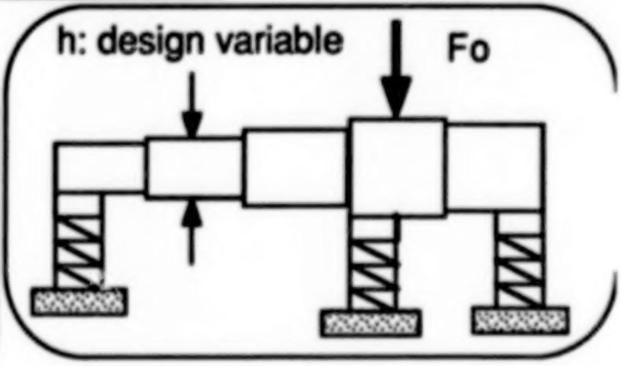

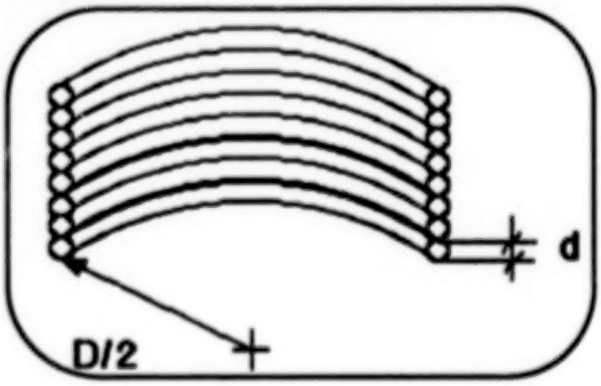

The 'min' intersection operator will be used to connect the sub-goals, i.e, the overall goal is

$$G=G_{susp}\cap G_{struct}\cap G_{spring},\quad \mu_G=\min\{\mu_{susp}, \mu_{struct}, \mu_{spring}\}$$

The objective in the suspension sub-problem (1) is the maximum force transmitted to the foundation by the three springs. The weight of the beam is the objective in the structure sub-problem. Although these are rather simple objectives for a fuzzy optimization problem, no significant loss of generality is introduced. Membership functions for these goals are shown below.

Problem 1.1 is special: it corresponds to the detailed design in the suspension design problem.The precise description of the spring (problem 1.1) becomes relevant only after some knowledge of the required stiffnesses is available (problem 1). This organization is present in typical design problems in which detailed design decisions are taken later in the design process. In this problem diameters D and d must be selected so that the spring stiffness matches the stiffness k prescribed by the problem (1) without exceeding limits on stress. The goal is set as

$$G_{spring}=G_{stiff}\cap G_{stress},\quad \mu_{spring}=\min\{\mu_{stiff}, \mu_{stress}\}$$

where

$$G_{stiff}=\{(D,d): k(D,d)\approx k\}$$

$$G_{stress}=\{(D,d): \sigma(D,d)\lesssim\sigma_Y\}$$

Membership functions for these sets are shown below.

$$\max_{k_1,k_2,k_3} \mu_{susp}$$
$$\delta_\Omega(h,k) \le \delta_{max}$$
$$k_{min} \le k \le k_{max}$$

$$\max_{h_1,h_2 \ldots h_5} \mu_{struct}$$
$$\sigma(h,k) \le \sigma_Y$$
$$\delta(h,k) \le \delta_{max}$$
$$h_{min} \le h \le h_{max}$$

$$\max_{D,d} \mu_{spring}$$
$$freq(D,d) \ge f_{min}$$
$$D_{min} \le D \le D_{max}$$
$$d_{min} \le d \le d_{max}$$

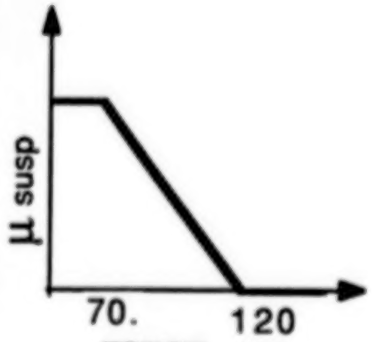

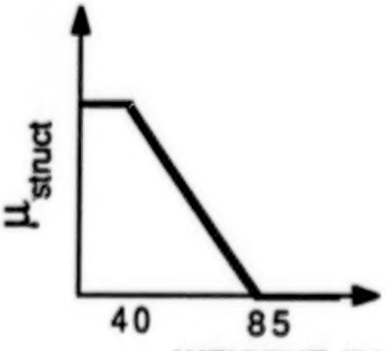

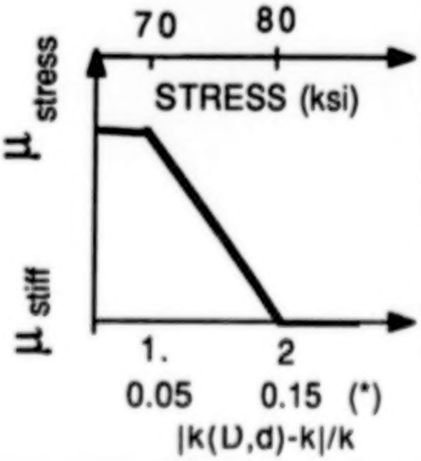

Solution history for the problem is shown in the figure below.

(0) μ_{susp} dominates. Problem 1 is solved with objective μ_G.

(1) $\mu_{susp} = \mu_{struct}$. Problem 2 is solved. Objective is μ_{struct} and μ_{susp} is not allowed to decrease (G_{susp} to worsen) more than 20%.

(2) $\mu_{susp} < \mu_{struct}$. Problem 1 i solved with objective μ_G.

(3) $\mu_{spring} = \mu_{susp}$. Problem 1.1 is solved with objective μ_{spring}. At the end of this step tighter restrictions on σ are imposed ((*) in membership function above).

(4) $\mu_{susp} < \mu_{struct}$ and a non-local constraint (maximum beam deflection) is active (figure). Problem 2 is solved to reduce this constraint. Notice that the convex approximation is effective to determine constraint activity.

(5) $\mu_{susp} = \mu_{struct}$. Problem 1 is solved with objective μ_G.

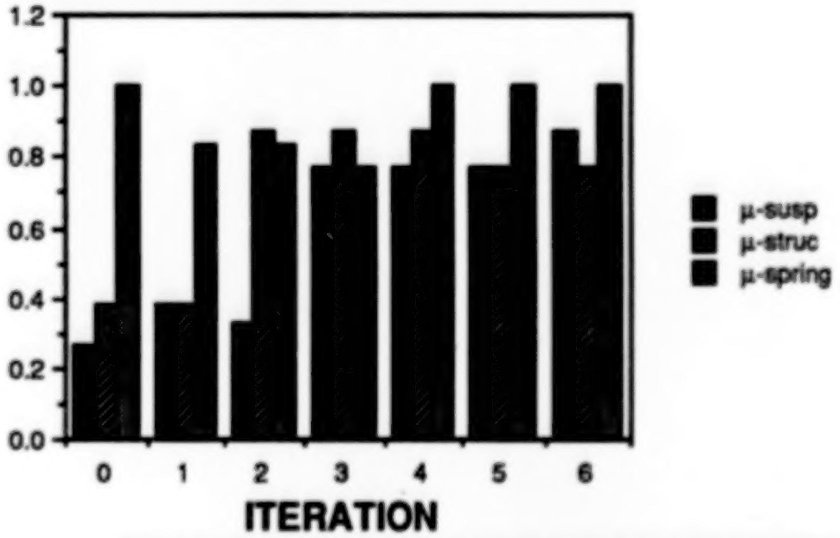

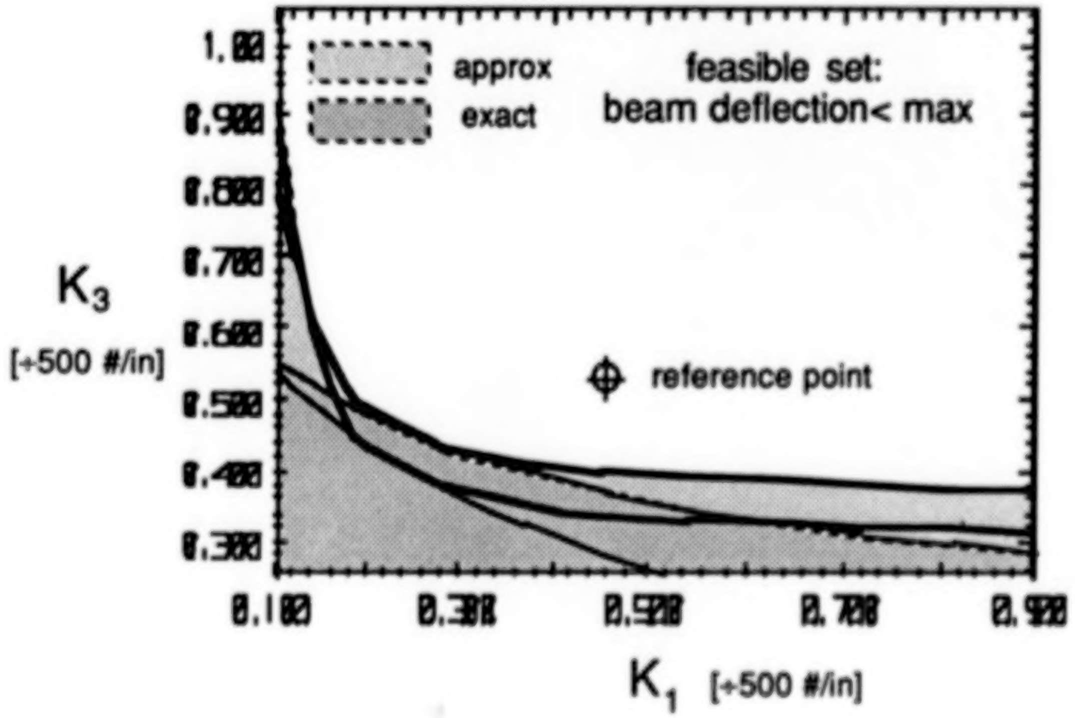

CONCLUSIONS

The introduction of fuzzy objective functions into the multilevel optimization problem adds a new dimension to the problem. Interactions among sub-problems can be represented as set operations on fuzzy sets, a feature that introduces flexibility and insight into the problem.

A more robust strategy to select the next active problem and objective needs to be developed. Heuristic approaches to determine constraint activity may prove useful here.

Some of the problems associated with keeping solutions feasible can be handled using convex approximations of non-local constraints. This is a promising approach, but one that needs further tests. More research is needed on issues such as how often sensitivity analyses must be performed to keep approximations accurate and how to determine appropriate step size limits.

ACKNOWLEDGEMENT

This material is based upon work supported by the National Science Foundation under Grant No. DME 8706902. This support is gratefully acknowledged.

BIBLIOGRAPHY

[1] Bellman, R.E. and Zadeh, L.,."Decision-making in a Fuzzy Environment," Management Science, 17(4), 1970, pp. B141-B164.

[2] Rao, S.S., "Multiobjective Optimization of Fuzzy Structural Systems," Int. J. for Numerical Methods in Eng., 24(6), 1987, pp. 1157-1171.

[3] Díaz, A., "Goal Aggregation in Design Optimization," Engineering Optimization , Vol. 13, 1988, pp. 257-273.

[4] Díaz, A., "Fuzzy Set Based Models in Design Optimization," Proceedings of the ASME Design Automation Conference, Orlando, Florida, Sept. 1988.

[5]Sobieszczanski-Sobieski, J."A Linear Decomposition Method for Large Optimization Problems-Blueprint for Development," NASA TM-83248, 1982.

[6] Haftka, "An Improved Computational Approach for Multilevel Optimum Design," J. Struct. Mechanics, Vol 12(2), 1984, pp. 245-261.

[7] Sobieszczanski-Sobieski, J., "Sensitivity Analysis and Multidisciplinary Optimization for Aircraft Design Recent Advances and Results," 16th Congress of the Intn'l Council of the Aeronautical Sciences, Jerusalem, Israel, 1988.

[8] Padula, S.L. and Sobieszczanski-Sobieski, J., "A Computer Simulator for Development of Engineering System Design Methodologies," ICED 87, Boston, MA, August 1987.

[9] Dubois, D. and Prade, H., "Criteria Aggregation and Ranking of Alternatives in the Framework of Fuzzy Set Theory," in H. Zimmermann, L. Zadeh, and B. Gaines, Eds., Fuzzy Sets and Decision Analysis, TIMS Studies in the Management Sciences, Vol. 20, 1984, pp. 209-240.

[10] Dubois, D. and Prade, H., "A Review of Fuzzy Set Aggregation Connectives," Information Sciences, 36, 1985, pp. 37,51.

[11] Parkinson, A., Balling, R., Wu, A. and Free, J. , "A General Strategy for Decomposing Large Design Problems Based on Optimization and Statistical Test Plans," ICED 87, Boston, MA, August 1987.

[12] Starnes, J.H. and Haftka, R.T., "Preliminary Design of Composite Wings for Buckling, Strength, and Displacement Constraints," J. Aircraft, 16(8), 1979, pp. 564-570.

[13] Fleury, C. and Braibant, V., "Structural Optimization: A New Method Using Mixed Variables," Int. J. for Numerical Methods in Eng., 23,1986, pp. 409,428.

[14] Sobieszczanski-Sobieski, J., "On the Sensitivity of Complex, Internally Coupled Systems," AIAA Paper 88-2378, AIAA/ASME/AHS 29th Structures, Structural Dynamics and Materials Conference, Williamsburg, VA, April 18-20, 1988.

A PENALTY APPROACH FOR NONLINEAR OPTIMIZATION WITH DISCRETE DESIGN VARIABLES

Dong K. Shin, Z. Gurdal, O.H.Griffin, Jr.
Department of Engineering Science and Mechanics
Virginia Polytechnic Institute & State University

INTRODUCTION

Most optimization techniques have been developed under the implicit assumption that the design variables are continuous-valued. For most practical optimization problems, however, the designer must choose the design variables from a list of commonly available values. The design variables such as cross-sectional areas of trusses, thicknesses of plates and membranes, fiber orientations and number of layers for laminated composite structures, fall into this category.

Although numerous algorithms for structural optimization problems have been developed, relatively little effort has been made for optimum structural design incorporating design variables with discrete values. The most common way of achieving a design with discrete-valued design variables is to round off the optimum values of the design variables, obtained by assuming them to be continuous variables, to the nearest acceptable discrete value. Although the idea is simple, for problems with a large number of design variables, selection of the discrete values without violating the design constraints can pose serious difficulties. More systematic methods are proposed in the research environment. Reinschmidt [1] used the Branch and Bound method for the plastic design of frames by posing the problem as an integer linear programming problem. Garfinkel and Nemhauser [2] showed the Branch and Bound method can also be used in solving convex nonlinear problems. This method forms new subproblems, called candidates, after obtaining the continuous optimum. These candidates exclude the infeasible (non-discrete) regions by branching, and bounds are used to rapidly discard many of the possible candidates without analyzing them due to the convexity of the problem. Schmit and Fleury [3] proposed a method in which approximation concepts and dual methods are extended to solve structural synthesis problems. In this technique, the structural optimization problem is converted into a sequence of explicit approximate primal problems of separable form. These problems are solved by constructing continuous explicit dual functions. Sizing type problems with discrete variables are solved successfully by this method. Another approach introduced by Olsen and Vanderplaats [4] used approximation techniques to develop subproblems suitable for linear mixed-integer programming methods. The solution is found by using two different softwares for continuous optimization and integer programming. Use of two different softwares, however, can be inconvenient for the practicing engineer. Also, the integer programming problems are difficult to handle.

This paper introduces a simple approach to minimization problems with discrete design variables by modifying the penalty function approach of converting the constrained problems into sequential unconstrained minimization technique (SUMT) problems [5]. It was discovered, during the course of the present work, that a similar idea was suggested by Marcal and Gellatly [6]. However, no further work has been encountered following Ref. [6]. In the following sections first, for the sake of clarity, a brief description of the SUMT is presented. Form of the penalty function for the discrete-valued design variables and strategy used for the implementation of the procedure are discussed next. Finally, several design examples are used to demonstrate the procedure, and results are compared with the ones available in the literature.

SEQUENTIAL UNCONSTRAINED MINIMIZATION TECHNIQUE

The SUMT algorithm transforms the constrained optimization problem into a sequence of unconstrained problems. The classical approach to using SUMT is to create a pseudo-objective function by combining the original objective function and the constraint equations. The constraints are added to the objective function in a way to penalize it if the constraint relations are not satisfied. That is, the constrained minimization problem,

$$\begin{array}{ll} \text{Minimize :} & F(X) \\ \text{Such that :} & g_j(X) \geq 0,\ j = 1, 2, \ldots, n_g \\ \text{where} & X = \{x_1, x_2, \ldots, x_n\}^T \\ & n \text{ : total number of design variables} \\ & n_g \text{ : number of constraints} \end{array} \tag{1}$$

is replaced by the following unconstrained one,

$$\text{Minimize :} \quad \Phi(X, r) = F(X) + r \sum_{j=1}^{n_g} y(g_j) \tag{2}$$

where $y(g_j)$ takes different forms depending on the method of penalty introduction [7]. The positive multiplier, r, in Eq. (2) controls the contribution of the constraint penalty terms. For a given value of the penalty multiplier, r, Eq. (2) describes the bounds of the feasible design space, often referred to as the response surface. As the penalty multiplier is decreased, the contours of the response surface conform with the original objective function and the constraints more closely. Therefore, minimization of the unconstrained problem is performed repeatedly as the value of r is decreased until the minimum value of the pseudo-objective function coincides with the value of the original objective function. Several response surfaces generated by using the extended interior penalty technique [7] for a problem with one design variable and a single constraint are shown in Figure 1.

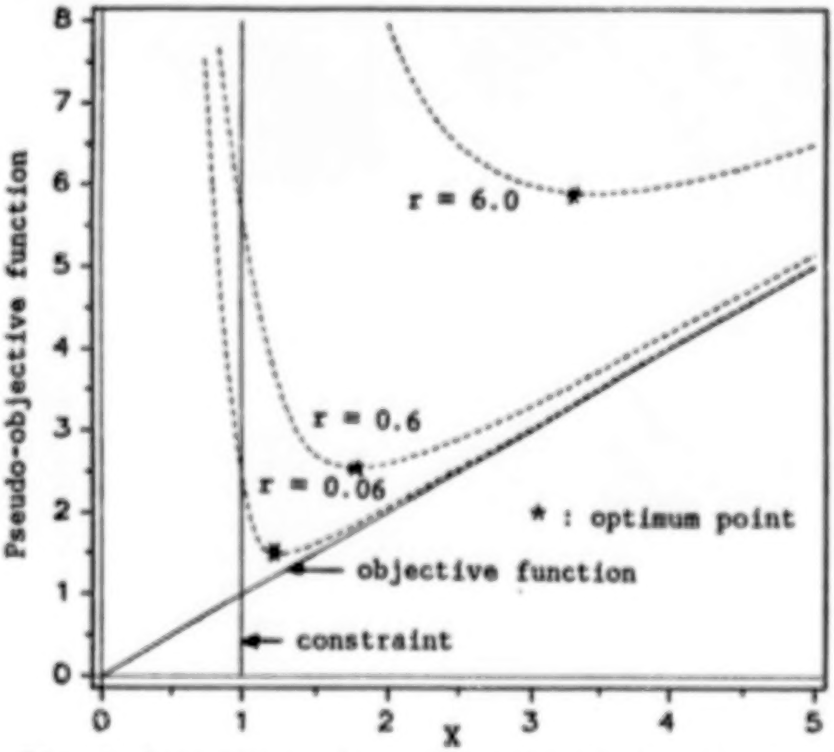

Fig. 1. Response surfaces for extended interior penalty method ($F = x$ subject to $g = x - 1.0 \geq 0$)

DISCRETE PENALTY FUNCTION

The basic idea behind the proposed method is to include additional penalty terms in the pseudo-objective function to reflect the requirement that the design variables take discrete values. The general formulation for a problem having discrete variables is presented below.

$$\begin{aligned} &\text{Minimize} &&: \quad F(X) \\ &\text{Subject to} &&: \quad g_j(X) \geq 0 \quad j = 1,2,\ldots,n_g \\ &\text{where} && \quad x_i = (d_{i1}, d_{i2}, \ldots, d_{iq})^T \\ & && \quad d_{ik} : \text{k-th discrete value of the i-th design variable} \\ & && \quad q : \text{number of discrete values for each design variable} \end{aligned} \tag{3}$$

In general, the number of available discrete values for each design variable may be different, or even in some cases continuous variation of some of the design variables may be allowed. The modified pseudo-objective function Ψ which includes the penalty terms due to constraints and the non-discrete values of the design variables is defined as

$$\Psi(X, r, s) = F(X) + r \sum_{j=1}^{m} p^x(g_j) + s \sum_{i=1}^{p} \Phi_d^i(X) \tag{4}$$

where r is the penalty multiplier for constraints, $p^x(g_j)$ is a quadratic extension function [8], s is the penalty multiplier for non-discrete values of the design variables, and $\Phi_d^i(X)$ denotes the penalty term for non-discrete values of the $i-$th design variable. Different forms for the discrete penalty function are possible. In the present study, the penalty terms $\Phi_d^i(X)$ are assumed to take the following sine-function form,

$$\Phi_d^i(X) = \frac{1}{2}\left(\sin \frac{2\pi[x_i - \frac{1}{4}(d_{ij+1} + 3d_{ij})]}{d_{ij+1} - d_{ij}} + 1\right) \tag{5}$$

The proposed functions $\Phi_d^i(X)$ penalize only non-discrete design variables and assure the continuity of the first derivatives of the modified pseudo-function at the discrete values of the design variables. The discrete penalty functions of the sine and elliptical forms are shown in Figure 2.

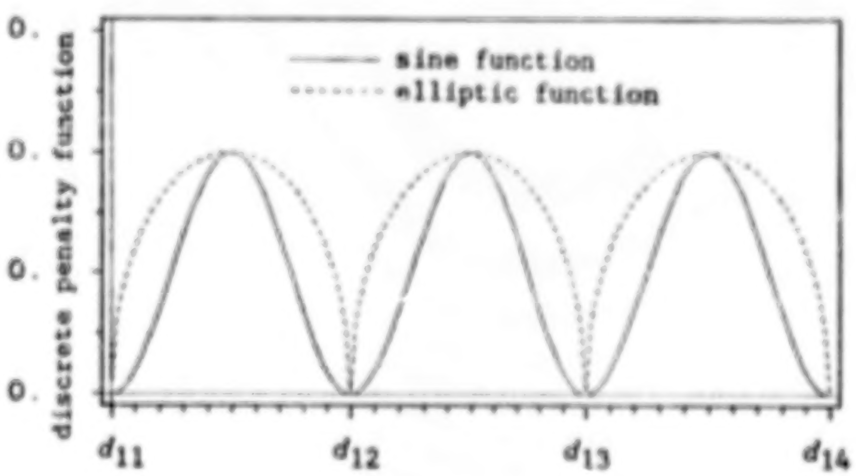

Fig. 2. Discrete penalty functions

257

SUMT WITH DISCRETE-VALUED DESIGN VARIABLES

The proposed method can be implemented with either exterior, interior, or extended interior penalty function approaches. The additional penalty terms for non-discrete design variables are incorporated to the optimization package NEWSUMT-A [9] which employs the extended interior penalty approach; hence, the following discussion is confined to the extended interior penalty technique. In equation (4), the response surfaces are determined according to the values of the penalty multipliers r and s since they control the amount of penalty for the constraints and for the non-discrete values, respectively. As opposed to the multiplier r, the value of the multiplier s is initially zero and is increased slowly from one response surface to another. One of the important factors in the application of the proposed method is to determine when to activate s, and how fast to increase it to obtain discrete optimum design. Clearly, if s is introduced too early in the design process, the design variables will be trapped by a local minimum resulting in a sub-optimal solution. To avoid this problem, the multiplier s has to be activated after several response surfaces which includes only constraint penalty terms. In fact, since the optimum design with discrete values is in the neighborhood of the continuous optimum, it may be desirable not to activate the penalty for the non-discrete design variables until a reasonable convergence to the continuous solution is achieved. This is especially true for problems with a large number of design variables and/or the intervals between discrete values are very close. The modified pseudo-objective function Ψ defined in equation (4) is shown in Figure 3 for a problem with one design variable and one constraint (See Example 1).

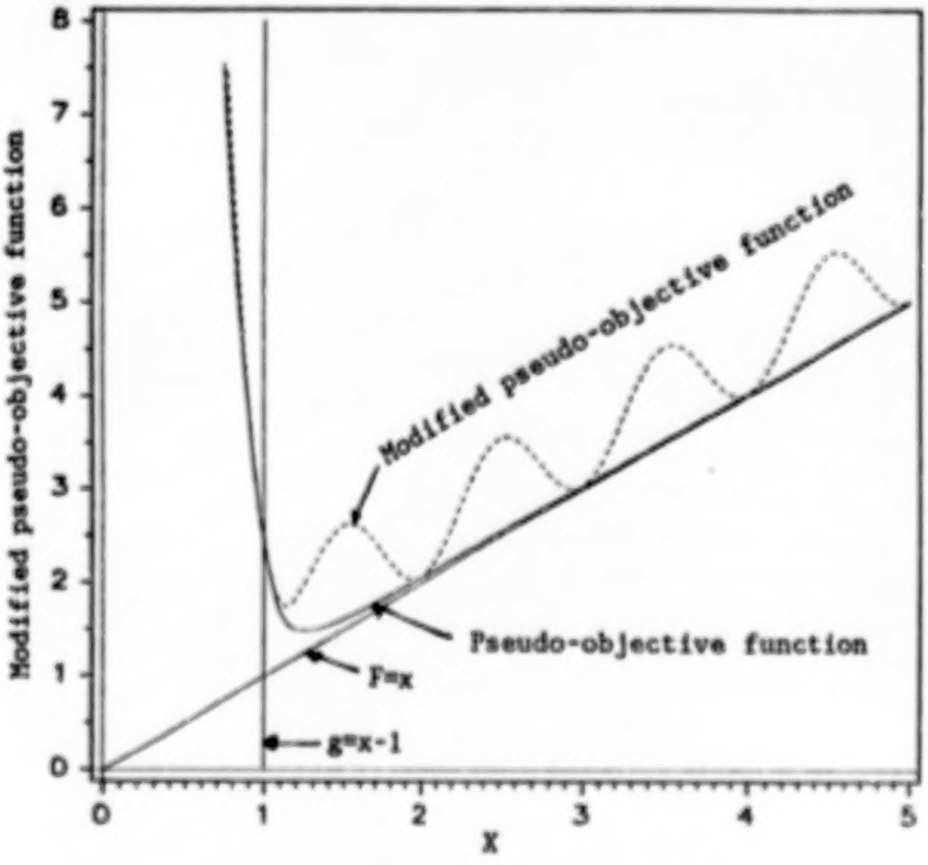

Fig. 3. Modified pseudo-objective function
($F = x$ subject to $g = x - 1.0 \geq 0$ and $x = 1, 2, 3, \ldots$)

DISCUSSION OF IMPLEMENTATION AND CONVERGENCE CRITERION

In using the SUMT, convergence is usually examined by comparing the total objective function with the corresponding value of the original objective function. A similar scheme is used to determine how close the design approaches to the continuous optimum before activating the discrete penalty. A criterion,

$$\epsilon_c = \frac{\text{amount of constraint penalty}}{\text{objective function}} \tag{6}$$

is used, where ϵ_c denotes the tolerance to activate the discrete optimization process.

One of the important aspects of the present procedure is to determine how big a penalty term to apply at the first discrete response surface. If too large s is applied at the first few discrete iterations, the design can be trapped at a local minimum. To prevent the design from stalling, s must be applied slowly. The magnitude of the non-discrete penalty multiplier, s, at the first discrete iteration, is calculated such that the amount of penalty associated with the non-discrete design variables is equal to the constraint penalty. As the iteration for discrete optimization proceeds, the non-discrete penalty multiplier for the new iteration, $s^{(i+1)}$, is calculated by multiplying the $s^{(i)}$ by 5. Increasing $s^{(i)}$ implies that the discrete values for design variables are becoming more important than the constraint violation as the discrete optimization process continues.

Another important aspect of the proposed procedure is how to control the other penalty multiplier for the constraints, r, during the discrete optimization process. If r is decreased for each discrete optimization iteration as for the continuous optimization process, the design can be stalled due to too strict penalty on constraint violation. On the other hand, if r is increased, the design may move away from the optimum resulting in a sub-optimal solution. Thus, it is logical to freeze the penalty multiplier r at the end of the continuous optimization process. However, the nearest discrete solution at this response surface may not be a feasible design, in which case the design is forced to move away from the continuous optimum by moving back to the previous response surface. This was achieved by increasing the penalty multiplier, r, by a factor of 10.

The solution process for the discrete optimization is terminated if the design variables are sufficiently close to the prescribed discrete values. The convergence criterion for discrete optimization used in this effort is

$$\epsilon_d = \sum_{i=1}^{n} \min(|x_i - d_{ij}|, |x_i - d_{ij+1}|) \tag{7}$$

where ϵ_d is the convergence tolerance.

During the discrete iteration process, it was experienced that some of the design variables were sometimes trapped at the middle of two discrete values, especially for a large value of penalty multiplier s. This is due to the vanishing nature of the first derivative of the sine function (5) at the mid-point. If it is detected that any one of the design variables is at the mid-point where the values of the first and second derivative of the sine function (5) approach 0 and -1, respectively, the trapping was avoided by removing the penalty terms for non-discrete values. This means only the original objective function and constraint penalty terms take part in the minimization process. The move direction is determined from the original response surface excluding the penalty terms due to non-discrete values. The flow chart for the proposed method combined with the extended interior approach is shown in Fig. 4.

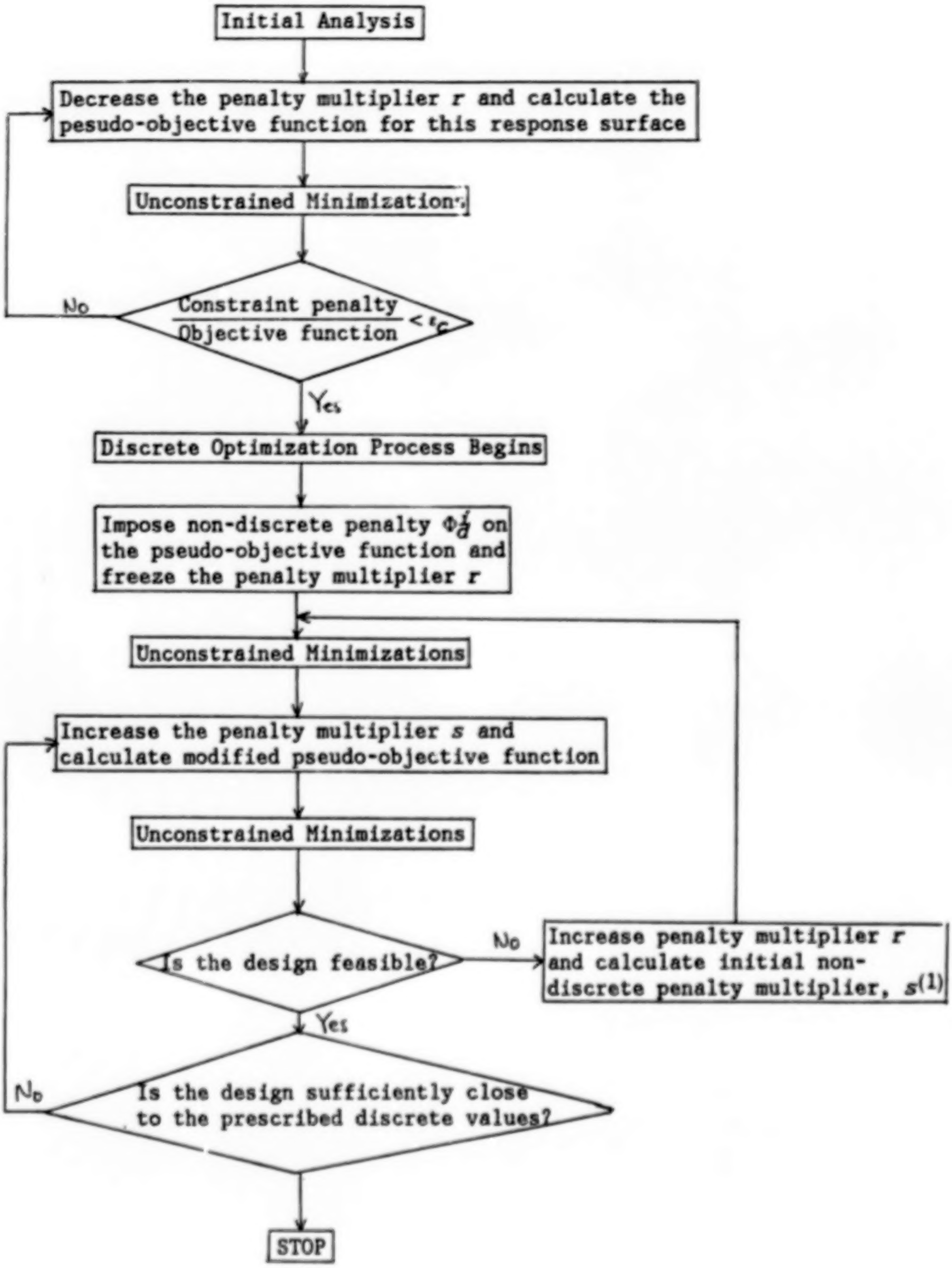
Initial Analysis
Decrease the penalty multiplier r and calculate the pesudo-objective function for this response surface
Unconstrained Minimizations
No
Constraint penalty / Objective function < ε_c
Yes
Discrete Optimization Process Begins
Impose non-discrete penalty Φ_d^j on the pseudo-objective function and freeze the penalty multiplier r
Unconstrained Minimizations
Increase the penalty multiplier s and calculate modified pseudo-objective function
Unconstrained Minimizations
Is the design feasible?
No
Increase penalty multiplier r and calculate initial non-discrete penalty multiplier, s(1)
Yes
No
Is the design sufficiently close to the prescribed discrete values?
STOP

Fig. 4. Flow Chart for Continuous and Discrete Optimization Process

EXAMPLES

All the results presented in this section are generated by using NEWSUMT-A modified with the proposed technique.

1. One Design Variable Problem

For pictorial demonstration, the following simple problem with one design variable and one constraint is presented.

$$\begin{aligned} &\text{Minimize :} && F = x \\ &\text{Subject to :} && g = x - 1.0 \geq 0 \\ &\text{where} && x = \{1.0,\ 2.0,\ \ldots.\} \end{aligned}$$

The process of the discrete optimization is shown in Fig. 5 for two different values of ϵ_c. For each discrete iteration, the amount of penalty on the non-discrete values is increased and the design converges to one of the discrete values. Fig. 5-(a) shows that the final design can be trapped at the local minimum if the discrete design process begins too early ($\epsilon_c = 0.5$). For this example, correct discrete optimum was obtained if $\epsilon_c < 0.5$.

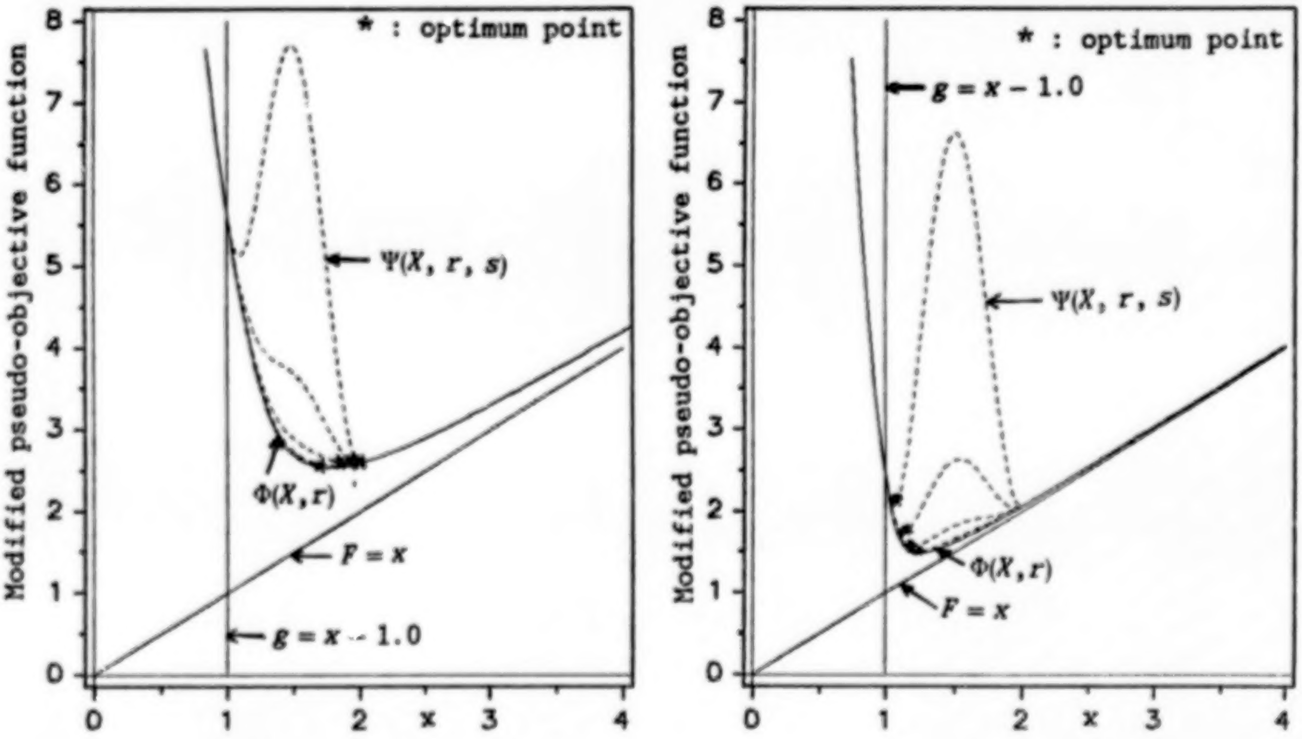

(a) $\epsilon_c = 0.5$ (b) $\epsilon_c = 0.1$

Fig. 5. Discrete optimization process for example 1

2. Three-bar Truss Problem

The indeterminate three bar truss as shown in Fig. 6 is subject to vertical and horizontal forces. The structural weight, W, is minimized under the constraint that the stress in all members should be smaller than the allowable stress, σ_0, in absolute magnitude. After nondimensionalization of the objective function and design variables ($F = \frac{\sigma_0 W}{P \rho l}$ and $x_i = \frac{a_i \sigma_0}{P}$), the optimum problem can be stated as

Minimize : $F = 2x_1 + x_2 + \sqrt{2}\,x_3$

Subject to :

$$g_1 = 1 - \frac{\sqrt{3}\,x_2 + 1.932x_3}{1.5x_1x_2 + \sqrt{2}\,x_2x_3 + 1.319x_1x_3} \ge 0$$

$$g_2 = 1 - \frac{0.634x_1 + 2.828x_3}{1.5x_1x_2 + \sqrt{2}\,x_2x_3 + 1.319x_1x_3} \ge 0$$

$$g_3 = 1 - \frac{0.5x_1 - 2x_2}{1.5x_1x_2 + \sqrt{2}\,x_2x_3 + 1.319x_1x_3} \ge 0$$

$$g_4 = 1 + \frac{0.5x_1 - 2x_2}{1.5x_1x_2 + \sqrt{2}\,x_2x_3 + 1.319x_1x_3} \ge 0$$

$$x_i = \{0.1,\ 0.2,\ 0.3,\ 0.5,\ 0.8,\ 1.0,\ 1.2\},\ i=1,2,3$$

The continuous optimum design is $F = 2.7336$, $x_1 = 1.1549$, $x_2 = 0.4232$ and $x_3 = 0.0004$. The discrete solution by the proposed method was found to coincide with the actual discrete optimum, $F = 3.0414$, $x_1 = 1.2$, $x_2 = 0.5$ and $x_3 = 0.1$ when $\epsilon_c \le 0.1$. For $\epsilon_c = 0.5$, the design was at a local minimum, $F = 3.1828$, $x_1 = 1.2$, $x_2 = 0.5$, and $x_3 = 0.2$. NEWSUMT-A program reached the continuous optimum in 7 response surfaces, whereas the discrete optimum was converged in 11, 11 and 13 response surfaces when $\epsilon_c = 0.5$, 0.1 and 0.01, respectively. The computing time for discrete design can be saved if the discrete iteration begins early, although it can result in local optimum.

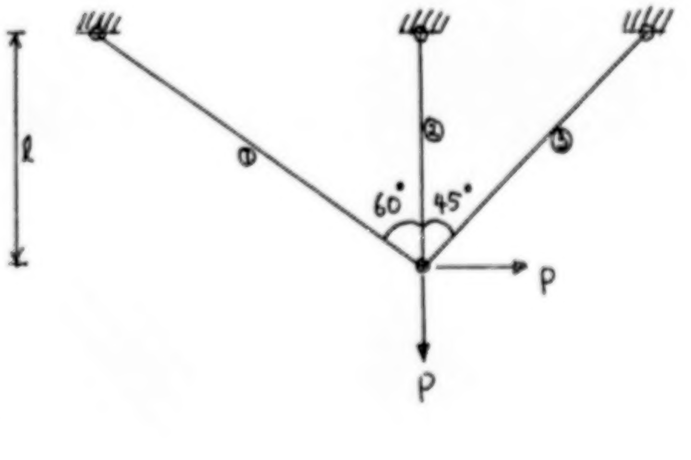

$|\sigma_i| \le \sigma_0$
ρ : mass density
a_i : cross-sectional area

Fig. 6. Three bar truss for example 2

3. Ten-Bar Truss Problem

The classical 10 bar truss is shown in Fig. 7. The design variables are the cross-sectional areas of the 10 bar. The structural weight, W, is minimized subject to a maximum stress limit of 25,000 psi and maximum displacement limit of 2.0 in. All design variables are assumed to take the discrete values, $x_i = \{ 0.1, 0.5, 1.0, 1.5, 2.0, 2.5, \ldots \}$. The discrete optimum solution obtained by proposed method is compared in Table 1 with other solutions by different techniques obtained from Reference [10]. The solution by the proposed method is different from all other solutions. The results by Branch & Bound, Ref. [3] and proposed method are slightly infeasible though negligible in engineering sense. It can be seen from Tab. 1 that the different starting point for discrete optimization, ϵ_c, can result in different discrete solutions. The continuous optimum was obtained in 7 response surfaces and discrete solutions were found in 10 and 13 response surfaces for ϵ_c =0.01 and 0.001, respectively. The continuous solution was obtained in 8 response surfaces and discrete solutions were found in 11 and 13 response surfaces for ϵ_c =0.01 and 0.001, respectively. With a relatively large number of design variables as this case, the continuous solution process has to be terminated in the close neighborhood of the continuous optimum.

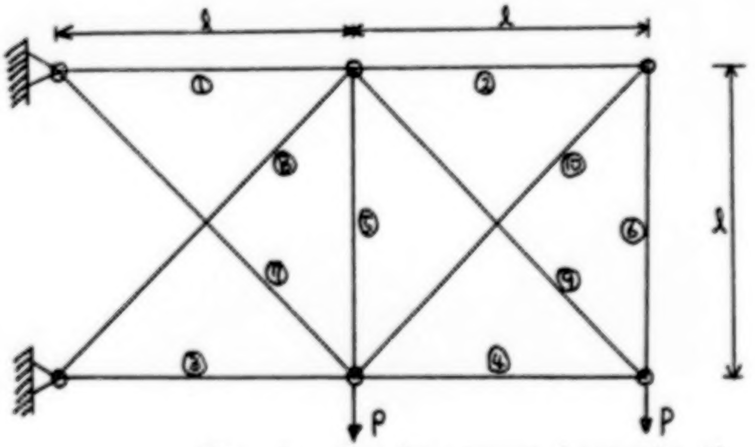

$E = 10^7$ psi
$\rho = 0.1$ lbm/in^3
P = 100 kip
l = 360 in

Fig. 7. Ten bar truss (example 3)

	Branch & Bound	Generalized Lagrangian	Dynamic Round-off	Schmit & Fleury	Proposed Method$^{(1)}$	Proposed Method$^{(2)}$
W	5059.9	5067.3	5077.9	5059.9	5059.9	5103.3
x_1	30.5	30.0	30.0	30.5	30.5	31.0
x_2	0.1	0.1	0.1	0.1	0.1	0.1
x_3	23.0	23.5	23.5	23.0	23.5	23.5
x_4	15.5	15.0	15.5	15.5	15.0	15.0
x_5	0.1	0.1	0.1	0.1	0.1	0.1
x_6	0.5	0.5	1.0	0.5	0.5	0.5
x_7	7.5	7.5	7.5	7.5	7.5	7.5
x_8	21.0	21.0	21.0	21.0	21.0	21.5
x_9	21.5	22.0	21.5	21.5	21.5	21.5
x_{10}	0.1	0.1	0.1	0.1	0.1	0.1

(1) : $\epsilon_c = 0.001$, (2) : $\epsilon_c = 0.01$

Table 1. Discrete solutions for 10 bar truss ($\epsilon_d = 0.001$)

CONCLUDING REMARKS

A simple penalty approach combined with the extended interior penalty function technique for the problems with discrete design variables was presented. Criteria for starting the discrete optimization and for convergence were proposed. The procedure was demonstrated on several numerical examples. It was found that the non-discrete penalty multiplier, *s*, has to be increased step-by-step and the continuous penalty multiplier, *r*, has to be relaxed in the discrete optimization process if the constraints are violated. If the problem has a large number of design variables and/or the intervals between prescribed discrete values are close, the penalty terms for non-discrete values have to be activated in the close neighborhood of the continuous optimum. While these preliminary results are encouraging, further numerical tests with more complex problems are required to use the proposed technique with confidence.

REFERENCES

1. Reinschmidt, K., "Discrete Structural Optimization," ASCE, J. Struct. Div., 97, 133-156, 1971.

2. Garfinkel, R. and Nemhauser, G., "Integer Programming," John Wiley, New York, 1972.

3. Schmit, L. and Fleury, C., "Discrete-Continuous Variable Structural Synthesis Using Dual Methods," AIAA J., Vol. 18, pp. 1515-1524, 1980.

4. Olson, G. R. and Vanderplaats, G. N., "A Method for Nonlinear Optimization with Discrete Design Variables," AIAA Paper No.87-0789, Dynamics and Materials Conference, April 6-8, 1987, Monterey, CA.

5. Fiacco, A. V. and McCormick, G. P., "Nonlinear Programming : Sequential Unconstrained Minimization Techniques," John Wiley, New York, 1968.

6. Marcal, P. V. and Gellatly, R. A., "Application of the Created Response Surface Technique to Structural Optimization," AFFDL-TR-68-150, Air Force Flight Dynamics Laboratory, WPAFB, Ohio, 1968.

7. Haftka, R. T. and Kamat, M. P., "Elements of Structural Optimization," Martinus Nijhoff Publishers, Boston, 1985.

8. Haftka, R. T. and Starnes, J. H., Jr., "Applications of a Quadratic Extended Penalty Function to Structural Optimization," AIAA J., Vol. 14, pp. 718-724, 1976.

9. Grandhi, R. V., Thareja, R. and Haftka, R. T., "NEWSUMT-A : A General Purpose Program for Constrained Optimization Using Constraint Approximation," ASME Journal of Mechanisms, Transmissions and Automation in Design, Vol. 107, pp. 94-99, March 1985.

10. Ringertz, U. T., "On Methods For Discrete Structural Optimization," Engineering Optimizations, Vol. 13, pp. 47-64, 1988.

MULTIPLIER–CONTINUATION ALGORITHMS FOR CONSTRAINED OPTIMIZATION

Bruce N. Lundberg*
Aubrey B. Poore** and Bing Yang**
Department of Mathematics
Colorado State University
Fort Collins, Colorado 80523

ABSTRACT

Several path following algorithms based on the combination of three smooth penalty functions, the quadratic penalty for equality constraints and the quadratic loss and log barrier for inequality constraints, their modern counterparts, augmented Lagrangian or multiplier methods, sequential quadratic programming, and predictor–corrector continuation are described. In the first phase of this methodology, one minimizes the unconstrained or linearly constrained penalty function or augmented Lagrangian. A homotopy path generated from the functions is then followed to optimality using efficient predictor–corrector continuation methods. The continuation steps are asymptotic to those taken by sequential quadratic programming which can be used in the final steps. Numerical test results show the method to be efficient, robust, and a competitive alternative to sequential quadratic programming.

---

*The work of the first author was partially supported by the National Aeronautics and Space Administration through NASA Grant # NGT–06–002–802. **The second and third authors were supported in part by the Air Force Office of Scientific Research through Grant # AFOSR–88–0059.

266

1. Introduction

Path following algorithms for the solution of constrained optimization have been revitalized in recent years, due in no small part to the claims and success of the Karmarkar algorithm in linear programming. The ones presented here can be viewed as a combination of various elements and techniques in nonlinear programming: three smooth penalty functions (quadratic penalty for equality constraints, quadratic loss and log barrier for inequality constraints), their more modern counterparts, augmented Lagrangian or multiplier methods, sequential quadratic programming (Newton's method), and predictor–corrector continuation methods for efficient path following. The objective in this work then is to describe this class of algorithms and to present numerical evidence of their efficiency, robustness, and potential.

One view (ref. 1) of these algorithms starts with the three aforementioned smooth penalty functions. One first performs an unconstrained or linearly constrained optimization of the penalty function. The minimizer then satisfies a set of first order necessary conditions (the gradient of the penalty function is zero when all constraints are incorporated into the penalty function) from which one can define an equivalent system of parameterized nonlinear equations. This system represents a perturbation of the Karush–Kuhn–Tucker first order necessary conditions, and the solution is followed to optimality using efficient predictor–corrector continuation methods. The simplest predictor–corrector steps are asymptotic to those taken in sequential quadratic programming, and thus the local convergence rates are the same as those of sequential quadratic programming. When shifts and weights are added to these three penalty functions and are adaptively chosen or updated during the optimization phase, one has the class of multiplier or augmented Lagrangian methods. Theoretically, one can expect a shorter path through the use of augmented Lagrangians (ref. 2, Theorem 12.2.1), which suggests that the use of these updates in the weights, scales, and shifts may be used to generate good paths to optimality.

A different perspective of these algorithms evolves from sequential quadratic programming (SQP) itself. These SQP methods perform exceptionally well in minimizing function evaluations, but may be slow since the combinatorial complexity of the inequality constraints is reflected in the subproblems at each step. Furthermore, they are currently restricted to small to medium size problems with promise for large scale applications (refs. 2 and 3). Augmented Lagrangian methods, on the other hand, are currently used effectively for large scale problems with structured sparsity arising, for example, from discretized partial differential equations. Also, augmented Lagrangians are often used as merit functions for globalizing sequential quadratic programming. However, the minimizer of the augmented Lagrangian at any given stage is not a solution of the original problem, and thus the homotopy between the minimizer of the augmented Lagrangian and sequential quadratic programming may be viewed as an intermediate globalization technique. We find this to be very efficient.

In the sections to follow, we briefly outline the methodology and present in section seven the results of our preliminary numerical testing.

2. Background and General Results

For expendiency and convenience of presentation, we present in this section the first order necesssary and second order sufficient conditions for the mathematical programming problem

$$\text{(2.1)} \qquad \operatorname{Min} \{ f(x) \mid h(x) = 0,\ g(x) \geq 0\}$$

where f: $\mathbb{R}^n \to \mathbb{R}^1$, h: $\mathbb{R}^n \to \mathbb{R}^q$ and g: $\mathbb{R}^n \to \mathbb{R}^p$ are assumed to be twice continuously differentiable in an open set Ω containing the feasible region $\mathcal{R} = \{ x \mid h(x) = 0, g(x) \geq 0 \}$. The Karush–Kuhn–Tucker first order necessary conditions state that in the presence of a constraint qualification, there exist multiplier vectors λ and μ such that

$$\text{(2.2)} \qquad F(x,\lambda,\mu) = \begin{bmatrix} \nabla\mathcal{L}(x,\lambda,\mu) \\ h(x) \\ Mg(x) \end{bmatrix} = 0$$

$$\mu \geq 0,\ g(x) \geq 0,$$

where $\mathcal{L} = f - h^T\lambda - g^T\mu$, $M = \operatorname{diag}(\mu)$, $\mu = (\mu_1,\dots,\mu_p)^T$, $\lambda = (\lambda_1,\dots,\lambda_q)$.

THEOREM 2.1 (ref. 4). Let (x_o,λ_o,μ_o) be a solution of $F(x,\lambda,\mu) = 0$. Assume f, g and h are twice continuously differentiable in a neighborhood of x_o and define two index sets $\bar{\mathcal{A}}$ and $\mathcal{A}$ and a corresponding tangent space $\bar{T}$ by

$$\bar{\mathcal{A}} = \{i\colon 1 \leq i \leq p,\ g_i(x_o) = 0\}, \qquad \mathcal{A} = \{i \in \bar{\mathcal{A}}\colon \mu_i^o \neq 0\},$$

$$\bar{T} = \{y \in \mathbb{R}^n\colon D_x h(x_o)y = 0,\ \ D_x g_i(x_o)y = 0 \ \ (i \in \bar{\mathcal{A}})\}.$$

Then a necessary and sufficient condition that $D_{(x,\lambda,\mu)}F(z_o,\lambda_o,\mu_o)$ be nonsingular is that each of the following three conditions hold:

(a) $\bar{\mathcal{A}} = \mathcal{A}$;

(b) $\{\{\nabla_x g_i(x_o)\}_{i\in\bar{\mathcal{A}}} \cup \{\nabla_x h_j(x_o)\}_{j=1}^{q}\}$ is a linearly independent collection of $q + |\bar{\mathcal{A}}|$ vectors where $|\bar{\mathcal{A}}|$ denotes the cardinality of $\bar{\mathcal{A}}$;

(c) the Hessian of the Lagrangian $\nabla_x^2\mathcal{L}$ is nonsingular on the tangent space $\bar{T}$ at (x_o,λ_o,μ_o).

Furthermore, if (b) remains valid, $\mu_o \geq 0$, $g(x_o) \geq 0$, and (a) and (c) are replaced by

(a') $\mu_i^o > 0$ for all $i \in \bar{\mathcal{A}}$,

(c) the Hessian of the Lagrangian $\nabla^2_x \mathcal{L}$ *is positive definite on the tangent space* $\bar{T}$ *at* (x_o,λ_o,μ_o),

then $D_{(x,\lambda,\mu)}F(x_o,\lambda_o,\mu_o)$ *is nonsingular and* x_o *is a local minimum of the nonlinear programming problem (2.1).*

We note that condition (a) is a complementarity condition, (b) is the linear independence constraint qualification, and (c) is a second–order condition.

3. Newton's Method for Nonlinear Programming

The objective of this section is to briefly review Newton's method (Newton–Lagrange or sequential quadratic programming) for the general nonlinear programming problem (2.1). The methods which we later present are asymptotic to Newton's method and, in fact, may be used in the last few iterations. The starting point for Newton's method is the first order necessary condition as stated in equation (2.2).

The motivation for Newton's method is to form a linear model suggested by Taylor's formula about the current point (x,λ,μ) and then solve this model for the linear increments $(\Delta x,\Delta\lambda,\Delta\mu)$. The difference between a nonlinear equations approach and that of constrained optimization is that one keeps a quadratic term in the complementarity condition:

$$(3.1)\quad F(x+\Delta x,\lambda+\Delta\lambda,\mu+\Delta\mu) = \begin{bmatrix} \nabla^2 L\Delta x - D_x h^T\Delta x - D_x g^T\Delta x + \nabla L \\ D_x h\Delta x + h \\ (M + \Delta M)(D_x g\Delta x + g) \end{bmatrix} + O(\Delta^2)$$

where $O(\Delta^2)$ refers to those increments $(\Delta x,\Delta\lambda,\Delta\mu)$ which are second order and higher. Note that the quadratic increment $\Delta M D_x g\Delta x$ has been retained, but the addition of such higher order terms will not affect the quadratic convergence of Newton's method. Setting this bracketed quantity to zero yields

$$\begin{aligned} &\nabla^2 L\Delta x - D_x h^T\Delta x - D_x g^T\Delta x = -\nabla L \\ &D_x h\Delta x + h = 0 \\ &(M + \Delta M)(D_x g\Delta x + g) = 0, \end{aligned}$$

which, if $\mu + \Delta\mu \geq 0$ is imposed, represent the first order optimality conditions for the quadratic programming subproblem

$$(3.2)\qquad \begin{aligned} \text{MIN}\quad & f + \nabla f^T\Delta x + (1/2)\Delta x^T\nabla^2 L\Delta x \\ \text{ST}\quad & D_x h\Delta x + h = 0 \\ & D_x g\Delta x + g \geq 0. \end{aligned}$$

Second order information for both the constraints and the objective function are built into the quadratic programming subproblem through the appearence of $\nabla^2 L$. The generic Newton's method with no safeguards is as follows:

ALGORITHM [NEWTON'S METHOD FOR NONLINEAR PROGRAMMING]

```
Initialize $x = x_o$, $\lambda = \lambda_o$, and $\mu = \mu_o$
For $k = 0,1,\ldots,$ until satisfied, do (a), (b), (c)
    (a) Compute $f = f(x_k)$, $h = h(x_k)$, $g = g(x_k)$, $\nabla f = \nabla f(x_k)$,
        $D_x h = D_x h(x_k)$, $D_x g = D_x g(x_k)$, $\nabla^2 L = \nabla^2 L(x_k, \lambda_k, \mu_k)$,
    (b) Solve (3.2) for the correction $\Delta x$ in $x_k$ and the multipliers
        $\mu_k + \Delta\mu \geq 0$ and $\lambda_k + \Delta\lambda$,
    (c) Update: $x_{k+1} = x_k + \Delta x$, $\lambda_{k+1} = \lambda_k + \Delta\lambda$, $\mu_{k+1} = \mu_k + \Delta\mu$.
```

The quadratic convergence of Newton's method for nonlinear equations is preserved for the nonlinear programming problem under conditions similar to those in nonlinear equations:

Theorem 3.1 [Convergence of Newton's Method]. *Let $\hat{x}$ be a local solution of the nonlinear programming problem, assume that f, g, and h are C^2 functions whose second derivatives are Lipschitz continuous in a neighborhood of $\hat{x}$, and suppose that the linear independence constraint qualification (condition (b) in Theorem 2.1) is satisfied. Then there exist multipliers $\hat{\lambda}$ and $\hat{\mu} \geq 0$ for which the Karush–Kuhn–Tucker conditions (2.2) are valid. If conditions (a') and (b') in Theorem 2.1 are satisfied, then there is a neighborhood N of $(\hat{x}, \hat{\lambda}, \hat{\mu})$ such that if (x_o, λ_o, μ_o) is in N, then the iterates (x_k, λ_k, μ_k) are defined, remain in N and converge quadratically to $(\hat{x}, \hat{\lambda}, \hat{\mu})$.*

As with Newton's method for nonlinear equations, there are the questions of linear algebra, updating techniques for quasi–Newton steps, and globalization methods. These questions are discussed, for example, in the review paper of Stoer (ref. 3), the book of Fletcher (ref. 2), and the references therein. Two commonly used merit functions for globalization are the L_1 penalty function

$$P = \nu f + (1/r)\, \Sigma\, |h_i(x)| + (1/r)\, \Sigma\, g_j(x)^-$$

and the augmented Lagrangian

$$L_a(x, \lambda, \mu, r) = f + (1/2r)\, \Sigma\, (h_i(x) - r\hat{\lambda}_i)^2 + (1/2r)\, \Sigma\, [(g_j(x) - r\hat{\mu}_j)^-]^2$$

where $g_j^-(x) = \mathrm{Min}\ \{\ g_j(x),\ 0\ \}$, r is the penalty parameter, and $\hat{\lambda}$ and $\hat{\mu}$ are the shifts or approximate multipliers. The use of the L_1 penalty function as a merit function for sequential quadratic programming has proved to be highly successful for small to medium problems. Augmented Lagrangians on the other hand have as their domain of application large scale problems such as those that appear in discretized partial differential equations; however, the function evaluation count on small to medium problems is not nearly as favorable as that of sequential quadratic programming (ref. 5). On the other hand, sequential quadratic programming may be slow in comparison to augmented Lagrangian methods, primarily due to the combinatorial complexity of the inequality constraints which persists in the quadratic subprograms. In this work we combine both approaches by using a few steps of augmented Lagrangians followed by a homotopy phase, and then sequential quadratic programming.

4. Homotopy Methods for Constrained Optimization

The idea of a homotopy method is to embed a difficult problem into a parameterized set of problems such that at one parameter value the problem is "easy" to solve and at another value one recovers the "difficult" problem. One then continues the solution of this parameterized system from the easy problem to the desired one. For nonlinear equations $F(x) = 0$, two commonly used homotopies are $G(x,t) = tF(x) + (1-t)(F(x) - F(a))$ (the global Newton homotopy) and $G(t,x) = tF(x) + (1-t)(x-a)$ (the regularizing homotopy). Indeed, at $t = 0$ these are easy to solve, while at $t = 1$ one recovers the original problem. These homotopy methods tend to be quite robust, but currently are not as efficient as the use of merit functions with a modified or quasi-Newton method. The homotopy methods discussed here are generally very efficient, but the the easy problem is not as easy as the above ones for nonlinear equations in that the "easy" problem requires the solution of an unconstrained or linearly constrained optimization problem.

To illustrate the idea and for later numerical comparisons, we first consider the mixed quadratic penalty–log barrier function

$$(4.1) \qquad P(x,r) = f + (1/2r)\ \Sigma\ h_i^2(x) - r\ \Sigma\ \ln(g_j(x))$$

or in the more general form

$$(4.2) \qquad \begin{aligned} P(x,\nu,\hat{\lambda},\mu,\sigma,\omega,\delta,r) = \nu f &+ (1/2r)\ \Sigma\ \sigma_i(\gamma_i h_i(x) - r\sigma_i^{-1}\hat{\lambda}_i)^2 \\ &- r\ \Sigma\ \omega_j\ \ln(g_j(x) + r\delta_j) \end{aligned}$$

wherein weights σ_i and ω_j, scales ν and γ_i, and shifts $\hat{\lambda}_i$ and δ_i have been introduced. The homotopy generated from this penalty function depends on the system parameters, which can be adaptively chosen during the optimization phase.

To explain how one can derive a homotopy, we consider the simpler form (4.1). At $r = r_0$, a minimizer, x_0, of this penalty function satisfies

$$\nabla P = \nabla f + \Sigma\, \nabla h_i (h_i/r) - \Sigma\, (r/g_j)\nabla g_j = 0,$$

which along with the definitions $\lambda_i = -h_i/r$ and $\mu_j = r/g_j$ yield an equivalent system of parameterized nonlinear equations

$$\begin{aligned} &\nabla L = 0, && L = f - h^T\lambda - g^T\mu \\ &h + r\lambda = 0, && \\ &Mg - re = 0, && M = \mathrm{diag}(\mu),\ e = (1,\ldots,1)^T. \end{aligned} \tag{4.3}$$

A solution to this parameterized system at $r = r_0$ is given by $\lambda = -h(x_0)/r$ and $\mu = r/g(x_0)$, componentwise. Furthermore, these equations represent the first order necessary conditions at $r = 0$ since $\mu(r) > 0$ for $r > 0$. Once the optimization phase is complete, continuation techniques can be used to track the solution to optimality at $r = 0$. Further discussion of this homotopy can be found in the work of Poore and Al-Hassan (ref. 1).

Another homotopy can be based on the quadratic penalty-loss function

$$P(x,r) = f + (1/2r)\, \Sigma\, h_i^2(x) + (1/2r)\, \Sigma\, [g_j^-(x)]^2 \tag{4.4}$$

or more generally, the augmented Lagrangian function,

$$\begin{aligned} L_a(x,\nu,\hat{\lambda},\hat{\mu},\sigma,\phi,\delta,\beta,r) = \nu f &+ (1/2r)\, \Sigma\, \sigma_i(\gamma_i h_i(x) - r\sigma_i^{-1}\hat{\lambda}_i)^2 \\ &+ (1/2r)\, \Sigma\, \phi_j[(\beta_j g_j(x) - r\phi_j^{-1}\hat{\mu}_j)^-\,]^2 \end{aligned} \tag{4.5}$$

where $g_j^-(x) = \mathrm{Min}\ \{\ g_j(x),\ 0\ \}$, weights ν, σ_i and ϕ_j, shifts $\hat{\lambda}_i$ and $\hat{\mu}_j$, and scales γ_i and β_j have been introduced. These parameters can again be adaptively chosen during the optimization phase. At a minimizer of the augmented Lagrangian L_a

$$\begin{aligned} \nabla L_a = \nu\nabla f &+ (1/r)\, \Sigma\, \nabla(\gamma_i h_i)(\sigma_i\gamma_i h_i(x) - r\hat{\lambda}_i) \\ &+ (1/r)\, \Sigma\, \nabla(\beta_j g_j)[(\phi_j\beta_j g_j(x) - r\hat{\mu}_j)^-\,] = 0. \end{aligned} \tag{4.6}$$

The definitions $\lambda = -(S\Gamma h - r\hat{\lambda})/r$ and $\mu = -(\phi B g - r\hat{\mu})^-/r$ along with this equation yield the equivalent system

$$
(4.7)\qquad
\begin{array}{ll}
\nabla L = 0, & L = \nu f - (\Gamma h)^T\lambda - (Bg)^T\mu \\
\Gamma h + S^{-1}r(\lambda - \hat{\lambda}) = 0 & S = \mathrm{diag}(\sigma) \\
\beta_j g_j(x) + \phi_j^{-1} r(\mu_j - \hat{\mu}_j) = 0 & \text{if } \beta_j g_j(x) < \phi_j^{-1} r\hat{\mu}_j \\
\mu_j = 0 & \text{if } \beta_j g_j(x) \geq \phi_j^{-1} r\hat{\mu}_j
\end{array}
$$

where $S = \mathrm{diag}\ (\sigma)$ and $\Phi = \mathrm{diag}\ (\phi)$ represent the weights and $\Gamma = \mathrm{diag}\ (\gamma)$ and $B = \mathrm{diag}\ (\beta)$ the scales. The usual updates for the multipliers $\hat{\lambda}$ and $\hat{\mu}$ (refs. 2 and 3) can be used in the optimization phase. Note that the use of different scales, weights, and updated multiplier approximations all change the homotopy path, and thus may be used to generate "good" paths. Furthermore, the ill-conditioning present in the penalty method is no longer present in the homotopies generated from these penalty functions. A final important modification to these homotopies is the normalization of the mulitpliers (ref. 1) to prevent multipliers tending to infinity, which happens generically when the linear independence constraint qualification is violated.

5. Continuation Methods

The system of parameterized equations posed in the previous section can be written as $G(z,r) = 0$ where r is the homotopy parameter and is arranged so that it goes from $r_o > 0$ to 0. The primary objective of this section is to briefly describe the methodology of traversing the path from $r_o = r_o$ to optimality at $r = 0$. The idea is to generate a sequence of points $\{(z_i,r_i)\}_{i=o}^{n}$ with $r_o = r_o$ and $r_n = 0$. To get from (z_i,r_i) to (z_{i+1},r_{i+1}), one first predicts a new point (z^p_{i+1},r^p_{i+1}) near the curve and then corrects back to the curve to obtain the desired (z_{i+1},r_{i+1}). Prediction is based on extrapolation of current and previous information about the solution. The extrapolation via polynomial interpolation of the solution values has been used for some time, but extrapolation of the tangents to the curve as is used here appears to be numerically more robust and efficient. A brief explanation of this methodology is given in the remainder of this section, but a more comprehensive explanation can be found in the works of Keller (ref. 6) and Shampine and Gordon (ref. 7).

A formal differentiation of $G(z,r) = 0$ with respect to a third variable s yields Davidenko differential equation

$$D_zG\,\frac{dz}{ds} + D_r\,\frac{dr}{ds} = 0,$$

where s can be chosen to be arclength by adding the normalization

$$\left\| \frac{dz}{ds} \right\|^2 + \left| \frac{dr}{ds} \right|^2 - 1 = 0.$$

Once an orientation, ie $\frac{dr}{ds}$ is positive or negative, is known and if D_zG is nonsingular, then one can write this system as the differential equation

$$\frac{dw}{ds} = f(w).$$

Thus given a point (w_k,s_k) on the curve, the diffential equation can be integrated to obtain

$$w(s_k + \Delta s) = w_k + \int_{s_k}^{s_k + \Delta s} f(w)\, ds$$

where f(w) denotes the tangent to the curve at the point w(s). If a polynomial $P_{k,m}$ of degree at most m is used to interpolate f at (w_{k-j},s_{k-j}) for j = o,...,m, the predicted solution is taken to be

$$w^P_{k+1} = w_k + \Delta s\ D(\Delta s),\quad D(\Delta s) = \frac{1}{\Delta s} \int_{s_k}^{s_k + \Delta s} P_{k,m}(s)\ ds.$$

Given an error tolerance, once can vary the order of this formula to achieve the largest stepsize, Δs, possible. This method varies from the standard Adams–Bashforth technique in that the stepsize and order are varied at each step.

Once a predicted point is obtained the correction back to the curve can be obtained in several ways. Two popular ones are the vertical correction, wherein the system of equations G(z,r) = 0 is solved with r fixed at the predicted value, and the correction in a hyperplane orthogonal to the predictor direction. In this latter method one solves the augmented system of equations

$$\begin{aligned} G(w) &= 0 \\ N(w) &= 0 \end{aligned}$$

where $N(w) = D^T(w - w^P_{k+1})$ represents the plane orthogonal to the predictor direction and passing the predicted point w^P_{k+1} and w = (z,r).

6. Relation to Sequential Quadratic Programming

The predictor–corrector method of the previous section gives steps toward the optimal solution and is, in fact, asymptotic to those obtained by sequential quadratic programming. The continuation phase may thus be viewed as a method for globalizing Newton's method. To explain the connection between the continuation phase with these two homotopies and sequential quadratic programming, we confine our attention in this section to the the homotopy generated by the quadratic penalty–log barrier function, ie.

274

$$\begin{aligned} &\nabla L = 0, && L = \nu f - h^T\lambda - g^T\mu \\ &h + r\lambda = 0 && \\ &Mg - re = 0 && M = \mathrm{diag}(\mu). \end{aligned}$$

The result is that a Newton step as defined from the solution of (3.2) is asymptotic to a vertical correction plus an Euler prediction as r tends to 0. More precisely, if $\Delta = (\Delta x, \Delta\lambda, \Delta\mu)$ denotes the Newton step as defined by the quadratic programming subproblems (3.2), $\Delta_1 = (\Delta x_1, \Delta\lambda_1, \Delta\mu_1)$, the Euler predictor or tangent to the curve with $\Delta r = -r$, and $\Delta_2 = (\Delta x_2, \Delta\lambda_2, \Delta\mu_2)$ the vertical correction with $\Delta r = 0$, then

$$\Delta = \Delta_1 + \Delta_2 + O(r\|\Delta\lambda_2\|, \|\Delta\|^2) \text{ as } r \to 0 \text{ and } \Delta \to 0.$$

A similar result applies for the quadratic penalty–loss function with the slight modification

$$\Delta = \Delta_1 + \Delta_2 + O(r\|\Delta\lambda_2,\Delta\mu_2\|) \text{ as } r \to 0.$$

This suggests that as soon as the predicted value reaches $r = 0$, one could just as effectively switch to sequential quadratic programming without a globalizer.

7. Numerical Examples

In this section we consider two approaches to constrained optimization based on the quadratic penalty–log barrier function and the augmented Lagrangian or shifted quadratic penalty–quadratic loss function. For the former we have previously compared the numerics and briefly summarize some of their properties (ref. 1). For the augmented Lagrangian approach we present some of our recent testing on some nontrivial test problems (ref. 5) to demonstrate the robustness, efficiency, and potential for the methodology.

For the quadratic penalty–log barrier function we first use the loss function $(g^-)^T g^-$ to generate a point $\hat{x}$ at which $g(\hat{x}) > 0$ or is at least close to feasible region $\{\ x : g(x) \geq 0\ \}$ and then define a δ so that $g(\hat{x}) + \delta > 0$. Then we use a quasi–Newton with a BFGS update to minimize the penalty function P function $P(x,r) = f(x) + h^T(x)h(x)/(2r) - r\Sigma \ln(g_i(x) + r\delta_i/r^o)$ at some value of the penalty parameter, say r_o, at which the problem is reasonably well conditioned. A quadratic–cubic line search and a Armijo stopping criterion (ref. 8), modified to maintain feasibility $(g(x) + \delta > 0)$ has been used to globalize the quasi–Newton method. Once the minimization problem is solved, continuation techniques are used to track the solution to optimality at $r = 0$. The initial value of $r_o = .1$ has been used in the numerical experiments reported in the table below under the heading PENCON, but scaling has not been used. Additional information can be found in (ref. 1).

For the quadratic penalty–loss function, scaling and adaptive choices of the weights and scales have been used. For this penalty function, one does not need an initial feasible point for the inequality constraints. Again the BFGS update has been used, but the line search has been modeled after that of Fletcher (ref. 2).

To get some estimation of the relative performance of this algorithm, we have solved several test problems from the book by W. Hock and K. Schittkowski (ref. 5) and give a comparative summary of the number of function evaluations in the table below. The function evaluation for the codes other than PENCON and LOSSCON are taken from (ref. 5). Consistent with those function evaluation counts, we count the evaluation of a p dimensional vector as p function evaluations; however, we do not count upper and lower bounds on variable since they are handled directly in the code and gradient evaluations of linear constraints are counted only once. The approximation of the Hessian of the Lagrangian in the continuation phase is based on finite differences (ref. 8).

CODE	**AUTHOR**	**METHOD**
VF02AD	Powell	Quadratic Approximation
OPRQP	Bartholomew–Biggs	Quadratic Approximation
GRGA	Abadie	Generalized Reduced Gradient
VF01A	Fletcher	Multiplier
FUNMIN	Kraft	Multiplier
FMIN	Kraft, Lootsma	Penalty
PENCON	Al–Hassan, Poore	Penalty–Continuation
LOSSCON	Lundberg, Poore, Yang	Loss Function–Continuation

CODE: PROB. NO.	**VF02AD**	**OPRQP**	**GRGA**	**VF01A**	**FUNMIN**	**FMIN**	**PENCON**	**LOSSCON**
5	16	16	86	32	38	200	26	16
10	48	126	678	280	554	687	88	63
12	48	132	277	300	492	306	130	68
13	180	300	192	565	928	4,178	269	209
14	36	126	108	192	726	838	107	91
15	30	165	508	377	496	2,464		113
19	78	1,785	314	838	3,339	661	423	304
20	160	200	102	383	728	4,094	282	104
29	52	206	646	421	482	414	155	162
118	**	1,800	3,857	**	**	**	2,804	

FUNCTION EVALUATION COUNT **indicates failure

Comparisons from this table illustrate that these penalty–continuation algorithms currently come in second and occasionally first and third; however, the methodology is quite robust, primarily because of the robustness of penalty paths leading to optimality and the robustness of the continuation methodology. The answers given by PENCON and LOSSCON have approximately twelve digits of accuracy on a 14+ digit CDC machine, whereas the remaining answers listed above are computed on a

10 digit machine (ref. 5) and those for VF02AD are generally to low accuracy. Furthermore, the quadratic penalty–loss function tends to perform a little better than the quadratic penalty – log barrier function with the current implementations. Scaling yields a significant improvement in some problems by reducing the number of function evaluations required in the unconstrained optimization phase and can reduce the number of steps taken in the continuation phase. The use of multiplier updates can also significantly reduce the length of the homotopy path but currently requires more function evaluations due to the reoptimization required after an update. These updates, however, may be useful for the large scale problems.

8. Summary and Conclusion

One of the objectives in this work has been to examine homotopy methods generated by three smooth penalty functions, the quadratic penalty for equality constraints and the log barrier and quadratic loss function for inequality constraints, and their modern counterparts, augmented Lagrangian or multiplier methods. We have shown that these methods are asymptotic to sequential quadratic programming and are competitive with these methods. However, considerable work will be required on large scale problems to assess their full potential.

The robustness and efficiency of this class of algorithms based on these smooth penalty functions, augmented Lagrangians, the derived homotopy, and predictor–corrector continuation techniques have been illustrated in Section 7. The methodology shows considerable promise and potential for solving constrained optimization problems; however, as with any method a word of caution is appropriate. One can construct simple examples illustrating the following situations for penalty paths: given $\epsilon > 0$ a penalty path may exist only for the penalty parameter $r \geq \epsilon$ or only for $r \leq \epsilon$, may not exist at all, may diverge, or may exist for $r > 0$ but the limit point at $r = 0$ is not a local minimum of the original problem. (When this last situation occurs, the Karush–Kuhn–Tucker equations have a singularity.) In spite of these examples penalty path following is a mathematically robust method of solving constrained optimization problems as is illustrated by the examples in Hock and Schittkowski (ref. 5), and these homotopy methods appear to make them efficient and a competitive alternative to the early stages of sequential quadratic programming.

REFERENCES

1. Poore, A.B., and Q. Al-Hassan, "The expanded Lagrangian system for constrained optimization problems", SIAM J. Control and Optimization, 2 (1988), 417–427.

2. Fletcher, R., Practical Methods of Optimization, Second Edition, John Wiley & Sons, Ltd., New York, 1987.

3. Stoer, J., "Principles of Sequential Quadratic Programming for Solving Nonlinear Programs", in: K. Schittkowski, ed., Computational Mathematical Programming, NATO ASI Series, Vol. F15, Springer-Verlag, Heidelberg, 1985.

4. Poore, A. B. and C. A. Tiahrt, "Bifurcation problems in nonlinear parametric programming", Mathematical Programming 39 (1987) 189–205.

5. Hock, W. and Schittkowski, K., Test Examples for Nonlinear Programming Code, Springer-Verlag, New York, 1981.

6. Keller, H. B., "Numerical solution of bifurcation and nonlinear eigenvalue problems", in P. Rabinowitz, ed., Applications of Bifurcation Theory, Academic Press, New York, pp. 359–384, 1977.

7. Shampine, L. F. and Gordon, M. K., Computer Solution of Ordinary Differential Equations: The Initial Value Problem, W. H. Freeman and Co., San Francisco, 1975.

8. Dennis, J. E. and Schnabel, R. B., Numerical Methods for Unconstrained Optimization and Nonlinear Equations, Prentice-Hall, Englewood Cliffs, NJ, 1983.

SESSION 13: SOFTWARE II

Chairmen: R. A. Canfield and J. L. Rogers, Jr.

A LARGE SCALE SOFTWARE SYSTEM FOR SIMULATION AND DESIGN OPTIMIZATION OF MECHANICAL SYSTEMS

Bernhard Dopker
and
Edward J. Haug
Center for Simulation and Design Optimization
and
Department of Mechanical Engineering
College of Engineering
The University of Iowa

INTRODUCTION

While the individual technologies of computers, computer graphics, and computational mechanics are well developed, these technologies have not yet been adequately exploited in support of mechanical system simulation and design optimization. Utilization of advanced computational tools by sophisticated development teams in the aerospace industry has demonstrated their potential, but they have not yet been brought to bear in mechanical system design environments, such as military vehicles. Mechanical design teams that currently fabricate and test prototypes should be able to carry out high resolution computer simulations long before committing to hardware. To meet this need and realize enormous cost and time savings, advanced methods and software must be developed and integrated to fully utilize emerging supercomputer and parallel processor architecture, computer graphics for communication, and data transfer between advanced large scale analysis programs.

Major developments have occurred in specialized analysis software, such as finite element structural analysis codes, kinematic and dynamic analysis codes, and control simulation codes. While vendors of CAD and CAE systems are beginning to include support for some specialized analysis software, the potential that exists for large scale interdisciplinary simulation and design optimization support to mechanical system design is virtually untapped. Significant research is contributing to disciplines that are required to meet the needs of mechanical system simulation and design optimization. Unfortunately, most of the research is being carried out by specialists with little or no communication among related disciplines. A simulation and design optimization software system is needed to accelerate interdisciplinary research and development (ref. 1).

CURRENT SIMULATION AIDS TO DESIGN

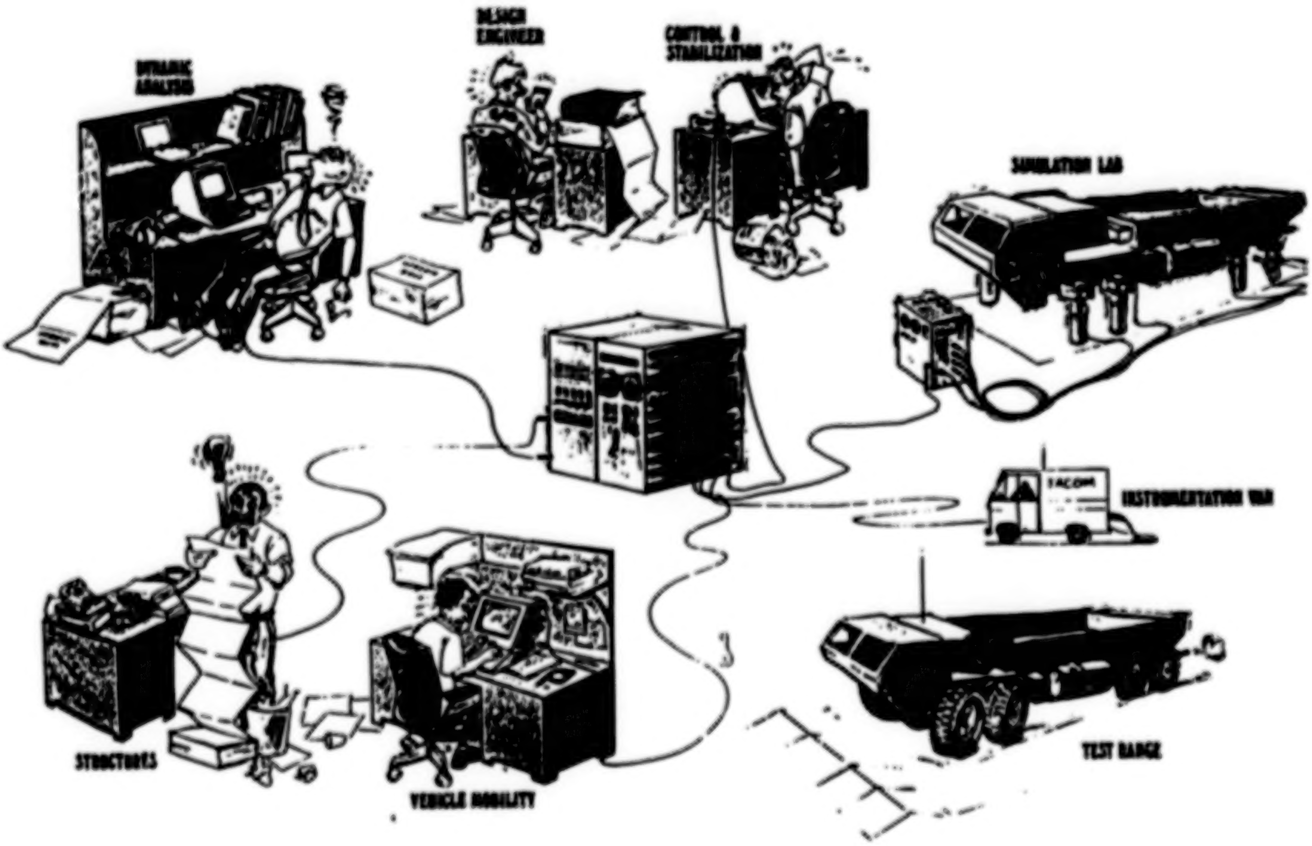

BEST COPY AVAILABLE

A SOFTWARE TEST BED

An NSF* Industry/University Cooperative Research Center was formed in 1987 to develop advanced mechanical system simulation methods and to implement them into a national research software system. An integrated software system for simulation and design optimization, including software such as finite element codes, kinematics and dynamics codes, control simulation codes, graphics based CAD/CAE codes, and design sensitivity analysis and optimization codes is being implemented. Emerging computer architectures, simulation methods, and data base management systems are being utilized. The goal is integration of discipline oriented software into a data base and command language system that permits research and development teams to carry out their work in an interdisciplinary environment.

This integrated software environment will, by necessity, be based on an underlying computational environment that consists of a network of heterogeneous computing elements. These may include personal computers, workstations, mainframe systems, parallel processors, supercomputers, and a variety of specialized servers for support of data base, graphics, and artificial intelligence activities. Thus, the software support system must be capable of supporting the integration of applications that consist of pieces running on different hardware platforms and under different operating system interfaces. This integration should be compatible with emerging standards for network computing (refs. 2, 3, and 4).

A National Software System For Mechanical System Simulation And Design Optimization

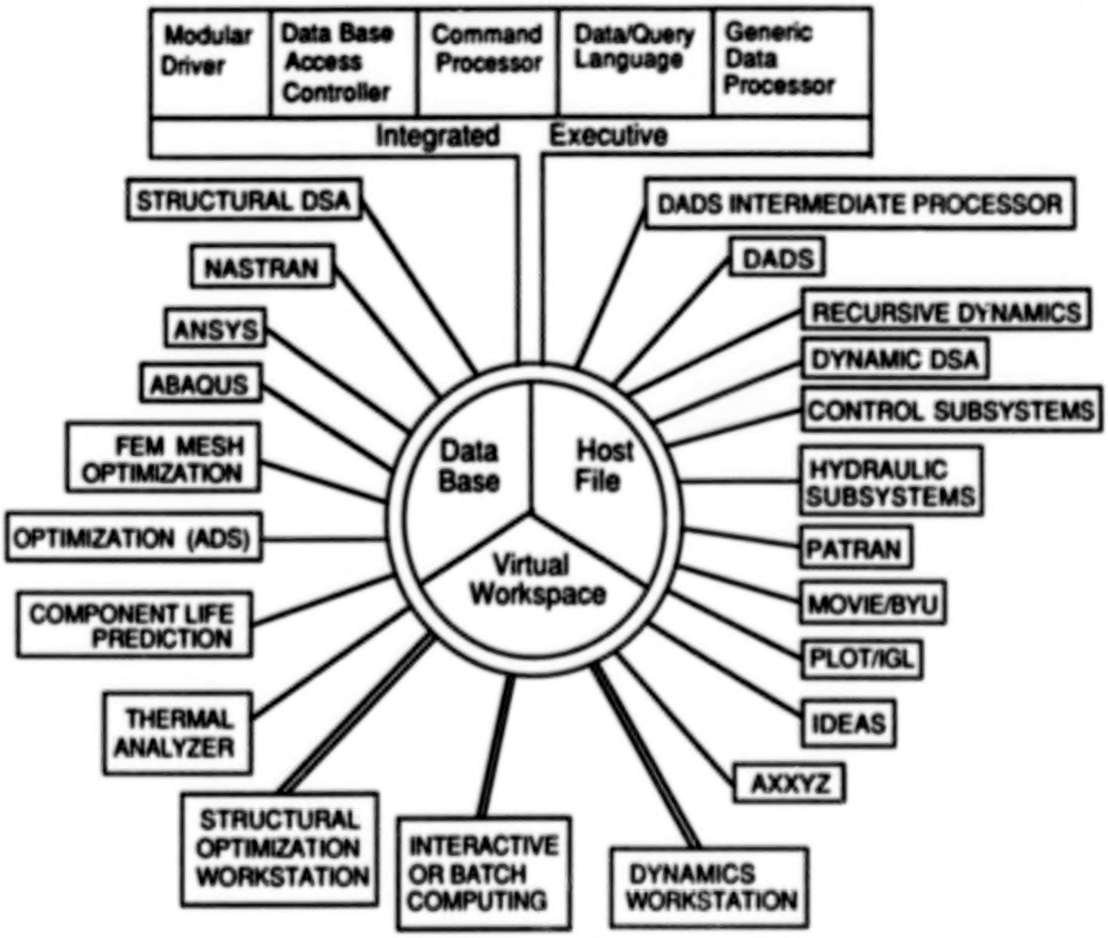
Modular Driver
Data Base Access Controller
Command Processor
Data/Query Language
Generic Data Processor
Integrated Executive
STRUCTURAL DSA
NASTRAN
ANSYS
ABAQUS
FEM MESH OPTIMIZATION
OPTIMIZATION (ADS)
COMPONENT LIFE PREDICTION
THERMAL ANALYZER
STRUCTURAL OPTIMIZATION WORKSTATION
INTERACTIVE OR BATCH COMPUTING
DYNAMICS WORKSTATION
AXXYZ
IDEAS
PLOT/IGL
MOVIE/BYU
PATRAN
HYDRAULIC SUBSYSTEMS
CONTROL SUBSYSTEMS
DYNAMIC DSA
RECURSIVE DYNAMICS
DADS
DADS INTERMEDIATE PROCESSOR
Data Base
Host File
Virtual Workspace

---

*National Science Foundation

THE INTEGRATED ANALYSIS CAPABILITY

As the basis for integrating the application codes, the Integrated Analysis Capability (IAC) developed by Boeing for NASA/Goddard, the SDI Office, and the Air Force is utilized (refs. 5 and 6). The objective of the IAC has been to provide a highly effective, interactive analysis tool for integrated, interdisciplinary analysis and design of large structures. Having the engineer-in-the-loop was an important design consideration. Emphasis has been placed on the capability to integrate new application programs into a uniform framework. The IAC has been focused on the technical disciplines of structures (both statics and dynamics), controls and thermodynamics. The Analysis Capability Executive (ACE) module, shown at the top of the figure, relies on the same set of standard IAC utilities that are documented and available for use by all modules in the system.

ACE contains a general driver code to execute other application modules; an input command processor that handles language syntax, prompting, help information, etc.; an extensive data/query management capability that allows the user to create, manipulate, and evaluate various types of data; and a generic data processor that allows the interface between the IAC and "foreign" module character formatted data. ACE is independent from any requirements of a particular application module. Multiple concurrent users may interface with IAC to perform both interactive and batch tasks.

The data base utilized by the IAC consists of three parts: (1) the IAC structured data base that allows for storage of data files in a structured form and provides some mathematical operations such as matrix additions and spreadsheet computations; (2) the IAC virtual workspace that allows storage of structured data temporarily and allows the same mathematical operations as on the IAC structured data base; and (3) the host directory of the computer operating system.

The IAC Database and Command Processor

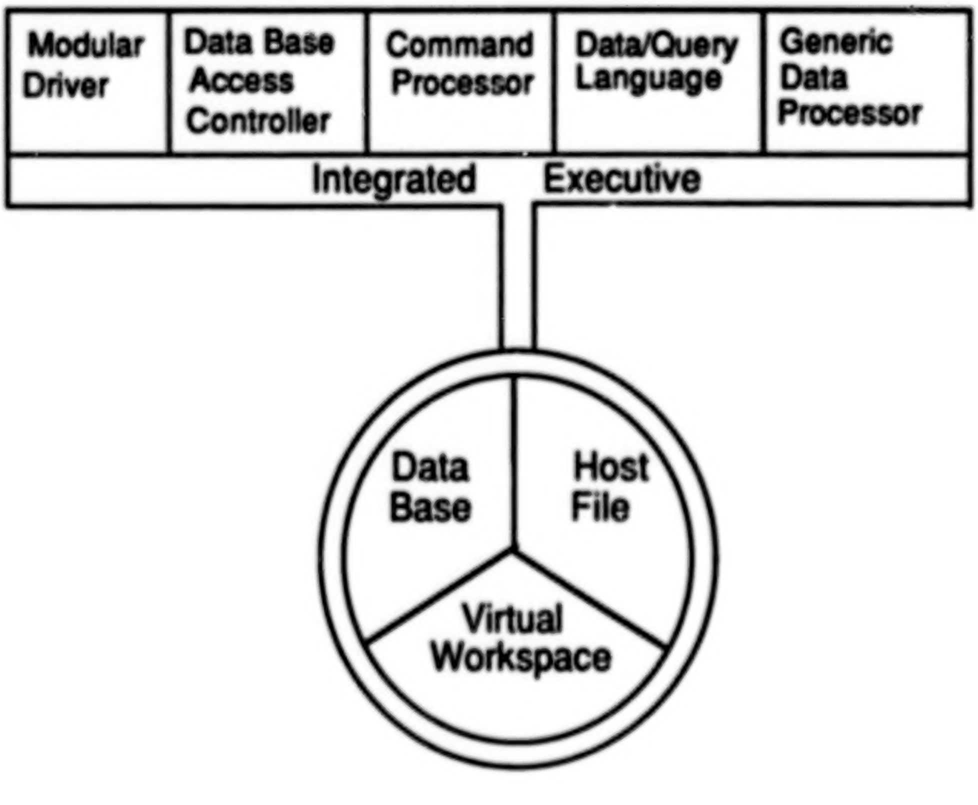

TOP DOWN DATA BASE DESIGN

The main criteria for developing the data base was to provide sufficient flexibility for extensions that may be required for later developments. To achieve this goal, an object oriented design methodology that is based on the object modeling technique was used to develop the data base (ref. 7). In an object oriented system, the external specifications are clearly separated from the internal implementation. A set of data and operations is associated with each object and related objects are grouped to facilitate reuse for similar code. A hierarchical organization of objects allows for top down design and utilization of the data base. That is, after the data associated with the highest level object is obtained, analysis codes that utilize these data may be executed, which in turn may create data associated with lower level objects.

As an example consider the figure below in which the data base for a vehicle is outlined. The highest object is the vehicle itself, which is an aggregation of the suspension subsystems, the frame, the steering mechanism, and many other objects. Even initial data associated with this object level hierarchy is sufficient for a crude system simulation, based on a rigid body dynamics model. If a more precise system simulation is required, the objects must be refined. For example, if the flexibility of a component must be considered, the object must again be refined. Now each object consists of subobjects for geometry data, dynamic data, and manufacturing data.

APPLICABILITY OF ANALYSIS TOOLS IN TOP DOWN DESIGN

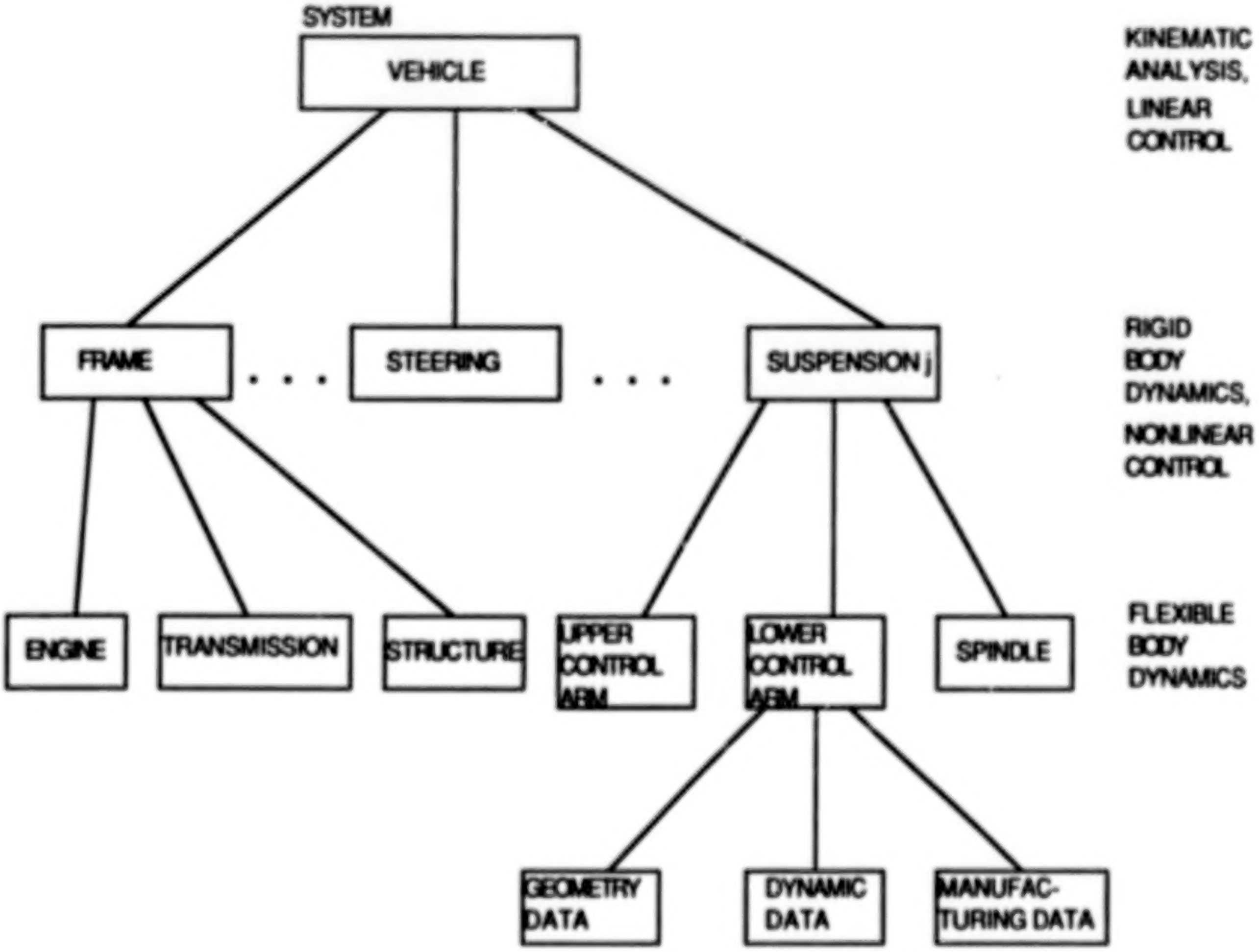
SYSTEM
VEHICLE
KINEMATIC ANALYSIS, LINEAR CONTROL
FRAME
. . .
STEERING
. . .
SUSPENSION j
RIGID BODY DYNAMICS, NONLINEAR CONTROL
ENGINE
TRANSMISSION
STRUCTURE
UPPER CONTROL ARM
LOWER CONTROL ARM
SPINDLE
FLEXIBLE BODY DYNAMICS
GEOMETRY DATA
DYNAMIC DATA
MANUFACTURING DATA

THE NETWORKING ENVIRONMENT

The analysis and design optimization system will be developed to handle local data bases that will assist designers in evaluating trial designs. Local area networks are being used to connect workstations, parallel computer(s), supercomputers, and other hardware, so computational tasks can be effectively distributed. Emerging tools such as user transparent distributed processing on workstation networks is being exploited.

The underlying software for such a network is (1) the Network File System (NFS) (ref. 2) that allows file access over a network of heterogeneous computers; (2) the Network Computing System (NCS) (ref. 3) that allows for distributed remote procedure calls; and (3) the X-Window system that allows creating windows and controls window management remotely (ref. 4).

A computer network is often composed of three components: a compute server, a data base server, and a user interface server. In the figure, the network environment at the Center for Simulation and Design Optimization at the University of Iowa is shown. As the computational server that will execute compute intensive tasks, such as finite element analysis or system dynamic simulation, the ALLIANT FX/8 and the ENCORE MULTIMAX are being used. As the data base server for long term data base storage, the VAX 11/780 is now being utilized. All user interface, modeling, and evaluation tools will be executed on a network of APOLLO workstations. For high performance graphics and real time animation, an IRIS 4D is being utilized.

I/UCRC COMPUTING ENVIRONMENT

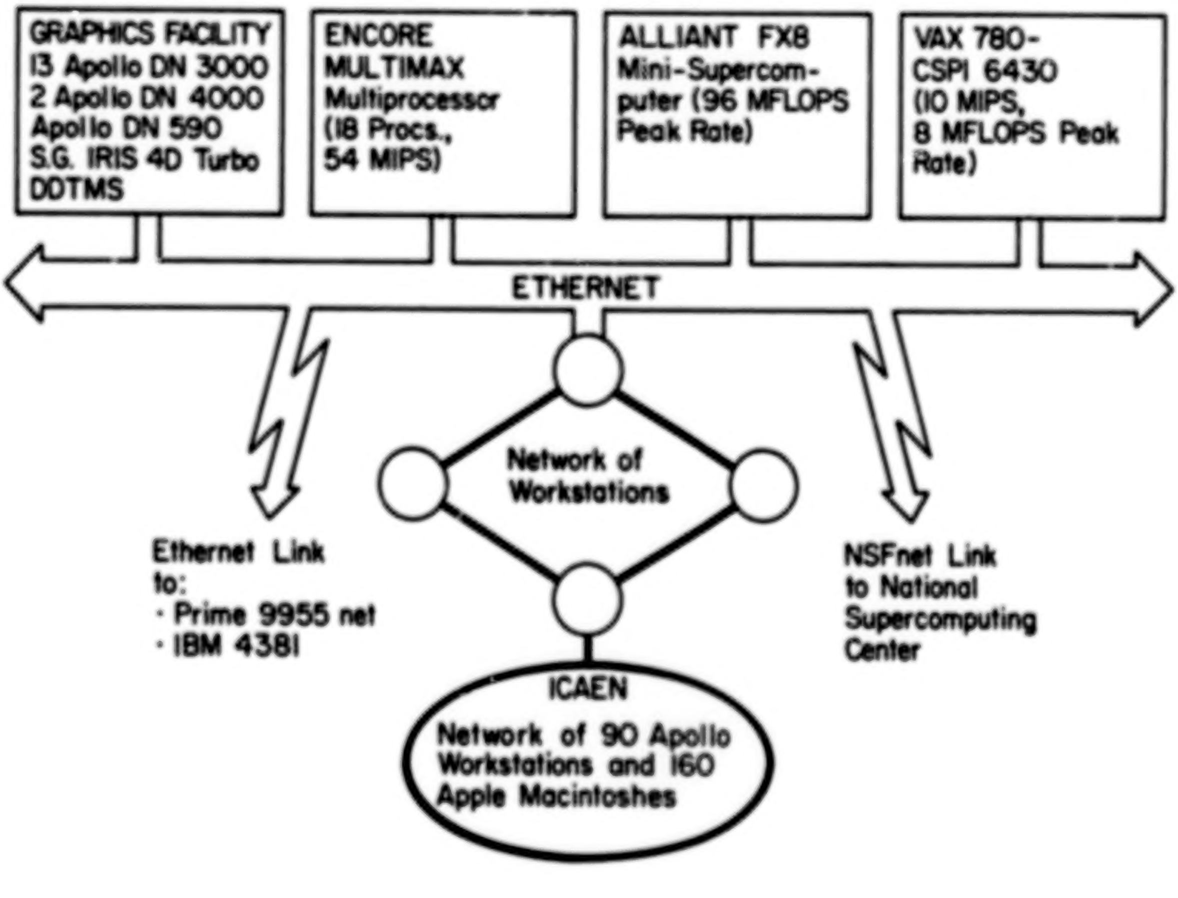
GRAPHICS FACILITY
13 Apollo DN 3000
2 Apollo DN 4000
Apollo DN 590
S.G. IRIS 4D Turbo
DDTMS
ENCORE
MULTIMAX
Multiprocessor
(18 Procs.,
54 MIPS)
ALLIANT FX8
Mini-Supercomputer (96 MFLOPS
Peak Rate)
VAX 780-
CSPI 6430
(10 MIPS,
8 MFLOPS Peak
Rate)
ETHERNET
Network of
Workstations
Ethernet Link
to:
· Prime 9955 net
· IBM 4381
NSFnet Link
to National
Supercomputing
Center
ICAEN
Network of 90 Apollo
Workstations and 160
Apple Macintoshes

RUN STREAMS

The term "run streams" refers to a standard or user defined sequence of IAC provided operations. A run stream is often designed to handle a class of problems that consists of a number of selectable options and variations, rather than a rigidly predefined and automated process. An engineer-in-the-loop mode of operation is therefore possible and encouraged.

The figure illustrates several standard run streams that have been defined to provide structural/system dynamics/controls/optimization capabilities. Besides the standalone (uncoupled) operation of each technology or major technical module, only the stress history and fatigue analysis run stream has been implemented. The other implementations are under development.

The IAC facilitates the flow of data between different modules or between a module and the user, by providing a central data base storage area, standard data structures and formats such as relations and arrays, and data management tools. Multi-user concurrent access to the data base is supported. The IAC allows cataloging of structured and unstructured data base files and, with each data structured catalog entry, textual information such as keywords and data titles and pointers to text files can be defined.

(I) LIFE PREDICTION RUN STREAM

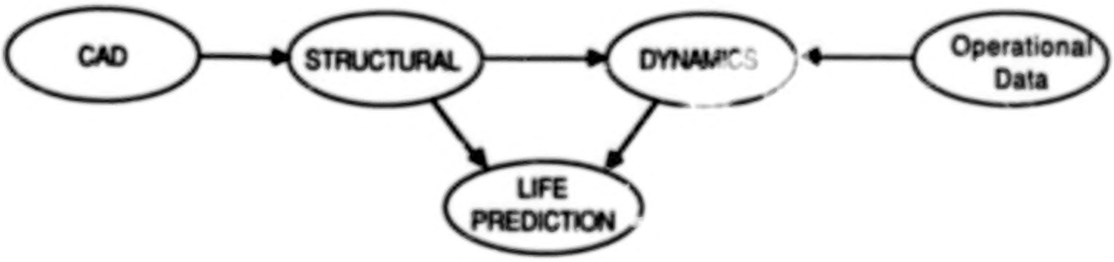
CAD
STRUCTURAL
DYNAMICS
Operational Data
LIFE PREDICTION

(II) STRUCTURAL OPTIMIZATION RUN STREAM

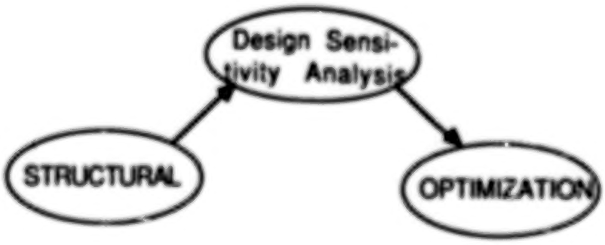
Design Sensitivity Analysis
STRUCTURAL
OPTIMIZATION

(III) CONTROL RUN STREAM

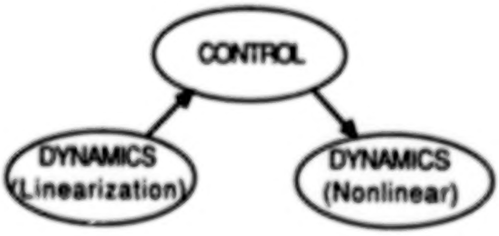
CONTROL
DYNAMICS (Linearization)
DYNAMICS (Nonlinear)

THE GRAPHICAL USER INTERFACE

A challenge for the analysis and design optimization system is to develop user interfaces that help the journeyman engineer take advantage of the network system (refs. 8 and 9). That is, the network system can be used by nonspecialist project engineers and will be flexible enough to fully exploit the network computing system (refs. 10 and 11). The overall integrated networked simulation and design optimization system will be set up in such a way that the experienced user can take full advantage of networks, whereas the inexperienced user need only know the concept and will employ a user friendly interface and support system to guide him through his applications.

The user interface is a multi-windowing system that executes on a workstation, where a variety of options will be laid out in a menu system and selections can be chosen by a mouse. The user interface menus are based on a user interface command language that (1) activates simulation, modeling, and evaluation tools and (2) provides numerical and graphical access to the data base.

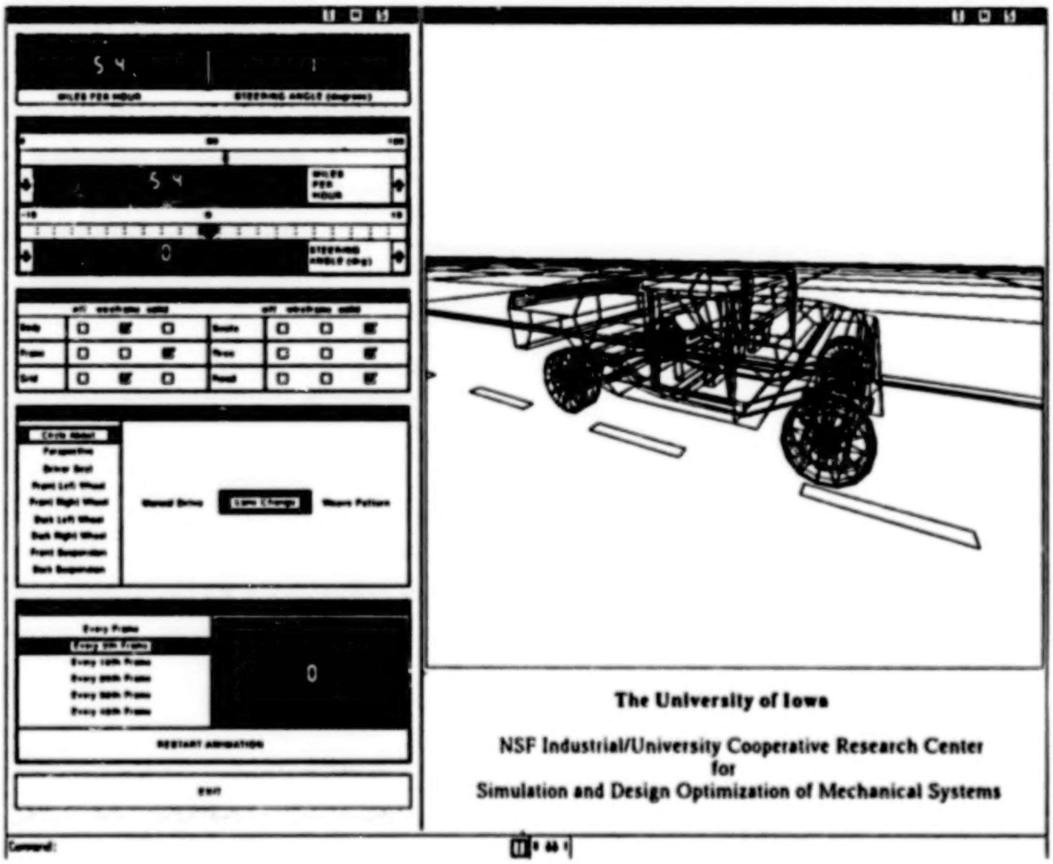

The University of Iowa

NSF Industrial/University Cooperative Research Center
for
Simulation and Design Optimization of Mechanical Systems

BEST COPY AVAILABLE

287

THE FUNCTIONALITY OF THE LIFE PREDICTION RUN STREAM

The data flow for computation of mechanical system component loads, stress histories, and fatigue life prediction is shown in the figure. The method is based on a coupled gross motion-flexible body dynamic simulation model, as described in refs. 12, 13, and 14.

Each individual component that is represented as a flexible body in the mechanical system must be identified. Either vibration mode or vibration modes combined with static correction modes are computed, using the finite element method, to represent the flexibility in the individual system components. Flexibility data preprocessing prepares the output data to be used in the dynamic simulation. A combination of rigid and flexible components may be used in the dynamic simulation of the mechanical system. Large displacements occur between points on different components, but linear elastic theory is adequate to describe the deformation of individual components. The dynamic simulation computes the loads on the individual components and the contribution of each deformation field on the total deformation of the system at each time step. After the stress fields associated with the individual vibration and static correction modes has been computed, they can be superposed according the contribution each deformation field had in the flexible deformation of the bodies in the dynamic simulation. This will provide a stress history that then may be used to predict the fatigue life of individual components. The data input and output for each individual component is defined in the figure.

Dynamic Stress and Fatigue Analysis Computation

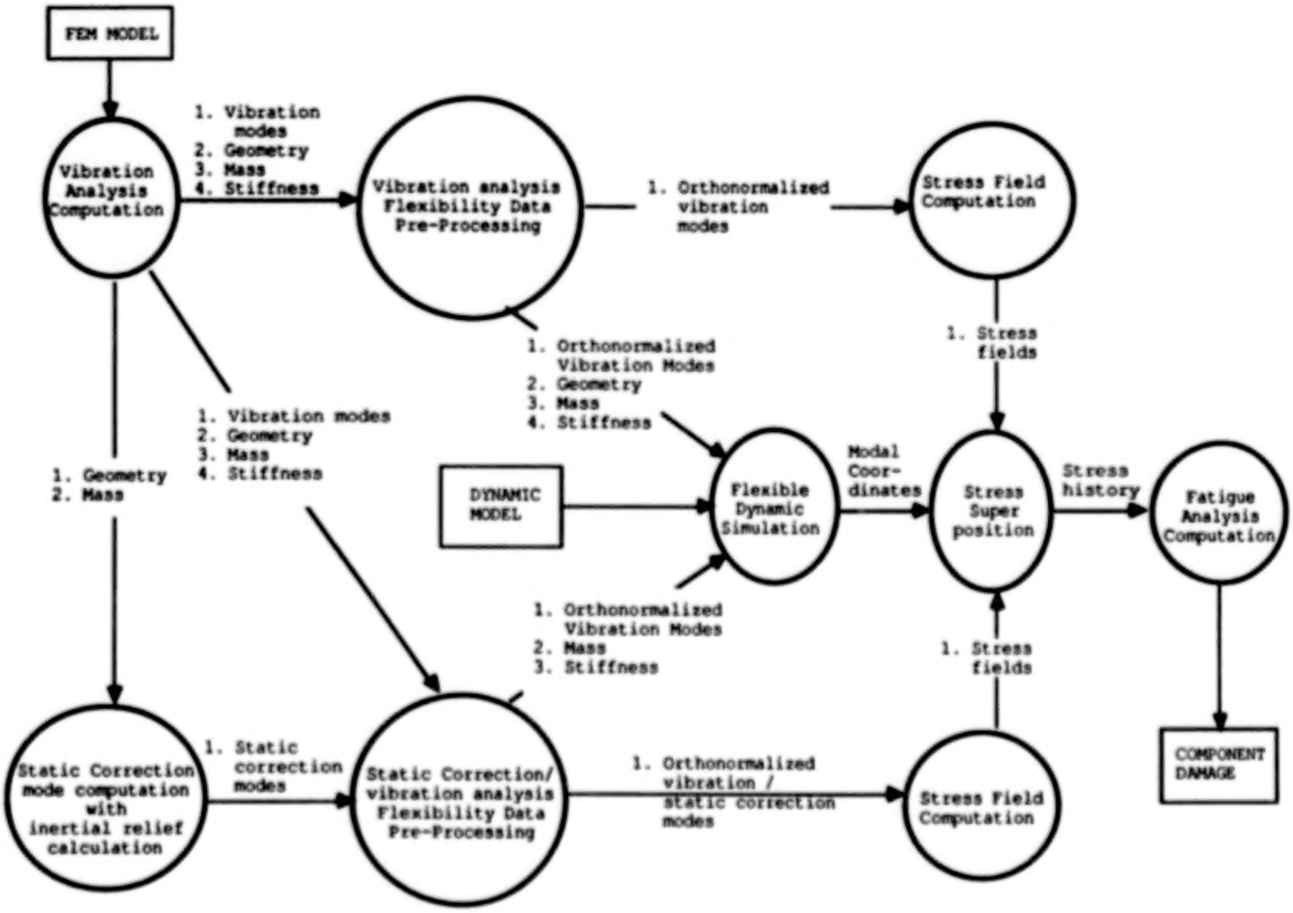
FEM MODEL
Vibration Analysis Computation
1. Vibration modes
2. Geometry
3. Mass
4. Stiffness
Vibration analysis Flexibility Data Pre-Processing
1. Orthonormalized vibration modes
Stress Field Computation
1. Stress fields
1. Orthonormalized Vibration Modes
2. Geometry
3. Mass
4. Stiffness
1. Vibration modes
2. Geometry
3. Mass
4. Stiffness
1. Geometry
2. Mass
DYNAMIC MODEL
Flexible Dynamic Simulation
Modal Coor-dinates
Stress Super position
Stress history
Fatigue Analysis Computation
1. Orthonormalized Vibration Modes
2. Mass
3. Stiffness
1. Stress fields
Static Correction mode computation with inertial relief calculation
1. Static correction modes
Static Correction/ vibration analysis Flexibility Data Pre-Processing
1. Orthonormalized vibration / static correction modes
Stress Field Computation
COMPONENT DAMAGE

THE IMPLEMENTATION OF THE LIFE PREDICTION RUN STREAM

Based on the data flow described above, a run stream for the computation of stress history and fatigue life of mechanical systems is shown in the figure. For vibration and static correction mode computation, the ANSYS finite element code was used. Relevant data from the ANSYS output file are written to the IAC data base. Data needed from ANSYS for the intermediate processor are read directly from the ANSYS output files. The output from the intermediate processor is written to the IAC data base. For the dynamic simulation function, the DADS code was utilized. Because DADS is a code in which only the executable is available, all data to and from the data base to the code must go through interface codes. One separate code was written and implemented in the IAC for (1) computing stress fields for a given displacement field, (2) computing stress field superposition, and (3) fatigue analysis. Because these codes were written by the Center, communication between the codes and the IAC data base was direct and no interface codes were needed.

PROGRAM ORGANIZATION

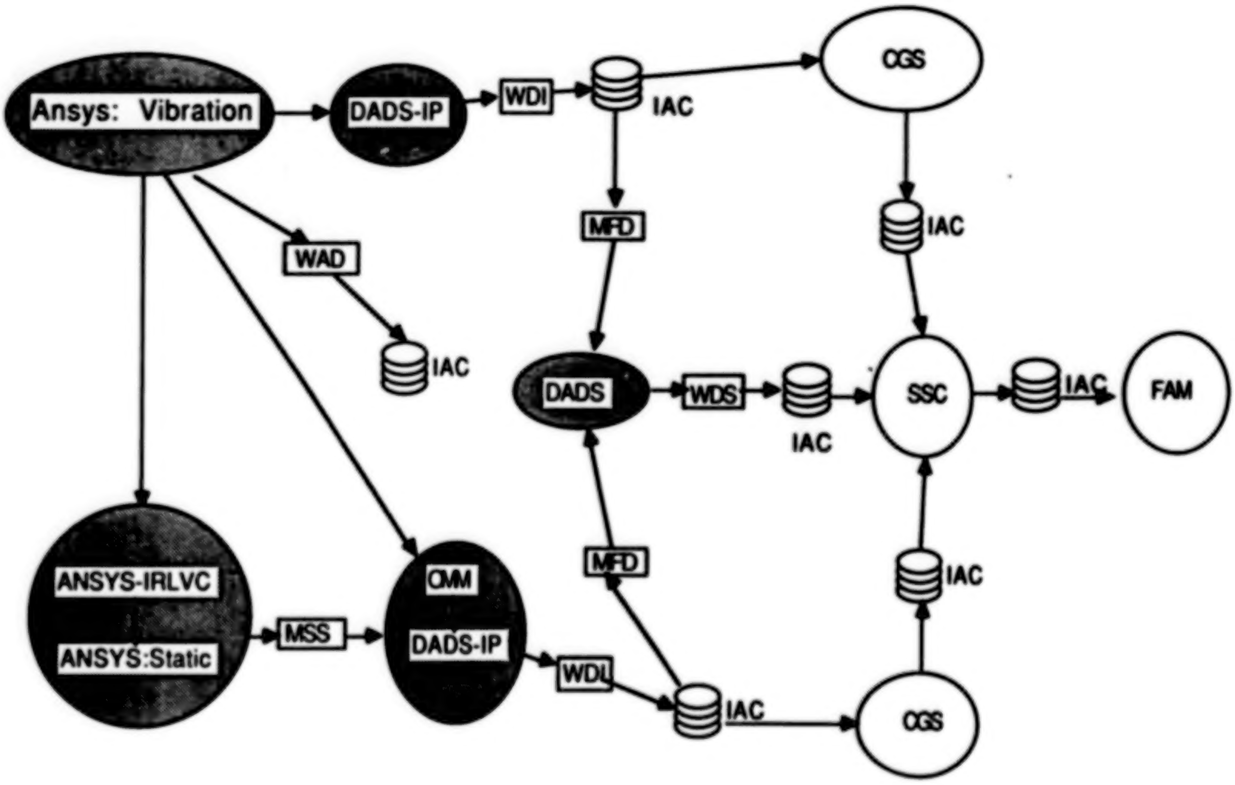
Ansys: Vibration
DADS-IP
WDI
IAC
CGS
MFD
IAC
WAD
IAC
DADS
WDS
IAC
SSC
IAC
FAM
ANSYS-IRLVC
ANSYS:Static
MSS
CMM
DADS-IP
WDL
MFD
IAC
IAC
CGS

THE HMMWV

The High Mobility Multipurpose Wheeled Vehicle (HMMWV) is used to demonstrate the applicability of the integrated, interdisciplinary system. It is 4.57 meters in length, 2.16 meters in width, and 1.76 meters in height and has a mass of 2340 kg. Bodies included in the dynamic model are the frame (including the nonstructural engine, transmission, and cab masses), control arms, and wheel assemblies. The HMMWV has four double-A-arm suspensions, each with two control arms and a wheel assembly. Hence, there are a total of thirteen bodies in the spatial model. Two spherical joints connect each control arm to beam elements that are attached to the chassis to represent bushing effects. Each control arm and the associated wheel assembly is connected by a spherical joint. In addition, there are distance constraints between each wheel assembly and the chassis, both in the front and in the rear, to represent steering tie rods.

The flexibility of the chassis is represented using 10 vibration modes. Flexible body simulations are performed with the vehicle traversing obstacles and rough terrains to account for use of the vehicle. Loads induced by ground roughness are transmitted through the tires and suspension subsystem to the chassis. A spatial dynamic simulation of the vehicle over multiple ground profiles is carried out using the DADS code to determine the deformation of the frame at each time step.

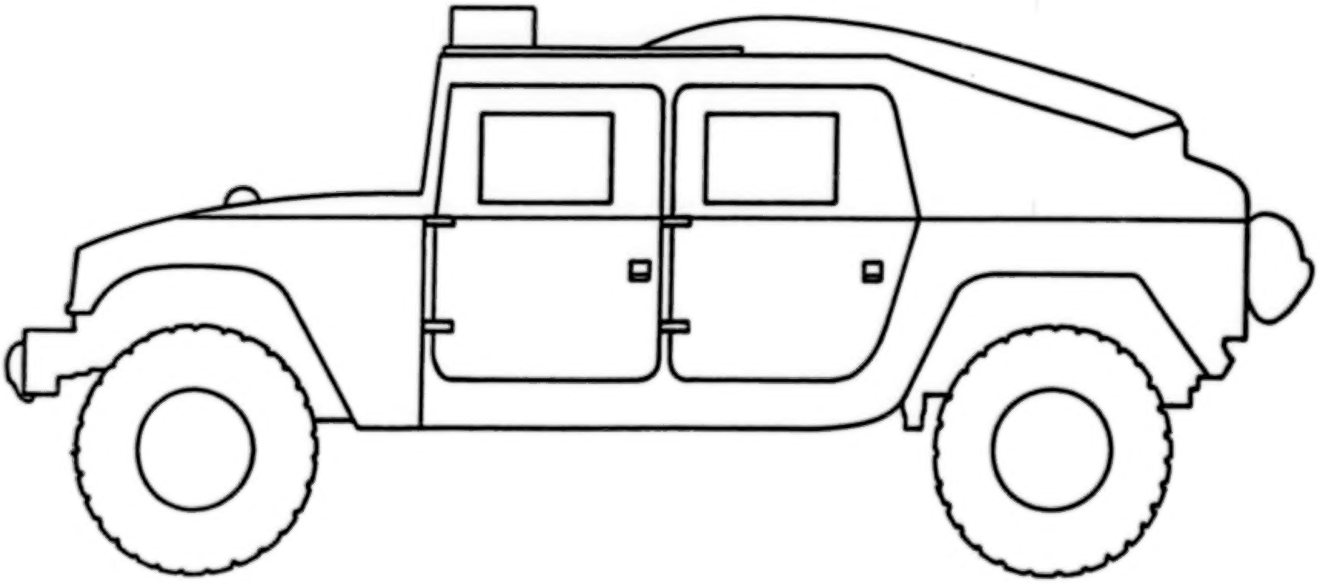

MODE ANALYSIS

The vehicle model consists of a frame and nonstructural masses. As illustrated below, the frame of the vehicle is comprised of two side rails, four suspension crossmembers, one transmission crossmember, two bumpers, and two braces. Nonstructural masses are attached to the frame to account for the engine-transmission and the cab. The engine-transmission is supported by three beams, to account for inertia loads that act on the frame, due to acceleration of the engine-transmission. Similarly, the cab is attached to the frame by six body mounts that are represented as beams.

The ANSYS finite element analysis program is employed for stress analysis. The generalized mass element in ANSYS is used to represent masses and inertias of the engine-transmission and the cab. The generalized mass element has three translational and three rotational degrees of freedom. Masses and rotary inertias are thus specified at nodal points that correspond to centers of mass of nonstructural masses. Beam-truss elements, with six degrees of freedom per node (Element types 4 and 44 in ANSYS), are used for modeling the side rails, crossmembers, bumpers, and braces. Material property data for AISI C1020 steel is input. A finite model of the frame with 56 elements, 49 nodes, and 294 degrees of freedom is adequate for this elementary structural model. Both the theoretical foundation and the implementation do not place any limitation on the model dimension. A refined FEM model of the frame is shown below.

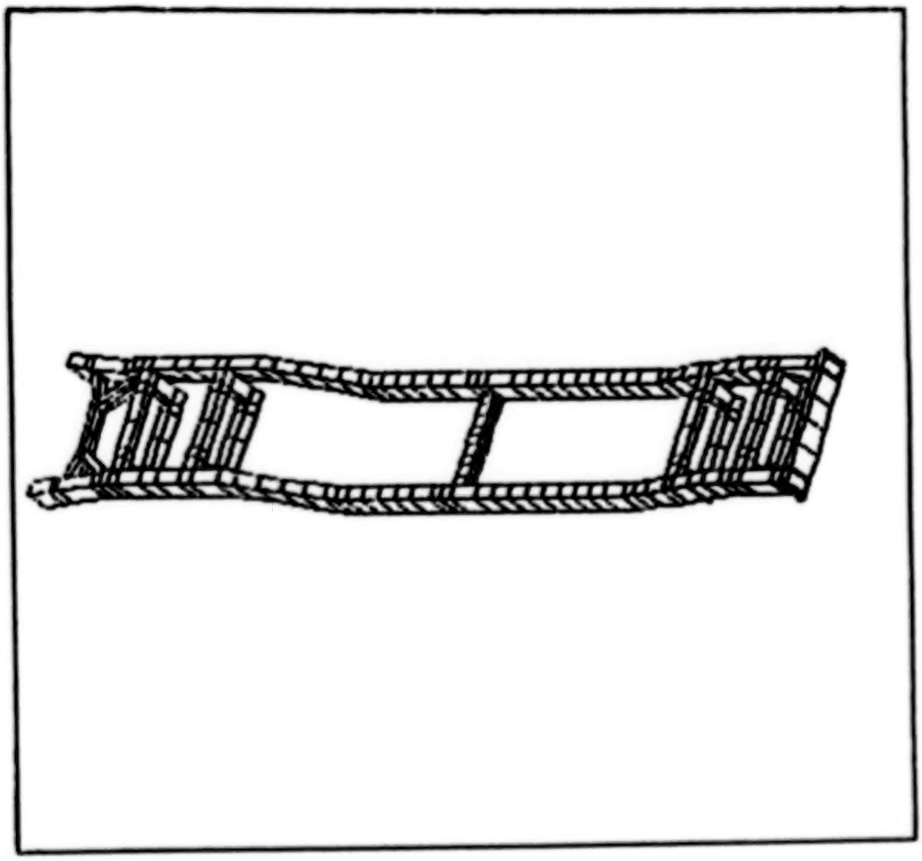

291

DYNAMIC STRESS HISTORY

As a typical dynamic simulation environment, the vehicle traverses a 4 in. high one sided bump with a speed of 22.5 mph. Because of this unsymmetrical terrain, the dynamic response and stress histories in the vehicle are unsymmetric. The simulation is carried out for 2.5 sec on a reporting time grid of 0.05 sec. Stress data are calculated for each node in each element.

As an example, the nominal strain history in the rearmost suspension crossmember, close to the lower corner bracket connection, is given. In the physical component, there is a hyperbolic notch. Large internal forces that vary with time occur here, due to large suspension and tire forces that are transmitted through the crossmember as the vehicle traverses the bump.

The insights and estimates of stress histories obtained in this analysis are of significant design value because they give the designer a clear idea of the effects of the coupled gross motion and flexible body dynamics on the system. This allows for improvement in design before building a prototype and testing, which significantly speeds up the design cycle.

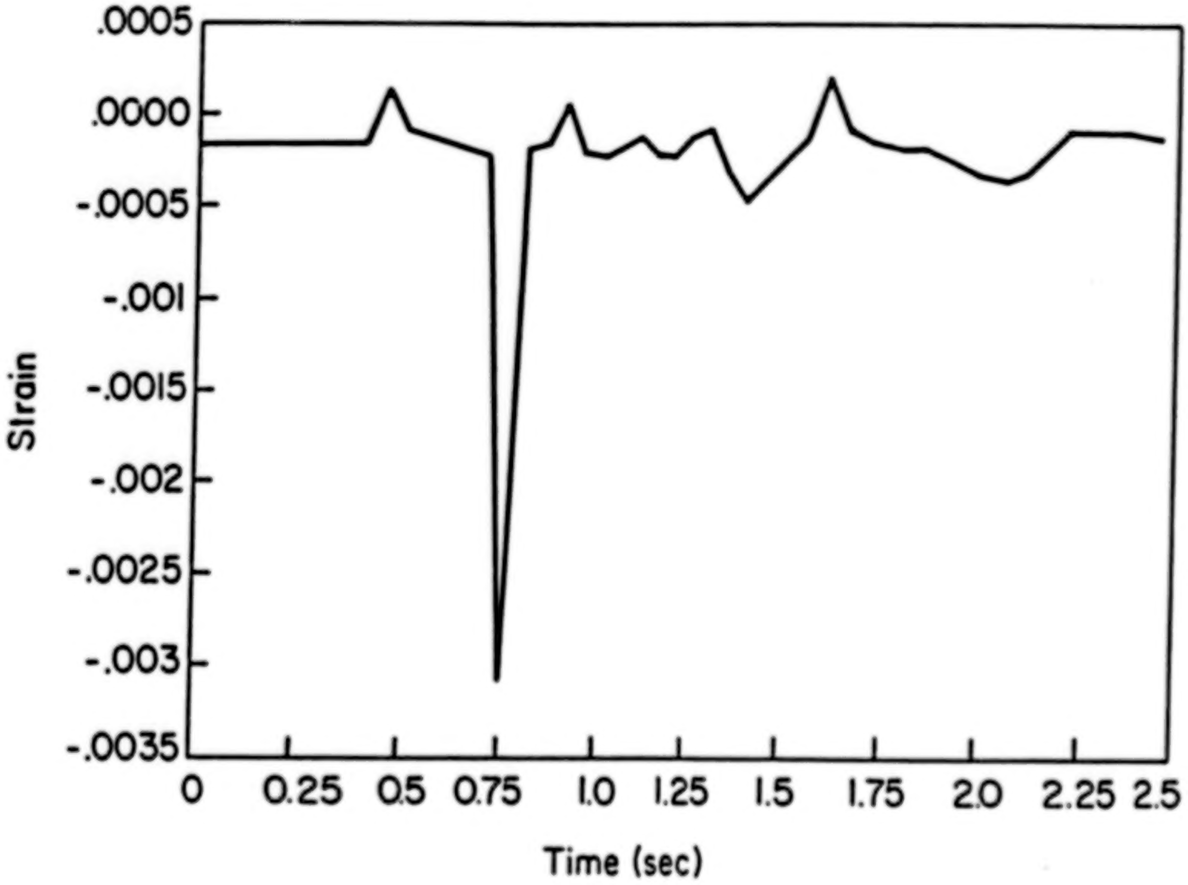

292

CONCLUSIONS

The concept of an advanced integrated, networked simulation and design system has been outlined. Such an advanced system can be developed utilizing existing codes without compromising the integrity and functionality of the system. An example has been used to demonstrate the applicability of the concept of the integrated system outlined here.

The development of an integrated system can be done incrementally. Initial capabilities can be developed and implemented without having a detailed design of the global system. Only a conceptual global system must exist. For a fully integrated, user friendly design system, further research is needed in the areas of engineering data bases, distributed data bases, and advanced user interface design.

The integrated system must be based on

- An integrated command processor and data base management system
- A network environment
- A graphical window based user interface

We concluded that

- Existing codes can be effectively utilized
- An interdisciplinary analysis system can be developed incrementally

REFERENCES

1. Dopker, B.: Developments in Interdisciplinary Software for Mechanical System Simulation and Design. Engineering with Computers, vol. 4, 1988, pp. 229-238.

2. Network File System (NFS), Sun Microsystems Inc., (Mountain View, California), 1987.

3. Network Computing System (NCS), Apollo Computer Inc., (Chelmsford, Massachusetts), 1987.

4. Scheifler, R.W.; and Gettys, J.: The X Window System. ACM Transactions on Graphics, vol. 5, 1986, pp. 79-109.

5. Vos, R.G.; Walker, W.J.; Beste, D.L.; Price, G.A.; Young, J.P.; and Frisch, H.P.: Development and Use of an Integrated Analysis Capability. AIAA/ASME/ASCE/AHS Structures, Structural Dynamics and Materials Conference (Lake Tahoe, Nevada), May 1983.

6. Vos, R.G.; Beste, D.L.; Gregg, J.; and Frisch, H.P.; and Sanborn, J.A.: Integrated Analysis Capability (IAC), Level 1.5. COSMIC Library, University of Georgia, (Athens, Georgia), 1985.

7. Blaha, M.R.; Premerlani, W.J.; and Rumbaugh, J.E.: Relational Database Design Using an Object-Oriented Methodology. Communications of the ACM, vol. 31, no. 4, 1988, pp. 414-427.

8. Woodward, W.S.; and Morris, J,W.: Improving Productivity in Finite Element Analysis Through Interactive Processing. Some Perspectives on CAD/CAM in Mechanical Engineering, (Ed.: Perrone, N.; and Magrab, E.B.), ASME PVP-vol. 87, 1984.

9. Wu, J.K.: Graphics-Based Mechanical System Simulation and Design Preprocessing. Proceedings of the 6th National Conference on University Programs in Computer Aided Engineering Design and Manufacturing, (Atlanta, Georgia), June 1988.

10. Dubetz, M.W.; Kuhl, J.G.; and Haug, E.J.: A Network Implementation of Real-Time Dynamic Simulation with Interactive Animated Graphics. Design Automation Conference, (Orlando, Florida), September 1988.

11. Dubetz, M.W.; and Haug, E.J.: Real-Time Dynamics Simulation - A Design Optimization Tool. Design Automation Conference, (Orlando, Florida), September 1988.

12. Liu, T.S.; Haug, E.J.; and Dopker, B.: A Dynamic Simulation Approach to Machine Component Life Prediction. Design Automation Conference, (Orlando, Florida), September 1988.

13. Stephens, R.I.; Dopker, B.; Haug, E.J.; Back, W.K.; Johnson, L.P.; and Liu, T.S.: Computational Fatigue Life Prediction of Welded and Non-Welded Ground Vehicle Components. Proceedings of the SAE Passenger Car Meeting, (Dearborn, Michigan), October 1987.

14. Liu, T.S.: Computational Methods for Life Prediction of Mechanical Components of Dynamic Systems. Ph.D. Thesis, The University of Iowa, (Iowa City, Iowa), December 1986.

The Role of Optimization in the Next Generation of Computer-based Design Tools

J.E. Rogan
School of Aerospace Engineering
Georgia Institute of Technology
Atlanta, Georgia 30332-0150

· 295

There is a close relationship between design optimization and the emerging new generation of computer-based tools for engineering design. With some notable exceptions, the development of these new tools has not taken full advantage of recent advances in numerical design optimization theory and practice. Recent work in the field of "design process architecture" has included an assessment of the impact of next-generation computer-based design tools on the design process. These results are summarized, and insights into the role of optimization in a design process based on these next-generation tools are presented.

Design optimization can be integrated into "intelligent" computer-based design tools as a constraint propagation mechanism. Design optimization techniques that offer significant potential for constraint propagation in next-generation computer-based design tools include the Schmit-Fleury technique for handling discrete constraints. Decomposition techniques provide a means for controlling the extent of constraint propagation in an "intelligent" computer-based design tool. The sensitivity of optimal solutions to problem parameters can be used to balance parallel constraint propagation tasks and to manage the iteration between levels of a multi-stage constraint propagation scheme.

Optimal sensitivity derivatives, combined with the use of the Schmit/Fleury technique to propagate design constraints, provide an algorithm for breaking a complex engineering problem into a sequence of design decisions. Why do this? The end product of design is not the "product definition". The result of a design effort is the *understanding* of the design issues gained by the design team. This understanding is represented by the signature of an engineer - certifying that in his or her professional opinion, the design is safe and will perform satisfactorily. This understanding is considerably enhanced through the execution of a step-by-step decision process. The development of a sequence of design decisions leading to an optimal (or near-optimal) solution can be thought of as one aspect of *meta design* - designing the design process.

An example problem has been worked out to illustrate the application of this technique. The example problem - layout of an aircraft main landing gear - is one that is simple enough to be solved by many other techniques. Although the mathematical relationships describing the objective function and constraints for the landing gear layout problem can be written explicitly and are quite straightforward, an approximation technique has been used in the solution of this problem that can just as easily be applied to integrate supportability or producibility assessments using theory of measurement techniques into the design decision-making process.

The design decision making process must be adapted to changes in requirements, goals and criteria, as well as to changing technologies. The primary way of accomplishing this adaptation is through design process planning. The "design of the design process" (meta design) is based on the structure of the problem. As used here, problem structure may include connectivity, monotonicity, and sensitivity of subproblem optimal solutions to problem parameters. The problem structure information is developed by the design team (which has to include manufacturing and support personnel, as well as the aerodynamicists, operations analysts, structural analysts, vendors, and others currently closely involved with the design project group), in a "Generate Design Alternatives" step of the design process (Figure 1). The meta design step ("Plan Design Decisions") was envisioned in reference 1 as taking place after design alternatives had been generated (and captured in a "design-in-process" object/knowledge/data base), and before design decisions were made.

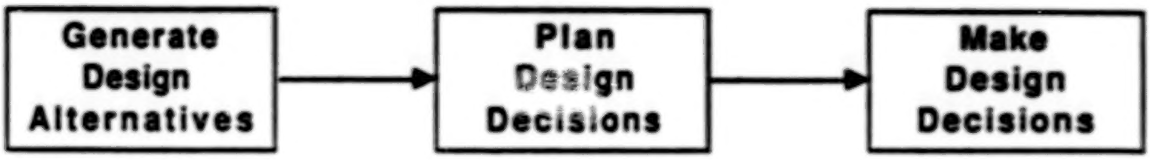

Figure 1. *"A/I Study"* (ref. 1) design process.

Some alternative approaches to accomplishing the meta design step have been investigated in the current study. The results of this effort have clarified the iterative nature of the relationship between meta design and design decision-making. This point of view is emphasized in Figure 2. Here the arrows (indicating sequence, not information flow) go *both* ways between meta design and design decision-making.

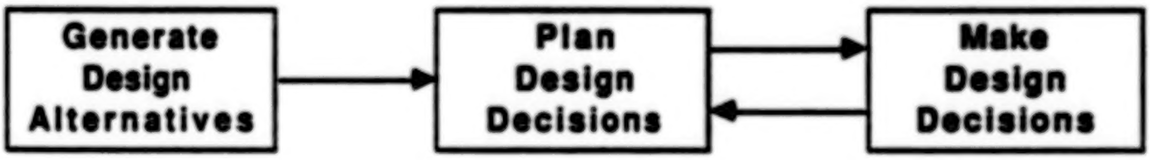

Figure 2. Meta design and decision-making are intertwined.

This study outlines one approach to accomplishing the development of such design tools. The approach is based on exploding a view of the "subtext" of design: the things designers do without thinking about them. The work so far has concentrated on *decision support* , i.e. once a design concept is defined, how does the designer plan and execute a design decision-making process? It should be emphasized that work on decision support for design should not take place in a vacuum relative to work on how design concepts are defined. Work supported by the NASA SBIR (Small Business Innovative Research) program and monitored through NASA Ames Research Center has addressed this need so far, and is also providing a vehicle for testing these ideas in prototype software (reference 2).

The basic idea is to formalize the design process planning and decision-making steps that designers go through. This approach provides an explicit mathematical model of the design decision-making process. Such a model is then accessible to analysis and criticism. Although concepts in this decision model are explained by reference to examples from "traditional" aircraft design, the nature of the model allows producibility and supportability considerations to be brought into the trade-off process at the same level as performance.

Design Planning and Meta Design

A procedure for meta design must take information from a description of alternative design concepts and formulate an interrelated set of design decisions based on this information. This seems to be a "trial and error" process now. The idea of a formal, structured approach to design process planning is not new. Several attempts have been made to come up with algorithms that use a model for the structure of the design-in-progress and some heuristic rules that (one hopes) characterize a desirable design process to structure design decisions.

Techniques for meta design that have been used in the past have included influence diagrams, interpretive structural modelling (ISM), the design structure system, monotonicity analysis, constraint propagation, and multilevel optimization using linear decomposition (MOLD). The techniques attack the problem at different stages. Some of the techniques, such as the design structure system, MOLD, constraint propagation, and monotonicity analysis, are primarily concerned with the individual design parameters and equations for design goals and constraints. Other techniques, such as influence diagrams and ISM, work at the level of design decisions.

An interesting contrast can be drawn between these various techniques based on their use of connectivity information contained in a network description of the design concept or decision process. MOLD, ISM, and the design structure system base their construction of a design decision-making plan primarily on this *topological* connectedness. On the other hand, monotonicity analysis is based on a mathematical *analysis* of the equations describing the design concept. Constraint propagation lies somewhere in the middle, using the topological connectedness as the basis for setting up a *computational agenda* (ref. 3) for solving the equations. Influence diagrams use the connectivity of relationships among design attributes, goals, and decisions to construct joint probability distributions for the effect of uncertainty in design attributes (or design evaluation results) on the attainment of design goals. A preliminary assessment of each of these techniques in terms of their application to meta design follows.

Influence diagrams (ref. 4) model all the elements of the design process, including design alternatives, goals, and design decisions. Relationships among these elements are modelled as probabilities. Before the influence diagram can be drawn, however, the basic decision structure must be known. Since *finding* this decision structure is one of the aims of meta design, the influence diagram technique does not appear to have immediate application to the meta design problem. There is, however, an interesting potential application of influence diagrams in assessing proposed decision structures for robustness against various known or suspected uncertainties. Such an assessment could be applied to eliminate design decision structures that are vulnerable to uncertainty from further consideration in the meta design process.

Interpretive Structural Modelling (refs. 5, 6) is based on the idea of exploiting priorities among decisions to construct a decision-making plan. ISM thus works at the level of design decisions. This level could be interpreted as choosing values for individual design attributes, or as determining the values for several tightly coupled attributes as part of an integral decision-making task. The method assumes a partial ordering of the decisions (i.e., the design decision-making process is thought of as a directed graph), and the structure of the decision-making plan is based almost entirely on this ordering. ISM addresses precisely the meta design problem. However, there are some limitations to the technique that must be addressed. First, since the decision structuring rules are strongly based on the idea of a partial ordering, we cannot model the process of "backing numbers out", i.e., inverting the design relationships, which is pervasive in aircraft design.

The design structure system (ref. 7) is based on the idea that if feedback from downstream choices is eliminated, a workable decision sequence can be identified. Structuring the adjacency matrix of the design problem to eliminate feedback loops results in a block-diagonal structure that is interpreted as defining the decision network. Problematically, the decision structure system algorithm may produce a single, highly coupled design decision when applied to aircraft preliminary design problems.

Monotonicity analysis (ref. 8) has been applied to identify active constraints and global monotonicities or degeneracies. Problems which are constraint-bound and can be solved as a system of simultaneous nonlinear equations can also be identified using this technique. The monotonicity analysis approach to identifying design decision structure introduces the

298

important idea that the *analytic* properties of design relationships (i.e. upper and lower bounds for independent variables and the signs of derivatives, which determine monotonicity properties) must enter into a successful method for structuring the design process, along with the topology (i.e. connectedness) of the network of design attributes and relationships among them.

Multilevel optimization by linear decomposition (refs. 9, 10, 11) introduces several important ideas. Decisions are modelled as mathematical optimization problems. A parameter passing algorithm is put forward to describe the iterative decision-making process. This approach has been further investigated (ref. 12), in which the non-hierarchical nature of complex design decision networks was illustrated by an in-depth example. Ref. 12 also explored an alternative way to group problem description elements into design decisions.

Even from this limited review of design process planning methodologies, it is clear that some model for the design decision-making process is needed. The model chosen as the basis for a meta design technique must be comprehensive enough to deal with discrete and continuous decision parameters, and with qualitative as well as quantitative design requirements, goals, and criteria. Means for distinguishing between desirable and undesirable design decision-making processes, compatible with the model for the design decision-making process, must be available.

The choice of mathematical optimization as a model for the design decision-making process has several advantages. Consideration of the design decision-making plan (the result of meta design) as an optimization procedure allows mathematically rigorous stability and rate of convergence criteria to be applied to distinguish between desirable and undesirable design decision-making processes. Design optimization is actually used in design practice, so that a meta design procedure based on this technique would not require an entirely new design toolkit to be transitioned to the design community. The techniques for analyzing parameter passing schemes in terms of optimal sensitivity derivatives can be readily applied to evaluate a prospective design decision-making plan. Finally, dual methods for design optimization are available that fit remarkably well with the meta design approach. Extensions to these methods are available that allow discrete parameters to be included in the decision-making process.

The most significant limitation of the design optimization model is, of course, the question of how to handle qualitative design considerations. Numerical ranking of alternative designs against qualitative criteria is one possible solution. "Quantifying the qualitative" raises significant issues in itself (ref. 13). However, a convincing argument can be made for including this approach as an integral part of the meta design procedure proposed in this study. The argument is made on the following points: First, the use of numerical rankings for qualitative criteria is well established in design practice (e.g., Cooper-Harper ratings, ref. 14. See also refs. 15, pg. 8-5; and 16). Second, representation and uniqueness problems almost certainly limit the applicability of measurement techniques to *relative* comparisons between design alternatives. Absolute predictions of product characteristics should probably not be based on these rankings alone. However, wind tunnel measurements of airplane drag are subject to this same restriction (ref. 17), and the wind tunnel is considered to be an invaluable tool for aircraft design.

The proposed technique for meta design will be described in detail by means of an aircraft layout example (see "Executing the design decision-making process", below). The technique is strongly based on the idea of structuring the design decision-making process to achieve stable convergence of the corresponding design optimization problem. The design process is structured dynamically as part of the solution to the design problem itself. To summarize the key elements of this approach:

- Model decisions as mathematical optimization problems.
- Use parameter passing to model the decision sequence.

249

- Handle uncertainty through error-bands on the location of constraints.
- Sequence decisions so that constraints imposed by previous decisions are not infeasible in later ones.
- Restrict allowable parameter passing topologies to those that are stable according to (ref. 12) (and other stability criteria).
- Formulate decisions dynamically as part of the solution process.
- Use dual methods to handle discrete parameters.
- Apply the theory of measurement to quantify qualitative attributes and relationships.

The technical approach for evaluating whether these recommendations are valid is that the resulting meta design approach should correspond to traditional design practices in interesting ways. Also, it must be clear how to bring qualitative assessments of downstream producibility and supportability issues into the trade-off process and to handle uncertainty in these assessments.

A Formal Algorithm using the Meta Design Approach

The problem is to select values for design decision attributes while meeting requirements, goals and criteria imposed on the design.

Considering this design problem as an optimization problem, we have

Problem *P* :

Minimize:

$\{f_a(x_{i_1}, \ldots, x_{i_r}),\ a \in \mathcal{F}\}$
a set of multiple objectives,

Subject to:

$\{g_b(x_{j_1}, \ldots, x_{j_s}) \geq 0,\ b \in \mathcal{G}\}$

with $x_i^{lower} \leq x_i \leq x_i^{upper}$

(equality constraints could be included in a similar fashion). The main feature of this problem to be emphasized here is that the objective and constraint functions do not usually depend on *all* of the design decision variables x_i, $i = 1, \ldots, n$.

The objectives fall into three broad categories (similar to those used by Taguchi, ref. 18), *minimize, maximize, and goal* . Formally, each type of objective can be handled as a minimization (for *maximize* objectives f, we minimize $-f$; for *goal* objectives, we minimize some measure of the departure from the goal value f^{goal}, such as $(f - f^{goal})^2$).

In the context of optimization theory, meta design involves partitioning the (large) optimization problem *P* into subproblems, and defining a convergent sequence for solving the subproblems. In general, there will be several design decision variables which appear in more than one subproblem. Values for these design decision variables will be determined by the solution of the first subproblem (in the solution sequence) in which these design decision variables appear. If a design decision variable x_i appears explicitly in a subproblem, but its value is determined outside of that subproblem, it is said to be a *parameter* in that problem.

Generally speaking, the imposition of any additional (active) constraint on an optimization problem will increase (i.e. worsen) the value that can be attained for minimization of the objectives of that problem. When a design decision variable x_i appears as a parameter in a problem P_j, a penalty will be incurred in the value of the objective function (relative to the objective function value which could be achieved if x_i were allowed to vary within the problem P_j). Sobieski, et al., (ref. 11) have developed techniques for evaluating the rate of change of the objective function of P_j with respect to changes in the value of x_i (as a parameter), subject to the conditions that optimality continues to hold and the active constraint set does not change. This *sensitivity of optimal solutions to problem parameters* technique provides us with a tool to assess the penalties associated with selecting a given solution sequence for the subproblems. This approach is referred to as a *parameter passing* technique, since the values of design decision variables determined by solution of subproblems are passed as parameters to subsequent subproblems.

There are a number of different ways to implement a meta design technique based on parameter passing, depending on the details of the formulation of the subproblems. Sobieski, et al. have investigated several alternative approaches (refs. 9 and 10), including formulating a penalty function from the constraints of a subsequent problem, P_2, and using the optimal sensitivity derivative of this penalty function to define a linear constraint in the prior problem, P_1. In this approach, P_1 (the prior problem) is then re-solved with the new "optimal sensitivity" constraint in order to force selection of a value of the parameter that will lead to a feasible solution downstream when P_2 is finally re-solved.

Two somewhat different approaches are presented here. The first approach represents an alternative to existing goal-programming techniques for solving multiobjective optimization problems. The second approach is based on the idea of *constraint propagation* . As mentioned earlier, the primary difference between the constraint propagation and goal-programming approaches is in the partitioning and formulation of the subproblems.

Each objective function f_a is assigned to a single subproblem (P_a) in the goal-programming type approach. The constraints belonging to this subproblem are those which have one or more design decision variables in common with the set of design decision variables appearing explicitly in f_a (this set of constraints is denoted $\mathcal{G}_a$). The total set of design decision variables for the problem P_a includes *all* design decision variables appearing in any of these constraints or in the objective function f_a , i.e.:

Problem P_a :

Minimize:

$$f_a\ (x_{i_1}, \dots, x_{i_r})$$

Subject to:

$$\{g_b\ (x_{i_1}, \dots, x_{i_r}, x_{j_1}, \dots, x_{j_s}) \geq 0,\ \ b \in \mathcal{G}_a\}$$

$$\text{with}\ \ x_i^{lower} \leq x_i \leq x_i^{upper}\ \ ,\ i \in \{i_1, \dots, i_r, j_1, \dots, j_s\}$$

(of course, not all of the x_i's have to appear explicitly in any given g_b . By definition, x_i , $i \in \{i_1, \dots, i_r\}$ all appear explicitly in f_a , and none of the x_i, $i \in \{j_1, \dots, j_s\}$ appear explicitly in f_a . This second group of design decision variables are the ones that come into the problem through the constraints.)

Subproblems formulated in this way may still be relatively large in terms of design decision variables. Using the idea of constraint propagation, we can formulate a subproblem corresponding to *each* design decision variable x_i as follows: Include each objective function and constraint in which x_i appears explicitly as part of the subproblem. The other design decision variables appearing explicitly in these objective and constraint functions will have to be included as well. Thus we end up with:

Problem P_i:

Minimize:

$\{f_a\ (x_{j_1}, \ldots, x_i, \ldots, x_{j_r}),\ a \in \mathcal{F}_i\}$

a set of multiple objectives,

Subject to:

$\{g_b\ (x_{k_1}, \ldots, x_i, \ldots, x_{k_s}) \geq 0,\ b \in \mathcal{G}_i\}$

with $x_k^{lower} \leq x_k \leq x_k^{upper}$ $k \in \{j_1, \ldots, j_r, \ldots, i, \ldots, k_1, \ldots, k_s\}$

Once the subproblems have been formulated, the basic idea of the meta design procedure is as follows (Figure 3): Each of the optimization problems P_i are initially assigned to determine a value for one or more of the decision design attributes x_i. Which attribute will be assigned to which problem, and the sequence in which the problems are to be solved, will be determined by comparing the solution to an optimization problem P_i in isolation, to the solution obtained when a decision design attribute x_p has been passed as a parameter from another optimization problem P_j (i.e. x_p is set equal to some value x_p^0 by solving P_j and then P_i is solved subject to the additional constraint $x_p = x_p^0$). A penalty associated with this parameter passing sequence is determined using the optimal sensitivity derivative (ref. 11) for the objective function of problem P_i with respect to the parameter x_p and the difference between the optimal value for the design decision variable x_p when P_i is solved in isolation (call this value x_p^*) and x_p^0 (the value of x_p determined by solution of P_j). For a given parameter passing scheme (including both: [1] the assignments of the determination of the decision design attributes to the optimization problems, and [2] the solution sequence for the optimization problems) a net penalty is calculated by summing the penalties associated with each parameter passing step. An optimal design process plan is one which minimizes this net penalty.

Executing the design decision-making process

The design problem of determining the location of the main landing gear (MLG) on an unlimited-class experimental racing aircraft (Figure 4) will be analyzed using the meta design approach. This design problem is extremely simple, yet elements of "quantifying the qualitative" are present. Producibility and operational characteristics are also significant elements of the problem.

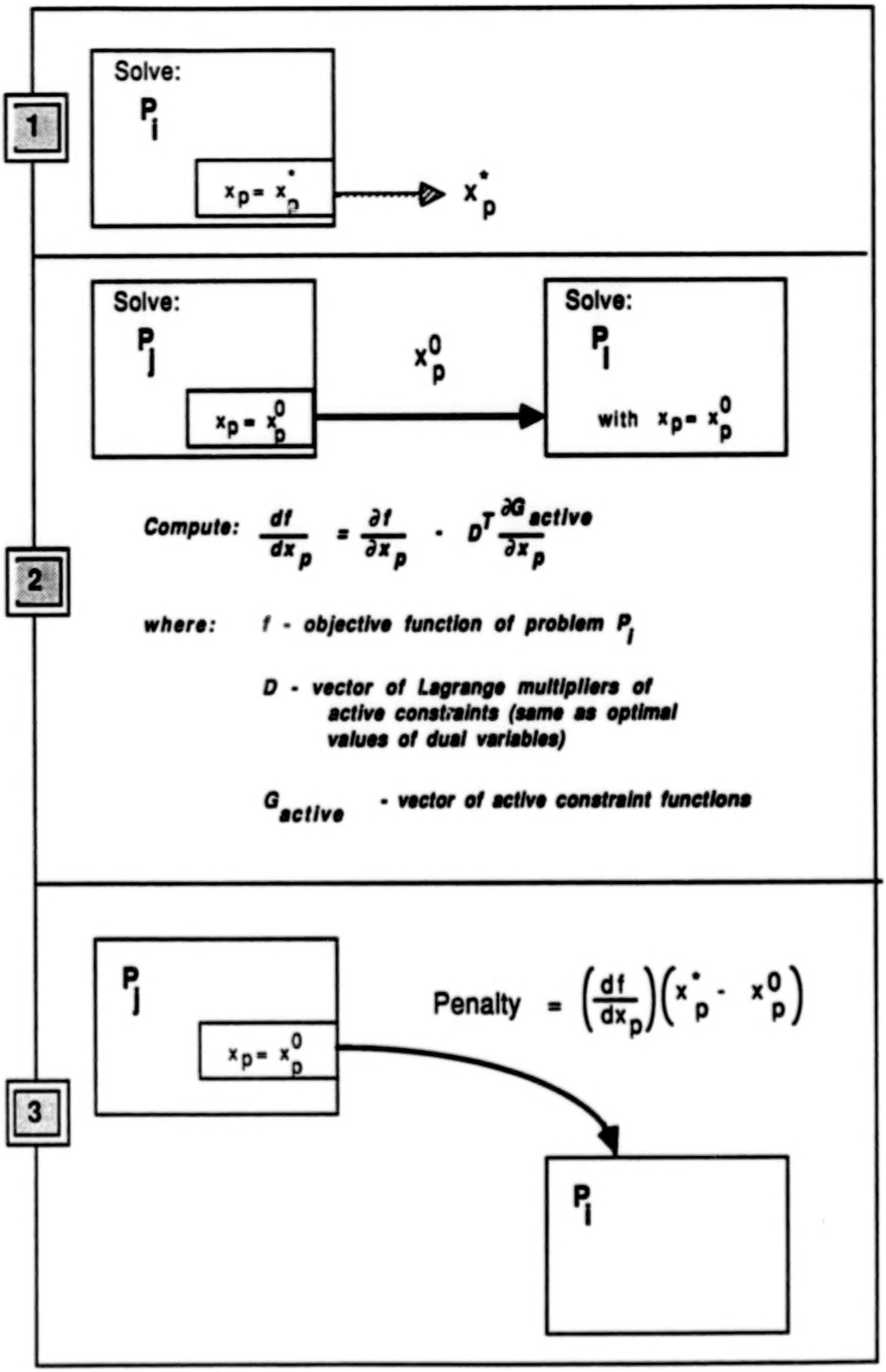
1
Solve:
P_i
$x_p = x_p^*$
x_p^*
2
Solve:
P_j
$x_p = x_p^0$
x_p^0
Solve:
P_i
with $x_p = x_p^0$
Compute: $\frac{df}{dx_p} = \frac{\partial f}{\partial x_p} - D^T \frac{\partial G_{active}}{\partial x_p}$
where: f - objective function of problem P_i
D - vector of Lagrange multipliers of active constraints (same as optimal values of dual variables)
G_{active} - vector of active constraint functions
3
P_j
$x_p = x_p^0$
Penalty $= \left(\frac{df}{dx_p}\right)\left(x_p^* - x_p^0\right)$
P_i

Figure 3. Overview of meta design Procedure.

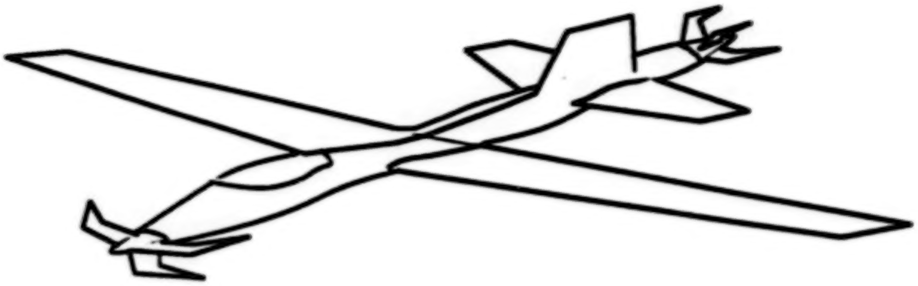

Figure 4. Unlimited-class experimental racing aircraft.

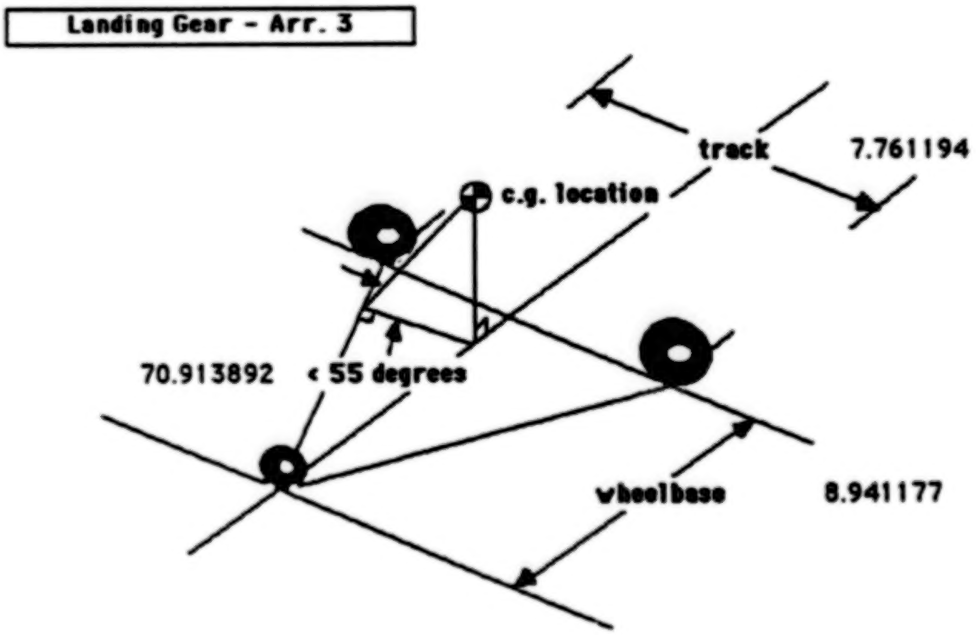
Landing Gear - Arr. 3
track
7.761194
c.g. location
70.913892
< 55 degrees
wheelbase
8.941177

Figure 5. Landing Gear Track Angle.

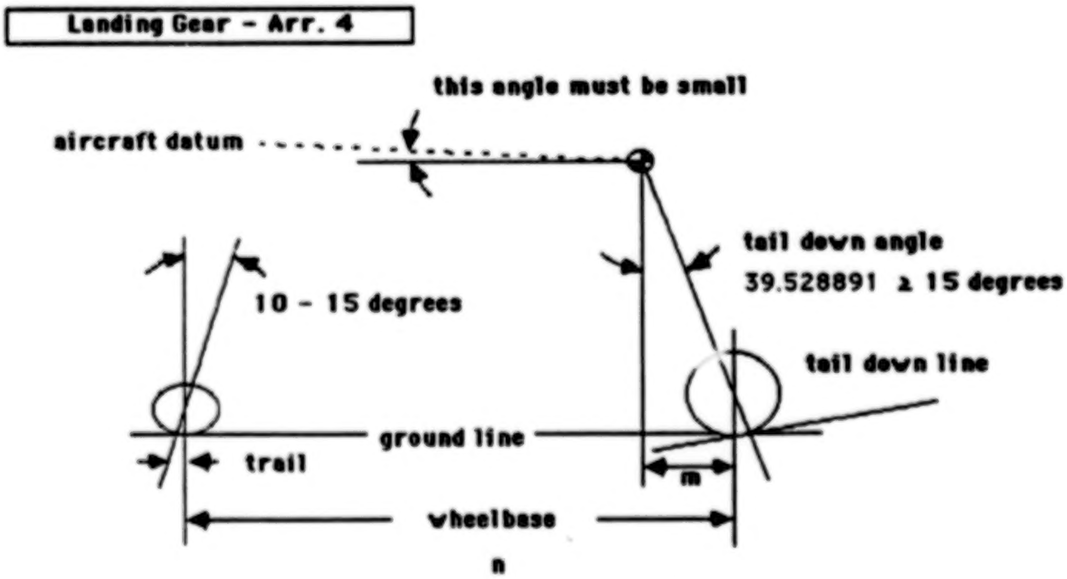
Landing Gear - Arr. 4
this angle must be small
aircraft datum
tail down angle
39.528891 ≥ 15 degrees
10 - 15 degrees
tail down line
ground line
trail
m
wheelbase
n

Figure 6. Landing Gear "Tail Down" Angle.

BEST COPY AVAILABLE

In design terms, early integration of producibility and supportability into the design process involves making design decisions that make the performance, cost and schedule of the aircraft *as insensitive as possible* to the details of how it will be manufactured, operated, and maintained. This point of view is based on the Taguchi (ref. 18) definition of quality as *robustness to "noise" or uncertainty*. Uncertainty refers to factors over which the designer has little or no control.

There are several failure modes that can occur when an aircraft is on the ground or when the aircraft is landing. When the aircraft is taxiing or parked on the airfield, a gust can tip the aircraft over about a line from the main landing gear wheel location to the nose wheel location. In order to avoid this, the *track angle* (Figure 5) is specified. Reference 19 gives a value of 55 degrees as the maximum allowable for this angle. Another failure mode can occur on landing. High performance aircraft often approach the runway and touch down at relatively high angles of attack. If the center of gravity is behind the vertical plane of the main landing gear wheels, the aircraft will encounter a moment which tends to sit the aircraft on its tail. This occurs as the weight of the aircraft is transferred from the wings to the landing gear. Restricting the angle between the center of gravity and the plane of the main landing gear wheels, as shown in Figure 6, will cause the aircraft to hit its tail on the runway (and presumably bounce back) before it can come to rest in a stable position on its tail.

One final consideration in landing gear location is considered in this example problem. The main landing gear must be retractable and must fit into a small space. Reliability, maintainability and cost will be adversely affected if complex retraction kinematics are required to accomplish this. Thus, *minimizing retraction complexity* is a goal for this example problem. In order to keep the analysis simple, retraction complexity is considered to be proportional to the distance from the main landing gear wheel to the closest fuselage frame forward of the wheel).

The example problem is then: to locate the main landing gear (in x,y,and z aircraft reference coordinates) in such a way as to minimize the retraction complexity, while satisfying constraints on "tail down angle" and "track angle". Side constraints on each of the design variables MLGx, MLGy, and MLGz, are derived as follows. The x coordinate of the aircraft c.g. (center of mass) location is at 9.5 ft. Thus a lower bound for MLGx is set at 10 ft. The upper bound is set at 15 ft. In a more detailed example, the upper bound would be related to the horizontal tail volume coefficient required to rotate the aircraft on takeoff. The lower bound for MLGy is set by the fuselage envelope at 1 ft. The upper bound for MLGy is related to the wing span and is set at 15 ft. The lower bound for MLGz is set by the shock strut length, which is related to the aircraft weight, design sink rate on approach, and landing gear design load factor, and is set at 4 ft. The upper bound for MLGz is related to maintenance access and is set at 7 ft. The statement of the example problem as an optimization problem is then:

Minimize: retractionComplexity (MLGx,MLGy,MLGz)

Subject to: trackAngle (MLGx,MLGy,MLGz) ≤ 55
tailDownAngle (MLGx,MLGy,MLGz) ≥ 15

$$10 \leq \text{MLGx} \leq 15$$
$$1 \leq \text{MLGy} \leq 15$$
$$4 \leq \text{MLGz} \leq 7$$

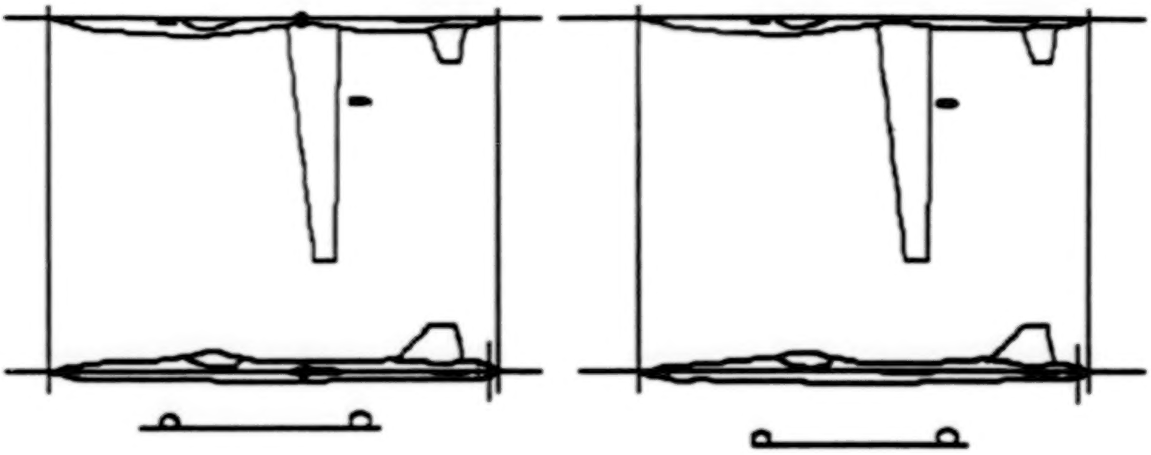

Landing Gear - Arr. 1

Landing Gear - Arr. 2

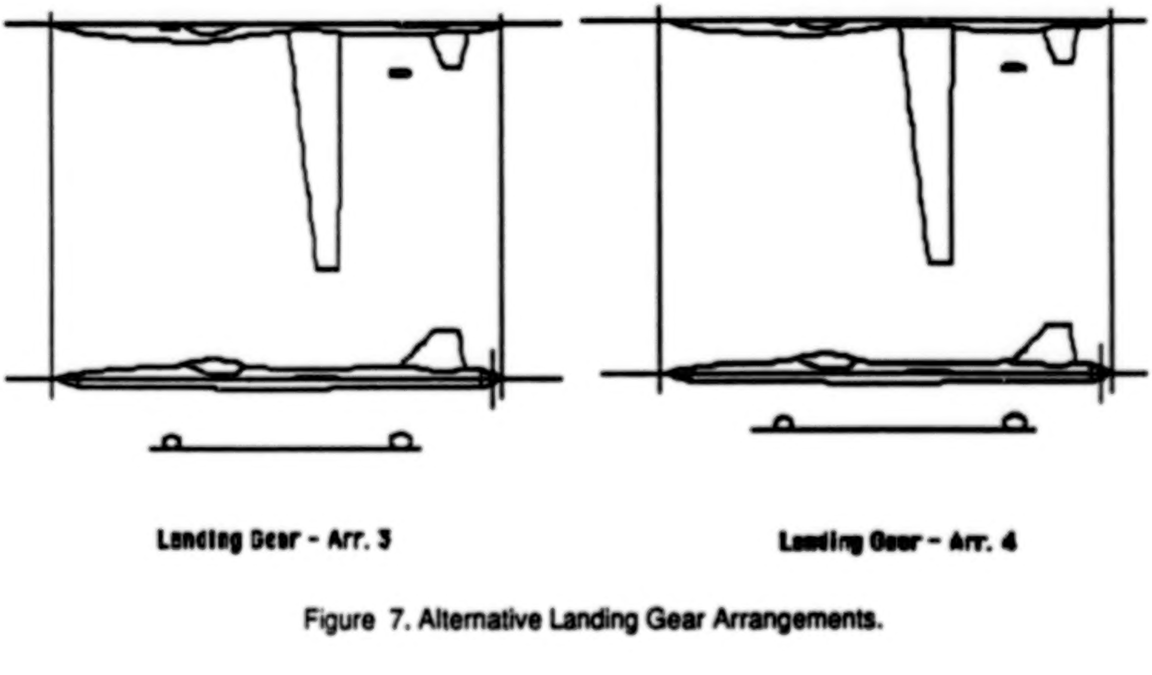

Landing Gear - Arr. 3

Landing Gear - Arr. 4

Figure 7. Alternative Landing Gear Arrangements.

Constructing Approximations

Simple mathematical expressions for retraction complexity, track angle and tail down angle as a function of MLGx, MLGy, and MLGz can be derived from the aircraft geometry. In the meta design procedure proposed here, these simple relationships are not used directly, but are approximated by functions that are linear either in the design variables, x_i, or in their inverses, $1/x_i$. As discussed in reference 20, this form of the approximations is separable and thus permits an explicit solution for the primal design variables in terms of the dual variables. The approximations are constructed by curve-fits to evaluation of the objectives and constraints on a set of alternative landing gear arrangements, as shown in Figure 7.

The process of constructing these approximations provides insights that are similar to those obtained through monotonicity analysis, although the approximations are only valid near the region of design space defined by the alternative configuration arrangements selected.

It should be emphasized that the use of these approximations allows performance and cost requirements to be balanced against a broad range of producibility and supportability requirements. Using the approximation technique, any aspect of the design that can be evaluated at some level can be brought into the trade-off process.

At least for this example problem, approximations can be found which provide a reasonably accurate *qualitative* picture of the design space (Figures 8 to 10). For meta design, this is probably accurate enough. These qualitative results are only valid locally, however, and can be quite inaccurate when extrapolated very much beyond the region of design space near the alternative configurations which were evaluated to construct the approximations (Figure 11).

In order for the dual objective function to be well-defined, the primal optimization problem must be *convex* (ref. 21). For the form of the approximations used here, this means that the coefficients of the design variables (or their inverses) must be positive if the constraint is "greater than or equal to". In the present study, this criterion was used to determine whether a constraint or goal design attribute was directly or inversely proportional to a decision design attribute. This approach was an unqualified success, as the correct (from the point of view of monotonicity) form of the approximation was deduced on the basis of this criterion in every case. (It is difficult if not impossible to ascertain this kind of information from the design evaluations alone for most arrangements of design points. An exception is, of course, a finite difference grid.)

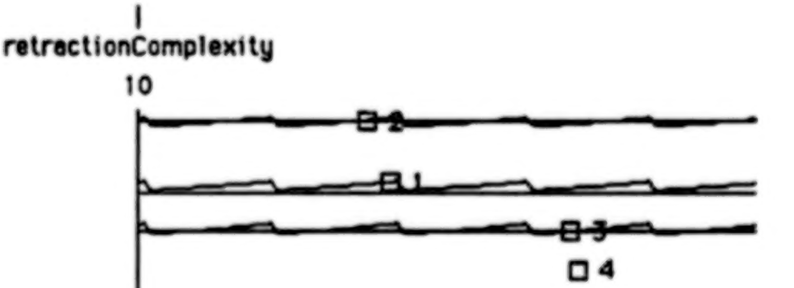

Figure 8. Retraction Complexity is (roughly) independent of MLGx.

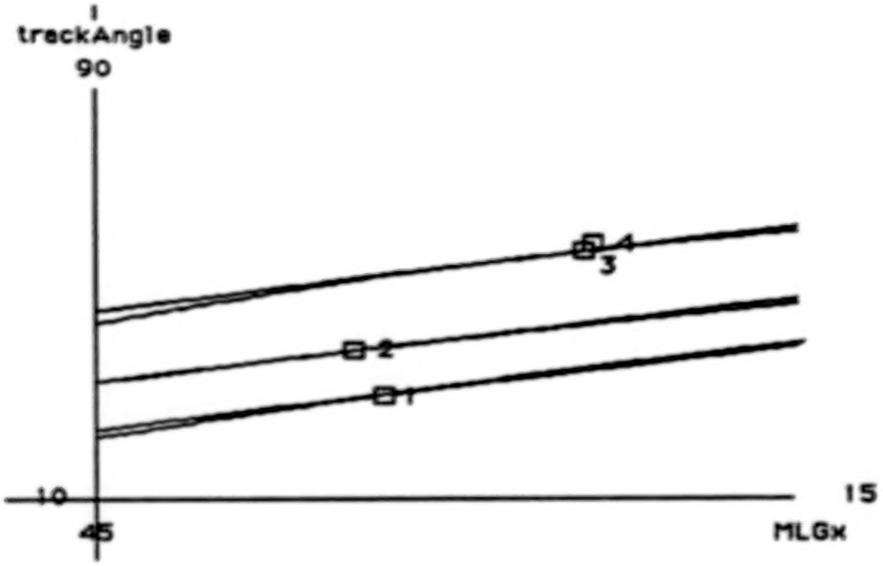

Figure 9. Track Angle is an increasing function of MLGx.

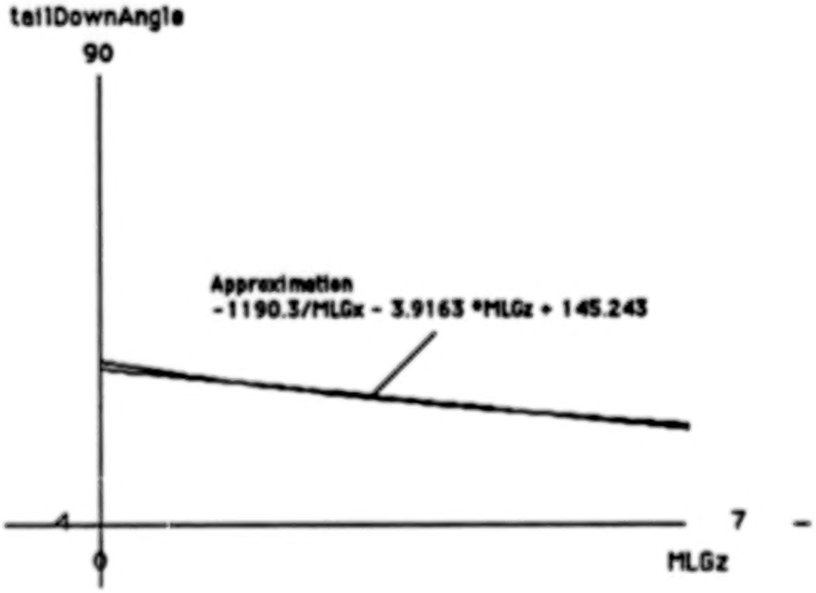

Figure 10. Tail Down Angle as a function of MLGz.

Formulation and Solution of Optimization Problems.

The initial structure of design decision-making tasks is based on the idea that goals (such as **minimize retraction Complexity**) and constraints (such as **tailDownAngle**) are *propagated* through choices of the design parameters **MLGx, MLGy and MLGz** (Figure 12). Thus the initial problem structure is as shown in Figure 13. There is a correspondence between optimization subproblem P1 and design variable MLGx in that problem P1 propagates goals and constraints that are linked in the "attribute-relationship diagram" of Figure 12 by the design variable MLGx. The meta design problem is to determine which of the optimization subproblems P1, P2 and P3 should determine which of the design variables MLGx, MLGy, and MLGz, and in what sequence. *Suprisingly, for this example, a design decision plan in which P1 determines MLGx, P2 determines MLGy, and P3 determines MLGz is not optimal.*

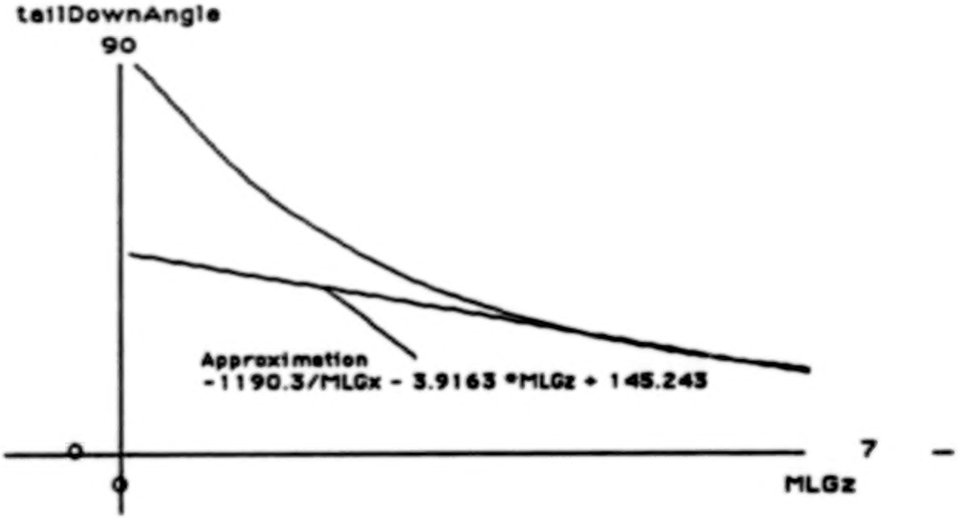

Figure 11. The approximations are not usually accurate globally.

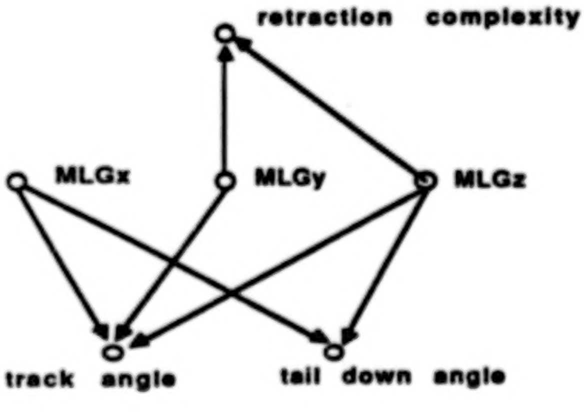

Figure 12. Attribute-relationship diagram for example problem.

The first step in the meta design procedure is to solve the individual optimization/constraint propagation problems P1, P2, and P3 as self-contained problems. This can be done very easily using the approximate forms for the goal and constraint design attributes. The method of ref. 20 is used here, with some changes. The first change is that the problems have been solved explicitly, rather than numerically, since this solution is straightforward. The second difference involves a simple extension of Schmit and Fleury's technique to handle a slightly broader range of forms for the constraint and goal approximations.

The initial solutions are

P1:
$d_1 = 0, d_2 = 0$

MLGx = 15, MLGy = 15, MLGz = 4.

P2:
d_1 = 0.1497
MLGx = 10, MLGy = 4.189, MLGz = 4

P3:
d_1= 0.1614, d_2 = 0.02626
MLGx = 10.39, MLGy = 4.351, MLGz = 4

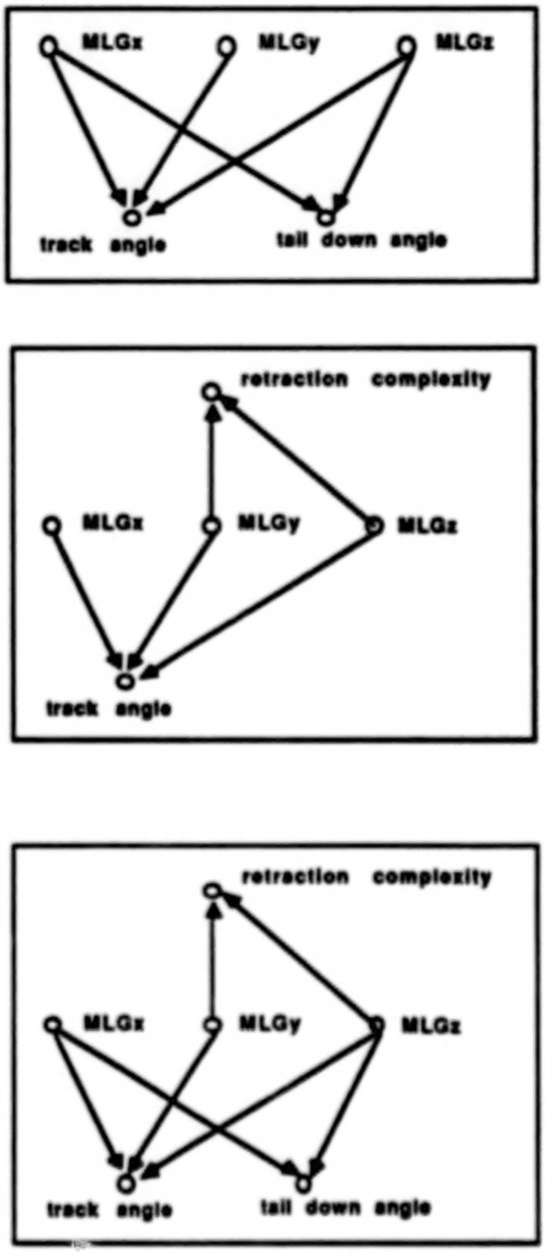
MLGx
MLGy
MLGz
track angle
tail down angle
retraction complexity
MLGx
MLGy
MLGz
track angle
retraction complexity
MLGx
MLGy
MLGz
track angle
tail down angle

Problem 1

Satisfy:
track angle ≤ 55
tail down angle ≥ 15

Problem 2

Minimize:
retraction complexity

Subject to:

track angle ≤ 55

Problem 3

Minimize:
retraction complexity

Subject to:

track angle ≤ 55
tail down angle ≥ 15

Figure 13. Optimization problem structure.

Evaluation of Parameter Passing Schemes

Once initial solutions to the constraint propagation/optimization problems P1, P2, and P3 have been obtained, we can begin to assess parameter passing schemes. The approach to accomplishing this is outlined in Figure 3. The purpose of computing the optimal sensitivity derivatives is to determine the penalties associated with each parameter passing scheme that is of interest (see, for example, Figure 14, where the penalties associated with passing MLGx as a parameter are labels on the directed arcs along which MLGx would be propagated).

Parameter passing schemes can be evaluated using the penalties summarized in Figure 14, Figure 15 and Figure 16. This has been done in Figure 17 for the most obvious parameter passing scheme (i.e. determining MLGx from problem P1, MLGy from P2, and MLGz from P3).

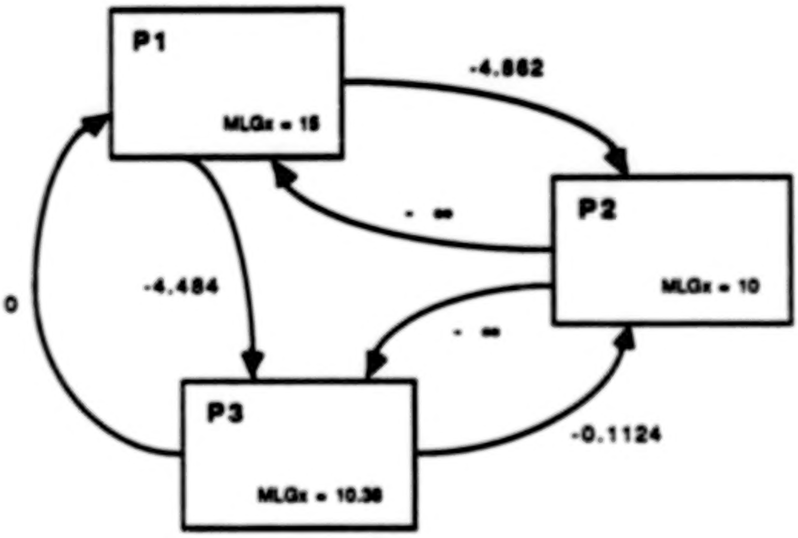

Figure 14. Penalties associated with passing MLGx as a parameter.

The penalty associated with passing MLGx as a parameter from P1 to P2 (Figure 17) is found to be -4.862 using Figure 14. The penalty for setting MLGy by solving problem P2 and passing the result to problem P1 is found (from Figure 15) to be 0. The net penalty for this parameter passing scheme is determined by summing individual penalties over all the arcs of the Figure 17 parameter passing diagram. If the net penalty is negative, the larger the absolute value of the net penalty, the more the solution of the global (i.e., including the whole network of problems) constraint propagation problem will depart from the locally (i.e., considering the individual problems in isolation) optimal solutions for the individual problems. The penalty calculated for the "naive" parameter passing scheme of Figure 17 is actually an upper bound for the loss of optimality. There may be some sequences of solution of the problems P1, P2, and P3 in which optimal solutions of prior problems may lead to infeasibility of subsequent ones. If this happens, the net penalty goes to -∞.

An improved parameter passing scheme for constraint propagation (Figure 18) can be found by thoughtful inspection of Figures 14, 15, and 16. In this scheme, P3 is solved first to find MLGx. The value 10.39 for MLGx is then passed as a parameter to problems P2 and P1. Solution of P2 then yields the value 4.351 for MLGy. Since this value is the same as the optimal value of MLGy for problem P3, there is no penalty associated with passing MLGy as a parameter from P2 to P3 (even though the optimal sensitivity derivative is not zero in this case). The solution to problem P1 is still feasible with MLGx = 10.39 and MLGy = 4.351, so there are no penalties associated with passing these parameters to problem P1.

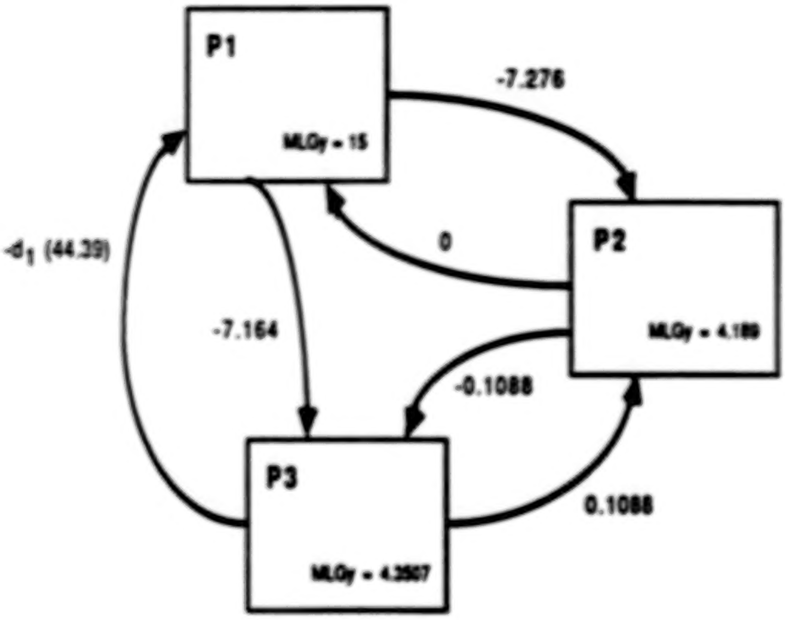
P1
MLGy = 15
-7.276
P2
0
MLGy = 4.189
$-d_1$ (44.39)
-7.164
-0.1088
P3
0.1088
MLGy = 4.3507

Figure 15. Penalties associated with passing MLGy as a parameter.

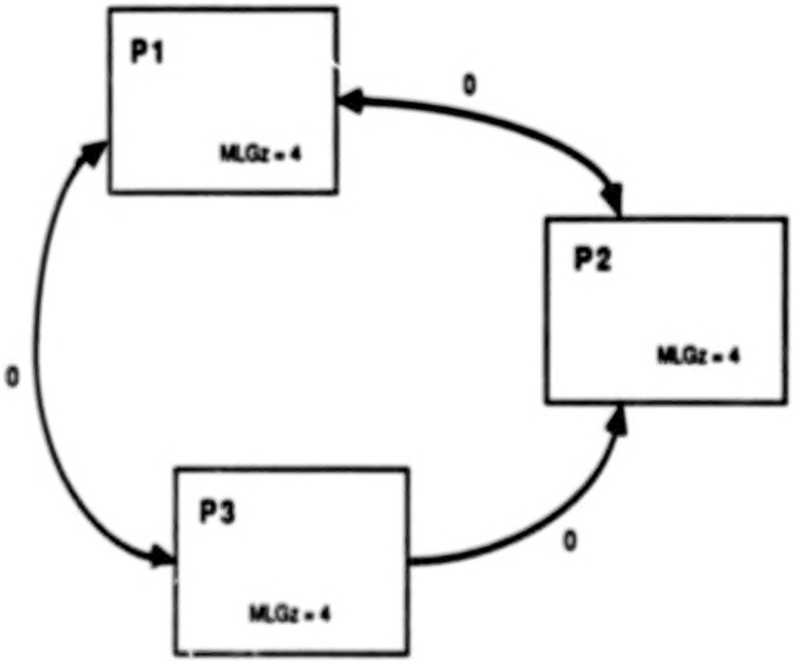
P1
MLGz = 4
0
P2
MLGz = 4
0
P3
0
MLGz = 4

Figure 16. Penalties associated with passing MLGz as a parameter.

312

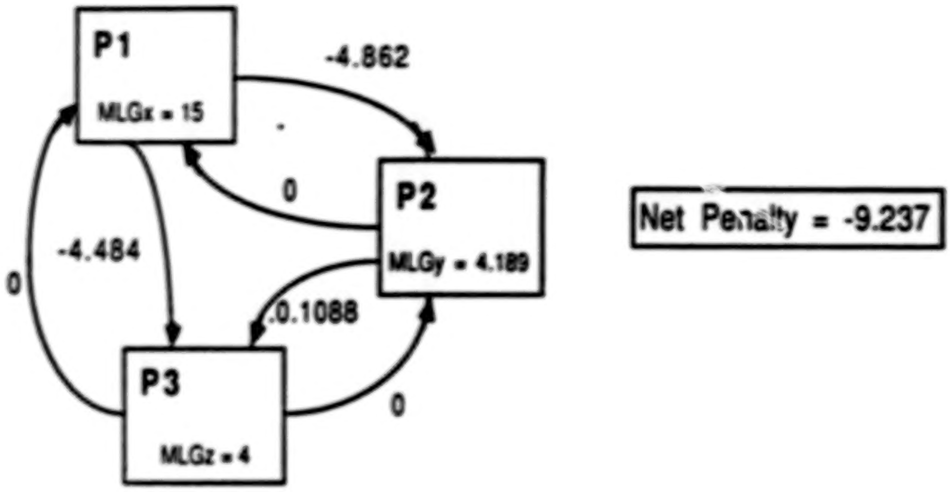

Figure 17. Naive constraint propagation scheme.

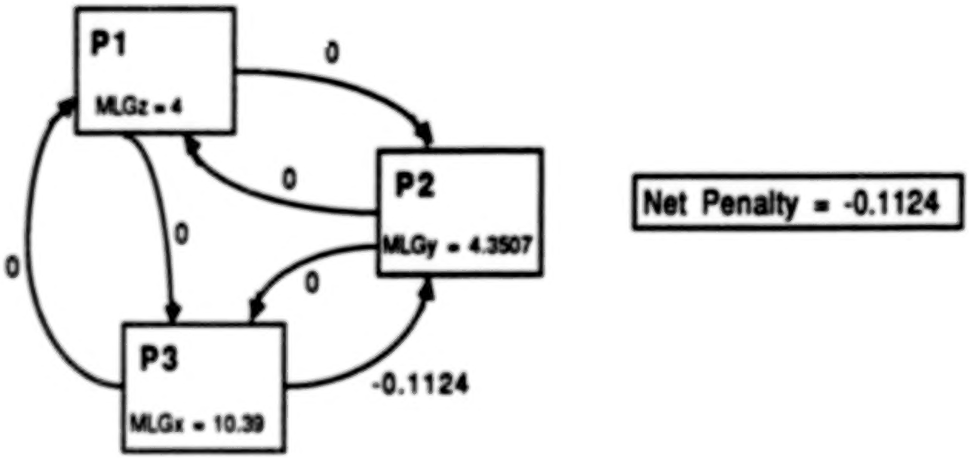

Figure 18. A greatly improved, possibly optimal scheme.

Conclusions

The working hypothesis on the application of parameter passing and constraint propagation ideas to meta design has been that: 1) an optimization problem could be associated with each design variable, 2) optimal sensitivity derivatives could be used in a straightforward way to identify a stable and convergent sequence for solving these problems. This example clearly indicates that the meta design problem is more subtle than was originally thought. At the same time, the example indicates that the meta design idea can be integrated with parameter selection techniques, such as Taguchi methods, through the use of approximations to goal and constraint design attributes. This approach has significant potential as a technique for performing trade-offs between performance, cost, schedule, producibility and supportability. In view of this, further investigation along the lines of this overall approach is likely to be productive. Thus it is important to highlight some of the questions raised by this example.

The formulation of the problems P1, P2, and P3 was based on the constraint propagation idea. P1 propagates constraints that are linked by MLGx, P2 those linked by MLGy, and P3 the constraints linked by MLGz. Yet, in the optimal parameter passing solution, P1 determines MLGx, and P3 determines MLGx, even though MLGx does not appear explicitly in the objective function for P3. This may be due to the fact that MLGz is in direct proportion to every constraint and goal design attribute where it appears, and thus is driven to its lower bound of

4. Thus, as a result of monotonicity, manipulating MLGz does not give the designer much leverage. Yet, from a constraint propagation point of view, MLGz is pivotal. P3 contains all of the design attributes (goals, constraints, and decision parameters) in the original problem. The fact that the constraint propagation problems derived from one of the decision variables are used to determine other decision variables also suggests that the technique of problem formulation requires further critical examination. Perhaps the point of view that the meta design process can indicate which information is required to determine which design decision attribute is more appropriate. Connectivity could then be used to show that it is not necessary to consider all possible permutations and combinations of constraints, goals, and design variables.

The size of the example problem was necessarily quite small. Several interesting potential applications of the meta design approach are slightly ouside its scope. For example, the dual method of Schmit and Fleury has been extended (ref. 20) to handle discrete variables. Demonstration of this capability would require only a marginal increase in problem size, to include, say, number of fuselage frames as a design variable. The discrete variable capability also makes it possible to bring qualitatively different design choices (by quantifying them using some representation). This could be investigated by including the issue of whether the landing gear should be attached to wing or fuselage as a decision variable (with discrete, specifically binary values).

Another aspect of the meta design procedure is that the meta design process clearly produces a solution to the design problem. How this would work on a larger, more complex problem is certainly of interest. Closely related to this issue is the approach that has been used in this study: the meta design technique has been developed and refined in this study through application to real (if extremely simple) design problems. Further investigations into meta design should follow the same basic approach: research priorities should be set by problems encountered in trying to apply the technique to design problems that are as realistic as possible.

The approximations to the constraint and goal design attributes were constructed from evaluations of candidate designs *without using the analytical relationships* . The fact that this aspect of the process was successfully accomplished suggests that the meta design process can now be applied to areas of producibility and supportability where analytical relationships are not available and judgments based on simulation and engineering or operational experience must be used to evaluate the design alternatives.

The decision-based model of the design process used in this study and elsewhere (c.f. ref. 16 promises to shed new light on the relationship between requirements definition and the design process. In fact, requirements are set by decisions. These requirements then appear as parameters in subsequent design decisions. Thus the relationship between requirements setting and design decisions can be studied using the meta design approach. In this context, the example problem implies some remarkable conclusions which merit further study. Considering requirements definition and design as a single, integrated problem to be decomposed using a meta design approach, it is clear that the problem does not have the simple, hierarchical structure (i.e. each requirement cannot be traced back to a single prior decision - see, for example, the complex decision network of ref. 12). The example problem indicates that, using meta design, we may be able to find a sequence of interleaving requirements setting and design decisions for which no iterative reallocation is necessary, assuming all of our information is accurate.

Integrating requirements-setting and design decision-making problems will make it necessary to deal with uncertainty in the values of the goal, constraint or decision design attributes. From the meta design point of view, this uncertainty may change the expected optimal decision-making sequence, perhaps even to an infeasible one. The meta design approach could be used to investigate the structural stability of the decision-making sequence as attributes subject to uncertainty are varied. This capability suggests a unique tool for balancing technical and schedule risk: the cost of reducing uncertainty in the attributes can be traded off against the schedule impact of a marginally workable decision sequence.

The meta design example also suggests that the problem of multiobjective programming, i.e. finding a Pareto-optimal ("balanced") decision solution when there are several conflicting goals, can be attacked by associating a constraint propagation problem with each goal and determining a decision sequence that balances the parameter passing penalties associated with each optimization subproblem.

References

1. Brei, M.L. et al, "Architecture and Integration Requirements for an ULCE Design Environment", IDA Paper P-2063, April 1988.

2. David Hall Consulting, "Development of a Micro-Computer based Integrated Design System for High Altitude Long Endurance Aircraft", NASA SBIR Contract final report, August, 1988.

3. Elias, Antonio L., "Knowledge Engineering of the Aircraft Design Process",Chapter 6 in Knowledge Based Problem Solving, Kowalic, J.S., ed., Prentice-Hall, Englewood Cliffs, New Jersey, 1985.

4. Rege, A., and Agogino, A.M., "Topological Framework for Representing and Solving Probabilistic Inference Problems in Expert Systems", Dept. of Mechanical Engineering, University of California, Berkeley, CA. Revision of paper of the same title presented at the 1986 International Computer Symposium, proceedings v.3, pgs. 1685-1691.

5. Malone, D.W., "An Introduction to the Application of Interpretive Structural Modeling", Proc. IEEE, v. 63, no. 3, March 1975, pgs. 397-404.

6. Warfield, J.N., ed., Annotated Bibliography of Publications, Institute for Advanced Study in the Integrative Sciences, George Mason University, December 1986.

7. Steward, D.V., "The Design Structure System: A Method for Managing the Design of Complex Systems", IEEE Trans. on Eng. Mgmt., v. EM 28, no. 3, August, 1981.

8. Michelena, Nestor F., and Agogino, Alice M., "Multiobjective Hydraulic Cylinder Design", Journal of Mechanisms, Transmissions, and Automation in Design, Vol. 110, March 1988. pgs. 81-87.

9. Sobieszczanski-Sobieski, J., "A Linear Decomposition Method for Large Optimization Problems - Blueprint for Development", NASA TM-83248, February, 1982.

10. Sobieszczanski-Sobieski, J., Barthelemy, J.-F. M., and Giles, G. L., "Aerospace Engineering Design by Systematic Decomposition and Multilevel Optimization", ICAS-84-4.7.3, September, 1984.

11. Sobieszczanski-Sobieski, J., Barthelemy, J.-F. M., and Riley, K. M., "Sensitivity of Optimum Solutions to Problem Parameters", AIAA 81-0548R, AIAA Journal, v. 20, n. 9, September 1982, pgs. 1291-1299.

12. Rogan, J. E., and Kolb, M. A., "Application of Decomposition Techniques to the Preliminary Design of a Transport Aircraft", NASA CR-178239, February 1987.

13. Cralley, W. E.; Owen, David; Kuenne, R., et al. (ULCE DSS Working Group), Decision Support Requirements in a Unified Life Cycle Engineering (ULCE) Environment, Volume I: An Evaluation of Potential Research Directions, Institute for Defense Analyses, IDA Paper P-2064, May 1988.

14. Roskam, Jan, Airplane Flight Dynamics and Automatic Flight Controls, Part I, Roskam Aviation and Engineering Corporation, Ottawa, Kansas, 1979. pg. 537.

15. Lockheed Missiles and Space Company, System Engineering Management Guide, Defense Systems Management College, Ft. Belvoir, VA. Contract MDA 903-82-C-0339, October 1983.

16. Mistree, Farrokh; Marinopoulos, Stergios; Jackson, David M.; and Shupe, Jon A., The Design of Aircraft Using the Decision Support Problem Technique, NASA CR 4134, April 1988. pg. 53.

17. Perkins, Courtland D.; and Hage, Robert E., Airplane Performance Stability and Control, Wiley & Sons, New York, 1949. pg. 111.

18. Anonymous, "Taguchi Methods Quality Engineering Executive Briefing", Center for Taguchi Methods, American Supplier Institute, Dearborn, Michigan, 1988.

19. Stinton, Darrol, The Design of the Aeroplane, Van Nostrand Reinhold, New York, 1983.

20. Fleury, C.; and Schmit, L. A., "Dual Methods and Approximation Concepts in Structural Synthesis", NASA CR-3226, 1980.

21. Luenberger, D.G., Linear and Nonlinear Programming, 2nd Edition, Addison-Wesley, 1984.

AN OVERVIEW OF THE DOUGLAS AIRCRAFT COMPANY AEROELASTIC DESIGN OPTIMIZATION PROGRAM (ADOP)

ALAN J. DODD
Douglas Aircraft Company, McDonnell Douglas Corporation
Long Beach, California

INTRODUCTION

This paper describes, from a program manager's viewpoint, the history, scope, and architecture of a major structural design program at Douglas Aircraft Company called ADOP -- Aeroelastic Design Optimization Program. Bruce A. Rommel discusses technical details and current and potential applications of the program in Douglas Paper 8102.*

The main businesses at Douglas' engineering division are design and analysis of large subsonic transport aircraft structures and development of existing designs. There is also a sustained effort at the advanced design level that involves subsonic and supersonic projects.

Since the mid 1950s, Douglas has maintained a generally uncoordinated research and development effort involving computerized methods for loads, statics, and dynamics. Plans for a comprehensive coordinated computational structural mechanics (CSM) effort were developed by Rommel in 1978. These plans were further refined for the (unsuccessful) proposal effort of 1982 for the Air Force contract which resulted in the Air Force Structural Optimization System (ASTROS). The ASTROS proposal led Douglas management to authorize full-scale development of ADOP, starting in late 1984.

ADOP was originally intended for the rapid, accurate, cost-effective evaluation of relatively small structural models at the advanced design level, resulting in improved proposal competitiveness and avoiding many costly changes later in the design cycle. Before release of the initial version in November 1987, however, the program was expanded to handle very large production-type analyses.

---

* Rommel, Bruce A. Meeting the Challenges with the Douglas Aircraft Company Aeroelastic Design Optimization Program (ADOP). Douglas Aircraft Company, Long Beach, California, DP 8102, September 1988. Presented to the Second NASA/Air Force Symposium on Recent Experiences in Multidisciplinary Analysis and Optimization, September 28-30, 1988. NASA CP-3031, 1988. (Page 1369 of this compilation.)

DESIGN AND ANALYSIS OF LARGE TRANSPORT AIRCRAFT

MODIFICATIONS TO EXISTING DESIGNS

ADVANCED PROJECTS -- AST, NASP, HSCT, PROPFAN

1982 -- "ASTROS" PROPOSAL

1985 -- FULL-SCALE ADOP DEVELOPMENT AUTHORIZED

REQUIREMENTS

The original Douglas requirement called for the rapid static and aeroelastic analysis and optimization of advanced design layouts. It was assumed that an accurate stiffened-shell, finite-element representation of the layout could be processed as a single entity. The available production analysis programs generally were not automatically interfaced, could not respond rapidly or cheaply enough for proposal or initial design purposes, and did not have optimization capabilities.

As soon as ADOP development started, it became clear that the automatic features of the program -- and particularly the use of a common finite-element model for static and aeroelastic analysis -- could also improve the efficiency and accuracy of production analyses. We were also asked to prepare for operations on a Cray XMP18. Therefore, a large detour was taken in the development schedule to expand the numerical method algorithms and data base utilities for out-of-core use.

It also became clear that our initial decision to use the in-house Computer Graphics Structural Analysis (CGSA) modeler program would limit ADOP applications. On a corporate-wide basis NASTRAN is often used, especially for dynamic analysis, so work was initiated on a NASTRAN-ADOP model translator.

ORIGINAL REQUIREMENT

- RAPID STATIC AND AEROELASTIC EVALUATION OF ADVANCED DESIGN LAYOUTS

SUBSEQUENT REQUIREMENTS

- LARGE-SCALE MODAL ANALYSIS
- CRAY APPLICATIONS
- INTERFACES WITH PATRAN AND NASTRAN

JUSTIFICATION

We were lucky at the start of ADOP planning in that Douglas was expanding rapidly, and our technical managers had research and development backgrounds and were sympathetic to the cause. The figure lists the main points used to justify what is, even for McDonnell Douglas Corporation, a large investment of research funds and manpower.

- Contracts may be won or lost at the proposal level, so it is essential that engineering inputs be as accurate and comprehensive as possible. An important factor at this stage is high-quality graphics.

- The cost of making design changes rises rapidly as the design cycle progresses. A program like ADOP allows correct design decisions to be made very early in the design process so that fewer changes are needed as the design matures.

- One reason that the existing analysis system cannot respond efficiently is the lack of an automated data interface between the loads, statics, and dynamics functions.

- Some managers advocated buying outside code and waiting for ASTROS. In reply, it was argued that to remain competitive it would still be necessary, even if ADOP were not being developed, to maintain a core group of engineer/programmers capable of evaluating and implementing state-of-the-art CSM programs and technology and capable of integrating new code with existing in-house analysis systems.

- None of these arguments would be valid were it not for the fact that significant and inexpensive computing power is now available and matrix methods to take advantage of this power are mature and accessible.

COMPETITIVE PROPOSAL WORK

A GOOD EARLY DESIGN = TIME AND COST SAVED LATER

NEED AN INTERDISCIPLINARY DATA BASE

NEED TO KEEP ABREAST OF TECHNOLOGY/PROGRAMS

NEED TO KEEP ABREAST OF COMPETITION

TECHNIQUES AND COMPUTING POWER NOW EXIST

DEVELOPMENT PHILOSOPHY

The objective of ADOP development is to produce user friendly code for the working engineer. There has been much discussion on the issue of user friendliness -- how much should the user be expected or required to know about the code and the methodologies incorporated? Fortunately, the ADOP control language, or ACL "DMAP" approach, allows the user to largely make that decision. He can pick up an existing "black box" ACL sequence or write his own.

Practical considerations dictate that existing modelers be used. We started with the in-house CGSA/CASD modeler but can now process NASTRAN bulk data sets from any compatible modeler.

Similarly, it makes practical sense to interface with existing in-house programs to generate weights and aerodynamics data. Much effort has been expended writing interfaces with these programs and persuading programmers to adopt ADOP data-management utilities for future work.

The main departure from existing practice is in the use of a common finite-element model for static and aeroelastic analysis. Currently, beam models are used for dynamics work, and the translation of data between models is a serious bottleneck. In practice, static analysis models are commonly finer than a one-for-one representation, which is more detailed than necessary for dynamic analysis and very expensive to process. This observation does not yet apply at the advanced design level, but in the future it may be necessary to supplement the static analysis model with a simpler, parallel version for dynamic analysis, or introduce comprehensive global/local analysis features to aid the static analysis of relatively coarse models.

The size of these models dictates that ADOP be optimized for mainframe or supercomputer applications. Douglas is an IBM house that has access to a Cray XMP18. There are no plans to adapt ADOP to mini- or personal computer installations.

As an aid to automating the design process, a comprehensive graphics capability has been specified. This encompasses some pre- and post-processor functions, but the main objective is to provide intermediate processing to aid in data generation, display, and transfer.

Literature reviews and practical experience suggested that the methodology to achieve these objectives was mature and readily available. It was decided to use consultants, when necessary, to ensure that the best available technology was incorporated. In practice, we repeatedly found that development, debugging, and adapting were necessary before existing methods or code could be incorporated in ADOP.

PROGRAM TO BE USER FRIENDLY
USE EXISTING PRE-PROCESSORS (CGSA, PATRAN)
INTERFACE WITH EXISTING IN-HOUSE DISCIPLINES
SAME MODEL FOR STATICS AND DYNAMICS
PROGRAM FOR MAINFRAMES -- NO PC VERSIONS
EXTENSIVE USE OF GRAPHICS DISPLAYS
MINIMAL METHOD DEVELOPMENT -- USE CONSULTANTS

PROGRAMMING TECHNIQUES

Most of the coding for ADOP is in FORTRAN 77, except for a new, C-coded graphics module called IMAGES -- Interactive Modal Aeroelastic Graphical Engineering System. The coding has been done by engineers rather than programmers, but with an awareness of the rules of structured programming and top-down programming. Most are common sense rules which nevertheless need to be emphasized. In essence, they are -- Plan what you are going to do, do it methodically, test it methodically, and establish programming rules so that the code can be modified and maintained as easily as possible. The system operates on IBM 3090 mainframes, which also act as a front-end processor to a Cray XMP18 at McDonnell Douglas in St. Louis.

Top-down programming concepts were applied to the overall design of the highly modular system, but we found that at the module level, the individual programmer must be free to do it his way -- bottom-up if necessary -- without having to plan every detail of the module before starting to code. The programmer must, of course, use the ADOP disk and memory management system (next page), which dynamically allocates virtual memory for array manipulation and provides for associated disk files. Arrays are tracked and manipulated by a comprehensive set of disk and core management utilities. Arrays are defined in detail (name, dimensions, type, and storage location) and the information stored in COMMON blocks. This is virtually the only use of COMMON in ADOP, and its use is transparent to module programmers.

The modules are called by a high-level ADOP control language (ACL), based originally on the Douglas FORMAT program and similar to NASTRAN DMAP and ASTROS MAPOL. At a still higher level, the ADOP run setup (interactive or batch), source deck updates, compiling and linking, and other functions are controlled by a series of TSO CLIST programs.

MODULAR ARCHITECTURE USING FORTRAN 77

IBM 3090 AND CRAY XMP18

DYNAMIC WORK ARRAY (ALMOST NO COMMON BLOCKS)

WORK ARRAY AND DISK MANAGEMENT UTILITIES

HIGH-LEVEL MATRIX/FUNCTION LANGUAGE (ACL)

PROGRAM CONTROL VIA TSO CLISTS

PROGRAM ARCHITECTURE

The figure is a simplified depiction of the ADOP architecture, showing the main data handling features and the relationship between ADOP and existing in-house codes. Starting from the top, basic configuration data is fed to the modeler and loads programs. Except for the generation of mass data, via IMAGES, from CASE, this step is not yet automated. Dataset names from the modeler and loads programs are input through ACL instructions and the datasets converted to ADOP format with translator modules. Program N5K was modified to directly produce data in ADOP format. Hopefully, the ADOP utilities will be adopted for new and updated programs. The ADOPGO CLIST asks the user for the ACL instruction dataset and output dataset names, then executes ADOP, either on line or batch.

Within the ADOP block, dynamic memory is allocated, and the ACL instruction list is compiled and passed as executable code to the execution monitor. The execution monitor allocates output and internally used files, and defines input files for the data base. Instructions are executed sequentially, ending with the WRAPUP module, which closes all files, prints lists of arrays on files and in memory, and exits back to the ADOPGO CLIST. Module architecture consists of driver subroutines or "task supervisors," which prepare input to and accept output from the "function subroutines," which ideally should be stand-alone code, independent of the ADOP system. Note that the only way a module should communicate with the data base is through the ADOP utilities.

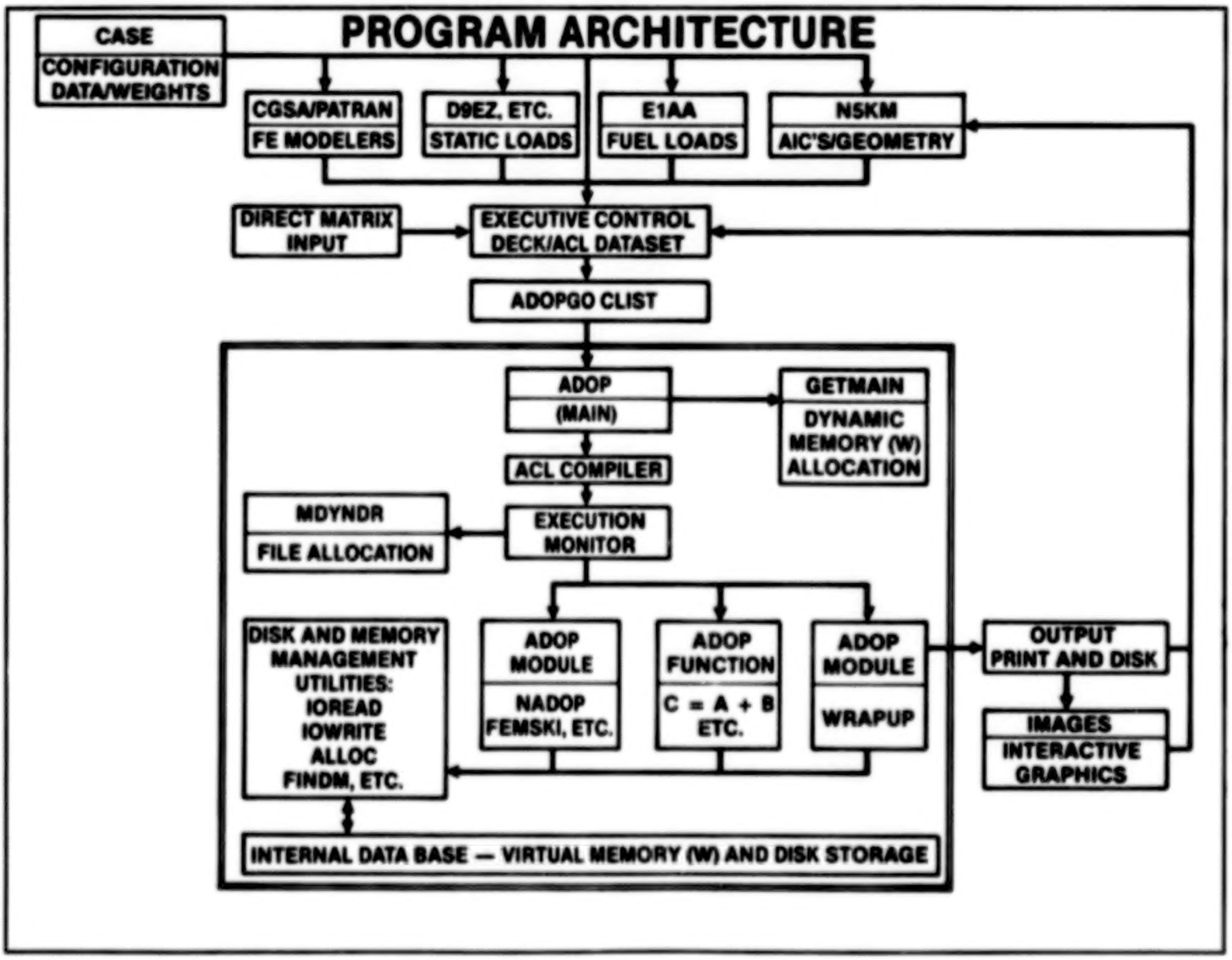
PROGRAM ARCHITECTURE
CASE
CONFIGURATION DATA/WEIGHTS
CGSA/PATRAN
FE MODELERS
D9EZ, ETC.
STATIC LOADS
E1AA
FUEL LOADS
N5KM
AIC'S/GEOMETRY
DIRECT MATRIX INPUT
EXECUTIVE CONTROL DECK/ACL DATASET
ADOPGO CLIST
ADOP
(MAIN)
GETMAIN
DYNAMIC MEMORY (W) ALLOCATION
ACL COMPILER
MDYNDR
FILE ALLOCATION
EXECUTION MONITOR
DISK AND MEMORY MANAGEMENT UTILITIES: IOREAD IOWRITE ALLOC FINDM, ETC.
ADOP MODULE
NADOP FEMSKI, ETC.
ADOP FUNCTION
C = A + B ETC.
ADOP MODULE
WRAPUP
OUTPUT PRINT AND DISK
IMAGES
INTERACTIVE GRAPHICS
INTERNAL DATA BASE — VIRTUAL MEMORY (W) AND DISK STORAGE

GRAPHICS

It was decided early in the ADOP planning process that interactive graphics should be emphasized as an aid to the automation process. After a false start using DYNA-MOVIE-BYU on an E&S 340 work station, we switched to a Silicon Graphics IRIS 3030 work station with a UNIX operating system. The comprehensive Silicon Graphics library firmware was used to write the new code for IMAGES.

The work station has sufficient capacity to operate independently of the IBM mainframe (unlike the E&S 340), but is linked to the IBM for file transfers to and from ADOP. A Seiko copier produces high-quality color screen images on paper or transparencies.

IMAGES performs the following functions:

- Display of the assembled FE model to allow visual checking for modeling errors and inconsistencies
- Definition of mass and weights data. Weights data is translated from the CASE model to the ADOP structural model and redefined as distributed or concentrated masses. Masses from other sources can be added at this stage. This data may be developed interactively on the IBM system, but the process is made much easier with the aid of IMAGES.
- Animated display of mode shapes and static deformations
- Color stress contours
- Graphical splining
- Aerodynamic data points generation

Some of these features -- model display and animated modes -- were initially regarded, perhaps cynically, as management and PR display tools, but they have become useful and popular for verifying the model and analyzing results. The animated modes display in particular has proved very useful for spotting "junk" modes, isolating modeling faults, and interpreting "good" modes.

SG 3030 IRIS WORK STATION (FIRMWARE-BASED, C LANGUAGE)

MODEL DEBUGGING

WEIGHTS/MASS DEFINITION

ANIMATED DISPLAY OF MODE SHAPES

GRAPHICAL SPLINING

AERODYNAMIC MODEL GENERATION

NUMERICAL METHODS

It is not the purpose of this presentation to detail the numerical methods incorporated in ADOP. The figure lists the chief methods currently operational. Future plans include comparisons of methods for accuracy, efficiency and applicability -- for example, Lanczos versus subspace iteration for modal analysis; optimality criteria versus numerical search methods for structural optimization.

As noted previously, it is often difficult to judge the relative merits of different methods just by studying the literature. Generally, the differences between established methods are not great and competing techniques often can be shown to differ only in the numerical "tricks" that are played.

The main area for improvement lies in the strategies employed in the use of the numerical methods -- for example, the wavefront method for solving the finite-element model equations versus the blocked skyline approach; the modal reduction approach for aeroelastic loads calculations versus calculations in discrete structural coordinates.

DISPLACEMENT METHOD STATIC ANALYSIS
- WAVEFRONT EQUATION SOLVER
- FULLY STRESSED DESIGN
- CONSISTENT OR DIAGONAL MASS MATRIX

LARGE ORDER MODAL ANALYSIS
- ACCELERATED SUBSPACE ITERATION
- RESTART
- INDEPENDENT RIGID BODY MODES
- NUMERICAL ERROR MONITORING

DYNAMIC RESPONSE
- DIRECT OR MODAL TRANSIENT RESPONSE
- AUTOMATED TIME HISTORY LOADING

GRAPHICAL SPLINING - HARDER, BEAM SPLINE

K-METHOD FLUTTER LOOP
- DAMPING VS. REDUCED FREQUENCY

NUMERICAL SEARCH
- ADS, CONMIN, ETC.
- SENSITIVITIES

SUMMARY

An Aeroelastic Design Optimization Program (ADOP) is currently being tested at Douglas Aircraft Company.

ADOP was originally intended as a relatively small-scale program to improve structural evaluations at the advanced design level. Soon after full-scale development began in 1985, it became clear that a large-scale capability was required and ADOP was expanded so that problem size is now limited only by available machine resources or cost.

ADOP drew upon experience with FORMAT, NASTRAN, and various in-house dynamics and flutter codes. The aim has been to incorporate state-of-the-art program architecture, numerical analysis, and nonlinear programming methods. Currently the main features of ADOP are

- A comprehensive disk and memory management system
- A high-level function language, ACL
- Large-order finite-element and modal analysis modules, FSD resizing and an automated flutter loop
- A graphics module, IMAGES, for intermediate data processing

To be accepted, a new program must make the analysts' job easier or have capabilities not otherwise available. ADOP offers these features, is well documented, reasonably user-friendly, and backed by expert assistance. In addition, the user may use modelers with which he is familiar.

Development is continuing...

ADOP IS UNDER TEST AT DOUGLAS AIRCRAFT COMPANY, LONG BEACH

EXPANDED FROM SMALL ADVANCED DESIGN CODE TO LARGE-SCALE GENERAL PURPOSE SYSTEM

STATE-OF-THE-ART AEROELASTIC ANALYSIS/OPTIMIZATION FEATURES

USER-ORIENTED

DEVELOPMENT IS CONTINUING

SESSION 14: DYNAMICS AND CONTROL OF FLEXIBLE STRUCTURES

Chairmen: J.-N. Juang and E. Livne

THE ROAD AHEAD

While much has been done, much remains to be done. We must complete work on our flutter optimization system. We must complete the static aeroelastic analysis and design package. We must develop a substructure capability for even larger finite-element models than we have currently analyzed. We must develop new procedures for global-local stress analysis to be used in analysis and design. We must initiate new work on aircraft structural loads. We must coordinate with new work being done in our Dynamics and Loads Research group on transonic flutter and aeroelastics. We must develop new procedures for fatigue life prediction, analysis, and design (Figure 9).

COMPLETE WORK JUST INITIATED

- INTERACTIVE GRAPHIC MODELER FOR AERO-MESH
- STATIC AEROELASTIC PACKAGE
- FLUTTER OPTIMIZER
- COMPOSITE FINITE ELEMENTS
- DIRECT INTEGRATORS FOR LARGE FINITE-ELEMENT MODELS

AREAS OF NEW WORK

- SUBSTRUCTURES, SUPERELEMENTS AND COMPONENT MODE SYNTHESIS
- GLOBAL/LOCAL STRESS ANALYSIS
- AIRCRAFT STRUCTURAL LOADS
- GEOMETRIC NONLINEARITY AND BUCKLING OPTIMIZATION
- TRANSONIC/SUPERSONIC FLUTTER AND AEROELASTIC ANALYSIS AND DESIGN
- FATIGUE LIFE, PREDICTION, ANALYSIS AND DESIGN

Figure 9

LOOKING BACK

Figure 8 shows the work completed and the work just initiated on the ADOP system. We have completed a large-order static and modal analysis system. We have demonstrated a fully stressed design capability for static strength. We have demonstrated a flutter analysis capability and computed design sensitivities for flutter and static strength. We have in place a time-domain integration system for modal models and work has been initiated on a direct integration package for large structural models. Work has been initiated on a new composite finite element library for analysis and design. We have in place a very powerful direct matrix abstraction language (ACL-DMAP), which in some respects is more powerful than the ASTROS-MAPOL or NASTRAN-DMAP languages. We have initiated work on the new static aeroelastic package, which will be coded largely in ACL-DMAP.

WORK COMPLETED

- LARGE ORDER STATIC ANALYSIS AND FSD DESIGN
- INTERFACE WITH SEMI-EMPIRICAL WEIGHTS PROGRAM
- LARGE-ORDER MODAL ANALYSIS
- FLUTTER ANALYSIS
- DIRECT MATRIX ABSTRACTION LANGUAGE (ACL-DMAP)
- TIME DOMAIN INTEGRATORS FOR MODAL MODELS

WORK JUST INITIATED

- INTERACTIVE GRAPHIC MODELER FOR AERO-MESH
- STATIC AEROELASTIC PACKAGE
- FLUTTER OPTIMIZER
- COMPOSITE FINITE ELEMENTS
- DIRECT INTEGRATORS FOR LARGE FINITE-ELEMENT MODELS

Figure 8

AERO-MESH MODELER FOR DOUBLET LATTICE AERODYNAMICS

In a recent development, work has been initiated to add an aero-mesh modeler to the IMAGES system for aeroelastic analysis and design. Neither PATRAN nor Douglas' Computer Graphics Structural Analysis (CGSA) program provides this kind of modeling capability. Currently, we are developing models from an existing data base of components of generic aircraft parts, as well as from three-view drawings. This new capability has been under development since July 15, 1988. Figure 7 shows the aero-mesh model being developed with this new Douglas graphics system.

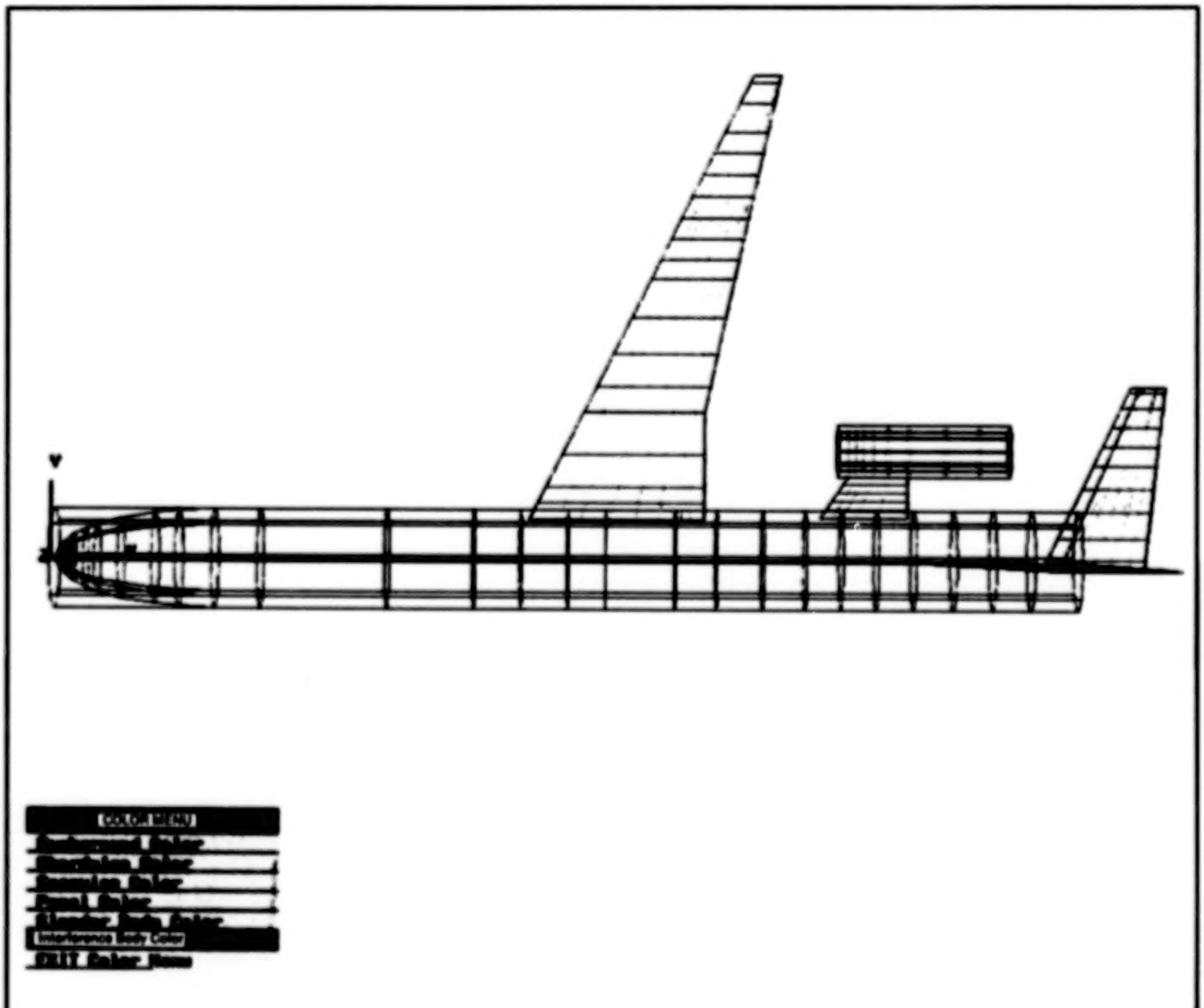

Figure 7

FLAP MODEL TIMING RESULTS

The modal analysis extracted eight modes. One of these is shown in Figure 6. ADOP's front-end processes include model translation from NASTRAN or CASD model files, joint instability identification and correction, equation count, node and element resequencing to minimize the wavefront and envelope size, and the generation of mass and stiffness matrix derivatives (scaled element arrays). These expensive front-end processes result in a well-structured data base for the numerically intensive modal analysis. ADOP uses an adaptive shift subspace iteration procedure for modal analysis. The actual modal analysis of this model was accomplished in 79.26 CPU minutes on the IBM 3090 computer, and 9.70 CPU minutes on the CRAY XMP-18. This speed-up factor of 8.2 is close to the maximum expected computational ratio for these single-CPU machines. Front processes were much lower, resulting in a speed-up factor of only about 2.3 between the CRAY XMP-18 and the IBM 3090. The modes extracted with ADOP were compared with the modes extracted with NASTRAN, resulting in errors of about one percent for all modes. The NASTRAN results were computed with both the Guyan reduction and Householder Givens in superelement procedures and with the NASTRAN block Lanczos procedure. The NASTRAN block Lanczos required 127.14 CPU minutes on the IBM 3090. Direct comparisons between the NASTRAN and ADOP run times are difficult to make because NASTRAN performed more shifts and computed more modes than did ADOP. Block Lanczos should be faster than subspace iteration, but the very efficient implementation of adaptive subspace in ADOP makes it very competitive with NASTRAN Block Lanczos.

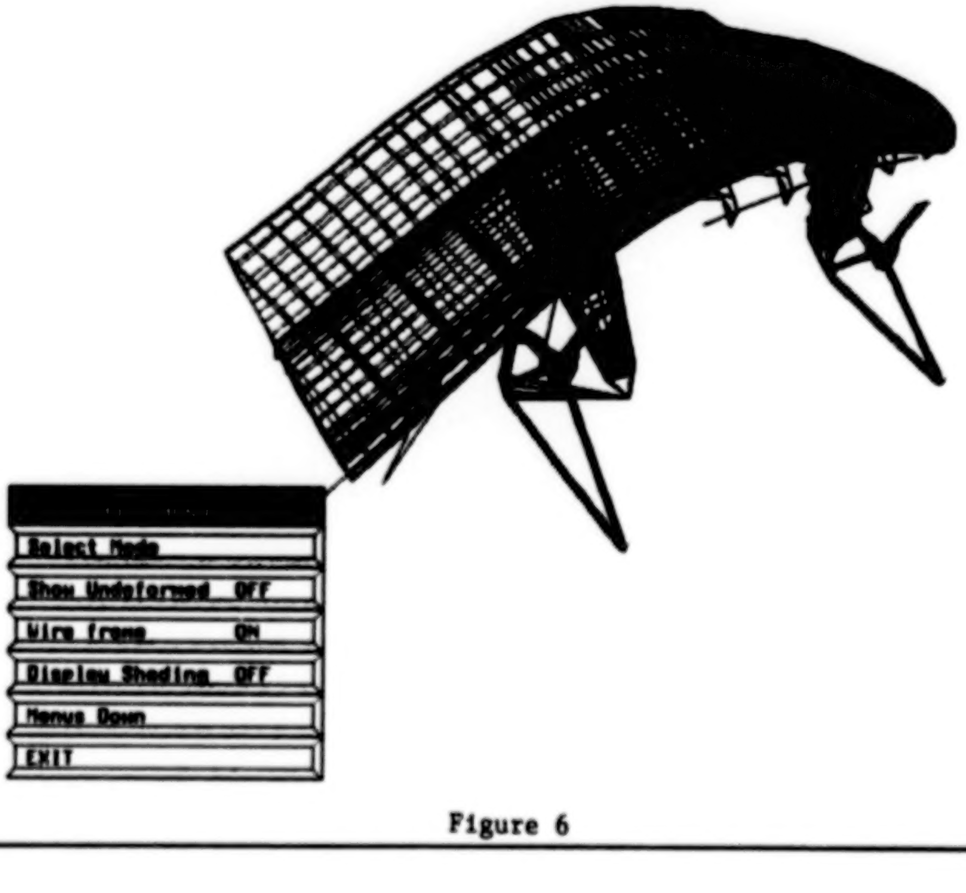

Figure 6

332

BEST COPY AVAILABLE

FLAP MODEL

In one of our first major ADOP applications we computed the modes of a flap model for an aircraft that we currently have under design and development (Figure 5). The widespread availability of computer graphics for finite element modeling has resulted in the development of very large structural models. This inboard flap model uses 35,523 DOF which is larger than the entire MD-83 model. With our first attempt at modal analysis of this model, we discovered numerous singularities. Many were traceable to an incompatible programming assumption: that all models should be able to take a general inertia loading at each node. Many of the bar elements in this model had section properties defined in only one direction. Furthermore, many dummy bar elements had been introduced as a modeling convenience that did not represent any real structure.

These fictitious structural elements and numerous boundary condition errors were the source of most of our problems. ADOP detects joint instability by considering the internal load paths resulting from all elements connected to each joint. Two approaches to automatic joint instability correction (NASTRAN Auto SPC) have been used in other programs. In one approach light stability springs are attached to the unstable nodes. In the other approach the unstable nodes are treated as skew nodes and the global DOF for these nodes are rotated so that the singular directions can be grounded out. In ADOP we had taken the the spring approach. This model showed us that this was a bad approach. As a result, ADOP was significantly reprogrammed to use the skew node approach. This corrected most of the problems. A modal analysis with ADOP was then performed and the modes reviewed with the IMAGES system. As a result, this fly-away vane deflection was discovered in some of the modes, as was an error in the model's boundary conditions. These errors were corrected and the modes recomputed.

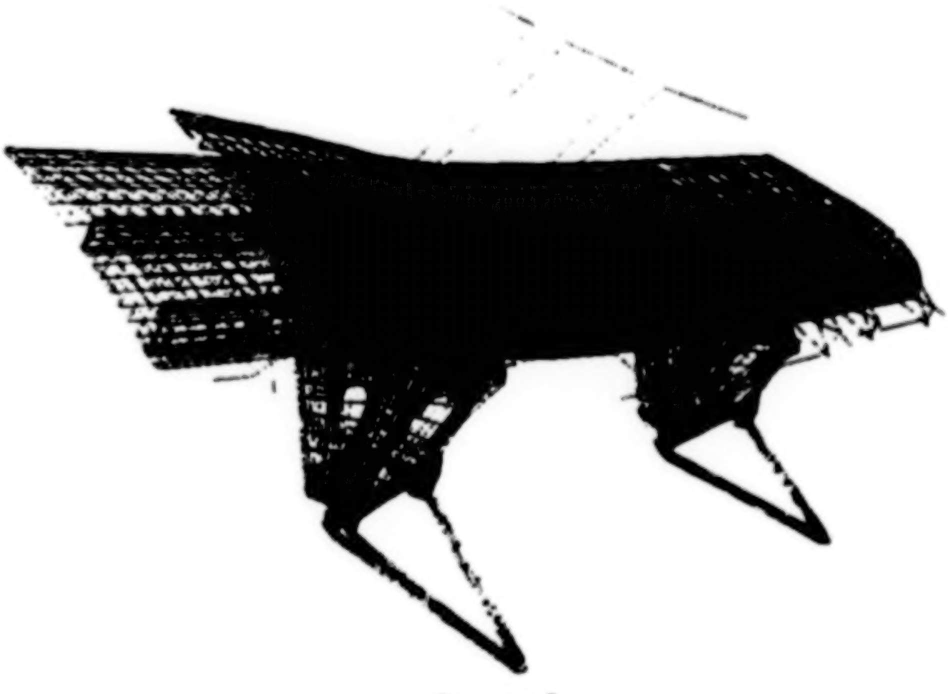

Figure 5

BEST COPY AVAILABLE

LARGE SCALE VERIFICATION MODEL (MD-80 SERIES)

When we started ADOP development, models like the one in Figure 4 - originally developed during the detailed design development of the MD-80 - were considered too large for use in any aeroelastic design optimization procedure. However, after we had developed procedures for weight and balance and large-scale modal analysis, we were challenged to test our procedures against real results from real aircraft. Since we don't do ground vibration tests on paper airplanes, we found ourselves translating this model, computing its weights, and calculating its modes. This model uses about 30,000 DOF and about 10 modes can be computed in about 1.5 hours on the IBM 3090 computer. Modal animation displays can be achieved, but view selection is much slower than for the smaller models. We divided the model into bays for weights analysis. When we translate the finite-element model we have only the finite-element weight. Other weights are determined by our semi-empirical weights program. This program computes the total bay weights and moment of inertia. From this data we compute the tear weight difference between the finite-element model and the bay weight. This is accomplished by dividing the model into bays with our IMAGES interactive graphics program. The tear weight is then distributed to the surface elements in each bay as a nonstructural mass. Major masses may be excluded from this distribution and lumped directly to one or more nodes using the IMAGES system. Passenger floor loading is assigned to the model using the IMAGES system.

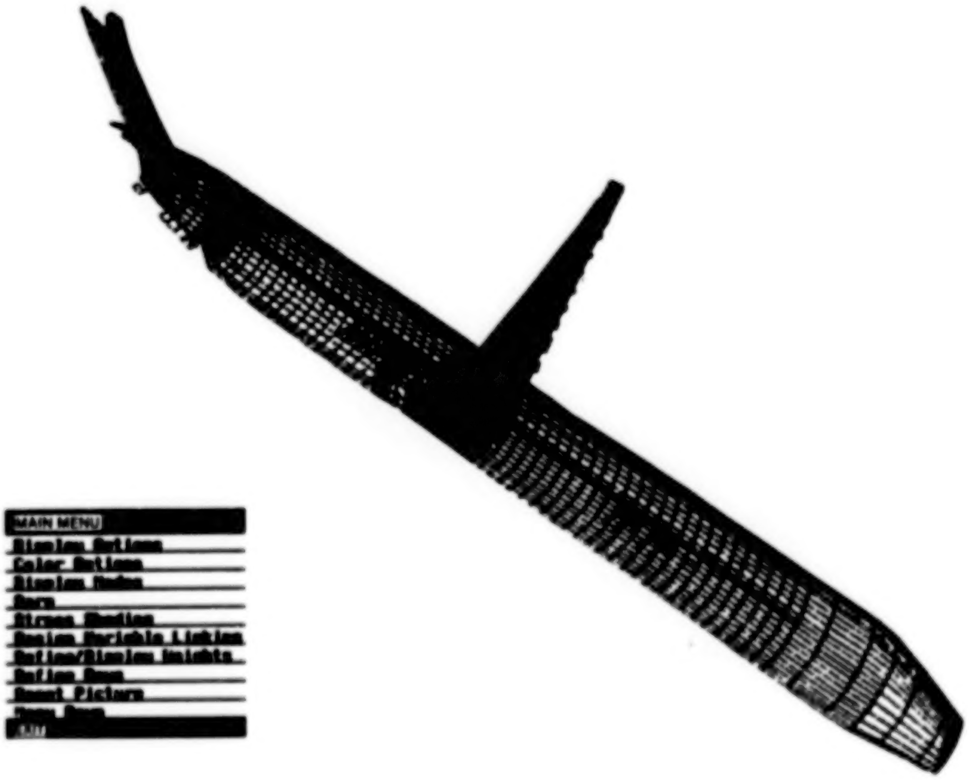

Figure 4

THE BIG TEST PROBLEM

The next test problem developed to test the ADOP program procedures was a complete aircraft model of a high-altitude hypersonic aircraft. Most advanced design study models use 5,000-10,000 DOF. Modal analysis of these models can be completed in a few minutes during a *TSO interactive session on the IBM 3090 computer without resorting to batch-mode processing. Such models can be rotated during animation, even with mirror imaging and solid rendering.

The model shown in Figure 3 was developed by Alan Dodd for an advanced design study. This configuration, which has many interesting design features such as the V-tail, was abandoned as impractical. It makes an ideal study model because no military or commercial trade secrets are revealed in its configuration. It was the first model with which we encountered significant modeling discrepancies with modal display. Some singular modes were developed that showed incorrect element nodal connectivity, even though an interactive graphics system was used to generate the model. These "marble modes" consisted of large deflections of a single node while the rest of the model was relatively stationary. Once these nodes and elements were defined, the modeling problems could be corrected. Subsequently, this condition was discovered in several other models developed for static strength analysis. The ability to compute and display the modes of large-scale, finite-element models has thus become a very valuable diagnostic tool for finite-element structural analysis. This was an unanticipated benefit of ADOP development.

---

*Time-Sharing Option

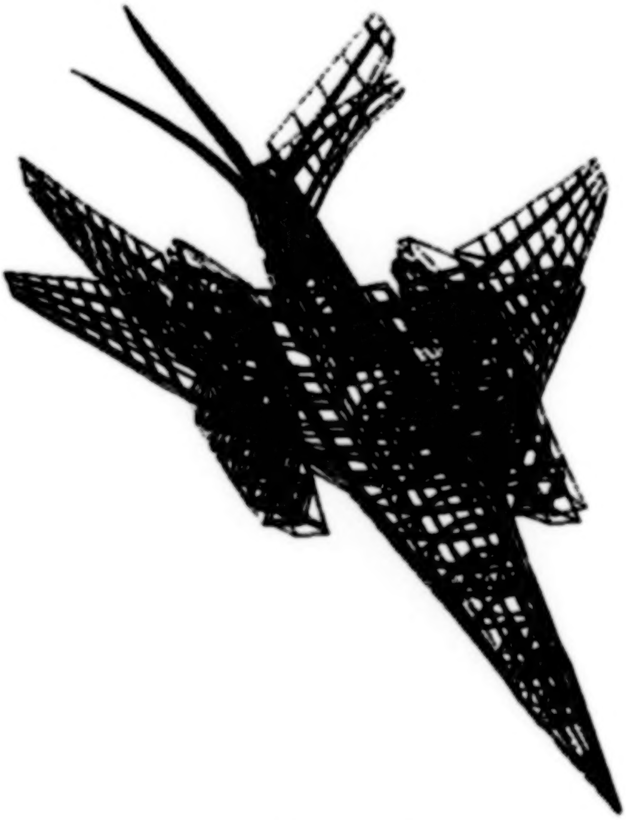

Figure 3

BEST COPY AVAILABLE

THE PILOT TEST PROBLEM (FIN OR SMALL WING)

Since the earliest days of ADOP development we have used the fin or small wing model to develop our data flows and procedures. This model is small enough so that much of the required data can be calculated by hand for verification. The amount of data is small enough that the procedure may, in many cases, be sight verified. Figure 2 depicts one of the simple wing modes. The mesh shown superimposed over the wire frame model is the aero control point mesh. It is a pseudo mesh generated to show how well the spline between the structural mesh and the aero mesh has fit the data. A Harder spline was used, and the fit was quite good even though the spline had to extrapolate beyond the domain of the structural box. This resulted in a slight cusping of the points farthest from the structural box. In general, the Harder spline will work best when no extrapolation is required and the splined points are near the data points. Even the higher frequency modes were fitted adequately with this spline; however, other spline procedures are being developed for use in ADOP. With this model we developed the animation of mode shapes with solid rendering as well as wire frame displays. The user may rotate during modal animation to better visualize the modes.

This same model was used to develop a stress contours post-processor display.

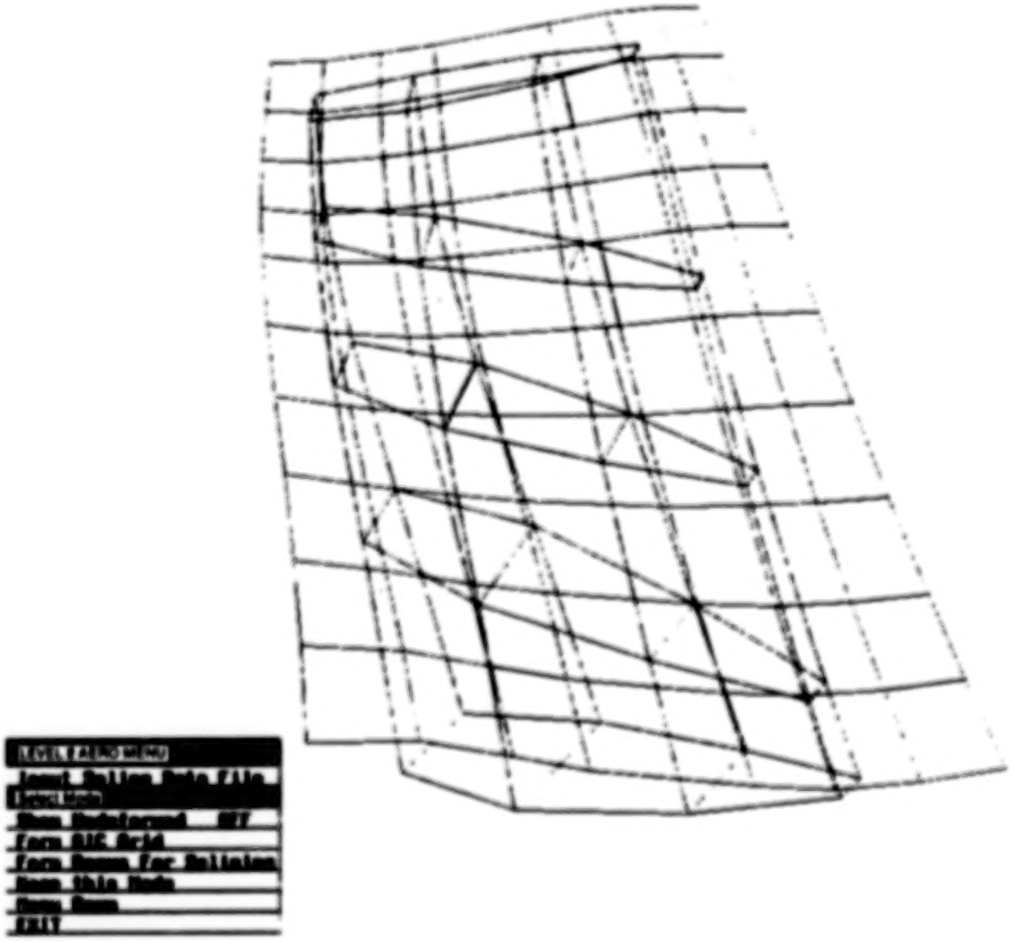

Figure 2

BEST COPY AVAILABLE

THE CHALLENGES OF AEROELASTIC DESIGN OPTIMIZATION

Aeroelastic design optimization for commercial aircraft must consider the full range of design loads and aeroelastic constraints. If significant constraints are omitted from the design optimization process, the result may be far from satisfactory and perhaps worse than a nonoptimal design obtained from conventional procedures. Fatigue is a major consideration: As shown in Figure 1, a design which is close to optimum for only a few load conditions may result in a severely short service life. Nearly 5,000 load conditions resulting from variations in speed, weight, maneuvers, and gust loads must be considered when designing a typical commercial aircraft. Typically, service lift goals are on the order of 60,000 flight hours, with 30,000 flights and landings over a service life of 20 years. To achieve these goals the fatigue life is normally set at about twice the number of flight hours and landings of the design service life. Recent experience indicates that these goals may double or even triple with the next generation of commercial aircraft.

To achieve these goals the analysis and design optimization program must be able to handle the large-scale, finite-element models required for detailed stress analysis. On the other hand, to automate the design process, common structural models for static strength, structural dynamics, flutter, and aeroelastic constraints are required. Critical flutter and aeroelastic constraints often arise near the region of transonic flight. A high-speed commercial transport to service the Pacific Basin will cruise at supersonic or even hypersonic speed, resulting in high heat loading conditions. Buckled skin finite elements used for high load conditions in static strength analysis are inappropriate for modal analysis resulting in a model dependency. Future aircraft will undoubtedly use more advanced composite materials to reduce weight and achieve desirable aeroelastic characteristics. It is with these considerations that we are developing an Aeroelastic Design Optimization Program at Douglas Aircraft Company.

CRITICAL LOAD CONDITIONS FOR STATIC STRENGTH (5,000 LOAD CASES)

FATIGUE DESIGN FOR A 20-YEAR SERVICE LIFE

- 60,000 FLIGHT HOURS/FATIGUE LIFE 120,000 HOURS
- 30,000 FLIGHTS/FATIGUE LIFE 60,000 FLIGHTS

LARGE FINITE-ELEMENT MODELS (10,000 - 60,000 DOF)

COMMON MODELS FOR STRENGTH AND FLUTTER DESIGN

DESIGN FOR TRANSONIC/SUPERSONIC TRANSPORTS

Figure 1

MEETING THE CHALLENGES WITH THE DOUGLAS AIRCRAFT COMPANY AEROELASTIC DESIGN OPTIMIZATION PROGRAM (ADOP)

BRUCE A. ROMMEL
Douglas Aircraft Company, McDonnell Douglas Corporation
Long Beach, California

OPTIMIZATION OF STRUCTURE
AND CONTROL SYSTEM

N. S. Khot
Air Force Wright Aeronautical Laboratories* (AFWAL/FIBR)
Wright-Patterson Air Force Base, Ohio

R. V. Grandhi
Department of Mechanical Systems Engineering
Wright State University, Dayton, Ohio

---

*Wright Research Development Center

INTRODUCTION

The objective of this study is the simultaneous design of the structural and control system for space structures. This study is focused on considering the effect of the number and the location of the actuators on the minimum weight of the structure, and the total work done by the actuators for specified constraints and disturbance. The controls approach used is the linear quadratic regulator theory with constant feedback. At the beginning collocated actuators and sensors are provided in all the elements. The actuator doing the least work is removed one at a time, and the structure is optimized for the specified constraints on the closed-loop eigenvalues and the damping parameters. The procedure of eliminating an actuator is continued until an acceptable design satisfying the constraints is obtained. The study draws some conclusions on the trade between the total work done by the actuators, and the optimum weight and the number of actuators.

OBJECTIVES

- Minimum weight design
- Simultaneous structural and control disciplines
- Closed–loop damping and eigenvalue requirements
- Effect of the number and location of actuators
- Study of the work done by actuators

OPTIMIZATION PROBLEM

Minimize W, weight of the structure, such that the constraints on the closed-loop frequencies, $\bar{\omega}_i$, and the closed-loop damping, $\bar{\xi}_i$, are satisfied. This optimization problem was solved by using the NEWSUMT-A program, which is based on the extended interior penalty function method with Newton's method of unconstrained minimization.

Structure/Control Optimization Problem

Minimize weight

$$W = \sum \rho_i A_i l_i \tag{1}$$

Such that

$$g_j(\bar{\omega}_i) \leq 0 \tag{2}$$

$$g_j(\xi_i) = 0 \tag{3}$$

$$g_j(A_i) \geq 0 \tag{4}$$

Where

$$g_j(\bar{\omega}_i) = \bar{\omega}_i - \bar{\bar{\omega}}_i \tag{5}$$

$$g_j(\xi_i) = \xi_i - \bar{\xi}_i \tag{6}$$

$$g_j(A_i) = A_i - \bar{A}_i(\text{min}) \tag{7}$$

347

CONTROL THEORY

In the state input Eq. 1 (below) (x) is the state variable vector and (f) is the input vector. The matrices [A] and [B] are the plant and input matrices. The plant matrix is a function of the structural frequencies. Eq. 2 defines the performance index where [Q] and [R] are the state and control weighting matrices. The result of minimizing the performance index and satisfying the input equation gives the state feedback control law given in Eq. 3. The Riccati matrix [P] in Eq. 4 is obtained by an interactive solution of the Algebraic Riccati equation.

Control System Design

State input equation

$$\{\dot{x}\} = [A]\{x\} + [B]\{f\} \tag{1}$$

Performance index

$$PI = \int_o^t \left(\{x\}^T[Q]\{x\} + \{f\}^T[R]\{f\}\right) dt \tag{2}$$

State feedback control law

$$\{f\} = -[\tilde{G}]\{x\} \tag{3}$$

Optimum gain matrix

$$[\tilde{G}] = [R]^{-1}[B]^T[P] \tag{4}$$

Algebraic Riccati equation

$$[A]^T[P] - [P][B][R]^{-1}[B]^T[P] + [P][A] + [Q] = 0 \tag{5}$$

CONTROL THEORY (CONC)

The optimal closed-loop system is defined in Eq. 1 (below). The solution to this equation is given in Eq. 3 where x(o) is the initial value of the state vector at time t = 0. The complex eigenvalues of the closed-loop matrix [Å] are defined in Eq. 5 where $\bar{\sigma}_i$ and $\bar{\omega}_i$ are the real and imaginary parts. Eq. 6 defines the closed-loop damping parameter.

Control System Design

Optimal closed–loop system

$$\{\dot{x}\} = [\overline{A}]\{x\} \tag{1}$$

$$[\overline{A}] = [A] - [B][\overline{G}] \tag{2}$$

Solution

$$\{x\} = e^{[\overline{A}]t}\{x(0)\} \tag{3}$$

$$e^{[\overline{A}]t} = 1 + \frac{\overline{A}t}{1!} + \frac{(\overline{A}t)^2}{2!} + \ldots \tag{4}$$

Closed–loop eigenvalues

$$\lambda_i = \overline{\sigma}_i \pm j\overline{\omega}_i \tag{5}$$

Damping parameter

$$\xi_i = -\frac{\overline{\sigma}_i}{(\overline{\sigma}_i^2 + \overline{\omega}_i^2)} \tag{6}$$

PROBLEM DESCRIPTION

This figure shows the finite-element model of ACOSS-FOUR. The number along the elements indicates the collocated actuator and sensor numbers. The structure has twelve degrees of freedom, and four masses of two units each are attached at nodes 1 through 4. The constraints imposed on the optimum design are $\omega_1 = 1.341$, ω_2, $\geq$, 1.6 and $\bar{\xi}_1 = 0.2574$. To calculate the work done by the actuators and study the transient response, an initial displacement of unit magnitude is given at node 2 in the x direction at time t = 0. The diagonal elements in the left top half of matrix [Q] are equal to the square of the structural frequencies, and the weighting matrix [R] is an identity matrix.

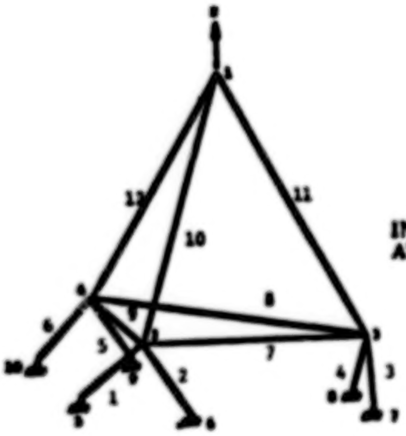

INITIAL UNIT DISPLACEMENT
AT NODE 2 AT T = 0.0

ACOSS FOUR (ACTUATOR LOCATIONS)

MINIMIZE THE WEIGHT WITH CONSTRAINTS ON

$$\bar{\omega}_1 = 1.341$$

$$\bar{\omega}_2 \geq 1.6$$

$$\bar{\xi}_1 = 0.2574$$

WEIGHTING MATRICES

$$Q = \left[\begin{array}{c|c} \ddots\ \omega^2\ \ddots & 0 \\ \hline 0 & \ddots\ I\ \ddots \end{array}\right]$$

$$R = \begin{bmatrix} \ddots\ I\ \ddots \end{bmatrix}$$

NUMERICAL RESULTS

This table gives the rank of the work done by each actuator for different designs. The first row gives the number of actuators as defined in the figure on the previous page. The first column on the left gives the number of actuators present in each design. The first design, 12*, is the initial design which is nonoptimum. All other designs are optimized. The design with 12 actuators was first obtained. It is seen that the ranking of the work done for the nonoptimum and optimum design with 12 actuators is not the same. In the optimum design the maximum work is done by actuator No. 7, and the least work by actuator No. 6. Hence, for the design with 11 actuators the sixth actuator was removed. This process was continued until a minimum weight design satisfying the constraints on the closed-loop eigenvalues and the damping parameters was obtained. The bottom row in the table shows the ranking of the work done by the actuators when five actuators are present. A design satisfying the constraints with less than five actuators could not be obtained.

RANK ORDER OF ACTUATOR INPUT

NUMBER OF ACTUATOR	1	2	3	4	5	6	7	8	9	10	11	12
12*	6	5	8	7	11	12	1	3	2	4	9	10
12	2	3	5	6	4	12	1	8	7	9	10	11
11	2	3	4	9	11		1	7	5	6	8	10
10	2	3	4	9			1	7	5	6	8	10
9	2	4	9	3			1	5	6	8	7	
8	2	4		3			1	5	6	8	7	
7	2	3		4			1	5	6		7	
6	1	3		6			2	4	5			
5	1	4					2	3	5			

*INITIAL DESIGN

NUMERICAL RESULTS (CONT)

This table summarizes the weight, the total work done by all the actuators and the magnitudes of the performance indices for each design. A minimum weight design with minimum total work done is obtained with 11 actuators. The weight and the total work done with 10 actuators are also nearly equal to the design with 11 actuators. So also for these designs, the magnitude of the performance index, PI, is the smallest.

PERFORMANCE INDEX, TOTAL WORK AND WEIGHT

NUMBER OF ACTUATORS	PI_1	PI_2	PI	TOTAL WORK	WEIGHT
12*	159.3	159.8	319.1	79.44	43.69
12	41.15	40.28	81.43	21.92	14.52
11	39.76	38.86	78.62	19.82	14.39
10	40.72	40.11	80.83	19.82	14.40
9	48.56	47.93	88.49	24.08	14.43
8	52.02	49.10	101.12	24.07	14.43
7	64.29	64.63	128.92	28.18	15.22
6	77.27	80.52	157.79	35.71	21.50
5	91.56	96.01	187.66	35.60	21.55

*INITIAL DESIGN

NUMERICAL RESULTS (CONT)

This table shows the percentage of work done by the first five actuators. The remaining actuators did less than 5% of the total work. For designs with more than six actuators, actuator No. 7 did the maximum work. For the remaining two cases with six and five actuators, actuator No. 1 did the maximum work.

PERCENTAGE OF WORK DONE BY THE ACTUATORS

NUMBER OF ACTUATOR	1	2	7	8	9
12*	5.5	6.5	30.2	12.2	24.0
12	17.0	11.0	34.0	5.1	3.3
11	21.0	15.0	35.0	5.0	5.8
10	21.0	16.0	31.0	4.0	6.3
9	17.0	8.0	37.0	6.2	5.3
8	18.0	9.0	40.0	6.5	6.3
7	25.0	11.0	39.0	7.3	5.8
6	36.0	11.0	26.0	10.0	8.2
5	37.0	11.0	29.0	14.0	8.0

*INITIAL DESIGN

NUMERICAL RESULTS (CONC)

This table shows the closed-loop damping parameters for all the designs for the 12 modes. The damping parameter associated with the first mode is equal to 0.25, indicating that this constraint is satisfied for all the designs. Comparing the damping parameters for all the designs, it is seen that as the number of actuators is reduced, the damping parameters associated with the unconstrained modes go on decreasing. For the designs with 11 and 10 actuators, the damping parameters associated with the first 5 modes are equal.

CLOSED-LOOP DAMPING PARAMETERS

12*	12*	11*	10*	9*	8*	7*	6*	5*
0.25	0.25	0.25	0.25	0.25	0.25	0.25	0.25	0.25
0.23	0.23	0.23	0.23	0.15	0.15	0.10	0.06	0.06
0.19	0.16	0.15	0.15	0.17	0.17	0.16	0.03	0.03
0.15	0.14	0.15	0.15	0.10	0.10	0.09	0.08	0.08
0.15	0.16	0.16	0.16	0.14	0.14	0.09	0.08	0.08
0.13	0.09	0.09	0.09	0.06	0.05	0.10	0.03	0.03
0.01	0.09	0.10	0.09	0.09	0.09	0.07	0.06	0.05
0.10	0.09	0.05	0.04	0.07	0.07	0.03	0.06	0.06
0.06	0.07	0.06	0.06	0.07	0.06	0.03	0.04	0.04
0.04	0.07	0.07	0.04	0.07	0.07	0.07	0.04	0.03
0.04	0.07	0.07	0.07	0.06	0.03	0.04	0.04	0.04
0.03	0.06	0.07	0.07	0.04	0.03	0.06	0.03	0.01

*NUMBER OF ACTUATORS

TRANSIENT RESPONSE

These two figures show the dynamic response of the designs with 10 actuators and 5 actuators. The transient response was simulated for a period of 25 seconds at a time interval t = 0.05 secs. The magnitude of the LOS (line-of-sight error) is given by the square root of the sum of the squares of the X and Y components of the displacement at node 1.

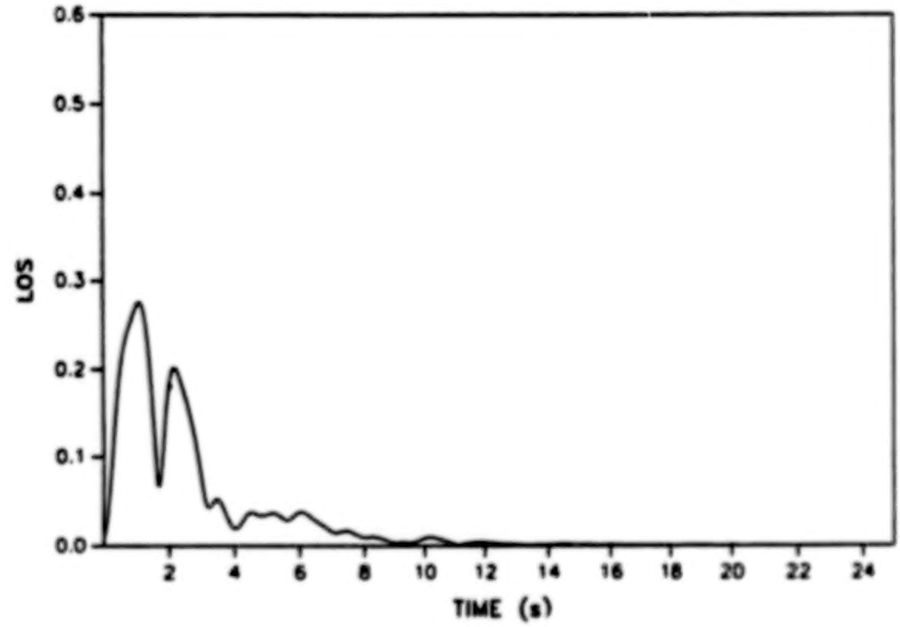
10 ACTUATORS

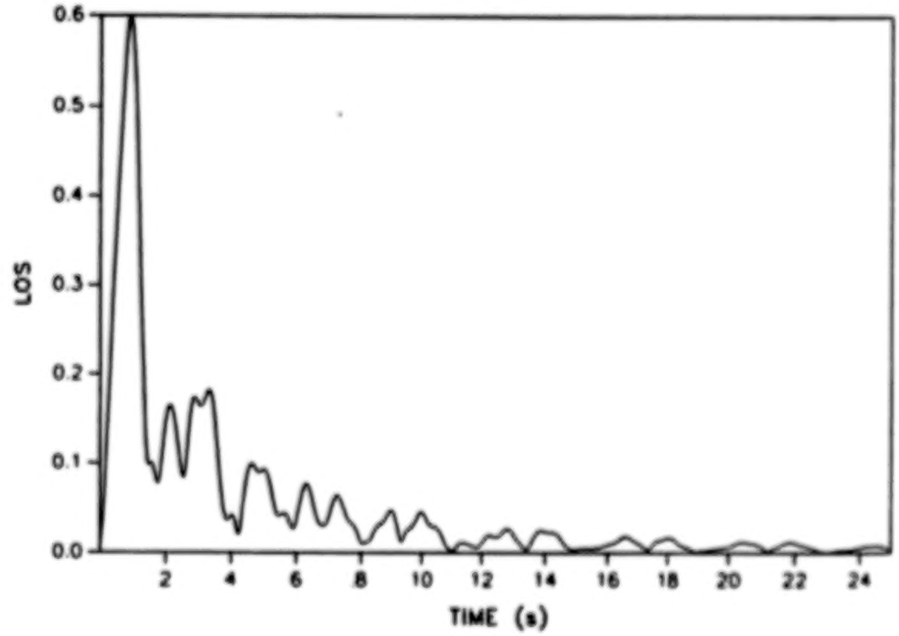
5 ACTUATORS

CONCLUSIONS

This work studied the optimum design of an ACOSS-FOUR structure starting with twelve actuators, one in each member. The performance index, the total work done by all the actuators, and the optimum weight satisfying the specified closed-loop requirements are compared. With a decrease in the number of actuators, the unconstrained damping values decreased substantially compared to twelve actuators. Due to this fact, the work done by the actuators increased to reduce the transient response or in effect to control the disturbance. The optimum weight realized increased to meet the specified closed-loop damping and eigenvalues. The closed-loop system performance index has also had similar effects. For 10 actuators, the total work, performance index and optimum weight were the best, but reducing the number of actuators beyond this number demanded increased work done by the controllers and an increase in the structural weight.

- Simultaneous structural and control optimization
  with closed–loop damping and eigenvalue requirements
- NEWSUMT–A — An optimizer for solving the problem
- Optimum number of actuators for best performance
- Fewer actuators provide less active damping
- Actuators closer to disturbance perform more work

STRUCTURAL OPTIMIZATION AND RECENT LARGE GROUND ANTENNA INSTALLATIONS*

Roy Levy
Jet Propulsion Laboratory
California Institute of Technology
Pasadena, California

---

*The research described in this paper was carried out by the Jet Propulsion Laboratory, California Institute of Technology, under a contract with the National Aeronautics and Space Administration.

NASA 70-METER ANTENNA CONSTRUCTION

Within the past several years, the Jet Propulsion Laboratory has designed and built major ground antenna structures in Spain, Australia, and California. One of the antennas at each location is a 70-meter-diameter structure that is a retrofit of the existing 64-meter antenna. The 64-meter existing antennas were first stripped back to a 34-meter interior and then completely new construction with deeper trusses was added to extend the interior to 70 meters. The 70-meter project included the rare opportunity to collect field data to compare with predictions of the finite-element analytical models. The new quadripod design was tested for its lower mode natural frequencies and the main reflector was measured by theodolite to determine deflections of subsets of the backup-structure deformations under load. The emphasis here will be to examine measurement results and possibly provide some appreciation of the relationship of predictions made from the design model to actual measurements.

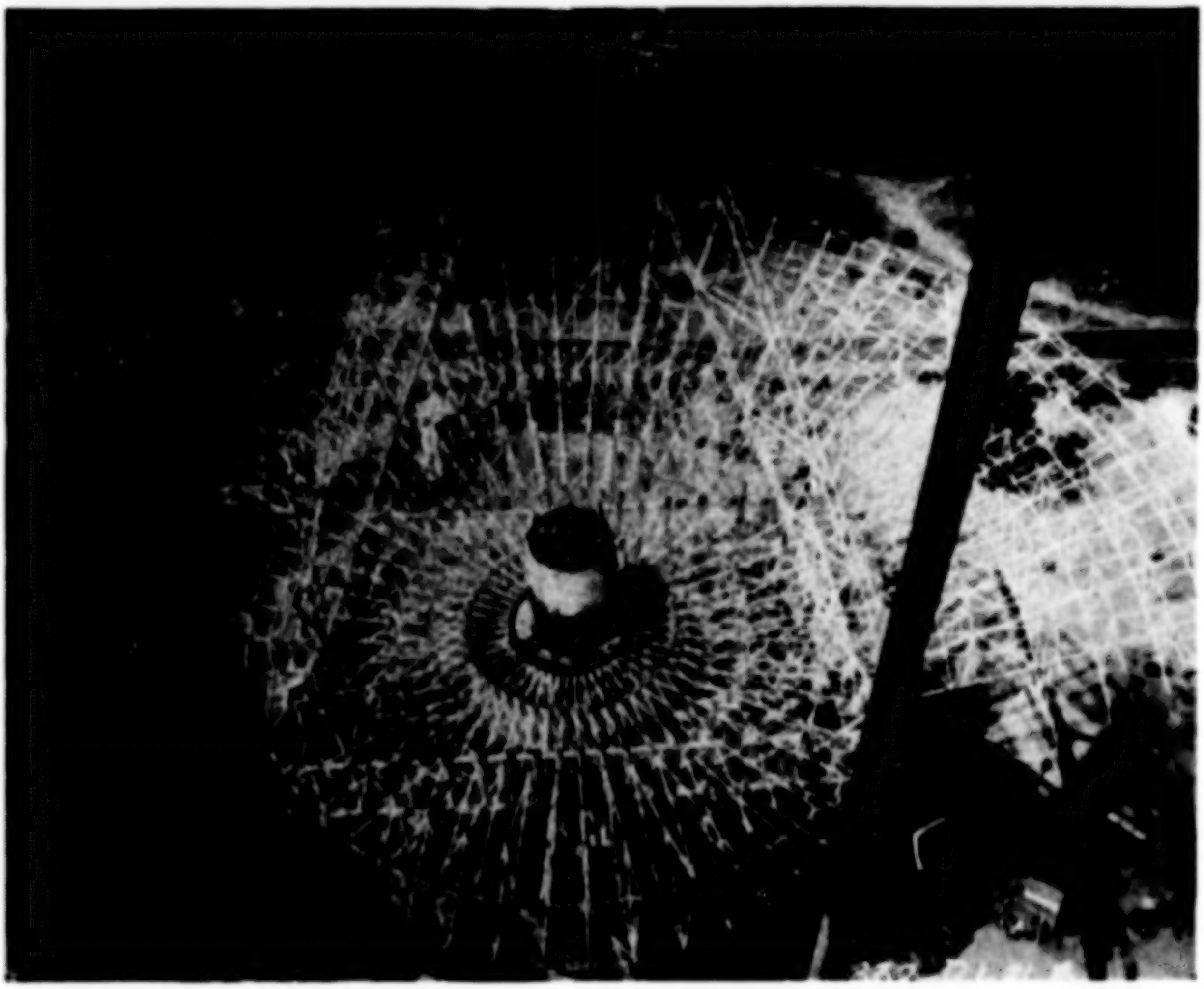

352

BEST COPY AVAILABLE

70-METER COMPLETED ANTENNA

All the 70-meter antennas are steerable both in elevation and azimuth and are characterized by extremely precise surface accuracy and boresight pointing error requirements. These requirements must be maintained for a spectrum of environmental wind and variable-attitude gravity loading. As an example of the required precision, the root-mean-square surface error (after a least-square fit (ref. 1) to an alternative rigid-body-shifted ideal surface) is only 20 to 50 millinches (mils). Furthermore, before any least-squares fitting, the maximum deflection at the 115-foot radius for the 70-meter antenna changes by only about 1.5 inches over the elevation angle range. The structure's contribution to the microwave beam pointing error should be only a few millidegrees, and this includes a penalty due to the rigid-body rotation of the best fitting surface.

BEST COPY AVAILABLE

ANTENNA OPTIMIZATION SOFTWARE

The diverse requirements of maintaining both the surface shape and the pointing accuracy constraints are in conflict when it comes to the design. Because of this, intuitive trial-and-error design and analysis procedures are both time consuming and likely to be unproductive. About 15 years ago, we began the development of our own special-purpose analysis and automated antenna-design-optimization software, called the "JPL-IDEAS" (Iterative Design of Antenna Structures) program. At the first public description (ref. 2) of the program, we were chagrined to learn that Grumman Aerospace had predated us in the use of the name "IDEAS" so that we immediately tacked on the "JPL-" prefix. Since then, there has been a proliferation of computer programs with this name, but the ambiguity does not yet seem to have caused confusion.

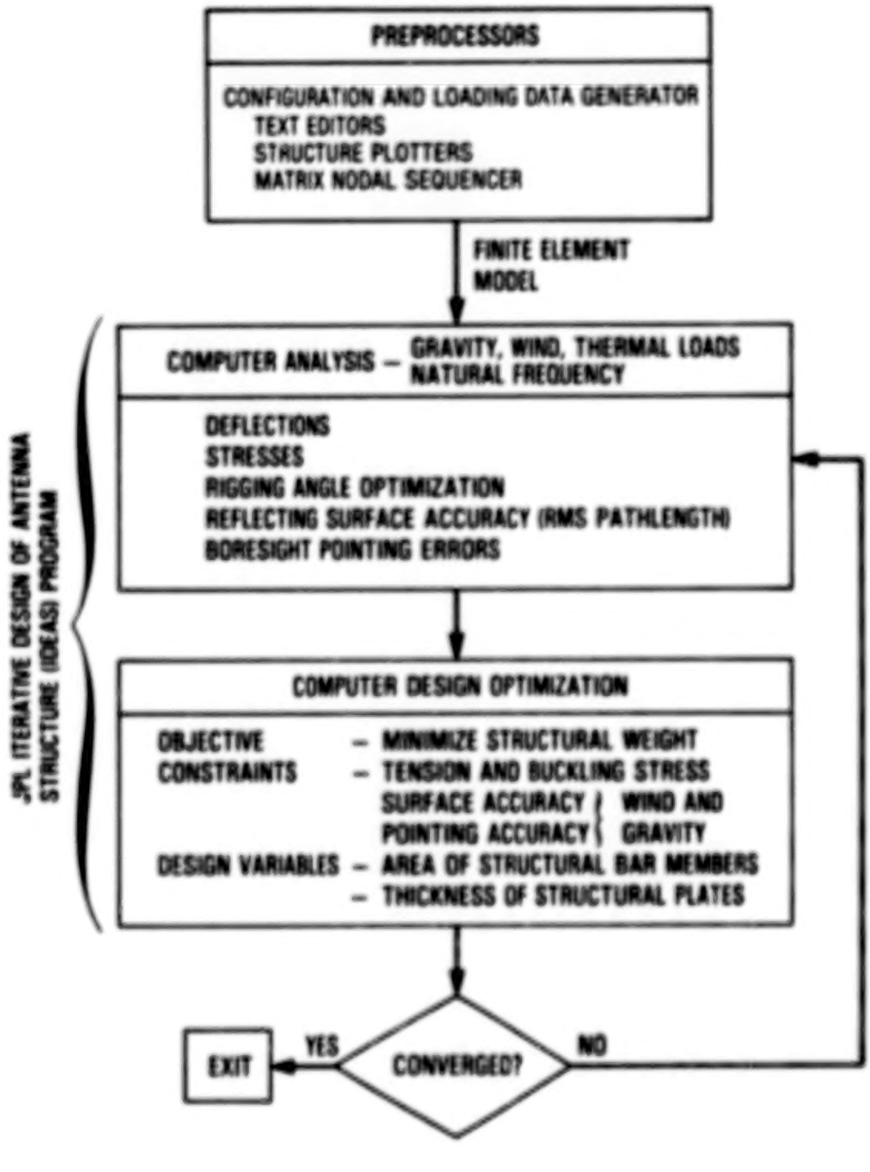
PREPROCESSORS
CONFIGURATION AND LOADING DATA GENERATOR
TEXT EDITORS
STRUCTURE PLOTTERS
MATRIX NODAL SEQUENCER
FINITE ELEMENT MODEL
COMPUTER ANALYSIS – GRAVITY, WIND, THERMAL LOADS
NATURAL FREQUENCY
DEFLECTIONS
STRESSES
RIGGING ANGLE OPTIMIZATION
REFLECTING SURFACE ACCURACY (RMS PATHLENGTH)
BORESIGHT POINTING ERRORS
COMPUTER DESIGN OPTIMIZATION
OBJECTIVE – MINIMIZE STRUCTURAL WEIGHT
CONSTRAINTS – TENSION AND BUCKLING STRESS
SURFACE ACCURACY
POINTING ACCURACY
WIND AND GRAVITY
DESIGN VARIABLES – AREA OF STRUCTURAL BAR MEMBERS
– THICKNESS OF STRUCTURAL PLATES
CONVERGED?
YES
NO
EXIT
JPL ITERATIVE DESIGN OF ANTENNA STRUCTURE (IDEAS) PROGRAM

ANTENNA STRUCTURAL DESIGN CONSTRAINTS

The compliance-type microwave performance requirements of maintaining a nearly ideal microwave reflecting surface figure and providing accurate pointing of the electronic beam lead to a specialized structural optimization formulation. The way we establish virtual ("dummy") loading vectors that allow us to derive the gradients of the compliance constraints and the procedures for applying optimality criteria, and finding the Lagrange multipliers has appeared in refs. 2 through 6. For convenient reference here, the figures below illustrate the nature of the structural deformations and geometric relationships involved in the surface path-length and pointing-error constraints.

PRIMARY COMPLIANCE CONSTRAINTS

- MICROWAVE PATH-LENGTH-ERROR CONSTRAINT
  - MAXIMUM PERMISSIBLE ROOT-MEAN-SQUARE PATH-LENGTH ERROR FROM A BEST-FITTING ALTERNATE SURFACE

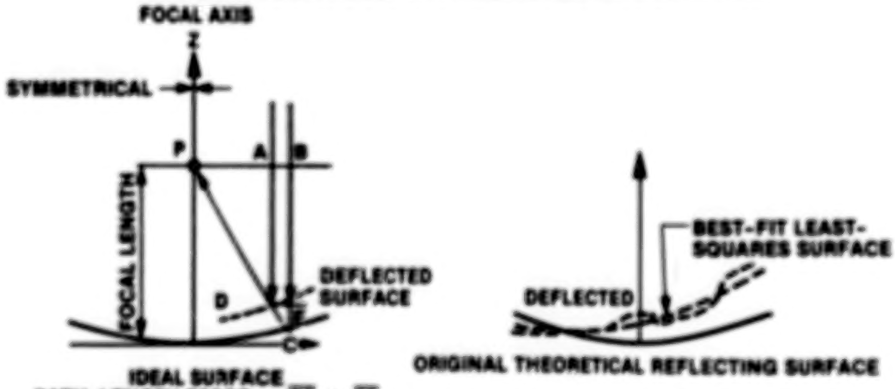
FOCAL AXIS
Z
SYMMETRICAL
P
A
B
FOCAL LENGTH
D
DEFLECTED SURFACE
E
C
IDEAL SURFACE
DEFLECTED
BEST-FIT LEAST-SQUARES SURFACE
ORIGINAL THEORETICAL REFLECTING SURFACE

PATH-LENGTH ERROR = $\overline{EC} + \overline{CD}$

- BORESIGHT POINTING-ERROR CONSTRAINT

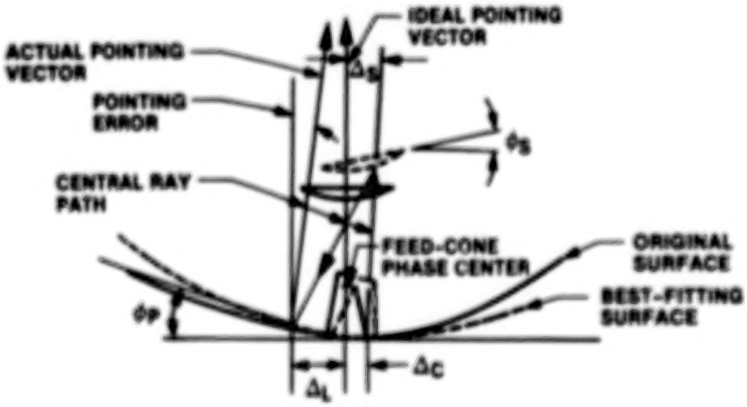
ACTUAL POINTING VECTOR
IDEAL POINTING VECTOR
Δ_S
POINTING ERROR
ϕ_S
CENTRAL RAY PATH
FEED-CONE PHASE CENTER
ORIGINAL SURFACE
BEST-FITTING SURFACE
ϕ_P
Δ_L
Δ_C

FIVE COMPONENTS OF ANTENNA POINTING ERROR

Δ_L - BEST-FIT PARABOLOID LATERAL VERTEX SHIFT
ϕ_P - BEST-FIT PARABOLOID AXIS ROTATION
Δ_S - SUBREFLECTOR LATERAL TRANSLATION
Δ_C - FEED-CONE LATERAL TRANSLATION
ϕ_S - SUBREFLECTOR ROTATION

DESIGN FOR MINIMUM NATURAL FREQUENCY

In addition to the antenna microwave performance constraints, there are requirements to maintain minimum natural frequencies in conjunction with control system instability. We found that the minimum natural frequency of the 70-meter structure was, for a decoupled quadripod mode, similar to that of the quadripod supported independently on a rigid foundation. This permitted a simplified design of the quadripod for minimum natural frequency: the quadripod was considered an isolated, stand-alone component. An algorithm to obtain maximum natural frequency for a prespecified structural mass was described in ref. 7 and executed with no difficulty. In the same reference and in others (refs. 8 and 9), it was found necessary to scale the design when the optimization was formed in the traditional way of minimizing the structural mass for a specified constraint on minimum natural frequency. Since then, the scaling requirement has been removed from our algorithm. We show the highlights of our more recent algorithm in the figure. With this formulation, the natural-frequency design case can be handled as another constraint case along with compliance and stress constraints in conventional optimality criteria problem formulations.

RAYLEIGH QUOTIENT, $\omega^2 = \dfrac{\phi^T K \phi}{\phi^T M \phi}$

$\dfrac{\partial \omega^2}{\partial a_i}$ LEADS TO: $\dfrac{1}{\underline{M}\, a_i} \times V_i$

WHERE $V_i = \phi^T k_i \phi - \omega^2 \phi^T m_i \phi$

NOMENCLATURE

K = STIFFNES MATRIX
M = MASS MATRIX
ω^2 = EIGENVALUE
ϕ = EIGENVECTOR
$\underline{M} = \phi^T M_i \phi$
a_i = DESIGN VARIABLE
k_i, m_i = ASSOCIATED WITH a_i
$\underline{M} = M_v + M_s$ WHERE M_v DOES NOT DEPEND ON a_i AND M_s DOES
L_i, E_i, γ_i = LENGTH, MODULUS, DENSITY ASSOCIATED WITH a_i
c_R, c_D = ELEMENT STRESS RESULTANTS FOR EIGENVECTOR

	DISPLACEMENT METHOD	FORCE METHOD
VIRTUAL WORK	$\phi^T K \phi$	$C_R\, C_D\, L/AE$

THEN $V_i = (L/aE)_i\, (c_R\, c_D')_i$, IN WHICH $C_D' = c_{D_i} - \omega^2 \phi^T m_i \phi\; (a/L\, C_R)_i$

LET $F_{ij} = \dfrac{C_R\, C_D'}{\underline{M}\, E}$, THEN $\dfrac{\partial \omega^2}{\partial a_i} = F_{ij}\, (L/a^2)_i$

FORM THE CONSTRAINT: $g_j = \omega_j^{*2} - \omega^2 < 0$, WHERE ω_j^* = PRESPECIFIED MINIMUM

THEN THE STANDARD OPTIMALITY CRITERION METHOD GIVES: $a_i' = (\sum_j (F_{ij}/\gamma)_i\, \lambda_j)^{1/2}$

IN THE SPECIAL CASE OF ONE FREQUENCY CONSTRAINT,

$\lambda^{1/2} = [\omega^{*2} - \omega^2\, M_v/M - (\sum V a'/a)_{\mathrm{BOUNDED}}] / (\sum F_{ij}\, L\, (F_{ij}/\gamma)^{1/2}/a^2$

OPTIMIZATION MODEL STATISTICS

The data show the relative complexity of the design-optimization problems. Both tabulations are for half-structure models with respect to one plane of symmetry. Most of our loadings are symmetrical with respect to this plane, but for design of the reflector for side wind loads, the design is automated for reflective symmetry and uses two different sets of boundary restraints. For the quadripod, we know that the lowest mode will be torsion with respect to its long axis; therefore, we design the quadripod for natural frequency with antisymmetric restraints at the plane of symmetry. On our UNISYS 1100/91 mainframe computer, a quadripod design is considered to be a small problem. However, the full 70-meter model design process is formidable. From 5 to 10 design cycles with about 10 to 15 path-length and pointing-error constraints could involve several hours of throughput and from $200 to $1000 in computer charges. The computer use is dominated by the analysis effort, which is dominated by decomposition of the stiffness matrix. Stress and Euler buckling constraints present no difficulties and these are handled as side constraints and readily treated by computing appropriate lower size bounds at each design cycle.

	HALF-STRUCTURE MODELS	
ITEM	QUADRIPOD	BACKUP STRUCTURE WITH QUADRIPOD
NODES	156	1986
UNCONSTRAINED DEGREES OF FREEDOM	420	5350
MAXIMUM NODAL WAVEFRONT	22	86
ROOT-MEAN-SQUARE NODAL WAVEFRONT	16	65
UNIVAC DECOMPOSITION TIME CPU, s	8	160
ROD ELEMENTS	443	6486
PLATES (TRIANGLE, SHEAR, QUADRILATERAL)	30	240
DESIGN VARIABLE GROUPS	42	708
UNEXCLUDED DESIGN VARIABLE GROUPS	39	435
WEIGHT OF STRUCTURE, kips	27	1235
PARASITIC WEIGHT, kips	11	635

IN-PLANT QUADRIPOD ASSEMBLY

The quadripod with its apex structure and a concrete weight to simulate the 12,000-pound subreflector were assembled at the fabricator's plant in Coslada, Spain, for a natural frequency test. The apex structure is about 85 feet above the foundation. Each leg is a four-post, trapezoidal cross-section tower. The posts are 5-inch by 3-inch rectangular tubes. The struts and diagonals are smaller square tubes. The two deep side faces and the widest end face are Pratt-Howe trusses, and the narrowest end faces are solid plates. Outrigger braces connected to the second lowest bay of the tower truss can be seen near the bottom.

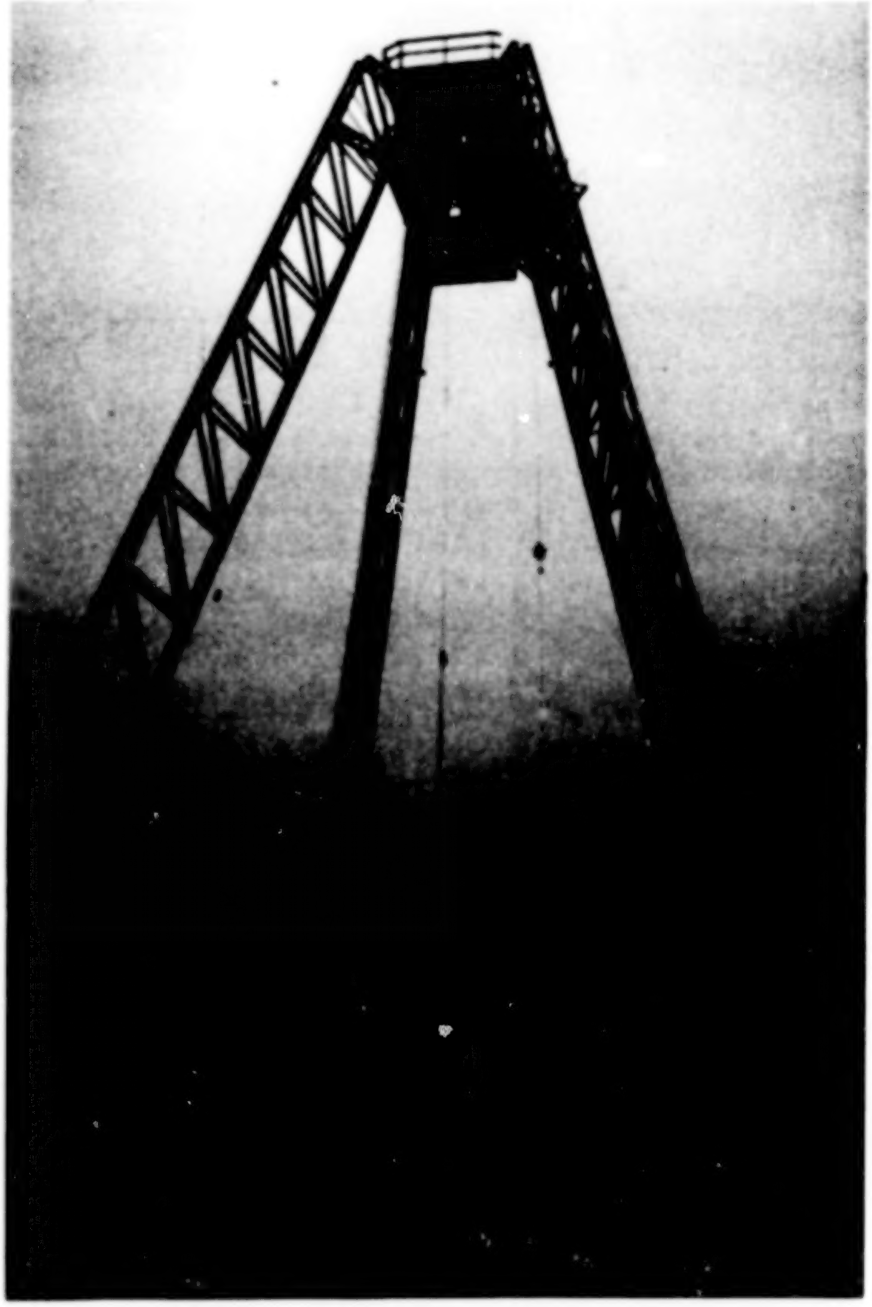

1400

BEST COPY AVAILABLE

OUTRIGGER BRACE CONNECTION

The bolts at this flange splice plate were drawn up tight, and welds were in place during one set of vibration tests and the bolts were removed and welds cut off during another set. Consequently, the tests were performed for two different structures; one set was with effective outrigger braces and the other was with the braces removed. The braces were added to the design when the computer optimization process made it evident that a 1.22-Hertz constraint goal for minimum natural frequency was almost unachievable because of a separate requirement for a narrow-leg cross section to reduce microwave blocking. The configuration with braces removed was tested to confirm that the frequency without braces was too low and that the braces, which tend to be both physical and esthetic nuisances, were really required.

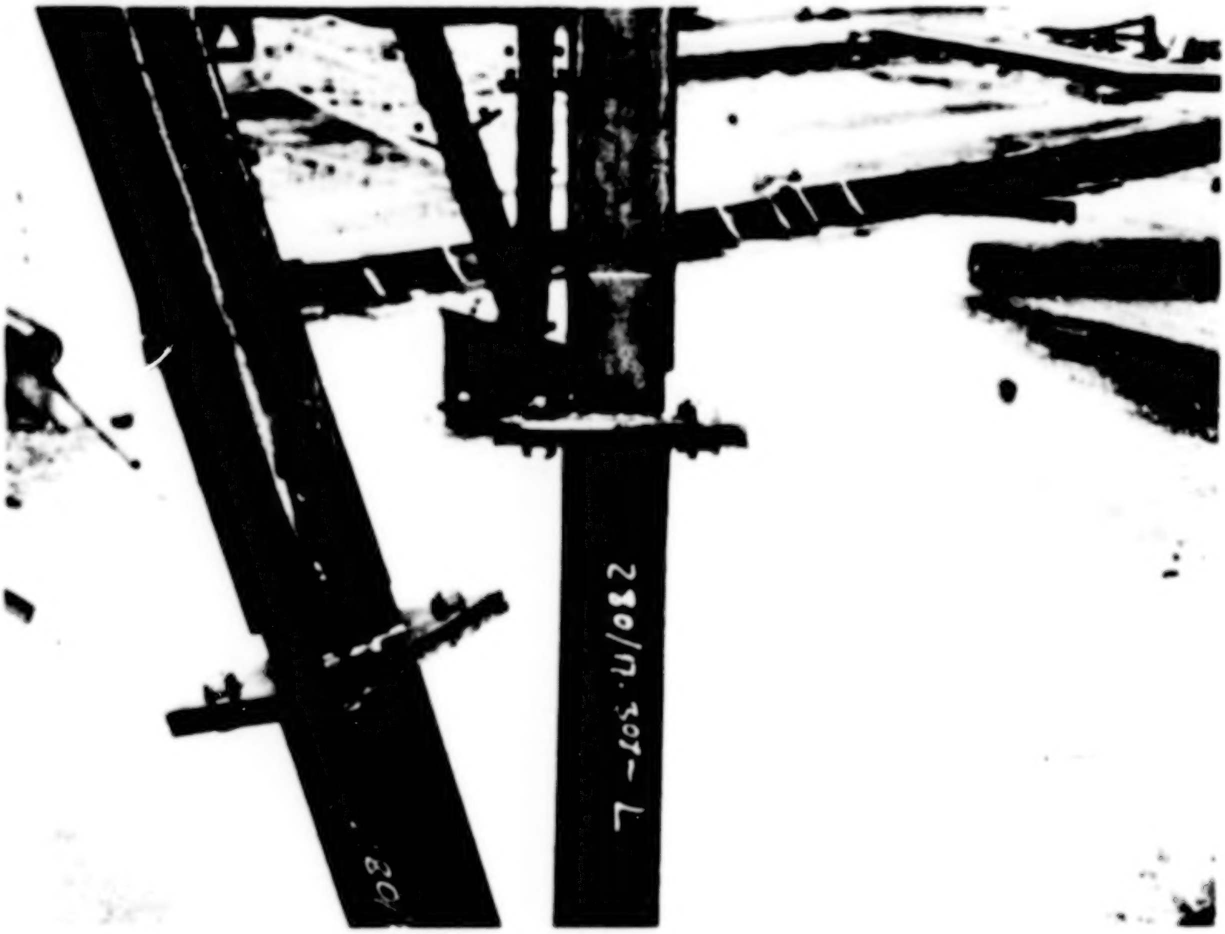

BEST COPY AVAILABLE

APERTURE BLOCKING SHADOW AND QUADRIPOD LEG PROFILE

The aperture blocking of the quadripod assembly consists of two types: plane wave and spherical wave. The plane wave is less important and it consists of the areas masked by the subreflector and the area determined by the projection of the legs on the aperture plane. The spherical wave area is much larger, beginning with a width equal to the leg width at the base of the leg and widening as rays from the focal point intersect the leg above the base and then fan out to reach the surface at points beyond the base.

The sketch of the leg cross-section trapezoids for the prior 64-meter antenna and the new 70-meter extension shows a much smaller profile for the 70-meter antenna. Consequently, the blocking effect of the 70-meter quadripod is 3.4% of the aperture; this provides a significant performance advantage with respect to the 6.3% shadow of the 64-meter quadripod. Nevertheless, and notwithstanding confirming analyses by the NASTRAN program, which was also used for buckling analyses, it was thought advisable to field-test the design predictions because of the unprecedented slim-leg profile.

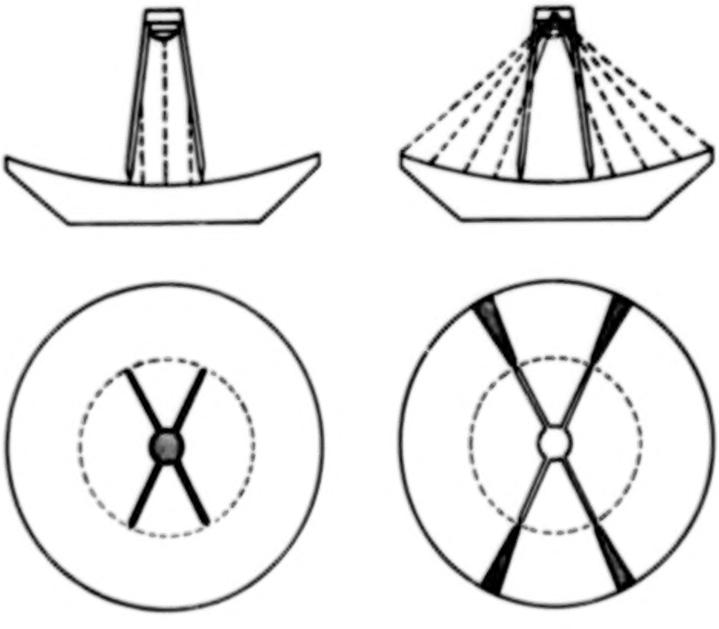

PLANE WAVE AND SPHERICAL WAVE BLOCKAGE

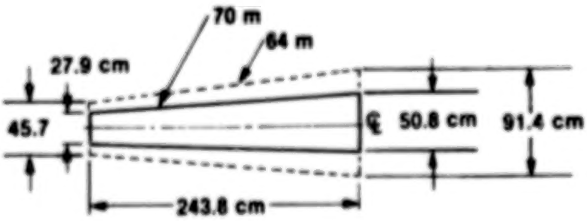

QUADRIPOD CROSS-SECTIONAL PROFILE

ACCELEROMETER AND SHAKER PLACEMENT

The vibration tests were conducted by Kinemetric, Inc., (ref. 10) of California. Ambient tests were first performed to locate the frequencies and characteristics of the lowest modes. This information was used to guide steady-state shaker-excited vibration sweeps that provided confirming information on frequencies, mode shapes, and damping ratios.

The figure shows the accelerometer and shaker locations used during the tests. The Y coordinate on the figure is in the antenna pitch direction, the X coordinate is in the side direction, and the Z coordinate is in the focal direction. Rotations about the Z axis when the antenna points to zenith and about the Y axis when the antenna points to the horizon directly couple with the servo azimuth drive system. At other elevations, components of these motions couple with the azimuth drive. Motions about the X axis can couple with the elevation drive at every antenna attitude.

The eight accelerometer stations A through H indicate possible locations for the instrumentation. Depending upon the particular test and mode shape anticipated from the finite-element model, accelerometers were oriented and reoriented along appropriate axes for each of the tests.

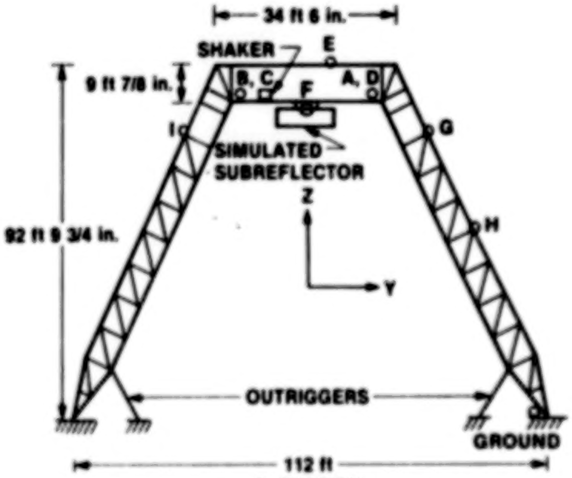
34 ft 6 in.
SHAKER
E
9 ft 7/8 in.
B, C
A, D
F
I
G
SIMULATED SUBREFLECTOR
Z
Y
H
92 ft 9 3/4 in.
OUTRIGGERS
GROUND
112 ft

ELEVATION

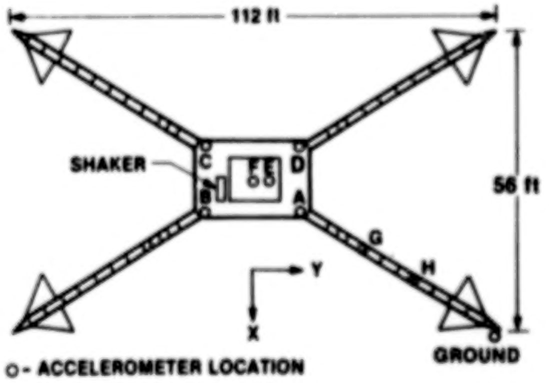
112 ft
SHAKER
C
F E
D
B
A
56 ft
G
H
Y
X
GROUND
○- ACCELEROMETER LOCATION

PLAN

TABULATIONS OF PREDICTED AND MEASURED FREQUENCIES

In addition to observing that the prediction models provide a reasonable representation of the measured frequencies, it can be seen that there really are two different structures (e.g., one without and one with outriggers) with significantly different frequencies. Consistent with the computer design, the outriggers are essential to achieving the 1.22-Hertz constraint.

Measured damping in most cases was less than 1%. The actual damping when on the antenna is likely to be less than measured because several connections that were bolted for the temporary assembly are fully welded at final assembly.

When comparing predictions with measurements, the idealizations made to expedite generating and processing the computer model are of two opposing types:

(1) The model is pin-jointed with 3 degrees of freedom per node. Almost all of the actual joints are fully shop or field welded. This would cause the structure to be stiffer than modeled.

(2) The elastic axes of all members are assumed to meet exactly at the nodal points in the model. The actual detailing and fabrication introduces some small eccentricities at the joints. This would cause the structure to be more compliant than modeled.

NO OUTRIGGER BRACES				WITH OUTRIGGER BRACES			
COMPUTER MODEL		MEASURED		COMPUTER MODEL		MEASURED	
Hz	DESCRIPTION	Hz	DESCRIPTION	Hz	DESCRIPTION	Hz	DESCRIPTION
0.64	TORSION	0.70	TORSION	1.30	TORSION	1.27	TORSION
1.29	X-TRANSLATION	1.36	X-TRANSLATION	1.97	X-TRANSLATION	1.76	X-TRANSLATION
1.55	LEG BENDING	1.74	LEG BENDING	2.72	Y AND PITCH	2.62	Y-TRANSLATION
1.73	LEG BENDING	1.89	LEG BENDING	3.01	LEG TWIST	3.14	LEG BENDING
1.84	LEG TWIST	2.00	LEG BENDING AND TORSION	3.09	LOCAL LEG TWIST	3.38	LEG BENDING
1.96	LEG TWIST	2.14	LEG BENDING AND TORSION	3.25	Y AND PITCH	3.59	LEG BENDING
2.14	LEG BENDING	2.26	LEG BENDING	3.56	Y		
2.15	LEG BENDING			3.79	LOCAL TWIST		
2.21	LEG, LOCAL			4.17	LEG BENDING	4.22	LEG BENDING
2.69	CANTILEVER PITCH	2.48	FIRST Y-TRANSLATION	4.24	LEG BENDING	4.60	LEG BENDING

MODE SHAPE, ELEVATION VIEW

In addition to comparing predicted with measured frequencies, a more stringent test would be to compare mode shapes. To do this, it is necessary to deal with the independent normalizations of the predicted and measured eigenvectors. Here, for each test, the set of mode shapes derived from accelerometer measurements was normalized to the largest component in the set. The corresponding subset of the prediction model eigenvectors was similarly and independently normalized to its own largest component. Consequently, measured and predicted mode shape displacements can be compared on the basis of both direction and, to some extent, magnitude.

The figures show first-mode eigenvector comparisons plotted to an enlarged scale on an elevation view of the quadripod. These are projections on the X-Z plane of the X-axis displacement components.

FIRST MODE - NO OUTRIGGER BRACES:
--- 0.70 Hz, MEASURED
— 0.84 Hz, PREDICTED

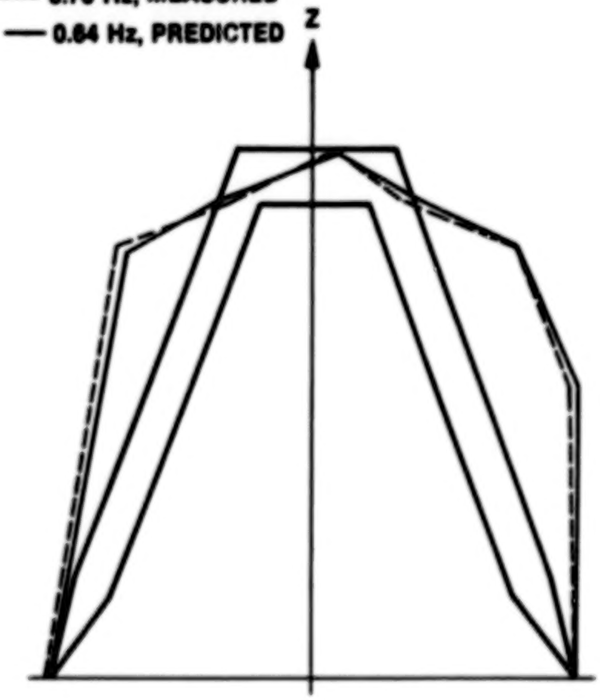

FIRST MODE - WITH BRACES:
--- 1.27 Hz, MEASURED
— 1.30 Hz, PREDICTED

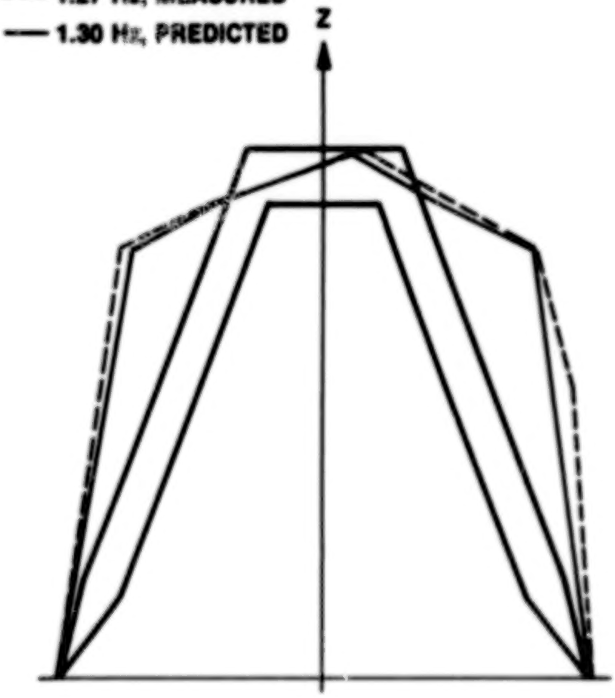

FIRST-MODE EIGENVECTOR COMPARISONS

The Z-axis eigenvector displacement components are usually insignificant in comparison to the X or Y components. Consequently, plotting mode-shape vectors as projected on the X-Y plane provides an almost complete picture of the vector. Notice that here the directions of prediction and measurement vector components are within a few degrees of coincidence and the magnitudes tend to agree also.

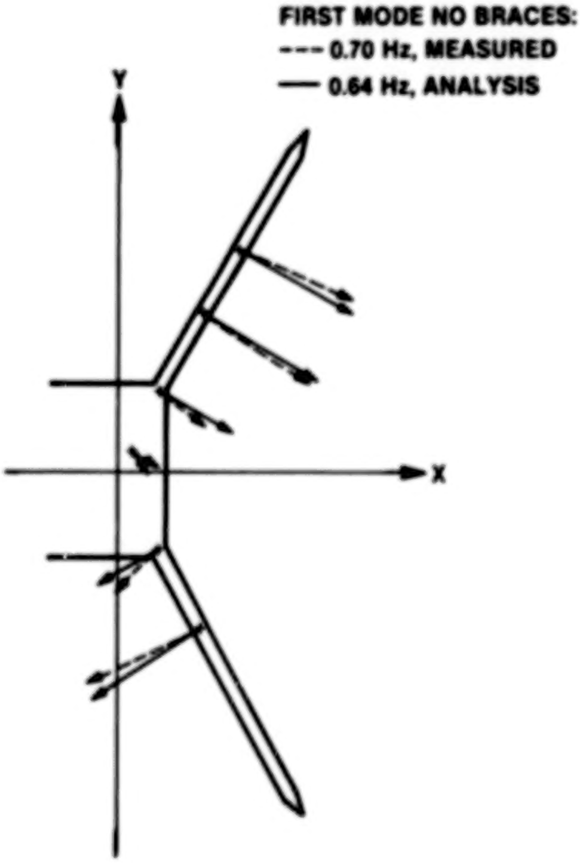
FIRST MODE NO BRACES:
--- 0.70 Hz, MEASURED
— 0.64 Hz, ANALYSIS
Y
X

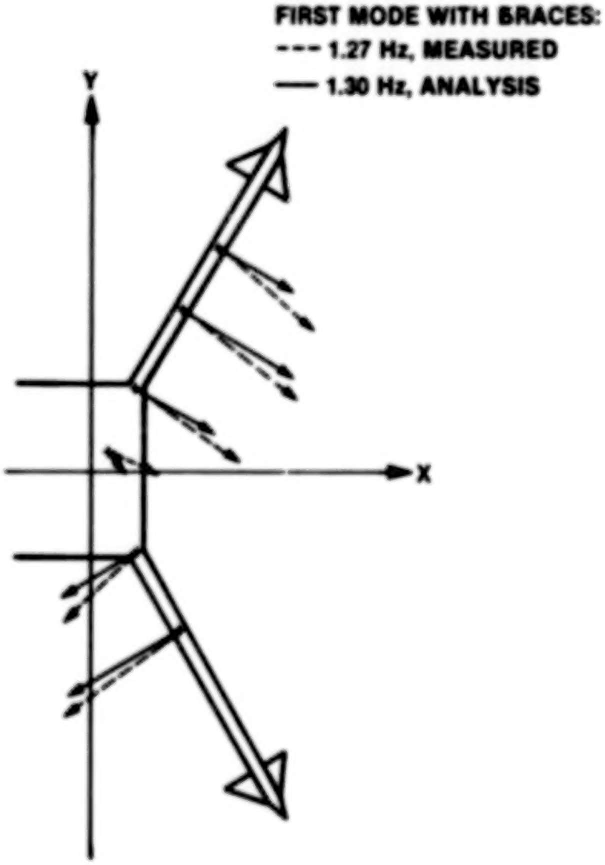
FIRST MODE WITH BRACES:
--- 1.27 Hz, MEASURED
— 1.30 Hz, ANALYSIS
Y
X

SECOND-MODE EIGENVECTOR COMPARISONS

The correspondence between second-mode predicted and measured eigenvectors is seen to be about as consistent in direction and magnitude as for the first mode.

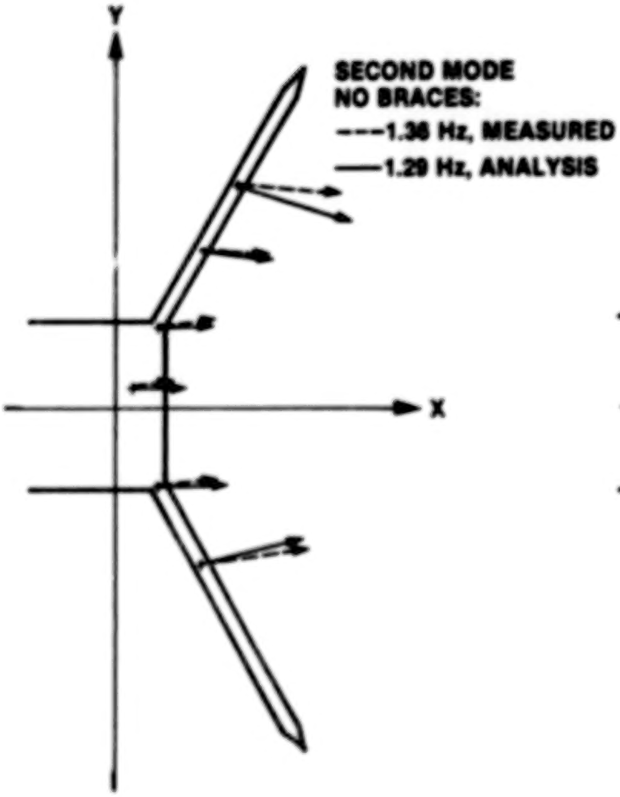
Y
X
SECOND MODE
NO BRACES:
---1.36 Hz, MEASURED
—1.29 Hz, ANALYSIS

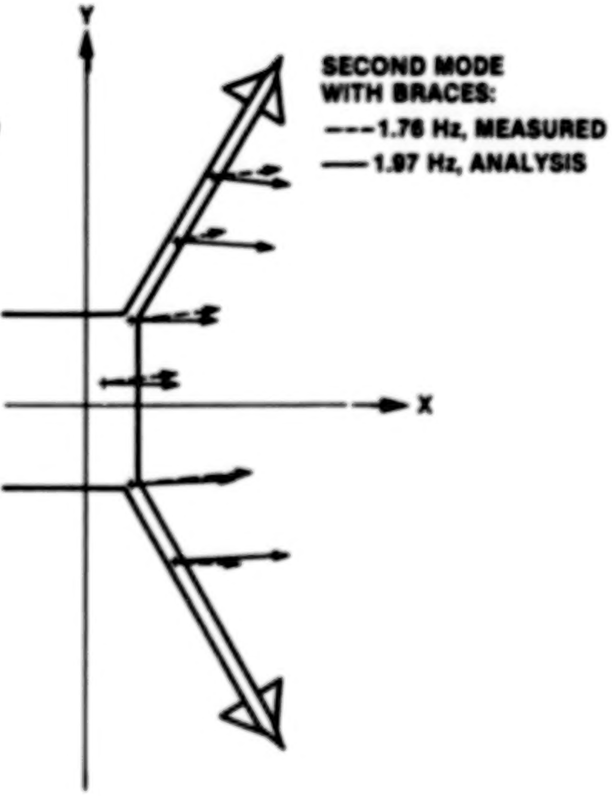
Y
X
SECOND MODE
WITH BRACES:
---1.76 Hz, MEASURED
—1.97 Hz, ANALYSIS

70-METER STRUCTURE

This is the assembled 70-meter structure with quadripod in place. The picture was taken from an erection crane prior to installation of the surface panels. The panels were installed subsequently with a precise ranging theodolite used to set target points on the panels to prescribed coordinates. The setting was done for convenience at the zenith (90-degree) elevation. Rather than setting the surface to the exact contour, the setting coordinates were adjusted by the computer model predictions of the changes from the 45-degree optimum "rigging" angle. Since the validity of biased panel setting depends upon the accuracy of the computer model prediction, and since there were questions about the achieved surface accuracy after the antenna went into operation, two types of field tests were performed. For one type, the antenna remained at the zenith elevation and a 10,000-pound load was applied at specific points of the structure; the change in theodolite reading under load was compared with model predictions. The second type consisted of theodolite measurements of differences in displacements of selected nodes of the structure at the zenith and 45-degree elevations. The changes in measurements at these two elevations were then compared with predictions from the model.

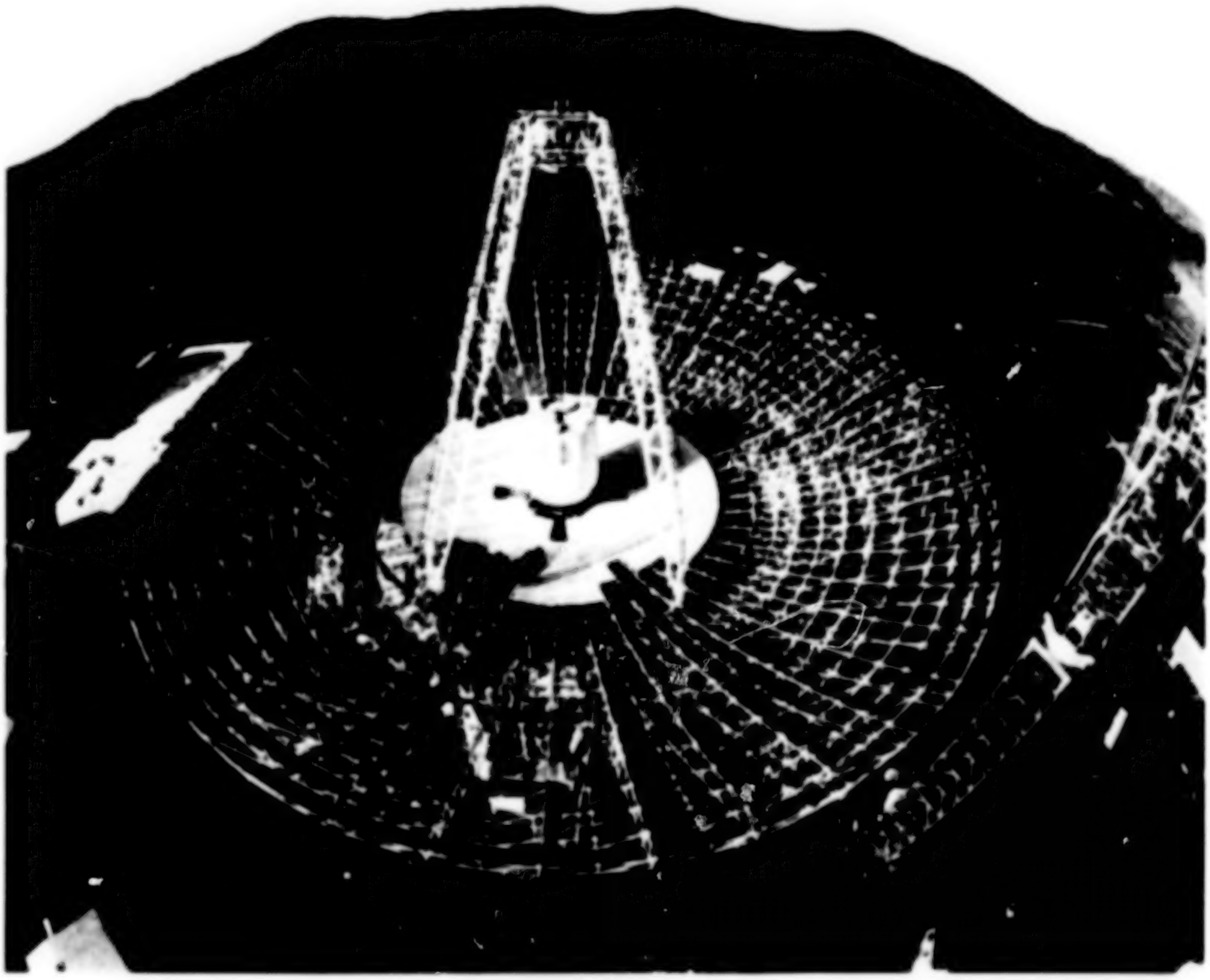

344

BEST COPY AVAILABLE

10,000-POUND PULL-TEST SETUP

The loads were all applied at the zenith elevation. One 10,000-pound load was applied in each test. The figure shows two application points and two load directions at each point. There were three candidate ribs for loading: the north rib (rib 1), the east rib (rib 25), and one other rib, called the "northeast rib" (rib 17) at 60 degrees from the north rib. Not all possible tests were completed. In particular, the B2 tests were abandoned because the deflections were too small for reliable measurements. Nevertheless, 12 load tests were completed; 6 before the panels were placed and 6 after. The panels are idealized in the computer model as parasitic, and the actual connections to the trusses are designed to avoid a load path through the panels. Unfortunately, there were not enough matching cases to determine if the panel effect on the deflections was significant. The limited information available indicates that any panel effect is of secondary order.

Several sets of theodolite reading repetitions were completed for a group of targets dispersed over the surface. Each target was read six times in each set of readings. It was determined that the standard error of theodolite reading repeatability was about 0.6 milligrads (2.5 arc seconds) and the error did not appear to be affected by the range to the target.

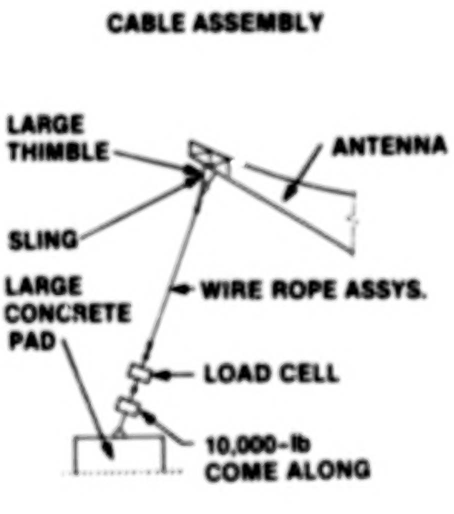

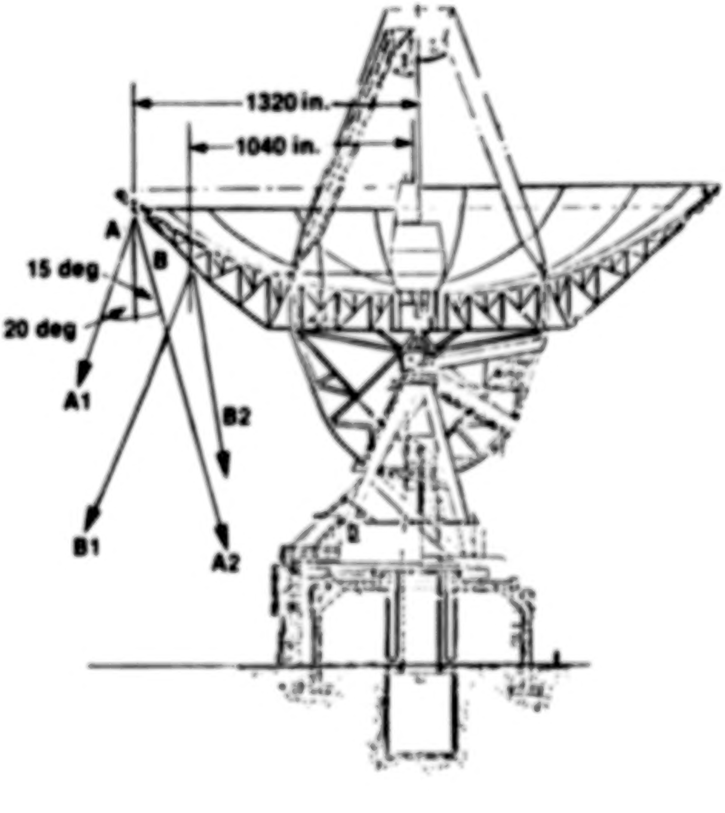

TEST LOAD ON NORTH RIB

The line-of-sight (LOS) offset is computed as the change in theodolite angle times the slant distance to the target point. This is test A1N (the A1 load of figure 15 on rib 1). The curves in the top plot contain points on the loaded rib. The curves in the bottom plot are the offsets for points on the outermost ring. The ribs are numbered 1 at the north, 25 at the east, 48 at the south, and -25 at the west. Any negative rib number is in the western half, and rib -47 is adjacent to rib 48.

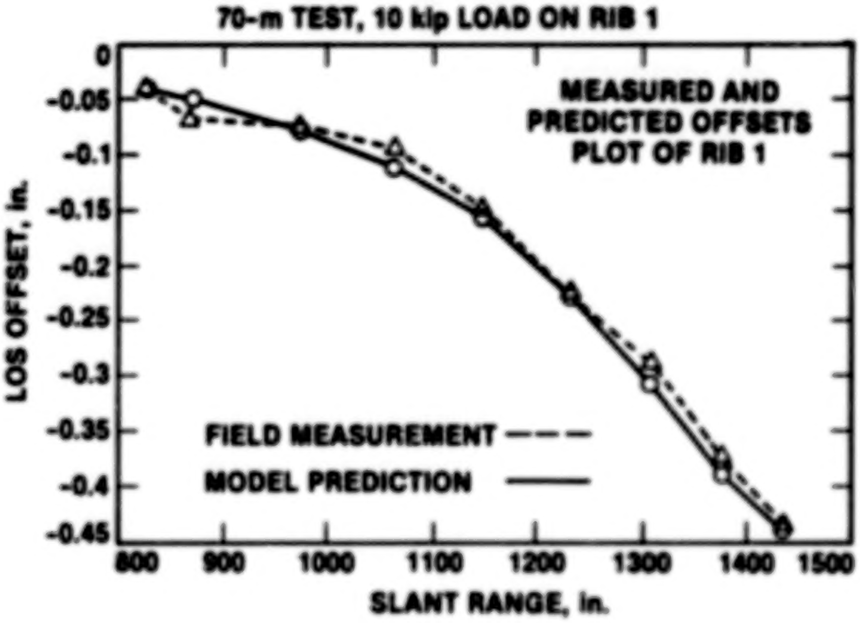

70-m TEST, 10 kip LOAD ON RIB 1

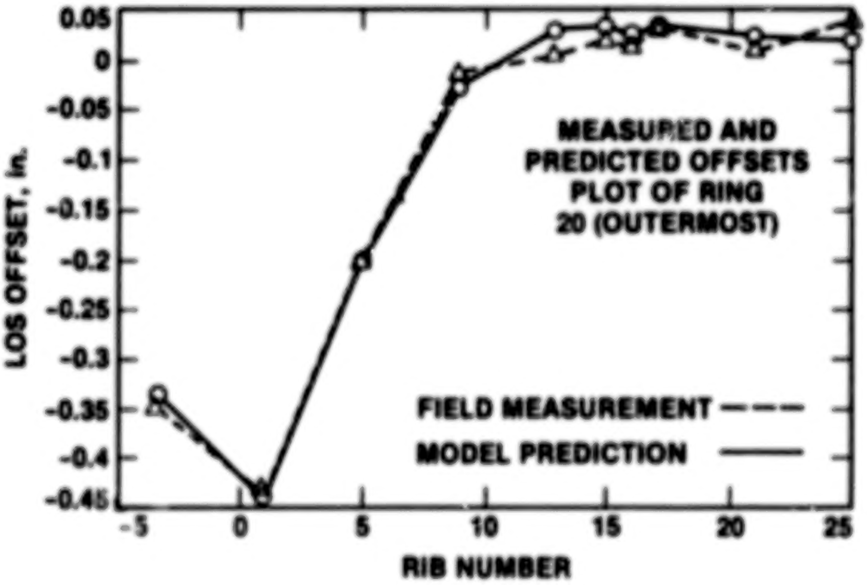

NORTH-RIB LOADING STATISTICAL ANALYSIS

One hypothesis that could be tested is that the model predictions and measurements agree, and the observed differences are due to the measurement error of the theodolite reading. Fortunately, we have a substantial amount of data on theodolite reading repeatability and therefore have a good idea of this standard deviation. Then, if we assume the reading errors have the normal distribution, we can compute the percentile bands of the expected differences between measurement and prediction.

In the top plot, the predictions are plotted on one axis and the measurement at the same point on the other. The units of plotting are in milligrads (1 grad = 0.9 degrees) of angle change. If there is perfect agreement, all points would fall on the 45-degree sloped line through the origin. On the other hand, since we do not expect perfect agreement because of theodolite reading variations, we should expect, for example, that about half the points would fall within the 50% confidence band (0.675 standard deviations) and not more than about 10% would fall outside of the 90% confidence band (1.675 standard deviations). The residual differences are shown on the bottom plot, and here, because of the scale, the confidence bands can be seen more clearly. The mode labels are equal to 100 times the rib number plus a two-digit ring identification. Of the 30 points plotted, 11 fall within the 50th percentile and 2 fall beyond the 90th percentile.

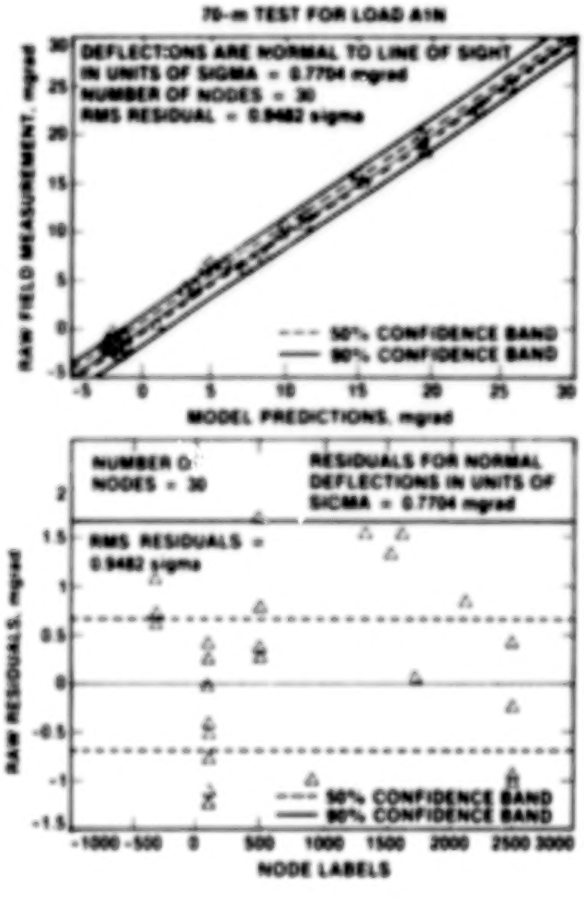

TEST LOADS ON EAST AND NORTHEAST RIBS

The agreement shown between measurements and predictions for these two loading cases and the previous cases (preceding figure), which are all Al type of pull loads, is representative of the full set of loading tests. The statistics and within-band counts for the two cases shown here would also be similar to those of the preceding figure.

A conclusion of the statistical evaluation of all of the processed data from the 12 loading cases is that the measurements agree with the predictions within reason. The differences at the points of maximum deflections are within 5% of the deflection. Of the variability between measurement and model, about 65% of the variance is measurement error and the remaining 35% is attributed to modeling error. Consequently, at the points of maximum deflections, the error in the model is not more than about 3%.

70-m TEST LOAD ON N.E. RIB

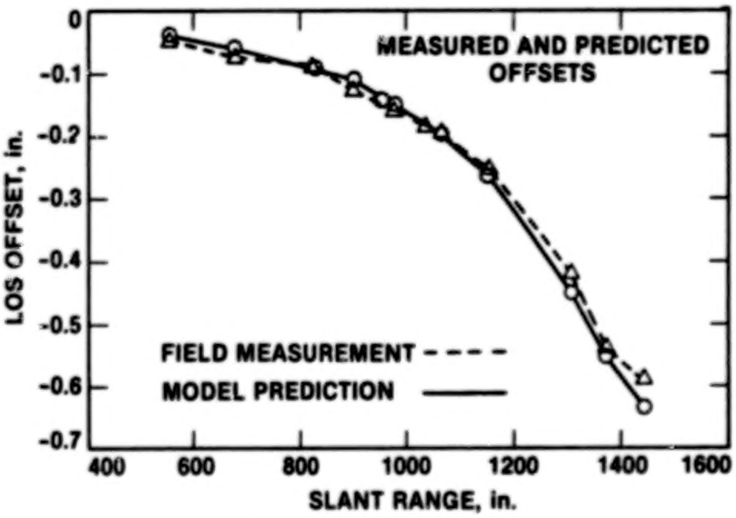

70-m TEST LOAD ON EAST RIB

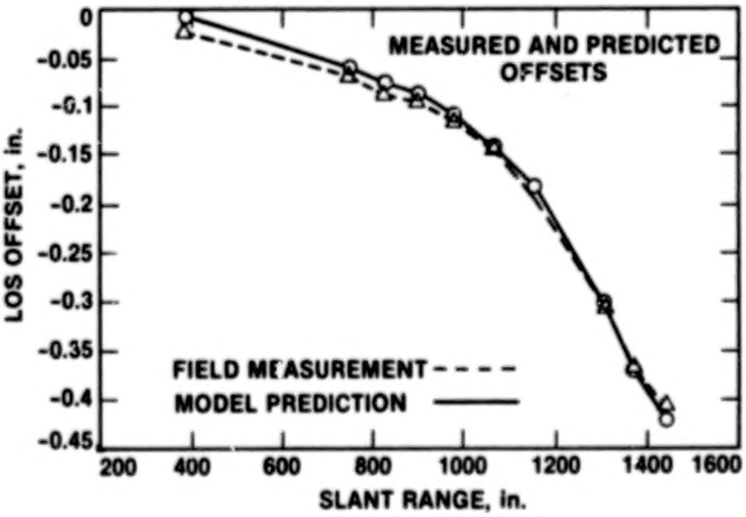

MAIN-RIB GRAVITY LOADING DIFFERENCES IN OFFSETS

The data here is obtained from theodolite measurements at 45-degree and zenith (or near zenith) theodolite measurements. The previously described pull loading tests were limited to a 10,000-pound change in load. Here the effect of the change in gravity loading is much larger and the deflections are from two to three times as large. Consequently, the theodolite repeatability errors are less significant and in many cases are much less than differences in measurement and model.

The loading that produces these offsets is due to the change in orientation of the gravity vector from the 88.5- to 45-degree elevations. One graph gives the offset in millidegrees of theodolite reading and the other graph converts the angle offset to linear projections from the theodolite line of sight. The two graphs give a different perspective of the differences between predictions and measurements. For example, the linear graph weights comparisons by the distance to the point and appears to smooth the angle graph. The linear graph is of most interest in considering differences in microwave path length from the ideal surface. The best fitting here applies to a rigid-body adjustment of the orientation of the field-measurement theodolite. This is necessary because in changing elevations we had no record of the changes in the displacements of the theodolite mounting point.

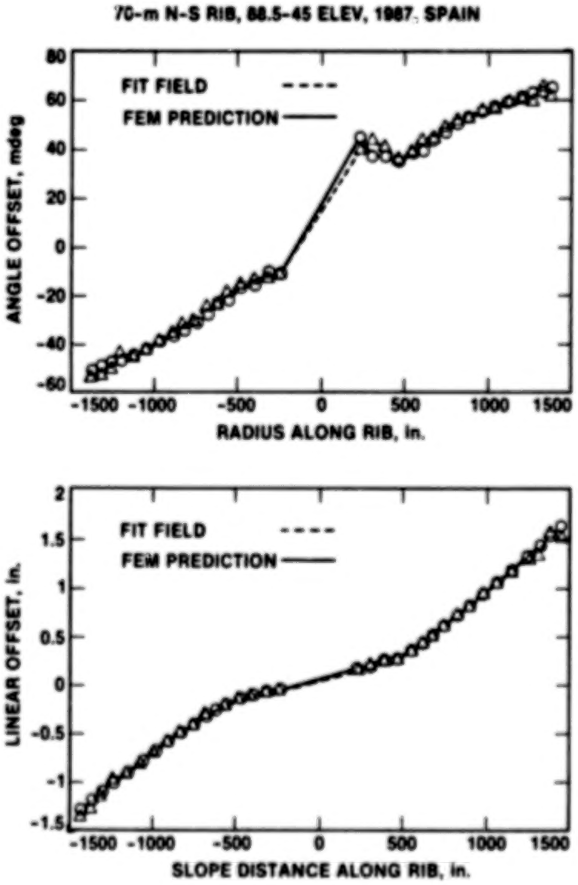

OUTER-RING GRAVITY LOADING DIFFERENCES IN OFFSETS

In addition to theodolite measurements of the main-rib offsets, another set of 90- and 45-degree elevation readings were taken at the two outermost rings (21 and 20) for a 360-degree dispersion of the ribs. Again, rib numbers 1 and 48 are at the north and south tips of the main rib of the preceding figure. The rib-20 plots have been lowered by 20 milligrads for clarity.

Here, and also on the previous curves, measurements and predictions appear to track each other well. The maximum differences between measurements and predictions are not more than about 1/8 inch and typically are much less than this. Nevertheless, as small as the discrepancies might appear here, they are larger than desirable for accurate prediction of microwave performance. The previously discussed set of 10,000-pound applied loading tests was undertaken in the attempt to obtain information to improve the model.

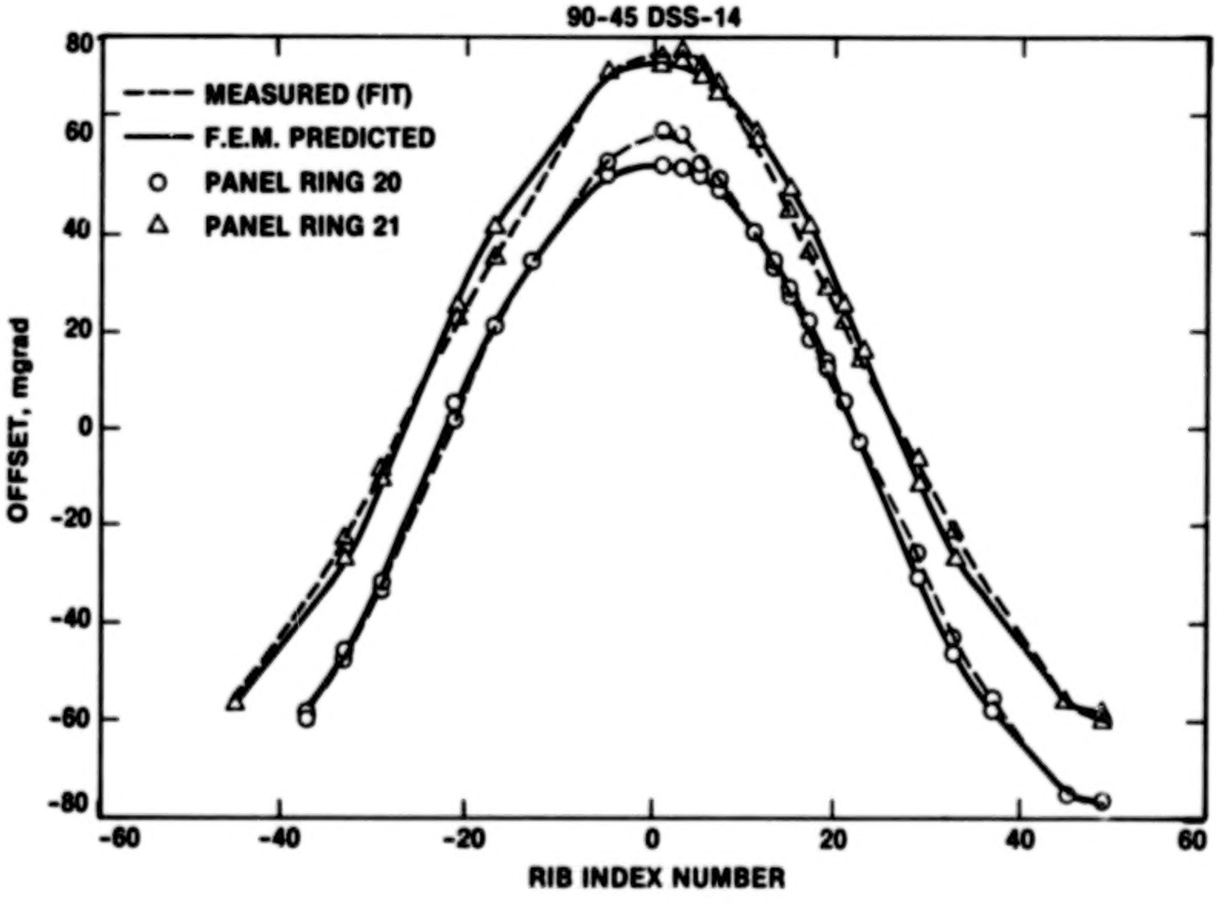

372

CONCLUSIONS

Considering that the quadripod computer model had known simplifying idealizations, the agreement of measurements with predictions was closer than both needed and expected.

There are some remaining puzzles in the reflector model. The models definitely capture the gross deflected shape but do not agree with the measurements to within current-day microwave frequency requirements for accuracy. Beyond the information presented here, a number of hypotheses have been proposed and tested as possible explanations. Some of these cover simplifying idealizations within the model and others cover model discrepancies. So far, none have been able to provide a satisfactory explanation. Our work is continuing and we look forward to obtaining microwave holography data shortly. This data will give us a complete map of the surface deformations at several different elevations and a much more complete picture than currently available through the limited number of theodolite measurements.

- **QUADRIPOD**
  - **MEASURED FREQUENCIES AND MODE SHAPES CONFIRM THE MODEL PREDICTIONS.**
  - **THE OUTRIGGERS ARE NECESSARY TO ACHIEVE THE REQUIRED MINIMUM NATURAL FREQUENCY.**
- **MAIN REFLECTOR**
  - **THE 10,000-lb LOAD TESTS SUPPORT THE HYPOTHESIS THAT THE MODEL REPRESENTS THE STRUCTURE.**
  - **THE CHANGE IN ELEVATION MEASUREMENTS INDICATE THAT THE MODEL REPRESENTS THE MEASURED GROSS DEFLECTION PATTERNS WITHIN REASON.**
  - **NOTWITHSTANDING THE GOOD REPRESENTATION OF GROSS DEFLECTIONS, THE RESIDUAL DEFLECTIONS ARE LARGER THAN DESIRABLE.**
- **CONCLUSION**
  - **FURTHER STUDY, AND POSSIBLY MORE DATA, MAY BE NEEDED TO EXPLAIN THE RESIDUAL ERRORS.**

REFERENCES

1. Utku, S., and Barondess, S. M. , Computation of Weighted Root-Mean-Square of Path Length Changes Caused by the Deformation and Imperfections of Rotational Paraboloidal Antennas. Technical Memorandum 33-118, Jet Propulsion Laboratory, Pasadena, California, March 1963.

2. Levy, R., Computer Design of Antenna Reflectors. AIAA/ASME/SAE, 14th SDM Conference, Paper 73-351, Williamsburg, Virginia, March 20-22, 1973.

3. Levy, R., and Melosh, R. J., Computer Design of Antenna Reflectors. Journal of the Structural Division, Proc. ASCE 99 (ST-11), Proc. Paper 10178, pp. 2269-2285, November 1973.

4. Schmit, L. A., and Fleury, C., Structural Synthesis by Combining Approximation Concepts and Dual Methods. AIAA Journal, Vol. 18, No. 10, pp. 1251-1260.

5. Levy, R., Optimization of Antenna Structure Design. Eighth Conference on Electronic Computation, ASCE, Houston, Texas, pp. 114-129, February 21, 1983.

6. Levy, R., and Parzynski, W., Optimality Criteria Solution Strategies in Multiple Constraint Design Optimization. AIAA Journal, Vol. 20, No. 5, pp. 708-715.

7. Levy, R., and Chai, K., Implementation of Natural Frequency Analysis and Optimality Criterion Design. Computers and Structures. Vol. 10, 1979, pp. 277-282.

8. Kamat, M. P., Venkayya, V., and Khot, N., Optimization with Frequency Constraints - Limitations. Journal of Sound and Vibration. 1983, Vol. 91, No. 1, pp. 147-154.

9. Grandhi, R., and Venkayya, V., Structural Optimization with Frequency Constraints. AIAA/ASME/ASCE/AHS, 28th SDM Conference, Paper 87-0787-CP, Monterey, California, April 6-8, 1987.

10. Vibration Measurements of Quadripod and Apex Structure for 70M Antenna, DSS-63. Kinemetric, Inc., 222 Vista Avenue, Pasadena, California, 91107, May 2, 1986.

A Novel Implementation of Method of Optimality Criterion in Synthesizing Spacecraft Structures with Natural Frequency Constraints

B. P. Wang
Department of Mechanical Engineering
The University of Texas at Arlington
Arlington, Texas

F. H. Chu
General Electric
Astro Space Division
Princeton, New Jersey

INTRODUCTION

In the design of spacecraft structures, fine tuning the structure to achieve minimum weight with natural frequency constraints is a time consuming process. In this paper, a novel implementation of the method of optimality criterion (OC) is developed. In this new implementation of OC, the free vibration analysis results are used to compute the eigenvalue sensitivity data required for the formulation. Specifically, the modal elemental strain and kinetic energies are used. Additionally, normalized design parameters are introduced as a second level linking that allows design variables of different values to be linked together. With the use of this novel formulation, synthesis of structures with natural frequency constraint can be carried out manually using modal analysis results. Design examples are presented to illustrate this novel implementation of the optimality criterion method.

PROBLEM STATEMENT

The optimal design problem to be solved is determination of the values of design variables such that the structure weight is minimized while maintaining a specified fundamental natural frequency of the system. The design variables are sizing of structural members, e.g. cross-sectional areas of truss elements; area moment of inertia of beam elements; and thickness of plate elements. Bounds on design variables are also considered.

FIND $X \in R^n$

TO MINIMIZE

$$W = W(X) \tag{1}$$

SUBJECT TO THE CONSTRAINTS

$$f_1 \geqslant f_{1d} \quad (\text{OR } \lambda_1 \geqslant \lambda_{1d}) \tag{2}$$

$$\text{AND} \quad X_L \leqslant X \leqslant X_U \tag{3}$$

NOTE THAT $f_1 = \sqrt{\lambda_1}/2\pi$

AND λ_1 IS RELATED TO THE DESIGN VARIABLE THROUGH THE EIGENVALUE PROBLEM

$$[K(X)]\{\phi_1\} = \lambda_1 [M(X)]\{\phi_1\}$$

OPTIMALITY CRITERION

The optimal design problem defined in the previous section can be solved by mathematical programming techniques. To derive a simpler approach, we will treat the frequency constraint defined in Eq. (2) as equality constraint. Additionally, the side constraints will be ignored for the time being. With these simplifications, the set of optimality criteria can be derived among the design variables by the Lagrange multiplier technique. The optimality criterion can be interpreted as:

> At the optimal design, the ratio of the eigenvalue sensitivity to weight sensitivity is a constant for all design variables.

FROM LAGRANGIAN:

$$L = W - \mu(\lambda_1 - \lambda_{1d})$$

THE OPTIMALITY CRITERION:

$$\frac{\partial L}{\partial X_i} = 0 \qquad (4)$$

LEADS TO

$$\frac{\partial W}{\partial X_i} - \mu \frac{\partial \lambda_1}{\partial X_i} = 0$$

OR

$$\frac{\partial \lambda_1 / \partial X_i}{\partial W / \partial X_i} = \frac{1}{\mu} = \text{CONSTANT} \qquad (5)$$

EQUATION (5) IS THE OPTIMALITY CRITERION AN OPTIMAL DESIGN MUST SATISFY.

BASIC REDESIGN ALGORITHM

Following the optimality criterion method suggested by Khot [1], linear recurrence relations can be developed based on Eq. (5). The Lagrange multiplier is computed by requiring that the updated design satisfy the frequency constraint. The basic redesign algorithm is summarized in Eqs. (6) and (7).

REDESIGN FORMULA:

$$(X_i)_{S+1} = (X_i)_S \left[\alpha + \mu(1-\alpha)\frac{G_i}{C_i}\right] \quad (6)$$

LAGRANGE MUTIPLIER:

$$\mu = \frac{\Delta\lambda + (1-\alpha)\Sigma G_i (X_i)_S}{(1-\alpha)\Sigma (G_i^2 \cdot X_i)_S / C_i} \quad (7)$$

$$\Delta\lambda = \lambda_{desired} - \lambda_{current}$$

APPROXIMATE EIGENVALUE SENTIVITY ANALYSIS

In the redesign algorithm, we need to know the derivatives of weight and eigenvalue with respect to the design variables. While the weight sensitivity is simple to calculate, the computation of eigenvalue sensitivity could be quite involved because of the need to know derivatives of element stiffness and mass matrices with respect to design variables. In this paper, we adopt an approximate approach for computing eigenvalue sensitivity which use elemental strain and kinetic energy in the vibration mode [2].

EIGENVALUE SENSITIVITY

GENERAL EQUATION:

$$\frac{\partial \lambda_1}{\partial X_i} = \frac{1}{M_1} \{\phi_1\}^T \left(\frac{\partial [K]}{\partial X_1} - \lambda_1 \frac{\partial [M]}{\partial X_1} \right) \{\phi_1\} \qquad (8)$$

SIMPLIFIED EQUATION [2]:

$$\frac{\partial \lambda_1}{\partial X_i} = \frac{2}{M_1} \left(\frac{\beta_i}{X_i} V_{1i1} - \frac{\gamma_i}{X_i} T_{1i1} \right) \qquad (9)$$

ASSUMPTIONS:

$$K_i = (X_i)^{\beta_i} K_i^* \qquad (10)$$

$$M_i = (X_i)^{\gamma_i} M_i^* \qquad (11)$$

SPECIAL CASE FOR:

1. TRUSS ELEMENTS
2. SYSTEM MASS MATRIX DOMINATED BY NON-STRUCTURE MASS

THEN

$$\frac{\partial \lambda_1}{\partial X_i} = \frac{2 V_{1i1}}{M_1 \cdot X_i} \qquad (12)$$

A NOVEL IMPLEMENTATION OF THE BASIC REDESIGN ALGORITHM

The redesign algorithm given by Eqs. (6) and (7) can be implemented easily for truss structure. For example, if one uses MSC/NASTRAN [3] for structural analysis, the strain energy and strain energy density can be obtained together with the modal analysis results. Using these data and assuming that a majority of the system weight is contributed from non-structural mass, the redesign algorithm can be implemented using the following procedures.

(1) PERFORM MODAL ANALYSIS WITH STRAIN ENERGY AND STRAIN ENERGY DENSITY CALCULATIONS.

(2) COMPUTE $C_i = \frac{\partial W}{\partial X_i}$ USING

$$C_i = \sum \rho_e (ESE)_e / (ESED_e \cdot X_e) \tag{13}$$

(3) COMPUTE $G_i = \frac{\partial \lambda_1}{\partial X_i}$ USING

$$G_i = 2 \sum (ESE_e / X_e M_1) \tag{14}$$

NOTE THAT THE SUBSCRIPT e REFERS TO ELEMENT NUMBER AND THE SUMMATIONS IN EQS. (13) AND (14) ARE OVER ALL THE ELEMENTS THAT ARE ASSIGNED AS DESIGN VARIABLE X_i.

(4) COMPUTE LAGRANGE MULTIPLIER USING EQ. (7).

(5) UPDATE THE DESIGN VARIABLES USING EQ. (6).

DESIGN EXAMPLE

The design procedure described in this paper has been applied to a truss structure shown below. The objective is to find the minimum weight design of the truss structure to maintain a specified fundamental natural frequency of the system. Starting from a uniform truss structure that satisfied the 5.7 Hz constraint on the fundamental natural frequency, the design is manually optimized by typical trade studies. The optimality criterion algorithm is then applied to this manually optimized structure to obtain an additional 25 pound saving in the structural weight. The comparison of the truss structures weights is shown in the table below.

DESIGN CASE	TRUSS STRUCTURE WEIGHT	f
UNIFORM TRUSS SIZE	2102.0 lbs	5.7 Hz
MANUALLY OPTIMIZED TRUSS SIZE	1014.0 lbs	5.7 Hz
OPTIMIZED TRUSS SIZE USING METHOD OF OC	989.0 lbs	5.7 Hz

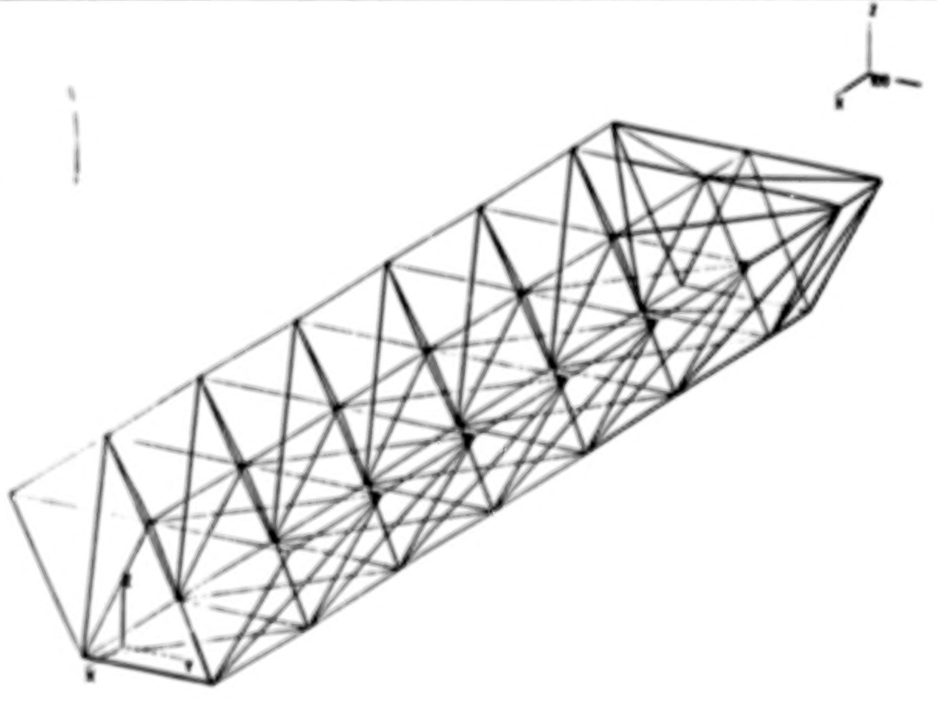

TRUSS STRUCTURE FOR OPTIMIZATION STUDY

BEST COPY AVAILABLE

CONCLUDING REMARKS

A method of optimality criterion was shown to be a powerful tool for minimum weight design of structures with constraint on fundamental natural frequency. With the new method of implementation presented in this paper, the design procedure can be carried out by simple calculations. The effectiveness of this approach has been demonstrated by a truss structure. This method can be extended to other types of structure elements using eigenvalue sensitivity formulation in Ref. [2].

REFERENCES

1. Khot, N., Optimality Criterion Methods in Structural Optimization. Chapter 5 of Foundations of Structural Optimazation: A Unified Approach, Edited by A.J. Morris, John Wiley and Sons, Ltd., 1982.

2. Wang B. P., On Computing Eigensolution Sensitivity Data Using Free Vibration Solutions. in Sensitivity Analysis in Engineering, NASA CP2457, 1987, pp. 223-245.

3. MSC/NASTRAN USER'S MANUAL, The MacNeal-Schwendler Co., 1982.

SYMBOLS AND ABBREVIATIONS

C_i = $\partial W/\partial X_i$ FOR CURRENT DESIGN
ESE_e = STRAIN ENERGY
$ESED_e$ = STRAIN ENERGY DENSITY
f_1 = FIRST NATURAL FREQUENCY
f_{1d} = DESIRED FIRST NATURAL FREQUENCY
G_i = $\partial \lambda_1/\partial X_i$ FOR CURRENT DESIGN
$[K(X)]$ = GLOBAL STIFFNESS MATRIX
$[M(X)]$ = GLOBAL MASS MATRIX
M_1 = GENERALIZED MASS OF THE FIRST MODE
R = SPACE OF DESIGN VARIABLES
T_{1i1} = TOTAL KINETIC ENERGY OF ELEMENTS ASSOCIATED WITH DESIGN VARIABLE i FOR MODE 1
V_{1i1} = TOTAL STRAIN ENERGY OF ELEMENTS ASSOCIATED WITH DESIGN VARIABLE i FOR MODE 1
W = STRUCTURE WEIGHT
X = DESIGN VARIABLE VECTOR
X_L = LOWER BOUNDS OF X
X_U = UPPER BOUNDS OF X
X_i = CURRENT DESIGN VARIABLE
$(X_i)_s$ = CURRENT DESIGN
$(X_i)_{s+1}$ = UPDATED DESIGN
λ = EIGENVALUE
α = RELAXATION FACTOR
ρ_e = WEIGHT DENSITY

COMPUTATIONAL EXPERIMENTS IN THE OPTIMAL SLEWING OF FLEXIBLE STRUCTURES

T. E. Baker and E. Polak
College of Engineering
University of California

1. INTRODUCTION

This paper reports on numerical experiments on the problem of moving a flexible beam. An optimal control problem is formulated and transcribed into a form which can be solved using semi-infinite optimization techniques. All experiments were carried out on a SUN 3 microcomputer.

2. PROBLEM STATEMENT

We consider the hollow aluminum tube depicted in figure 1. The tube is one meter long, has a cross-sectional radius of 1.0 cm, and a thickness of 1.6 mm. Attached to one end of the tube is a mass of 1 kg, and attached to the other end is a shaft connected to a motor. For simplicity, we assume that the torque produced by the motor can be directly controlled. Our aim is to determine the torque necessary to rotate the tube and bring it to rest. The maximum torque produced by the motor is 5 newton-meters. The equations of motion determined by application of the standard Euler-Bernoulli tube with Kelvin-Voigt visco-elastic damping are:

$$m w_{tt}(t,x) + CI w_{txxxx}(t,x) + EI w_{xxxx}(t,x) - m\Omega^2(t) w(t,x) = -m u(t) x, \quad x \in [0,1] \tag{1a}$$

with boundary conditions:

$$w(t,0) = 0, \quad w_x(t,0) = 0, \quad CI w_{txx}(t,1) + EI w_{xx}(t,1) = 0. \tag{1b}$$

$$M[\Omega^2(t) w(t,1) - w_{tt}(t,1) - u(t)] + CI w_{txxx}(t,1) + EI w_{xxx}(t,1) = 0, \tag{1c}$$

where $w(t,x)$ is the displacement of the tube from the *shadow tube* (which remains undeformed during the motion) due to bending as a function of time and distance along the tube; $u(t)$ is the torque applied by the motor, and $\Omega(t)$ is the resulting angular velocity (in radians per second). We shall denote by $\Theta(t)$ the angular displacement of the rigid body (in radians). The values for the parameters in (1a) - (1c) are: $m = .2815$ kg/m, $C = 6.89 \times 10^7$ pascals/sec., $E = 6.89 \times 10^9$ pascals, $I = 1.005 \times 10^{-8} m^4$, $M = 1.00$ kg. These values are from the CRC Handbook of Material Science. The tube is very lightly damped (0.1 percent).

We consider three problems:

P_1: Minimize the time required to rotate the tube 45 degrees, from rest to rest, subject to the given torque constraint.

P_2: Minimize the total energy required to rotate the tube 45 degrees, from rest to rest, subject to the given torque constraint and the maneuver time not exceeding a given bound.

P_3: Minimize the time required to rotate the tube 45 degrees, from rest to rest, subject to the given torque constraint and an upper bound on the potential energy due to deformation of the tube throughout the entire maneuver.

3. MATHEMATICAL FORMULATION OF THE THREE PROBLEMS

We will formulate the above problems P_1, P_2, and P_3 in the form of the following canonical optimization problem:

$$P_0: \min_{T \in \mathbf{R}_+,\, u \in G_T} \{ g^0(u,T) \mid g^j(u,T) \le 0, j \in \underline{m} \} \tag{2}$$

where $\mathbf{R}_+ \triangleq \{ \gamma \in \mathbf{R} \mid \gamma > 0 \}$, $\underline{m} \triangleq \triangleq \{ 1, 2, \cdots m \}$,

$$G_T \triangleq \{ u \in L_\infty[0,T] \mid |u(t)| \le 5, t \in [0,T] \}, \tag{3}$$

and $g^j : G_T \times T \to \mathbf{R}$ is continuously differentiable for $j \in \{ 0, 1, \cdots, m \}$. We define $\psi(u,T) \triangleq \max_{j \in \mathbf{m}} \{ g^j(u,T) \}$ and $\psi_+(u,T) \triangleq \max \{ 0, \psi(u,T) \}$.

We shall be making use of the following functions. First, let T denote the final time. Then we define

$$g^1(u,T) \triangleq T. \tag{4}$$

The input energy is defined as the integral of the square of the input; hence we define

$$g^2(u,T) \triangleq \int_0^T u(t)^2 dt. \tag{5}$$

Next we define

$$g^3(u,T) \triangleq (\Theta(T) - \pi/4)^2 \tag{6}$$

to be the square of the angular error at the final time. We say that *the tube is at rest* when the total energy of the tube is zero. This energy is composed of the energy due to rigid body motion and energy due to vibration and deformation. Rigid body energy at final time is proportional to the square of the angular velocity. Hence we define

$$g^4(u,T) \triangleq \Omega(T)^2. \tag{7}$$

The kinetic energy due to vibration of the tube at time t is given by

$$K(t,u) \triangleq \frac{m}{2} \int_0^1 w_t(t,x)^2 dx, \tag{8}$$

and the potential energy due to deformation of the tube at time t is given by

$$P(t,u) \triangleq \frac{EI}{2} \int_0^1 w_{xx}(t,x)^2 dx. \tag{9}$$

We now define

$$g^5(u,T) \triangleq K(T,u), \qquad g^6(u,T) \triangleq P(T,u). \tag{10}$$

The tube is at rest if $g^4(u,T) = g^5(u,T) = g^6(u,T) = 0$.

For problem $\mathbf{P}_3$, we require that the potential energy due to the tube deformation be within a specified range throughout the entire maneuver. This constraint has the form $P(t,u) \le f(t)$ for all $t \in [0,T]$, where $f(\cdot)$ is a given positive bound function. This is a *state-space constraint*, and does not fit the canonical form P_0. However, we can replace it by an equivalent form which requires that we define

$$g^7(u,T) \triangleq \int_0^T [\max\{ P(t,u) - f(t) \ , \ 0 \}]^2 \tag{11}$$

Then, since $P(t,u)$ is continuous, $g^7(u,T) = 0$ if and only if $P(t,u) \leq f(t)$ for all $t \in [0,T]$.

It can be shown that $g^j : G_T \times T \rightarrow \mathbb{R}$ is continuously differentiable (in the L_∞ topology) in u and t for all $j \in \{1, 2, \cdots 7\}$. To conform with the format of problem $\mathbf{P}_0$, we relax each of the equality constraints by a small amount. The relaxation can be be chosen to be sufficiently small so as not to matter from a practical point of view. The three problems now acquire the following mathematical form

$$\mathbf{P}_1\text{:}\ \min\{ g^1(u,T) \mid g^3(u,T) - \varepsilon \leq 0,\ g^4(u,T) - \varepsilon \leq 0,\ g^5(u,T) - \varepsilon \leq 0,\ g^6(u,T) - \varepsilon \leq 0,\ u \in G_T \} \tag{12}$$

$$\mathbf{P}_2\text{:}\ \min\{ g^2(u,T) \mid g^1(u,T) - T_f \leq 0,\ g^3(u,T) - \varepsilon \leq 0,\ g^4(u,T) - \varepsilon \leq 0,\ g^5(u,T) - \varepsilon \leq 0,\ g^6(u,T) - \varepsilon \leq 0,\ u \in G_T \} \tag{13}$$

$$\mathbf{P}_3\text{:}\ \min\{ g^1(u,T) \mid g^3(u,T) - \varepsilon \leq 0,\ g^4(u,T) - \varepsilon \leq 0,\ g^5(u,T) - \varepsilon \leq 0,\ g^6(u,T) - \varepsilon \leq 0,\ g^7(u,T) - \varepsilon \leq 0,\ u \in G_T \} \tag{14}$$

In our experiments, we set $\varepsilon = 10^{-4}$. Thus, with this relaxation, we are requiring that the final value of the angle Θ be in the interval $[45 - 0.5, 45 + 0.5]$ degrees.

By adding an additional state variable $z(t)$, with $\dot{z}(t) \equiv 0$, the above problems can be recast as *fixed time problems* on the interval $[0,1]$ in which one has to determine not only the (time scaled) control $u(t)$, but also T, the initial value of $z(t)$ which acts as a time scale factor, and, in fact, is also the final time. Although the *abstract form* of the fixed time, scaled problems

$$\bar{\mathbf{P}}_0\text{:}\ \min_{u \in G, T \in \mathbb{R}_+} \{ \bar{g}^0(u,T) \mid \bar{g}^j(u,T) \leq 0, j \in \mathbf{m} \}, \tag{15}$$

where $G \triangleq G_1$, is indistinguishable from that of the free time problem, the fixed time problem does not lead to the serious convergence problems that are associated with the discretization of free time problems.

4. THE ALGORITHM

To solve the above problems in fixed time form, we use an extension of the Mayne-Polak phase I - phase II algorithm [1]. The algorithm first determines a search direction and then a step size to update the design parameters $u(\cdot)$ and T. The algorithm requires an initial guess $T \geq 0$ and $u \in G$. We state this algorithm in *conceptual form*.

Conceptual Algorithm

Data: $T_0 \in \mathbb{R}, u_0 \in G,\ \alpha \in (0,1),\ \beta \in (0,1),\ \rho > 0$

Step 0: $i = 0$.

Step 1: Compute search direction $\delta u_i = v_i - u_i$, $\delta T_i = \tau_i - T_i$ and the optimality function $\theta(u_i, T_i)$, where v_i, τ_i are the solutions of the program

$$\theta(u_i, T_i) \triangleq \min_{v \in G, \tau \in \mathbb{R}_+} \{ \frac{1}{2} \| v - u \|^2 + \frac{1}{2} \| \tau - T_i \|^2 + \max_{j \in \mathbf{m}} \{ -\rho \psi_+(u_i, T_i) + \langle \nabla g^0(u_i, T_i), \begin{bmatrix} v - u_i \\ \tau - T_i \end{bmatrix} \rangle ; g^j(\hat{u}_i, T_i) + \langle \nabla g^j(u_i, T_i), \begin{bmatrix} v - u_i \\ \tau - T_i \end{bmatrix} \rangle - \psi_+(u_i, T_i) \} \} \tag{16}$$

Step 2: Compute the stepsize $\lambda_i \in S \triangleq \{ \lambda \in \{ 0, 1, \beta, \beta^2, \cdots \} \}$ such that

if $\psi(u_i, T_i) > 0$ (at least one constraint is violated)

$$\lambda_i = \max \{ \lambda \in S \mid \psi(u_i + \lambda \delta u_i, T_i + \lambda \delta T_i) - \psi(u_i, T_i) \le \alpha \lambda \theta(u_i, T_i) \} \tag{17a}$$

if $\psi(u_i, T_i) \le 0$, ((u_i, T_i) is feasible)

$$\lambda_i = \max \{ \lambda \in S \mid g^0(u_i + \lambda \delta u_i, T_i + \lambda \delta T_i) - g_0(u_i, T_i) \le \alpha \lambda \theta(u_i, T_i) \text{ and } \psi(u_i + \lambda \delta u_i, T_i + \lambda \delta T_i) \le 0 \} \tag{17b}$$

Step 3: Set $u_{i+1} = u_i + \lambda_i \delta u_i$. $T_{i+1} = T_i + \lambda_i \delta T_i$.

Step 4: Set $i = i + 1$; go to Step 1. ■

The function $\theta(\cdot, \cdot)$ is called an optimality function. It has two important properties: (i) For all $T > 0$ and $u \in G$, $\theta(u, T) \le 0$, and (ii) if $\theta(u_i, T_i) < 0$, then (u_i, T_i) is not optimal and $(v_i - u_i, \tau_i - T_i)$, where (v_i, τ_i) is the solution of (16), is a direction of descent for ψ if (u_i, T_i) is not feasible and for g^0 otherwise. The following theorem can be deduced from the results in [1].

Theorem 1: If $\{ (u_i, T_i) \}$ is a sequence generated by the conceptual algorithm and $(\hat{u}, \hat{T})$ is an accumulation point of this sequence, then $\theta(\hat{u}, \hat{T}) = 0$. ■

The above algorithm is called a *conceptual* algorithm because we cannot solve system (1a) - (1c) exactly, and hence we cannot evaluate $g^j(u, T)$ or $\nabla g^j(u, T)$ exactly. Furthermore, since u is an infinite dimensional design vector, it can only be entered into a computer in discretized form. Hence, in practice, we must use an *implementable* algorithm which accepts approximations. The algorithm that we use adjusts integration precision adaptively, along the lines described in [2, 3 Appendix A]. To discretize the PDE in space, we use the finite element method. Since the PDE is fourth order in space, it is necessary to use elements of at least second order. We have chosen Hermite splines as basis elements. The input $u \in G$ is discretized in time and Newmark's method is applied to evaluate the resulting system of ordinary differential equations. For a specific number of finite elements, p, and a number of time steps, n, the resulting discretized problem has the form:

$$\mathbf{P}_{n,p}: \min_{u \in G^n, T \in \mathbb{R}_+} \{ g^0_{n,p}(u, T) \mid g^j_{n,p}(u, T) \le 0, j \in \mathbf{m} \}, \tag{18}$$

where $G^n \triangleq \{ u \in \mathbb{R}^n \mid |u^j| \le 5, j \in \mathbf{n} \}$.

The resulting problem $P_{n,p}$ is finite dimensional and can be solved by computer. Problem $\mathbf{P}_{n,p}$ always has a solution because the set G^n is bounded. However, at first examination, it is not clear how solutions to $\mathbf{P}_{n,p}$ relate to the solution to $\bar{\mathbf{P}}_0$. Fortunately, it is possible to establish the following theorem which is an extension of the results in [2, 3].

Theorem 2: Let $(u_{n,p}, T_{n,p})$ be a solution to $\mathbf{P}_{n,p}$. If $(\hat{u},\hat{T})$ is an accumulation point of $\{ (u_{n,p}, T_{n,p}) \}$ as $n \to \infty, p \to \infty$, then $(\hat{u},\hat{T})$ is a solution to $\bar{P}_0$. ■

Implementable Algorithm

The implementable algorithm continues solving problem $\mathbf{P}_{n,p}$ until a test indicates that both n and p must be incremented, i.e., the implementable algorithm increases the discretization in time and space adaptively. When the algorithm is far from a solution, it is less important that the partial differential equations be solved exactly. By using a coarse discretization in the early iterations, we save in two ways: the effort in solving the differential equations is smaller, and the number of design parameters (the size of the discretized control) is much smaller. The test for precision refinement monitors the progress in the reduction of $\psi(u, T)$, when (u, T) is infeasible, or in the reduction of $g^0(u, T)$, when (u, T) is feasible. When that reduction is smaller than a parameter $\gamma > 0$, both the number of finite elements and time steps are doubled while γ is halved. The following theorem can be obtained by extending the results in [2, 3 Appendix A].

Theorem 3: Let $\{ (u_i, T_i) \}$ be the sequence produced by the implementable algorithm with the refinement criterion above. Then the discretization becomes infinitely refined as $i \to \infty$, and any accumulation point of $\{ (u_i, T_i) \}$, $(\hat{u},\hat{T})$, satisfies the optimality condition $\theta(\hat{u},\hat{T}) = 0$. ■

5. COMPUTATIONAL RESULTS

The results presented here are for the case in which the $\Omega^2(t)$ terms are neglected in equation (1a) - (1c). Similar results have been obtained by performing experiments for the case in which the $\Omega^2(t)$ terms are included.

Problem $\mathbf{P}_1$:

For simplicity, we choose the zero function as initial control and 2 for an initial value for the maneuver time.

Figure 2 is a graph of the control after 150 iterations. The number of time steps is 256 and the number of finite elements is 48.

Figure 3a is a graph of $\psi_{n,p}(u, T)$ as a function of the iteration number. Figure 3b shows $\psi_{n,p}(u, T)$ for the first 15 iterations. The initial discretization is 32 time steps and 6 finite elements. The discretization is refined at iterations 67, 99, and 123. After precision refinement, algorithm finds a feasible value for the control and final time for the new problem $\mathbf{P}_{n,p}$ in only a few additional iterations. At each refinement the value of $\psi_{n,p}$ increases. This is due to improvement in the accuracy of the evaluation of the partial differential equation. This increase in $\psi_{n,p}$ decreases each time the discretization is refined and we can show that in the limit the increase is zero.

Figure 4 is the graph of the cost as a function of iteration number.

Figure 5 is the graph of $w(t, 1)$, the displacement of the tip of the tube, from the *shadow tube*, as a function of time. There is a maximum displacement of the tip of about 5 mm. This is within the range of validity of the Euler-Bernoulli model. The tip displacement is large between 0.36 seconds and 0.437 seconds.

Figure 6 is a profile of the tube deformation, $w(t, x)$ (see figure 1), during this interval. The total time for the entire maneuver is 0.7886 seconds.

Problem P_2:

Formulating the slewing problem as a minimum time problem has two drawbacks. First, the solution to the problem is a bang-bang control (figure 2). Bang-bang controls may be undesirable because they may cause premature aging of the equipment. Furthermore, bang-bang controls tend to excite the high-frequency modes of the system. High-frequency modes are less well modeled by system (1a) - (1c), and it is therefore best not to excite them. Second, the simple minimum time formulation does not take into account the amount of energy expended in performing the maneuver. In certain applications, the total energy available may be limited, while the total time of the slewing motion is less critical. Fortunately, both of the problems arising from minimum time control can be mitigated by reformulating the problem. We minimize the total input energy while constraining the final time to be less that a specified amount.

Figure 7 is the graph of the control produced by minimizing the total input energy while constraining the final time to be less than 0.800 seconds. The resulting final time is 0.800 seconds. This is an increase of only 1.4 percent in the final time. The control has become much smoother and the total energy is reduced from 19.15 to 15.72, a reduction of 18 percent.

Figure 8 is the graph of the control for final time being 1.00 second. This is an increase of 27 percent in time over the minimum time case, but the total energy is reduced to 7.27, a decrease of 62 percent.

Problem P_3:

In Figure 9, curve A is the graph of the potential energy of the tube as a function of time for the control generated in solving the minimum time problem $\mathbf{P}_1$. In problem $\mathbf{P}_3$, we have the additional requirement to keep the potential energy, which is a measure of the total tube deformation, below the parabola (B) for all time.

Figure 10 shows the optimal bang-bang control for problem P_3. The optimal final time for this case is 0.8177 seconds, an increase of 3.7 percent over the solution of problem $\mathbf{P}_1$.

Figure 11 shows the potential energy curve for the optimal control (Figure 10).

6. ACKNOWLEDGEMENT

The authors wish to thank Prof. C. A. Desoer for his assistance in preparing this manuscript. This research was supported by the National Science Foundation grant ECS-8517362; the Air Force Office Scientific Research grant 86-0116; and the Office of Naval Research contract N00014-86-K-0295.

REFERENCES

[1] D. Q. Mayne and E. Polak, "An Exact Penalty Function Algorithm for Control Problems with State and Control Constraints," *IEEE Trans. on Control*, Vol. AC-32, No. 5, pp. 380-388, 1987.

[2] R. Klessig and E. Polak, "An Adaptive Algorithm for Unconstrained Optimization with Applications to Optimal Control", *SIAM J. Control*, Vol. 11, No. 1, pp. 80-94, 1973.

[3] E. Polak, "Computational Methods in Optimization: A Unified Approach", Academic Press, 329 pages, 1971.

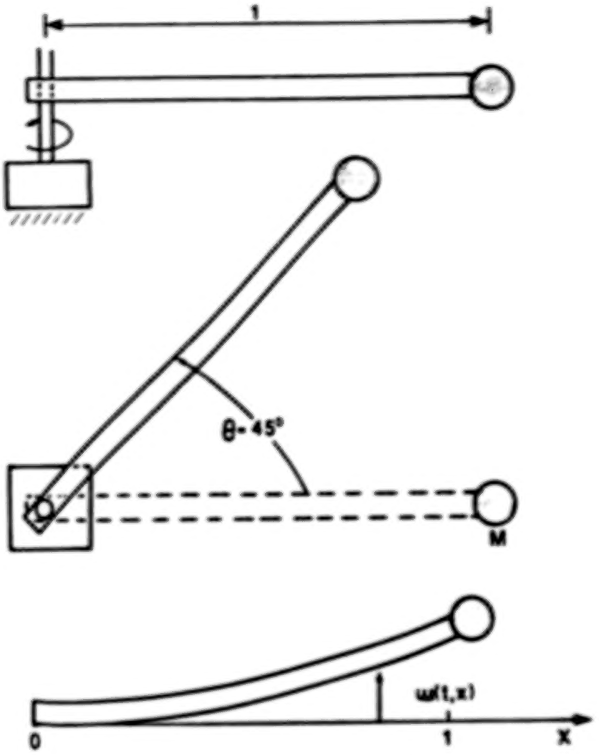
1
θ= 45°
M
w(t,x)
0
1
X

Figure 1 - Configuration of slewing experiment.

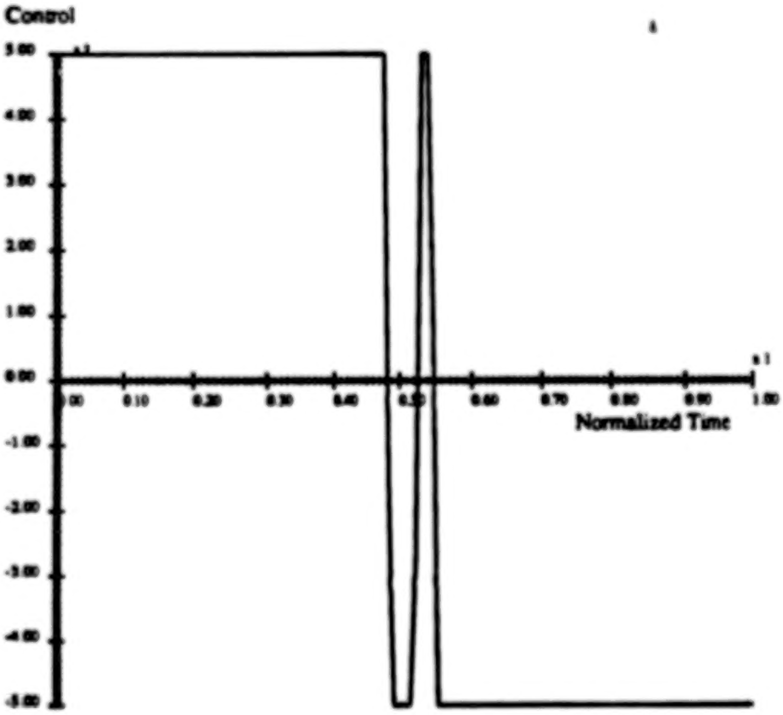

Figure 2 - Problem 1 control.

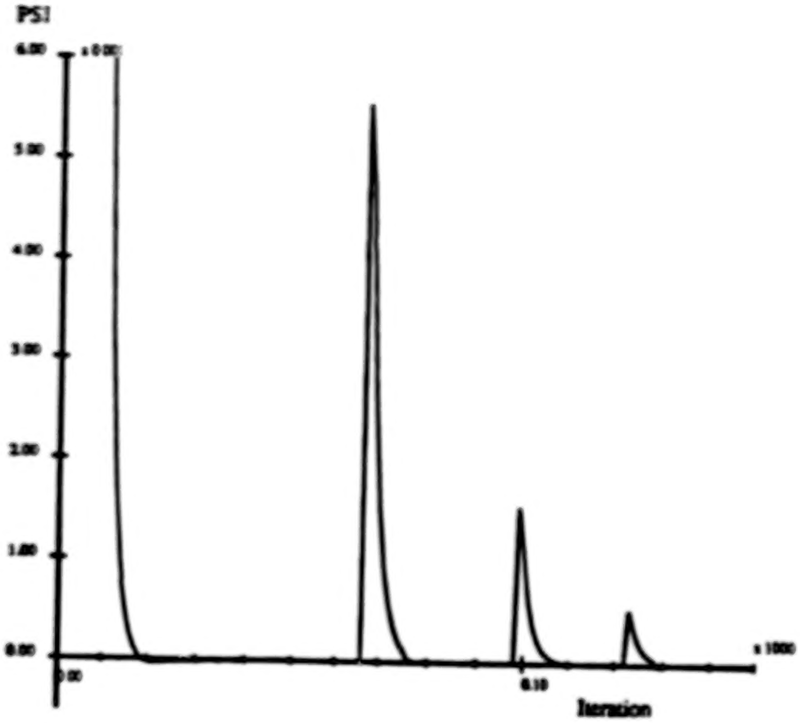

Figure 3a - Problem 1 PSI.

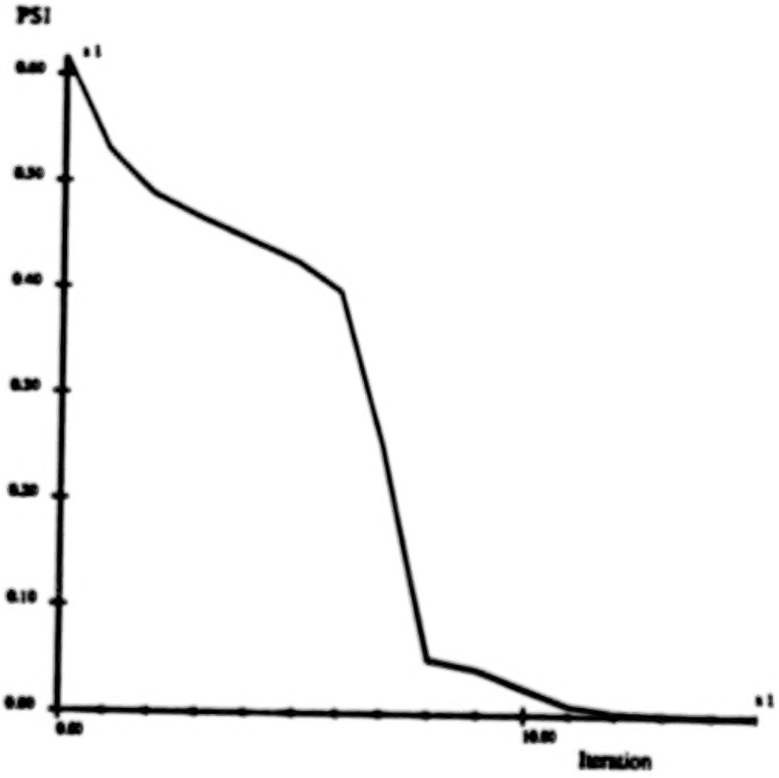

Figure 3b - Problem 1 PSI.

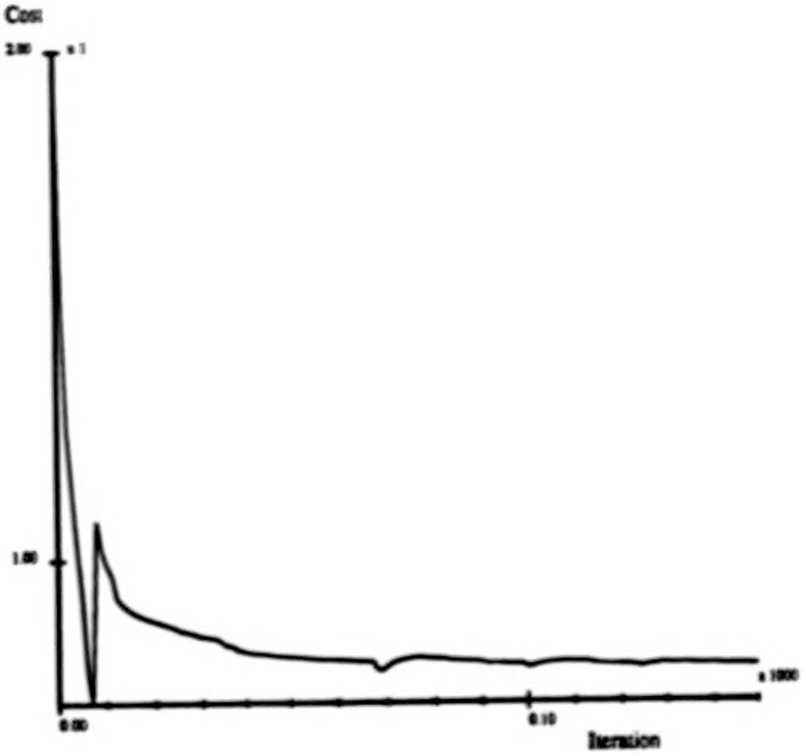

Figure 4 - Problem 1 cost.

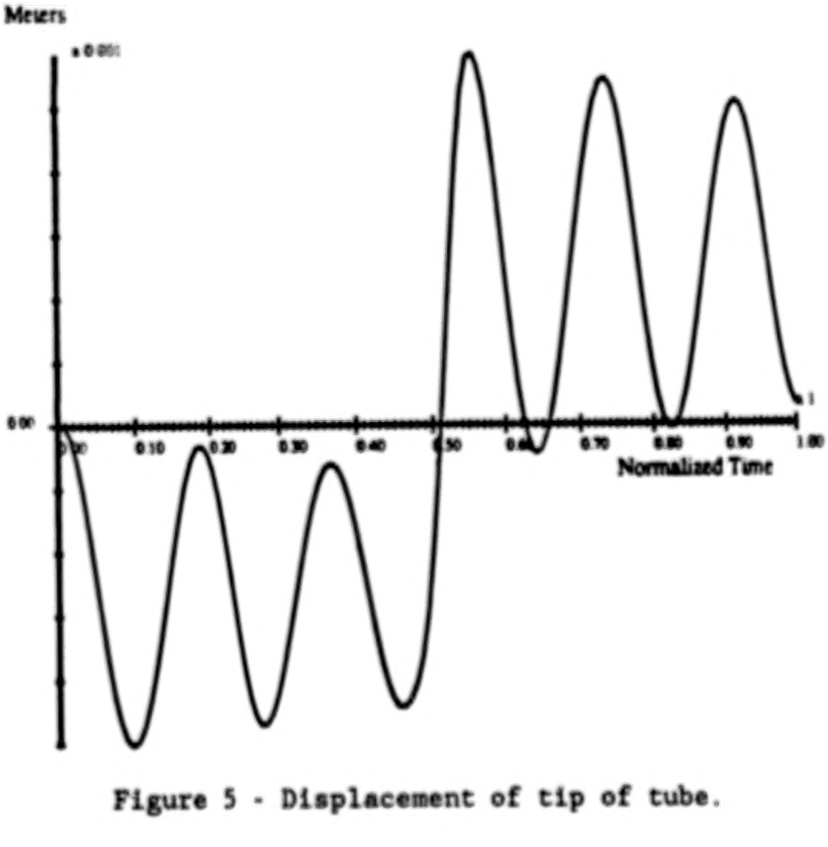

Figure 5 - Displacement of tip of tube.

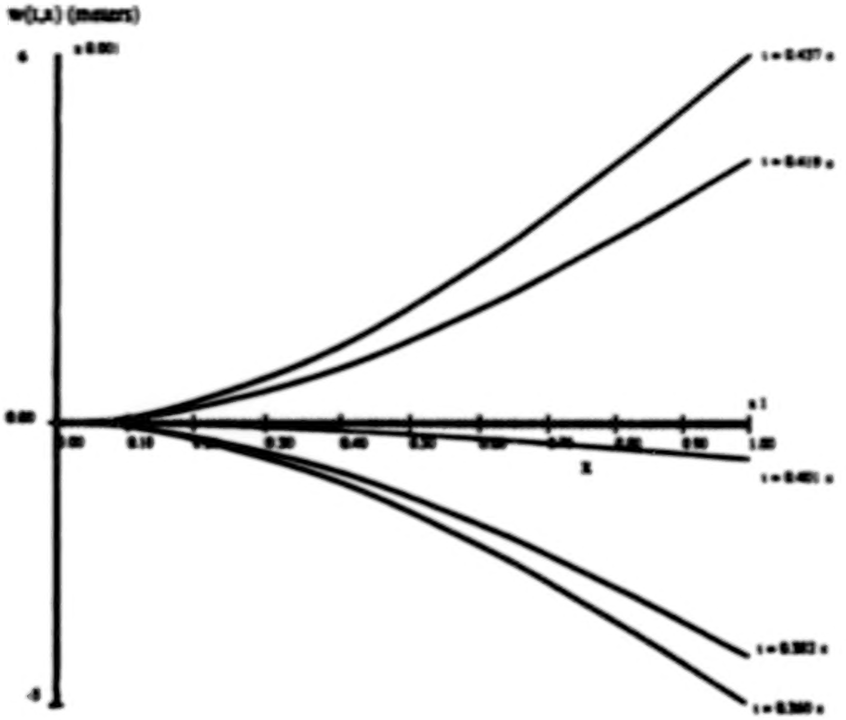

Figure 6 - Beam profile.

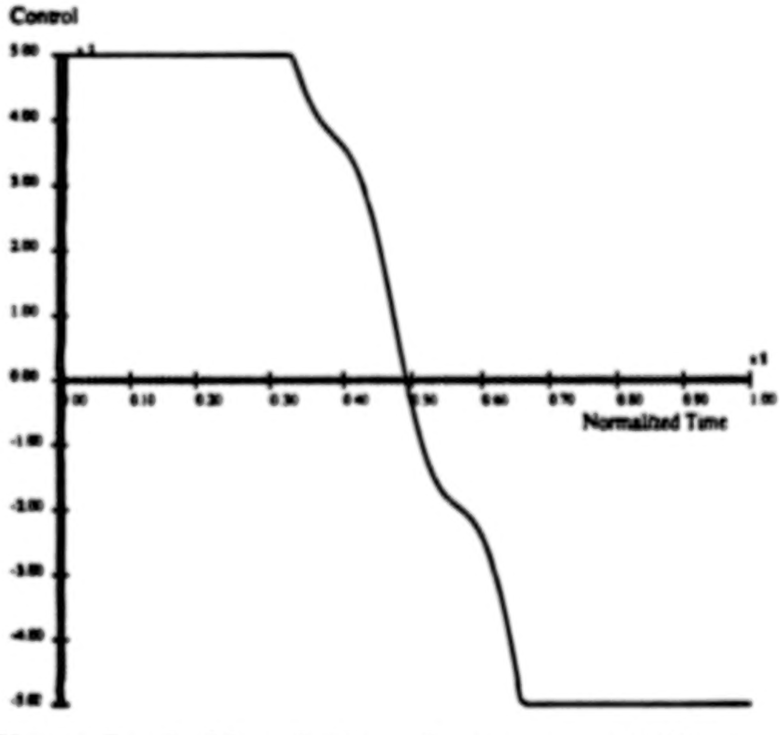

Figure 7 - Problem 2 time of maneuver = 0.800 seconds.

394

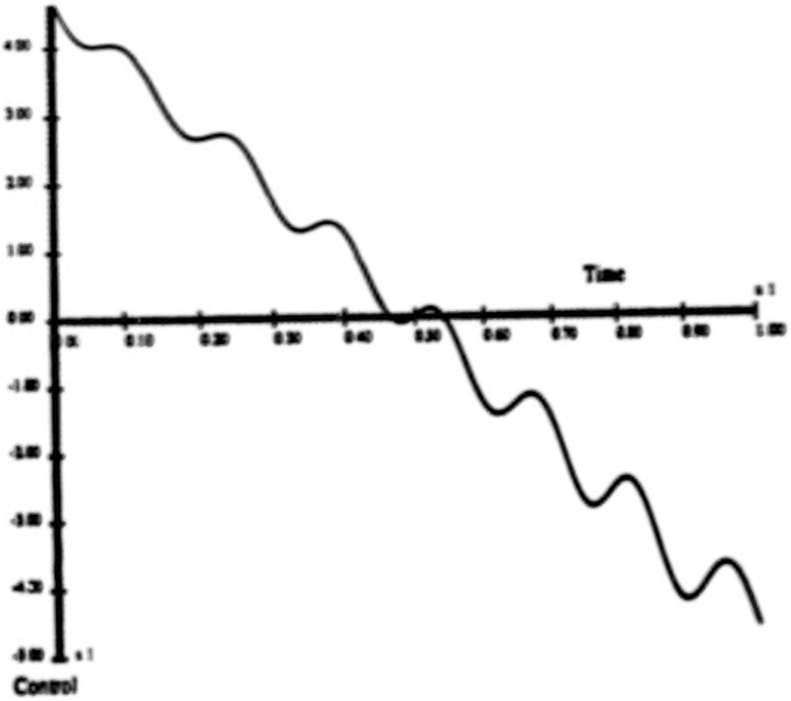

Figure 8 - Problem 2 time of maneuver = 1.000 seconds.

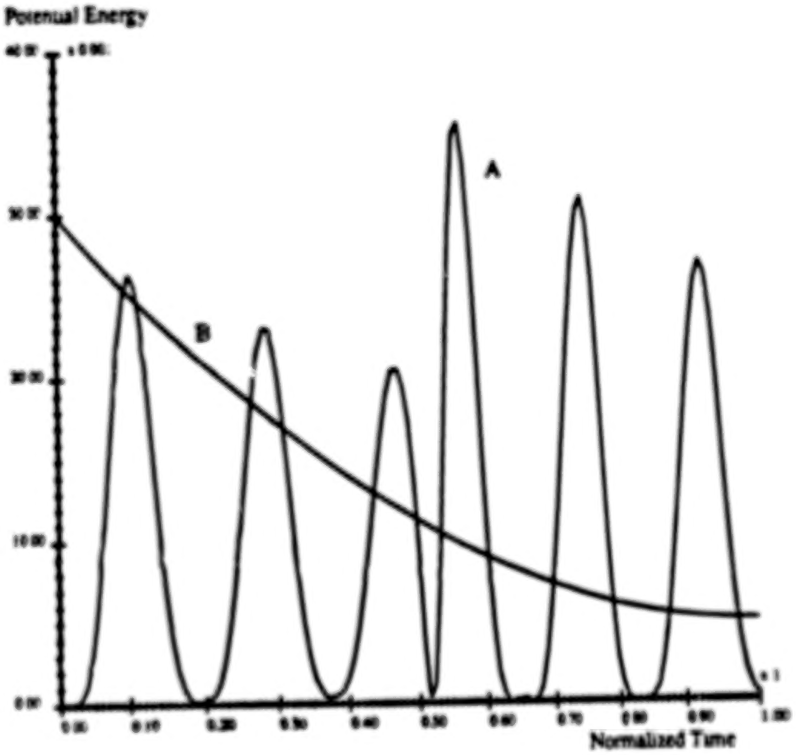

Figure 9 - Problem 1 potential energy.

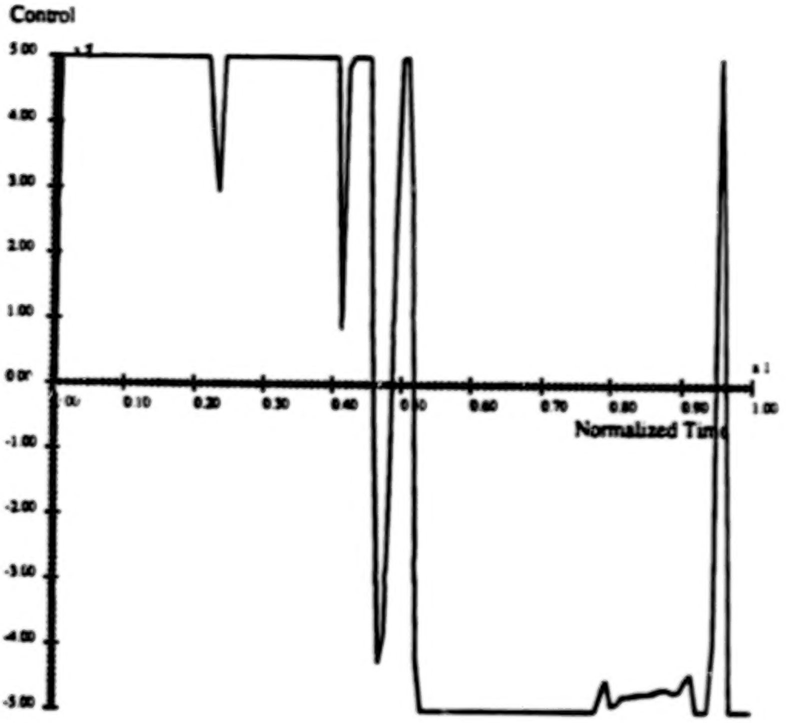

Figure 10 - Problem 3.

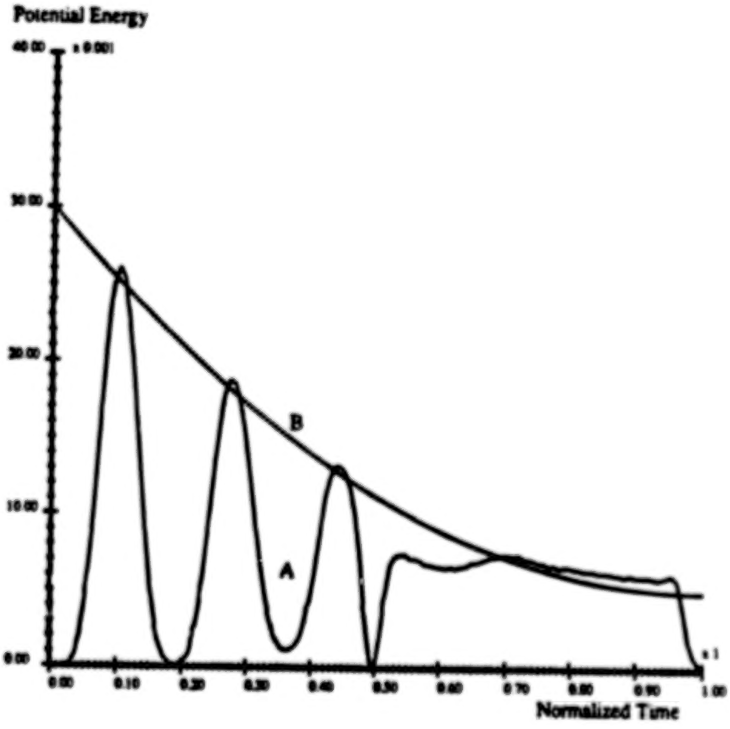

Figure 11 - Problem 3 potential energy.

OPTIMAL PLACEMENT OF EXCITATIONS AND SENSORS BY SIMULATED ANNEALING

M. Salama, R. Bruno, G-S. Chen, and J. Garba
Applied Technologies Section
Jet Propulsion Laboratory
California Institute of Technology

BACKGROUND

It is often desired in many applications to optimally select the locations of a given number of discrete actuators and response measurements. For example, ground modal testing involves the determination of the structural dynamic characteristics (frequencies, modes, and damping) from forced vibration tests. The locations of excitations and measurements are usually assigned on the basis of skilled engineering insight. After intensive processing and review of the test data, it may be further required to perform additional testing for a different set of excitation and measurement locations. The process is repeated until satisfactory results have been obtained for all modes of interest.

Repeated experimentation and data review is a luxury that cannot be afforded in the on-orbit verification of the dynamics of complex large structures which have been assembled or deployed for the first in space in their service configuration. Especially in the latter case, it is essential to determine in advance the number and locations of required excitations such that the quality and quantity of information derived from a single set of measurements are maximized.

When the locations available for placement of the excitation and measurement devices are spatially continuous, the usual gradient - based optimization methods can be used successfully to determine the optimum locations. However, when the available locations are spatially discrete, the problem becomes one of integer or combinatorial optimization. Except for the simplest cases, combinatorial optimization problems tend to be nonconvex and to require the evaluation of very large numbers of combinations of possible locations - thus becoming computationally intractable. Their exact solution is usually not possible with reasonable expenditure of computing resources. Thus instead of seeking the exact optimum, one must resort to suboptimal approximate techniques, most of which are heuristically-based [1, 2, 3]. In this paper, we further pursue the method of simulated annealing of Ref. [3] with the objective of (1) exploring a number of improvements which aim at incorporating knowledge about the structural characteristics in the random search of the simulated annealing method, and (2) applying the technique to the problem of finding the optimal location of passive dampers.

OPTIMIZATION STATEMENT

The optimal placement problem at hand may be stated as follows:

Given I^* sensors that may be placed at any of I possible discrete locations, and given J^* actuators that may be placed at any of J possible discrete locations, find the combination of location $C(I^*, J^*)$, $I^* \epsilon I$, $J^* \epsilon J$ which extremize an objective function $E(I^*, J^*)$, Figure 1.

The specific choice of the objective function E, and whether it should be maximized or minimized is problem dependent. It may be taken to represent a structural property or a response quantity. And just as in the continuous optimization problems, side constraints may be imposed on the design variables (locations of I^* and J^*) or any function thereof $h(I^*, J^*)$. In some cases, the design variables may consist of sensor locations only or actuator locations only. When both are present, their co-location may be admitted.

$$\text{Find } C(I^*, J^*);\ I^* \epsilon I;\ J^* \epsilon J \tag{1}$$

$$\text{Such that } E(I^*, J^*) \rightarrow \text{ EXTREMUM} \tag{2}$$

$$\text{Side constr. } \overline{h} \geq h(I^*, J^*) \geq \underline{h} \tag{3}$$

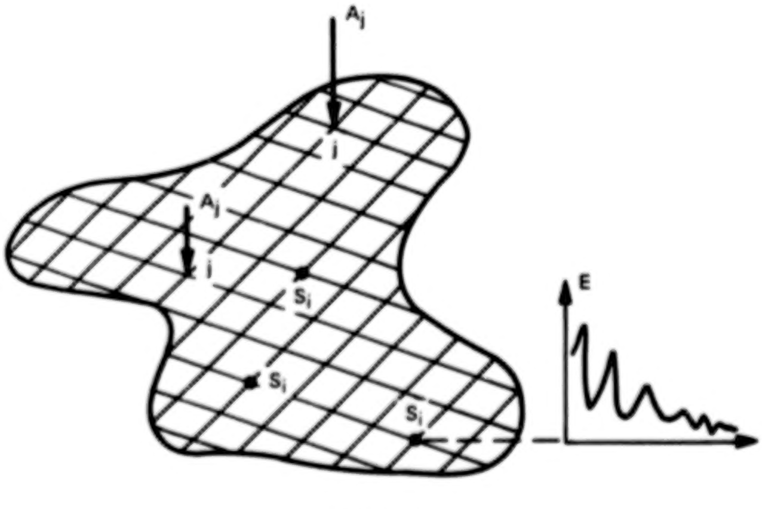

Figure 1.

COMPUTATIONAL COMPLEXITY

Through enumeration, it is possible to determine the exact solution to the problem stated previously by evaluating the objective function for every possible combination of I* sensor locations and J* actuator locations. This is a combinatorial optimization problem for which the number of possible combinations that must be examined can be found from

$$\eta^* = \frac{I!}{I^*!(I-I^*)!} \times \tfrac{1}{2} \left[\frac{J!}{J^*!(J-J^*)!} + 1\right] \tag{4}$$

The (½) and (+1) account for Maxwell's reciprocity theorem relating locations of actions and response. Table 1 below gives numerical values for η^* for various parameter values. Clearly, the number of possible combinations that must be evaluated becomes extremely large rather rapidly for problems with relatively small order.

Table 1

I	I*	J	J*	η^*
5	3	5	2	55
20	5	20	2	1.48×10^6
100	10	50	5	1.84×10^{19}
1000	100	500	10	$\sim \infty$

Intractable, Except for Simplest Cases

ITERATIVE IMPROVEMENT TECHNIQUES

Most conventional techniques for finding approximate solutions to combinatorial optimization problems are built around the idea of iterative improvements. Starting with an initial solution, iterative improvement techniques repeatedly consider changes in the current solution and accept only those that improve the objective function, see Figure 2. The disadvantage of these techniques is that they usually get trapped in a local optimum. Without a mechanism to allow climbing out of local optima, they will fail to discover more global ones. The simulated annealing technique provides such a mechanism and may be considered a variation on iterative improvement algorithms.

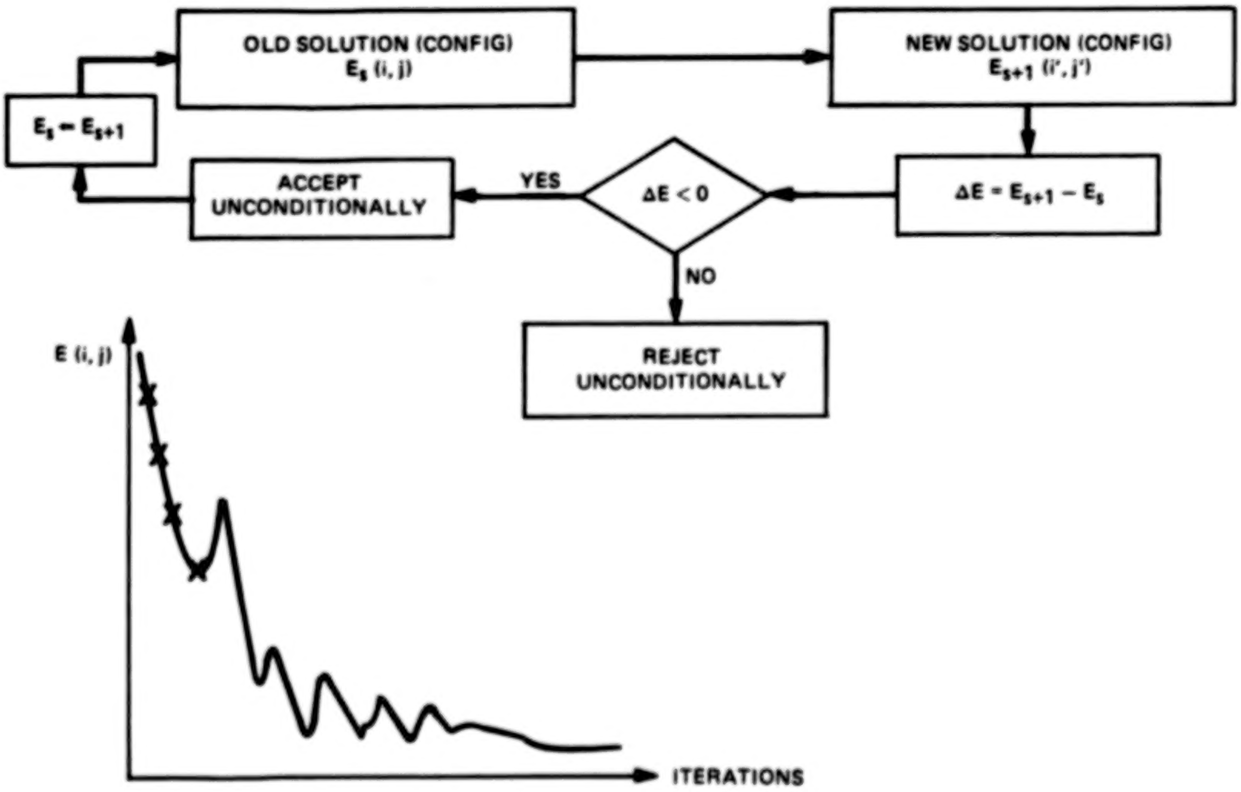
OLD SOLUTION (CONFIG)
$E_s(i, j)$
NEW SOLUTION (CONFIG)
$E_{s+1}(i', j')$
$E_s \leftarrow E_{s+1}$
ACCEPT UNCONDITIONALLY
YES
$\Delta E < 0$
$\Delta E = E_{s+1} - E_s$
NO
REJECT UNCONDITIONALLY
E (i, j)
ITERATIONS

Figure 2.

THE SIMULATED ANNEALING HEURISTIC

In trying to numerically simulate the behavior of atoms of a body in thermal equilibrium at finite temperature, Metropolis et al. [4] observed that · at high temperature T_h the atoms are randomly arranged in a state of disorder whose energy level is high. Following Figure 3, as the temperature T_h is cooled to T_o, the atoms migrate to a more ordered state having low energy level. The final degree of order depends on the cooling rate. Too fast cooling (quenching) is characterized by a monotonic decrease in energy to an intermediate state of semi-order. On the other hand slow cooling (annealing) is characterized by a general decrease in energy accompanied by occasional small energy increases whose rate of occurrence may be estimated by the probability density

$$P = 1/(e^{\Delta E/K_B T}) \qquad (5)$$

where ΔE is the change in energy, K_B is a Boltzmann constant, and T is the current temperature. At the low temperature end of the annealing process the system's energy reaches a much lower value (ground state) and the atomic arrangement reaches a much higher degree of order (Crystaline) than in the rapid quenching regime. Annealing, therefore, allows achieving a more global energy optimum than is possible by the local optimum provided by rapid quenching.

Use of the annealing simulation algorithm as an optimization tool is, therefore, built on the premise that in anticipation of reaching a more globally optimum solution, we must occasionally accept deteriorating ones. The probability of accepting deteriorating solutions is given by Equation (5). And it is these probabilistic jumps that allow the solution to climb out of local optima.

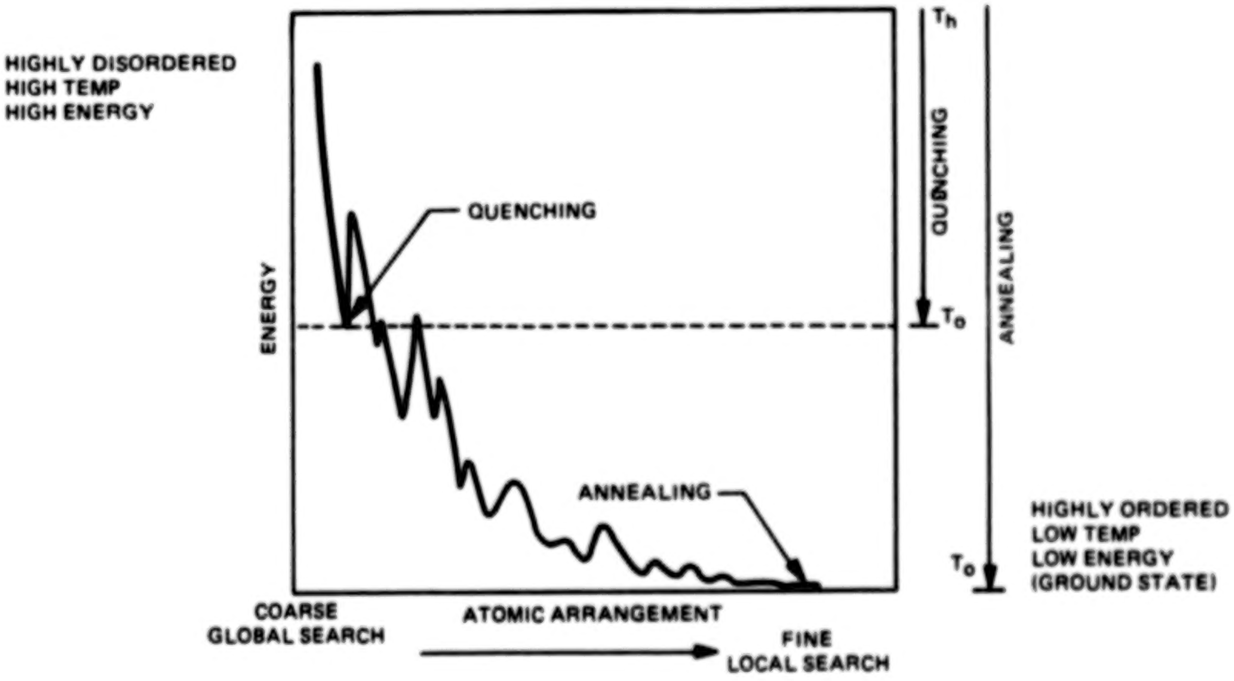
HIGHLY DISORDERED
HIGH TEMP
HIGH ENERGY
QUENCHING
ENERGY
ANNEALING
T_h
QUENCHING
T_o
ANNEALING
T_o
HIGHLY ORDERED
LOW TEMP
LOW ENERGY
(GROUND STATE)
COARSE
GLOBAL SEARCH
ATOMIC ARRANGEMENT
FINE
LOCAL SEARCH

Figure 3.

SIMULATED ANNEALING ALGORITHM

The flow chart in Figure 4 outlines steps of the simulated annealing heuristic just described. It differs from the iterative improvements algorithm mainly in the introduction of the probability function which controls the frequency of accepting deteriorating solutions. As an optimization tool, the simulated annealing method does not involve any actual annealing or temperature. The product K_BT is replaced by θ which may be viewed as a pseudo temperature, a parameter that controls the frequency of accepting deteriorating solution during the optimization process. Notice that the probability density function P, ranging from 1.0 to zero, is highest at high pseudo temperature θ_h, (i.e., at the beginning of the optimization iterations). The algorithm therefore begins with a coarse global search where more deteriorating solutions are accepted (P = 50% to 80%), and gradually ends up with fine local search where only improving solutions are accepted. As the optimization procedure continues iteratively, new solutions or configurations must be generated. For the type of problems under consideration, a new solution or configuration is defined by a set of locations for I* sensors and J* excitations. In an earlier application of the method [3], new solutions were generated from the current one by moving the J* excitations one at a time randomly to any of the remaining (J-J*) unassigned locations, and moving the I* sensors one at a time randomly to any of the remaining (I-I*) unassigned locations. Variations on this scheme will be explored subsequently.

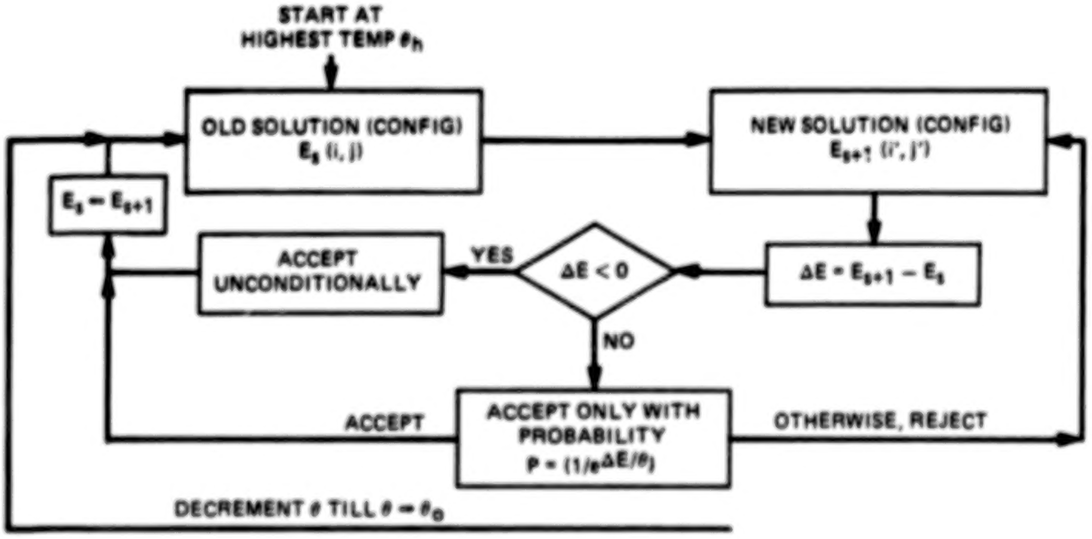
START AT
HIGHEST TEMP θ_h
OLD SOLUTION (CONFIG)
E_s (i, j)
NEW SOLUTION (CONFIG)
E_{s+1} (i', j')
$E_s = E_{s+1}$
ACCEPT UNCONDITIONALLY
YES
$\Delta E < 0$
$\Delta E = E_{s+1} - E_s$
NO
ACCEPT
ACCEPT ONLY WITH PROBABILITY
$P = (1/e^{\Delta E/\theta})$
OTHERWISE, REJECT
DECREMENT θ TILL $\theta = \theta_0$

Figure 4.

OPTIMAL LOCATIONS OF PASSIVE DAMPERS

1. DESCRIPTION

The cantilevered truss shown in Figure 5 consists of 58 axial members connecting 23 pinned joints with 114 unrestrained degrees of freedom. The modal masses are not uniformly distributed; 55% of the mass is concentrated near the free tip. The first nine undamped frequencies and a qualitative description of their corresponding modes are listed in Table 2. While the first few modes are primarily global in nature, higher modes of the truss are primarily local with much of the strain energy tending to be concentrated at members near the free tip. Assuming no inherent structural damping, we wish to place a limited number of passive dampers N_D along some members of the truss so as to achieve a desired level of modal damping ζ_i in any specified mode i. If we further assume that the target modal damping ζ_i per cycle is to be adjusted so that the total decay over one second of time is constant = 17.4% for any mode, then $\zeta_i = .174/\Omega_i$. These are also listed in Table 2.

Table 2

Mode No.	1	2	3	4	5	6	7	8	9
Freq. (Hz)	8.7	15.5	33.0	60.0	71.3	74.2	79.5	88.2	95.1
Mode Type	1^{st} xz	1^{st} xy	1^{st} torsion	Comb. xy xz	2^{nd} xz	local bending & twisting almost near tip			
Target Modal Damping ζ_i	2%	1.12%	.53%	.29%	.24%	.23%	.22%	.20%	.18%

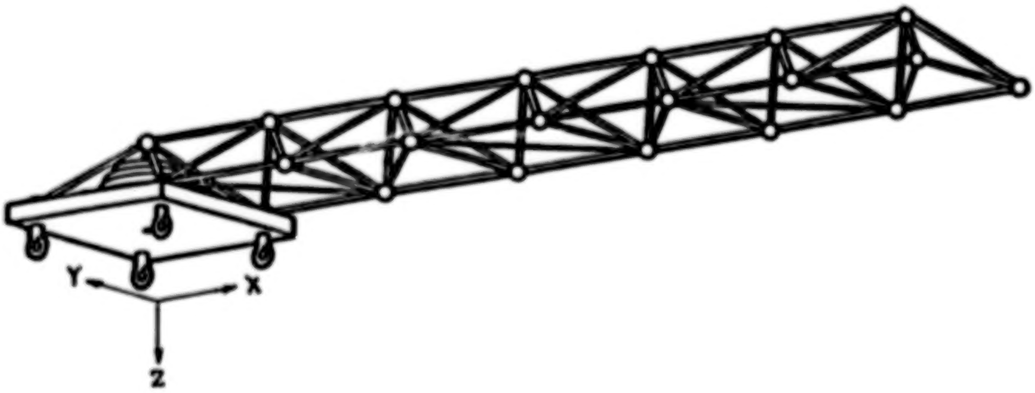

Figure 5.

2. PERFORMANCE INDEX

With the quantities defined below, one may define the performance index J_e as a measure of performance over all N_m modes under consideration. Maximization of J_e over all possible combinations of N_D damper locations will insure the highest possible modal damping ζ_i for modes $i=1,\ldots,N_m$.

The specific form of the performance index J_e below is motivated by the fact that for $r=2$, $N_m=2$, a geometrical interpretation can be given: if e_1 and e_2 represented two perpendicular sides of a triangle, the maximum value for J_e for a constant $(e_1 + e_2)$ will occur when $e_1 = e_2$. This interpretation may be generalized to any hyper-dimension N_m and for any $r>2$. More importantly, this means that maximization of J_e will insure the maximization of all e_i quantities more equally. The higher the r-values, the more sensitive will J_e be to small changes in e_i. In the following numerical results, $r=4$ was used.

DEFINE: $\zeta_o = 5\%$ - percent damping provided by any of N_D passive damping elements

ϵ_{ij} - strain energy ratio imparted in mode i to truss member j

ζ_i - percent modal damping computed for mode i

$$= \sum_{j=1}^{N_D} \zeta_o \, \epsilon_{ij}$$

$e_i = \zeta_i/\bar{\zeta}_i$ - normalized modal damping for mode i

OBJECTIVE: maximize the performance index J_e

$$J_e = \left(\frac{1}{N_m} \sum_{i=1}^{N_m} (e_i)^{1/r}\right)^r \qquad r \geq 2 \qquad (6)$$

3. NUMERICAL RESULTS

In what follows, two cases are considered. They differ in the number of passive elements N_D used, and the number of modes N_m targeted for modal damping alteration. In case 1, four passive damping elements are used to achieve the target modal damping in the first three modes. In case 2, six passive damping elements are used to achieve the target modal damping in all nine modes. The optimal locations found by the simulated annealing technique are indicated in Figure 6 by 1 and 2, for case 1 and case 2, respectively. The corresponding modal damping values are given by mode for each case in Table 3. Note that all target values have been exceeded for both cases, except for mode 3 in the second case. This could also be satisfied with the addition of a seventh damper.

Table 3

	Mode No.	1	2	3	4	5	6	7	8	9
Case 1 $N_D=4$ $N_m=3$	Target $\bar{\zeta}_i$	.02	.0112	.0053	.0029	.0024	.0023	.0022	.0020	.0018
	Computed ζ_i $i=1,..3$	.0207	.0203	.0065						
Case 2 $N_D=6$ $N_m=9$	Computed ζ_i $i=1,...,9$	.0208	.0193	.0038	.0330	.0160	.0341	.0304	.0393	.0201

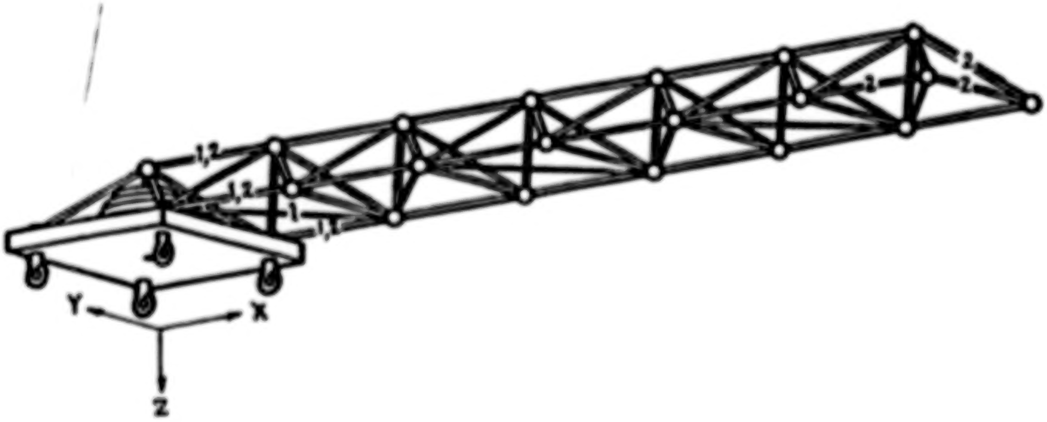

Figure 6.

ITERATION HISTORY FOR FOUR PASSIVE DAMPING ELEMENTS

An insight into how the algorithm converges can be gained by examination of the iteration history in Figure 7 for four passive damping elements. Convergence was achieved after about 200 solutions steps. As a result of the probability function used, the solutions began with large variations (in both amplitude and frequency) about a trend line (dotted). Gradually, these variations are damped out. Note that an enumeration (exact) solution to this problem would require 58!/[4!(58-4)!] = 424,270 evaluations.

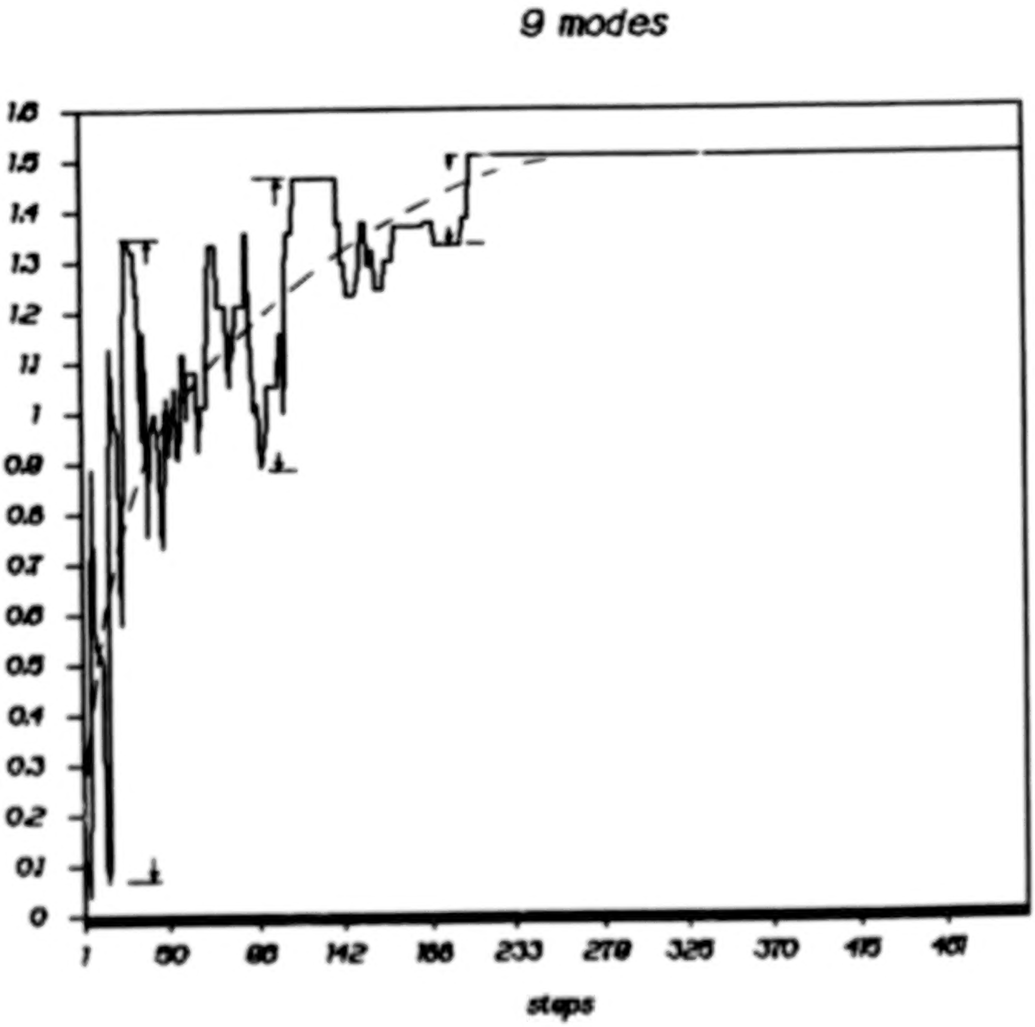

Figure 7.

OPTIMAL PLACEMENT OF EXCITATIONS & SENSORS

In this section, we revisit the previously solved example of the COFS space truss [3], with the aim of introducing a number of improvements in the policy of generating new solutions during the simulated annealing optimization. The objective here is to place I* sensors and J* actuators so as to maximally observe all first thirteen modes of the 960 degrees of freedom truss structure. In general, all $N=960$ degrees of freedom are possible sites for excitation and sensing. In practice, however, only a subset I are allowed for sensing using I* sensors ($I^* \epsilon\ I\ \epsilon\ N$), and only a subset J are allowed for excitation using J* actuators ($J^* \epsilon\ J\ \epsilon\ N$). Co-location of sensors and actuators is admitted, and only one sensor and one actuator may be placed at a degree of freedom.

Taking the kinetic energy $E_i{}^j$ measured at degree of freedom i due to excitation at degree of freedom j to be the observer for the selected $N^*=13$ modes, one can form the objective function to be maximized as given below. Instead of the kinetic energy $E_i{}^j$, one may choose to observe the square of the displacement $U_i{}^j$. The general form of the objective function remains the same, but the optimal locations are expected to be different. This is illustrated by the numerical results in Figure 8 for the three cases listed in Table 4 below.

OBJECTIVE: Place a Given Number of Sensors and Excitations
so as to Maximally Observe a Given Number of Modes.

$$\underset{I^*,J^*}{\text{Max}} \left[\sum_{n}^{N^*} \sum_{m}^{N^*} \left(\sum_{j=1}^{J^*} \sum_{i=1}^{I^*} E_i{}^j \right)^{1/r} \right]^r, \ (I^* \epsilon\ I\ \epsilon\ N), \ (J^* \epsilon\ J\ \epsilon\ N)$$

$$E_i{}^j = \tfrac{1}{2}\, \dot{U}_m \,\text{diag}\, \phi_m(j)\, \phi_{im}^T\, m_i\, \phi_{in} \text{diag}\, \phi_n(j)\, \dot{U}_n = \text{Energy Transf. Funct.}$$

$$U_i{}^j = U_m \,\text{diag}\, \phi_m(j)\, \phi_{im}^T\, \phi_{in} \text{diag}\, \phi_n(j)\, U_n = \text{Displacement Transf. Funct.}$$

Table 4

Case	N	I	J	N*	I*	J*
1	960	480	480	13	12	2
2					24	2
3					12	4

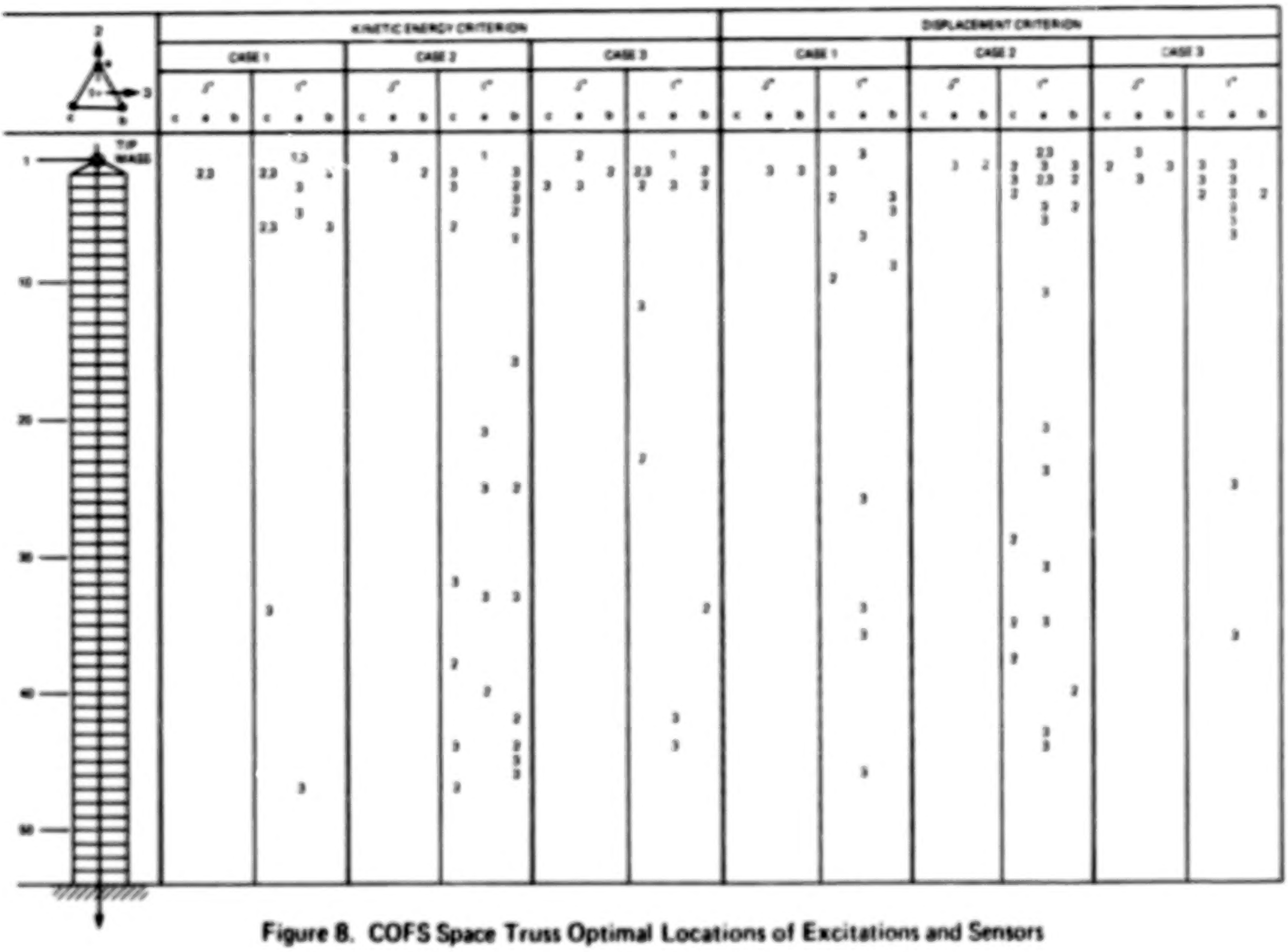
KINETIC ENERGY CRITERION
DISPLACEMENT CRITERION
CASE 1
CASE 2
CASE 3
CASE 1
CASE 2
CASE 3
TIP MASS
1
10
20
30
40
50

Figure 8. COFS Space Truss Optimal Locations of Excitations and Sensors

BEST COPY AVAILABLE

GENERATING NEW SOLUTIONS

One of the key steps in the simulated annealing technique deals with how to create a new solution from the current one. In the examples discussed so far this was done by moving the J^* excitations one at a time randomly to the remaining $(J-J^*)$ unassigned locations, and moving the I^* sensors one at a time randomly to the remaining $(I-I^*)$ unassigned locations.

The following additional rules are now introduced to lend some insightful knowledge of the solution behavior into the otherwise highly randomized moves above.

1. RULES

   a. Limit the excitation and sensor assignments to a smaller set of degree of freedom D^* having relatively high modal displacements. $D^* \supsetneq D_1, D_2, \ldots D_{N^*}$, where D_i set contains $\overline{N}$ degree-of-freedom $(\overline{N} \ll N)$ with the largest displacement magnitudes in mode i. The size $\overline{N}$ is empirically chosen to be the largest of $\frac{1}{2}\sqrt{IxI^*}$ and $\frac{1}{2}\sqrt{JxJ^*}$.

   b. From the expressions for E_i^j one can show that $(E_i^j)_{i-j} \geqslant (E_i^j)_{i \neq j}$. Thus co-locating the J^* excitations and I^* sensors (whenever possible) will give the largest observable response. If $I^* \neq J^*$, the remaining ones are assigned independently.

   c. As new solutions are generated, keep track of the best one so far. When θ is decremented, use this best solution as the starting point for the current temperature range.

Incorporation of the above rules in the policy for generating new solutions alter the simulated annealing implementation details - but not its basic philosophy. The changes are shown in Figure 9.

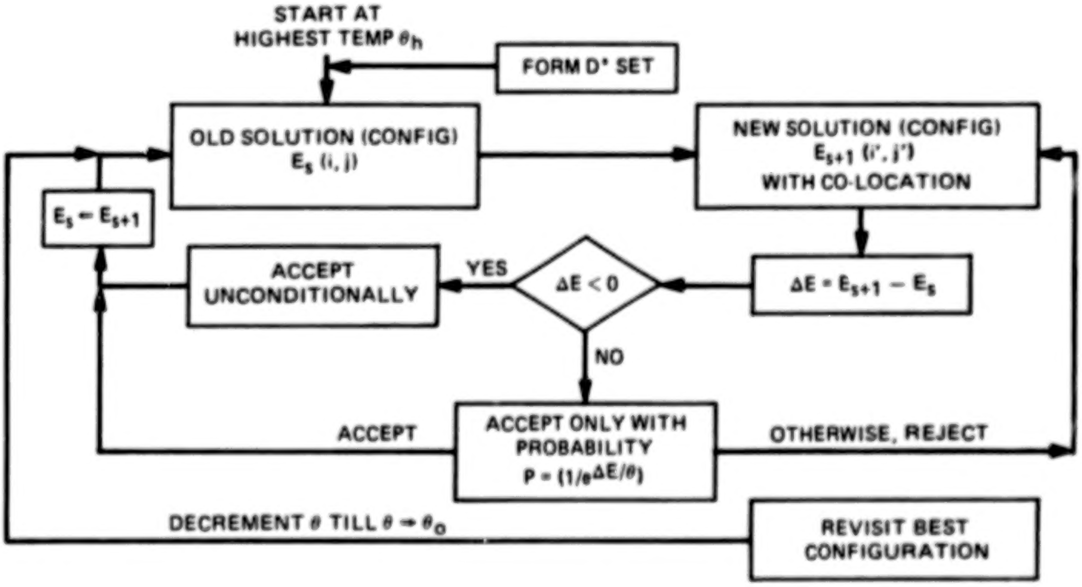
START AT
HIGHEST TEMP θ_h
FORM D* SET
OLD SOLUTION (CONFIG)
$E_s(i, j)$
NEW SOLUTION (CONFIG)
$E_{s+1}(i', j')$
WITH CO-LOCATION
$E_s \leftarrow E_{s+1}$
ACCEPT UNCONDITIONALLY
YES
$\Delta E < 0$
$\Delta E = E_{s+1} - E_s$
NO
ACCEPT
ACCEPT ONLY WITH PROBABILITY
$P = (1/e^{\Delta E/\theta})$
OTHERWISE, REJECT
DECREMENT θ TILL $\theta \rightarrow \theta_0$
REVISIT BEST CONFIGURATION

Figure 9.

412

2. NUMERICAL RESULTS

To assess the effect of the new solution generation rules of the previous section, the three cases of Table 4 were resolved with and without these rules. Table 5 compares the two sets of results using two measures: the maximum observed energy achieved at the end of the optimization schedule, and the CPU time required. The trend strongly supports the conclusion that the suggested rules help the simulated annealing algorithm in achieving more superior optima while requiring generally less computing time.

Figure 10 compares the set of actuator and sensor locations corresponding to the cases in Table 5.

Table 5

Max. Observed Energy for 13 Modes
(-:-) CPU Time

	Without New Rules	With New Rules
Case 1	5.37 (1:28)	6.61 (1:26)
Case 2	6.87 (2:18)	7.71 (2:24)
Case 3	9.62 (4:54)	9.72 (3:36)

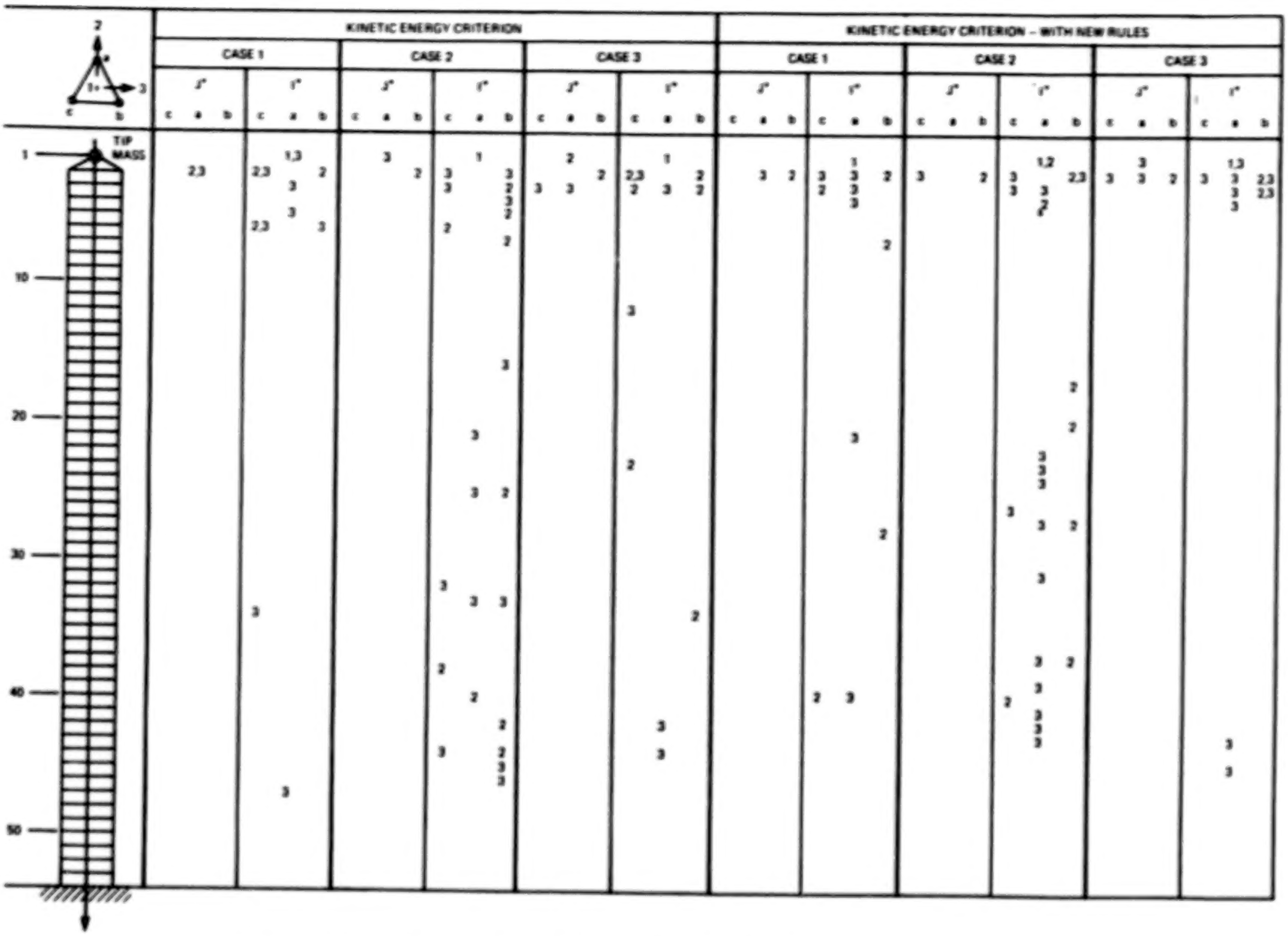
KINETIC ENERGY CRITERION
KINETIC ENERGY CRITERION – WITH NEW RULES
CASE 1
CASE 2
CASE 3
c a b
TIP MASS
1
10
20
30
40
50

Figure 10. COFS Space Truss Optimal Locations of Excitations and Sensors

414

CONCLUSIONS

The optimal placement of discrete actuators and sensors is posed as a combinatorial optimization problem. Two examples for truss structures were used for illustration; the first dealt with the optimal placement of passive dampers along existing truss members, and the second dealt with the optimal placement of a combination of a set of actuators and a set of sensors. Except for the simplest problems, an exact solution by enumeration involves a very large number of function evaluations, and is therefore computationally intractable. By contrast, the simulated annealing heuristic involves far fewer evaluations and is best suited for the class of problems considered. As an optimization tool, the effectiveness of the algorithm is enhanced by introducing a number of rules that incorporate knowledge about the physical behavior of the problem. Some of the suggested rules are necessarily problem dependent.

ACKNOWLEDGMENT

This work was carried out at the Jet Propulsion Laboratory, California Institute of Technology under contract with NASA. The effort was sponsored by S. Venneri, Office of Aeronautics and Space Technology.

REFERENCES

1. Skelton, R. and DeLorenzo, M.,k "Selection of Noisy Actuators and Sensors in Linear Stochastic System," Journal of Large Scale Systems, Theory and Applications, pp. 109-136, 1983.

2. Haftka, R. and Adelman, H., "Damping and Control of Spacecraft Structures: Selection of Actuator Locations for Static Shape Control of Large Space Structures by Heuristic Integer Programming," Computers and Structures, Vol. 20, No. 1-3, pp. 575-582, 1985.

3. Salama, M., Rose, T., and Garba, J., "Optimal Placement of Excitations and Sensors for Verification of Large Dynamical Systems," 28th AIAA/ASME/ASCE/AHS Structures, Structural Dynamics and Materials Conference, Paper No. 87-0782, Monterey, CA, April 1987.

4. Metropolis, N., Rosenbluth, A., Rosenbluth, M., Teller, A., and Teller, E., "Equations of State Calculations by Fast Computing Machines," Journal of Chemical Physics, Vol. 21, No. 6, pp. 1087-1092, June, 1953.

EXPERIENCES IN APPLYING OPTIMIZATION TECHNIQUES TO CONFIGURATIONS FOR THE CONTROL OF FLEXIBLE STRUCTURES (COFS) PROGRAM

Joanne L. Walsh
National Aeronautics and Space Administration
Langley Research Center
Hampton, Virginia 23665

416

EXPERIENCES IN APPLYING OPTIMIZATION TECHNIQUES TO CONFIGURATIONS FOR THE CONTROL OF FLEXIBLE STRUCTURES (COFS) PROGRAM

INTRODUCTION

Over the last two decades an extensive amount of work has been done in developing and applying mathematical programming methods to the optimum design of structures (refs. 1-11). In the past, optimization techniques have been applied mainly in the conceptual (refs. 2 and 6) and preliminary design (refs. 7 and 8) phases with few applications to realistic problems such as those found in references 9-11. In reference 2 Ashley discusses the lack of applications of optimization techniques to realistic problems. Generally, transforming a realistic problem into a mathematical programming formulation is difficult and a high degree of engineering judgment and experience is needed. Also the choice of an objective function is not always obvious. Ashley offers three reasons why classically optimized structures are not being found in actual service: first, developmental engineers are sometimes reluctant to try "new and unfamiliar" methods; second, they sometimes find it difficult to translate realistic design or operational requirements into a mathematical programming formulation; and third, they sometimes find it easier to perform many finite element parametric analyses than learn optimization software. The latter is especially true when a designer is faced with time and schedule deadlines and will often choose to perform parametric studies rather than try formal optimization procedures.

This paper will address several of these issues - namely the objective function choice and the difficulty of translating realistic design requirements into a mathematical programming formulation. The paper will also show that optimization procedures can also be helpful later in the postdesign phase.

The purpose of the paper is to relate experiences gained in applying optimization procedures to design large flexible spacecraft for the Control of Flexible Structures (COFS) program. First some background and a brief discussion of the motivation behind the COFS work will be presented. Next the paper will discuss two studies using optimization techniques related to the COFS project which address the issue of objective function choice. In the first study an optimization procedure was developed for frequency spacing for a simple model of a COFS-II configuration. The next study involved an optimization procedure for a detailed model of the COFS-I configuration in connection with a buckling deficiency problem. The third study describes a redesign activity of the COFS-I mast in which optimization techniques were used to redesign the mast structure using the same design requirements as the contractor who originally designed the mast using parametric studies. Finally the paper will relate some experiences and insights gained in incorporating into a structural optimization procedure requirements that are realistic and which were continually being modified as the study was being conducted.

417

CONTROL OF FLEXIBLE STRUCTURES (COFS)

As spacecraft structural concepts increase in size, complexity, and flexibility, a need exists to develop and validate analytical methods to design and assess the performance of such spacecraft. The Control of Flexible Structures (COFS) research program shown in figure 1 was initiated by the NASA Office of Aeronautics and Space Technology (OAST) to develop a validated technology data base for understanding the structural response, pointing and shape control, suppression of inherent dynamic responses, and avoidance of undesirable interaction between flexible structures and controls. Information on the COFS program can be found in references 12-19. Shown in the figure are two projects in the COFS program. First the COFS-I Project was to involve a series of on-ground and in-flight tests to investigate the dynamics/control interactions utilizing a beam. Second the COFS-II project was to build on the control technology developed in COFS-I project to investigate three-dimensional dynamics/control interactions.

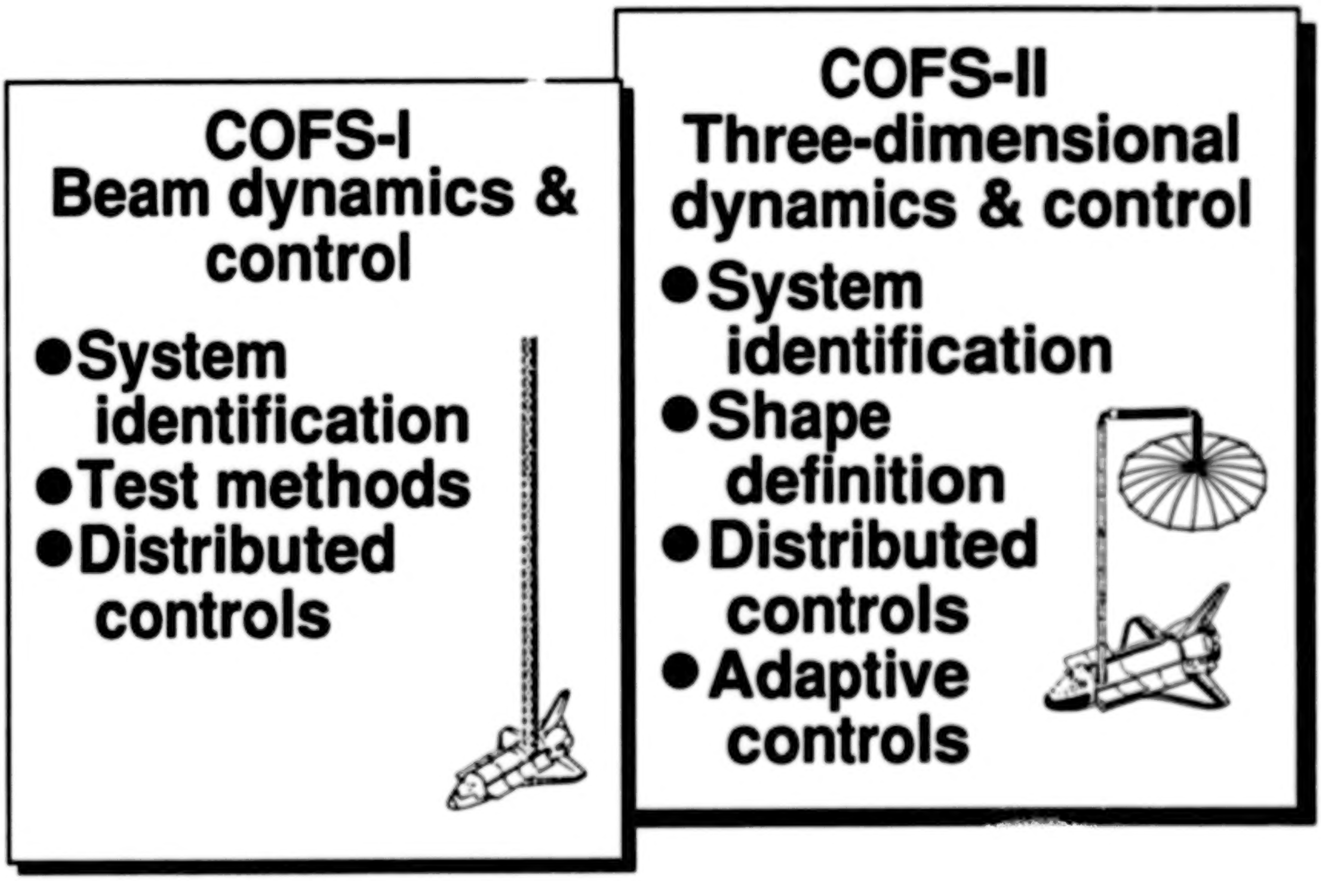
COFS-I
Beam dynamics & control
● System identification
● Test methods
● Distributed controls
COFS-II
Three-dimensional dynamics & control
● System identification
● Shape definition
● Distributed controls
● Adaptive controls

FIGURE 1

MOTIVATION FOR COFS OPTIMIZATION

The COFS structure is to be designed to have closely coupled vibration modes (fig. 2). This is contrary to the normal process in which the designer seeks widely spaced frequencies as he tries to control rigid body motions and avoid control/structures interactions. However, the COFS program requires a structure which has closely spaced frequencies in order to challenge control law and system identification methodology. The need for a method to systematically design large spacecraft with closely spaced frequencies was the motivation for the initial optimization work for frequency spacing of COFS.

- **COFS required closely spaced frequencies to challenge:**
  - **Control law synthesis**
  - **System identification**
- **Need**

Systematic method to design large space systems (LSS) for close-spacing of vibration frequencies

FIGURE 2

OVERVIEW OF OPTIMIZATION PROCEDURES FOR COFS STUDIES

An optimization procedure (fig. 3) was developed which systematically designed a large space system with closely spaced frequencies. The procedure uses the general-purpose finite-element analysis program Engineering Analysis Language (EAL, ref. 20) and a combination of the general-purpose optimization program CONMIN (ref. 21) and piecewise linear approximate analyses for the optimization. The eigenvalue analysis and constraint calculations are performed using EAL. The EAL system contains individual processors that communicate through a data base containing data sets. The data sets typically contain data describing the finite-element model of the structure (such as geometry) as well as response information that is accumulated during the execution of the processors. The processors can be executed in any appropriate sequence, and a sequence of processor executions is denoted as a "runstream". The EAL system also uses a set of flexible FORTRAN-like statements called executive control system (ECS) commands. These commands allow branching, testing data, looping, and calling runstreams (similar to calling FORTRAN subroutines). The EAL processors, with the appropriate ECS commands organized as runstreams are used to calculate the eigenvalues, eigenvectors, constraints, objective function and derivatives of these quantities. CONMIN is a general-purpose optimization program that performs constrained minimization using a usable-feasible directions search algorithm. In the search for new design variable values, CONMIN requires derivatives of the objective function and constraints. The user has the option of either letting CONMIN determine the derivative by finite differences or supplying derivatives to CONMIN. The latter method will be used herein. In the approximate analysis method, previously calculated derivatives of the objective function and constraint functions with respect to the design variables are used for linear extrapolation of these functions. The assumption of linearity is valid over a suitably small change in the design variable values and will not introduce a large error into the analysis provided the changes are small. This approximate analysis will be referred to as a "piecewise linear approximation." Errors which may be introduced by use of the piecewise linear approach are controlled by imposing "move limits" on each design variable during a design cycle. A move limit which is specified as a fractional change, δ, of each design variable value (for this work, δ=0.1) is imposed as an upper and lower design variable bound on each cycle. These move limits must not exceed the absolute design variable values. Details of the algorithm are contained in reference 11.

- **Use formal mathematical programming techniques**
- **Combine EAL, CONMIN, and approximate analyses**
- **Free vibration eigenvalue problem**

$$\left([K]-\omega_j^2[M]\right)\{\theta\}_j=0$$

- **Eigenvalue derivative**

$$\frac{\partial\omega_j^2}{\partial V_K}=\{\theta\}_j^T\left(\frac{\partial[K]}{\partial V_K}-\omega_j^2\frac{\partial[M]}{\partial V_K}\right)\{\theta\}_j$$

FIGURE 3

COFS-II FREQUENCY SPACING STUDY

The purpose of the COFS-II frequency study was to develop the methodology for systematically obtaining two pairs of closely-spaced frequencies. A conceptual design of a candidate COFS-II configuration is shown in figure 4. The configuration consisted of a mast, a boom, and a structure attached to the tip (such as an antenna).

Earlier unpublished parametric studies[*] using a simple model indicated the most suitable frequency pairs for close-spacing are the third frequency, f_3, with the fourth frequency, f_4, and the fifth frequency, f_5, with the sixth frequency, f_6. The third mode is characterized by bending and twisting of the mast and rigid body movement of the boom. The fourth mode is characterized by first in-plane bending of the mast and first in-plane bending of the boom. The fifth mode is characterized as second in-plane bending of the mast and second in-plane bending of the boom. The sixth mode is characterized by second out-of-plane bending coupled with torsion of the mast and first out-of-plane bending of the boom. These parametric studies verified the feasibility of closely spacing two pairs of frequencies and led to the development of an optimization procedure to systematically closely space pairs of frequencies. More details on the COFS-II frequency spacing optimization study can be found in reference 22.

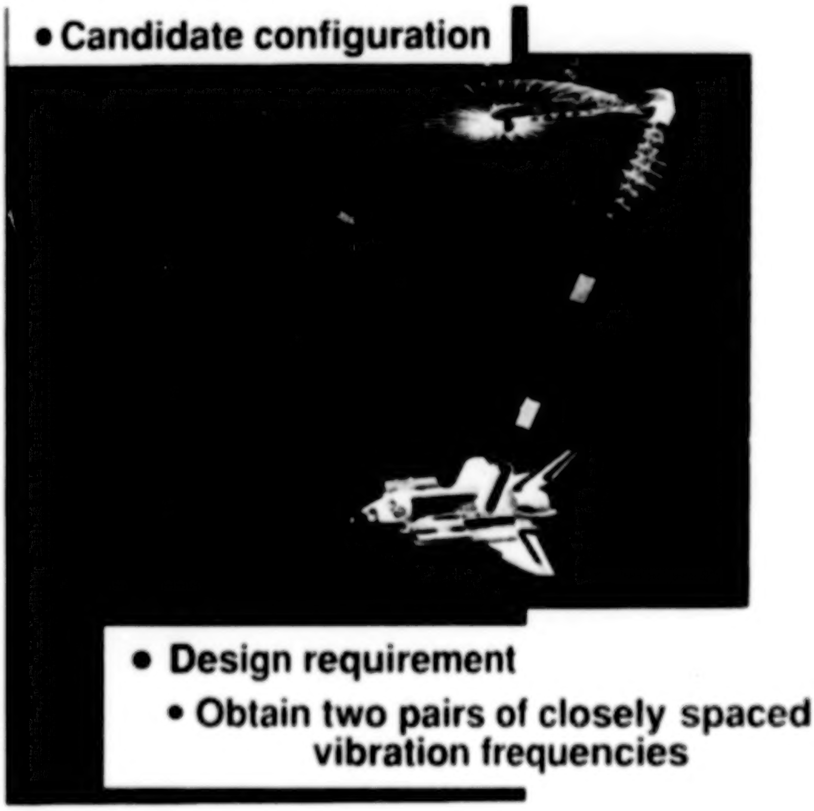

- Candidate configuration

- Design requirement
  - Obtain two pairs of closely spaced vibration frequencies

FIGURE 4

---

[*] Carried out and communicated to the author by Dr. Michael F. Card of the NASA Langley Research Center.

BEST COPY AVAILABLE

COFS-II MODEL FOR FREQUENCY SPACING STUDY

The simple model of a COFS-II configuration shown on the right in figure 5 was used in this study. The model which is based on the geometry derived from reference 23 is modeled as an equivalent beam with 17 joints. More detail on the model can be found in reference 22. The properties of the mast are fixed except for the length L_1. In the beam segment from the top of the mast to the tip of the boom, none of the properties are fixed.

The six design variables are shown below: the mast length (L_1), the boom length (L_2), the boom cross-sectional area (A), the two boom area moments of inertia (I_{yy} and I_{zz}), and the concentrated mass (M) at the tip of the beam. Since the structure is to be deployable to an arbitrary length in increments of two-bay lengths and must fold inside a canister on the Shuttle, the mast length L_1 is allowed to vary between 40 and 60 meters and the boom length L_2 between 1 and 25 meters. The tip mass, M, representative of an attachment such as an antenna is allowed to vary between 10 and 30 kg. The range of values for A, I_{yy}, and I_{zz} are chosen to prevent mode switching (i.e. want to ensure f_3 is paired with f_4 and f_5 is paired with f_6).

Design variables

L_1 - mast length

L_2 - boom length

A - boom cross-sectional area

I_{yy}, I_{zz} } Boom moments of inertia

M - mass attached to end of boom

Model

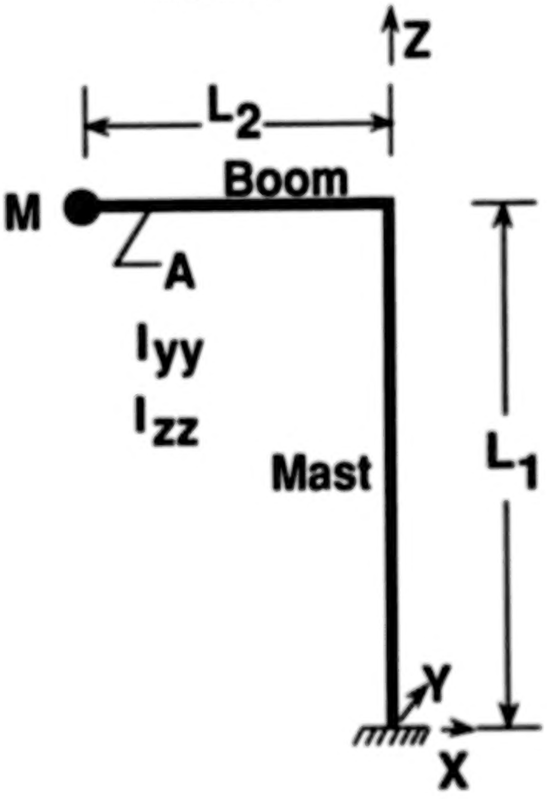

FIGURE 5

OPTIMIZATION FORMULATIONS FOR COFS-II FREQUENCY SPACING STUDY

Two optimization formulations (fig. 6) were tried for the COFS-II study. Since the aim of the study was to develop the methodology for closely-spacing two pairs of frequencies, the optimization problem was first formulated in terms of a frequency spacing objective function (Formulation 1). The objective function was defined so that minimizing the objective function would cause the close-spacing of the frequency pairs. The only constraints on the problem were upper and lower bounds on the design variables denoted by ϕ_{i_L} and ϕ_{i_U}, respectively. The second formulation (Formulation 2) was a more conventional structural optimization formulation in which mass was minimized. The design requirements include two pairs of adjacent frequencies to be closely spaced - i.e., f_3 and f_4 be within a specified arbitrarily small ε_1 while f_5 and f_6 be within a specified arbitrarily small ε_2. These latter conditions are modeled as constraints in the optimization along with upper and lower bounds on the design variables denoted by ϕ_{i_L} and ϕ_{i_U}, respectively. For both formulations the design variables are L_1, L_2, A, I_{YY}, I_{ZZ}, and M (fig. 5).

	Formulation 1	**Formulation 2**
Objective function	$\left[\left(\frac{f_6-f_5}{f_6}\right)^2+\left(\frac{f_4-f_3}{f_4}\right)^2\right]^{1/2}$	**Mass**
Constraints	$\varphi_{i_L} \leq \varphi_i \leq \varphi_{i_u}$	$\varphi_{i_L} \leq \varphi_i \leq \varphi_{i_u}$ $\left\lvert\frac{f_4-f_3}{f_4}\right\rvert \leq \varepsilon_1$ $\left\lvert\frac{f_6-f_5}{f_6}\right\rvert \leq \varepsilon_2$
Design variables (φ_i)	$L_1, L_2, A, I_{yy}, I_{zz}, M$	

FIGURE 6

COFS-II OPTIMIZATION RESULTS

Results of the optimization procedure using Formulation 2 are shown in figure 7. Plots of vibrational frequency as a function of design cycle are shown on the left. A design cycle is a finite element analysis followed by an optimization step. As shown in the figure the first pair of frequencies (f_3 and f_4) are closely spaced after 5 design cycles. After about 16 design cycles, both pairs of frequencies are closely spaced. A detailed discussion of why the optimization procedure is able to closely space the first pair of frequencies (f_3 and f_4) so quickly but requires 11 more cycles to closely space the second pair of frequencies (f_5 and f_6) can be found in reference 22. A plot of the mass as a function of design cycle is shown on the right. The optimization procedure obtains a design which is able to closely-space two pairs of adjacent frequencies and provides some reduction in total mass (approximately 11 kg). Results for Formulation 1 are not shown since this formulation was not successful. The reasons for this will be discussed in figure 8.

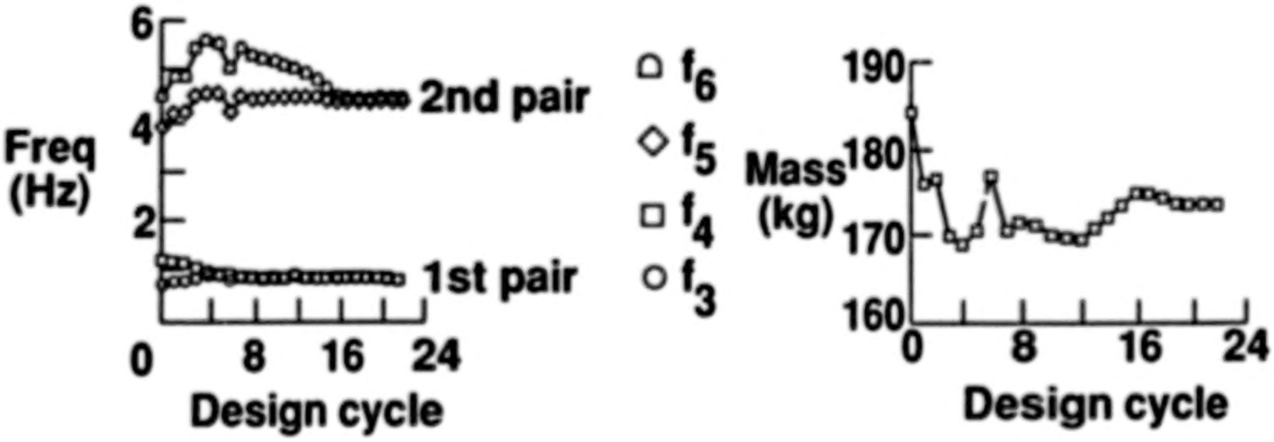

FIGURE 7

OBSERVATIONS FROM THE COFS-II FREQUENCY SPACING STUDY

Of the two optimization formulations tried for the COFS-II frequency spacing study only Formulation 2 was successful. With Formulation 1 the optimizer initially had some success in closely spacing one pair of frequencies (f_3 and f_4) for the first several cycles. When the optimizer tried to closely space the second pair of frequencies (f_5 and f_6), the first pair separated. At first it was thought it might not be possible to closely space f_5 and f_6 so two separate optimization problems were tried - one where one pair of frequencies (f_3 and f_4) were to be paired and one where the frequencies (f_5 and f_6) were to be paired. It was found that both pairs could be closely spaced separately. As a result, the second formulation (Formulation 2) was developed in which frequency spacing conditions were formulated as constraints. This formulation was successful. In retrospect one difficulty with Formulation 1 may have been due to the use of CONMIN with no constraints (other than side constraints on the design variables). Since CONMIN uses the method of usable feasible directions, it tends to follow active constraints in its search for an optimum. However by examining the plots (fig. 7) for Formulation 2, it appears that a stronger reason why Formulation 1 did not work was that the pairings were conflicting. The optimizer could not adjust the spacing of one pair without hurting the spacing of the second pair. However, when the pairings were used as constraints, the optimizer increased the spacing between the second pair of frequencies (f_5 and f_6) to decrease the spacing between the first pair (f_3 and f_4) and then finally decreased the spacing between the second pair later (around cycle 16) in the optimization process.

- **Formulation 1**
  - **No convergence**
  - **Only one pair of frequencies could be closely spaced at a time**
    - **CONMIN performs best for constrained problems**
    - **Conflicting goals in objective function**
- **Formulation 2**
  - **Converged**
  - **Two pairs of frequencies closely spaced**
  - **Observation of convergence behavior revealed reason for poor convergence of Formulation 1**

FIGURE 8

COFS-I BUCKLING DEFICIENCY STUDY

The next study involved the COFS-I flight mast shown fully deployed from the Space Shuttle in figure 9. The mast is approximately 60 meters long and consists of 54 bays of single-laced latticed beams with unequal area longerons (two "weak" longerons and one "strong" longeron). The "strong" longeron is located on the centerline of the Shuttle. The longerons have different cross-sectional areas to promote the coupling between modes. Further details of the COFS-I flight mast can be found in references 15, 16, and 19.

The mast was originally designed using parametric studies to have one pair of closely spaced frequencies (the first torsional and the second bending frequencies). It was subsequently determined that there were some deficiencies with the original design. In particular, the diagonal members of the original COFS-I design might buckle during deployment. There was also a concern that individual member frequencies might interact with global frequencies of the mast (i.e. be in the bandwidth which was to be tested in the flight experiment). An in-house redesign team was formed to address these issues. As part of this effort, an optimization procedure based on the previous COFS-II study was formulated and applied using a detailed model of the original COFS-I configuration to determine if it was possible to meet the additional design requirements and maintain the close-spacing of the frequencies. The design requirements, shown below, are that the first natural frequency of the diagonal be greater than 15 Hz, the first torsional and second bending frequencies be within one percent, the first natural frequency of the mast be greater than 0.18 Hz, minimum gage conditions (e.g. diagonal wall thickness be greater than 0.56mm), and the condition that the "weak" and "strong" longerons remain the same. For this study the mast was analyzed at its fully deployed position. It was felt that addressing the individual member frequency concern would also help alleviate the buckling during deployment concern.

- **Issues - original design deficient**
  - **Potential buckling of diagonal during deployment**
  - **Interaction of individual member frequencies with global frequencies**
- **Design requirements**
  - **1st natural frequency of diagonal ≥ 15 Hz (local frequency and buckling requirements)**
  - **1st torsion and 2nd bending frequencies within 1%**
  - **1st natural frequency of mast ≥ 0.18 Hz**
  - **Minimum gage, e.g. diagonal wall thickness ≥ 0.56mm**
  - **"Weak"/"strong" longerons**

FIGURE 9

BEST COPY AVAILABLE

COFS-I MODEL FOR BUCKLING DEFICIENCY STUDY

A finite element model of the entire COFS-I mast and Shuttle consisting of 360 joints is used in this study. The Shuttle is modeled as a stick model with very stiff beam elements. The battens, longerons, and diagonals of the mast are modeled by tubes which have bending, torsional, and axial stiffnesses. The model includes lumped masses to represent hinges, deployer retractor assembly, sensor and actuator platforms, etc. Further details of the finite element model can be found in reference 19.

Shown on the left of figure 10 is a typical 2-bay segment of the mast. In order to have minimal impact on the original design, a limited number of quantities are allowed to vary. The number of bays, all lengths of individual members (battens, longerons, and diagonals), and all physical properties of the battens are held constant. The outer radii of the longerons are also held constant to permit the mast to fold into a canister in the Shuttle without redesigning the hinges. The inner radii (R_S and R_W) of the longerons and the inner and outer radii of the diagonals (R_D and R_O, respectively) are allowed to vary in order to meet the design requirements discussed above. The four design variables are shown on the right.

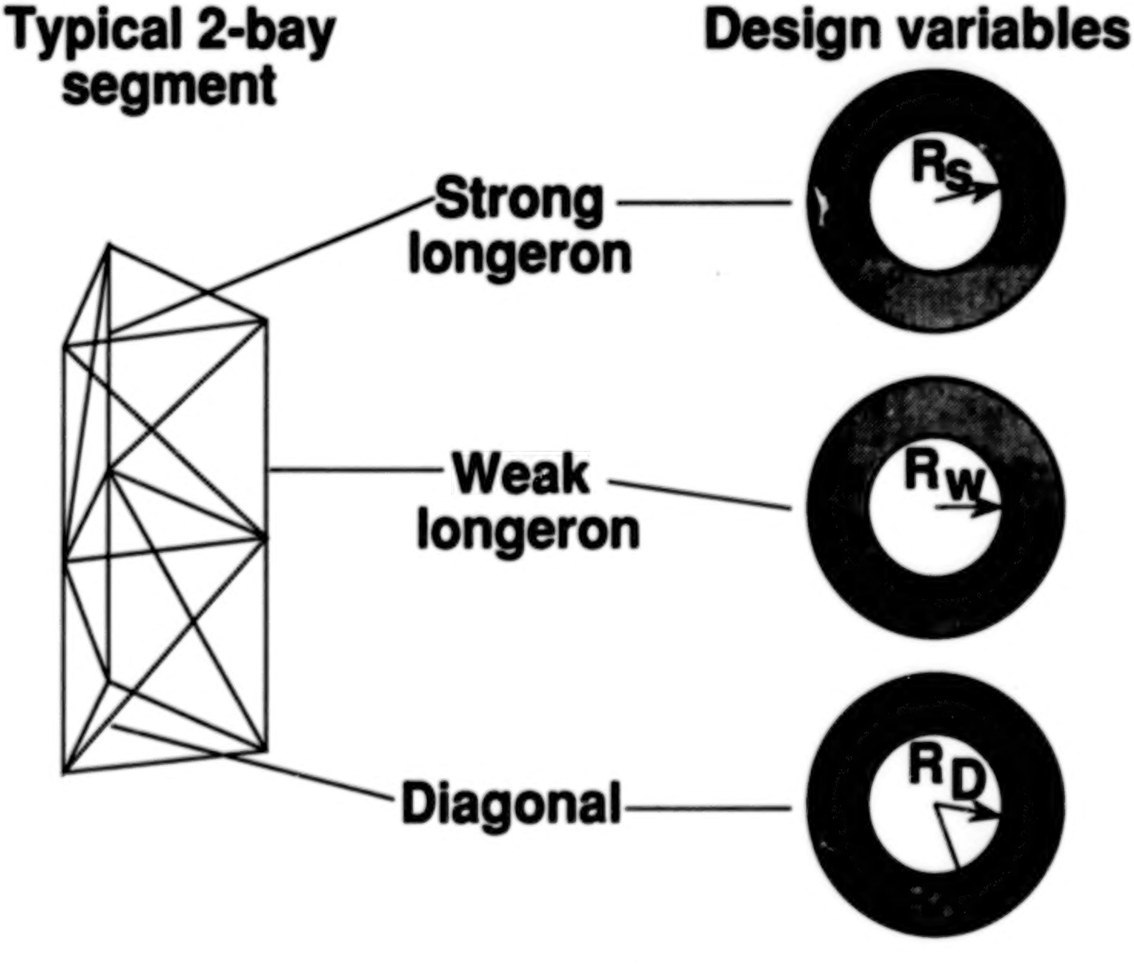

FIGURE 10

427

OPTIMIZATION FORMULATIONS FOR COFS-I BUCKLING DEFICIENCY STUDY

The two optimization formulations used for the COFS-I buckling deficiency study are shown in figure 11. The major difference between the two formulations was in the choice of objective function. In Formulation 1, the objective function was the total mass with frequency spacing used as a constraint. In Formulation 2 the objective function was a measure of the spacing between the first torsional and second bending frequencies denoted by f_T and f_B, respectively. No limitations on the mass were included. The design variables (R_S, R_W, R_D, and R_O) and the remaining constraints were the same for both formulations. The first constraint is that the first natural frequency (f_D) of the diagonal be greater than 15 Hz. The diagonal frequency is calculated from a simple formula based on assumptions of simply-supported ends with the mass of the hinge concentrated at the center of the diagonal (ref. 24). This requirement is a stiffness constraint to ensure that individual member frequencies of the diagonals are outside the mast frequency range in which frequencies are to be closely spaced (to preclude interaction of member frequency upon the global frequency). Although individual member frequencies of the longerons and battens are also of concern, it is felt that individual member frequencies of the diagonals are most likely to be in the mast frequency range due to their length and the large mass of the hinge. The next requirement is that the first natural frequency (f_1) of the mast be greater than 0.18 Hz. This requirement assures that the frequencies of the mast do not couple with those of the Shuttle control system. Another requirement is that the inner radius R_W of the weak longeron be at least 0.254mm larger than the inner radius R_S of the strong longeron (this is the "weak"/"strong" longeron design requirement shown on the previous figure). The last requirement is a minimum gage requirement on the wall thickness (Δt) of the diagonal members (the minimum wall thickness must be greater than 0.56mm). In addition side constraints (lower and upper limits denoted by ϕ_{i_L} and ϕ_{i_U}, respectively) were imposed on the design variables.

	Formulation 1	Formulation 2
Objective function	Mass	$\left[\left(\frac{f_T - f_B}{f_T}\right)^2\right]^{1/2}$
Design variables (φ_i)	R_S, R_W, R_D, R_O	R_S, R_W, R_D, R_O
Constraints	$\left\lvert\frac{f_T - f_B}{f_T}\right\rvert \leq 0.01$	
	$f_D \geq 15$ Hz	$f_D \geq 15$ Hz
	$f_1 \geq 0.18$ Hz	$f_1 \geq 0.18$ Hz
	min. gage	min. gage
	$(R_W - R_S \geq \Delta)$	$(R_W - R_S \geq \Delta)$
	$\Delta t_D \geq 0.56$mm	$\Delta t_D \geq 0.56$mm
	$\varphi_{i_L} \leq \varphi_i \leq \varphi_{i_u}$	$\varphi_{i_L} \leq \varphi_i \leq \varphi_{i_u}$

FIGURE 11

OPTIMIZATION RESULTS FROM COFS-I BUCKLING DEFICIENCY STUDY

Results for the COFS-I buckling deficiency optimization study using Formulation 1 are given in figure 12. Plots which show convergence of the COFS-I design give the designer insight into the design process by allowing him to see trade-offs between design requirements. The optimization procedure begins with four satisfied design requirements (two of which are active). As shown on the upper left, initially the frequencies f_B (second bending) and f_T (first torsional) are closely spaced and the Shuttle requirement on the first natural frequency f_1 of the mast is active (f_1=0.188Hz). As seen in the upper right figure, the requirement on the weak and strong longerons (R_W-R_S) and the diagonal wall thickness (R_O-R_D) are satisfied with the latter requirement being active. However, from the lower left figure, initially the diagonal frequency (f_D=11.5 Hz) is lower than the required value of 15 Hz. As stated earlier, the diagonal frequency requirement was not considered in the original design. As the optimization process proceeds, the values of the design variables are changed until the diagonal frequency requirement is satisfied (lower left). The two frequencies (f_B and f_T, upper left) are not as close as they were initially since the diagonal frequency works against this requirement. Specifically, when the diagonal frequency f_D is increased by an increase in stiffness, the first torsional frequency f_T is also increased. The "dips" in the diagonal frequency and the frequency pairs at cycles 9, 13, and 20 are partly due to the optimizer which attempts to satisfy all constraints even at the expense of increasing the objective function and partly due to the linearization of the problem. The optimizer concentrates on satisfying the diagonal frequency constraint until cycle 8, when it tries to satisfy the frequency spacing requirement. The optimizer chooses values for the four radii which closely space the frequencies (see cycle 9, upper left), but those choices lower the diagonal frequency (cycle 9, lower left). Now the optimizer tries to satisfy this diagonal frequency constraint which, as mentioned previously, works against the frequency spacing requirement (see upper left, cycles 10-12). This same process occurs again at cycles 13 and 20. The spacing of the two frequencies (f_B and f_T) cannot be made closer than 0.18 Hz. The "dips" are also due to the linearization of the problem. During the optimization process, "mode switching" occurs at cycles 9, 13, and 20. For example, if at the beginning of the cycle, the second bending mode is associated with f_{10} and the first torsional mode is associated with f_{11}, changes in the radii can cause the second bending mode to be associated with f_9 and the torsional mode with f_{11}. However, the optimizer is choosing values for the design variables based on derivative information at the start of the cycle (i.e. which mode is torsional and which mode is second bending). This is rectified when a full analysis is performed. The design process is also being limited by the minimum gage requirements - namely, R_D and R_W are at their upper and lower bounds, respectively. The inner radius, R_W, is within 0.25 mm of minimum gage (limited by the fourth design requirement upper right). A plot of the objective function (mass of the Mast) as a function of design cycle is shown on the lower right of figure 12. The optimization procedure obtains a design for the mast which better satisfies the design requirements at the expense of an additional 40 kg of mass. This increase in mass from the original design is mainly due to the diagonal frequency requirement.

OPTIMIZATION RESULTS FROM COFS-I BUCKLING STUDY (Formulation 1)

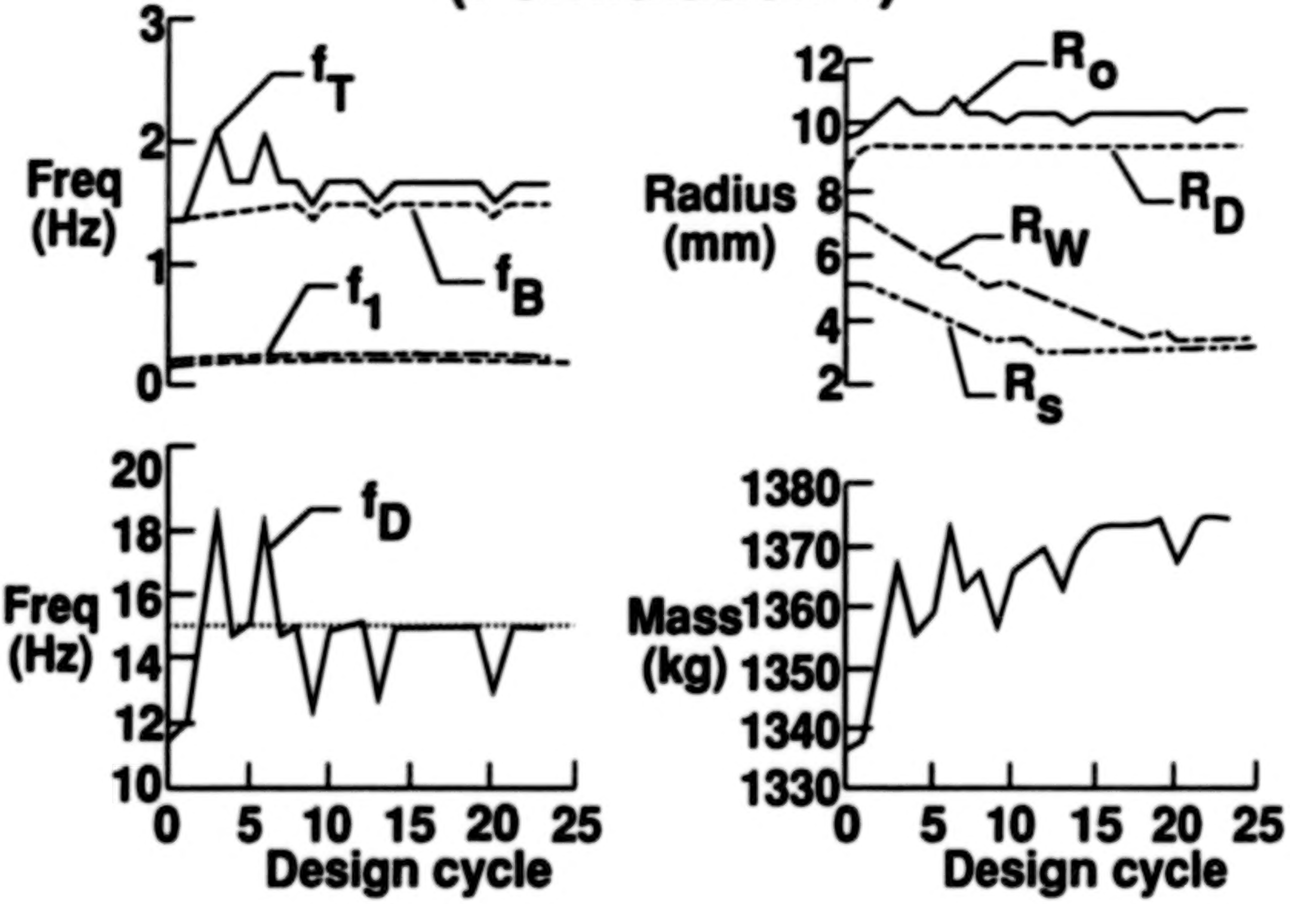

FIGURE 12

OBSERVATIONS FROM COFS-I BUCKLING DEFICIENCY STUDY

As shown in figure 13, in the previous study (COFS-II), two formulations were tried. Unlike the previous study, both formulations were successful and converged to the same design. From both studies, it is concluded that no feasible design exists which can be obtained by simply varying longeron radii and diagonal tube thickness within the prescribed limits. Therefore, there is a need for more design freedom in the optimization procedure in order to achieve a fully satisfactory design.

- Two formulations used for frequency spacing
  - Constraint-based (successful)
  - Objective function-based (successful)
- Formulations gave identical results
- Results showed need for more design freedom

FIGURE 13

COFS-I STRUCTURAL REDESIGN ACTIVITY

In May 1987 a problem (fig. 14) arose during the final experiment definition phase of the COFS-I project before the system requirement review. The project faced severe cost overruns and possible failure to meet schedule deadlines. In addition there were concerns whether the mast would meet some design requirements. An activity at Langley addressed these concerns. This section of the paper will describe the role of optimization in that activity.

In order to meet the proposed design and science requirements, the mast had been designed with a high modulus material (P75 graphite) in the longerons. This material had never been flight tested and there was concern for its performance. If this high modulus material (P75) could be replaced by a lower modulus material (HMS4 graphite) which had been flight qualified, flown, and could still meet all the design and science requirements (close-spacing of two adjacent frequencies), then there could be a cost savings. If the science requirements could not be met using the 54-bay length with the lower modulus material, the question was how short would the mast have to be to use the lower modulus material. These issues had to be addressed and answered in a very short time (originally approximately six weeks). Finally, there was to be minimal impact on the existing design. For example, no hinge or individual length changes were permitted. The deployment mechanism constrained length changes to 2-bay increments.

- **Issues - cost savings associated with material choice**
  - **Candidate material (P75) has desirable characteristics**
    - **High modulus**
    - **Resulting design meets science requirements**
  - **Alternate material (HMS4) has lower modulus but**
    - **flight qualified**
    - **flight experience**
- **Could HMS4 be used?**
- **Would mast need to be shortened to permit HMS4 to be used and still meet science requirements?**
- **Short time frame for decisions**
- **Minimal impact on existing design**
  - **no hinge changes**
  - **no individual length changes**
  - **no outer diameter changes**

FIGURE 14

APPROACH

To address the issues described in figure 14 and meet schedule deadlines, the optimization procedures discussed previously were extended to included redesigning the mast to see if the lower modulus material could be used for the longerons. As shown in figure 15, the approach to the problem was first to identify the design requirements used to design the mast originally and then incorporate as many of these requirements as possible into an optimization procedure. Since there was to be a minimal impact on the existing design, only the inner radii of the longerons and diagonals and modulus of the longerons were allowed to vary. The optimizer would determine the modulus and wall thicknesses of the longerons and the wall thickness of the diagonal. The radius of the diagonal elements was allowed to change since from the previous COFS-I study it was known that the diagonal radius would have to change in order to satisfy the individual member frequency requirement. Once the optimum modulus and wall thicknesses of the longerons and diagonals were found, the closest ply layup would then be determined manually . The ease of manufacturing would also be verified. If this design looked "good" from the ease of a manufacturing point of view, this design would be offered as a possible replacement for the COFS-I mast design. If the design looked "bad" from the ease of manufacturing point of view, then a parameter such as wall thickness (possibly a new design variable) would be added and the optimization procedure would be repeated. There was also the possibility that new design requirements could be imposed.

- Extend optimization procedures developed in two previous studies
- Identify design requirements used for existing design
- Incorporate as many requirements as possible in extremely short time
- Address material issue:
    - Use optimization procedure to determine modulus and wall thickness
    - Manually determine ply layup
    - Verify manufacturability

FIGURE 15

DESIGN REQUIREMENTS

The design requirements which were used in the COFS-I structural redesign activity are shown in figure 16. On the left are the flight mast requirements which the design must meet. The first requirement is that the first natural frequency (f_1) of the mast be between 0.15 Hz and 0.2 Hz. This requirement assures that the frequencies of the mast avoid those of the Shuttle control system. The second requirement is that the first torsional and the higher of the second bending frequencies be approximately equal for a beam three bays shorter than its fully deployed length. The third requirement is that the first natural frequency (f_D) of the diagonal be greater than 18 Hz. This requirement was to assure that the diagonal frequency would be above the bandwidth which would be tested in the flight experiment. The fourth requirement is that the fundamental bending frequencies about the two principal axes be "distinctly different". In addition the mast must be able to withstand a tip deflection of 0.2m and a tip rotation of 2 degrees when fully deployed.

Shown on the right is how the mast design requirements were interpreted and implemented in the optimization procedure. There were some differences between these requirements and those used in the optimization procedure. Some of these changes were due to a better interpretation of the design requirements and some were due to the imposition of new requirements during the redesign activity. To save time and analysis effort, all design requirements were implemented at the fully deployed length so that only one finite element model would be required. The first difference shows up in the bounds on the first natural frequency. The same lower bound of 0.18 Hz used in the previous studies was used here, but the upper bound was changed from 0.2 Hz to 1 Hz when it was found that using 0.2 Hz as the upper bound prevented the optimizer from finding a feasible design. Later, it was determined that there was no reason why an upper bound of 1.0 Hz should not be used. In most cases the optimum designs gave a value of approximately 0.28 Hz for the first frequency. The tip rotation and tip deflection requirements were replaced by constraints on the Euler buckling loads in individual members. The critical Euler buckling loads $P_{S,cr}$, $P_{W,cr}$, and $P_{D,cr}$ for a strong longeron, weak longeron, and diagonal member respectively had to be greater than corresponding loads in the member denoted by P_S, P_W, and P_D (determination of these loads proved to be a challenge and will be discussed shortly in the observations section). A weight restriction on the mast was also added to the design requirements. The mast must fit inside a canister on a platform in the Shuttle. There were restrictions on how much weight this platform could hold due to launch and landing loads. The weight requirement was expressed in terms of the tubing weight (longerons, diagonals, and battens). Minimum gage wall thicknesses were also imposed.

434

DESIGN REQUIREMENTS

Mast's Requirements	Optimization Implementation
1st natural frequency of mast greater than 0.15 Hz and less than 0.2 Hz	$0.18 \le f_1 \le 1.0$ Hz
1st torsion and higher one of 2nd bending frequencies be approximately equal for beam 3 bays shorter than fully deployed length	$\left\lvert \frac{f_T - f_B}{f_T} \right\rvert \le \varepsilon$
1st natural frequency of diagonal greater than 18 Hz	$f_D \ge 18$ Hz
Fundamental bending frequencies about the 2 principal axes be "distinctly different"	"Weak"/"strong" longeron requirement, $R_W - R_s \ge \Delta$
Fully deployed mast withstand tip deflection of 0.2 m and tip rotation of 2 degrees	$P_{s,cr} \ge P_s$, $P_{w,cr} \ge P_w$, $P_{D,cr} \ge P_D$
	Weight of tubing $\le \overline{W}$ Minimum gage wall thickness

FIGURE 16

COFS-I STRUCTURAL REDESIGN ACTIVITY OPTIMIZATION FORMULATIONS

The two optimization formulations developed for the COFS-I structural redesign activity are shown below in figure 17. Both formulations have the frequency spacing as the objective function and the same set of constraints. They differ in the number of design variables. As noted below the pairs of frequencies to be closely-spaced and some of the constraint limits are expressed in generic terms (e.g. f_A, f_B, P_S, P_W, P_D, $\overline{W}$, and $\overline{\Delta t_D}$). No single optimization formulation can be shown as in the previous studies since design requirements shown on the previous page and even design variables were continually augmented and clarified throughout the study. Some of the changes were due to a better interpretation of the mast design requirements. While other changes were due to the addition of new requirements which should have been included, still other changes involved insights which came from some of the results of the optimization procedure.

Shown below are two of the formulations used. Formulation 1 addressed the issues discussed in figure 14. During the study several "what if" questions arose. For example, instead of trying to closely space the first torsional and second bending frequencies, could the third torsional and second bending be closely spaced. Another question was could the diagonal frequency be even higher than 18 Hz. This led to several studies where the diagonal frequency lower limit was 20, 25 and even 30 Hz. In addition, from the results of Formulation 1 (four design variables), the question was asked what if the material in the diagonal were changed to the same material (HMS4 graphite) as the longerons, could the 54 bay length be used for the mast, and if, not what length could be used and still meet all the design requirements. This led to Formulation 2 (five design variables) shown on the right of figure 17. In addition, the minimum diagonal wall thickness was adjusted due to questions about the ease of manufacturing (handling qualities) of tubes with ply layups corresponding to the optimum wall thickness and modulus determined by the optimizer. The tubing weight limit $\overline{W}$ was a function of the mast length.

	Formulation 1	**Formulation 2**
Objective function	$\left[\left(\frac{f_A - f_B}{f_A}\right)^2\right]^{1/2}$	$\left[\left(\frac{f_A - f_B}{f_A}\right)^2\right]^{1/2}$
Design variables (φ_i)	R_S, R_W, R_D, E_L	R_S, R_W, R_D, E_L, E_D

Constraints
(Both Formulations)

$$0.18\text{ Hz} \le f_1 \le 1.0\text{ Hz}$$
$$f_D \ge 18\text{ Hz}$$
$$R_W - R_s \ge \Delta$$
$$P_{s,cr} \ge P_s$$
$$P_{W,cr} \ge P_W$$
$$P_{D,cr} \ge P_D$$
$$W \le \overline{W}$$
$$\Delta t_D \ge \overline{\Delta t_D}$$
$$\varphi_{i_L} \le \varphi_i \le \varphi_{i_U}$$

FIGURE 17

SUMMARY OF CASES STUDIED

As mentioned on figure 17 many different cases were optimized during the COFS-I structural redesign activity. Figure 18 presents a summary of the cases studied during the redesign activity. The cases optimized included different material for the longerons and diagonals, different frequencies to be closely spaced (first torsional and second bending frequencies or third torsional and second bending frequencies), various minimum values for the diagonal frequencies (18, 20, 25, and 30 Hz) and different minimum diagonal wall thicknesses (20 mils, 30 mils, and 40 mils). In addition, the cases mentioned above were optimized for different mast lengths, i.e. number of bays (42, 44, 46, 48, 50, 52 and 54 bays).

- **Different materials (P75, HMS4)**
- **Different frequencies to be paired**
- **Different diagonal frequency lower limits**
- **Different wall thickness limits**
- **Different Mast lengths**

FIGURE 18

RESULTS OF COFS-I STRUCTURAL REDESIGN ACTIVITY

During the redesign activity over 60 optimum designs were obtained. Nine "official redesigns" were obtained. By "official" it is meant that these designs warranted further analyses to see if they met additional requirements such as ease of manufacturing not included in the optimization procedure. These "official" redesigns were for HMS4 graphite. The optimization procedure was formulated, implemented, and results obtained in less than four months (figure 19).

- **Total number of optimized designs obtained - 60**
- **Nine candidate redesigns produced**
    - **All used HMS4**
    - **All met design requirements**
- **Accomplished in less than four months**

FIGURE 19

TYPICAL OPTIMIZATION RESULTS FOR COFS-I STRUCTURAL REDESIGN ACTIVITY

Over 60 optimum designs were obtained during the COFS-I structural redesign activity. Figure 20 presents optimization results for one of the nine "official" redesign candidates. This design is for a mast with 42 bays, HMS4 material in the longerons and diagonals, a maximum diagonal wall thickness of 40 mils, and a tubing weight limit of 125 kgs. The first torsional f_T and second bending f_B frequencies were to be closely spaced. The diagonal frequency f_D had to be greater than 18 Hz. The limit loads in the longerons and diagonals were 16000N for P_S and P_W and 1955N for P_D.

Design variable and objective function histories are shown in the upper half of figure 20. Histories of the two frequencies (f_T and f_B) comprising the objective function are also given. Design requirement histories are shown in the lower half of the figure. To increase the second bending frequency f_B, the optimizer increased the longeron modulus E_L to its upper limit and decreased the inner radii of the longerons (R_W and R_S). To lower the first torsional frequency f_T, the optimizer decreased the diagonal modulus E_D to its optimum value. R_D and R_S reached their respective lower limits.

The effect of these design variable changes on the design requirements is shown in the lower portion of figure 20. The diagonal frequency f_D and the first natural frequency f_1 met the requirements throughout the design process (with initial values of 22.5 Hz and 0.23 Hz and final values of 19.4 Hz and 0.27 Hz, respectively). The buckling loads in the strong longeron ($P_{S,cr}$) and the diagonal ($P_{D,cr}$) were adequate throughout the design process. The strong longeron buckling $P_{S,cr}$ increased from an initial value of 16258N to a final value of 20820N and both its modulus (E_L) and wall thickness increased. Since the modulus was at its upper limit after three cycles, the optimizer increased the wall thickness of the longeron (i.e., by decreasing the inner radius R_S) to raise the second bending frequency f_B. Initially with the HMS4 material, the constraint on the buckling load in the weak longeron was violated ($P_{W,cr} = 13906N$). The optimizer satisfied this constraint by increasing the wall thickness of the weak longeron (i.e. decreasing the inner radius R_W). In the final design, the buckling load requirements for both the weak and strong longerons ($P_{S,cr} = 20820N$ and $P_{W,cr} = 20305N$, respectively) were well satisfied. However, the buckling load in the diagonal (denoted by $P_{D,cr}$) was at its limiting value of 1955N. The optimizer increased the tubing weight W from an initial value of 92.5 kg to its upper limit of 125 kg to satisfy the buckling load constraints and increase the second bending frequency f_B. In the final design the diagonal wall thickness denoted by Δt_D (lower right) was at its minimum value. The "weak"/"strong" longeron requirement (R_W-R_S) kept R_W from reaching its lower limit.

TYPICAL OPTIMIZATION RESULTS FOR COFS-I STRUCTURAL REDESIGN ACTIVITY
42 Bay Mast

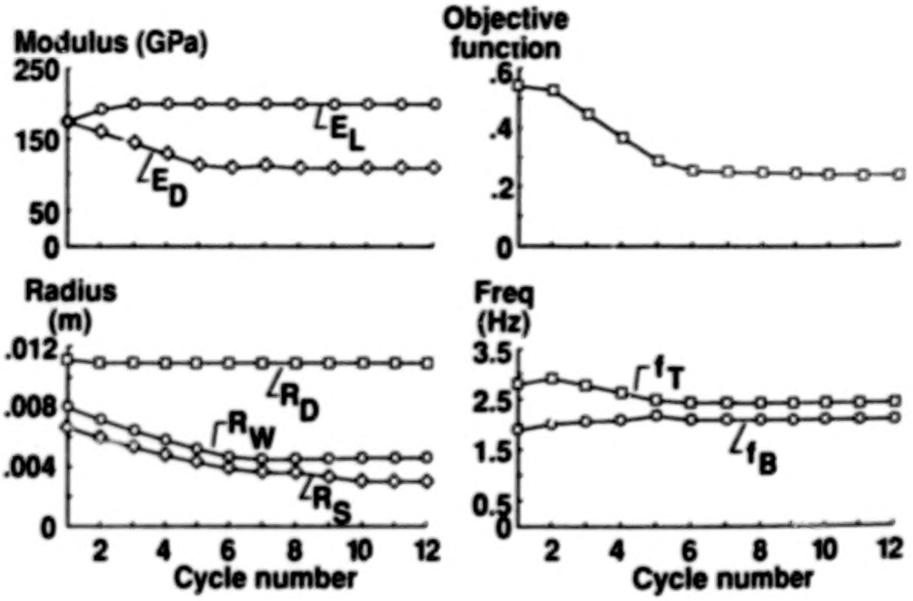

TYPICAL OPTIMIZATION RESULTS FOR COFS-I STRUCTURAL REDESIGN ACTIVITY, CONCLUDED
42 Bay Mast

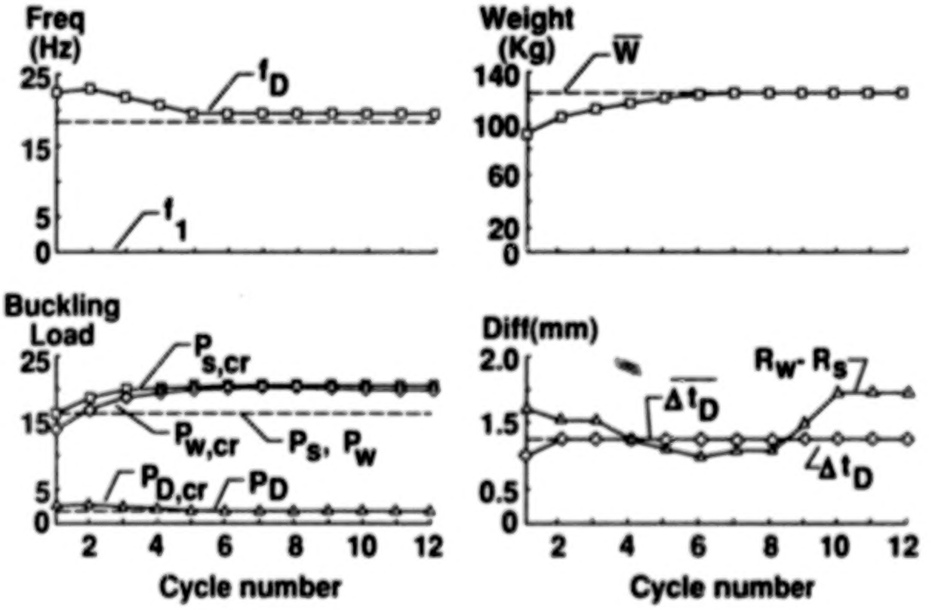

FIGURE 20

OBSERVATIONS FROM COFS-I STRUCTURAL REDESIGN ACTIVITY

As shown in figure 21, the use of optimization techniques can be extremely helpful when applied to an actual design activity such as the one just described. Once the procedure is developed, the designer is able to look at different options and answer "what if" questions he may not have time to answer by doing parametric studies. Since convergence is rapid (usually in less than 12 cycles), the optimization procedure allows the designer to look at many different options in a very short time. The designer is offered many avenues he may not have in a normal redesign activity when faced with time limitations and confined to using only parametric studies. Even infeasible designs can be important since they give the designer options he could have if willing to relax some of the design requirements. For example, if he were willing to accept a lower diagonal frequency than originally specified, he might obtain a candidate design with a longer mast.

Needless to say, optimization procedures are not a substitute for engineering judgment. The designer must be able to interpret and incorporate design requirements into the procedure. Sometimes this is not an easy task. For example, the buckling load requirement (the Euler buckling load greater than the limit load in the member) proved to be a troublesome constraint. Initially, a simplifying assumption was made to meet schedule deadlines. The limit load was defined as a safety factor (2.8) times the working load in the member. This working load was determined by applying the tip rotation and tip deflection requirement (fig. 17). Assuming that the limit loads varied in the analysis but were constant in the derivative calculations made it easy to obtain the derivatives of the constraints, but the constraint functions determined by the linear Taylor series approximations were inaccurate. Allowing these limit loads to vary during the derivative calculations made the calculations more costly in computer time and convergence, but the approximate constraint functions were more accurate. The limit loads were nevertheless very sensitive to changes in the design variables and the optimization procedure had trouble converging to a feasible design. The procedure appeared to be converging very slowly and there was no time to complete the convergence since deadlines were approaching. At the same time, communication with the contractor resulted in a better interpretation of how to obtain these limit loads. Since the hinges were already designed to withstand given loads, it was decided to use these same loads as limit loads for the longerons and diagonal. After this, the optimization procedure converged rapidly (less than 12 cycles).

A final observation is that optimization practitioners must be aware of the ease of manufacturing designs. Consideration of handling qualities led to an increase in the minimum wall thickness for the diagonals. Questions about the wall thickness of the longerons being too thick (could graphite tubes with very small inner diameters be manufactured?) led to changes in lower bounds on the design variables (inner radii).

OBSERVATIONS FROM COFS-I STRUCTURAL REDESIGN ACTIVITY

- Optimization can be powerful tool for practical engineering decisions
- Designer can look at different alternatives ("what if" questions)
- Designer can quickly determine effect of different options on design
- Infeasible design also important - give designer options if willing to relax a design requirement

BUT

- Not a substitute for engineering judgment - examples
  - Buckling load constraint determinations
  - Manufacturing considerations

FIGURE 21

SUMMARY

The paper described experiences gained in optimizing Control of Flexible Structures (COFS) configurations. Optimization procedures were developed to systematically provide closely spaced vibration frequencies. The optimization procedures combined a general-purpose finite-element program for eigenvalue and sensitivity analyses with formal mathematical programming techniques. The formal mathematical programming technique combined a general-purpose optimization program and approximate analyses.

Results were presented for three studies. The first study used a simple model of a typical COFS-II configuration to obtain a design with two pairs of closely spaced frequencies. Two formulations were developed: an objective function-based formulation; and a constraint-based formulation for the frequency spacing. It was found that conflicting goals were handled better by a constraint-based formulation. The second study used a detailed model of the COFS-I configuration. The structure was to be designed to have one pair of closely spaced frequencies while satisfying requirements on local member frequencies and manufacturing tolerances. Two formulations were again developed. Both the constraint-based and the objective function-based formulations performed reasonably well and converged to the same results. However, no feasible design solution existed which satisfied all the design requirements for the choices of design variables and the upper and lower design variable values used. It was concluded that more design freedom was needed to achieve a fully satisfactory design. The third study was part of a redesign activity in which a detailed model was used and actual design requirements were incorporated. The use of optimization in this redesign activity allowed the project engineers to investigate numerous options (such as number of bays, material, minimum wall thickness, minimum diagonal wall thicknesses) over a relatively short period of time. The procedure provided data (60 designs in a four month period) for judgments on the effects of different options on the design. Finally the optimization results permitted examination of various alternatives and answers to many "what if" questions in a relatively short time. (See figure 22.)

- **Related experiences in optimizing COFS structures**
- **Many "what if" questions were answered**
- **Proper problem formulation-important**
  - **Objective function selection**
  - **Design variable selection**
  - **Conflicting goals work best as constraints**
- **Optimization found to be powerful tool in engineering design process**

FIGURE 22

443

REFERENCES

1. Venkayya, V. B.: Structural Optimization: A Review and Some Recommendations. International Journal for Numerical Methods in Engineering, vol. 13, 1978, pp 203-228.

2. Ashley, H.: On Making Things the Best - Aeronautical Use of Optimization. Journal of Aircraft, vol. 19, no. 1, 1982.

3. Vanderplaats, G. N.: Structural Optimization - Past, Present, and Future. AIAA Journal, Vol. 20, No. 7, July 1982.

4. Sobieszczanski-Sobieski, J. (compiler): Recent Experiences in Multidisciplinary Analysis and Optimization. NASA CP-2327, Parts 1 and 2, 1984.

5. Sobieszczanski-Sobieski, J.: Structural Optimization Challenges and Opportunities. Presented at Int. Conference on Modern Vehicle Design Analysis, London, England, June 1983.

6. Rao, S. S.: Automated Optimum Design of Wing Structures - Deterministic and Probabilistic Approaches. NASA TM-84475, 1982.

7. Sobieszczanski, Jaroslaw; McCullers, L. Arnold; Ricketts, Rodney H.; Santoro, Nick J.; Beskenis, Sharon D.; and Kurtze, William L.: Structural Design Studies of a Supersonic Cruise Arrow Wing Configuration. Proceedings of the SCAR Conference - Part 2, NASA CP-001, 1977, pp.659-683.

8. Sobieszczanski-Sobieski, J.: An Integrated Computer Procedure for Sizing Composite Airframe Structures. NASA TP-1300, 1979.

9. Wrenn, G. A.; and Dovi, A. R.: Multilevel Decomposition Approach to the Preliminary Sizing of a Transport Aircraft Wing. AIAA/ASME/ASCE/AHS 28th Structures,Structural Dynamics and Materials Conference. Paper No. 87-0714-CP. Monterey, California, April 6-8, 1987.

10. Barthelemy, J.-F. M.; Chang, K. J.; and Rogers, Jr., J. L.: Structural Optimization of an Alternate Design for the Space Shuttle Solid Rocket Booster Field Joint. NASA TM-89113, February 1987.

11. Walsh, Joanne L.: Application of Mathematical Optimization Procedures to a Structural Model of a Large Finite-Element Wing. NASA TM-87597, 1986.

12. Hanks, B. R.: Control of Flexible Structures (COFS) Flight Experiment Background and Description. Large Space Antenna Systems Technology 1984. NASA CP-2368, Part 2, December 1984, pp 893-902.

13. Allen, John L.: COFS-I - Beam Dynamics and Control Technology Overview. NASA/DOD Control/Structures Interaction Technology 1986. NASA CP-2447, Part 1,November 1986, pp. 221-232.

14. Horner, G. C.: COFS-I Research Overview. NASA/DOD Control/Structures Interaction Technology 1986. NASA CP-2447, Part 1, November 1986, pp. 233-251.

15. Talcott, Ronald C.; and Shipley, John W.: Description of the MAST Flight System. NASA/DOD Control/Structures Interaction Technology 1986. NASA CP-2447, Part 1, November 1986, pp. 253-263.

16. Lenzi, David C.; and Shipley, John W.: MAST Flight System Beam Structure and Beam Structural Performance. NASA/DOD Control/Structures Interaction Technology 1986. NASA CP-2447, Part 1, November 1986, pp. 265-279.

17. Pyle, Jon S.; and Montgomery, Raymond: COFS-II 3-D Dynamics and Controls Technology. NASA/DOD Control/Structures Interaction Technology 1986. NASA CP-2447, Part 1, November 1986, pp. 327-345.

18. Letchworth, Robert; and McGowan,Paul E.: COFS-III Multibody Dynamics & Control Technology. NASA/DOD Control/Structures Interaction Technology 1986. NASA CP-2447, Part 1, November 1986, pp. 347-370.

19. Horta, Lucas G.; Walsh, Joanne L.; Horner, Garnett C.; and Bailey, James P.: Analysis and Simulation of the MAST (COFS-I Flight Hardware). NASA/DOD Control/Structures Interaction Technology 1986. NASA CP-2447, Part 1, November 1986, pp. 515-532.

20. Whetstone, W.D.: EISI-EAL Engineering Analysis Language Reference Manual - EISI-EAL System Level 2091. Engineering Information Systems, Inc., July 1983.

21. Vanderplaats, Garret N.: CONMIN - A FORTRAN Program for Constrained Function Minimization - User's Manual. NASA TM X-62282, 1973.

22. Walsh, Joanne L.: Optimization Procedure to Control the Coupling of Vibration Modes in Flexible Space Structures. AIAA/ASME/ASCE/AHS 28th Structures, Structural Dynamics and Materials Conference. Paper No. 87-0826-CP. Monterey, California, April 6-8, 1987. (Also available as NASA TM-89115, February 1987).

23. Card, M. F.; Anderson, M. S.; and Walz, J. E.: Dynamic Response of a Flexible Beam. NASA TM-86441, May 1985.

24. Hurty, Walter C.; and Rubinstein, Moshe E.: Dynamics of Structure. Prentice-Hall, Inc., 1965.

AN IMPROVED ALGORITHM FOR OPTIMUM STRUCTURAL DESIGN WITH MULTIPLE FREQUENCY CONSTRAINTS

Oliver G. McGee[1] and Khing F. Phan[2]

Department of Civil Engineering
The Ohio State University
Columbus, Ohio 43210

---

[1] Assistant Professor
[2] Graduate Research Associate

444.

SUMMARY

This paper presents an optimality criterion (OC) method for minimum-weight design of structures having multiple constraints on natural frequencies. In this work a new resizing strategy is developed based on "relaxation" techniques. A computationally adaptive control parameter is used in conjunction with existing OC recursive formulae to promote convergence of optimum structural designs. Some considerations regarding the coupling of the modified Aitken accelerator with the OC method are discussed. Improved and rapidly converged minimum-weight designs are obtained when using an under-relaxed recursive scheme combined with the modified Aitken accelerator.

INTRODUCTION

In recently published literature regarding structural optimization with multiple frequency constraints [1,2], the algorithms were applied to truss systems, taking advantage of their special characteristics (i.e., single design variable per element, structural matrices linearly proportional to the design variables, constant stress elements, etc.). In search for optimal values of design parameters in minimum weight design the iterative approach based on alternately satisfying the constraints (scaling) and applying an "optimality criterion" (resizing) may give oscillatory results which might not converge; or they may converge to local extrema at the expense of an increased number of iterations.

The resizing formulae used in [1,2] employed an exponential control parameter as the step size. The control parameter was reduced to stabilize the iterative design cycle and to assure convergence. Basically, the control parameter was kept constant through all the iterations, as the structural weight was continually reduced; or if a sudden rise in the weight was observed, the iterative design cycle was momentarily stalled and the control parameter was reduced until a decrease in the weight was obtained. For various single and multiple frequency constraint conditions, optimum designs were presented. Although, the final designs being the real optimum were questionable.

In this work a new resizing strategy is developed based on "relaxation" techniques. A computationally adaptive control parameter is used in conjunction with OC recursive formulae currently used to obtain minimum weight design of truss system [1-3]. The new control parameter is adjusted by monitoring the local histories of scaled weights calculated in the iterative design cycle. As the step size is reduced, the rate of convergence is reduced. Hence, the convergence rate is increased using an acceleration technique. The modified Aitken accelerator [4,5] is implemented to extrapolate values of structural weight from the local history of the design cycle to accelerate convergence towards an optimal design. Structural element sizes and natural frequencies are presented for optimally designed truss systems under various frequency constraint conditions. Design cycle histories of structural weights and control parameters are charted to compare the performance of different recursive strategies to modify the design variables and to estimate the Lagrange multipliers.

FREQUENCY ANALYSIS

The square of the j^{th} natural frequency for the case of undamped vibration of a discretized structure can be written as

$$\omega_j^2 = \{q_j\}^T[K]\{q_j\} \qquad (1)$$

where [K] is the stiffness matrix, and $\{q_j\}$ is the j^{th} vibration mode normalized with respect to the total mass, $[M]=[M_s+M_c]$, consisting of structural and nonstructural mass. The gradient of the natural frequency with respect to the design variables x_i (member cross-sectional areas) is obtained by differentiating Eq. (1). The result is

$$(\omega_j^2)_{,x_i} = (1/x_i)\,[\{q_j\}_i^T[k_i]\{q_j\}_i - \omega_j^2\{q_j\}_i^T[m_i]\{q_j\}_i] \qquad (2)$$

where $\{q_j\}_i$, $[k_i]$, and $[m_i]$ denote components of the structural matrices associated with the i^{th} element x_i, and ( ), represents a partial differentiation.

OPTIMIZATION PROCEDURE

The optimization problem is defined as

minimize the structural weight

$$W(x_i) = \rho_i\ l_i\ x_i \qquad (i=1,2,\ldots,n) \qquad (3)$$

subject to m constraints

$$\begin{aligned} g_j(x_i) &= \omega_j - \omega_j^* = 0 \qquad (j=1,2,\ldots,k) \\ g_j(x_i) &= \omega_j - \omega_j^* < 0 \qquad (j=k+1,\ldots,m) \end{aligned} \qquad (4)$$

where ρ_i is the mass density, x_i is the design variable, and l_i is the length of the element. In Eq. (4) ω_j and ω_j^* are the actual and the desired values of the frequency constraints. In addition, minimum limits are prescribed on the design variables: $x_i > x_i^1$.

Using Eqs. (3) and (4), the Lagrangian function, L, can be written as

$$L(x_i, \lambda) = \rho_i\ l_i\ x_i - \lambda_j\ (\omega_j - \omega_j^*)$$
$$(i=1,2,\ldots,n) \qquad (j=1,2,\ldots,m) \qquad (5)$$

where λ_j are the Lagrange multipliers.

Differentiating Eq. (5) with respect to the design variables and setting the resulting equations to zero, the optimality criterion can be written as:

$$e_{ij}\,\lambda_j = 1 \qquad (i=1,2,\ldots,n\ ;\ j=1,2,\ldots,m) \tag{6}$$

where

$$e_{ij} = \frac{(\omega_j)_{,xi}}{(W)_{,xi}} \tag{7}$$

where the Lagrangian energy density, e_{ij}, represents the ratio of the gradient for the natural frequency constraint (Eq. 2) to the gradient of the objective function, given as $(\rho_i l_i)$.

Using Eq. (6), one can write recursive relations to modify the design variables. Recursive relations to estimate the Lagrange multipliers can be written by assuming that all the constraints in Eq. (4) are equality constraints [3]. In either case these recursive relations can be written in an exponential or a linearized form. In the exponential recursive relations the design variables (or Lagrange multipliers) are modified by multiplying them by a quantity which is equal to unity at the optimum, and in the linear recursive relations the design variables (Lagrange multipliers) are modified by adding a quantity which is equal to zero at the optimum. Note that the linear recursive relation for the Lagrange multipliers is an approximation to a set of linear equations that can be used to determine the Lagrange multipliers [1,3]. Nonetheless, it is possible to promote the convergence of these relations by incorporating a simple technique known as relaxation. Such a modification is used in this work:

To modify the design variables:

$$x_i^{k+1} = x_i^k + s\,[(e_{ij}\,\lambda_j)_k^{(1/r)} - 1]\,x_i^k \tag{8}$$

$$x_i^{k+1} = x_i^k + s\,[\{1 + (1/r)\,(e_{ij}\,\lambda_j - 1)\}_k - 1]\,x_i^k \tag{9}$$

To estimate the Lagrange multipliers:

$$\lambda_j^{k+1} = \lambda_j^k + s\,[(\lambda_j\ /\ \lambda_j^*)_k^{(1/b)} - 1]\,\lambda_j^k \qquad ; \quad (b=1/r) \tag{10}$$

$$\lambda_j^{k+1} = \lambda_j^k + s\,[\{(b+1)/b\} - (1/b)(\lambda_j\ /\ \lambda_j^*)_k^{(1/b)} - 1]\,\lambda_j^k \tag{11}$$

where the superscripts k and k+1 denote iteration numbers. The quantity (1/r), is the step size used in the algorithms reported in [1,2]. In the present algorithm this step size is immobilized by setting it to a constant value, 1/r=0.5. Alternatively, a more adaptive control parameter s, is utilized. At the beginning of the design cycle the control parameter is set to unity. Henceforth, the value of s is adjusted by monitoring the local histories of structural weights calculated in the iterative design cycle. For structural weight histories exhibiting an oscillatory pattern of convergence, an optimal value of s is chosen using the following algorithm: If $W^{k+1} > (1/2)[W^{k} - W^{k-1}]$ or $W^{k+1} > W^{k} > W^{k-1}$ and the current value of s is above a specified minimum value, then s is reduced to s/2. (For structural weight histories displaying a pattern of convergence other than oscillatory, the algorithm can be appropriately refined. At the optimum the optimality criterion (Eq. 6) and the constraints (Eq. 4) are satisfied. Hence, Eqs. (8-9) converge to $x_i^{k+1} = x_i^{k}$ and Eqs. (10-11) converge to $\lambda_j^{k+1} = \lambda_j^{k}$.

The jth Lagrange multiplier for the jth frequency constraint also can be approximated by a simple expression derived from a single constraint condition [2,6]

$$\lambda_j = W / \omega_j^2 \, m_1 \tag{12}$$

where

$$m_1 = \frac{q_j^T [M_s] q_j}{q_j^T [M] q_j} \tag{13}$$

Equation (12) is used as initial values in the recursive Eqs. (10-11).

After the structural members are modified using Eqs. (8) or (9), they are uniformly scaled by a factor f_j corresponding to the j^{th} frequency constraint. The relationship between the unscaled design x_i and the scaled design x_i^* is given by

$$x_i^* = f_j x_i \tag{14}$$

The scale factor f_j is computed as follows [2,6]:

$$f_j = \frac{m_1 R_j^2}{1 - R_j^2 m_2} \quad , \quad R_j^2 m_2 < 1$$

$$f_j = R_j^2 \quad , \quad \text{otherwise} \tag{15}$$

where

$$m_2 = \frac{q_j^T [M_c] q_j}{q_j^T [M] q_j} \tag{16}$$

and R_j^2 represents the frequency target ratio given by

$$R_j^2 = \omega_j^{2*} / \omega_j^2 \tag{17}$$

In search for optimal values of design parameters in minimum weight design the iterative approach based on alternately satisfying the constraints (Eqs. 14-17) and applying the optimality criterion (Eqs. 6) may give oscillatory results which might not converge; or they may converge to local extrema at the expense of an increased number of iterations. The control parameter s, adopted in Eqs. (8-11) controls the step size of the recursive relations and stabilizes the convergence of the iterative design cycle. A drawback is that the convergence rate is slowed as the control parameter is reduced. This is primarily due to the fact that a smaller value of s reduces gains towards meeting the optimality condition. Hence, the convergence rate of the iterative process is improved with two-fold objectives in mind: (1) maintaining as large of a value for s as possible during the design cycle, and (2) extrapolating structural information from the local history of the design cycle to accelerate the convergence rate.

MODIFIED AITKEN ACCELERATOP

The convergence rate of the iterative process can be enhanced by using an accelerator. An appropriate one has been proposed by Boyle and Jennings [4,5]. The Aitken accelerator is a numerical technique whereby three consecutive results of an iterative process are extrapolated to obtain improved results on the assumption that the error curve of the iterative process decays exponentionally. The adaptability of Aitken's accelerator for the computer, however, is unpredictable given the possibility of a singular denominator in the predictor algorithm. Nonetheless, a modified Aitken accelerator was developed by Jennings [5] for general multivariable iterative problems. The predictor algorithm for the modified Aitken accelerator requires only one division as opposed to one for each variable and allows the divisor to be chosen to avoid the possibility of a zero value.

In this work, local histories of structural weight are monitored for convergence patterns which are not monotonic. If the structural weight histories before the current design exhibit an oscillatory pattern of convergence and show a mark increase in value, then continued computations with the current design are bypassed while an improved design (i.e., one that will result in a reduced scaled weight) is obtained using the modified Aitken accelerator.

Let x_i^{k-3}, x_i^{k-2}, and x_i^{k-1} be design variables obtained from three consecutive iterations of the design cycle and let x_i^k be the desired variables for a current design. By letting

$$d_1 = x_i^{k-2} - x_i^{k-3} \qquad\qquad d_2 = x_i^{k-1} - x_i^{k-2} \qquad (18)$$

the adopted procedure [5] for finding an improved (accelerated) design x^*, may be written as

$$x_i^* = x_i^{k-1} + Sd_2 \qquad (19)$$

where S, is defined as the acceleration factor

$$S = (d_2 - d_1)^T(-d_2)[(d_2 - d_1)^T(d_2 - d_1)]^{-1} \qquad (20)$$

In general, x_i^* satisfies neither the optimality condition (Eq. 6) nor the frequency constraints. Nonetheless, the design cycle is continued after an acceleration by applying the optimality condition with the improved design x_i^a:

$$x_i^k = x_i^a + s\,[(e_{ij}\,\lambda_j)_a^{(1/r)} - 1]\,x_i^a \tag{21}$$

$$x_i^k = x_i^a + s\,[\{1 + (1/r)\,(e_{ij}\,\lambda_j - 1)\}_a - 1]\,x_i^a \tag{22}$$

$$\lambda_j^k = \lambda_j^a + s\,[(\omega_j\,/\,\omega_j^*)_a^{(1/b)} - 1]\,\lambda_j^a \quad ; \quad (b=1/r) \tag{23}$$

$$\lambda_j^k = \lambda_j^a + s\,[\{(b+1)/b\} - (1/b)(\omega_j\,/\,\omega_j^*)_a^{(1/b)} - 1]\,\lambda_j^a \tag{24}$$

The kth design is then scaled to satisfy the constraints using Eq. (14). (Note that the control parameter s is appropriately adjusted as previously outlined.)

OPTIMIZATION ALGORITHM

The main steps of the present optimization algorithm are

(1) Assign uniform sizes to all elements (set s=1, k=1).
(2) Perform frequency analysis (Eqs. 1-2)
(3) Scale the design until frequency constraints are obtained within the required accuracy (Eqs. 14-17).
(4) Calculate the scaled weight of the structure using (Eq. 3) and the scaled design variables (Eq. 14).
(5) For iteration k=4 or greater, check for oscillatory convergence pattern of scaled weights in the last three consecutive k-1, k-2, k-3 iterations. If this is the case, then apply the modified Aitken accelerator to obtain an improved design (Eq. 19) and modify the design variables using Eqs. (20 or 21 and 12, 22 or 23). Else continue to step (6).
(6) Determine the Lagrange multipliers (Eqs. 10,11 or 12).
(7) Modify the design variables (Eqs. 8 or 9).
(8) Repeat steps 2, 3 and 4.
(9) For iteration k=3 and greater: If $W^{k+1} > (1/2)\,[W^k - W^{k-1}]$ or $W^{k+1} > W^k > W^{k-1}$ and s > specified minimum value, then s is equal to s/2 and go to step 7; Else go to step 5.
(10) Steps 5-9 represent one iteration in the design cycle history.
(11) Repeat until difference in weight is less than specified tolerance.

RESULTS AND DISCUSSIONS

The effectiveness of the above algorithm was demonstrated by designing a 10 member truss (Figure 1), a classical problem in the structural optimization literature [1-3]. The elastic modulus was 10^7 psi, and the weight density was 0.1 psi. A nonstructural mass of 2.588 lb-sec²/in was added to the four free nodes. All the member cross-sectional areas were given uniform sizes for an initial design. During the design cycle history, a lower limit value of 0.1 in² was imposed on member sizes. The natural frequencies and mode shapes were computed using a Jacobi method.

Table 1 presents initial and final frequencies and structural weight at the optimum design for various frequency constraint conditions. Table 2 gives the optimum member sizes. As indicated in Tables 1 and 2, Eq. 8 was used to modify designs and Eq. 12 was used to estimate the Lagrange multipliers. Reference [2] presents optimization studies using similar formulae for the same ten member truss subjected to the same constraint conditions. In Tables 1 and 2 these results are shown in parentheses for comparison with those obtained in the present analysis.

The ten member truss was designed with both single and multiple frequency constraint conditions (Tables 1 and 2). The first set of results (Case 1) was obtained with a single constraint on the second frequency ($\omega_2=10.0$Hz). The next three sets of results involved multiple frequency constraints: (Case 2) $\omega_1=7.0$Hz, $\omega_2>15.0$Hz; (Case 3) $\omega 1=7.0$Hz, $\omega_2>15.0$Hz, $\omega_3>20.0$Hz; (Case 4), $\omega_1>3.5$Hz, $\omega_2>10.0$Hz, $\omega_3>14.0$Hz.

At the initial design the structural weight was 4000 lbs. Furthermore, the first eight frequencies were on the average approximately 4.26 percent higher than those of reference [2]. Resulting design weights obtained by the present analysis were significantly lower than those obtained in [2]. For example, Cases 1 and 4 showed mark improvements in structural weight with approximately 15.7 and 15.88 percent decreases, respectively. Additionally, the first eight frequencies calculated for Cases 1 and 4 were decreased by an average of approximately 11.13 and 12.63 percent, respectively. For Case 4 the constraint on the first and second frequencies was met to within 6 and 3.5 percent, respectively. The third frequency constraint in Case 4 was completely satisfied, as well as the second frequency constraint in Case 1. In Case 2 a 3.01 percent decrease from the weight reported in [2] was calculated, while a 9.78 percent decrease in weight was obtained for Case 3. For the calculated frequencies in Cases 2 and 3, there was less than 1 average percent change from those reported in [2].

Reference [1] presents optimization studies of a thirty-eight member truss (Figure 2) with multiple frequency limits. The elastic modulus and weight density of the material were 10^7 psi and 0.1 lb/in^3, respectively. At nodes 8 and 14 a nonstructural mass of 0.5 lb-sec^2/in was included. Lower limit on the design variables was 0.005 in^2.

Tables 3 and 4 show design cycle histories of structural weight and frequencies of a 38 member truss when a specified band between the square of the first and second frequency is increased: [(Case i) $\omega_1{}^2=2500$rad^2/sec^2, $\omega_2{}^2>2500$rad^2/sec^2; (Case ii) $\omega_1{}^2=2500$rad^2/sec^2, $\omega_2{}^2>3000$rad^2/sec^2, respectively.] The first set of results were obtained by the present analysis using Eq. (8) to modify the design variables and Eq. (12) to estimate the Lagrange multipliers. The asterisk associated with an iteration indicates the use of the modified Aitken's accelerator (Eq. 19) and the corresponding Eqs. (21-24). The second set of results was taken from reference [1]. Khot [1] reported real optimum designs because the minimum weights obtained were equal to the dual weight of the structure, which was the difference between the total weight and the weight of passive elements (such as elements at minimum gage).

From Tables 3 and 4 it is seen that with the relative areas of all members equal to unity the initial scaled weight of the structure was 27.74 compared to 52.30 obtained in [1]. The present authors could not reach any justifiable conclusions for the difference. However, it is seen that the weights obtained in this work quickly converged to a 8.61 percent lower weight for Case (i) (Table 3). Comparing the results for Case (ii) (Table 4), it is seen that the present algorithm calculated a 7.04 percent decrease in weight.

The example ten bar truss was redesigned with the constraints of Case 4. The two recursive relations used to modify the design variables were (1) the exponential relation (Eq. 8); (2) the linear relation (Eq. 9). The Lagrange multipliers for the above two cases were determined by using (1) the approximate relation [2] (Eq. 12); (2) the exponential relation (Eq. 10); (3) the linear relation (Eq. 11).

The design cycle history of structural weights using combinations of the above recursive formulae (Cases A-F) is given in Table 5. This table also contains CPU time (sec) using double precision arithmetic on a 32-bit IBM machine. Table 6 gives design cycle histories of the control parameter s, used in Cases A-F. (Note that the control parameter is not used in Eq. (12) of Cases A-B). The iteration history for the six cases is shown in Figure 3. At this time it is premature to draw general conclusions at this time on which case performs the best in a wide variety of design situations. Although all the cases appear to illustrate an average degree of convergence, a value of s near unity is preferred in Eq. (8 or 9) because this ensures a larger contribution in satisfying the optimality condition. This inevitably leads to a more rapid convergence to a lower weight. Hence, Case B appears to perform the best for the example problem.

The example thirty-eight bar truss was redesignedwith the constraints of Cases (i) and (ii). The design cycle history of structural weights using the recursive Cases A-F is given in Tables 7 and 8. The iteration history for the six cases is shown in Figures 4 and 5. In Figure 4, all the recursive cases appear to converge with Case A producing the lowest weight. The curve for Case B displays the most stable convergence. As the frequency band is increased in Figure 5, all the cases appear to converge to the same weight, but the path of convergence is more dispersed.

CONCLUSIONS

In this paper, minimum weight designs of truss systems with multiple frequency constraints were obtained using OC methods with a new resizing strategy based on relaxation techniques. A computationally adaptive control parameter was used in conjunction with available OC recursive formulae. To increase the overall rate of convergence, the modified Aitken accelerator was employed during the design cycle. Several recursive schemes to modify the design variables and to estimate the Lagrange multipliers have been compared. It is premature to generally state which scheme was superior for frequency constraint design problems until more case studies are complete. Minimum weight designs were obtained for various frequency constraint conditions, even though their design may be undesirable due to other practical considerations. Practical extensions of this work call for including displacement constraints.

ACKNOWLEDGMENTS

This research effort has been supported by the Air Force Office of Scientific Research at Air Force Wright Aeronautical Laboratories, WPAFB, Ohio. The authors gratefully acknowledge the helpful assistance given by Dr. R.S. Sandhu, Professor, Department of Civil Engineering at The Ohio State University.

REFERENCES

1. Khot, N.S., "Optimization of structures with multiple frequency constraints", Computer and Structures, Vol. 20, No. 5, p. 869-876 (1985).

2. Grandhi, R.V. and Venkayya, V.B., "Structural optimization with frequency constraints", 26th Structural, Dynamics and Materials Conference, Monterey, California (1986).

3. Khot, N.S., "Optimality criterion methods in structural optimization, foundations of structural optimization: a unified approach" (Ed. by A.J. Morris), p. 99-235, Wiley, New York (1986).

4. Jennings, A., "Accelerating the convergence of matrix iterative processes", J. Inst. Maths. Applics., Vol. 8, p. 99-110 (1971).

5. Boyle, E.F. and Jennings, A., "Accelerating the convergence of elastic-plastic stress analysis", Int. J. Num. Meth. Engng., Vol. 7, p. 232-235 (1973).

6. Venkayya, V.B. and Tischler, V.A., "Optimization of Structures with Frequency Constraints", Computer Meth. for Nonlinear Solids and Structural Mech., ASME, AMD-54, p. 239-259, (1983).

BEST COPY AVAILABLE

Table 1 Ten Bar Truss

*Initial and Final Frequencies (Hz) in Different Constraint Conditions**

Frequency No.	Initial Design	$\omega_2 = 10.0$	$\omega_1 = 7.0$ $\omega_2 \geqslant 15.0$	$\omega_1 = 7.0$ $\omega_2 \geqslant 15.0$ $\omega_3 \geqslant 20.0$	$\omega_1 \geqslant 3.5$ $\omega_2 \geqslant 10.0$ $\omega_3 \geqslant 14.0$
1	9.18 (8.96)	3.04 (3.26)	7.00 (7.00)	7.00 (7.00)	3.71 (4.40)
2	27.31 (27.08)	10.00 (10.00)	15.45 (15.58)	16.30 (15.61)	10.35 (12.14)
3	29.79 (27.45)	10.00 (10.19)	17.36 (16.93)	20.15 (20.17)	14.00 (14.00)
4	53.87 (51.25)	11.44 (16.01)	18.83 (18.75)	20.24 (20.77)	14.33 (17.89)
5	61.06 (58.00)	12.86 (18.08)	28.36 (29.13)	29.08 (28.76)	16.84 (19.58)
6	68.35 (64.73)	17.34 (22.96)	29.71 (30.30)	29.88 (29.76)	19.52 (22.96)
7	69.95 (66.87)	26.01 (25.21)	47.70 (46.93)	48.52 (53.88)	30.33 (34.01)
8	82.11 (80.85)	26.81 (27.25)	50.31 (49.67)	51.41 (56.03)	31.84 (35.72)
Weight (lb)	4000.0 (4000.0)	256.7 (304.5)	1137.3 (1172.6)	1180.4 (1308.4)	411.5 (489.17)

Notes :

* present analysis using exponential resizing and approximate Lagrange multiplier formulae.

( ) via reference [2].

Table 2 Ten Bar Truss
Optimum Design Variables (in^2) in Different Constraint Conditions[*]

Element No.	$\omega_1 = 10.0$	$\omega_1 = 7.0$ $\omega_2 \geq 15.0$	$\omega_1 = 7.0$ $\omega_2 \geq 15.0$ $\omega_3 \geq 20.0$	$\omega_1 \geq 3.5$ $\omega_2 \geq 10.0$ $\omega_3 \geq 14.0$
1	0.887 (0.910)	5.769 (5.511)	5.254 (5.672)	1.021 (2.306)
2	0.889 (0.821)	1.944 (1.937)	2.446 (3.823)	1.211 (1.304)
3	0.887 (0.910)	5.769 (5.511)	5.254 (5.672)	1.021 (2.306)
4	0.889 (0.821)	1.944 (1.937)	2.446 (3.823)	1.211 (1.304)
5	0.360 (0.768)	0.125 (0.207)	0.125 (0.646)	0.213 (0.639)
6	0.208 (0.570)	0.448 (0.414)	0.720 (0.321)	0.343 (0.557)
7	0.788 (0.712)	3.302 (3.616)	3.739 (4.191)	1.661 (1.029)
8	0.788 (0.712)	3.302 (3.616)	3.739 (4.191)	1.661 (1.029)
9	0.276 (0.581)	2.211 (2.414)	2.109 (1.604)	0.605 (0.800)
10	0.276 (0.581)	2.211 (2.414)	2.109 (1.604)	0.605 (0.800)
Weight (lb)	256.7 (304.5)	1137.3 (1172.6)	1180.4 (1308.4)	411.5 (489.17)

Notes :
- * present analysis using exponential resizing and approximate Lagrange multiplier formulae
- ( ) via reference [2].

Table 3 Thirty-Eight Bar Truss
Design Cycle History for $\omega_1^2 = 2500$ and $\omega_2^2 \geq 2500$ $(rad/sec)^2$

Iter. No. *	ω_1^2	ω_2^2	Weight (lbs)	Iter. No. +	ω_1^2	ω_2^2	Weight (lbs)
1	2500	3667	27.74	1	2500	8560	52.30
2	2500	2907	25.74	2	2500	6451	39.41
3	2500	3111	30.65	3	2500	5061	33.29
4	2500	4497	* 28.56	4	2500	4326	31.01
5	2500	3435	26.29	5	2500	4033	29.83
6	2500	2759	25.26	6	2500	3706	28.94
7	2500	2507	24.93	7	2500	3314	28.26
				8	2500	2880	27.72
				9	2500	2537	27.36
				10	2500	2501	27.29
				11	2500	2500	27.28

Notes :
- * present analysis using exponential resizing and approximate Lagrange multiplier
- + via. reference [1]
- * with acceleration

Table 4 Thirty-Eight Bar Truss
Design Cycle History for $\omega_1^2 = 2500$ and $\omega_2^2 \geqslant 3000$ $(rad/sec)^2$

Iter. # No.	ω_1^2	ω_2^2	Weight (lbs)	Iter. + No.	ω_1^2	ω_2^2	Weight (lbs)
1	2500	3667	27.74	1	2500	8560	52.30
2	2578	3000	26.58	2	2500	6451	39.41
3	2500	3789	26.89	3	2500	5061	33.29
4	2500	3123	* 25.77	4	2500	4326	31.01
				5	2500	4033	29.83
				6	2500	3706	28.94
				7	2500	3314	28.26
				8	2500	3016	27.80
				9	2500	2998	27.72
				10	2500	2999	27.72
				11	2500	3000	27.72

Notes :
- # present analysis using exponential resizing and approximate Lagrange multiplier
- + via. reference [1]
- * with acceleration

Table 5 Ten Bar Truss

Design Cycle History of Structural Weight
Using Various OC Recursive Formulae
$\omega_1 \geqslant 3.5$, $\omega_2 \geqslant 10$ & $\omega_3 \geqslant 14$ Hz.

Iter. #	A	B	C	D	E	F
1	778.192	469.222	778.192	469.222	778.192	469.222
2	646.754	502.846	647.753	533.498	647.753	533.498
3	750.374	606.414	744.672	674.662	744.672	672.496
4	* 445.400	436.027	* 439.545	628.077	* 439.545	618.992
5	467.874	463.789	528.799	462.462	511.869	457.601
6	* 438.693	* 442.361	* 407.225	484.560	* 409.063	458.850
7	436.855	422.566	448.569	491.267	436.235	* 455.656
8	425.245	404.818	* 430.650	* 480.714	* 430.713	454.152
9	422.174		427.603	472.686	418.765	450.901
10	421.555		414.426	465.015	406.346	447.713
11	416.449		418.468	457.683		444.588
12	411.556		* 415.834	450.670		441.523
13			414.329			438.518
14						435.571
15						432.681
16						429.847
17						427.068
c.p.u. (sec.)	(3.16)	(1.86)	(3.33)	(3.17)	(2.28)	(3.99)

Notes :
- A exponential resizing/approximate Lagrange multiplier formulae
- B linear resizing/approximate Lagrange multiplier formulae
- C exponential resizing/exponential Lagrange multiplier formulae
- D linear resizing/exponential Lagrange multiplier formulae
- E exponential resizing/linear Lagrange multiplier formulae
- F linear resizing/linear Lagrange multiplier formulae
- * with acceleration

Table 6 Ten Bar Truss

Design Cycle History of Control Parameter β
Using Various OC Recursive Formulae
$\omega_1 \geq 3.5$, $\omega_2 \geq 10$ & $\omega_3 \geq 14$ *Hz.*

Iter. #	A	B	C	D	E	F
1	1.	1.	1.	1.	1.	1.
2	1.	1.	1.	1.	1.	1.
3	1.	1.	1.	1.	1.	1.
4	0.5	1.	0.5	1.	0.5	1.
5	0.5	1.	0.5	1.	0.5	1.
6	0.5	0.5	0.5	0.125	0.5	1.
7	0.25	0.5	0.125	0.0625	0.125	0.0625
8	0.125	0.5	0.125	0.0625	0.125	0.0313
9	0.0625		0.125	0.0625	0.125	0.0313
10	0.0625		0.125	0.0625	0.125	0.0313
11	0.0625		0.0156	0.0625		0.0313
12	0.0625		0.0156	0.0625		0.0313
13			0.0156			0.0313
14						0.0313
15						0.0313
16						0.0313
17						0.0313

Notes :
A exponential resizing/approximate Lagrange multiplier formulae
B linear resizing/approximate Lagrange multiplier formulae
C exponential resizing/exponential Lagrange multiplier formulae
D linear resizing/exponential Lagrange multiplier formulae
E exponential resizing/linear Lagrange multiplier formulae
F linear resizing/linear Lagrange multiplier formulae
* with acceleration

Table 7 Thirty-Eight Bar Truss

Design Cycle History of Structural Weight
Using Various OC Recursive Formulae
$\omega_1^2 = 2500$ & $\omega_2^2 \geq 2500$ $(rad/sec.)^2$

Iter. #	A	B	C	D	E	F
1	27.742	30.186	25.741	26.965	25.741	26.965
2	25.741	26.965	30.653	25.293	30.653	25.293
3	30.653	25.379	215.117	29.667	215.117	29.322
4	* 28.564	25.613	34.820	* 27.886	34.820	* 27.636
5	26.288	* 25.438	31.565	26.434	31.565	26.264
6	* 25.259	25.297	26.756	25.500	26.756	25.376
7	24.928		25.119	25.153	25.119	25.044

Notes :
A exponential resizing/approximate Lagrange multipier formulae
B linear resizing/approximate Lagrange multipier formulae
C exponential resizing/exponential Lagrange multipier formulae
D linear resizing/exponential Lagrange multipier formulae
E exponential resizing/linear Lagrange multiplier formulae
F linear resizing/linear Lagrange multiplier formulae
* with acceleration

Table 8 Thirty-Eight Bar Truss
Design Cycle History of Structural Weight
Using Various OC Recursive Formulae
$\omega_1^2 = 2500$ & $\omega_2^2 \geqslant 3000$ $(rad/sec.)^2$

Iter. #	A	B	C	D	E	F
1	27.742	30.186	26.888	26.965	26.888	26.965
2	26.577	26.965	29.175	32.344	29.278	32.344
3	26.888	28.090	37.388	32.410	211.307	32.518
4	* 25.776	* 27.450	27.629	26.922	72.092	26.964
5		26.287	26.085	25.920	* 31.820	
6		26.154			* 27.844	
7		25.987			26.752	
8					25.976	

Notes :
A exponential resizing/approximate Lagrange multipier formulae
B linear resizing/approximate Lagrange multiplier formulae
C exponential resizing/exponential Lagrange multiplier formulae
D linear resizing/exponential Lagrange multiplier formulae
E exponential resizing/linear Lagrange multiplier formulae
F linear resizing/linear Lagrange multiplier formulae
* with acceleration

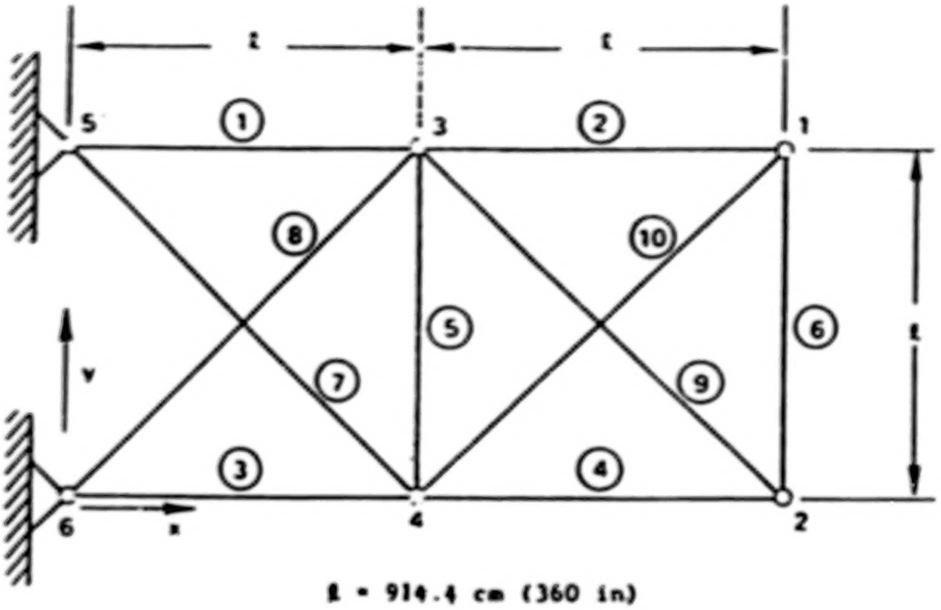
ℓ
ℓ
5
①
3
②
1
⑧
⑩
⑤
⑥
ℓ
y
⑦
⑨
③
④
6
x
4
2

ℓ = 914.4 cm (360 in)

Figure 1 Ten bar truss

Element	Connecting Nodes	Element	Connecting Nodes	Element	Connecting Nodes
1	1-2	14	7-9	27	13-16
2	1-3	15	7-10	28	14-15
3	1-4	16	8-9	29	14-16
4	2-3	17	8-10	30	15-17
5	2-4	18	9-11	31	15-18
6	3-5	19	9-12	32	16-17
7	3-6	20	10-11	33	16-18
8	4-5	21	10-12	34	17-19
9	4-6	22	11-13	35	17-20
10	5-7	23	11-14	36	18-19
11	5-8	24	12-13	37	18-20
12	6-7	25	12-14	38	19-20
13	6-8	26	13-15		

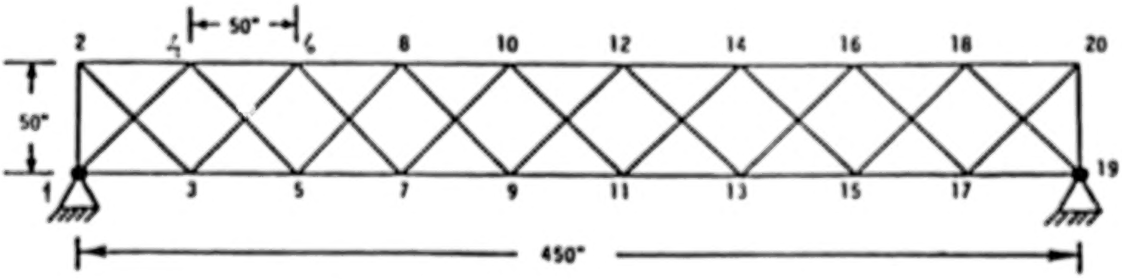
2
4
50"
6
8
10
12
14
16
18
20
50"
1
3
5
7
9
11
13
15
17
19
450"

Figure 2 Thirty-eight bar truss

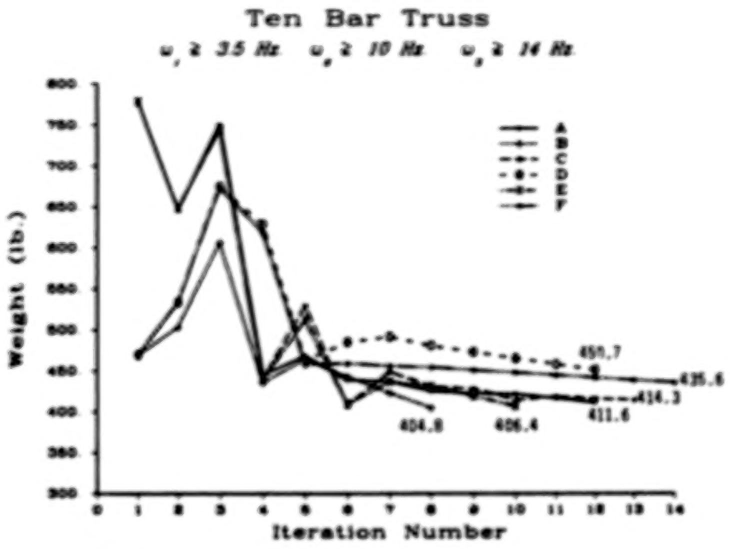

Notes :

A : exponential resizing/approximate Lagrange multiplier formulae
B : linear resizing/approximate Lagrange multiplier formulae
C : exponential resizing/exponential Lagrange multiplier formulae
D : linear resizing/exponential Lagrange multiplier formulae
E : exponential resizing/linear Lagrange multiplier formulae
F : linear resizing/linear Lagrange multiplier formulae

Figure 3 Iteration history for ten bar truss with multiple frequency constraints

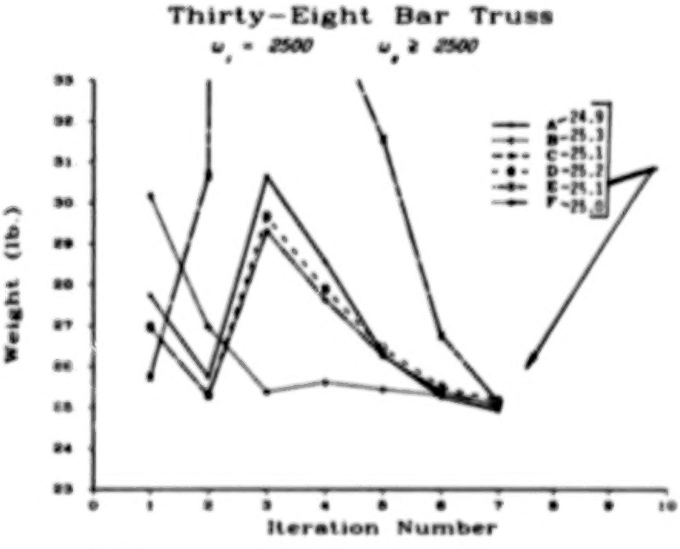

Notes :

A : exponential resizing/approximate Lagrange multiplier formulae
B : linear resizing/approximate Lagrange multiplier formulae
C : exponential resizing/exponential Lagrange multiplier formulae
D : linear resizing/exponential Lagrange multiplier formulae
E : exponential resizing/linear Lagrange multiplier formulae
F : linear resizing/linear Lagrange multiplier formulae

Figure 4 Iteration history for thirty-eight bar truss with multiple frequency constraints

BEST COPY AVAILABLE

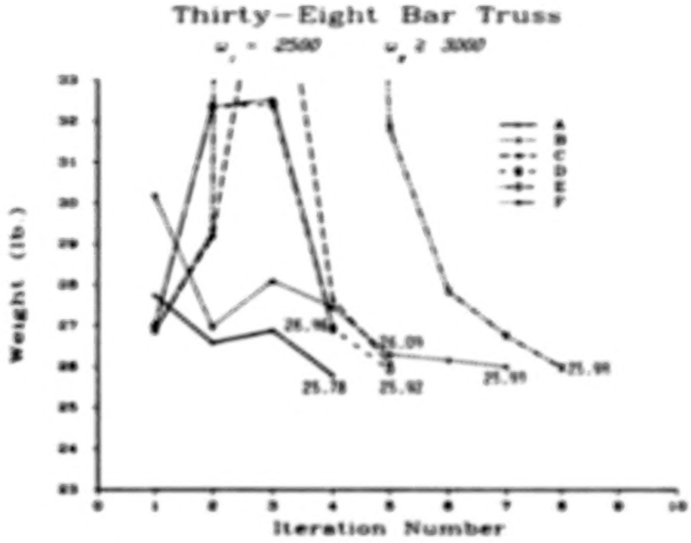

Notes :

A : exponential resizing/approximate Lagrange multiplier formulae
B : linear resizing/approximate Lagrange multiplier formulae
C : exponential resizing/exponential Lagrange multiplier formulae
D : linear resizing/exponential Lagrange multiplier formulae
E : exponential resizing/linear Lagrange multiplier formulae
F : linear resizing/linear Lagrange multiplier formulae

Figure 5 Iteration history for thirty-eight bar truss with multiple frequency constraints

463

BEST COPY AVAILABLE

Structural Damage Assessment as an Identification Problem [*]

P. Hajela and F.J. Soeiro
Aerospace Engineering, Mechanics & Engineering Science
University of Florida, Gainesville, Florida

---

[*] Paper was submitted for presentation at conference but could not be presented due to time restrictions.

Abstract

Damage assessment of structural assemblies is treated as an identification problem. A brief review of identification methods is first presented with particular focus on the output error approach. The use of numerical optimization methods in identifying the location and extent of damage in structures is studied. The influence of damage on eigenmode shapes and static displacements is explored as a means of formulating a measure of damage in the structure. Preliminary results obtained in this study are presented and special attention is directed at the shortcomings associated with the nonlinear programming approach to solving the optimization problem.

Introduction

Structural systems in a variety of applications including aerospace vehicles, automobiles, civil engineering structures such as tall buildings, bridges and offshore platforms, accumulate damage during their service life. From the standpoint of both safety and performance, it is desirable to monitor the occurrence, location, and extent of such damage. System identification methods, which may be classified in a general category of nondestructive evaluation techniques, can be employed for this purpose. Using experimental data, such as eigenmodes, static displacements and damping factors, and an analytical structural model, parameters of the structure such as its mass, stiffness and damping characteristics can be identified. The approach is one where the structural properties of the analytical model are varied to minimize the difference between the analytically predicted and empirically measured response. In this process, the number of equations describing the system is typically different from the number of unknowns, and the problem reduces to obtaining the best solution from the available data.

The genesis of identification methods in structural analysis can be traced to the model determination and model correction problems. The underlying philosophy in these efforts was that a reasonably close analytical model of the structural system was available, and that deviations in the analytical response from the measured response could be used to implement corrections in the model to account for these variations. This resulted in the adoption of a standard strategy wherein the change in the analytical model was minimized to obtain a match between analytical and empirical data. For the class of problems for which it was intended, the method has enjoyed a fair degree of success. A large body of identification work has been based on measurements of eigenmodes of the structure, and this is philosophically the right approach as eigenmodes reflect the global behavior of the structure. However, some reservations about this approach do exist, as these modes are sensitive to the physical boundary conditions that exist on the experimental model, and are not accounted for in the analytical model.

The problem of damage assessment in structures by identification methods is similar to the one described above. However, the approach of minimizing changes in the analytical model is no longer applicable, as significant variations can be introduced locally due to damage in a structural component. In the present work, damage in the structure is represented by a reduction in the elastic properties of the material, and these are designated as design variables of the optimization problem. Both eigenmodes and static structural deflections are used in the identification process. The use of static structural displacements as the measured response is a departure from the standard practice of using vibration modes. Since these displacements are reflective of the applied loading, an auxiliary problem in their use is one of determining the load conditions which are best suited for a global model identification.

Subsequent sections of this paper are devoted to the review of identification methods and their prior applications in structural damage assessment. The approach used in the current work is then presented, with special emphasis on the numerical efficiency aspects of the optimization problem. In particular, the use of a reduced set of dominant design variables and constructing equivalent reduced order models for damage assessment is explored with some success.

System Identification

The veracity of analytical models is usually determined by comparing the response predicted by the model with the response observed in tests or during operation. Although measurements are in themselves imprecise due to the equipment errors and data acquisition techniques used, reasonable bounds can be imposed within which the experimental data is expected to lie. The difference between the measured and analytical data may be large enough to be considered unacceptable. In this case, if there is sufficient confidence in the experimental data, identification methods can be invoked to improve the analytical model. This subject is not new and several studies pertinent to the field are documented in the literature [1-5]. In some cases, experimental data may even be used to deduce an analytical model which eludes analytical derivation.

The data utilized in identification may include both input and output measurements, or, some system dependent characteristics such as modal parameters, which in turn are functions of the input-output measurements. A priori knowledge about the behavior of the system may also be available in the form of an analytical model. In the case of discrete structural dynamic systems, the model consists of linear second order differential equations. The mass, damping and stiffness matrix elements constitute the parameters to be identified.

Identification techniques may be classified in many different ways. Such classification is typically based on the type of data used, on the type of system being identified, or on the type of formulation employed [6]. Three of the more important formulations used in identification of structural systems are briefly discussed in the following paragraphs. These are the equation error approach, the output error approach and the minimum deviation approach.

In the equation error approach, equations describing the system response are explicitly stated. The system parameters, which are typically coefficients in such equations, are then selected to minimize the error in satisfying the system equations with a set of measured input-output data. Consider a linear differential equation represented in a functional form as follows.

$$f(c_1,c_2,x,t)=g(t) \tag{1}$$

Here, c_1 and c_2 are considered as the unknown system parameters, and $x(t)$ and its derivatives represent the system response at a time t; $g(t)$ is the forcing function. The system response and the loading is explicitly measured over some characteristic time period. An objective function, which is the measure of residual errors in the system equations for given values of the parameters, is formulated as follows:

$$F = \{ \int_0^T (f(c_1,c_2,x_m,t) - g_m(t))^2 \, dt \} \tag{2}$$

This function is then extremized by differentiating with respect to each system parameter and equating to zero. The approach results in the same number of equations as coefficients to be determined and is therefore regarded as a direct method. In eqn. (2), subscript m denotes measured response, and T denotes the characteristic period over which measurements are made.

The output error approach selects some system characteristic response as the entity for which a match between the analytical prediction and experimental measurements is considered to reflect a good analytical model. An objective function is formulated that is typically an averaged least-squares measure as follows.

$$F = \int_0^T (x_m(t) - x(t))^2 \, dt \tag{3}$$

The analytical model from which x(t) is obtained, contains system parameters which are adjusted to minimize the function F. In structural dynamics identification problems, system eigenmodes are generally selected as the characteristic response quantities used to identify the model.

The minimum deviation approach is frequently used in structural identification problems. In this approach, deviation of the system parameters from initial assumed values is minimized, subject to the constraints that the system equations be satisfied. An illustration of this approach in structural applications is in the determination of changes in the elastic stiffness matrix. In such applications, the mass matrix is assumed to be accurately defined. A weighted matrix norm of the difference between the a priori and corrected stiffness matrices is minimized in the identification process. This norm can be written as

$$F = \| \, M^{-1/2} \, (\, K - \bar{K} \,) \, M^{-1/2} \, \| \tag{4}$$

where M is the mass matrix, K is the desired stiffness matrix, and $\bar{K}$ is the a priori stiffness matrix. This minimization is subject to the constraint that the modified stiffness matrix remain symmetric. An incomplete set of eigenmodes is measured, and these eigenmodes are required to satisfy the eigenvalue equation and be orthogonal to the modified stiffness matrix. This results in the following equality constraints:

$$\phi^T K \phi = \Omega^2 \tag{5}$$

$$K = K^T \tag{6}$$

$$K\phi = M\phi\Omega^2 \tag{7}$$

In the above equations, ϕ is an nxp modal matrix and Ω^2 is a diagonal matrix of eigenvalues for the p measured modes; n is the number of degrees of freedom for the structural dynamic system. The constraints are incorporated into the objective function by means of Lagrange multipliers, and the application of the optimality condition yields a close form expression for the corrected stiffness matrix as follows:

$$K = K - K\phi\phi^T M - M\phi\phi^T K + M\phi\phi^T K\phi\phi^T M + M\phi\Omega^2\phi^T M \tag{8}$$

Damage Assessment

The foregoing discussion outlines various identification techniques and their applicability in predicting changes in a structural configuration. This approach has been employed for detecting changes in the analytical model due to structural damage. The requirements of the identification problem are to use experimental data to determine if the structure is damaged and to further detect the extent and location of that damage.

A major structural failure in the form of a macroscopic rupture can be visually observed. However, changes in the structural load carrying capacity that is localized to an internal structural component may not be detected as easily. As weight considerations dictate the use of lighter, more flexible and actively stiffened structures, it has become increasingly important to develop a consistent approach that would allow real time detection and correction for structural damage.

The use of identification techniques to detect damage has been recently attempted [7-8], but with limited success. Chen and Garba [7] discuss the use of measured eigenmodes to determine the changes in the stiffness matrix, assuming no changes in the mass matrix with damage. They employ the use of a direct optimization method, in which an Euclidean norm of the changes in the stiffness matrix is minimized, subject to the constraints that the modified system matrices produce the measured eigenmodes. This is an application of the minimum deviation approach described in the previous section. The number of unknown elements of the modified stiffness matrix is typically much larger than the number of equations available. An infinite number of solutions is possible in the optimization problem, and this difficulty is clearly evidenced by the results obtained.

Smith and Hendricks [8] report the evaluation of a similar method and another that uses linear perturbations of system submatrices and an energy distribution analysis to detect damage. Both methods show appreciable problems in detecting damage. Another shortcoming of these methods, based on the minimum deviation approach, is the fact that it fails in showing damage clearly. The stiffness matrix has several entries which depend on the elastic and geometric properties of the structure as well as on structural element connectivity. There are overlaps in the matrix due to the contribution of different members sharing the same node, which makes it difficult to identify where damage is occurring. Also, the minimum deviation approach tries to deviate the minimum from the a priori model. In this kind of problem, the a priori model is the original stiffness matrix corresponding to the undamaged structure. The damage may be quite severe and located in different members of the structure. The changes in the stiffness matrix may be significant, thereby increasing the possibility that this approach may not be able to give good results.

In a finite element formulation, structural characteristics are defined in terms of the stiffness, damping, and mass matrices [K], [C] and [M], respectively. The governing equation of equilibrium for a dynamical system involves each of these matrices, and can be written as

$$[M]\{\ddot{x}\} + [C]\{\dot{x}\} + [K]\{x\} = \{P(t)\} \quad (9)$$

where $\{x\}$ is the displacement vector, and $\{P(t)\}$ is the vector of applied loads. The eigenvalue problem can be stated in terms of the system matrices, eigenvalues ω_i^2, and the corresponding eigenmodes ϕ_i as follows:

$$([K] - \omega_i^2 [M])\{\phi_i\} = \{0\} \quad (10)$$

The static load-deflection relation only involves the system stiffness matrix.

$$[K]\{x\} = \{P\} \quad (11)$$

It is clear from these equations that a change in the system matrices results in a changed response, and this difference can be related to changes in specific elements of the system matrices. Since internal structural damage typically does not result in a loss of material, we will assume the mass matrix to be a constant. The stiffness matrix can be expressed as a function of the sectional properties A,I, and J, the element dimensions denoted by t and L, and by extensional and shear modulii E and G, respectively.

$$[K] = [K(A,I,J,L,t,E,G)] \quad (12)$$

In the present work, changes in these quantities due to damage are lumped into a coefficient d_i that is used to multiply the extensional modulus E_i for the particular element. These d_i's constitute the design variables for the optimization problem. If the measured and analytically determined static displacements or eigenmodes are denoted by $\{y_m\}$ and $\{y_a\}$, respectively, the optimization problem can be stated as finding a vector of d_i (and hence the analytical stiffness matrix) that minimizes the quantity

$$\sum_i \sum_j (y_m^{ij} - y_a^{ij})^2 \quad (13)$$

where i represents the degree of freedom, and j denotes the static loading condition or a particular eigenmode. This minimization requires that $\{y_a\}$ be obtained from the eigenvalue problem or the load deflection equations using the [K] matrix that must be identified. Lower and upper bounds of 0 and 1 were established for the design variables d_i.

The nonlinear programming solution to the damage detection problem can be computationally demanding, and approximations were used to circumvent this problem. The first approach was one in which a select number of dominant variables were used in the optimization, based on the magnitude of the search direction. This set of dominant variables was periodically revised with a new assessment of the dominance.

The second approach was one in which equivalent reduced order models were constructed. Consider the truss shown in Figure 1, subjected to tensile and bending loads. An equivalent beam model (figure 2), with an independent axial and bending stiffness for each section, can be obtained to simulate the behavior of the truss structure. Each section corresponds to one bay in the truss. The degrees of freedom and number of design variables for the beam are 15 and 5, and this compares with 20 degrees of freedom and 25 design variables for the original truss structure. The equivalent section is first used to identify the section in which damage exists. This gives us a reduced set of variables to work with in the actual structure, and convergence to the correct stiffness matrix is far more efficient.

Recognition of the fact that measured data often cannot be obtained for all nodes and degrees of freedom, the identification problem was also carried out with a reduced set of measurements. The results of this implementation were encouraging.

In working with static displacements as the measured response, careful consideration must be given to the fact that the applied loading is not one that allows only a few members of the structural system to participate in the load carrying process. This issue has been studied in extensive detail and results are presented in [9].

Numerical Examples

The procedure described in the preceding section was implemented on a VAX 11-750 computer. The Davidon-Fletcher-Powell variable metric method was used for function minimization and a finite element analysis program EAL [10] was used to obtain the structural response. The simulated measured data was the finite element solution obtained for the damaged structure, corrupted by a random noise signal.

The method developed for damage detection has been applied to a series of representative truss models and semimonocoque structures. A twenty five bar truss shown in Fig.1 was damaged in element 11 by reducing its Young's modulus to 0.0 . The first four eigenmodes were used to detect the extent and location of damage in the structure, and the results are shown in Table 1. The same problem was solved using static displacements for the indicated static loading, and these results are shown in Table 2. This example was repeated with the use of master design variables and was more efficient from the standpoint of computational effort. An equivalent beam with five elements, each corresponding to one bay of the truss is created (Fig.2). The problem is then solved in two steps. The first step is the use of the reduced order model to detect the area of damage in the five element beam. The second step entails the detection of damage in the original structure with reduced number of design variables.

Another representative example is that of a semimonocoque wing box structure (Fig.3) consisting of axial rod elements and membrane elements. Membrane element 2 was damaged and the identification of damage conducted with the use of static displacements. Table 3 summarizes the results for this example, clearly indicating the need for applying a torque that forces the membrane to participate more equitably in the load bearing process. This case also represents the successful use of a reduced set of experimental measurements in the damage detection process. In this 54 d.o.f system, only 9 displacements were employed: 3 horizontal displacements in the middle of the upper panel and 3 vertical displacements at each edge of the upper panel. In using static displacements for damage assessment purposes, critical members are more easily detected. This is reassuring from the standpoint of safety in the structure.

The iterative optimization methods used in this approach are clearly susceptible to convergence to a local optimum. One approach that circumvents the problem of nonconvexities in the design space [11] is presently under development and will be used in future work.

Conclusions

This paper presents an approach for damage detection in structures based on identification techniques. The different identification methods are discussed with particular focus on the output error approach. Both eigenmodes and static displacements are used in the identification procedure, with the static displacements providing the advantage of lower computational cost and easier measurement. Approximation concepts have been introduced to decrease the computational cost such as equivalent structures with less d.o.f and master displacements. The approach has given extremely encouraging results and has proved to be very flexible. Future work will include the study of damage detection in composite materials that are extensively used in aerospace structures. Damping also promises to be a good parameter for damage assessment as it represents an energy dissipation process that may be influenced by microscopic or macroscopic damage.

References

1. A. Berman and W.G. Flannelly, "Theory of Incomplete Models of Dynamic Structures", AIAA Journal, Vol. 9 ,No. *, Aug 1971, pp1481-1487.

2. A. Berman and E.J. Nagy, "Improvement of a Large Analytical Model Using Test Data", AIAA Journal, Vol. 21, No. 8, 1983, pp1168-1173.

3. M. Baruch, "Optimal Correction of Mass and Stiffness Matrices Using Measured Modes", AIAA Journal, Vol. 20, No.11, 1982, pp1623-1626.

472

4. A.M. Kabe, "Stiffness Matrix Adjustment Using Mode Data", AIAA Journal, Vol.23, No. 9, 1985, pp1431-1436.

5. C.B. Yun and M. Shinozuka, "Identification of Nonlinear Structural Dynamic Systems", Journal of Structural Mechanics, Vol. 8, 1980, pp187-203.

6. S. Hanagud, M.Meyyappa and J.I. Craig, "Identification of Structural Dynamic Systems", Recent Trends in Aeroelasticity, Structures and Structural Dynamics, Florida Presses, 1987.

7. J.C. Chen and J.A. Garba, "On Orbit Damage Assessment for Large Space Structures", Proceedings of the 28th SDM Conference, Monterey, California, April 1987.

8. S.W. Smith and S.L. Hendricks, "Evaluation of Two Identification Methods for Damage Detection in Large Space Structures", Proceedings of the 6th VPI&SU/AIAA Symposium on Dynamics and Control of Large Structures, 1987.

9. P. Hajela and F.J. Soeiro, "Structural Damage Detection Based on Static and Modal Analysis", in review for the 30th AIAA/ASME/ASCE/AHS/ASC SDM Conference, Mobile, Alabama, April 1989.

10. D. Whetstone, "SPAR - Reference Manual", NASA CR-145098-1, February 1977.

11. P. Hajela, "Genetic Search - An Approach to the Nonconvex Optimization Problem", in review for presentation at the 30th AIAA/ASME/AHS/ASCE SDM Conference, Mobile, Alabama, April 1989.

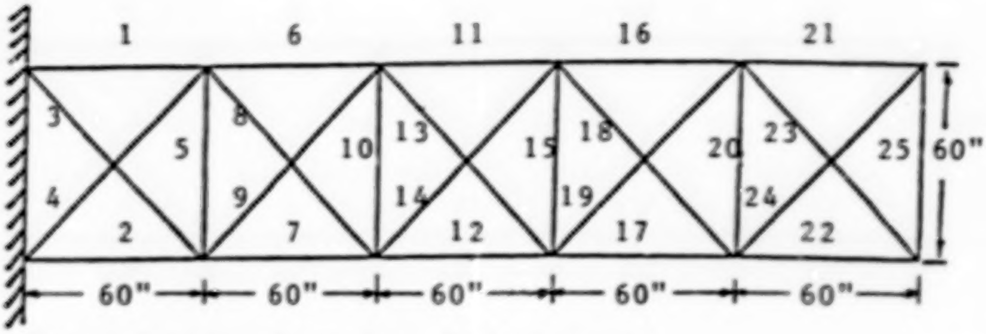
1
6
11
16
21
3
5
8
10
13
15
18
20
23
25
60"
4
9
14
19
24
2
7
12
17
22
60"
60"
60"
60"
60"

Fig.1 Twenty five bar planar truss

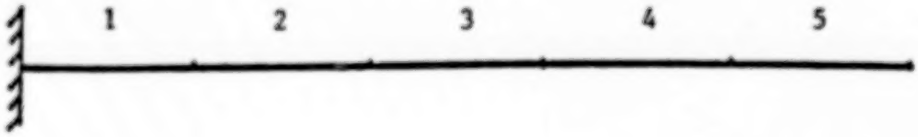

Fig.2 Equivalent five element beam model for the twenty five bar truss

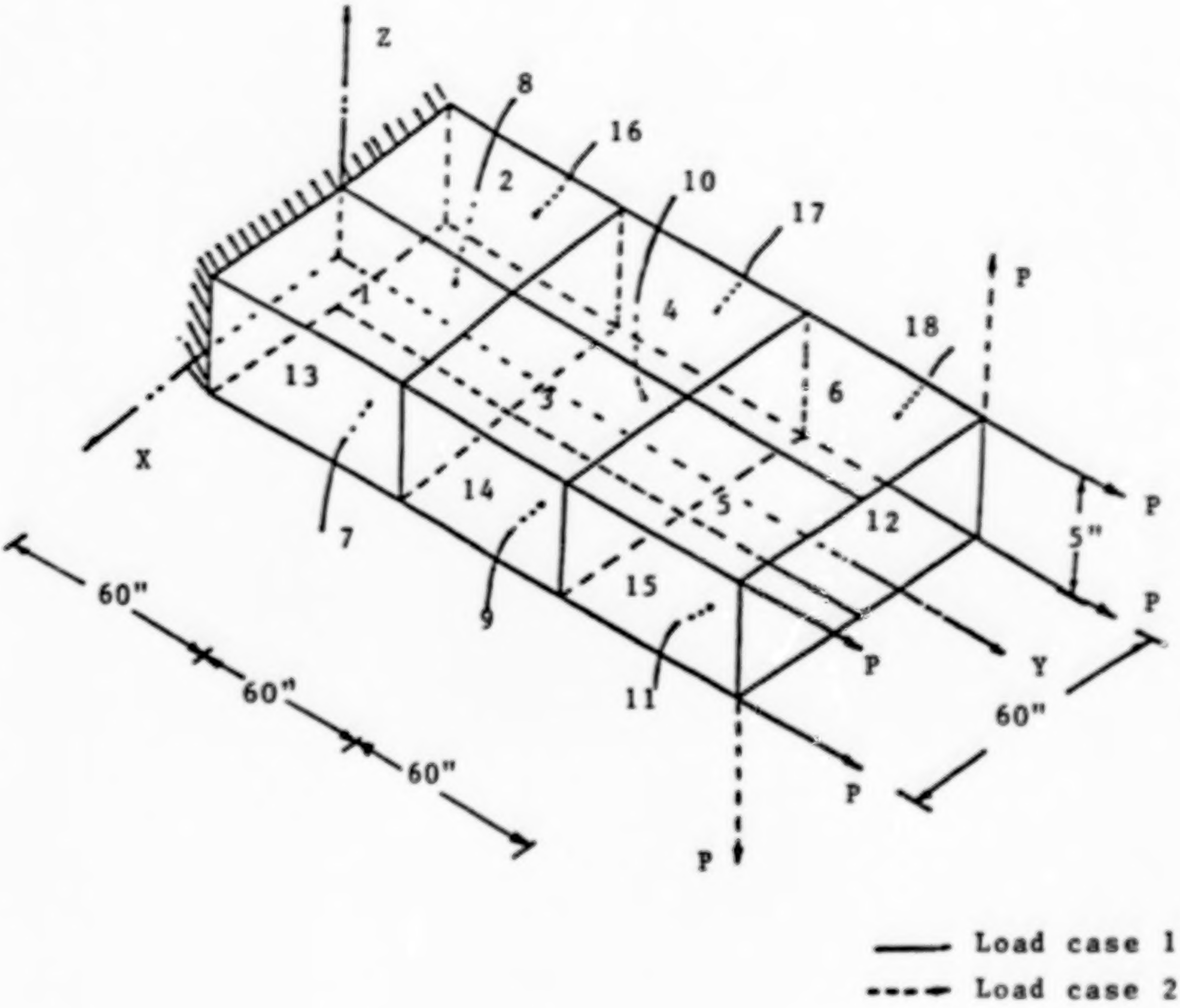
Z
8
16
2
10
17
1
4
18
P
13
3
6
X
14
5
12
P
5"
7
P
60"
15
9
P
Y
11
60"
60"
60"
P
P
Load case 1
Load case 2

Fig.3 Semimonocoque wing box model

OPTIMIZATION RESULTS

VARIABLE	LOWER BOUND	VALUE	UPPER BOUND
1	0.00000E+00	0.92536E+00	0.10000E+01
2	0.00000E+00	0.93169E+00	0.10000E+01
3	0.00000E+00	0.93320E+00	0.10000E+01
4	0.00000E+00	0.91196E+00	0.10000E+01
5	0.00000E+00	0.96094E+00	0.10000E+01
6	0.00000E+00	0.87899E+00	0.10000E+01
7	0.00000E+00	0.96327E+00	0.10000E+01
8	0.00000E+00	0.10000E+00	0.10000E+01
9	0.00000E+00	0.87905E+00	0.10000E+01
10	0.00000E+00	0.98613E+00	0.10000E+01
11	0.00000E+00	0.00000E+00	0.10000E+01
12	0.00000E+00	0.89017E+00	0.10000E+01
13	0.00000E+00	0.85975E+00	0.10000E+01
14	0.00000E+00	0.91797E+00	0.10000E+01
15	0.00000E+00	0.10000E+01	0.10000E+01
16	0.00000E+00	0.85562E+00	0.10000E+01
17	0.00000E+00	0.90889E+00	0.10000E+01
18	0.00000E+00	0.92100E+00	0.10000E+01
19	0.00000E+00	0.98278E+00	0.10000E+01
20	0.00000E+00	0.10000E+01	0.10000E+01
21	0.00000E+00	0.10000E+01	0.10000E+01
22	0.00000E+00	0.93679E+01	0.10000E+01
23	0.00000E+00	0.93863E+01	0.10000E+01
24	0.00000E+00	0.94524E+01	0.10000E+01
25	0.00000E+00	0.10000E+01	0.10000E+01

Table 1. Twenty five bar truss - results using eigenmodes

OPTIMIZATION RESULTS

VARIABLE	LOWER BOUND	VALUE	UPPER BOUND
1	0.00000E+00	0.10000E+01	0.10000E+01
2	0.00000E+00	0.10000E+01	0.10000E+01
3	0.00000E+00	0.10000E+01	0.10000E+01
4	0.00000E+00	0.10000E+01	0.10000E+01
5	0.00000E+00	0.99410E+00	0.10000E+01
6	0.00000E+00	0.74186E+00	0.10000E+01
7	0.00000E+00	0.10000E+00	0.10000E+01
8	0.00000E+00	0.10000E+00	0.10000E+01
9	0.00000E+00	0.10000E+00	0.10000E+01
10	0.00000E+00	0.98792E+00	0.10000E+01
11	0.00000E+00	0.17763E-01	0.10000E+01
12	0.00000E+00	0.91020E+00	0.10000E+01
13	0.00000E+00	0.99999E+00	0.10000E+01
14	0.00000E+00	0.94951E+00	0.10000E+01
15	0.00000E+00	0.99196E+00	0.10000E+01
16	0.00000E+00	0.73150E+00	0.10000E+01
17	0.00000E+00	0.90617E+00	0.10000E+01
18	0.00000E+00	0.95281E+00	0.10000E+01
19	0.00000E+00	0.98696E+00	0.10000E+01
20	0.00000E+00	0.10000E+01	0.10000E+01
21	0.00000E+00	0.96812E+01	0.10000E+01
22	0.00000E+00	0.99026E+00	0.10000E+01
23	0.00000E+00	0.96977E+00	0.10000E+01
24	0.00000E+00	0.95638E+00	0.10000E+01
25	0.00000E+00	0.99999E+00	0.10000E+01

Table 2. Twenty five bar truss - results using static displacements

Element No. (Panel)	Design Variables (d_i) using static response		
	Load 1 only	Load 1 & 2	Exact sol.
1	1.0000	1.0000	1.0000
2	0.1240	0.1020	0.1000
3	0.9601	1.0000	1.0000
4	0.7720	1.0000	1.0000
5	0.9585	1.0000	1.0000
6	0.9837	0.9999	1.0000
7	0.9736	1.0000	1.0000
8	1.0000	1.0000	1.0000
9	0.9954	1.0000	1.0000
10	0.8713	1.0000	1.0000
11	0.9979	1.0000	1.0000
12	0.8984	1.0000	1.0000
13	0.9999	1.0000	1.0000
14	0.9998	1.0000	1.0000
15	0.9981	1.0000	1.0000
16	0.9926	0.9702	1.0000
17	1.0000	1.0000	1.0000
18	0.9855	0.9999	1.0000

Table 3. Results for the 54 d.o.f. semimonocoque wing box model using static displacements for damage detection

Recent Developments in Large-Scale Structural Optimization *

V.B. Venkayya

Flight Dynamics Laboratory
Air Force Wright Aeronautical Laboratories †
Wright-Patterson AFB, Ohio

---

[*] This paper arrived during the printing process and was originally included in Session I.

[†] Wright Research Development Center

ABSTRACT

This paper presents a brief discussion of mathematical optimization and the motivation for the development of more recent numerical search procedures. A review of recent developments and issues in multidisciplinary optimization are also presented. These development are discussed in the context of the preliminary design of aircraft structures. A capability description of programs FASTOP, TSO, STARS, LAGRANGE, ELFINI and ASTROS is included.

INTRODUCTION

The notion of an optimum solution to an engineering problem is intriguing and has been investigated for a long time. The strongest cantilever beam in bending and constant shear as formulated by Galileo Galilei was also an optimum design for minimum weight under a uniform stress constraint. Galileo's problem was probably one of the earliest structural optimization problems. However, the roots for the development of mathematical optimization started after the introduction of calculus by Newton and/or Leibniz during the latter part of the 17th Century. The min-max conditions (from calculus) as defined by the gradients of the function with respect to the independent variables provided the necessary conditions for optimal solutions. The function itself represented a measure of the performance of the system, while the independent variables spanned the design space. The min-max conditions, in their original form, are only of limited, interest because they addressed only the unconstrained optimization problems, which are of little interest in true engineering optimization. The extension of simple mini-max conditions to constrained optimization problems is through the formulation of an augumented Lagrangian function which consists of both the objective and constraint functions with additional variables called Lagrangian multipliers. There are as many Lagrangian multipliers as there are constraint functions. The Lagrangian multipliers serve two purposes: a) they are weighting factors in establishing the importance of the various constraints at different regions of the design space; b) they are also a link between the objective and the constraint functions in the augumented Lagrangian function. One way of looking at this latter connection is the dimensional compatibility of the objective function and the constraint functions in an augmented Lagrangian function. The Lagrangian multipliers are the dual variables, while the original variables in the objective and constraint functions are the primal variables. Determination of both these variables constitutes the solution of the optimization problem.

The emergence of the calculus of variations (attributed to Bernoulli, Euler and Lagrange during the 17th/18th Century) represents the beginning of the golden age of mathematical optimization. The brachistochrone problem and its many variations provided an intellectual challenge to such great mathematicians as the Bernoulli brothers, Leibniz, L'Hôpital and Newton. Variational calculus is basically a generalization of the elementary theory of minima and maxima. However, variational methods deal with the extremum of a function of functions. The resulting solution is not an extremum point but one or more functions, and they are represented by differential equations. The solution of these differential equations represents the optimal path or all the optimal points in the domain of definition.

Variational methods have applications in many disciplines such as solid mechanics, fluid mechanics, fluid-structure interaction, optics, flight mechanics, optimal controls and general engineering optimization problems. The formulation of the Euler-Lagrange equations in the 18th Century represented the most far reaching advance in variational calculus. Most of the field equations of rational mechanics can be derived from the Euler-Lagrange equations. The next major advance in variational methods was the "principle of least action" as originally derived by Euler and later improved and expanded to a wider class of forces by Hamilton. It is subsequently known as Hamilton's principle. Most of the dynamic system equations based on Newton's Laws can be derived from Hamilton's principle of least action. A further extension of the principle of least action is the formulation of Lagrange's equation which is the basis for an elegant description of Newtonian dynamics. Reference 1 provides a lucid description of the development of variational methods with details of the mathematical formulation.

Even though variational methods are the basis for all optimization problems, they present numerous difficulties in practical applications. The Euler-Lagrange equations

490

which express the extremum conditions yield one or more differential equations for solution. Most often they are nonlinear differential equations. The solution of nonlinear differential equations in closed form is difficult except in the case of very simple problems. Even when there are solutions, the continuity and differentiability requirements severely restrict the range of their application. A numerical approach to the solution of variational equations involves an approximation of derivatives by differences and integrals by sums. The accuracy, time steps and convergence become serious impediments to a reliable solution. Multidisciplinary design as an optimization problem becomes even more intractable in the context of variational calculus. Each discipline generates different orders and characteristics of the differential equations, and their interface is often difficult because the requirements of differentiability and continuity cannot be satisfied easily. Moreover modern digital computers are geared for the direct solution of algebraic equations rather than differential equations. The solution of differential equations on a digital computer involves an additional step of converting them into algebraic equations through approximations which do not always guarantee the desired accuracy or the stability of convergence.

It became apparent in the 1950's that high speed digital computers can provide unprecedented opportunities for the solution of complex engineering problems. The result is the development of finite element, finite difference and other discrete methods for the analysis and numerical search techniques for optimization problems. A common feature of these new methods is that they reduce the field equations to algebraic form instead of ingro-differential form. The algebraic equations are readily amenable to solution on high speed digital computers.

The basic concept of numerical search techniques for optimization problems is very simple. It involves a point by point search for the optimum in an n-dimensional design space. In its simplest form a numerical search procedure consists of four steps when applied to unconstrained minimization problems:

i. Selection of an initial design in the n-dimensional space where n is the number of variables.

ii. A procedure for the evaluation of the function (objective function) at a given point in the design space.

iii. Comparison of the current design with all the preceding designs.

iv. A rational way to select a new design and repeat the process.

The constrained minimization requires an additional step for the evaluation of the constraints. This step is for determining whether the design is feasible (does not violate the constraints).

The numerical search procedure as outlined here appears deceptively simple. However, actual implementation to practical design problems poses many difficult questions which cannot be answered easily. Even a cursory examination of the procedure reveals a number of uncertainties. For example, how is the initial design selected and what effect will it have on the outcome of the search? If there is a unique optimum, the intial design should not effect the final result. However, it is well known that most nonlinear optimization problems will have multiple optimums, and the initial design would only guarantee the nearest optimum. Even if there is a unique optimum, the initial design will certainly effect the number of points to be searched. The next pertinent question is what is a rational way to select the new designs and how does it effect the final outcome. This is the most serious issue and incites more passion than a rational discussion among the algorithm developers. The simplest, but probably a mindless way, is to select new design points at random. This procedure may be acceptable when the dimensionality of the design space is small and the objective and constraint functions evaluation is simple and computationally inexpensive. A more rational approach to the search strategy is to take advantage of the gradient information of the objective and constraint functions to reach the optimum. The next question is where to stop the search. The obvious answer is when the optimality conditions are satisfied. In the case of unconstrained minimization, the necessary conditions for the optimum are the standard min-max criterion of calculus. For constrained minimization problems the same min-max conditions are also valid with the augumented Lagrangian function. In the presence of multiple optimums this procedure can only guarantee the local optimum. The only way to investigate other solutions is by starting at different initial points and hope to cover the rest of the design space. Even though the numerical search procedures lack the elegance of variational methods, they are simple in concept and flexible in implementation in multidisciplinary design.

ISSUES IN MULTIDISCIPLINARY DESIGN OPTIMIZATION

Design optimization in an interdisciplinary setting is one of the most promising fields at present both in basic research and exploratory development. As systems become more and more complex, a creative designer needs to supplement intuition with computational tools in order to verify the validity of new concepts. Recent developments in computer hardware and related software offer great opportunities for integration of the relevant disciplines to simulate the true environment of aerospace vehicles. The goal of modern design is to optimize the total system rather than the individual components. The conflicting requirements of the subsystems can be handled much more effectively in an integrated design.

As lofty as this goal might be, progress has been very slow in achieving the objectives of interdisciplinary design. The obvious difficulty is the vast scope of individual disciplines and the inability to comprehend complex interactions. For example, a typical aircraft design encompasses at least aerodynamics, structures, controls and propulsion.

Each of the disciplines presents numerous computational issues on their own. When combined, their interaction further compounds the problem. Even the definition of a simple merit function, the constraints, and the variables that respond to the requirements of all the disciplines is not an easy matter. The weight of the structure may be the most appealing merit function for a structural designer. The lift and/or drag may be the concern of an aerodynamicist. Some stability or performance criterion may be a suitable merit function for a control designer, while the thrust to weight ratio may be the interest of the propulsion designer. The definition of the constraints and the variables similarly add to the complexity.

A closer examination of the design process in the context of an aircraft wing (and other lifting surfaces) optimization can lead to a better appreciation of the complex interactions. In particular the coupling between aerodynamics, structures, and controls is very strong in high peformance aircraft. The elements of structural optimization with due consideration to this coupling are shown schematically in Fig. 1. It is assumed that a structural concept definition preceded this discussion, and a reasonable mathematical model of the structure is available for preliminary design.

The loads definition is a complex process in an aircraft design. This information can be derived from knowledge of the expected maneuvers. The maneuver loads have generally two components: The inertia loads from the aircraft acceleration and the lift and drag forces from the aerodynamics. They are calculated at the peak condition of each maneuver and used as static airloads. These loads are used in conjunction with the static and dynamic aeroelastic conditions in optimization. The airloads are computed on the entire lifting surface (aerodynamic model). The structural box normally constitutes only a fraction of the lifting surface, and the two models (the aero model and the structural model)

Interdisciplinary Design

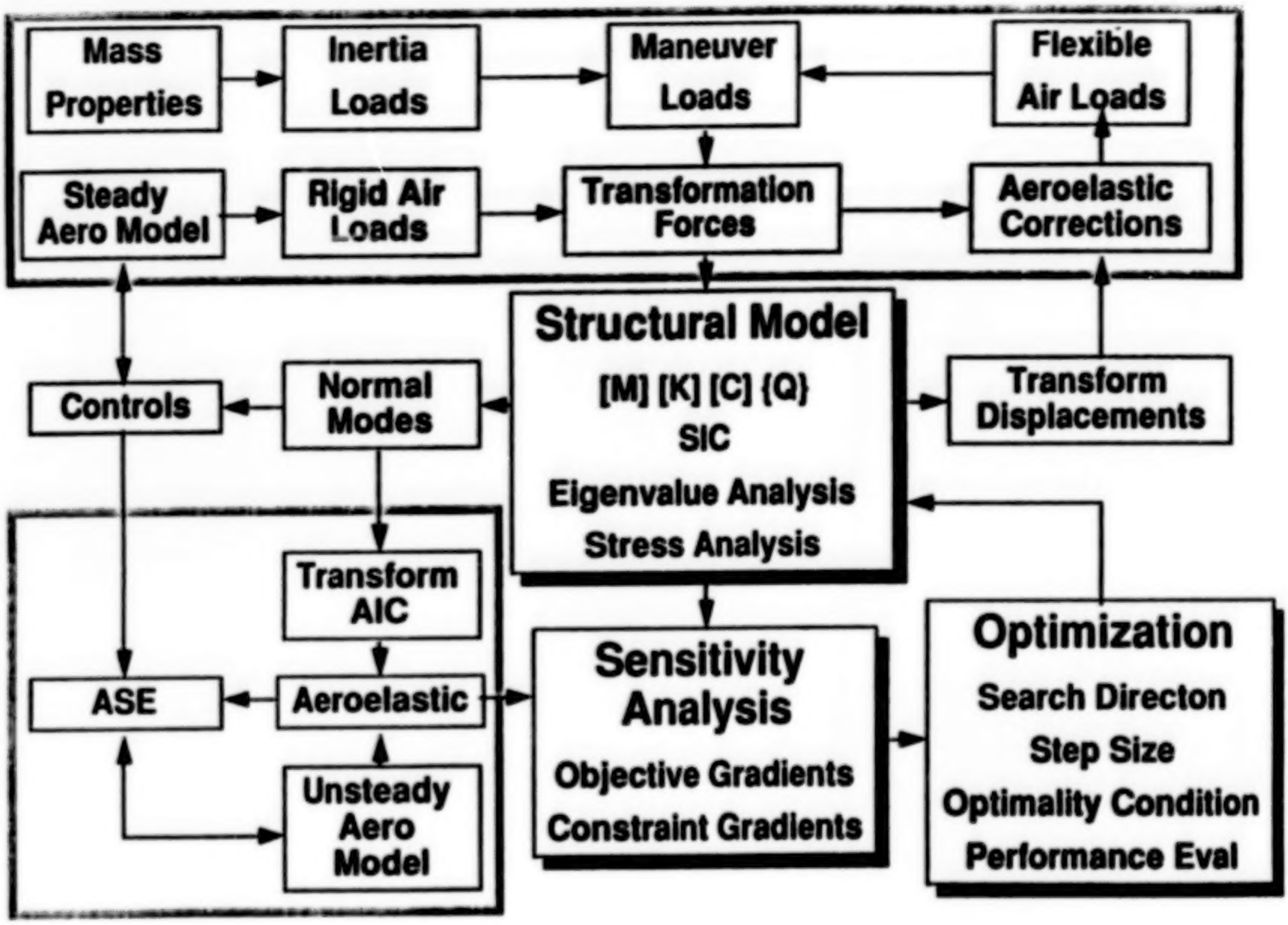
Mass Properties
Inertia Loads
Maneuver Loads
Flexible Air Loads
Steady Aero Model
Rigid Air Loads
Transformation Forces
Aeroelastic Corrections
Structural Model
[M] [K] [C] {Q}
SIC
Eigenvalue Analysis
Stress Analysis
Controls
Normal Modes
Transform Displacements
Transform AIC
ASE
Aeroelastic
Unsteady Aero Model
Sensitivity Analysis
Objective Gradients
Constraint Gradients
Optimization
Search Directon
Step Size
Optimality Condition
Performance Eval

FIGURE 1

are not the same. To make the two models compatible, two types of transformations (one preceding and one after the analysis) must be devised. One transformation involves the generation of an equivalent load system from the airloads to the structual grid loads. The theoretical basis of this transformation is somewhat nebulous and open to controversy. The assumptions made in deriving this transformation can adversely effect the local behavior of the structure. Optimization can further aggravate the situation by propagating the errors. The second transformation involves an interpolation/extrapolation of the displacements from the structural box to the aerodynamic surface. The purpose of this extrapolation is to determine the change in angle of attack (due to deformation) which effects the air flow on the wing. Many software systems such as NASTRAN and ASTROS use a spline extrapolation for this purpose. In many instances the approximations in this extrapolation seem to break down and produce spurious results. Even though the loads and the displacement transformations appear to be innocuous, they are one of the serious impediments to integration. The technology of maneuver loads calculation is one of the major stumbling blocks. This is particularly so in the supersonic range. Aeroelasticity and aeroservoelasticity are emerging technologies, and they need further validation. Dimensionality is a serious limitation in optimization algorithms. This limitation is of particular significance in the optimization of composites where the number of design variables increases rapidly. These are some of the issues which need further resolution for an effective application of multidisciplinary optimization.

STATUS OF MULTIDISCIPLINARY OPTIMIZATION

Interest in multidisciplinary design has been widespread for over 20 years. A number of optimization programs for the preliminary design of aircraft structures were developed in the past and are being developed at present. A brief review of these optimization systems is provided in the remainder of this paper. A list of programs reviewed in this paper is as follows:

- ASOP-FASTOP(2,3)
- TSO(4,5)
- STARS(6,7)
- LAGRANGE(8,9)
- ELFINI(10)

485

- ASTROS[11,12]

ASOP-FASTOP PROGRAM

The ASOP (Automated Structural Optimization Program) and FASTOP (Flutter And Strength Optimization Program) programs were the earliest attempts to automate the preliminary design function of lifting surfaces. These programs were originally intended for the modest integration of structures, aerodynamics and optimization. The original objectives of these programs were very ambitious but with very limited resources for development. However, these programs were very effective and established the feasibility of integrating the three disciplines. They are the forerunners for the more recent systems. The objectives of even recent systems are not significantly different from those of FASTOP. A summary of FASTOP capabilities and shortcomings is provided here.

- Structural Model
    - Elements
        Membrane Quadrilateral
        Membrane Triangle
        Shear Panel
        Rod
        Bar
    - Materials
        Isotropic and Layered Composites
- Air Loads
    Steady Aerodynamics
    Distribution of Vortices - Subsonic
    Distribution of Sources - Supersonic
- Inertia Loads
    Maneuver Defined by
    Vehicle Load Factors
    Angular Accelerations and Velocities
- Aerodynamics and Structure Interface
    A beaming procedure to the structural grid points nearest to the panel center of pressure.
- Aeroelasticity
    Unsteady Aerodynamics

    - Kernel Function - Subsonic
    - Doublet-Lattice - Subsonic
    - Mach-Box - Supersonic
    - Flutter Solution
    - K-Method
    - P-K Method
- Optimization
    - Stress-Ratio Type
- Objective Function
    - Weight
- Constraints
    - Strength, Stiffness and Aeroelasticity

The major contribution of FASTOP is that it established the feasibility of integrating structures, aerodynamics and aeroelasticity. It is a relatively unsophisticated program from the point of view of software design. It is a difficult program to adapt to changes in computer operating systems. A number of aerospace companies have used the FASTOP system, and even today it is considered to be a very good capability.

TSO PROGRAM

The TSO (Tailored Structural Optimization) program was developed for the tailoring of composites for aircraft wing type structures. It is intended primarily for making rapid design trades in order to establish performance trends while optimizing the composite layup. Structures, aerodynamics, aeroelasticity (with the capability to model multiple control surfaces), sensitivity analysis and optimization are the disciplines integrated in this program.

SPECIFIC DETAILS

- Structural Model
    - Smeared Plate and Raleigh-Ritz Procedure
    - Single Trapezoidal Surface
    - Polynomial Variation of Thickness
- Materials
    - Isotropic and Layered Composites
- Air Loads

A Finite Element Lifting Surface Procedure - ROT

- Inertia Loads
  - Maneuver Specified
- Aeroelasticity
  - Assumed Downwash Pressure Distributions
- Optimization
  - Unconstrained Minimization with Penalty
  - Davidson-Fletcher-Powell Modification for Search
- Objective Function
  - Weight
- Constraints
  - Strength
  - Stiffness
  - Static and Dynamic
  - Aeroelasticity

TSO is one of the most widely used programs for the aeroelastic tailoring of lifting surfaces with layered composites. One of the serious deficiencies of TSO is the structures model. Equivalent plate idealization does not fully capture the internal behavior of a wing structure. It needs extensive lumping before optimization and unlumping after optimization. Nevertheless, it is an extremely good capability for establishing overall design trends.

STARS PROGRAM

STARS - (STructural Analysis and Redesign System) is a structural optimization system originally developed at RAE. Later development was transfered to SCICON Ltd. This program is of interest to aircraft companies in Europe, in particular, British Aerospace in England and MBB in Germany. The original STARS was primarily a structural optimization program. It was intended for structural weight minimization with strength, stiffness and frequency constraints. The program has limited structural analysis internally (RAE analysis) but depends on programs like NASTRAN for large scale applications. Versions of the program at MBB and British Aerospace include a flutter optimization capability. To the author's knowledge the program does not have the capability to calculate static air loads.

SPECIFIC DETAILS

- Stuctural Model
    - Elements

        When used in conjunction with NASTRAN, it has access to all the NASTRAN elements. RAE analysis consists of the following elements:

        Membrane Quadrilateral - Bending
        Rod
        Bar-Box Beam
        Shear Panel
        Triangular Elements
- Materials

    Isotropic, Anisotropic and Layered Composites
- Air Loads

    The author is not aware of air loads capabilities.
- Aeroelasticity

    Versions at British Aerospace and MBB have aeroelasticity.
- Optimization

    Stress Ratio Module
    Pseudo-Newton Module
    Optimality Criterion Module
- Objective Function

    Weight
- Constraints

    Strength
    Stiffness
    Frequency
    Flutter (British Aerospace and MBB)

The STARS system will continue to be and further develop into a sophisticated structural optimization system if British Aerospace enhances the aerodynamics capability. It is also being used by MBB-civilian division.

LAGRANGE PROGRAM

Messer Schmitt-Bolkow-Blohm in Germany has invested considerable resources in the development of LAGRANGE, a structrual optimization system. It contains most of the capabilities necessary for the integration of aerodynamics, structures and controls in an optimization setting. It appears that the system has been operational at MBB for over a year. However, it is not clear from the two references, 6 and 7, whether LAGRANGE is an integrated (structures, aerodynamics, optimization, etc.) system or an interface between programs such as NASTRAN, TSO (modified at MBB), ASAT (modified FASTOP) etc. These references contain excellent design studies, and they can be the basis for comparison with the designs obtained from other multidisciplinary optimization systems.

SPECIFIC DETAILS

- Structural Model

  It is not clear if the structural analysis module is external to the system. If NASTRAN is the main driver for the structural analysis, then the system has access to all the elements necessary for the optimization of aircraft structures.

- Materials

  Isotropic
  Anisotropic
  Layered Composites

- Air Loads

  Similar to FASTOP and TSO with signficant enhancements.

- Inertia Loads

  Maneuvers defined by
  Vehicle Load Factors
  Angular Accelerations and Velocities

- Aerodynamics and Structure Interface

  A beaming procedure similar to FASTOP (assumption).

- Aeroelasticity

  It is assumed that it is similar to FASTOP with significant enhancements.

- Optimization

  Sequential Quadratic Programming
  Generalized Reduced Gradients

- Objective Function

    Weight

- Constraints
    - Strength
    - Displacements
    - Frequencies
    - Static Aeroelastic Efficiencies

The LAGRANGE program is expected to have a significant impact on future multidisciplinary optimization developments. This judgment is based on published design studies using the program.

ELFINI - STRUCTURAL OPTIMIZATION SYSTEM AT DASSAULT

ELFINI is an integrated finite element analysis and optimization system under development at Dassault for over a decade. It is an excellent example of what a sustained long term investment can do to design productivity. It appears that ELFINI's interface is not limited to finite element pre and post processing systems. The Three-D graphics system CATIA with extensive mesh generation capability can be used in conjunction with the finite element pre and post processors to generate a data stream for analysis and optimization. ELFINI integrates the structures, aerodynamics and controls for aircraft structures design. ELFINI has the most extensive applications history starting with its use in the design of Dassault's mirage series fighters to more recent systems like RAFALE (the most recent DASSAULT fighter with extensive use of composites) and HERMES (European Space Shuttle). Both military and civilian applications are cited.

SPECIFIC DETAILS

- Structural Model
    - Rod
    - Bar
    - Membrane Triangle
    - Membrane Quadrilateral
    - Shear Panel
    - Buckling Plate - Triangle and Quadrilateral.
    - There are additional elements but they are not relevant in optimization.
- Material
    - Isotropic

  - Anisotropic
  - Layered Composites
- Aerodynamics
  - Extensive Aeroelasticity Capability
  - Not clear about integrated air loads capability.
- Optimization
  - Conjugate Projected Gradient
- Objective Function
  - Weight
- Constraints
  - Strength
  - Displacements
  - Frequencies
  - Buckling of the Elements
  - Buckling of the Structure
  - Static and Dynamic Aeroelastic Constraints
- Graphics Interface
  - Extensive graphics interface in pre and post processing and geometric modeling.

Like the program LAGRANGE, ELFINI is expected to play an important role in the development of integrated design systems by providing an applications data base. The most impressive features of ELFINI are its extensive graphics interface and its applications in a practical design environment.

ASTROS - AUTOMATED STRUCTURAL OPTIMIZATION SYSTEM

This program was developed over the past five years. The program was released to industry in July 1988. This program is a follow-up of a series of optimization programs (ASOP-FASTOP-TSO-ASTROS) sponsored by the Flight Dynamics Laboratory at Wright-Patterson AFB. Development of software standards for integrated design systems is one of the significant contributions of ASTROS. This is in the tradition of the development of NASTRAN. ASTROS' "MAPOL" executive system and Computer Aided Design Data Base (CADDB) are supported by six engineering modules which are important in the integrated design of aircraft structures. Figs. 2-4 show the schema, the architecture and the engineering modules.

SPECIFIC DETAILS

- Structures Model
    - Rod
    - Bar
    - Membrane Triangle
    - Membrane Quadrilateral
    - Shear Panel
    - QUAD4 - Bending and Membrane Quadrilateral
- Materials
    - Isotropic
    - Anisotropic
    - Layered Composites
- Aerodynamics
    - Air Loads - Steady Aerodynamics
    - USSAERO - Woodward Aerodynamics
    - Aeroelasticity - Unsteady Aerodynamics integrated into ASTROS
    - Doublet Lattice - Subsonic
    - CPM - Supersonic
- Optimization
    - ADS
    - Optimality Criterion (Planned)
- Objective Function
    - Weight
- Constraints
    - Strength
    - Stiffness
    - Frequencies
    - Static and Dynamic Aeroelastic Constraints
- Graphics Interface
    - Data input and output similar to NASTRAN.
    - Pre and post processors for NASTRAN are applicable.

With the ASTROS program release to industry, a number of applications and results are expected in the near future. The program is being updated for new releases after quality assurance testing. The formulation of a users group and procedures for submitting an SPR

AUTOMATED STRUCTURAL OPTIMIZATION SYSTEM

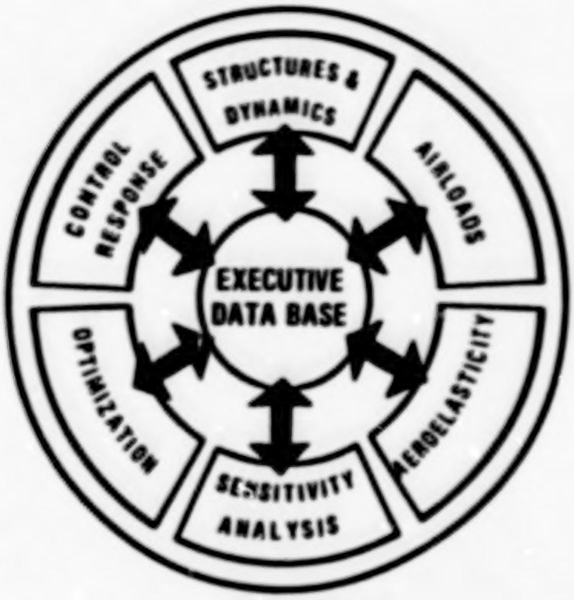
STRUCTURES & DYNAMICS
AIRLOADS
AEROELASTICITY
SENSITIVITY ANALYSIS
OPTIMIZATION
CONTROL RESPONSE
EXECUTIVE DATA BASE

FIGURE 2

ASTROS ARCHITECTURE

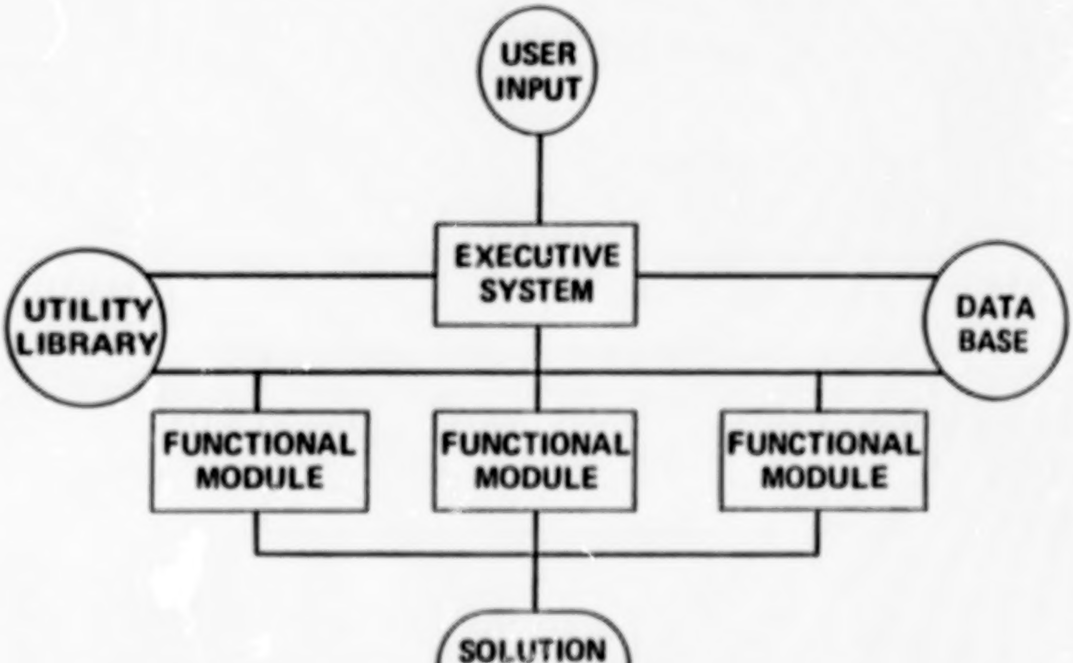
USER INPUT
EXECUTIVE SYSTEM
UTILITY LIBRARY
DATA BASE
FUNCTIONAL MODULE
FUNCTIONAL MODULE
FUNCTIONAL MODULE
SOLUTION RESULTS

FIGURE 3

ENGINEERING DISCIPLINES

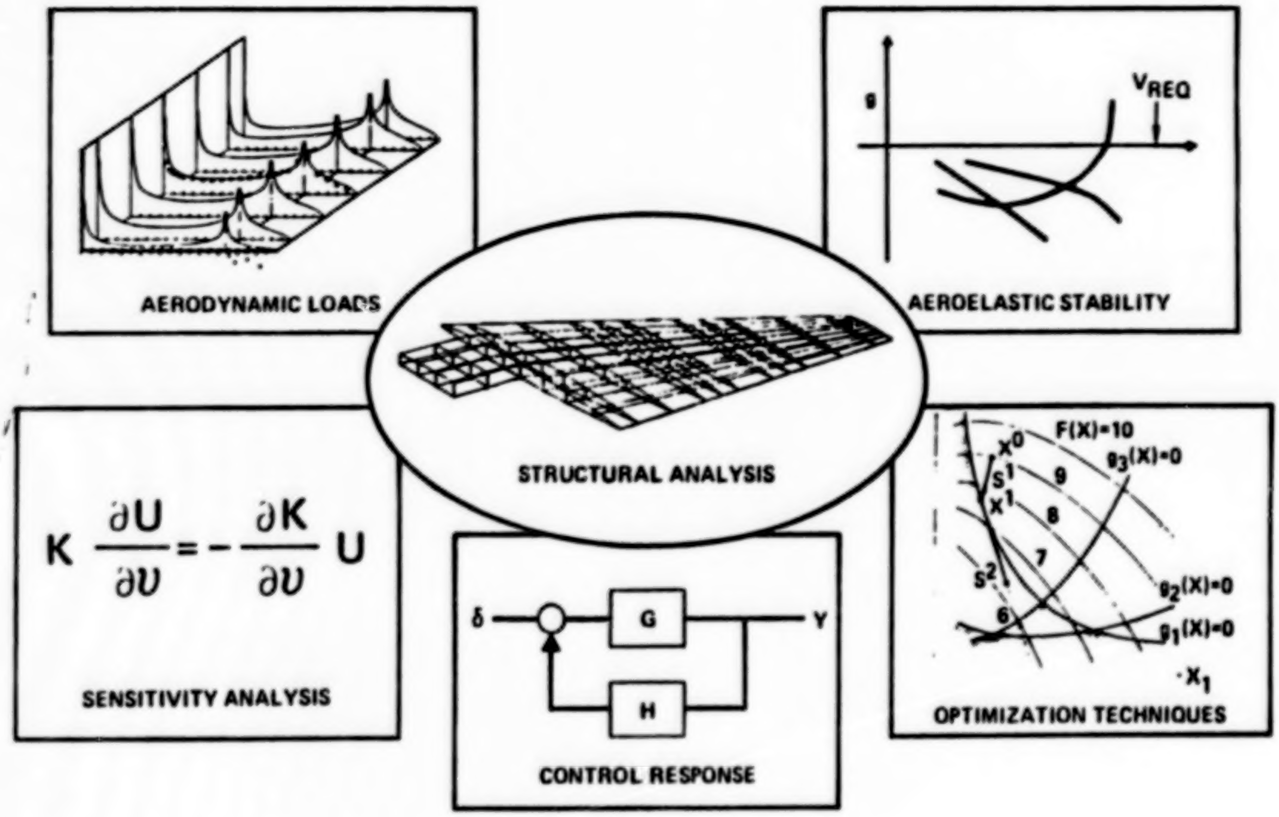
AERODYNAMIC LOADS
g
V_{REQ}
AEROELASTIC STABILITY
STRUCTURAL ANALYSIS
$K \frac{\partial U}{\partial \upsilon} = - \frac{\partial K}{\partial \upsilon} U$
SENSITIVITY ANALYSIS
δ
G
Y
H
CONTROL RESPONSE
F(X)=10
X^0
$g_3(X)=0$
S^1
X^1
9
8
7
S^2
6
$g_2(X)=0$
$g_1(X)=0$
X_1
OPTIMIZATION TECHNIQUES

FIGURE 4

BEST COPY AVAILABLE

(Software Problem Report) and a DER (Documentation Error Report) are being worked out.

CONCLUSIONS

With the release of all these new systems, the concept of multidisciplinary optimization has the potential to become reality. The growth of an applications data base in the next few years will not only help fine-tune the systems but also will provide valuable lessons for future developments. The expected release of MSC-NASTRAN with optimization will be a significant development in the direction of establishing standards for multidisciplinary optimization. The developments in new computers and the interest in integrated design will provide excellent opportunities for making the computer-aided design a reality. Reference 13 contains a capability summary of many of the systems.

REFERENCES

1. Smith, D. R., "Variational Methods in Optimization," Prentice-Hall Inc., Englewood Cliffs, NJ, 1974.

2. Isakson, G., Pardo, H., Lerner, E., and Venkayya, V., "ASOP-3: A Program for the Optimum Design of Metallic and Composite Structures Subjected to Strength and Deflection Constraints," AIAA Paper 77-378; also published in the Journal of Aircraft, July 1978, pp. 422-428.

3. Wilkinson. K., Markowitz, J., Lerner, E., Chipman, R., George, D., and Schriro, G., "An Automated Procedure for Flutter and Strength Analysis and Optimization of Aerospace Vehicles," Vol. I - Theory, Vol. II - Program User's Manual, Air Force Flight Dynamics Laboratory, AFFDL-TR-75-137, Dec. 1975.

4. McCullers, L. A., and Lynch, R. W., "Dynamics Characteristics of Advanced Filamentary Composite Structures," AFFDL-TR-73-111, Volume II, September 1974.

5. Lynch, R. W., Rogers, W. A., and Brayman, W. W., "Aeroelastic Tailoring of Advanced Composite Structures for Military Aircraft," Vol. I - General Theory, Vol. II - Wing Preliminary Design, Vol. III - Modifications and User's Guide for Procedure TSO: AFFDL-TR-76-100, April 1977.

6. Bartholomew, P., Morris, A. J., "STARS: A Software Package for Structural Optimization," Proceedings of the International Symposium on Optimum Structural Design, Oct 1981, University of Arizona.

7. Wellen. H., and Bartholomew, P., "Structural Optimization in Aircraft Construction," Proceedings of the NATO Advanced Study Institute - Computer Aided Structural and Mechanical Systems - Editor: Carlos A. Mota Soares - Springer-Verlag, 1987, pp 955-970.

8. Sensburg, O., Fullhas, K., and Schmidinger, G., "Interdisciplinary Design of Aircraft Structures for Minimum Weight," A paper presented at AIAA/ASME/ASCE/AHS/ACS 29th Structures, Structural Dynamics and Materials Conference, Williamsburg, VA, April 18-20, 1988.

9. Kneppe, G., Kramer, J., and Winkler, E., "Structural Optimization of Large Scale Problems Using MBB-LAGRANGE," Paper presented at the Fifth World Congrress and Exhibition on Finite Element Methods, Salzburg/Austria, October 5-9, 1987.

10 Lecina, G., and Petian, C., "Advances in Optimal Design with Composite Materials," Proceedings NATO - Advanced Study Institute - Computer Aided Optimal Design - Structural and Mechanical Systems - Editor: Carlos A. Mota Soares - Troia, Portugal, June 29 - July 11, 1986.

11 Neill, D. J., Johnson, E. H., and Canfield, R. A., "ASTROS - A Multidisciplinary Automated Structural Design Tool," Paper presented at AIAA/ASME/ASCE/AHS 28th Structures, Structural Dynamics and Materials Conference, Monterey, CA, April 6-8, 1987.

12. Johnson, E. H., Neill, D. J., and Venkayya, V. B., ASTROS: Theoretical Manual - User's Manual - Applications. AFWAL-TR-88-3028, December, 1988.

13. Hornlein, H. R. E. M., "Take-off in Optimum Structural Design," Proceedings of NATO Advanced Study Institute - Editor: Carlos A. Mota Soares - Troia, Portugal, June 29 - July 11, 1986.

★U.S. GOVERNMENT PRINTING OFFICE: 1989 -627-064/ 86029

NASA
National Aeronautics and Space Administration

Report Documentation Page

1. Report No.
NASA CP-3031, Part 3

2. Government Accession No.

3. Recipient's Catalog No.

4. Title and Subtitle
Recent Advances in Multidisciplinary Analysis and Optimization

5. Report Date
April 1989

6. Performing Organization Code

7. Author(s)
Jean-François M. Barthelemy, Editor

8. Performing Organization Report No.
L-16568

10. Work Unit No.
506-43-41-01

9. Performing Organization Name and Address
NASA Langley Research Center
Hampton, Virginia 23665-5225

11. Contract or Grant No.

12. Sponsoring Agency Name and Address
National Aeronautics and Space Administration
Washington, DC 20546-0001
and
Wright Research Development Center
Wright Patterson AFB, OH 45433

13. Type of Report and Period Covered
Conference Publication

14. Sponsoring Agency Code

15. Supplementary Notes
Conference Co-Chairmen:
Jaroslaw Sobieski, NASA Langley Research Center
Laszlo Berke, NASA Lewis Research Center
Vipperla Venkayya, Air Force Wright Aeronautical Laboratory

16. Abstract

This three-part document contains a collection of technical papers presented at the Second NASA/Air Force Symposium on Recent Advances in Multidisciplinary Analysis and Optimization, held September 28-30, 1988 in Hampton, Virginia. The topics covered include: Helicopter Design, Aeroelastic Tailoring, Control of Aeroelastic Structures, Dynamics and Control of Flexible Structures, Structural Design, Design of Large Engineering Systems, Application of Artificial Intelligence, Shape Optimization, Software Development and Implementation, and Sensitivity Analysis.

17. Key Words (Suggested by Author(s))
Optimization
Synthesis
Systems
Sensitivity
Computers

18. Distribution Statement
Unclassified - Unlimited
Subject Category 05

19. Security Classif. (of this report)
Unclassified

20. Security Classif. (of this page)
Unclassified

21. No. of pages
529

22. Price
A23

NASA FORM 1626 OCT 86

For sale by the National Technical Information Service, Springfield, Virginia 22161-2171

NASA-Langley, 1989

**National Aeronautics and
Space Administration
Code NTT-4**

**Washington, D.C.
20546-0001**

**Official Business
Penalty for Private Use, $300**

National Aeronautics and Space Administration

WASHINGTON, D.C. 20546

OFFICIAL BUSINESS
Penalty For Private Use $300.00

POSTAGE AND FEES PAID
NATIONAL AERONAUTICS AND
SPACE ADMINISTRATION
PERMIT NO. G27

U.S.MAIL

SPECIAL FOURTH CLASS MAIL
BOOK

1S 001 CR3031-111E9C417S00237ED
GOVERNMENT PRINTING OFFICE
LIBRARY PROGRAMS SERVICE/SLIR
ACQUISITIONS SECTION
WASHINGTON DC 20401

NASA

POSTMASTER: **If Undeliverable (Section 158
Postal Manual) Do Not Return**

799

END

DATE FILMED

12-19-91